WOODHEAD PUBLISHING SERIES IN BIOMATERIALS

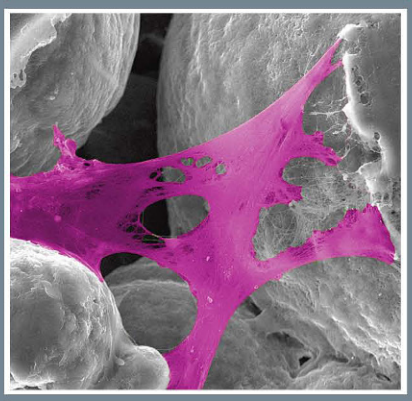

Biomedical Foams for Tissue Engineering Applications

Edited by Paolo A. Netti

WP
WOODHEAD PUBLISHING

Biomedical Foams for Tissue Engineering Applications

Related titles:

Novel biomaterials for bone regeneration
(ISBN 978-0-85709-804-7)

Bone substitute biomaterials
(ISBN 978-0-85709-497-1)

Silk biomaterials for tissue engineering and regenerative medicine
(ISBN 978-0-85709-699-9)

Woodhead Publishing Series in Biomaterials: Number 76

Biomedical Foams for Tissue Engineering Applications

Edited by
Paolo A. Netti

AMSTERDAM • BOSTON • CAMBRIDGE • HEIDELBERG • LONDON
NEW YORK • OXFORD • PARIS • SAN DIEGO
SAN FRANCISCO • SINGAPORE • SYDNEY • TOKYO
Woodhead Publishing is an imprint of Elsevier

Woodhead Publishing is an imprint of Elsevier
80 High Street, Sawston, Cambridge, CB22 3HJ, UK
225 Wyman Street, Waltham, MA 02451, USA
Langford Lane, Kidlington, OX5 1GB, UK

British Library Cataloguing-in-Publication Data
A catalogue record for this book is available from the British Library.

Library of Congress Control Number: 2013956584

ISBN 978-0-85709-696-8 (print)
ISBN 978-0-85709-703-3 (online)

For information on all Woodhead Publishing publications visit our website at http://store.elsevier.com/

Typeset by Newgen Knowledge Works Pvt Ltd, India

Printed and bound in the United Kingdom

Contents

Contributor contact details

(* = main contact)

Editor

P. A. Netti
Department of Chemical, Materials and Production Engineering and Interdisciplinary Research Centre on Biomaterials (CRIB)
University of Naples Federico II
Piazzale Tecchio 80
80125 Naples, Italy

E-mail: nettipa@unina.it

and

Center for Advanced Biomaterials for Health Care (IIT@CRIB)
Istituto Italiano di Tecnologia
Largo Barsanti e Matteucci 53
80125 Naples, Italy

E-mail: paolo.netti@iit.it

Chapter 1

A. Salerno
Center for Advanced Biomaterials for Health Care (IIT@CRIB)
Istituto Italiano di Tecnologia
Largo Barsanti e Matteucci 53
80125 Naples, Italy

E-mail: asalerno@unina.it

P. A. Netti*
Department of Chemical, Materials and Production Engineering and Interdisciplinary Research Centre on Biomaterials (CRIB)
University of Naples Federico II
Piazzale Tecchio 80
80125 Naples, Italy

E-mail: nettipa@unina.it

and

Center for Advanced Biomaterials for Health Care (IIT@CRIB)
Istituto Italiano di Tecnologia
Largo Barsanti e Matteucci 53
80125 Naples, Italy

E-mail: paolo.netti@iit.it

Chapter 2

V. Guarino and L. Ambrosio*
Institute of Composite and Biomedical Materials
National Research Council of Italy
Piazzale Tecchio 80
80125 Naples, Italy

E-mail: ambrosio@unina.it

Chapter 3

A. Salerno*
Center for Advanced Biomaterials for Health Care (IIT@CRIB)
Istituto Italiano di Tecnologia
Largo Barsanti e Matteucci 53
80125 Naples, Italy

E-mail: asalerno@unina.it

P. A. Netti
Department of Chemical, Materials and Production Engineering and Interdisciplinary Research Centre on Biomaterials (CRIB)
University of Naples Federico II
Piazzale Tecchio 80
80125 Naples, Italy

E-mail: nettipa@unina.it

and

Center for Advanced Biomaterials for Health Care (IIT@CRIB)
Istituto Italiano di Tecnologia
Largo Barsanti e Matteucci 53
80125 Naples, Italy

E-mail: paolo.netti@iit.it

Chapter 4

M. Madaghiele, L. Salvatore and A. Sannino*
Department of Engineering for Innovation
University of Salento
Via per Monteroni
73100 Lecce, Italy

E-mail: alessandro.sannino@unisalento.it

Chapter 5

E. M. Prieto and S. A. Guelcher*
Department of Chemical and Biomolecular Engineering
Vanderbilt University
PMB 351604
2301 Vanderbilt Place
Nashville, TN 37235, USA

E-mail: edna.m.prieto@vanderbilt.edu; scott.guelcher@vanderbilt.edu

Chapter 6

S. Iannace* and L. Sorrentino
Institute of Composite and Biomedical Materials
National Research Council
Piazzale E. Fermi 1
80055 Portici (NA), Italy

E-mail: iannace@unina.it

E. Di Maio
Department of Chemical, Materials and Production Engineering
University of Naples Federico II
Piazzale Tecchio 80
80125 Naples, Italy

Chapter 7

A. Hoppe and A. R. Boccaccini*
Institute of Biomaterials
Department of Materials Science and Engineering
University of Erlangen-Nuremberg
Cauerstrasse 6
91058 Erlangen, Germany

E-mail: aldo.boccaccini@ww.unierlangen.de

Chapter 8

F. Baino* and C. Vitale-Brovarone
Institute of Materials Physics and Engineering
Applied Science and Technology Department
Politecnico di Torino
Corso Duca degli Abruzzi 24
10129 Torino, Italy

E-mail: francesco.baino@polito.it

Chapter 9

S. Sprio, M. Sandri, M. Iafisco and S. Panseri
Institute of Science and Technology for Ceramics
National Research Council
Via Granarolo 64
48018 Faenza (RA), Italy

G. Filardo, E. Kon and M. Marcacci
Rizzoli Orthopaedic Institute
Laboratory of Biomechanics and Technology Innovation
Via Di Barbiano 1/10
40136 Bologna, Italy

A. Tampieri*
Institute of Science and Technology for Ceramics
National Research Council
Via Granarolo 64
48018 Faenza (RA), Italy

E-mail: anna.tampieri@istec.cnr.it

Chapter 10

M. P. Ginebra* and E. B. Montufar
Biomaterials, Biomechanics and Tissue Engineering Group
Department of Materials Science and Metallurgical Engineering
Technical University of Catalonia
Av. Diagonal 647
08028 Barcelona, Spain

E-mail: maria.pau.ginebra@upc.edu

Chapter 11

M. Shah Mohammadi
Department of Mining and Materials Engineering
McGill University
M.H. Wong Building
3610 University Street
Montreal, QC H3A 0C5, Canada

M. N. Bureau
National Research Council of Canada
Boucherville, QC J4B 6Y4, Canada

S. N. Nazhat*
Department of Mining and Materials Engineering
McGill University
M.H. Wong Building
3610 University Street
Montreal, QC H3A 0C5, Canada

E-mail: Showan.Nazhat@Mcgill.ca

Chapter 12

S. Van Vlierberghe, G.-J. Graulus, S. Keshari Samal, I. Van Nieuwenhove and P. Dubruel
Polymer Chemistry & Biomaterials Group
Ghent University
Krijgslaan 281 (Building S4-Bis)
B-9000 Ghent, Belgium

E-mail: Sandra.VanVlierberghe@UGent.be

Chapter 13

F. Causa*
Department of Chemical, Materials and Production Engineering and Interdisciplinary Research Centre on Biomaterials (CRIB)
University of Naples Federico II
Piazzale Tecchio 80
80125 Naples, Italy

E-mail: causa@unina.it

and

Center for Advanced Biomaterials for Health Care (IIT@CRIB)
Istituto Italiano di Tecnologia
Largo Barsanti e Matteucci 53
80125 Naples, Italy

E-mail: filippo.causa@iit.it

N. Gargiulo
Department of Chemical, Materials and Industrial Production Engineering
University of Naples Federico II
Piazzale Tecchio 80
80125 Naples, Italy

E. Battista
Center for Advanced Biomaterials for Health Care (IIT@CRIB)
Istituto Italiano di Tecnologia
Largo Barsanti e Matteucci 53
80125 Naples, Italy

P. A. Netti
Department of Chemical, Materials and Production Engineering and Interdisciplinary Research Centre on Biomaterials (CRIB)
University of Naples Federico II
Piazzale Tecchio 80
80125 Naples, Italy
E-mail: nettipa@unina.it

and

Center for Advanced Biomaterials for Health Care (IIT@CRIB)
Istituto Italiano di Tecnologia
Largo Barsanti e Matteucci 53
80125 Naples, Italy

E-mail: paolo.netti@iit.it

Woodhead Publishing Series in Biomaterials

1 **Sterilisation of tissues using ionising radiations**
Edited by J. F. Kennedy, G. O. Phillips and P. A. Williams
2 **Surfaces and interfaces for biomaterials**
Edited by P. Vadgama
3 **Molecular interfacial phenomena of polymers and biopolymers**
Edited by C. Chen
4 **Biomaterials, artificial organs and tissue engineering**
Edited by L. Hench and J. Jones
5 **Medical modelling**
R. Bibb
6 **Artificial cells, cell engineering and therapy**
Edited by S. Prakash
7 **Biomedical polymers**
Edited by M. Jenkins
8 **Tissue engineering using ceramics and polymers**
Edited by A. R. Boccaccini and J. Gough
9 **Bioceramics and their clinical applications**
Edited by T. Kokubo
10 **Dental biomaterials**
Edited by R. V. Curtis and T. F. Watson
11 **Joint replacement technology**
Edited by P. A. Revell
12 **Natural-based polymers for biomedical applications**
Edited by R. L. Reiss et al.
13 **Degradation rate of bioresorbable materials**
Edited by F. J. Buchanan
14 **Orthopaedic bone cements**
Edited by S. Deb
15 **Shape memory alloys for biomedical applications**
Edited by T. Yoneyama and S. Miyazaki
16 **Cellular response to biomaterials**
Edited by L. Di Silvio
17 **Biomaterials for treating skin loss**
Edited by D. P. Orgill and C. Blanco

18 **Biomaterials and tissue engineering in urology**
Edited by J. Denstedt and A. Atala
19 **Materials science for dentistry**
B. W. Darvell
20 **Bone repair biomaterials**
Edited by J. A. Planell, S. M. Best, D. Lacroix and A. Merolli
21 **Biomedical composites**
Edited by L. Ambrosio
22 **Drug–device combination products**
Edited by A. Lewis
23 **Biomaterials and regenerative medicine in ophthalmology**
Edited by T. V. Chirila
24 **Regenerative medicine and biomaterials for the repair of connective tissues**
Edited by C. Archer and J. Ralphs
25 **Metals for biomedical devices**
Edited by M. Ninomi
26 **Biointegration of medical implant materials: Science and design**
Edited by C. P. Sharma
27 **Biomaterials and devices for the circulatory system**
Edited by T. Gourlay and R. Black
28 **Surface modification of biomaterials: Methods analysis and applications**
Edited by R. Williams
29 **Biomaterials for artificial organs**
Edited by M. Lysaght and T. Webster
30 **Injectable biomaterials: Science and applications**
Edited by B. Vernon
31 **Biomedical hydrogels: Biochemistry, manufacture and medical applications**
Edited by S. Rimmer
32 **Preprosthetic and maxillofacial surgery: Biomaterials, bone grafting and tissue engineering**
Edited by J. Ferri and E. Hunziker
33 **Bioactive materials in medicine: Design and applications**
Edited by X. Zhao, J. M. Courtney and H. Qian
34 **Advanced wound repair therapies**
Edited by D. Farrar
35 **Electrospinning for tissue regeneration**
Edited by L. Bosworth and S. Downes
36 **Bioactive glasses: Materials, properties and applications**
Edited by H. O. Ylänen
37 **Coatings for biomedical applications**
Edited by M. Driver

38 **Progenitor and stem cell technologies and therapies**
Edited by A. Atala
39 **Biomaterials for spinal surgery**
Edited by L. Ambrosio and E. Tanner
40 **Minimized cardiopulmonary bypass techniques and technologies**
Edited by T. Gourlay and S. Gunaydin
41 **Wear of orthopaedic implants and artificial joints**
Edited by S. Affatato
42 **Biomaterials in plastic surgery: Breast implants**
Edited by W. Peters, H. Brandon, K. L. Jerina, C. Wolf and V. L. Young
43 **MEMS for biomedical applications**
Edited by S. Bhansali and A. Vasudev
44 **Durability and reliability of medical polymers**
Edited by M. Jenkins and A. Stamboulis
45 **Biosensors for medical applications**
Edited by S. Higson
46 **Sterilisation of biomaterials and medical devices**
Edited by S. Lerouge and A. Simmons
47 **The hip resurfacing handbook: A practical guide to the use and management of modern hip resurfacings**
Edited by K. De Smet, P. Campbell and C. Van Der Straeten
48 **Developments in tissue engineered and regenerative medicine products**
J. Basu and J. W. Ludlow
49 **Nanomedicine: Technologies and applications**
Edited by T. J. Webster
50 **Biocompatibility and performance of medical devices**
Edited by J.-P. Boutrand
51 **Medical robotics: Minimally invasive surgery**
Edited by P. Gomes
52 **Implantable sensor systems for medical applications**
Edited by A. Inmann and D. Hodgins
53 **Non-metallic biomaterials for tooth repair and replacement**
Edited by P. Vallittu
54 **Joining and assembly of medical materials and devices**
Edited by Y. (Norman) Zhou and M. D. Breyen
55 **Diamond-based materials for biomedical applications**
Edited by R.Narayan
56 **Nanomaterials in tissue engineering: Fabrication and applications**
Edited by A. K. Gaharwar, S. Sant, M. J. Hancock and S. A. Hacking
57 **Biomimetic biomaterials: Structure and applications**
Edited by A. J. Ruys
58 **Standardisation in cell and tissue engineering: Methods and protocols**
Edited by V. Salih

59 **Inhaler devices: Fundamentals, design and drug delivery**
Edited by P. Prokopovich
60 **Bio-tribocorrosion in biomaterials and medical implants**
Edited by Y. Yan
61 **Microfluidic devices for biomedical applications**
Edited by X.-J. James Li and Y. Zhou
62 **Decontamination in hospitals and healthcare**
Edited by J. T. Walker
63 **Biomedical imaging: Applications and advances**
Edited by P. Morris
64 **Characterization of biomaterials**
Edited by M. Jaffe, W. Hammond, P. Tolias and T. Arinzeh
65 **Biomaterials and medical tribology**
Edited by J. Paolo Davim
66 **Biomaterials for cancer therapeutics: Diagnosis, prevention and therapy**
Edited by K. Park
67 **New functional biomaterials for medicine and healthcare**
E.P. Ivanova, K.Bazaka and R. J. Crawford
68 **Porous silicon for biomedical applications**
Edited by H. A. Santos
69 **A practical approach to spinal trauma**
Edited by H. N. Bajaj and S. Katoch
70 **Rapid prototyping of biomaterials: Principles and applications**
Edited by R.Narayan
71 **Cardiac regeneration and repair Volume 1: Pathology and therapies**
Edited by R.-K. Li and R. D. Weisel
72 **Cardiac regeneration and repair Volume 2: Biomaterials and tissue engineering**
Edited by R.-K. Li and R. D. Weisel
73 **Semiconducting silicon nanowires for biomedical applications**
Edited by J. L. Coffer
74 **Silk biomaterials for tissue engineering and regenerative medicine**
Edited by S. Kundu
75 **Novel biomaterials for bone regeneration: Novel techniques and applications**
Edited by P. Dubruel and S. Van Vlierberghe
76 **Biomedical foams for tissue engineering applications**
Edited by P. Netti
77 **Precious metals for biomedical applications**
Edited by N. Baltzer and T. Copponnex
78 **Bone substitute biomaterials**
Edited by K. Mallick

79 **Regulatory affairs for biomaterials and medical devices**
Edited by S. Amato and R. Ezzell
80 **Joint replacement technology Second edition**
Edited by P. A. Revell
81 **Computational modelling of biomechanics and biotribology in the musculoskeletal system: Biomaterials and tissues**
Edited by Z. Jin
82 **Biophotonics for medical applications**
Edited by I. Meglinski
83 **Modelling degradation of bioresorbable polymeric medical devices**
Edited by J. Pan
84 **Perspectives in total hip arthroplasty: Advances in biomaterials and their tribological interactions**
S. Affatato

This page intentionally left blank

Part I

Fundamentals, properties and modification of biomedical foams

This page intentionally left blank

1

Introduction to biomedical foams

A. SALERNO, Center for Advanced Biomaterials for Health Care (IIT@CRIB), Istituto Italiano di Tecnologia, Italy and P. A. NETTI, Center for Advanced Biomaterials for Health Care (IIT@CRIB), Istituto Italiano di Tecnologia, Italy

DOI: 10.1533/9780857097033.1.3

Abstract: Biocompatible and biodegradable foams are key components for tissue substitution for *in vitro* and *in vivo* tissue engineering applications, as well as for biosensing and diagnostic. The aims of this chapter are (i) to illustrate the evolution of the biomedical foam concept and its function from the beginning to the current applications; (ii) to provide an overview on traditional and advanced materials and processes for the design and fabrication of biomedical foams; and (iii) to describe some of the most important current applications of biomedical foams.

Key words: tissue engineering, bioactivated materials, biodegradable foams, biomedical foams, cell-instructive materials, microscaffolds, scaffold fabrication.

1.1 Introduction

Due to their unique properties, porous materials have been widely used for biomedical applications requiring a three-dimensional (3D) porous network coupled with good mechanical properties, controlled degradation and biocompatibility. These applications include, among others: (i) porous biomedical devices and prostheses; (ii) scaffolds for *in vitro* cell culture and *in vivo* tissue-induced regeneration; (iii) macro-, micro- and nano-particulate foams for drug delivery, diagnostic and sensing, and, ultimately (iv) 3D culture platforms, for the investigation of cancer development and response to drug.

The performance of these biomedical foams – and therefore their field of application – resides in the sapient control over the different features and functionalities of the foams, which, in turn, depends on the appropriate selection of materials and fabrication processes. For example, in designing porous scaffolds for tissue engineering, the porous structure, including surface-to-volume ratio, pore size and interconnection degree, is a key factor in controlling cell behaviour and new tissue development (Karangeorgiu,

2005; Salerno *et al*., 2009a). Improving further the functionality of the foams integrating the control over cell fate through the spatial and chronological control of morphogen and growth factor delivery from the scaffolding material is now warranted (Sands, 2007; Biondi, 2008; Chan and Mooney, 2008).

Several processing techniques have been developed and are currently available for fabricating biomedical foams with specific control over their morphological, micro- and nano-structural features and degradation (Chevalier *et al*., 2007; Guarino *et al*., 2008). Furthermore, the advance in toxic-free and low-temperature processes allows for the controlled sequestration and release of bioactive moieties (LaVan *et al*., 2003).

Within the past decade, the 'explosion' of computer-aided approaches, microfabrication technologies and microfluidic strategies has noticeably increased the resolution achievable over biomedical foam architecture and composition (Hollister, 2005; Choi *et al*., 2007; Sands and Mooney, 2007; Melchels *et al*., 2010). This improvement has given an additional impulse in the biomedical field to elucidate several mechanisms underlying cell/material interactions and, ultimately, to develop multifunctional foams and scaffolds with improved performance.

At present, great efforts are being devoted to the design and fabrication of miniaturized foams with properties down to the nanometric scale that are able to combine technological potential with biochemical and biophysical cues. These multifunctional devices can serve different purposes, starting from building blocks for *in vitro* cell culture and *in vivo* tissue regeneration, to sensors and actuators to improve health status, and provide prophylactic or therapeutic treatment *in situ*.

This chapter aims to provide an overview of the history and evolution of biomedical foams, from the perspective of the materials, fabrication technologies and past, present and possible future applications.

1.2 Evolution of biomedical foams

The history of biomedical foams started rather shortly after the discovery of the first implantable biomaterials. Biomaterials initially developed for use inside the human body were selected and designed in order to match the biophysical properties of the replaced tissue, and to induce a minimal toxic response by the host (Hench and Polak, 2002). Suitable implants were fabricated mainly from materials used and developed for different applications, such as metals, ceramics and thermosetting polymers, which ensured an adequate inertness when in contact with the body's aggressive environment (Table 1.1 and Fig. 1.1).

Recreating a porous structure on the surface of bone and vascular prosthetic devices was proposed to improve the bonding between prosthesis and surrounding tissues, and to overcome clinical problems related to implant

Table 1.1 Evolution of materials, fabrication, property and application of biomedical foams

Evolution of biomedical foams	Materials	Manufacturing	Key features	Application	Reference
(I) Requirement: Achieve a suitable combination of physical properties to match those of the replaced tissue with a minimal toxic response in the host. Approach: Stable implant and prosthesis for restoration of tissue diseased function.	Metals: stainless steel, cobalt chrome, titanium Ceramics: alumina, zirconia Thermosetting polymers: polyamides, polyurethanes, polyethylene terephthalate	Freeze drying Particles sintering Phase inversion Reverse templating Spraying Textiles	Low porosity Micrometric pore size (hundreds of microns) High mechanical strength or flexibility	Permanent implants and coating for soft and hard tissues	Poth *et al*. (1955); Nilles and Coletti (1973)
(II) Requirement: Improve the integration with the physiological environment. Approach: Synthesis of bioactive and biodegradable materials with controlled chemistry and microstructural properties.	Metals: magnesium Ceramics: silicate-, borate- and calcium phosphate-glasses Polymers: biodegradable synthetic (polyanhydrides, polyesters, polyurethanes) and natural (collagen, fibrin, hyaluronic acid, alginate, silk, chitosan, zein) Composites: polymer/ceramic micro- or nano-particles	Emulsion Freeze drying Gas foaming Particles sintering Phase inversion Reverse templating SFF Spraying Textiles	Biodegradation High (99%) to low porosity; nano- to micro-metric pore size resolution; pore shape and aspect ratio Soft-to-hard mechanical properties Bioactive surface to improve cell/tissue compatibility	Scaffolds and particles for cell culture: stem cell, osteoblast, chondrocytes, fibroblast, axon Implantable scaffolds: dermis, bone, cartilage, vessel, nerve, muscle	Mikos *et al*. (1993); Chen *et al*. (2002); Gomes *et al*. (2002); Mathieu *et al*. (2006); Chevalier *et al*. (2007); Guarino *et al*. (2008); Melchels *et al*. (2010); Choi *et al*. (2012) Rezwan *et al*. (2005)

(*Continued*)

Table 1.1 (*Continued*)

Evolution of biomedical foams	Materials	Manufacturing	Key features	Application	Reference
(III) Requirement: Elicit specific biological responses at the molecular level. Approach: Bioactive and biomimetic materials able to promote and guide specific cellular processes.	Ceramics: gene-activated and drug releasing glasses Polymers: drug releasing, surface-functionalized polyesters; DNA and Peptide-based materials	Bioprinting Microfluidic Phase separation Particles sintering Reverse templating Self-assembly SFF	Enzymatic biodegradation Micro- and nano-metric architecture Mechanotransduction Multiple drug releasing capability Bioactive surface	Scaffolds to study cell behaviour Advanced scaffolds for tissue repair Micro- and nano-foams for drug and cell delivery, biosensing, and diagnostic	Chan (2008) Fischbach (2007) Kloxin *et al*. (2009) Lee *et al*. (2010) Lutolf and Hubbell (2005) Mironov *et al*. (2009) Pathi *et al*. (2010) Perez and Regev (2012)

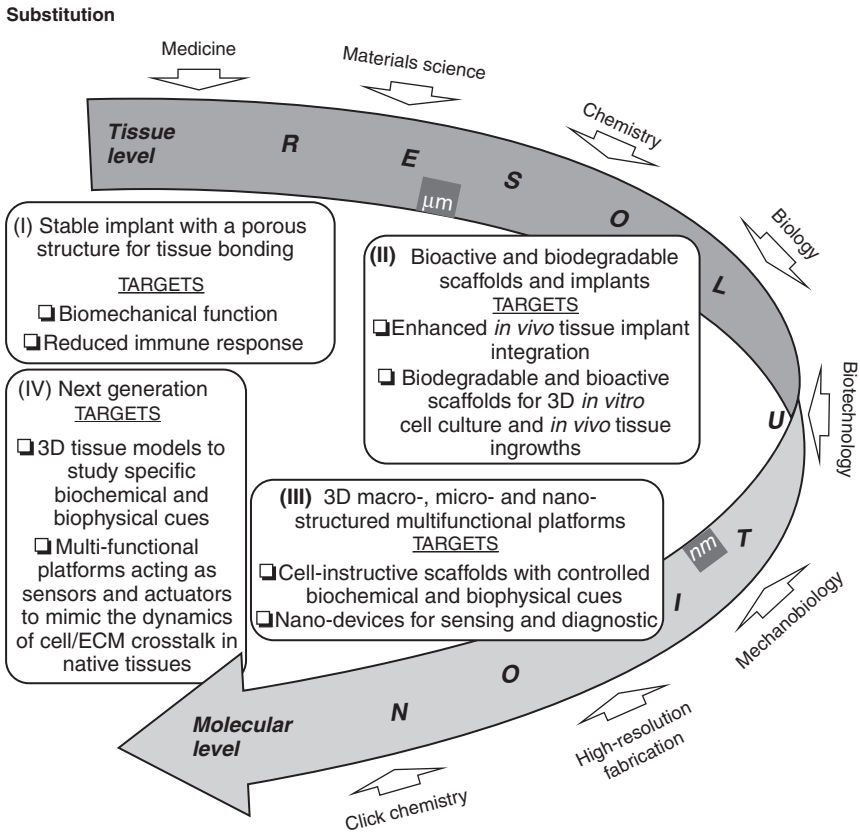

1.1 Scheme of the evolution of biomedical foams from tissue substitution to repair/regeneration.

mobility and stabilization (Poth *et al*., 1955; Nilles and Coletti, 1973). For instance, Nilles and Coletti (1973) demonstrated that bone prostheses characterized by open porous surfaces can induce tissue ingrowth at the interface and, therefore, improve their biomechanical performance as compared to non-porous ones. The efficacy of this approach is demonstrated by the fact that modern implants still follow this design principle and features.

Although inert foams allowed the fabrication of prostheses able to replace the mechanical functionality of tissues such as bone, the absence of biologically active surfaces render these materials unable to control the biological response at the interface between implant and surrounding tissue (Hench, 1998; Hench and Polak, 2002). As a direct consequence, an avascular, collagenous fibrous capsule that is typically 50–200 µm forms all around the implant, leading to several complications and, ultimately, to implant failure.

Improvement of biomedical foams occurred mainly between 1980 and 2000, when novel bioactive materials were developed with the aim of enhancing integration with the surrounding tissue. This was achieved by using, among others, bioactive ceramics and biodegradable polymers obtained from both synthetic and natural resources. The philosophy of these novel materials is that the body should no longer adjust to the materials, but that the materials should interact with the biological components, developing features that improve their response. An example of these materials are bioactive ceramics, such as bioglasses, that promote the *in vitro* and *in vivo* deposition and formation of a biological hydroxyapatite layer at the material surface, thus providing a biochemical bonding with the surrounding tissues (Hench, 1998). Bioglasses were used, for example, to coat the porous surface of metallic prostheses, which found clinical use in a variety of orthopaedic and dental applications (Cao and Hench, 1996).

Another advance was the development of biomaterials that exhibited clinically relevant chemical breakdown and degradation. These materials, mainly composed of biodegradable polymers and composites with ceramic particles, were engineered to provide a final solution to the foreign-body reaction, as they have the potential of being ultimately replaced by regenerating tissues (Hench and Polak, 2002).

The development of bioactive and biodegradable biomaterials in the 1980s coincided with the birth of tissue engineering science and the first significant paradigm shift of biomedical foams, from substitution to repair/regeneration (Fig. 1.1). During two decades, from 1980 to 2000, great efforts were devoted to designing 3D porous biodegradable substrates, named scaffolds, able to stimulate transplanted cells to regenerate biological tissues with defined sizes and shapes (Langer and Vacanti, 1993). In particular, the scaffold is intended as a three-dimensional temporary support for cells growth and proliferation, while its degradation and mechanical properties are tailored until the formation of a self-supporting newly generated matrix.

Collagen sponge was among the first scaffolds used in tissue engineering for the regeneration of skin-equivalent tissue of full thickness for the treatment of ulcers and acute wounds (Bell *et al.*, 1981). Furthermore, porous scaffolds made of a wide range of synthetic and natural polymers, bioactive glasses and their composites were prepared, and their regeneration potential was assessed by using different cell lines and *in vivo* models. In particular, great effort was devoted to finding the optimal combination of scaffold composition, degradation rate, pore structure and mechanical properties for the repair/regeneration of tissues such as bone, cartilage, blood vessels, nerve and derma.

Most importantly, cultivating cells on porous scaffolds evidenced several technological problems related to *in vitro* cell seeding and survival within

the 3D porosity. Indeed, inadequate fluid transport and cell viability inside cell/scaffold constructs may result in a necrotic core and the formation of inhomogeneous tissues. Technological approaches based on the use of bioreactors for dynamic cell seeding and cultivation represented a step forward to a more controllable and reliable *in vitro* tissue regeneration (Martin *et al*., 2004). Indeed, these bioreactors can improve cell distribution and colonization within the scaffold and, to date, are essential component of *in vitro* tissue engineering scaffold-based strategies.

The optimization of scaffold fabrication and culture conditions allowed new tissue synthesis both *in vitro* and *in vivo*. However, researchers observed that the biophysical and biochemical properties of these tissues were significantly different from those observed in native conditions. This was ascribed to the fact that cells in native tissues are exposed to a highly dynamic and complex array of biophysical and biochemical signals, originating from the extracellular matrix (ECM). The ECM is the main regulatory and structural component of the tissues, and is composed of fibrous proteins, proteoglycans and glycoproteins (Chan and Mooney, 2008). The ECM signals are transmitted to the outside of a cell by various cell surface receptors and integrated by intracellular signalling pathways, finally regulating gene expression and cell phenotype (Lutolf and Hubbell, 2005). Then, the ultimate decision of a cell to migrate, proliferate, differentiate or perform other specific functions is regulated by this cell/ECM crosstalk. Furthermore, the bidirectional nature of this crosstalk, whereby a cell continuously modifies the properties of the ECM, stimulated further research towards developing scaffolds able to be remodelled by the cells. In particular, over the last decade the concept of cell guidance in tissue regeneration was discussed and revised, and new knowledge of the complex features of cell–material interaction has been disclosed and elucidated (Causa *et al*., 2007).

Advancement in chemistry, materials science and nanotechnology allowed studying cell–material interactions by designing and fabricating platforms presenting predefined spatial and temporal patterns of many different biochemical and biophysical signals (Lo *et al*., 2000; Hersel *et al*., 2003; Martínez *et al*., 2009; Guarnieri *et al*., 2010; Sharma and Snedeker, 2010; Ventre *et al*., 2012). Cell culture onto the surface of 2D platforms of controlled properties was performed to assess cell response to a wide range of material properties, including topography (Martínez *et al*., 2009), stiffness (Lo *et al*., 2000), molecular cues such as cell adhesion peptides (Hersel *et al*., 2003; Guarnieri *et al*., 2010), as well as combination of biophysical and biochemical properties (Sharma and Snedeker, 2010).

It is, however, important to point out that in native tissues cell fate is governed by a plethora of 3D biophysical and biochemical signals in continuous spatial and temporal evolution. Furthermore, the translation of biochemical and biophysical information from 2D platforms to 3D porous scaffolds is

rather difficult. Mimicking the functionality of the ECM by using synthetic analogues able to replicate all of the complex biochemical and biophysical functions of ECM is far from being achieved, and represents a great challenge for the tissue engineering community. Recent technological progress has allowed the design and fabrication of three-dimensional scaffolds with high resolution of biophysical and biochemical signal presentation, therefore suitable to test novel molecularly tailored biomaterials for tissue engineering. Such examples are (Table 1.1 and Fig. 1.1): (i) drug releasing scaffolds able to stimulate cell differentiation and tissue vascularization (Shea *et al*., 1999; Huang *et al*., 2002; Ungaro *et al*., 2006; Jeon *et al*., 2007; Tayalia and Mooney, 2009); (ii) photodegradable poly ethylene glycolate (PEG)-based hydrogels that can be manipulated to induce molecular-scale degradation and consequent stem cell spreading, migration or ECM elaboration at any time of culture (Kloxin *et al*., 2009); (iii) 3D porous scaffolds with both precisely engineered architecture and tailored surface topography to study the role of surface topography on stem cells differentiation (Mata *et al*., 2009); (iv) scaffolds with precise pore structure prepared using two-photon polymerization to study cell migration (Tayalia *et al*., 2008) and; (v) gene-activated scaffolds to study cell recruitment and transfection (Orsi *et al*., 2010).

In the past decade, the impressive increase of high resolution technologies and processes able to control biomaterial chemistry and physical properties down to micrometric and nanometric scales has opened new routes for the application of biomedical foams. Porous devices miniaturized from the macroscale (higher than 1 mm) to the microscale (0.1–100 μm) have received great attention as microscaffolds for cell transplantation and drug release (Urciuolo *et al*., 2010; Chen *et al*., 2011; Choi *et al*., 2012). Furthermore, nanoscale (down to 1–100 nm) foams ultimately promise integrated implantable systems that can monitor health status and provide prophylactic or therapeutic treatment *in situ* (LaVan *et al*., 2003).

It is clear that the synthesis of new materials and the development of advanced manufacturing processes are key requirements for the successful implementation of tissue engineering approaches and, ultimately, for the introduction of biomedical foams into the clinic.

1.3 Materials for fabricating biomedical foams

A biomaterial can be defined as ‘a nonviable material used in a medical device, intended to interact with biological systems’ (Williams, 1986). It is, therefore, easy to imagine that the topic ‘biomaterial’ is highly interdisciplinary as it resides, among others, at the interface between chemistry, engineering, materials science, biology and medicine, with considerable input from government-regulated administrations.

Biomaterials are the constituent of biomedical foams and, ideally, must be accurately designed and fabricated in order to fulfil a series of properties. These include (i) biocompatibility intended as the capability to perform with an appropriate host response in a specific application; (ii) biodegradability without producing toxic degradation by-products; (iii) processability to manufacture biomedical devices and foams of desired internal structure and external shape; (iv) being sterilizable by using process technologies appropriate for biological uses; and, ultimately, (v) being able to provide mechanical properties tailored for the required application.

In this section we aim to provide a comprehensive and concise description of the different classes of biomaterials that have been used to fabricate biomedical foams. Both biologically derived and synthetic materials have been extensively explored in tissue engineering and scaffold fabrication. Depending on the field of application, biomedical devices and foams may be designed and fabricated using all the existing material classes, namely metals, ceramics and polymers, as well as their combinations.

1.3.1 Metals

Metals are the most frequently used biomaterials to replace structural components of the human body. This is because, compared to polymeric and ceramic materials, they are very reliable from the viewpoint of mechanical performance. In particular, metals possess tensile strength, fatigue strength, and fracture toughness properties that make them excellent candidates for the fabrication of medical devices for the replacement of hard tissues such as artificial hip joints, bone plates, coronary stents and dental implants (Niinomi, 2008).

Type 316L stainless steels, cobalt–chromium–molybdenum alloys, commercially pure titanium and Ti–6Al–4V alloys are typical metallic biomaterials used for implant devices (Sumita *et al.*, 2004). Although originally developed for industrial purposes, these materials have been employed for biomaterial purposes due to their relatively high corrosion resistance and excellent mechanical properties. Through a wide range of alloying, annealing and surface treatment technologies, the biological performance of metallic biomaterials can be specifically tailored for the specific application. Stainless steels, such as type 316L austenitic steel, are among the most used metallic biomaterials because of their inferior costs of fabrication, compared to cobalt–chromium alloys and titanium alloys (Sumita *et al.*, 2004; Niinomi, 2008). However, great efforts have been also made to develop nickel-free stainless steels, which may provide enhanced corrosion resistance by using different austenitic stabilizers, such as nitrogen and manganese (Sumita *et al.*, 2004).

Recently, a novel class of metallic biomaterials, based on magnesium and its alloys, has been developed in order to manufacture biodegradable bone lightweight implants. Indeed, magnesium is an essential element for human metabolism and is characterized by 4.5 times lower density than steel. This aspect can allow for the fabrication of implants with mechanical properties closer to that of bone tissue, and therefore improved mechanical integration (Staiger *et al.*, 2006). Because of the fast corrosion of pure magnesium *in vivo* (of the order of few months), small amounts of caesium, cadmium, aluminium, manganese or rare earth elements have been used as additives for the preparation of magnesium alloys with slower degradation (down to 1 year) (Staiger *et al.*, 2006).

1.3.2 Ceramics

The most commonly used ceramic biomaterials are alumina, zirconia, calcium phosphates, bioactive glasses, glass ceramics and carbon. Alumina and zirconia are used in total joint prostheses and dental implants because of their bioinertness, high wear resistance, strength and their relatively low friction.

Due to their chemical similarity to the inorganic phase of bone, inorganic biomaterials such as calcium phosphates (e.g. hydroxyapatite and α- and β-tricalcium phosphate), have been more intensively investigated in respect to their possible application as bone scaffolds (Hoppe *et al.*, 2011). These materials are bioactive, osteoconductive and are able to bond directly to bone. Ceramic implants for osteogenesis are based mainly on hydroxyapatite, since this is the inorganic component of bone (Karangeorgiou and Kaplan, 2005). Hydroxyapatite is also used in plasma-sprayed titanium alloys for load-bearing orthopaedic implants, promoting the formation of a strong bond between the mineralized bone tissue and the implant, and shortened healing times (Jandt, 2007). Tricalcium phosphates are also advantageous when used as bone cements and implant materials, because they offer a higher solubility than, for example, stoichiometric hydroxyapatite (Jandt, 2007).

Bioactive glasses contain SiO_2, Na_2O, CaO and P_2O_5, the major component being SiO_2, and represent another important group of inorganic, bioactive biomaterials used as bone scaffolds (Hench, 1998; Hoppe *et al.*, 2011). Bioactive glasses are osteoinductive and, when exposed to biological fluid, show the ability to form a carbonated hydroxyapatite layer that serves as a bonding interface between the implant and the surrounding bone. Silica-rich scaffolds evidence excellent new bone forming ability and resorption rates directly dependent on the silica content (Karangeorgiou and Kaplan, 2005). Nevertheless, mechanical fragility remains one of the

main limitations of ceramic biomaterials and their foams for load-bearing applications.

1.3.3 Polymers

Polymers are mostly made of organic components and are characterized by macromolecular properties comparable to lipids, proteins and polysaccharides, which are key functional organic components of the biological environment. Further advantages of polymeric biomaterials are their relatively simple processability and their broad range of application, spanning from non-degradable implants to controlled degradable biomedical devices.

Non-degradable polymers, such as ultra-high molecular weight poly(ethylene), are widely used in applications requiring excellent mechanical and corrosion resistance. These include low-friction inserts for load-bearing surfaces in total joint arthroplasty and acetabular cups in hips or in knee prostheses (Jandt, 2007). Further polymeric biomaterials used are poly(ethylene terephthalate) and poly(tetrafluoroethylene) for vascular prosthesis, poly(methylmetacrylate) as bone cements, dental composites and intraocular lenses, and poly(urethanes) for vascular prostheses (Lloyd *et al*., 2001; Salacinski *et al*., 2001; Webb and Spencer, 2007).

Both synthetic polymers and biologically derived (or natural) polymers have been extensively investigated as biodegradable polymeric biomaterials. Materials from natural resources, such as collagen and hyaluronic acid, possess the great advantage of biological recognition, because of the presence of receptor-binding ligands inside their chemical structure. Conversely, synthetic biomaterials may overcome the problems related to purification immunogenicity and pathogen transmission and may also provide a greater control over the properties of biomedical devices.

Natural polymers can be considered as the first biodegradable biomaterials used clinically. Purified ECM components or decellularized ECMs derived from animals have been widely investigated in tissue engineering. Indeed, even if they are subjected to purification and sterilization treatments, these materials retain important characteristics of the physical and chemical structure of the native ECM. Owing to their similarity to the ECM, natural polymers may also avoid the stimulation of chronic inflammation or immunological reactions and toxicity, often detected with synthetic polymers (Mano *et al*., 2007). Although decellularized ECM has been successfully used as a scaffold for soft tissue applications (Voytik-Harbin *et al*., 1998), single purified ECM components, such as collagen, hyaluronic acid and fibrin, can be combined appropriately to create more controlled and standardized materials that are potentially less immunogenic and have a similar structure to native ECM (Chan and Mooney, 2008). Animal- or

vegetal-derived proteins have been shown to be potentially viable as scaffolds for tissue engineering applications. Silk proteins, for example, contain a high content of β-sheet sequences that make this polymer particularly suitable for high-strength and slow-degradation purposes (Rockwood *et al*., 2011). Alginate and chitosan, which are glycans extracted from brown algae and the exoskeletons of shellfish, respectively, have gained popularity because of their biocompatibility, ease of processing and ability to encapsulate cells and bioactive molecules (Mano *et al*., 2007; Nair and Laurencin, 2007). Natural proteins such as gelatin and zein have been also investigated as biomaterial scaffolds for applications spanning from soft to hard tissue regeneration (Chang *et al*., 2003; Wang *et al*., 2007).

A variety of biodegradable synthetic polymers, including poly(α-esther)s, such as polyglycolide, polylactides, polycaprolactone and their co-polymers, polyanhydrides and poly(propylene fumarate) have also been extensively investigated for biomedical applications (Nair and Laurencin, 2007; Chan and Mooney, 2008). The application of synthetic biodegradable polymers in the tissue engineering field provides several advantages. First of all, these materials can be synthesized in a variety of chemical structures, enabling the possibility to easily tailor their microstructural and degradation behaviour. Furthermore, the Federal Drug Administration approval of some of them may allow fabrication of biomedical devices and foams suitable to be introduced into the market. The unspecific interaction with cells represents to date the main limitation of foams prepared starting from synthetic polymers (Nair and Laurencin, 2007).

The ability to control the shape and structure of biomolecules, such as proteins and DNA, and the evolution-optimized chemical functions of biomaterials, make biomolecules attractive building blocks for functional biomedical foams.

The custom-design of proteins by taking advantage of nature's protein synthesis machinery allows material scientists to genetically engineer novel, well-defined and multifunctional materials. Peptides and proteins self-assemble into distinct structures (e.g. β-sheets and α-helices) because of van der Waals and ionic interactions at the molecular level. Depending on the amino acid sequence, the same set of amino acids can create a virtually unlimited range of protein materials with various structures. Protein-based materials can be derived by cloning sequences from organisms that naturally produce the protein or, for more controlled material properties, by engineering plasmids that code only the desired amino acid sequences (van Hest and Tirrell, 2001). Tuning the primary peptide sequence of these materials also allows developing biomaterials that self-assemble *in situ* under appropriate physiological conditions (Caplan *et al*., 2002; Hartgerink *et al*., 2002).

Like peptide-based materials, DNA is increasingly being investigated as a biomaterial, because the material properties can be controlled by defining

sequences of nucleotides as building blocks. DNA is a versatile building material for nanoconstruction because of its remarkable molecular recognition capability and well-predicted duplex conformation. A number of DNA motifs that can assemble into well-defined nanostructures in Mg^{2+} containing buffer solution have been engineered. The negative charge of DNA can also be utilized to fabricate long nanofibers in Ca^{2+} solutions that can serve to fabricate composites containing $CaCO_3$ nanotubes and nanowires (He *et al.*, 2007).

1.3.4 Composites

Although each biomaterial class has unique advantages for tissue engineering applications, each also has intrinsic drawbacks, depending on its nature and fabrication process. A possible solution for overcoming this limitation is to combine two or more materials in order to design and fabricate a multiphase composite taking the advantages of the single components.

Natural bone matrix is a typical example of organic/inorganic composite material made of collagen and mineral (apatites). This natural composite material has an excellent balance between strength and toughness, superior to both its individual components.

Being similar to the major inorganic component of natural bone, inorganic compounds, such as hydroxyapatite or calcium phosphate, in the form of micro- and nano-particles, can be dispersed inside a polymeric matrix to improve foam mechanical properties and degradation kinetics (Murugan and Ramakrishna, 2005; Salerno *et al.*, 2010a). Furthermore, the interaction between ionic dissolution products of ceramics and cell metabolic activity has been also reported to promote cell differentiation and tissue neo-vascularization (Gerhardt *et al.*, 2011; Hoppe *et al.*, 2011).

Another example of composites is ceramic coating to increase the osseointegration of other biomaterials. Collagen scaffolds have been coated with hydroxyapatite to improve its osseointegration capacity by means of the surface formation of a bioactive apatite layer (Karangeorgiou and Kaplan, 2005). Fibre reinforced composites may be also tailored to mimic the anisotropy occurring in natural tissues such as bone, finally improving the biomechanical response of porous scaffolds (Jandt, 2007).

1.4 Manufacturing processes for biomedical foams and scaffolds

In native biological tissues, the 3D organization of cells and ECM provides tissues with biophysical and biochemical properties suitable to exploit appropriate function within the body. As in the native tissue, the ideal

scaffold for tissue engineering should be able to allow for the correct 3D localization and development of cells and ECM by means of appropriate cues – chemical, biochemical and biophysical. In particular, scaffolds for tissue engineering must be characterized by a porous network of open pores with appropriate size, distribution, shape, surface texture and topography. Concomitantly, the chemical composition of the scaffold material, its surface chemistry and mechanical function, as well as its ability to sequestrate and deliver bioactive factors (e.g. growth factors, ions) to the cells also are key requirements for tissue engineering applications.

Engineering porous scaffolds with tailored properties strongly depend on the manufacturing technique. In this section, a description of traditional and advanced scaffold manufacturing processes is reported, discussing their advantages and current limitations.

1.4.1 Traditional manufacturing techniques

Conventional techniques for porous scaffold fabrication include textile technologies, porogen leaching, thermodynamic-based processing of polymeric solutions such as gas foaming, phase separation and freeze drying, as well as microsphere sintering.

Textile technologies were among the first approaches for fabricating porous scaffolds for cell culture and *in vivo* implantation. Indeed, fibres may provide a large surface area/volume that is beneficial for protein adsorption and cell adhesion. Fibre meshes consisting of woven or knitted synthetic fibres made of polyglycolic acid, polylactic acid or their co-polymers have been investigated for cell transplantation and regeneration of various tissues such as nerve, skin, ligament and cartilage (Chen *et al.*, 2002). Increased structural stability of textile scaffolds can be achieved by fibre bonding techniques based on the melting and linking of the polymeric fibres at the cross points (Mikos *et al.*, 1993).

The method of reverse templating was first described by Mikos *et al.* (1994) to fabricate highly porous (up to 93%) biodegradable polylactic acid foams. The process involves the preparation of polymeric solutions containing appropriate salt (sodium chloride, sodium tartrate or sodium citrate) particles, followed by the setting of the polymer and the dissolution of the salt. This technique has been successively applied to different classes of biomaterials, such as synthetic and natural polymers (Gomes *et al.*, 2002; Guarino *et al.*, 2008), ceramics (Chevalier *et al.*, 2007) and metals (Staiger *et al.*, 2006) to fabricate scaffolds and porous implant for biomedical applications. Further improvements over pore architecture control and mechanical function for load-bearing applications have been reported by the use of continuous porogens (Salerno *et al.*, 2009b).

Gas foaming, phase separation and freeze drying techniques create porous scaffolds by inducing thermodynamic instabilities in multi-phase polymeric systems. In the gas foaming process, a blowing agent is dissolved inside the biomaterials at high pressure, typically in the range of 10–30 MPa, followed by a controlled pressure drop to ambient pressure. This depressurization starts the nucleation and growth of pores inside the material (Salerno *et al.*, 2009a). The absence of toxic chemicals and the optimization of processing temperatures can offer the great advantage of preserving polymer structure and fabricating bioactive and biomimetic scaffolds (Mathieu *et al.*, 2006).

Phase separation and freeze drying are thermodynamic-based processes typically used for fabricating porous polymeric scaffolds by using organic solvents. In these techniques, the synthetic or natural polymer is dissolved in the solvent and the solution brought into a thermodynamically unstable state by decreasing the temperature or adding a non-solvent. This step leads to the formation of a multi-phase system characterized by polymer-rich and polymer-lean phases. The subsequent removal of the solvent from the system induces the crystallization of the polymer-rich phase and the formation of the porous network in the polymer-lean phase. Depending on the polymer–solvent choice and phase separation conditions, highly porous scaffolds, up to 99%, with random or oriented pores can be produced (Guarino *et al.*, 2008).

Microsphere-based tissue engineering scaffold designs have attracted significant attention in recent years, as the microspheres as building blocks offer several benefits, including ease of fabrication, control over morphology and physicochemical characteristics, and versatility in controlling the release kinetics of encapsulated factors (Shi *et al.*, 2010; Salerno *et al.*, 2012). The properties of the scaffold, in turn, can be tailored by the selection of the raw material as well as by altering the microsphere design and fabrication method.

1.4.2 Advanced manufacturing of biomedical foams and scaffolds

Solid freeform fabrication

One of the common shortcomings of the fabrication technologies discussed above is the difficulty of fabricating scaffolds with predefined reliable and reproducible internal morphology and external shape. To overcome these limitations, in the last decade computer-aided design and manufacturing (CAD-CAM) approaches, namely solid freeform fabrication (SFF), have been implemented to manufacture tissue engineering porous scaffolds with complex architecture and full pore interconnectivity starting from a computer-generated CAD model of the scaffold. The scaffold is then built by

using layered manufacturing strategies. Commercially available CAM systems may be categorized into three major groups based on the way materials are deposited (Hollister, 2005): (i) laser-based machines that either photopolymerize liquid monomer or sinter powdered materials; (ii) the printing of a chemical binder onto powdered material or directly printing wax, and; (iii) nozzle-based systems, such as Bioplotter, that are able to print biological cells as well as a range of biomaterials.

These hierarchical computational techniques have allowed design of three-dimensional anatomic scaffolds from polymers, hydrogels, ceramic and even metal biomaterials and characterized by a porous architecture that balances function and mass transport (Hollister, 2005; Li *et al*., 2005; Simon *et al*., 2007). Because of their highly ordered microstructures and full pore interconnectivity, SFF scaffolds often endowed mechanical properties and biological performance better than those achievable by using traditional approaches (Hollister, 2005).

Stereolithography was developed by 3D Systems in 1986, being the first commercially available SFF technique. The manufacturing of porous scaffolds by stereolithography is based on the layer-by-layer spatially controlled solidification of a liquid resin by photo-polymerization using a computer-controlled laser beam or a digital light projector (Melchels *et al*., 2010). A post-curing polymerization is often necessary after draining and washing-off the excess of resin, in order to complete the conversion of un-reacted material. To date, stereolithography has been applied to fabricate porous scaffolds made of poly(propylene fumarate) for bone tissue engineering (Cooke *et al*., 2003), polytrimethylene carbonate for drug delivery application (Jansen *et al*., 2010), as well as poly(ethylene oxide) and poly(ethylene glycol) hydrogels-cell constructs for soft tissue engineering (Dhariwala *et al*., 2004). Recently, microstereolithographic approaches have been also proposed in order to improve the resolution of stereolithographic scaffolds down to few micrometres (Bertsch *et al*., 2003).

Two-photon polymerization, which belongs to the class of stereolithographic techniques, uses multi-photon excitation of photoinitiator molecules to induce polymerization of a resin. Due to the non-linear nature of two-photon absorption, the resolution of the polymerization volume can be beyond the diffraction limit, resulting in photopolymerized materials with resolution down to 100 nm (Lee *et al*., 2008). Although the majority of two-photon polymerization works focused on cell culture on 2D substrates with three-dimensional nano-/micro-structures, some pioneering works also used two-photon polymerization for fabricating 3D porous scaffolds for cell culture and migration (Tayalia *et al*., 2008). Wylie and Shoichet (2008) also proposed the use of two-photon technique to imprint amines micropatterns inside agarose hydrogel, which can serve as reactive sites for

further water-based chemistry and may also create cell adhesion patterns inside agarose scaffolds.

Robotic additive biofabrication, named bioprinting, has emerged as a flexible tool in tissue engineering with potential to build organs or viable tissues (Mironov *et al*., 2009; Norotte *et al*., 2009). Bioprinting uses a computer-controlled 3D printing device to accurately deposit cells and biomaterials into precise geometries – the goal being the creation of anatomically correct structures. A computer-assisted design can be used to guide the placement of specific types of cells and polymers into precise geometries that mimic natural tissue/organ structure. Although, to date, a complete organ has not been printed yet, bioprinting approaches have been reported for the manufacturing, among others, of vascular structures (Norotte *et al*., 2009). The broad spectrum of potential applications and rapidly growing toolboxes of biofabrication approaches can make this technique one of the leading platforms of next scaffold and tissue manufacturing.

High resolution integrated approaches

The increasing demand for nano- and micro-metric controlled 3D scaffolding materials for tissue engineering has led to the development of integrated approaches that combine high resolution 2D structure manufacturing with layer-by-layer assembly. These approaches differ from those of SFF because the 'multi-layer scaffolds' are built in a semi-automated two-step process. This approach has been used for constructing, among others, complex three-dimensional microfluidic scaffolds for tissue vascularization (Vacanti *et al*., 2010) as well as biomimetic and bioactive scaffolds with precise micro-architecture and surface micro- and nano-textures for controlled cell ingrowth and differentiation (Mata *et al*., 2009). In particular, Mata and co-workers have recently proposed a novel 3D production technique that combines microfabrication and soft lithography to construct high resolution porous scaffolds. This technique consists of dual-sided moulding and stacking of polydimethylsiloxane (PDMS) layers characterized by predefined and precise micro-architectures and surface micro-textures and obtained by PDMS replication of photopatterned SU8 layers. The results of their work corroborates those widely reported in 2D that appropriately patterned scaffold surfaces can promote and guide cell adhesion, migration and osteogenic differentiation in three dimensions (Mata *et al*., 2009).

Although integrated approaches can be useful for manufacturing scaffolds with micro- and nano-metric pore surface resolution, there is still the need for improved approaches for a precision layer positioning, as well as a consistent layer bonding and automated assembly.

1.5 Scaffolds for *in vitro* cell culture

Engineering of tissues for therapeutic applications by means of culturing transplanted cells within 3D porous scaffolds is one of the most investigated approaches of the tissue engineering research. Indeed, the creation of biological tissues *in vitro* is desirable for their potential use as replacements for full animal models in basic biological studies and pharmacological and toxicological screens, and as replacement tissues for clinical applications.

In vivo, cell behaviour is the result of a cascade of events that relies on the interaction between cells and the 3D microenvironment, comprising the ECM, surrounding cells and molecular cues. In order to recapitulate the *in vivo* milieu, a key issue is to understand how cells respond to such microenvironmental stimuli by determining cell–scaffold crosstalk dynamics. This aspect is essential towards developing cell-instructive materials able to guide successful tissue regeneration.

To date, the effect of scaffolds features, namely composition, degradation, pore structure and mechanical properties on *in vitro* tissue formation has been assessed extensively for different cell–scaffold combinations. For instance, it has been reported that scaffold-induced regeneration *in vitro* can be optimized by selecting the constituent material and, in turn, surface chemistry, degradation rate and mechanical properties (Lee *et al*., 2001; Hu *et al*., 2003; Sung *et al*., 2004). Furthermore, the pore structure, namely porosity, pore size, shape and interconnectivity, act in synergy with the other parameters by controlling cell spatial distribution, infiltration and the transport of fluids, such as nutrients and oxygen, across the entire cell–scaffold constructs (Guarino *et al*., 2008, Salerno *et al*., 2010b).

Major obstacles to the *in vitro* generation of functional tissues and their widespread clinical use are related to a limited understanding of the regulatory role of specific physicochemical culture parameters on tissue development (Martin *et al*., 2004). Furthermore, it has long been known that the supply of oxygen and soluble nutrients becomes critically limiting for the *in vitro* culture of 3D tissues of thickness higher than 200 μm (Salerno *et al*., 2010b). Bioreactors, are devices which able to provide a tight control and monitoring of biological and biochemical processes, have been developed aimed at overcoming limitations of static cultures by providing a dynamically stimulating environment for improved cell behaviour and new tissue development. In particular, bioreactors have demonstrated great potential for (i) improving cell seeding uniformity, proliferation and ECM biosynthesis within the entire scaffold pore structure characterized by different physical and chemical properties, and (ii) stimulating mechanically transplanted cells to induce correct cell differentiation and tissue development (Martin *et al*., 2004; Mauney *et al*., 2004).

Surface modification of porous scaffolds to control protein adsorption and cell interaction is also an important aspect for *in vitro* strategies. Chemical modifications of synthetic polymers with entire ECM molecules or relevant peptide or glycan fragments, such as arginine–glycine–aspartic acid (RGD), have been used to mediate specific mechanisms of cell adhesion and to control tissue morphogenesis (Chan and Mooney, 2008). This has been almost exhaustively achieved in the case of 2D platforms, allowing the building of a broad library of cell-responsive material properties. For example, it has been demonstrated that the type of peptides used, their density and spatial distribution at the micro- and nano-scale, significantly affect cell responses (Ratner and Bryant, 2004; Hildebrand *et al*., 2006). The possibility to extend these procedures to immobilize functional motifs on 3D porous scaffold surfaces has been mainly investigated by means of post-treatments on settled scaffolds. These approaches, involving the dipping of the scaffolds inside reactive solutions of appropriate compositions for a definite time, was successfully used for fabricating RGD-functionalized poly epsilon-caprolactone (PCL) scaffolds prepared via SFF technique for improved fibroblast attachment (Gloria *et al*., 2012), as well as chitosan/poly(lactic acid–glycolic acid) sintered microsphere scaffolds for bone tissue engineering (Jiang *et al*., 2009). It is, however, important to point out that, to date, the precise translation of the information achieved in 2D to the cell culture in 3D is still far to be achieved, as it requires high-throughput approaches of combinations and screening of 3D microenvironmental variables.

Considerable knowledge on *in vitro* new tissue formation has been also obtained by cell culture within hydrogel scaffolds. Indeed, hydrogels are mainly composed of water (99%) inside a highly dense nanofibrous polymeric network, thereby providing a biomimetic environment for cell culture. Furthermore, these materials can be synthesized and processed under physiological conditions and with functionalities adjustable to obtain cell and tissue specificity (Drury and Mooney, 2003; Lutolf and Hubbell, 2005). Lutholf and Hubbell (2005) fabricated polyethylene glycol-based synthetic hydrogels containing proteolytic domains inside the chemical structure to study cell migration by means of proteolytic degradation of the 3D fibrous structure. This way, the biomaterial becomes the recipient of information produced by cells and can be remodelled depending on the amount of proteases produced during cell migration. Many hydrogels can be also polymerized in the presence of cells, thereby ensuring a uniform cellular distribution throughout the three-dimensional network (Khetani and Bhatia, 2006). Hydrogels have also been used to test the effect of spatially and temporally controlled three-dimensional gradients of biomolecules on cell fate to finally control tissue development and regeneration. Such examples are photodegradable poly(ethylene glycol)-based hydrogels with local control of stiffness and cell-adhesive peptide ligands to influence chondrogenic

differentiation of encapsulated stem cells (Kloxin *et al*., 2009), as well as gene-activated 3D matrices for cell recruitment (Orsi *et al*., 2010).

1.6 Scaffolds for *in vivo* tissue-induced regeneration

Achieving *in vivo* tissue-induced regeneration for injured tissues and/or organs by means of porous scaffolds represents the most important goal of tissue engineering. In general, optimal scaffolds for the *in vivo* tissue repair/regeneration must serve four primary purposes: (i) they must define a space that will shape the regenerating tissue; (ii) they must provide temporary structural function in the implantation site while tissue regenerates; (iii) they must stimulate the progressive formation of a functional new tissue within the pore structure and; (iv) they must degrade progressively, matching the rate of new tissue growth, without releasing toxic by-products.

Since scaffold-based approaches were first proposed in tissue engineering, a massive research effort has been carried out about the effect of scaffold composition, microstructure and degradation on *in vivo* tissue-induced regeneration. Materials from synthetic or natural resources, as well as multiphase composites, have been implanted in well-established *in vivo* models for the repair/regeneration of tissues such as bone, cartilage and skin (Staiger *et al*., 2006; Mano *et al*., 2007; Nair and Laurencin, 2007).

The presence of the pore structure and the maintenance of sufficient structural integrity are critical aspects for *in vivo* implantation. Indeed, porosity is necessary for initial cell attachment and migration, and for mass transfer of nutrients and metabolites, and provides sufficient space for development and later remodelling of the organized tissue (Karangeorgiu and Kaplan, 2005). Concomitantly, the structural integrity may permit cell and tissue remodelling until achieving stable biomechanical conditions and vascularization at the host site. As the degree of remodelling depends on the tissue itself and its host anatomy and physiology, scaffold degradation and concomitant evolution of structural properties must be accurately controlled for the envisioned application.

In general, scaffold implantation triggers a series of body responses which are included in the so-called 'foreign-body reaction', characterized by nonspecific protein adsorption to the scaffold surface and the adhesion of a number of different cells to the scaffold, such as monocytes/macrophages, leukocytes and platelets. If the inflammation persists, the macrophages fuse together to form giant cells, finally leading to the formation of a collagenous capsule surrounding the implant (Ratner and Bryant, 2004). It is therefore clear that to induce successful tissue regeneration *in vivo* the scaffolds must be able to control the biological response induced by them.

One of the most investigated strategies to address this issue has been the modification of the surface properties of porous scaffolds to guide protein

adsorption. Initial protein–material interactions are crucial, as they control and guide cell attachment and adhesion processes. Cell adhesion to adsorbed proteins is mediated through integrin and other receptors located within the cell membrane (García, 2005). Therefore, it is universally recognized that controlling protein adsorption on the surface of biomaterials may be critical in controlling and directing cell response to biomaterials.

A plethora of techniques has been developed in order to modify surface characteristics, including biomaterial chemistry, wettability and morphology and to improve *in vivo* tissue-induced regeneration. Bioactivation of polymeric scaffolds by means of micro- and nano-metric fillers incorporation represents one of the most used approaches for bone regeneration. Indeed, the inorganic phase may improve the deposition of new bone inside the implant and the consequent integration of the scaffold with the surrounding tissue. A comprehensive account of this topic can be found in the review of Rezwan and co-workers (2005). Chemical grafting has been also proposed to improve the functionality of implanted scaffolds. This approach involves activating the surface with reactive groups followed by grafting the desired functionality to the surface. Short oligopeptides exhibiting specific binding domains, as well as whole proteins such as fibronectin, vitronectin, laminin and collagen, have been attached to the surface of the scaffolds to support cells and present an instructive background to guide their behaviour. Zheng and co-workers (2012) improved the functionality of polycaprolactone vascular graft by means of RGD coating. The obtained implants showed decreased occlusion, improved haemocompatibility, enhanced cell infiltration and homogeneous distribution, compared to untreated implants. Although this approach still remains popular owing to its comparative simplicity, its efficacy requires tight control over the composition of the adsorbed protein layer to stimulate a constructive cell response, favouring wound repair and tissue integration. Conversely, proteins in an unrecognizable state may indicate foreign materials to be isolated or removed. Concomitantly, it is worth noting that the *in vivo* efficacy of these approaches has yet to be demonstrated. In particular, further efforts and well-characterized animal implantation models are necessary to provide a correlation between surface functionality and short-term *in vivo* response, as well as to demonstrate that this approach can be also efficacious for the control of long-term *in vivo* cellular responses.

Functional porous biomaterials must also be capable of undergoing an active transformation from one state to another in the presence of biological systems. For instance, the transformation from an injectable state to a solid state is highly beneficial for use in minimally invasive surgical procedures to alleviate problems associated with implantation of prefabricated scaffolds. Injectable materials can also be combined with cells and bioactive molecules to improve regeneration.

The injectability of a scaffold is generally related to the rheological properties of the formulations, and the setting time of the precursors is determined by the structure/composition of the formulations and their processing conditions (Hou *et al*., 2004). Among the different biomaterials, calcium phosphate cements are among the most investigated as injectable foams for minimally invasive bone regeneration. Indeed, these materials offer the possibility of combining bioactivity, injectability and *in situ* self-setting properties coupled with a macro- and nano-porous structure for bone cell adhesion and tissue ingrowth. Calcium phosphate cements can undergo a self-setting process within the body after injection, based upon the cementing action of acidic and basic calcium phosphate compounds once wet with body fluids. The setting time can be also adjusted by addition of manipulator compounds to the wetting medium (Hou *et al*., 2004). Injectable scaffolds have also been fabricated by using thermally or photochemically activated polymers (Hou *et al*., 2004; Kim *et al*., 2009). Kim and co-workers (2009) developed a novel pH- and thermo-sensitive hydrogel as an injectable scaffold for autologous bone tissue engineering. The pH/thermo-sensitive polymer was synthesized by adding pH-sensitive sulfamethazine oligomers to both ends of a thermo-sensitive poly(ε-caprolactone-co-lactide)–poly(ethylene glycol)–poly(ε-caprolactone-co-lactide) block copolymer. After *in vivo* implantation in mice, scaffold containing mesenchymal stem cells evidenced mineralized tissue formation and high levels of alkaline phosphatase activity in the mineralized tissue.

In vivo implantation of cell-seeded porous scaffolds belongs to the so-called 'cell therapy' and has been proposed as a suitable approach to improve implant bonding and integration to the surrounding tissue, as well as new tissue vascularization. The positive effect of seeding cells within porous scaffolds before implantation has been reported for different scaffolds and tissues, such as bone (Savarino *et al*., 2007), cartilage (Vinatier *et al*., 2009) and muscle (Levenberg *et al*., 2005). For instance, Savarino and co-workers (2007) combined polycaprolactone scaffolds with bone marrow-derived mesenchymal stem cells for bone regeneration. Compared to the neat scaffold, the cell-seeded scaffold improved new tissue formation into the macropores of the implant and neo-tissue vascularization after implantation in rabbits. Similarly, Levenberg and co-workers (2005) demonstrated that mouse myoblasts and endothelial cells can be co-cultured *in vitro* within a polylactic acid scaffold to improve the *in vivo* vascularization, blood perfusion and survival of muscle tissue constructs after transplantation in mice. It is important to point out that scaffold-based cell therapies require appropriate cell culture techniques, which are technically demanding, to achieve the desired tissue maturation before implantation.

1.7 Platforms for the controlled delivery of bioactive agents

Drug delivery systems have already had an enormous impact on medical technology, greatly improving the performance of many existing drugs and enabling the use of entirely new therapies. Polypeptide growth factors are powerful regulators of biological functions. They modulate many cellular functions including migration, proliferation, differentiation and survival. Therefore, additional direction over cell fate, beyond control of biomaterials chemistry, can be achieved through the spatially and temporally controlled incorporation and release of morphogens and growth factors (Sands and Mooney, 2007; Biondi *et al*., 2008).

The design of biocompatible foams – able to sequester and deliver bioactive molecules in a controlled fashion – is a key issue in tissue engineering and the biomedical field, and has been the object of extensive investigation. Bolus administration of growth factors cannot be effective in several approaches because of the uncontrollable diffusion rate and of the enzymatic digestion or deactivation (Biondi *et al*., 2008). Conversely, drug delivery foams can prevent drug inactivation that, conversely, occurs in contact with biological environments, during the whole release duration. Moreover, local delivery and prolonged exposition of the bioactive molecules is necessary to minimize the release of the agent to non-target sites, and support tissue regeneration that normally occurs over long time frames. Some examples of application of drug delivery biomedical foams are scaffolds for cell therapy and tissue regeneration, oral drug administration via microparticles and porous nanoparticles for drug/gene delivery and sensing applications.

Drug encapsulation can be achieved by simply dispersing the bioactive agent inside the matrix, as widely reported in the case of hydrogels. Alternatively, biomaterials can also be modified to interact with bioactive molecules, thereby achieving a better control over their release. For instance, signals can be released upon degradation of a linking tether or the matrix itself that immobilizes the molecule within the biomaterial, as in the case of heparin-binding drugs (Jeon *et al*., 2007). The number of binding sites, the affinity of the signal for these sites, and the degradation rate of the scaffold, are key parameters controlling the amount of bound signal and its release profile (Biondi *et al*., 2008; Chan and Mooney, 2008).

Drug delivery technologies can be of help in designing bioactive porous scaffolds in which low or high molecular weight molecules, such as DNA, growth factors and regulators of the inflammation response should be locally released in a chrono-programmed fashion (Shea *et al*., 1999; Tayalia and Mooney, 2009). Ungaro and co-workers (2006) fabricated drug releasing scaffolds by incorporating poly(lactic-co-glycolic acid) (PLGA)

microspheres inside collagen and hyaluronic acid hydrogels. By tuning the pore structure of both microspheres and the scaffolds, the authors were able to adjust the releasing rate as requested by the specific application. Incorporating drug-loaded microspheres inside a porous matrix also gives the opportunity of a multiple sequential delivery of growth factors, thereby mimicking naturally occurring processes during tissue regeneration and vascularization (Tayalia and Mooney, 2009). Porous synthetic scaffolds have been also fabricated for the controlled release of growth factors able to recruit mesenchymal stem cells from the host and limit scar tissue formation when implanted *in vivo* for cartilage regeneration (Huang *et al*., 2002). In principle, this approach can overcome the complex and expensive steps of *in vitro* cell seeding within porous scaffolds before implantation.

Particulate foams also found large applications for oral administration of drugs in medical therapies. Oral ingestion is the predominant, easy route for drug delivery because it allows for the immediate release of the desired dosage, minimizing the fluctuations in drug concentrations in the body, reducing the administration frequency and, ultimately, leading to improved patient compliance. Adequate control of the gastric residence time, combined with time-controlled drug release patterns, can significantly increase the bioavailability of the drug and, thus, the efficiency of the medical treatment (Streubel *et al*., 2006). Particulate foams can be very useful for this purpose, because they can be designed to float when in contact with the gastric fluids, thereby increasing the control of resident time.

Efforts to miniaturize drug delivery particulate devices from the macroscale (> 1 mm) to the microscale (0.1–100 μm) or nanoscale (1–100 nm) can potentially allow for the target delivery of precise dose of the drug, reducing the possibility of missing or erring in a dose.

Drug releasing nanoparticles are already in use in several areas of drug delivery and cosmetics. Usually smaller than 100 nm, nanoparticles are obtained by forming nanocrystals or drug–polymer complexes or by creating nanoscale shells (such as liposomes) that entrap drug molecules. Because of their size, they are often taken up by cells, whereas larger particles would be excluded or cleared from the body. Small molecules, peptides, proteins and nucleic acids can be loaded into nanoparticles that are not recognized by the immune system and that can be targeted to particular tissue types (LaVan *et al*., 2003).

Tailored nanoparticles structures offer unique characteristics to design drug delivery carriers for a particular therapy. The *in vivo* use of porous nanoparticles as therapeutic and diagnostic agents is of intense interest, owing to their unique properties such as large surface areas, tunable pore sizes and volumes, and well-defined surface properties for site-specific delivery and for hosting molecules of various sizes, shapes and functionalities. Magnetic and/or luminescent functionalities can be further incorporated

within nanoparticles to combine drug releasing with sensing and diagnostics. Among the different materials for nanoparticle fabrication, a growing interest on porous ceramic biocompatible nanoparticles such as silica, titania and alumina has recently emerged. The mesoporous structure of silica nanoparticles can be particularly interesting for drug releasing, because the release profile can be controlled either by the size or the morphology of the pores, with no need for additional chemical modification (Slowing *et al.*, 2007). The rich chemistry of silica also allows for many other possible manipulations to yield more complex systems, capable of performing more elaborate tasks. An example is the fabrication of mesoporous dye-doped silica nanoparticles decorated with multiple magnetite nanocrystals for simultaneous enhanced magnetic resonance imaging, fluorescence imaging and drug delivery (Lee *et al.*, 2010).

Among the various types of nanomaterials, dendrimers and carbon nanotubes have also recently attracted increasing attention as drug delivery devices in the biomedical research.

Dendrimers are a new class of porous polymeric systems characterized by an inner core surrounded by a series of functional branches providing high specific surface and large functional sites for loading drug molecules. The high level of control over dendrimers' size, shape, branching length/density and their surface functionality permits the encapsulation of bioactive agents directly into the interior of the dendrimers or their chemically attached/physical adsorption onto the dendrimer surface, with the option of tailoring the carrier to the specific needs and therapeutic applications.

Carbon nanotubes are well-ordered, hollow porous nanomaterials consisting of carbon atoms and can be described as rolled graphene sheets held together by van der Waals interactions. Carbon nanotubes possess outstanding properties and a unique physicochemical architecture, which may serve as an alternative platform for the delivery of various therapeutic molecules.

For more details about dendrimers and carbon nanotubes for biomedical applications and drug delivery, the reader can consult two review papers that have been recently reported, by Svenson and Tomalia (2012) and Perez and Regev (2012), respectively.

1.8 Microscaffolds for *in situ* cell delivery and tissue fabrication

Porous microparticles have been the subject of intensive research by the tissue engineering community in view of their uses, among others, as drug and cell delivery carriers and building blocks for bottom-up scaffold design and tissue fabrication (Biondi *et al.*, 2008; Urciuolo *et al.*, 2010; Salerno

et al., 2012). Indeed, microparticles can be fabricated starting from different biomaterials, while their composition, size, shape, microstructure and drug releasing capability can be controlled, selecting appropriately the fabrication technique and the processing conditions. Furthermore, the recent development of microfluidic techniques holds great promise in both the fields of drug delivery and tissue engineering, allowing for a very precise control, down to a nanoscale resolution, over the biophysical and biochemical properties of microparticles (Marre and Jensen, 2010).

Microparticulate foams were originally used as carriers for *in vitro* cell expansion and have since recently been serving as cell delivery systems for cell therapy to regenerate tissue at the site of trauma with minimally invasive procedures (Fig. 1.2). Microparticulate foams can be a substrate on which cell populations can attach and migrate, can be implanted with a combination of specific cell types as a cell delivery vehicle and can also be used as a drug carrier system to activate a specific cellular function in the localized region.

Depending on the required application, cells can be encapsulated inside the microparticles or seeded on their pore surface.

Temporary encapsulation of cells in microparticles may protect the cells from short-term environmental effects – such as those associated with the delivery to the regeneration site – and avoid the use of immunosuppressive agents, which may potentially have severe toxic effects (Hernández *et al*., 2010). Alginate, chitosan and hyaluronic acid are the most investigated hydrogel materials for cell encapsulation and have been used as stem cell carriers for *in vivo* bone and cartilage repair (Drury and Mooney, 2003; Hernández *et al*., 2010). Microparticles can also be used as vehicles of growth factor, thus enhancing the therapeutic potential of transplanted cells (Hernández *et al*., 2010; Huang and Fu, 2010; Rahman *et al*., 2010). In an interesting study, Rahman and co-workers (2010) encapsulated mouse embryonic stem cells within VEGF-functionalized agarose particles to improve blood vessel formation.

In addition to incorporating the living material, some approaches employ porous microparticles as microscaffolds, where cells are attached to the surface and inner pore structure.

Microscaffolds can be fabricated by use of techniques such as reverse templating, gas foaming and emulsion-freeze drying (Kim *et al*., 2006; Hong *et al*., 2009; Ambrosch *et al*., 2012; Choi *et al*., 2012). For example, Hong and co-workers (2009) have recently reported the fabrication of porous PCL-bioactive apatite microscaffolds with interconnected tubular pores for bone tissue engineering by using camphene as a non-toxic porogen.

Several studies have highlighted the importance of the pore structure of microscaffolds on their regenerative potential. *In vitro* cell studies with human keratinocytes and fibroblasts have demonstrated that microparticles

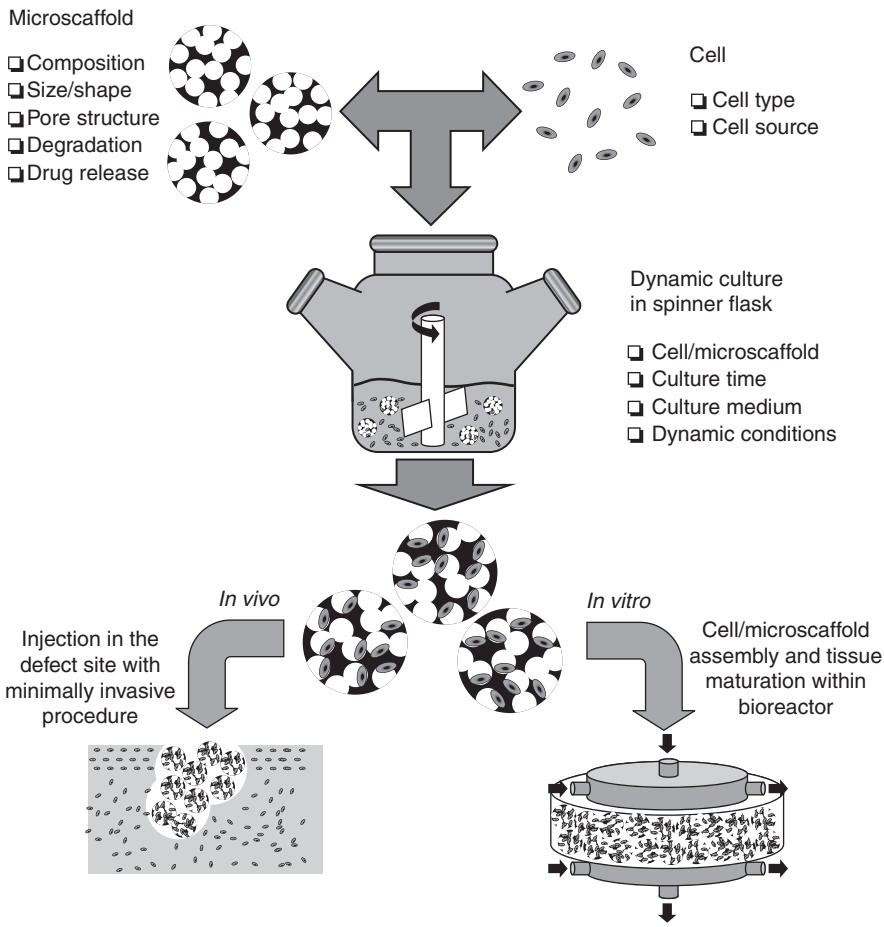

1.2 Microscaffold approaches for *in vitro* and *in vivo* tissue regeneration.

with a multicavity surface seem optimal to facilitate cell attachment and proliferation, uniform cell distribution, and ultimately skin regeneration (Huang and Fu, 2010). Similarly, chondrocytes cultured on porous PLGA microscaffolds enhanced significantly *in vivo* neo-cartilage formation, compared to non-porous ones (Choi *et al*., 2012). In addition to the formation of a porous structure, a tight control over microscaffold pore size is also essential. Indeed, it has been reported that the increase in pore size from 13 μm to 36 μm increased in turn the viability and infiltration of fibroblasts (Choi *et al*., 2012).

Gelatin is the most investigated biomaterials for microscaffold fabrication. Indeed, gelatin is highly biocompatible and can be processed to fabricate microparticles of controlled size and pore structure as well as degradation

kinetic. Furthermore, porous gelatin microscaffolds are also available on the market (CultiSpher, from Percell Biolytica).

One of the most novel and promising applications of microscaffolds is their use as building blocks for *in vitro* engineering of viable tissue equivalents (Fig. 1.2). In this 'bottom-up' approach, cells are isolated, expanded and seeded onto biodegradable microscaffolds in a dynamic culture. The cell-seeded microscaffolds, named microtissues, are then placed in a dynamic culture chamber where they assemble to form a macrotissue (Urciuolo *et al*., 2010; Chen *et al*., 2011). Assembling is the result of cell–cell and cell–ECM interactions across the microtissues. The degradation of the biomaterial finally provides the formation of a tailor-made biological tissue.

Besides offering the possibility of creating *de novo* biological tissues with biomimetic composition and architectural features, this approach can potentially generate viable 3D tissues with no limitation in size, overcoming the drawbacks of classical tissue engineering approaches. Tissue constructs resulting from this bottom-up approach include skin (Huang and Fu, 2010), derma (Urciuolo *et al*., 2010), bone and cartilage (Sommar *et al*., 2010; Chen *et al*., 2011).

A critical step towards the optimization of the final properties of the new-engineered tissue is related to the spatial distribution of the microtissues inside the construct and the culture conditions selected for tissue maturation. To date, macrotissue formation has been achieved by simply transferring a suspension containing the microtissues inside a culture chamber, while the possibility to manipulate microtissues for achieving a micrometric spatial resolution has not yet been reported in literature. However, the rapid development of techniques for the precise building of macrostructures from the bottom up, such as microfluidic devices (Chung *et al*., 2008) and SFF fabrication (see paragraph 3 for more details) can allow for a more complex manipulation of the micro- and macro-environment of the macrotissue. For instance, SFF techniques have been recently applied to fabricate tissues and organs by printing and assembling tissue spheroids or cells encapsulated inside hydrogels (Norotte *et al*., 2009). Concomitantly, the design of bioreactors for dynamic cultures of microtissues and for macrotissue maturation, coupled with the optimal selection of culture conditions, can permit the control of the biological fusion of the cell-seeded microparticles and, ultimately, the mechanical properties and the composition of the macrotissue (Urciuolo *et al*., 2010).

1.9 Three-dimensional tumour models

Three-dimensional scaffolds represent highly innovative tools for recreating tumour microenvironmental conditions in culture to study the development and evolution of cancer and to test suitable chemotherapies. Compared to

conventional 2D cultures, tumour cells maintained in 3D scaffold-based models exhibit characteristics that are more representative of their behaviour *in vivo* (Fischbach *et al*., 2007; Pathi *et al*., 2010). In recent years, 3D tumour cell culture approaches have dramatically improved our understanding of the role of 3D culture on tumour cells. These newly developed tumour models have demonstrated great utility in the investigation of cancer progression and are also used as a new test system for antitumour drugs. Porous scaffolds prepared starting from natural polymers such as collagen, chitosan and alginate have been investigated as 3D templates for tumour models. For instance, Mitsiades and co-workers (2000) developed a 3D cancer model by co-culturing human osteoblasts and cancer cells within a collagen scaffold. The construct was prepared by mixing osteoblasts with a collagen solution, followed by scaffold setting and subsequent inoculation with cancer cells. In the majority of cases, the inoculation of cancer cells induced a blastic reaction, evidenced by an increased osteoblast proliferation and a higher collagen density. Fischbach and co-workers (2007) used a porous PLGA scaffold prepared via gas foaming and salt leaching to study the angiogenic characteristics of transplanted cancer cells. *In vitro* culture was optimized in order to induce a central hypoxia within the cell/scaffold construct to mimic 3D tumour-like tissue context. By correlating *in vitro* and *in vivo* models, the authors were able to study the angiogenic characteristics of tumour cells and the effect of chemotherapy agents on tumour progression. In order to provide a more reliable model to study bone metastasis, Pathi and co-workers (2010) compared the behaviour of cancer cells within non-mineralized or mineralized polymeric scaffolds. As a result, the authors observed improved tumour cell adhesion, proliferation and secretion of pro-osteoclastic interleukin-8 in mineralized tumour models, demonstrating the role of hydroxyapatite on neoplastic and metastatic growth of cancer cells in bone.

1.10 Conclusion

This chapter describes the evolution of biomedical foams from tissue substitutions to repair/regeneration applications.

Biomedical foams were first used in implantology in order to improve the biomechanical performance of orthopaedic and vascular prostheses. Taking advantage of the possibility to induce *in vivo* tissue ingrowth at the implant/tissue interface, these materials provided prostheses with more stable fixation and enhanced life.

In the 1980s, the development of bioactive and biodegradable materials expanded the field of application of biomedical foams, from substitution to repair/regeneration. In particular, great efforts were devoted by the tissue engineering community to the design of porous biodegradable scaffolds for

in vitro cell culture and *in vivo* tissue-induced regeneration. Different classes of materials, of natural and synthetic origins, were selected and processed using various manufacturing techniques. These scaffolds were characterized to assess the effect of their composition and microstructural properties on their biocompatibility. At the same time, biotechnology and mechanobiology advances allowed for the design and fabrication of bioreactors able to improve *in vitro* cell seeding and cultivation and to provide more reliable conditions for tissue regeneration.

Finally, during the last decade, the concept of cell guidance in tissue regeneration has been extensively discussed and progressively revised as new knowledge of the complex features of cell–material interaction has been disclosed and elucidated. Biomedical foams able to mimic the biochemical and biophysical cues of native ECM have been designed aiming to improve the biological functionalities of new-engineered tissues. This has been possible thanks to the development of high resolution and automated scaffold manufacturing, able to recreate cell-niches and to test the effect of spatially and temporally controlled signals on cell fate. Furthermore, by means of miniaturization techniques and molecularly-engineered biomaterials, micro- and nano-metric multifunctional foams have been obtained, holding promise for use as platforms for *in vivo* diagnostic and repair.

1.11 References

Ambrosch, K., Manhardt, M., Loth, T., Bernhardt, R., Schultz-Siegmund, M. and Hacker, M. C. (2012) 'Open porous microscaffolds for cellular and tissue engineering by lipid templating', *Acta Biomater*, **8**, 1303–1315.

Bell, E., Ehrlich, H. P., Buttle, D. J. and Nakatsuji, T. (1981) 'Living tissue formed *in vitro* and accepted as skin-equivalent tissue of full thickness', *Science*, **211**, 1052–1054.

Bertsch, A., Jiguet, S., Bernhard, D. and Renaud, P. (2003) 'Microstereolithography: a review', *Materials Research Society Symposium Proceedings*, 758 Rapid Prototyping Technologies Symposium, 3–5 December 2002, Boston, Massachusetts, 1–13.

Biondi, M., Ungaro, F., Quaglia, F. and Netti, P. (2008) 'Controlled drug delivery in tissue engineering', *Adv Drug Deliv Rev*, **60**, 229–242.

Cao, W. and Hench, L. L. (1996) 'Bioactive materials', *Ceramic Int*, **22**, 493–507.

Caplan, M. R, Schwartzfarb, E. M., Zhang, S. G., Kamm, R. D. and Lauffenburger, D. A. (2002) 'Control of self-assembling oligopeptide matrix formation through systematic variation of amino acid sequence', *Biomaterials*, **23**, 219–227.

Causa, F., Netti, P.A. and Ambrosio, L. (2007) 'A multi-functional scaffold for tissue regeneration: The need to engineer a tissue analogue', *Biomaterials*, **28**, 5093–5099.

Chan, G. and Mooney, D. J. (2008) 'New materials for tissue engineering: towards greater control over the biological response', *Trends Biotechnol*, **26**, 382–392.

Chang, W. H., Chang, Y., Lai, P. H. and Sung, H. W. (2003) 'A genipin-crosslinked gelatin membrane as wound-dressing material: *in vitro* and *in vivo* studies', *J Biomater Sci Polym Ed*, **14**, 481–495.

Chen, G., Ushida, T. and Tateishi, T. (2002) 'Scaffold design for tissue engineering', *Macromol Biosci*, **2**, 67–77.

Chen, M., Wang, X., Ye, Z., Zhang, Y., Zhou, Y. and Tan, W. (2011) 'A modular approach to the engineering of a centimeter-sized bone tissue construct with human amniotic mesenchymal stem cells-laden microcarriers', *Biomaterials*, **32**, 7532–7542.

Chevalier, E., Chulia, D., Pouget, C. and Viana, M. (2007) 'Fabrication of porous substrates: A review of processes using pore forming agents in the biomaterial field', *J Pharm Sci*, **97**, 1135–1154.

Choi, N. W., Cabodi, M., Held, B., Gleghorn, J. P., Bonassar, L. J. and Stroock, A. D. (2007) 'Microfluidic scaffolds for tissue engineering', *Nature Mater*, **6**, 908–915.

Choi, S., Zhang, Y., Yeh, Y., Wooten, A. L. and Xia, Y. (2012) 'Biodegradable porous beads and their potential applications in regenerative medicine', *J Mater Chem*, **22**, 11442–11451.

Chung, S. E., Park, W., Shin, S., Lee, S. A. and Kwon, S. (2008) 'Guided and fluidic self-assembly of microstructures using railed microfluidic channels', *Nat Mater*, **7**, 581–587.

Cooke, M. N., Fisher, J. P., Dean, D., Rimnac, C. and Mikos, A. G. (2003) 'Use of Stereolithography to manufacture critical-sized 3D biodegradable scaffolds for bone ingrowth', *J Biomed Mater Res B Appl Biomater*, **64B**, 65–69.

Dhariwala, B., Hunt, E. and Boland, T. (2004) 'Rapid prototyping of tissue-engineering constructs, using photopolymerizable hydrogels and stereolithography', *Tissue Eng*, **10**, 1316–1322.

Drury, J. L. and Mooney, D. J. (2003) 'Hydrogels for tissue engineering: scaffold design variables and applications', *Biomaterials*, **24**, 4337–4351.

Fischbach, C., Chen, R., Matsumoto, T., Schmelzle, T., Brugge, J. S., Polverini, P. J. and Mooney, D. J. (2007) 'Engineering tumors with 3D scaffolds', *Nat Met*, **4**, 855–860.

García, A. J. (2005) 'Get a grip: integrins in cell–biomaterial interactions', *Biomaterials*, **26**, 7525–7529.

Gerhardt, L., Widdows, K. L., Erol, M. M., Burch, C. W., Sanz-Herrera, J. A., Ochoa, I., Stämplfly, R., Roqan, I. S., Gabe, S., Ansari, T. and Boccaccini, A. R. (2011) 'The pro-angiogenic properties of multi-functional bioactive glass composite scaffolds', *Biomaterials*, **32**, 4096–4108.

Gloria, A., Causa, F., Russo, T., Battista, E., Della Moglie, R., Zeppetelli, S., De Santis, R., Netti, P. A. and Ambrosio, L. (2012) 'Three-dimensional poly(ε-caprolactone) bioactive scaffolds with controlled structural and surface properties', *Biomacromolecules*, DOI: 10.1021/bm300818y.

Gomes, M. E., Godinho, J. S., Tchalamov, D., Cunha, A. M. and Reis, R. L. (2002) 'Alternative tissue engineering scaffolds based on starch: processing methodologies, morphology, degradation and mechanical properties', *Mater Sci Eng C*, **20**, 19–26.

Guarino, V., Causa, F. Salerno, A., Ambrosio, L. and Netti, P. A. (2008) 'Design and manufacture of microporous polymeric materials with hierarchal complex structure for biomedical application', *Mater Sci tech*, **24**, 1111–1117.

Guarnieri, D., De Capua, A., Ventre, M., Borzacchiello, A., Pedone, C., Marasco, D., Ruvo, M. and Netti, P. A. (2010) 'Covalently immobilized RGD gradient on PEG hydrogel scaffold influences cell migration parameters', *Acta Biomater*, **6**, 2532–2539.

Hartgerink, J. D., Beniash, E. and Stupp, S. I. (2002) 'Peptide-amphiphile nanofibers: a versatile scaffold for the preparation of self assembling materials', *Proc Natl Acad Sci USA*, **99**, 5133–5138.

He, Y., Tian, Y., Chen, Y., Ye, T. and Mao, C. (2007) 'Cation-dependent switching of DNA nanostructures', *Macromol Biosci*, **7**, 1060–1064.

Hench, L. L. (1998) 'Bioceramics', *J Am Ceram Soc*, **81**, 1705–1728.

Hench, L. L. and Polak, J. M. (2002) 'Third-generation biomedical materials', *Science*, **295**, 1014–1017.

Hernández, R. M., Orive, G., Murua, A. and Pedraz, J. L. (2010) 'Microcapsules and microcarriers for in situ cell delivery', *Adv Drug Del Rev*, **62**, 711–730.

Hersel, U., Dahmen, C. and Kessler, H. (2003) 'RGD modified polymers: biomaterials for stimulated cell adhesion and beyond', *Biomaterials*, **24**, 4385–4415.

Hildebrand, H. F., Blanchemain, N., Mayer, G., Chai, F., Lefebvre, M. and Boschin, F. (2006) 'Surface coatings for biological activation and functionalization of medical devices', *Surf Coat Tech*, **200**, 6318–6324.

Hollister, S. J. (2005) 'Porous scaffold design for tissue engineering', *Nat Mater*, **4**, 518–524.

Hong, S., Yu, H. and Kim, H. (2009) 'Tissue engineering polymeric microcarriers with macroporous morphology and bone-bioactive surface', *Macromol Biosci*, **9**, 639–645.

Hoppe, A., Güldal, N. S. and Boccaccini, A. R. (2011) 'A review of the biological response to ionic dissolution products from bioactive glasses and glass-ceramics', *Biomaterials*, **32**, 2757–2774.

Hou, Q., De Bank, P. A. and Shakesheff, K. M. (2004) 'Injectable scaffolds for tissue regeneration', *J Mater Chem*, **14**, 1915–1923.

Hu, Y., Winn, S. R., Krajbich, I. and Hollinger, J. O. (2003) 'Porous polymer scaffolds surface-modified with arginine-glycine-aspartic acid enhance bone cell attachment and differentiation *in vitro*', *J Biomed Mater Res A*, **64A**, 583–590.

Huang, Q., Goh, J. C. H., Huthmacher, D. W. and Lee, E. H. (2002) '*In Vivo* mesenchymal cell recruitment by a scaffold loaded with transforming growth factor b1 and the potential for in situ chondrogenesis', *Tissue Eng*, **8**, 469–484.

Huang, S. and Fu, X. (2010) 'Naturally derived materials-based cell and drug delivery systems in skin regeneration', *J Contr Rel*, **142**, 149–159.

Jandt, K. D. (2007) 'Evolutions, revolutions and trends in biomaterials science–A perspective', *Adv Eng Mater*, **9**, 1035–1050.

Jansen, J., Boerakker, M. J., Heuts, J., Feijen, J. and Grijpma, D. W. (2010) 'Rapid photocrosslinking of fumaric acid monoethyl ester-functionalized poly(trimethylene carbonate) oligomers for drug delivery applications', *J Contr Rel*, **147**, 54–61.

Jeon, O., Song, S. J., Kang, S., Putnam, A. J. and Kim, B. (2007) 'Enhancement of ectopic bone formation by bone morphogenetic protein-2 released from a heparin-conjugated poly(L-lactic-co-glycolic acid) scaffold', *Biomaterials*, **28**, 2763–2771.

Jiang, T., Khan, Y., Nair, L. S., Abdel-Fattah W. I. and Laurencin, C. T. (2009) 'Functionalization of chitosan/poly(lactic acid-glycolic acid) sintered microsphere

scaffolds via surface heparinization for bone tissue engineering', *J Biomed Mater Res Part A*, **93A**, 1193–1208.

Karangeorgiou, V. and Kaplan, D. (2005) 'Porosity of 3D biomaterial scaffolds and osteogenesis', *Biomaterials*, **26**, 5474–5491.

Khetani, S. R. and Bhatia, S. N. (2006) 'Engineering tissues for *in vitro* applications', *Curr Opin Biotech*, **17**, 524–531.

Kim, T. K., Yoon, J. J., Lee, D. S. and Park, T. G. (2006) 'Gas foamed open porous biodegradable polymeric microspheres', *Biomaterials*, **27**, 152–159.

Kim, H. K., Shim, W. S., Kim, S. E., Lee, K., Kang, E., Kim, J., Kim, K., Kwon, I. C. and Lee, D. S. (2009) 'Injectable in situ–Forming pH/thermo-sensitive hydrogel for bone tissue engineering', *Tissue Eng*, **15**, 923–933.

Kloxin, A. M., Kasko, A. M., Salinas, C. N. and Anseth, K. S. (2009) 'Photodegradable hydrogels for dynamic tuning of physical and chemical properties', *Science*, **324**, 59–63.

Langer, R. and Vacanti, J. P. (1993) 'Tissue engineering', *Science*, **260**, 1920–1926.

LaVan, D. A., McGuire, T. and Langer, R. (2003) 'Small-scale systems for *in vivo* drug delivery', *Nat Biotec*, **21**, 1184–1191.

Lee, C. R., Grodzonsky, A. J. and Spector, M. (2001) 'The effects of cross-linking of collagen-glycosaminoglycan scaffolds on compressive stiffness, chondrocyte-mediated contraction, proliferation and biosynthesis', *Biomaterials*, **22**, 3145–3154.

Lee, K., Kim, R. H., Yang, D. and Park, S. H. (2008) 'Advances in 3D nano/microfabrication using two-photon initiated polymerization', *Progr Polym Sci*, **33**, 631–681.

Lee, J. E., Lee, N., Kim, H., Kim, J., Choi, S. H., Kim, J. H., Kim, T., Song, I. C., Park, S. P., Moon, W. K. and Hyeon, T. (2010) 'Uniform mesoporous dye-doped silica nanoparticles decorated with multiple magnetite nanocrystals for simultaneous enhanced magnetic resonance imaging, fluorescence imaging, and drug delivery', *J Am Chem Soc*, **132**, 552–557.

Levenberg, S., Rouwkema, J., Macdonald, M., Garfein, E., Kohane, D. S., Darland, D. C., Marini, R., Van Blitterswijk, C., Mulligan, R. C., D'Amore, P. and Langer, R. (2005) 'Engineering vascularized skeletal muscle tissue', *Nat Biotech*, **23**, 879–884.

Li, J. P., De Wijn, J. R., Van Blitterswijk, C. A. and De Groot, K. (2005) 'Porous Ti6Al4V scaffolds directly fabricated by 3D fibre deposition technique: Effect of nozzle diameter', *J mater Sci Mater Med*, **16**, 1159–1163.

Lloyd, A. W., Faragher, R. G. A. and Denyer, S. P. (2001) 'Ocular biomaterials and implants', *Biomaterials*, **22**, 769–785.

Lo, C., Wang, H., Dembo, M. and Wang, Y. (2000) 'Cell movement is guided by the rigidity of the substrate', *Bioph J*, **79**, 144–152.

Lutolf, M. P. and Hubbell, J. A. (2005) 'Synthetic biomaterials as instructive extracellular microenvironment for morphogenesis in tissue engineering', *Nature Biotech*, **23**, 47–55.

Mano, J. F., Silva, G. A., Azevedo, H. S., Malafaya, P. B., Sousa, R. A., Silva, S. S., Boesel, L. F., Oliveira, J. M., Santos, T. C., Marquas, A. P., Neves, N. M. and Reis, R. L. (2007) 'Natural origin biodegradable systems in tissue engineering and regenerative medicine: present status and some moving trends', *J R Soc Interface*, **4**, 999–1030.

Marre, S. and Jensen, K. F. (2010) 'Synthesis of micro and nanostructures in microfluidic systems', *Chem Soc Rev*, **39**, 1183–1202.

Martin, I., Wendt, D. and Heberer, M. (2004) 'The role of bioreactors in tissue engineering', *Trends Biotech*, **22**, 80–86.

Martínez, E., Engel, E., Planell, J. and Samitier, J. (2009) 'Effects of artificial micro- and nano-structured surfaces on cell behaviour', *Ann Anatomy*, **191**, 126–135.

Mata, A., Kim, E. J., Boehm, C. A., Fleischman, A. J., Muschler, G. F. and Roy, S. (2009) 'A three-dimensional scaffold with precise micro-architecture and surface micro-textures', *Biomaterials*, **30**, 4610–4617.

Mathieu, L. M., Mueller, T. L., Bourban, P., Pioletti, D. P., Müller, R. and Månson, J. E. (2006) 'Architecture and properties of anisotropic polymer composite scaffolds for bone tissue engineering', *Biomaterials*, **27**, 905–916.

Mauney, J. R., Sjostorm, S., Blumberg, J., Horan, R., O'Leary, J. P., Vunjak-Novakovic, G., Volloch, V. and Kaplan, D. L. (2004) 'Mechanical stimulation promotes osteogenic differentiation of human bone marrow stromal cells on 3-D partially demineralized bone scaffolds *in vitro*', *Calcif Tissue Int*, **74**, 458–468.

Melchels, F. P. W., Feijen, J. and Grijpma, D. W. (2010) 'A review on stereolithography and its applications in biomedical engineering', *Biomaterials*, **31**, 6121–6130.

Mikos, A. G., Bao, Y., Cima, L. G., Ingber, D. E., Vacanti, J. P. and Langer, R. (1993) 'Preparation of poly(glycolic acid) bonded fiber structures for cell attachment and transplantation', *J Biomed Mater Res*, **27**, 183–189.

Mikos, A. G., Thorsen, A. J., Czerwonka, L. A., Bao, Y., Langer, L., Winslow, D. N. and Vacanti, J. P. (1994) 'Preparation and characterization of poly(l-lactic acid) foams', *Polymer*, **35**, 1068–1077.

Mironov, V., Trusk, T., Kasyanov, V., Little, S., Swaja, R. and Markwald, R. (2009) 'Biofabrication: a 21st century manufacturing paradigm', *Biofabrication*, **1**, 022001.

Mitsiades, C., Sourla, A., Doillon, C., Lembessis, P. and Koutsilieris, M. (2000) 'Three-dimensional type I collagen co-culture systems for the study of cell-cell interactions and treatment response in bone metastases', *J Musculoskelet Neuronal Interact*, **1**, 153–155.

Murugan, R. and Ramakrishna, S. (2005) 'Development of nanocomposites for bone grafting', *Comp Sci Tech*, **65**, 2385–2406.

Nair, L. S. and Laurencin, C. T. (2007) 'Biodegradable polymers as biomaterials', *Progr Polym Sci*, **32**, 762–798.

Niinomi, M. (2008) 'Metallic biomaterials', *J Artif Organs*, **11**, 105–110.

Nilles, J. L. and Coletti, J. R. (1973) 'Biomechanical evaluation of bone-porous material interfaces', *J Biomed Mater Res*, **7**, 231–251.

Norotte, C., Marga, F. S., Niklason, L. E. and Forgacs, G. (2009) 'Scaffold-free vascular tissue engineering using bioprinting' *Biomaterials*, **30**, 5910–5917.

Orsi, S., De Capua, A., Guarnieri, D., Marasco, D. and Netti, P. A. (2010) 'Cell recruitment and transfection in gene activated collagen matrix', *Biomaterials*, **31**, 570–576.

Pathi, S. P., Kowalczewski, C., Tadipatri, R. and Fischbach, C. (2010) 'A novel 3-D mineralized tumor model to study breast cancer bone metastasis', *Plos One*, **5**, e8849.

Perez, S. and Regev, O. (2012) 'Carbon nanotubes as nanocarriers in medicine', *Curr Op Coll Interf Sci*, **17**, 360–368.

Poth, E. J., Johnson, J. K. and Childers, J. H. (1955), 'The use of plastic fabrics as arterial prostheses', *Ann Surg*, **142**, 624–632.

Rahman, N., Purpura, K. A., Wylie, R. G., Zandstra, P. W. and Shoichet, M. S. (2010) 'The use of vascular endothelial growth factor functionalized agarose to guide pluripotent stem cell aggregates toward blood progenitor cells', *Biomaterials*, **31**, 8262–8270.

Ratner, B. D. and Bryant, S. J. (2004) 'Biomaterials: Where we have been and where we are going', *Annu Rev Biomed Eng*, **6**, 41–75.

Rezwan, K., Chen, Q. Z., Blaker, J. J. and Boccaccini, A. R. (2005) 'Biodegradable and bioactive porous polymer/inorganic composite scaffolds for bone tissue engineering', *Biomaterials*, **27**, 3413–3431.

Rockwood, D. N., Preda, R. C., Yücel, T., Wang, X., Lovett, M. L. and Kaplan, D. L. (2011) 'Materials fabrication from Bombyx mori silk fibroin', *Nat Protoc*, **6**, 1612–1631.

Salacinski, H. J., Goldner, S., Giudiceandrea, A., Hamilton, G., Seifalian, A. M., Edwards, A. and Carson, R. J. (2001) 'The mechanical behavior of vascular grafts: A review', *J Biomater Appl*, **15**, 241–278.

Salerno, A., Di Maio, E., Iannace, S. and Netti, P. (2009a) 'Engineering of foamed structures for biomedical application', *J Cell Plast*, **45**, 103–117.

Salerno, A., Oliviero, M., Di Maio, E., Iannace, S. and Netti, P. (2009b) 'Design of porous polymeric scaffolds by gas foaming of heterogeneous blends', *J Mater Sci: Mater Med*, **20**, 2043–2051.

Salerno, A., Zeppetelli, S., Di Maio, E., Iannace, S. and Netti, P. (2010a) 'Novel 3D porous multi-phase composite scaffolds based on PCL, thermoplastic zein and ha prepared via supercritical CO_2 foaming for bone regeneration', *Comp Sci Tech*, **70**, 1838–1846.

Salerno, A., Guarnieri, D., Iannone, M., Zeppetelli, S. and Netti, P. A. (2010b) 'Effect of micro- and macroporosity of bone tissue three-dimensional-poly(ε-Caprolactone) scaffold on human mesenchymal stem cells invasion, proliferation, and differentiation *in vitro*', *Tissue Eng*, **16**, 2661–2663.

Salerno, A., Levato, R., Mateos-Timoneda, M., Engel, E., Netti, P. A. and Planell, J. (2012) 'Modular polylactic acid microparticle-based scaffolds prepared via microfluidic emulsion/solvent displacement process: Fabrication, characterization, and *in vitro* mesenchymal stem cells interaction study', *J Biomed Mater Res Part A*, **101A**, 720–732, DOI: 10.1002/jbm.a.34374.

Sands, R. W. and Mooney, D. J. (2007) 'Polymers to direct cell fate by controlling the microenvironment', *Curr Op Biotech*, **18**, 448–453.

Savarino, L., Baldini, N., Greco, M., Capitani, O., Pinna, S., Valentini, S., Lombardo, B., Esposito, M. T., Pastore, L., Ambrosio, L., Battista, S., Causa, F., Zeppetelli, S., Guarino, V. and Netti, P. (2007) 'The performance of poly-ε-caprolactone scaffolds in a rabbit femur model with and without autologous stromal cells and BMP4', *Biomaterials*, **28**, 3101–3109.

Sharma, R. I. and Snedeker, J. G. (2010) 'Biochemical and biomechanical gradients for directed bone marrow stromal cell differentiation toward tendon and bone', *Biomaterials*, **31**, 7695–7704.

Shea, L. D., Smiley, E., Bonadio, J. and Mooney, D. J. (1999) 'DNA delivery from polymer matrices for tissue engineering', *Nat Biotech*, **17**, 551–554.

Shi, X., Ren, L., Tian, M., Yu, J., Huang, W., Du, C., Wang, D. and Wang, Y. (2010) '*In vivo* and *in vitro* osteogenesis of stem cells induced by controlled release of drugs from microspherical scaffolds', *J Mater Chem*, **20**, 9140–9148.

Simon, J. L., Michna, S., Lewis, J. A., Rekow, E. D., Thompson, V. P., Samy, J. E., Yampolsky, A., Parsons, J. R. and Ricci, J. L. (2007) '*In vivo* bone response to 3D periodic hydroxyapatite scaffolds assembled by direct ink writing', *J Biomed Mater Res*, **83A**, 747–758.

Slowing, I. I., Trewyn, B. G., Giri, S. and Lin, V. S. (2007) 'Mesoporous silica nanoparticles for drug delivery and biosensing applications', *Adv Func Mater*, **17**, 1225–1236.

Sommar, P., Pettersson, S., Ness, C., Johnson, H., Kratz, G. and Junker, J. P. E. (2010) 'Engineering three-dimensional cartilage- and bonelike tissues using human dermal fibroblasts and macroporous gelatine microcarriers', *J Plast Reconstr Aest Surg*, **63**, 1036–1046.

Staiger, M. P., Pietak, A. M., Huadmai, J. and Dias, G. (2006) 'Magnesium and its alloys as orthopedic biomaterials: A review', *Biomaterials*, **27**, 1728–1734.

Streubel, A., Siepmann, J. and Bodmeier, R. (2006) 'Drug delivery to the upper small intestine window using gastroretentive technologies', *Curr Op Pharm*, **6**, 501–508.

Sumita, M., Hanawa, T. and Teoh, S. H. (2004) 'Development of nitrogen-containing nickel-free austenitic stainless steels for metallic biomaterials-review', *Mater Sci Eng C*, **24**, 753–760.

Sung, H. Meredith, C., Johnson, C. and Galis, Z. S. (2004) 'The effect of scaffold degradation rate on three-dimensional cell growth and angiogenesis', *Biomaterials*, **25**, 5735–5742.

Svenson, S. and Tomalia, D. A. (2012) 'Dendrimers in biomedical applications—reflections on the field', *Adv Drug Del Rev*, **64**, 102–115.

Tayalia, P., Mendonca, C. R., Baldacchini, T., Mooney, D. J. and Mazur, E. (2008) '3D cell-migration studies using two-photon engineered polymer scaffolds', *Adv Mater*, **20**, 4494–4498.

Tayalia, P. and Mooney, D. J. (2009) 'Controlled growth factor delivery for tissue engineering', *Adv Mater*, **21**, 3269–3285.

Ungaro, F., Biondi, M., D'angelo, I., Indolfi, L., Quaglia, F., Netti, P. A. and La Rotonda, M. I. (2006) 'Microsphere-integrated collagen scaffolds for tissue engineering: Effect of microsphere formulation and scaffold properties on protein release kinetics', *J Contr Rel*, **113**, 128–136.

Urciuolo, F., Imparato, G., Palmiero, C., Trilli, A., Netti, P. A. (2010) 'Effect of Process Conditions on the Growth of Three-Dimensional Dermal-Equivalent Tissue Obtained by Microtissue Precursor Assembly', *Tissue Eng*, **17**, 155–164.

Vacanti, J. P., Shin, Y. M., Ogilvie, J., Svy, A., Maemura, T., Ishii, O., Kaazempur-Mofrad, M. R., Borenstein, J. T., King, K. R., Wang, C. and Weinberg, E. (2010) 'Fabrication of vascularized tissue using microfabricated two-dimensional molds', US patent, 2010/0267136 A1.

van Hest, J.C.M. and Tirrell, D.A. (2001) 'Protein-based materials, toward a new level of structural control', *Chem Commun*, **19**, 1897–1904

Ventre, M., Causa, F. and Netti, P. (2012) 'Determinants of cell-material crosstalk at the interface: towards engineering of cell instructive materials', *J R Soc Interface*, **9**, 2017–2032.

Vinatier, C., Mrugala, D., Jorgensen, C., Guicheaux, C. and Noël, D. (2009) 'Cartilage engineering: a crucial combination of cells, biomaterials and biofactors', *Trends Biotech*, **27**, 308–314.

Voytik-Harbin, S. L., Brightman, A. O., Waisner, B. Z., Robinson, J. P. and Lamar, C. H. (1998) 'Small intestinal submucosa: A tissue-derived extracellular matrix that promotes tissue-specific growth and differentiation of cells *in vitro*', *Tissue Eng*, **4**, 157–174.

Wang, H., Gong, S., Lin, Z., Fu, J., Xue, S., Huang, J. and Wang, J. (2007) '*In vivo* biocompatibility and mechanical properties of porous zein scaffolds', *Biomaterials*, **28**, 3952–3964.

Webb, J. C. J. and Spencer, R. F. (2007) 'The role of polymethyl methacrylate bone cement in modern orthopaedic surgery', *J Bone Joint Surg Br*, **89-B**, 851–857.

Williams, D. F. (1986) '*Definitions in biomaterials. Progress in Biomedical Engineering*', Vol. **4**. Amsterdam: Elsevier. 72.

Wylie, R. G. and Shoichet, M. S. (2008) 'Two-photon micropatterning of amines within an agarose hydrogel', *J Mater Chem*, **18**, 2716–2721.

Zheng, W., Wang, Z., Song, L., Zhao, Q., Zhang, J., Li, D., Wang, S., Han, J., Zheng, X., Yang, Z. and Kong, D. (2012) 'Endothelialization and patency of RGD-functionalized vascular grafts in a rabbit carotid artery model', *Biomaterials*, **33**, 2880–2891.

2

Properties of biomedical foams for tissue engineering applications

V. GUARINO and L. AMBROSIO,
National Research Council of Italy, Italy

DOI: 10.1533/9780857097033.1.40

Abstract: Over the last decade, there has been a significant progress towards the development of foams, or porous scaffolds, for a wide variety of biomedical applications. The manipulation of material chemistry and processing technologies allows for the design of tailor-made devices with peculiar mechanical morphological and functional properties for different applications. Here, we propose a complete review of materials recently used in the development of biomedical foams highlighting the relevance of some properties such as degradability or mechanical properties on the suitability of foams for the repair and regeneration strategies.

Key words: biomaterials, porous materials, biomedical foams.

2.1 Introduction

The state-of-the-art in biomaterial design has continuously evolved over the last decades to offer a portfolio of innovative devices to support the functionalities of natural tissues. In recent years, there has been increasing importance attached to materials that might be used in biomedical areas. After an early empirical phase of biomaterial selection based on availability, design attempts have been primarily focused on either achieving structural/mechanical performance or on rendering biomaterials inert and thus unrecognizable as foreign bodies by the immune system. Traditionally, biomaterials were used as implants in the form of sutures, bone plates, joint replacements, ligaments, vascular grafts, heart valves, intraocular lenses, dental implants, and medical devices such as pacemakers and biosensors (Griffith, 2000; Härtl *et al.*, 2004; Staiger *et al.*, 2006). Moreover, biomaterials have played a critical role in biomedical applications by acting as synthetic frameworks, namely scaffolds, matrices, and foams able to guide the mechanisms of tissue regeneration.

Hence, significant advances have been made in 3D porous structures – foams and scaffolds – to support the regeneration of various tissues including

skin and cartilage (Horch *et al.*, 2005), bone and ligaments (Guarino *et al.*, 2007), liver (Allen and Bhatia, 2002), heart valves and arteries (Nerem and Ensley, 2004; Leora *et al.*, 2005), bladder (Pattison *et al.*, 2005), pancreas (Kin *et al.*, 2008), nerves (Yu and Bellamkonda, 2003), corneas (Doillon *et al.*, 2003), and various other soft tissues (Guan *et al.*, 2005).

The main goal in design and developing biomedical devices is to restore the function and mobility of the native tissue that is to be replaced. In order to select an ideal biomaterial for biomedical applications, specific property requirements must be fulfilled. More generally, an ideal biomaterial should be biocompatible and bioadhesive, possess adequate mechanical properties to tolerate the applied physiological load, be corrosion/wear resistant and, finally, show good bioactivity to ensure sufficient bonding at the material/tissue interface. The criteria for selecting the materials as biomaterials are based on their chemistry, molecular weight, solubility, shape and structure, hydrophilicity/hydrophobicity, lubricity, surface energy, water absorption degradation, and erosion mechanism.

Commonly, materials for biomedical use can be divided into five major classes: metals, ceramics, natural polymers, synthetic polymers, and composites (Hench, 1998). Here, it is intended to discuss the main features of biomedical foams, describing how the peculiar properties of materials influence specific foam functions, and so directing their use towards different fields of application.

2.2 Metals for biomedical foam fabrication

Over the last few decades, a large number of metals and applied materials have been developed, with significant improvements of various properties, for a wide range of medical applications. Compared to other biomaterials, such as ceramics and polymers, the metallic biomaterials offer a wider range of mechanical properties (Table 2.1), such as high strength, ductility, fracture toughness, hardness, and formability, as well as corrosion resistance and biocompatibility. These are required properties for most load-bearing applications in fracture fixation and bone replacement (total joint arthroplasty) (Breme and Biehl, 1998; Hallab *et al.*, 2004).

Traditionally, metal implants are made of stainless steel, cobalt alloys, or titanium or its alloy nitinol. Stainless steels are preferentially used for fracture fixation devices because they exhibit high elastic modulus and tensile strength, and possess good ductility, which allows them to be cold-worked and fairly biocompatible. However, the main disadvantage of using stainless steel as biomaterial is still seen to be its fatigue limits and relative expense. Meanwhile, cobalt alloys also show high elastic modulus, strength and hardness, and are highly corrosion resistant (Singh and Dahotre, 2007). These properties allow cobalt alloys to be chosen to serve as artificial joints or

Table 2.1 Summary of mechanical properties of alloys and metal foams for biomedical use

Materials	Density (g/cm^3)	Elastic modulus (GPa)	Max elongation (%)	Yield stress (Mpa)	Ultimate tensile stress (MPa)	References
Dense bone (Cortical)	1.8–2.0	35–283	–	104–114	5–23	Black and Hastings, 1998
Porous bone (Spongy)	1.0–1.4	1.5–38	–	–	0.01–1.5	Black and Hastings, 1998
Ti6Al4V	4.43	114	–	760–880	830–1025	ASTM, 2003
316L SS	8.0	190		200–300	450–650	ASTM, 2003
Pure Mg annealed foams	1.74	45	–	160	90	ASTM, 2003
MgZnMnCa alloy (Cast)	1.58	–	9	70	90	ASM, 2005
Mg, 0.5 Ca, 2.0 Zn, 1.2 Mn foams						
WE43 Mg alloy foams	1.84	44	2	170	220	ASTM, 2001

total joint prostheses, and also for dental applications. However, they possess low ductility, and are difficult to process by traditional routes.

Alternatively, titanium and its alloys have been used extensively as bone substitutes (even under load-bearing conditions), spinal cages, and dental implants (Lin *et al.*, 2007). In particular, titanium is currently used for the production of orthopaedic implants where direct contact occurs between bones and implant surfaces (Giannoni *et al.*, 2009). Metals are also used for spinal fixation, acetabular hip prostheses, dental implants, permanent osteosynthesis plates, and intervertebral discs (Likibi *et al.*, 2005; Chaudhari *et al.*, 2011).

Indeed, titanium and some of its alloys provide many advantages, such as excellent biocompatibility, high strength-to-weight ratio, low elastic modulus, and superior corrosion resistance, required for dental and orthopaedic implants (Ramaswamy *et al.*, 2009). Alloying elements, i.e. Zr, Nb, Ta, Sn, Mo and Si, would lead to superior improvement in properties of titanium for biomedical applications. These alloys may be easily prepared in many different shapes and textures without affecting its biocompatibility (Kasemo and Lausmaa, 1988).

However, most titanium implants consist of dense components, which lead to problems such as bone resorption and implant loosening due to biomechanical mismatch of the elastic modulus (Baril *et al.*, 2011). To overcome these problems, porous structures are being investigated extensively, since a reduction in elastic modulus can be coupled with bone integration through tissue in-growth (Spoerke *et al.*, 2005). Scientific advancements have been made to fabricate porous scaffolds that mimic the architecture and mechanical properties of natural bone. The porous structure provides the necessary framework for the bone cells to grow into the pores and integrate with host tissue, known as osteointegration. In particular, several factors are crucial for promoting cell growth, vascularization and the supply of nutrients, including pore shape and size – between 100 and 500 μm – over their interconnectivity and homogeneous spatial distribution into the scaffold. Besides, it is well known that bone in-growth into porous structures provides a strong implant/bone bond, preferably when pores are three-dimensionally interconnected, because the pore interconnection provides enough space for the attachment and proliferation of new bone tissues and facilitate the transport of body fluids (Vasconcellos *et al.*, 2008).

In this context, appropriate mechanical properties, such as lower elastic moduli with respect to the bulk metal, also better mimic the bone response so minimizing or eliminating the stress-shielding problem. Indeed, the main concern regarding the application of bulk (dense) metallic biomaterials is their higher stiffness than bone. The magnitude of elastic modulus for bulk metallic implant materials overcomes that of cortical bone by far, and results in a failed stress transmission from biomaterial to bone, the so-called

stress-shielding effect. The stress shielding may lead to bone resorption or even fretting, due to micro-motions occurring at the bone/implant interface (Kawalec *et al.*, 1995).

In other words, the traditional metallic bone implants are dense and often suffer from the problems of adverse reaction, biomechanical mismatch, and lack of adequate space for new bone tissue to grow into the implant. Hence, the idea of preparing a porous material arises to bridge this biomechanical mismatch. A decrease in elastic modulus (or lowering the stiffness) would result in a higher elastic elongation of the cells in the vicinity of the implant, thereby stimulating bone formation by producing calcium (Natali and Meroi, 1989). In this context, the modulation of metal properties by adapting specific processing routes may offer the opportunity to tailor physical and mechanical properties, as well as biocompatibility, of the final device.

New processes have recently been developed to synthesize biomimetic porous titanium scaffolds for bone replacement through powder metallurgy, an efficient technique for manufacturing these complex shapes with interconnected pores without the need for machining steps (Li *et al.*, 2006). In particular, the space holder sintering method is capable of adjusting the pore shape, the porosity, and the pore size distribution, notably within the range of 200–500 μm as required for osteoconductive applications. Moreover, the powder metallurgy technique seems to be particularly advantageous because of its processing route and cost. In powder metallurgy, pores can originate from the particle compacting arrangement or from changes in this arrangement, when decomposition of spacer particles causes increasing porosity, and from solid-state diffusion in the sintering step (Ramakrishnan, 1983). Finally, the porous structure must also present adequate mechanical strength, since large pores have a deleterious effect on the scaffold's mechanical properties (Elzey and Wadley, 2001). The gradient of maximum porosity must be adjusted adequately with respect to porosity and pore size, in order to ensure the scaffold's acceptable mechanical strength.

In this context, porous shape memory alloy (SMA) scaffolds have recently achieved a considerable success for the design of new implantable devices, due to the combination of their unique mechanical and functional properties, i.e. shape memory effect and superelasticity, and low elastic modulus combined with new bone tissue in-growth ability and vascularization. These attractive properties are of great benefit to the healing process for implant applications.

The shape memory effect of SMAs provides a possibility of preparing self-expanding, self-compressing, and other functional implants (Duerig *et al.*, 1996); the superelasticity of SMAs can match the mechanical deformation behaviour of bone, which has a recoverable strain of 2% (Zelazny *et al.*, 2011). The main properties of SMAs are explained by martensitic transformation – from austenite to martensite, and vice versa – which can

differentially occur as a function of composition and metallurgical treatments, which dramatically affects the phase transition temperatures (Kim *et al.*, 2008).

Among the SMAs, nitinol is a shape memory metal which is strongly emerging for use in bone plates, because it provides a compressive force on the fracture, resulting in faster healing (Kawaguchi *et al.*, 2011). NiTi alloys with porous structure have also exhibited excellent bone in-growth ability, and elastic modulus similar to natural bone (Drozdov, 1995). In comparison with dense NiTi alloys, the mechanical properties of porous NiTi SMA can be easily controlled by modulating the porous characteristics, including porosity, pore shape, pore size, and aspect ratio (Xiong *et al.*, 2008a, 2008b). In this case, the high melting temperature of NiTi-based alloys (approximately 1310°C) makes liquid-state foaming processing methods (such as foaming of melts with blowing agents – e.g. TiH_2 – or injecting a gas into melts) inapplicable due to the extreme chemical reactivity with crucibles and atmospheric gases, and the relatively high density of the NiTi (6.45 g cm^{-3})-based alloy. To overcome these difficulties, researchers have resorted to solid-state foaming processing methods, mainly powder metallurgical techniques including conventional sintering (CS) (Li *et al.*, 1998), self-propagating high-temperature synthesis (SHS) (Biswas, 2005), hot isostatic pressing (HIP) (Yuan *et al.*, 2004), and spark plasma sintering (SPS) (Zhao *et al.*, 2005).

It has been also demonstrated that shape memory behaviour and superelasticity, bone-resembling yield strength and elastic modulus, concur to characterize the success of porous NiTi-based SMA in terms of *in vitro* and *in vivo* biocompatibility (Prymak *et al.*, 2005; Zhu *et al.*, 2008). In particular, these materials overcome the most common problems of metallic materials, such as corrosion or wear which generally provoke any negative tissue reaction, so limiting their employment as biomaterials in the human body (Buehler *et al.*, 1963).

In this context, degradable implants made of metal can be considered as a novel concept, which actually opposes the established assumption 'metallic biomaterials must be corrosion resistant' (Hermawan and Mantovani, 2009). In terms of mechanical properties, biodegradable metals are more suitable than biodegradable polymers when a high strength to bulk ratio is required, such as for internal bone fixation screws/pins and coronary stents.

More recently, biodegradable metals have showed an interesting mechanical property close to that of human bone with tailored degradation behaviour, required for porous scaffolds in bone regeneration. Indeed, the major challenge in scaffold design is to achieve adequate initial strength and stiffness and to maintain them during the stage of healing or neotissue generation throughout the scaffold degradation process (Chen *et al.*, 2002). However, biodegradable polymers generally show poor mechanical properties, often

unable to achieve the required level of strength and Young's modulus for hard tissue applications such as bone. Contrariwise, the inherent strength and ductility possessed by metals are the key features that make them appealing for hard tissue applications (Farack *et al*., 2011).

Magnesium- (Mg-) based and iron- (Fe-) based metals, alloyed with other chemical elements including rare earth elements (Witte *et al*., 2005), Calcium (Ca) (Zhang and Yang, 2008), pure Fe (Peuster *et al.*, 2006), or Mn (Schinhammer *et al.*, 2010), have been preferentially used for bone replacement scaffolds. Indeed, Mg ions largely found in bone tissue are an essential element in the human body, and their presence is beneficial to preserve bone strength (Vormann, 2003), while many studies have recognized the osteoconductive potential to actively stimulate bone growth (Witte *et al*., 2005; Guarino *et al.,* 2012). Fe ions are also essential elements, playing a significant role in the human body as metabolism mechanisms for transport, activation, and storage of molecular oxygen, reduction of ribonucleotides and dinitrogen, and decomposition of lipid, protein, and DNA damage (Mueller *et al*., 2006). Combining their excellent mechanical properties and degradability, Mg- and Fe-based alloys are emerging as a potential alternative to polymer-based composites for making scaffold for bone regeneration application. Their use in orthopaedic implants is mainly due to their supportive physical properties to human bones. Indeed, the elastic modulus of pure Mg is close to that of cortical and cancellous bones, and can be further improved by alloying and thermo-mechanical processes. Moreover, the addition of alloying elements such as aluminium, silver, indium, silicon, tin, zinc, and zirconium could improve both the strength and elongation of Mg alloys (Gu *et al.,* 2009) and their ductility (Li *et al*., 2008). Fe alloys show higher elastic modulus (211 GPa) than Mg (41 GPa) and its alloys (44 Gpa) and 316L stainless steel (190 Gpa) (Ryan *et al*., 2006).

However, they showed evidence that pronounced inflammatory response and systemic toxicity were not observed up to 18 months of the study. Hence, the use of Fe alloys for the scaffold production is still strongly limited. Only recently, Farack (Farack *et al*., 2011) have investigated the use of Fe foams coated with calcium phosphate for bone replacement scaffold. They have demonstrated that human mesenchymal stem cells proliferated and differentiated preferentially onto hydroxyapatite (HA)-coated Fe foams, confirming the ability of HA to enhance bioactivity despite inhibiting the degradation of Fe foams. In this context, the introduction of other metallic elements may contribute to optimize the degradation kinetics and mechanical properties of Fe foams for bone applications. For example, the addition of phosphorus elements allows fabrication of open porous Fe-phosphorous, which shows a faster *in vitro* degradation than pure Fe, increased compressive yield up to 11 MPa (higher than that of pure Fe of 2.4 MPa), and Young's modulus of 2.3 GPa (comparable to that of typical bone) (Quadbeck *et al*., 2010).

2.3 Ceramics and glass for biomedical foam fabrication

Bioceramics identifies the subclass of ceramic materials that can be used inside the body without rejection, due to their biocompatibility, low density, chemical stability, and high wear resistance. They generally show a refractory behaviour in nature and possess high compressive strength required to replace or fix hard connective tissues such as bones, joints, or teeth. Examples of bioceramics are alumina, zirconia, titania, HA, and calcium phosphate (CaP) (Minay and Boccaccini, 2005). As for the fabrication of biomedical foams, the most common classification of ceramic materials distinguishes between CaPs and bioglasses.

CaPs are generally preferred for tissue repair applications, mainly for their compositional similarity to the mineral phase of bone (Kalita *et al.*, 2007). Indeed, the rationale for the use of CaPs derives from their promising response in terms of biocompatibility, osteoconductivity, and biodegradability. At present, CaPs such as HA produced from natural sources (i.e., corals) have been reportedly used for orthopaedic bone-defect reconstruction (Vaccaro, 2002). These porous coral HA scaffolds are reported to exhibit a hydrothermal exchange reaction, thereby converting porous coralline skeletal materials into HA that has similar microstructure as the initial carbonate skeletal material (Mangano *et al.*, 2003). However, the major drawback for the use of coralline HA is the inability to control the pore size and chemical composition, thereby resulting in unpredictable outcomes. In order to take advantage of the CaP biocompatibility, more recently, many researchers have turned their attention towards the use of synthetic CaP for the engineering of trabecular bone-like scaffolds (Zyman *et al.*, 1998). The most widely used CaP-based bioceramics are HAP and β-tricalcium phosphate (β-TCP). HA has the chemical formula $Ca_{10}(PO_4)_6(OH)_2$, the Ca/P ratio being 1.67, and possesses a hexagonal structure, making it the most stable phase among various CaPs. Contrariwise, β-tricalcium phosphate (β-TCP) represented by the chemical formula $Ca_3(PO_4)_2$, presents a Ca/P ratio equal to 1.5 and X-ray patterns consistent with a pure hexagonal crystal structure, although the related α-TCP is monoclinic. Differences in crystal structure and chemical composition influence the dissolution rate of β-TCP ceramic, much faster than HA, thus promoting a more efficient bone bonding.

Hence, other CaPs particles – not only HA – may be considered for the bioactive potential. Besides, the chemical composition of native HA – the main mineral component of bone tissue and teeth – differs from that of synthetic HA, due to the presence of several ionic substitutions in the 3D crystal, (i.e., CO_3^{2-}, F^-, Mg^{2+}, and Na^+), which play an important role in the biological responses of bone cells as a function of their spatial distribution

and their concentration in the tissue (Elliott, 1994). For example, many authors have demonstrated that carbonates have a strong influence on the growth of apatite crystals (Ikoma *et al.*, 2001), sodium plays a role in bone remodelling (Heaney, 2006), and the fluoride ions prevent the development of dental caries (Featherstone, 1999). Recently, other authors have demonstrated that the presence of metal ions (i.e., Mg^{2+}, Zn^{2+}, Sr^{2+}) is essential to assure a stimulatory effect on bone formation *in vitro* and *in vivo*. In particular, magnesium-doped HA particles promote osteoblast function, actively participate in bone regeneration (Dasgupta *et al.*, 2010), and play a key role in bone metabolism. This effect is mainly evident during the early stages of osteogenesis, with the stimulation of osteoblast proliferation (Bigi *et al.*, 1992), due to the enhanced osteoconductivity and resorption of ion-doped particles in comparison to stoichiometric HA (Rude and Gruber, 2004; Landi *et al.*, 2008).

Recently, several processes have been optimized to impart a controlled-pore architecture to bioactive ceramic materials. The method of gel-casting foams has shown suitability for the manufacture of strong and reliable macroporous ceramics that have great potential to replace bone tissue. The process yields non-cytotoxic compounds in various porosity fractions, optimized strength, and open spherical pores, as shown in earlier work (Sepulveda *et al.*, 2000a). For bone repair strategies, macropores arranged to form a highly interconnected network are required to provide in-growth access of surrounding host tissues, facilitating further deposition of newly formed tissue in the spherical cavities. Additionally, the intricate shape of the walls provides a framework that supports the organization of growing tissue, improving biological fixation, and avoiding drawbacks that may result from implant mobility (Kienapfel *et al.*, 1999). Therefore, porous HA has been also manufactured via foaming of aqueous ceramic suspensions and setting via gel casting of organic monomers (Sepulveda *et al.*, 2000b). This technique involves foaming of ceramic suspensions or swelling of ceramic green bodies via gas evaporating chemical reactions from organic and inorganic sources. Some foaming agents tested were hydrogen peroxide, carbonate salt, and baking powder. They were added to the HA slurries while stirring to let it foam, and then subjected to polymerization followed by sintering (Woyansky *et al.*, 1992). The porous HA obtained has pore sizes of 30–600 μm (Aoki *et al.*, 2004).

Tamai *et al.* (2002) developed a modified version of the ceramics foaming method they called '*foam-gel*' technique. This technique involves a cross-linking polymerization step that gelatinizes the foam-like HA slurry in a rapid manner, thus promoting the formation of an interconnected porous structure. The wall surface of the device obtained is very smooth, and HA particles are aligned closely with one another and bound tightly. With an average pore size of 150 μm, and average interpore connections at 40 μm,

this device is favourable for interpore cell migration or tissue in-growth. Gel casting of foams can be applied to produce ceramic scaffolds with high mechanical strength. The disadvantage of this technique is that it typically results in a structure of poorly interconnected pores and non-uniform pore size distribution. For these reasons, porous HA commonly cannot be used for load-bearing applications, but is used to fill only small bone defects and for artificial bone substitutes. Besides, a successful development of porous bone substitutes with optimal properties requires perfect control of morphological properties, i.e., pore volume, mean pore, and interconnection sizes. In particular, dimension and morphology of pores are crucial factors for an excellent osteointegration (Le Huec *et al.*, 1995; Gauthier *et al.*, 1998). The minimum pore size required to enable in-growth of the surrounding bone together with blood supply is about 100–150 μm for macropores (Hulbert *et al.*, 1972), and even with pores as small as 50 μm osteoconduction, it is still possible (Chang *et al.*, 2000).

Some reports have stated that it should be 200–500 μm for colonization of osteoblast in the pores, fibrovascular in-growth, and finally the deposition of the new bone (Flatley *et al.*, 1983) In order to match these morphological requirements, a useful approach for fabricating porous ceramic foams consists in the use of polymers via the replication of a polymeric sponge substrate to produce reticulated open-celled porous ceramics. The polymeric sponge method, as this method is named, is performed by impregnating porous polymeric substrates (sponges) with HA slurry. Porous HA prepared via the polymeric sponge method has shown well-interconnected pores but has poor mechanical strength for load-bearing applications. It was shown that the polymeric sponge method results in a proper pore size distribution, as osteoconduction requires. This is characterized by the existence of micro/meso/macropores with an adequate degree of interconnection (Tampieri *et al.*, 2001). This method allows control of rheological properties of the ceramics powder suspension by varying the characteristics of starting powders. By varying the characteristics of the starting powders, that is powders 20% and 80% of crystallinity degree, the rheological properties of the ceramics powder suspension can be controlled (Guicciardi *et al.*, 2001). Moreover, some authors have demonstrated the possibility of preparing HA ceramics with crystallinity and porosity gradients that mimic the physicochemical features of cortical and spongy bones. In this case, the foams show tortuous frameworks and large interconnected pores which support cell attachment and organization into 3D arrays to form new tissue. Once *in vivo*, HA foam implants are progressively filled with mature new bone tissue and osteoid after the period of implantation, without any immune or inflammatory reactions, thus confirming the high osteoconductive potential and high biocompatibility of HA and the suitability of foam network in providing good osteointegration.

Alternatively, bioactive glasses are ideal materials because they rapidly bond to bone and degrade over time, releasing soluble silica and calcium ions that are thought to stimulate osteoprogenitor cells (Jones *et al.*, 2010). Bioactive glasses have been shown to bond with bone more rapidly than other bioactive ceramics (Oonishi *et al.*, 1997, 2000) and to stimulate human osteoblast cells at the genetic level, which has been attributed to soluble silica and calcium ions being released from the glasses after implantation (Xynos *et al.*, 2001). Their bioactivity is directly related to the chemical substitution of silicon (or silicate groups) for phosphorous (or phosphate groups) (Patel *et al.*, 2002), which led to the development of successful clinical products. Indeed, silicon plays an essential role in bone formation, because it is involved in the calcification process of young bones (Carlisle, 1970). Firstly, the presence of silicon in biological ceramics and glasses has a significant effect on the osteogenesis process. Indeed, it has been demonstrated that the incorporation of silicon into apatites induces the formation of higher amounts of bone tissue than non-doped apatites (Patel *et al.*, 2002). Moreover, silicon improves materials' bioactivity by leading to the formation of Si–OH groups on the material surface. These groups trigger the nucleation and formation of apatite layers on the surface, improving the material–bone bonding. Bioglasses containing SiO_2 are able to stimulate the tissue regeneration by inducing the formation of surface active layers (Anderson and Kangansniemi, 1991; Cao and Hench, 1996) based on carbonated HA (CHA) similar to the native bone apatite. Hence, bioglasses have been successfully used in low load-bearing material applications for bone repair in dental and orthopaedic surgery (Schepers *et al.*, 1991; Stanley *et al.*, 1997).

Process developments in foaming, solid freeform fabrication, and nanofibre spinning have now allowed the production of porous bioactive glass scaffolds from both melt- and sol–gel-derived glasses (Hench *et al.*, 1998). Initially, melt-derived bioactive glasses, such as the original bioglass composition, have been commercially available, but several difficulties have been detected to fabricate porous scaffolds, due to crystallization phenomena of bioglass and similar compositions crystallize during the sintering process. More recently, sol–gel strategies have allowed this problem to be overcome. Indeed, they assure the preparation of hierarchical pore structure comprising interconnected macropores with interconnected diameters exceeding 100 μm in size that is thought to be needed for vascularized bone in-growth, and an inherent nanoporosity of interconnected mesopores (2–50 nm) which is beneficial for the attachment of osteoprogenitor cells. These peculiar morphology features are usually generated by controlled foaming strategy, further added to the sol–gel process: in particular, the hydrolysed sol phase can be foamed by vigorous agitation in air with the aid of a surfactant. In this context, the surfactant lowers the surface tension and temporally stabilizes

the foam (Jones *et al*., 2006). The result is a hierarchical pore structure of macropores interconnected by nanoporosities which show characteristic size scales of pores independently tailored. Macropores may affect cell response and tissue in-growth, while nanoporosity affects surface area, degradation rate, and cellular attachment. Indeed, as they degrade they release soluble silica and calcium ions that can stimulate osteogenic cells to bone in-growth. However, this does not compromise the mechanical response of scaffolds which show characteristic properties falling in the range of cancellous bone (Rainer *et al*., 2008). Hence, the interest in composite bioglasses is progressively increasing, to fill the mechanical gap of bioglasses alone. Tough composites can be produced using a biodegradable polymer matrix including polylactide (PLA) and polyglycolide (PGA) and their copolymers polyglycolic acid (PLGA) with bioactive glass particles as the filler phase (Rezwan *et al*., 2006) which concur to increase the stiffness and compressive strength of the polymer matrix.

2.4 Degradable polymers for biomedical foam fabrication

General criteria to select a biomaterial for the development of 3D porous foams are to match the mechanical properties and the degradation rate. Polymers can be classed into degradable and non-degradable. Degradable ones will be the focus of this section, as they can be totally removed from human bodies as foreign bodies. It is obvious from the recent literature on clinical engineering (Ranade, 1990) that there is an increasing interest in several degradable and resorbable biomaterials due to their peculiar biological properties (Rezwan, 2006). Much of this interest has been stimulated by recent breakthroughs in tissue engineering techniques, whereby resorbable scaffold materials are used as a support matrix or as a substrate for the delivery of cultured cells or for three-dimensional tissue reconstruction (Freed *et al.*, 1994; Hutmacher *et al.*, 1996). Recently, an equal interest has been directed towards the use of biodegradable polymers in controlled drug delivery strategies from polymer-based carriers (Langer, 1990). Hence, the demand for degradable polymers with improved physical, mechanical, chemical, and biological properties is dramatically increasing, thanks to the use of multi-component systems with multi-scale degradation kinetics as smart solutions for the design of temporary devices for tissue repair and regeneration (Holy *et al.*, 2003).

The term '*biodegradable polymer*' refers to the susceptibility of a polymer to be decomposed by living organisms or by environmental factors. According to the American Society for Testing and Materials (ASTM) standard definition, biodegradable means capable of undergoing decomposition into CO_2, CH_4, H_2O, inorganic compounds or biomass (Smith, 2005).

However, in terms of their use in tissue engineering, biodegradable polymers could be decomposed into biologically acceptable molecules (without the production of harmful intermediates) which could be metabolized and removed from the body via natural pathway (metabolism or excretion) (Vert, 2005). In this context, different degradable and non-degradable polymers have been widely investigated as biomaterials because of their ease of manufacturability, low cost, and adequate mechanical and physical properties. Among them, two types of polymers can be distinguished: natural and synthetic polymers (Yang *et al.*, 2001; Guarino *et al.*, 2007). Natural polymers, i.e., collagens, starch, chitin, and chitosan, are totally recognized by the biological microenvironment, thus making them useful in the regeneration of several tissues (i.e., nerve, skin, cartilage, and bone). Despite many advantages offered by materials from natural sources, notably biological recognition, synthetic polymers offer greater advantages than natural ones, in that they can be tailored to give a wider range of properties. In particular, some drawbacks in terms of mechanical properties often require the use of synthetic polymers which combine improved chemical stability and tailored degradation histories, ensuring a higher durability *in vivo*. The use of synthetic material has been extensively exploited for two important reasons. First, the immunogenic and purification issues relating to natural biomaterials are only partially overcome by recombinant protein technologies. Secondly, there is a relevant interest in controlling the material properties, and to tailor performance in terms of tissue response. Hence, synthetic materials satisfy this demand thanks to their highly chemically programmable and reproducible properties.

However, some limitations in terms of cell recognition impose the need to improve their physical and chemical performance, by modification or combination with natural source materials to generate their semi-synthetic counterparts (Langer and Tirrell, 2004). Due to these peculiar degradation properties, several polymers have been designed in the form of 3D foams by various processing strategies, such as CO_2 foaming (Salerno *et al.,* 2008).

2.4.1 Natural polymers

Natural polymers may be defined as the biodegradable biomaterials clinically used '*par excellence*' (Nair and Laurencin, 2007). Indeed, natural materials, owing to their bioactive properties, have better interaction with the cells, which allows them to enhance the cells' performance in a biological system. In order to perform a rough classification, it is possible to distinguish between proteins (silk, collagen, gelatin, fibrinogen, elastin, keratin, actin, and myosin), polysaccharides (cellulose, amylose, dextran, chitin, and glycosaminoglycans), and polynucleotides (DNA, RNA) (Yannas, 2004).

Polysaccharides, in particular, have some excellent properties which make them a polymer group with important features for widest medical application (Hon, 1996), including non-toxicity (monomer residues are not hazardous to health), water solubility or high swelling ability by simple chemical modification, stability to pH variations, and a broad variety of chemical structures. This versatility makes these materials able to overcome disadvantages such as low mechanical, temperature and chemical stability, and proneness to microbial and enzymatic degradation, which can generally limit their use as three-dimensional foams.

Alginates are naturally produced polysaccharides that have been finding increasing applications in the biotechnology field. They belong to a family of linear copolymers of β-D-mannuronic acid and α-L-guluronic acid residues, which can be arranged in different proportions and sequences along the polymer chain (Smidsrod and Draget, 1996; Gombotz and Wee, 1998). Sodium alginate and most other alginates from monovalent metals are soluble in water, forming solutions of considerable viscosity. Due to their suitable rheological properties, alginates have long been used in the pharmaceutical industry as thickening or gelling agents, as colloidal stabilizers, and as blood expanders. More recently, alginate foams are attracting most attention, due to many new possibilities for overcoming today's biomedical challenges in areas such as tissue engineering, wound management, anti-adhesion, *in vitro*/*in vivo* cell support, medical implants, and controlled drug release *in situ*. This is assured by their peculiar properties in terms of flexibility and pliability which preserve the structural integrity and tensile strength required for *in vitro* and *in vivo* applications. Unlike other foams, alginate foams are biocompatible, do not exhibit handling brittleness, can be manufactured by inexpensive methodologies, and sterilized using common sterilization techniques.

The most common technique for production of alginate foams is freeze drying. Ionically-gelled alginate foams with interconnected pores can be made with controllable pore size, pore-wall thickness, and elasticity by changing formulation and processing parameters (Shapiro and Cohen, 1997). Frequently, this technique is combined with the use of porogen salts or gas expansion through covalently cross-linked gels in order to create a macroporous architecture. Moreover, alginate may be easily blended with other natural polymers such as gelatin in bead form, or cationic polymers such as chitosan (Barbetta *et al.*, 2009; Hwang *et al.*, 2010).

Recently, alginate foams provided several benefits as immobilization matrices (Melvik and Dornish, 2004) able to entrap drugs, particulates and living cells within the tailored pores of the foam, so allowing cell proliferation in three dimensions (Hegge *et al.*, 2010). Moreover, they really imitate the natural environment needed to support differentiated cells by the possibility of modulating the elasticity/stiffness of the foam.

Among polysaccharides, hyaluronic acids or hyaluronan have been alternatively used in biological context due to large availability *in vivo* in the form of polyanion and not in the protonated acid form (Liao *et al.*, 2005). Hyaluronan is a naturally occurring non-sulphated glycosaminoglycan and a major macromolecular component of the intercellular matrix of most connective tissues such as cartilage, vitreous of the human eye, umbilical cord, and synovial fluid (Liao *et al.*, 2005). From chemical point of view, it is a linear polysaccharide consisting of alternating disaccharide units of α-1,4-D-glucuronic acid, and β-1,3-N-acetyl-D-glucosamine, linked by $\beta(1\rightarrow3)$ bonds (Laurent *et al.*, 1995) and plays many physiological roles including tissue and matrix water regulation, structural and space-filling properties, lubrication, and a number of macromolecular functions (Liao *et al.*, 2005). The peculiar viscoelastic properties of hyaluronan enable its use as a lubricant and shock absorber in synovial fluid (Nishinari and Takahashi, 2003). Moreover, several hyaluronan formulations have been mainly studied for drug delivery, implantable delivery devices, and for gene delivery (Liao *et al.*, 2005). More recently, hyaluronan has been successfully used to develop foams in the form of benzyl ester of hyaluronic acid (HYAFFs) to engineer synthetic cartilage or menisci (Kon *et al.*, 2008), and to regenerate bone at the osteochondral level (Guarino *et al.*, 2010).

It is recognized that the type and extent of chemical esterification of hyaluronan considerably affect the biological properties of these materials, offering a range of polymers either favouring or, conversely, inhibiting the adhesion of certain types of cell (Campoccia *et al.*, 1998). An advantage of HYAFF-based scaffolds is their good cell adhesiveness, even in the absence of any coating or surface conditioning treatment often required by other widely used support matrices, such as those made of polyglycolic and polylactic acid (Solchaga *et al.*, 2005). They are sufficiently stable in aqueous solution to allow incubation with cells for over 3 weeks. Once wet, the benzyl ester loses part of its mechanical strength, more so than other completely synthetic materials. However, under *in vitro* cell culture conditions, the material maintains its structural integrity, can easily be handled, and does not contract as some collagen-based materials do in *in vitro* studies on hyaluronic-acid-based membranes (Chiari *et al.*, 2008).

However, one of the drawbacks of the natural-origin polymers still consists in their possible batch variation. To prevent these issues, recombinant protein technologies have recently been used to finely control monodispersity and precisely define polymer properties in terms of crosslinking groups, binding moieties at specific sites along the polypeptide chain or their programmable degradation rates, thus providing the opportunity to bioengineer protein-based polymers of well-defined and complex structure (Rodríguez-Cabello *et al.*, 2005). In particular, recombinant polymers, also termed 'Recombinamers' in recent publications (Rodríguez-Cabello *et al.*, 2009),

are macromolecules produced using recombinant DNA technology by introducing a desired gene into the genetic content of a host organism such as micro-organisms, plants or other eukaryotic organisms. Elastin-like recombinant polymers (ELR), which form a subclass of protein-based recombinant polymers, are composed of the pentapeptide repeat Val-Pro-Gly-Xaa-Gly (VPGXG), which mimics the sequence of hydrophobic domains of tropoelastin, where X represents any natural or modified amino acid except proline. This peculiar composition allows mimicking functional properties of natural proteins with an absolute control of the amino-acid sequence and a complete absence of randomness (Patel *et al.*, 2006). Recently, ELRs have been foamed by freeze-drying strategies in combination with collagen to realize scaffolds for tissue regeneration (Garcia *et al.*, 2009). The enzymatic chemical crosslinking with mTGase assures optimal *in vitro* biocompatibility of the device. Meanwhile, the introduction of elastic-like elements coupled to collagen macromolecules significantly enhances the mechanical response of the scaffold as required for load-bearing applications. Lastly, this concurs to improve the ultimate response of cells, thus making this scaffold an attractive platform for the regeneration of different tissues.

2.4.2 Synthetic polymers

An alternative solution to the use of natural polymers is represented by synthetic polymers, which can be produced under controlled conditions to exhibit in general predictable and reproducible mechanical and physical properties such as tensile strength, elastic modulus, and degradation rate. Possible risks, such as toxicity, immunogenicity, and favouring of infections, are lower for pure synthetic polymers with constituent monomeric units having a well-known and simple structure (Rezwan *et al.*, 2006). The most used biodegradable synthetic polymers for 3D foaming scaffolds in tissue engineering are saturated polyhydroxyesters, including poly(lactic acid) (PLA) and poly(glycolic acid) (PGA), as well as poly(lactic-coglycolide) (PLGA) copolymers (Jagur-Grodzinski, 1999; Seal *et al.*, 2001). Due to their properties, PLA and PGA have been used in products and devices, as being degradable they have been approved by the US Food and Drug Administration. PLA and PGA can be processed easily and their degradation rates, physical and mechanical properties are adjustable over a wide range by using various molecular weights and copolymers. Indeed, the chemical properties of these polymers allow hydrolytic degradation through de-esterification. Once degraded, the monomeric components of each polymer are removed by natural pathways. The body already contains highly regulated mechanisms for completely removing monomeric components of lactic and glycolic acids. However, these polymers undergo a bulk erosion

process, such that they can cause scaffolds to fail prematurely. In addition, abrupt release of these acidic degradation products can cause a strong inflammatory response (Bergsma *et al.*, 1993; Martin *et al.*, 1996). Polyester degradation occurs by uptake of water followed by the hydrolysis of esters. This mechanism is generally affected by several factors, including chemical composition, processing history, molecular weight and polydispersity (Mw/Mn), environmental conditions, crystallinity and porosity, especially in the case of 3D foams (Heidemann *et al.*, 2001).

In the light of these considerations, aliphatic polyesters can therefore exhibit quite distinct degradation kinetics. PGA, for example, is a stronger acid and is more hydrophilic than PLA, which is partially hydrophobic due to its methyl groups. Moreover, PLA can be cleared through the tricarboxylic acid cycle while PGA is converted to metabolites or eliminated by other mechanisms, further explaining why PGA degrades faster than PLA. Hence, PLGA, a copolymer of PLA and PGA, may show intermediate degradation rates that can be modulated as a function of the relative fraction of hydrophobic/hydrophilic phases, crystallinity, and composition of chains (i.e. contents in L-LA and D-LA, and/or GA units) (Andrew *et al.*, 2001). Indeed, the amount of D- or mesolactide present in the L-PLA polymer changes the properties significantly in terms of melting temperature, crystallization rate and therefore processability and properties of foams. For example, the higher the D-isomer content in the polymer, the lower are the crystallization rate and the melting point. All these parameters are fundamental to balance the process conditions during the foaming process. Of particular significance for applications in tissue engineering are debris and crystalline by-products, as well as particularly acidic degradation products of aliphatic polyesters, such as PLA, PGA, polycaprolactone (PCL) and their copolymers that have been implicated in adverse tissue reactions (Yang *et al.*, 2001). This is the result of the heterogeneous degradation of these polymers, which occurs faster inside than at the exterior by the competition of the next two phenomena: the easier diffusion of soluble oligomers from the surface into the external medium than from inside, and the neutralization of carboxylic end groups located at the surface by the external buffer solution (*in vitro* or *in vivo*). The combination of these events contributes to reduce the acidity at the surface, instead enhancing the degradation rate by autocatalysis due to carboxylic end groups in the bulk (Jagur-Grodzinski, 1999). It is evident that the advance of hydrolysis reactions is strictly related to the ease of fluids to diffuse into the polymer chains, which is mainly determined by the relative fraction of amorphous/crystalline regions. Indeed, crystal segments are chemically more stable than amorphous segments and reduce water permeation into the matrix in combination with ionic strength, temperature, and pH of the medium. In this context, other compounds, i.e., CaPs or bioactive glasses, may be further incorporated to stabilize the environment conditions

surrounding the polymer in order to control its degradation. This counteracting effect of the acidic degradation of biodegradable polymers represents one of the main reasons to move towards the design of composite materials.

2.5 Polymer-based composites for biomedical foam fabrication

Development of composite foams is currently attractive, as advantageous properties of two or more types of materials can be combined to better suit the mechanical and physiological demands of the host tissue. Lee *et al.* (2006) showed the optimization of process preparation of 100% open-pore foams in a wide range of gas-foaming processing conditions by mixing softer/harder immiscible phases of few microns into the polymeric matrix. Soft phases concur to the mechanism of pore opening by decreasing the pore-wall strength, also increasing the foam expansion ratio. Likewise, the presence of a harder second phase also facilitates the pore-wall opening, because of the different deformation behaviour with respect to the matrix (Lee *et al.*, 2005).

Similar approaches based on composite materials have been successfully applied in scaffold design for tissue engineering. Indeed, taking advantage of the formability of polymers by most recognized foaming and scaffold manufacturing processes, the addition of bioactive polymers of ceramic phases allows improving the ultimate mechanical and biological performance of the device. For instance, the integration of CaP particles, such as HA within PCL matrix, currently represents one of the most effective strategies to make PCL implants more 'biologically informative' (Guarino *et al.*, 2012). Indeed, CaPs traditionally used in a range of orthopaedic and dental applications (Marcacci *et al.*, 1999) more recently, may be advantageously used to design bioactive scaffolds in bone tissue engineering because of their inherent bioactivity, namely the ability to form chemical bond with bone (Habibovic *et al.*, 2008) and osteoconductivity, namely the capability of supporting bone growth (LeGeros, 2002).

As for the bioactive 3D porous foams, ceramic filler may act also as a reinforcement system that is able to significantly improve mechanical properties (Guarino *et al.*, 2008a). Meanwhile, PCL matrix, as a binder, plays a protective function of ceramic particles, so preventing any problems associated with brittleness and difficulties in shaping hard ceramic materials to fit bone defects (Coombes and Meikle, 1994).

However, it can often impair bioactive potential by reducing particle exposure at the interface (Rizzi *et al.*, 2001). Moreover, addition of bioactive phases to bioresorbable polymers can also alter the polymer degradation behaviour, by allowing rapid exchange of protons in water for alkali

in the ceramic glasses (Li and Chang, 2005). In particular, the inclusion of bioactive glasses has been shown to modify surface and bulk properties of composite scaffolds by increasing the hydrophilicity and water absorption of the hydrophobic polymer matrix, thus altering the scaffold degradation kinetics (Lu *et al*., 2003). For example, Boccaccini *et al*. have demonstrated that the inclusion of 45S5 bioglass particles allows for the increase of water absorption compared to pure polymer foams of poly-DL-lactide acid (PDLLA) (Boccaccini and Maquet, 2003) and PLGA (Maquet *et al.*, 2004). Other studies have reported that polymer composites, filled with HA particles, hydrolysed homogeneously, due to water penetrating the interfacial regions (Li and Chang, 2005). Ideally, the degradation and resorption kinetics of composite scaffolds are designed to allow cells to proliferate and secrete their own extracellular matrix, while the scaffolds gradually vanish, leaving space for new cell and tissue growth. In this context, the physical support provided by the 3D foam has to be maintained until the engineered tissue has sufficient mechanical integrity to support itself (Niemela *et al.*, 2005). However, the most synthetic matrices generally show hydrophobic surfaces which makes unfavourable basic cell interaction mechanisms (i.e., adhesion, proliferation) than on hydrophilic surfaces (Vandiver *et al.*, 2005). The inclusion of bioactive solid signals into the polymer matrix may allow supporting the creation of a strong bond with the living host bone at the scaffold/implant interface thanks to an improved wettability ascribable to the presence of the apatite particles (De Aza *et al.*, 2003). Hence, synthetic polymer matrices made of biocompatible polyesters (i.e., polycaprolactone, polylactide acid) have generally demonstrated a tendency to be inert and to promote the formation of encapsulated fibrous tissues, thereby resulting in significant bone formation. Contrariwise, the inclusion of CaP particles into biodegradable porous foams may concur to promote the bone osteogenesis, as studied in the case of porous PCL/HA foams obtained by phase inversion and salt leaching techniques (Guarino *et al.*, 2008a). The presence of stoichiometric HA particles enhances the scaffold bioactivity and human osteoblast cell response, evidencing their role as '*bioactive solid signals*' in the promotion of surface mineralization and, consequently, on the cell–material interaction.

In particular, the biological study performed on foams with different PCL/HA volume ratio, double scale of pore sizes and fully interconnected porosities, has shown that stromal cells from bone marrow (bMSC) were able to adhere and grow on PCL-based scaffolds at any HA content, so demonstrating their '*nature*' as a precursor with high replicative potential. Indeed, even though cultured *in vitro* in static conditions, without additional stimulants (e.g., growth factors), bMSC adhered during the first four weeks of culture, showing a cuboidal appearance on the polymer surface, which is a typical feature of mature osteoblasts. However, in some cases, the presence

of HA into PCL scaffolds only slightly affects the biological response so that the viability and MSC differentiation seem to be not directly related to the amount of HA in the porous matrix (Russias *et al.*, 2006). Beyond the osteoconductive enhancement, the relative amount of HA is relevant in affecting the intrinsic mechanical response of the composite scaffolds and their degradation properties.

Several papers have demonstrated the active role of CaP fillers on *in vitro* degradation mechanisms by the simultaneous assessment of the influence of scaffold morphology and its physicochemical properties (Guarino *et al.*, 2009). The addition of HA particles was found to slightly modify the pore morphology with a small reduction of the average pore size. More interestingly, other studies on the scaffold mass losses have evidenced that the presence of apatite phases embedded in the PCL matrix drastically increases the polymer crystallinity degree, promoting the formation of more densely packed crystalline phases within the composite with a lower amount of amorphous regions which are potentially more susceptible to hydrolytic attacks due to a better accessibility of the ester linkage (Guarino *et al.*, 2009). In this case, the increase in crystallinity of polymer matrix in HA-loaded scaffolds hinders the degradation of the composites, preferentially deflecting the fluids at the polymer/ceramic interface, which are more susceptible to hydrolytic attack.

Meanwhile, the use of rigid bone-like particles embedded into a polymer matrix evidently improve the mechanical properties, as recommended in the use of composite scaffolds as a substrate for hard tissue replacement (Kikuchi *et al.*, 1997; Khan *et al.*, 2004).

However, the contribution of mechanical response due to the ceramic phase may be partially hindered by the presence of macro- and microstructured pores, which even represent a basic requirement to induce the regeneration mechanisms in tissue engineering applications. For this reason, the further integration of biodegradable PLA fibres into the PCL matrix allows improving the mechanical response of the scaffolds, providing spaces required for cellular in-growth and matrix production. Added bioactive apatite-like particles generating needle-like crystals of calcium-deficient HA similar to natural bone apatite also interact with the fibre-reinforced polymer matrix, further enhancing the mechanical response in compression by up to an order of magnitude (Guarino and Ambrosio, 2008b). However, HA-loaded polymer matrices have recently shown an adverse reaction due to a non-homogeneous distribution of ceramic particles in the polymeric matrix which dramatically compromises both the mechanical performance and the bioactive potential of the composite scaffolds (Guarino *et al.*, 2007).

The polymer matrix degradation, for example, causes a faster escape of HA particles, creating voids within the polymeric structure (Guarino *et al.*,

2009). This evidently affects the mechanical response of the scaffolds, influencing their integrity at longer times of the *in vitro* culture.

Alternatively, chemically inspired approaches based on the sol–gel transition and colloidal precipitation of CaPs may efficiently improve the particles' dispersion, directly controlling the sizes of precipitated grains through the interaction between calcium and phosphate precursors under controlled temperature and pH conditions (Huang *et al.*, 2000). The sol–gel reaction allows finely dispersing CaP nanoparticles into a polymer such as polycaprolactone (PCL) matrix, with an expected improvement of the functional features (i.e., mechanical response, bioactivity) as reported in previous work (Raucci *et al.*, 2010a). Moreover, this technique assures a more efficacious compensation of acidosis, due to the acidic release from the polymer matrix through the alkaline CaP, minimizing the undesired phenomena of pH decay during the *in vitro* (Raucci *et al.*, 2010b) or *in vivo* experiments (Martin *et al.*, 1996).

2.6 Conclusions and future trends

In recent years, the world of biomaterials has been extended from purely synthetic materials to synthetic/biological material hybrids, whose design and engineering simultaneously have encompassed bioactivity and biodegradability. In particular, this recent biomaterial progress is ascribable to the growing requirement of controlling increasingly complex biological responses, in terms of ion interactions and growth factor incorporation.

In this chapter, innovative materials among metals, ceramics, polymers, and composites have been reviewed to fabricate 3D porous foams for tissue repair and regeneration. As for the repair, new discoveries in the materials field mainly concern implantable devices with tailored chemical and physical properties as well as smart mechanical behaviour which has to adapt to the native properties of surrounding tissue during the healing (i.e., shape memory foams). As for tissue engineering, polymer and composite materials currently represent the most interesting strategy for fabricating reproducible bioactive and bioresorbable 3D foams with tailored porosity and pore structure, which are able to maintain their structure and integrity for predictable times, even under load-bearing conditions and to incorporate biomolecules to support specific cellular events (Guarino *et al.*, 2007). This is also permitted by recent improvement in process technologies which concur to better control shapeability, bioactive behaviour and biodegradation kinetics. Moreover, they provide the opportunity to modulate specific properties of different material classes in the case of composites, so obtaining optimum performance in terms of porosity and structure interconnection. However, many different approaches are continually looking to satisfy all

the complex requirements regarding structure and function of biomedical foams. Today, a fruitful way could consist of identifying suitable processes able to really control pore structure, mechanical and degradation properties in order to understand the cell regeneration and degradation product transport in the porous structure. From a materials point of view, biodegradable metals are currently emerging as a valid alternative for scaffolds in tissue engineering. The integration of biodegradable polymers or ceramics and drugs could be another interesting direction to explore. Future trends should be inspired from mechanically superior metals and the excellent biocompatibility and biofunctionality of ceramics and polymers to obtain the most desirable clinical performance of the implants.

2.7 References

Allen J W and Bhatia S N (2002) 'Engineering liver therapies for the future', *Tissue Eng*, **8**(5), 725–737.

Anderson O H and Kangansniemi L (1991)'Calcium phosphate formation at the surface of bioactive glass *in vivo*', *J Biomed Mater Res*, **25**, 1019–1030, (DOI:10.1002/jbm. 820250808).

Andrew S D, Phil G C and Marra K G (2001) 'The influence of polymer blend composition on the degradation of polymer/hydroxyapatite biomaterials', *J Mater Sci: Mater Med*, **12**, 673–677.

Aoki S, Yamaghuci S, Nakahira A and Suganuma K (2004) 'Preparation of porous calcium phosphate using a ceramic foaming technique combined with a hydrothermal treatment and the cell response with incorporation of osteoblast like cells', *J Cer Soc Jpn*, **112**, 193–199.

ASTM (2003) 'Standard specification for wrought 18chromium- 14nickel-2.5molybdenum stainless steel bar and wire for surgical implants (UNS S31673)', Tech Rep F138, ASTM International, West Conshohocken, Pa, USA.

ASM (2005) *ASM Handbook*: '*Properties and Selection: Nonferrous Alloys & Special Purpose Materials*', Vol. **2**, Ohio, USA, ASM International, Materials Park.

ASTM (2001) 'Standard specification for magnesium-alloy sand castings', Tech Rep B80, West Con-shohocken, Pa, USA, ASTM International.

Barbetta A, Barigelli E and Dentini M (2009) 'Porous alginate hydrogels: synthetic methods for tailoring the porous', *Biomacromolecules*, **10**, 2328–2337.

Baril E, Lefebvre L P and Hacking S A (2011) 'Direct visualization and quantification of bone growth into porous titanium implants using micro computed tomography', *J Mater Sci Mater Med*, **22**(5), 1321–1332.

Bergsma E J, Rozema F R, Bos R R M and Debruijn W C (1993) 'Foreign body reaction to resorbable poly(L-lactic) bone plates and screws used for the fixation of unstable zygomatic fractures', *J Oral Maxillofac Surg*, **51**, 666–670.

Bigi A, Foresti E, Gregorini R, Ripamonti A, Roveri N and Shah J S (1992) 'The role of magnesium on the structure of biological apatites', *Calcif Tissue Int*, **50**, 439–444.

Biswas A (2005) 'Porous NiTi by thermal explosion mode of SHS: processing, mechanism and generation of single phase microstructure', *Acta Mater*, **53**(5), 1415–1425.

Black J and Hastings G (1998) '*Handbook of Biomaterial Properties*', London, UK, Chapman and Hall.

Boccaccini A R and Maquet V (2003) 'Bioresorbable and bioactive polymer/Bioglass(R) composites with tailored pore structure for tissue engineering applications', *Compos Sci Technol*, **63**, 2417–2429.

Breme J and Biehl V (1998) 'Metallic Biomaterials', in Black J and Hastings G (eds.), *Handbook of Biomaterial Properties*, London, Chapman and Hall, 135–144.

Buehler W, Gilfrich J and Wiley R (1963) 'Effect of low temperature phase changes on the mechanical properties of alloys near composition of TiNi', *J Appl Phys*, **34**, 1475–1477.

Campoccia D, Doherty P, Radice M, Brun P, Abatangelo G and Williams D F (1998) 'Semisynthetic resorbable materials from hyaluronan esterification', *Biomaterials*, **19**, 2101–2127.

Cao W and Hench L L (1996) 'Bioactive materials', *Ceram Int*, **22**, 493–507, (DOI:10.1016/0272-8842(95)00126-3).

Carlisle E M (1970) 'Silicon: a possible factor in bone calcification', *Science*, **167**, 279–280, (DOI:10.1126/science.167.3916.279).

Chang B S, Lee C K, Hong K S, Youn H J, Ryu H S, Chung S S and Park K W (2000) 'Osteoconduction at porous hydroxyapatite with various pore configurations', *Biomaterials*, **21**, 1291–1298.

Chaudhari A, Braem A, Vleugels J, Martens J A, Naert I, Cardoso M V and Duyck J (2011) 'Bone tissue response to porous and functionalized titanium and silica based coatings', *PLoS One*, **6**(9), e24186.

Chen G, Ushida T and Tateishi T (2002) 'Scaffold design for tissue engineering', *Macromol Biosci*, **2**, 67–77.

Chiari C, Koller U, Kapeller B, Dorotka R, Bindreiter U and Nehrer S (2008) 'Different behavior of meniscal cells in collagen II/I,III and Hyaff-11 scaffolds *in vitro*', *Tissue Eng A*, **14**, 1295–1304.

Coombes A G A and Meikle M C (1994) 'Resorbable synthetic polymers as replacements for bone graft', *Clin Mater*, **17**, 35–67.

Dasgupta S, Banerjee S S, Bandyopadhyay A and Bose S (2010) 'Zn- and Mg-doped hydroxyapatite nanoparticles for controlled release of protein', *Langmuir*, **26**(7), 4958–4964.

De Aza P N, Luklinska Z B, Santo C, Guitian F and De Aza S (2003) 'Mechanism of bone-like formation on a bioactive implant *in vivo*', *Biomaterials*, **24**, 1437–1445.

Doillon C J, Watsky M A, Hakim M, Wang J, Munger R, Laycock N, Osborne R and Griffith M (2003) 'A collagen-based scaffold for a tissue engineered human cornea: physical and physiological properties', *Int J Art Org*, **26**(8), 764–773.

Drozdov I A (1995) 'Formation of intermetallics in a porous powder titanium-nickel diffusion couple', *Sov Powder Metall*, **34**, 282.

Duerig T W, Pelton A R and Stöckel D (1996) 'The utility of superelasticity in medicine', *Biomed Mater Eng*, **6**, 255–266.

Elliott J C (1994) 'Structure and chemistry of the apatites and other calcium orthophosphates', in *Studies in Inorganic Chemistry*, Amsterdam, Elsevier, 18.

Elzey D M and Wadley N G (2001) 'The limits of solid state foaming', *Acta Mater*, **49**, 849–859.

Farack J, Wolf-Brandstetter C, Glorius S, Nies B, Standke G, Quadbeck P, Worch H and Scharnweber D (2011) 'The effect of perfusion culture on proliferation and differentiation of human mesenchymal stem cells on biocorrodible bone replacement material', *Mater Sci and Eng B*, **176**, 1767–1772.

Featherstone J D B (1999) 'Prevention and reversal of dental caries: role of low level fluoride', *Community Dent Oral Epidemiol*, **27**, 31–40.

Flatley T J, Lynch K L and Benson M (1983) 'Tissue response to implants of calcium phosphate ceramics in the rabbit spine', *Clin Orthop*, **179**, 246–252.

Freed L E, Vunjak-Novakovic G, Biron R J, Eagles D B, Lesnoy D C, Barlow S K and Langer R (1994) Biodegradable polymer scaffolds for tissue engineering', *Bio/Technol*, **12**, 689–695.

Garcia Y, Hemantkumar N, Collighan R, Griffin M, Rodriguez-Cabello J C and Pandit A (2009) '*In vitro* characterization of a collagen scaffold enzymatically cross-linked with a tailored elastin-like polymer', *Tissue Eng A*, **15**, 887–899.

Gauthier O, Bouler J, Aguado E, Pilet P and Daculsi G (1998) 'Macroporous biphasic calcium phosphate ceramics: influence of macropore diameter and macroporosity percentage on bone ingrowth', *Biomaterials*, **19**, 133–139.

Giannoni P, Muraglia A, Giordano C, Narcisi R, Cancedda R, Quarto R and Chiesa R (2009) 'Osteogenic differentiation of human mesenchymal stromal cells on surface-modified titanium alloys for orthopedic and dental implants', *Int J Artif Organs*, **32**(11), 811–820.

Gombotz W R and Wee S F (1998) 'Protein release from alginate matrices', *Adv Drug Deliv Rev*, **31**, 267–285.

Griffith L G (2000) 'Polymeric biomaterials', *Acta Mater*, **48** (1), 263–277.

Gu X, Zheng Y, Cheng Y, Zhong S and Xi T (2009) '*In vitro* corrosion and biocompatibility of binary magnesium alloys', *Biomaterials*, **30**(4), 484–498

Guan J, Fujimoto K L, Sacks M S and Wagner W R (2005) 'Preparation and characterization of highly porous, biodegradable polyurethane scaffolds for soft tissue applications', *Biomaterials*, **26**(18), 3961–3971.

Guarino V, Causa F and Ambrosio L (2007) 'Bioactive scaffolds for bone and ligament tissue', *Expert Rev Med Dev*, **4**(3), 405–418.

Guarino V, Causa F, Netti P A, Ciapetti G, Pagani S, Martini D, Baldini N and Ambrosio L (2008a) 'The role of hydroxyapatite as solid signal on performance of PCL porous scaffolds for bone tissue regeneration', *J Biomed Mater Res B Appl Biomater*, **86B**, 548–557.

Guarino V and Ambrosio L (2008b) 'The synergic effect of polylactide fiber and calcium phosphate particles reinforcement in poly ε-caprolactone based composite scaffolds', *Acta Biomater*, **4**, 1778–1787.

Guarino V, Taddei P, Di Foggia M, Fagnano C, Ciapetti G and Ambrosio L (2009) 'The influence of hydroxyapatite particles on *in vitro* degradation behaviour of PCL based composite scaffolds', *Tissue Eng A*, **15**, 3655–3668.

Guarino V, Gloria A, De Santis R and Ambrosio L (2010) 'Composite hydrogels for scaffold design, tissue engineering and prostheses', in Ottenbrite R M, Park K and Okano T (eds.), *Biomedical Applications of Hydrogels Handbook*, Vol. **3**, 227–245.

Guarino V, Scaglione S, Sandri M, Alvarez-Perez M A, Tampieri A, Quarto R and Ambrosio L (2012) 'MgCHA particles dispersion in porous pcl scaffolds: *in vitro* mineralization and *in vivo* bone formation', *J Tissue Eng and Reg Med*, (DOI: 10.1002/term.1521).

Guicciardi S, Galassi C, Landi E, Tampieri A, Satou K and Pezzoti G (2001) 'Rhelogical characteristics of slurry controlling the microstructure and the compressive strength behaviour of biomimetic hydroxyapatite', *J Mater Res*, **16**, 163–170.

Habibovic P, Kruyt M C, Juhl M V, Clyens S, Martinetti R, Dolcini L, Theilgaard N and van Blitterswijk C A (2008) 'Comparative *in vivo* study of six hydroxyapatite-based bone graft substitutes', *J Orthop Res*, **26**, 1363–1370.

Hallab N J, Jacobs J J and Katz J L (2004) 'Application of materials in medicine, biology and artificial organs: orthopedic applications', in Ratner B D, Hoffman A S, Schoen F and Lemons J E (eds.), *Biomaterials Science: An Introduction to Materials in Medicine*, Hench, Elsevier Academic Press, 526–555.

Härtl A, Schmich E, Garrido J A, Hernando J, Catharino S C R, Walter S, Feulner P, Kromka A, Steinmüller D and Stutzmann M (2004) 'Protein-modified nanocrystalline diamond thin films for biosensor applications', *Nature Mat*, **3**, 736–742.

Heaney R P (2006) 'Role of dietary sodium in osteoporosis', *J Am Coll Nutr*, **25**, 271–276.

Hegge A B, Andersen T, Melvik J E, Kristensen S and Tønnesen H H (2010) 'Evaluation of novel alginate foams as drug delivery systems in antimicrobial photodynamic therapy (aPDT) of infected wounds – an *in vitro* study: studies on curcumin and curcuminoides XL', *J Pharm Sci*, **99**, 3499–3513.

Heidemann W, Jeschkeit S, Ruffieux K, Fischer J H, Wagner M, Kruger G, Wintermantel E and Gerlach K L (2001) 'Degradation of poly(D,L)lactide implants with or without addition of calcium phosphates *in vivo*', *Biomaterials*, **22**, 2371–2381.

Hench L L (1998) 'Biomaterials: a forecast for the future', *Biomaterials*, **19**(16), 1419–1423.

Hench L L, Wheeler D L and Greenspan D C (1998) 'Molecular control of bioactivity in sol-gel glasses', *J Sol-Gel Sci Technol*, **13**, 245–250.

Hermawan H and Mantovani D (2009) 'Degradable metallic biomaterials: The concept, current developments and future directions', *Minerv Biotecnol*, **21**, 207.

Holy E, Fialkov J A, Davies J E and Shoichet M S (2003) 'Use of a biomimetic strategy to engineer bone', *J Biomed Mater Res A*, **15**, 447–453.

Hon D S (1996) 'Cellulose and its derivatives: structures, reactions, and medical uses', in Dumitriu S (ed.), *Polysaccharides in Medicinal Applications*, New York, USA, Marcel Dekker, 87–105.

Horch R E, Kopp J, Kneser U, Beier J and Bach A D (2005) 'Tissue engineering of cultured skin substitute', *J Cell and Mol Med*, **9**(3), 592–608.

Huang L Y, Xu K W and Lu J (2000) 'A study of the process and kinetics of electrochemical deposition and the hydrothermal synthesis of hydroxyapatite coatings', *J Mater Sci Mater Med*, **11**, 667–673.

Hulbert S F, Morisson S J and Klawitter J J (1972) 'Tissue reaction to three ceramics of porous and nonporous structures', *J Biomed Mater Res*, **6**, 347–374.

Hwang C M, Sant S, Masaeli M, Kachouie N N, Zamanian B, Lee S H and Khademhosseini A (2010) 'Fabrication of three-dimensional porous cell-laden hydrogel for tissue engineering', *Biofabrication*, **2**, 1–12.

Ikoma T, Kubo Y, Yamazaki A, Akao M and Tanaka J (2001) 'Effect of carbonate contents on crystal structure of A-type carbonate apatites', in Giannini S and

Moroni A (eds.), *Bioceramics*, Zurich, Trans Tech Publications Ltd, Vol. 13, 191–194.

Jagur-Grodzinski J (1999) 'Biomedical application of functional polymers', *Reactive Funct Polym*, **39**, 99–138.

Jones J R, Ehrenfried L M and Hench L L (2006) 'Optimising bioactive glass scaffolds for bone tissue engineering', *Biomaterials*, **27**(7), 964–973.

Jones J R, Lin S, Yue S, Lee P D, Hanna J V, Smith M E and Newport R J (2010) 'Bioactive glass scaffolds for bone regeneration and their hierarchical characterisation'. *Proc Inst Mech Eng*, *H: J Eng Med*, **224**, 1373.

Kalita S J, Bhardwaj A and Bhatt H A (2007) 'Nanocrystalline calcium phosphate ceramics in biomedical engineering', *Mater Sci Eng C*, **27**, 441–449.

Kasemo B and Lausmaa J (1988) 'Biomaterial and implant surfaces: a surface science approach', *Int J Oral Maxillofac Implants*, **3**, 247–259.

Kawaguchi T, Shimizu H, Lassila L V, Vallittu P K and Takahashi Y (2011) 'Effect of surface preparation on the bond strength of heat-polymerized denture base resin to commercially pure titanium and cobalt-chromium alloy', *Dent Mater J*, **30**(2), 143–150.

Kawalec J S, Brown S A, Payer J H and Merritt K (1995) Mixed-metal fretting corrosion of Ti_6Al_4V and wrought cobalt alloy', *J Biomed Mater Res*, **29**, 867–873.

Khan Y M, Katti D S and Laurencin C T (2004) 'Novel polymer-synthesized ceramic composite-based system for bone repair: An *in vitro* evaluation', *J Biomed Mater Res A*, **69**, 728–737.

Kienapfel H, Sprey C, Wilke A and Griss P (1999) 'Implant fixation by bone ingrowth', *J Arthroplasty*, **14**(3), 355–368.

Kikuchi M, Cho S B, Suetsugu Y and Tanaka J (1997), '*In vitro* tests and *in vivo* tests developed TCP/CPLA composites', *Bioceramics*, **10**, 407–410.

Kim J I, Nam T H, Lee Y J and Miyazaki S (2008) 'Effect of annealing on shape memory characteristics of Ti–50.85 at. %Ni alloy', *Funct Mater Lett*, **1**(3), 209–213.

Kin T, O'Neil J J, Pawlick R, Korbutt G S, Shapiro A M J and Lakey J R T (2008) 'The use of an approved biodegradable polymer scaffold as a solid support system for improvement of islet engraftment', *Artif Org*, **32**(12), 990–993.

Kon E, Chiari C, Marcacci M, Delcogliano M, Salter D M, Martin I, Ambrosio L, Fini M, Tschon M, Tognana E, Plasenzotti R and Nehrer S (2008) 'Tissue engineering for total meniscal substitution: animal study in sheep model', *Tissue Eng A*, **14**, 1067–1080.

Landi E, Logroscino G, Proietti L, Tampieri A, Sandri M and Sprio S (2008) 'Biomimetic Mg-substituted Hydroxyapatite: from synthesis to *in vivo* behaviour', *J Mater Sci Mater Med*, **19**, 239–247.

Langer R (1990) 'New methods of drug delivery', *Science*, **249**,1527–1533.

Langer R and Tirrell D A (2004), 'Designing materials for biology and medicine', *Nature*, **428**, 487–492.

Laurent T C, Laurent U B G and Fraser J R E (1995) 'Functions of hyaluronan', *Ann Rheum Dis*, **54**, 429–432.

Le Huec J C, Schaeverbeke T, Clement D, Faber J and Le Rebeller A (1995) 'Influence of porosity on the mechanical resistance of hydroxyapatite ceramics under compressive stress', *Biomaterials*, **16**(2), 113–118.

Lee P C, Wang J and Park C B (2006) 'Extrusion of microcellular open-cell LDPE-based sheet foams', *J Appl Polym Sci*, **102**, 3376–3384.

Lee P C, Wang J and Park C B (2005) 'Extruded open-cell foams using two semi-crystalline polymers with different crystallization temperatures', *Ind Eng Chem Res*, **45**, 175–181.

LeGeros R Z (2002) 'Properties of osteoconductive biomaterials: calcium phosphates', *Clin Orthop Relat Res*, **395**, 81–98.

Leora J, Amsalema Y and Cohen S (2005) 'Cells, scaffolds, and molecules for myocardial tissue engineering', *Pharmacol Therapeut*, **105**(2), 151–163.

Li B Y, Rong L J and Li Y Y (1998) 'Porous NiTi alloy prepared from elemental powder sintering', *J Mater Res*, **13**, 2847–2851.

Li H Y and Chang J (2005) 'pH-compensation effect of bioactive inorganic fillers on the degradation of PLGA', *Compos Sci Technol*, **65**, 2226–2232.

Li J P, Li S H, Van Blitterswijk C A and De Groot K (2006) 'Cancellous bone from porous Ti_6Al_4V by multiple coating technique', *J Mater Sci Mater Med*, **17**, 179–185.

Li Z, Gu X, Lou S and Zheng Y (2008) 'The development of binary Mg–Ca alloys for use as biodegradable materials within bone', *Biomaterials*, **29**(10), 1329–1344.

Liao Y H, Jones S A, Forbes B, Martin G P and Brown M B (2005) 'Hyaluronan: pharmaceutical characterization and drug delivery', *Drug Deliv*, **12**, 327–342.

Likibi F, Assad M, Coillard C, Chabot G and Rivard C H (2005) 'Bone integration and apposition of porous and non porous metallic orthopaedic biomaterials', *Ann Chir*, **130**, 235–241.

Lin C Y, Wirtz T, La Marca F and Hollister S J (2007) 'Structural and mechanical evaluations of a topology optimized titanium interbody fusion cage fabricated by selective laser melting process', *J Biomed Mater Res A*, **83**(2), 272–279.

Lu H H, El-Amin S F, Scott K D, Laurencin C T (2003) 'Three-dimensional, bioactive, biodegradable, polymer-bioactive glass composite scaffolds with improved mechanical properties support collagen synthesis and mineralization of human osteoblast-like cells *in vitro*', *J Biomed Mater Res Part A*, **64A**, 465–474.

Mangano C, Bartolucci E G and Mazzocco C (2003) 'A new porous hydroxyapatite for promotion of bone regeneration in maxillary sinus augmentation: clinical and histologic study in humans', *Inter J Oral Maxillofac Implants*, **18**, 23–30.

Maquet V, Boccaccini A R, Pravata L, Notingher I and Jerome R (2004) 'Porous poly([alpha]-hydroxyacid)/Bioglass(R) composite scaffolds for bone tissue engineering. I: Preparation and *in vitro* characterisation', *Biomaterials*, **25**, 4185–4194.

Marcacci M, Kon E, Zaffagnini S, Giardino R, Rocca M, Corsi A, Benvenuti A, Bianco P, Quarto R, Marin I, Muraglia A and Cancedda R (1999) 'Reconstruction of extensive long-bone defects in sheep using porous hydroxyapatite sponges', *Calcif Tissue Int*, **64**, 83–90.

Martin C, Winet H and Bao J Y (1996) 'Acidity near eroding polylactide polyglycolide *in vitro* and *in vivo* in rabbit tibial bone chambers', *Biomaterials*, **17**(24), 2373–2380.

Melvik J E and Dornish M (2004) 'Alginate as a carrier for cell immobilisation', in Nedovic V and Willaert R (eds.), *Fundamentals of Cell Immobilisation Biotechnology*, Dordrecht, Kluwer Academic Publishers, 33–51.

Minay E J and Boccaccini A R (2005) 'Metals', in Hench L L and Jones J R (eds.), *Biomaterials, artificial organs and tissue engineering*, England, Woodhead Publishing Limited.

Mueller P P, May T, Perz A, Hauser H and Peuster M (2006) 'Control of smooth muscle cell proliferation by ferrous iron', *Biomaterials*, **27**(10), 2193–2200.

Nair L S and Laurencin C T (2007) 'Biodegradable polymers as biomaterials', *Prog Polym Sci*, **32**, 762–798.

Natali A N and Meroi E A (1989) 'A review of biomedical properties of bone as a material', *J Biomed Eng*, **11**, 212–219.

Nerem R M and Ensley A E (2004) 'The tissue engineering of blood vessels and the heart', *Am J Transplant*, **4**(6), 36–42.

Niemela T, Niiranen H, Kellomaki M and Tormala P (2005) Self-reinforced composites of bioabsorbable polymer and bioactive glass with different bioactive glass contents. Part 1: Initial mechanical properties and bioactivity, *Acta Biomater*, **1**, 235–242.

Nishinari K and Takahashi R (2003) 'Interaction in polysaccharide solutions and gels', *Curr Opin Colloid Interface Sci*, **8**, 396–400.

Oonishi H, Kushitani S, Yasukawa E, Iwaki H, Hench L L, Wilson J, Tsuji E I and Sugihara T (1997) 'Particulate bioglass compared with hydroxyapatite as a bone graft substitute', *Clin Orthop Relat Res*, **334**, 316–325.

Oonishi H, Hench L L, Wilson J, Sugihara F, Tsuji E, Matsuura M, Kin S, Yamamoto T and Mizokawa S (2000) 'Quantitative comparison of bone growth behavior in granules of bioglass (R), A-W. glass-ceramic, and hydroxyapatite', *J Biomed Mater Res*, **51**(1), 37–46.

Patel N, Best S M, Bonfield W, Gibson I R, Hing K A, Damien E and Revell P A (2002) 'A comparative study on the *in vivo* behavior of hydroxyapatite and silicon substituted hydroxya patite granules', *J Mater Sci Mater Med*, **13**(12), 1199–1206.

Patel A, Fine B, Sandig M and Mequanint K (2006) 'Elastin biosynthesis: the missing link in tissue-engineered blood vessels', *Cardiovasc Res*, **71**, 40–49.

Pattison M A, Wurster S, Webster T J and Haberstroh K M (2005), 'Three-dimensional, nano-structured PLGA scaffolds for bladder tissue replacement application', *Biomaterials*, **26**(15), 2491–2500.

Peuster M, Hesse C, Schloo T, Fink C, Beerbaum P and von Schnakenburg C (2006) 'Long-term biocompatibility of a corrodible peripheral iron stent in the porcine descending aorta', *Biomaterials*, **27**(28), 4955–4962.

Prymak O, Bogdanski D, Koller M, Esenwein S A, Muhr G, Beckmann F, Donath T, Assad M and Epple M (2005) 'Morphological characterization and *in vitro* biocompatibility of a porous nickel–titanium alloy', *Biomaterials*, **26**, 5801–5807.

Quadbeck P, Hauser R and Kummel K (2010) 'Iron based cellular metals for degradable synthetic bone replacement', *Proc Powder Metal World Cong* (PM10), 10–14 October 2010, Florence, Italy.

Rainer A, Giannitelli S M, Abbruzzese F, Traversa E, Licoccia S and Trombetta M (2008) 'Fabrication of bioactive glass–ceramic foams mimicking human bone portions for regenerative medicine', *Acta Biomater*, **4**, 362–369.

Ramakrishnan K (1983) 'Hystory of powder metallurgy', *Indian J Hist Sci*, **18**(1), 109–114.

Ramaswamy Y, Wu C and Zreiqat H (2009) 'Orthopedic coating materials: considerations and applications', *Expert Rev Med Devices*, **6**(4),423–430.

Ranade V V (1990) 'Drug delivery systems: 3B. Role of polymers in drug delivery', *J Clin Pharmacol*, **30**, 107–120.

Raucci M G, Guarino V and Ambrosio L (2010a), 'Hybrid composite scaffolds prepared by sol-gel method for bone regeneration', *Compos Sci Technol*, **70**, 1861–1868.

Raucci M G, D'Antò V, Guarino V, Sardella E, Zeppetelli S, Favia P and Ambrosio L (2010b) 'Biomineralized porous composite scaffolds prepared by chemical synthesis for bone tissue regeneration', *Acta Biomater*, **6**, 4090–4099.

Rezwan K, Chen Q Z, Blaker J J and Boccaccini A R (2006), 'Biodegradable and bioactive porous polymer/inorganic composite scaffolds for bone tissue engineering', *Biomaterials*, **27**, 3413–3431.

Rizzi S C, Heath D J, Coombes A G A, Bock N, Textor M and Downes S (2001) 'Biodegradable polymer/hydroxyapatite composites: surface analysis and initial attachment of human osteoblasts', *J Biomed Mater Res*, **55**, 475–486.

Rodríguez-Cabello J C, Martín L, Alonso M, Arias F J and Testera A M (2009) 'Recombinamers as advanced materials for the post-oil age', *Polymer*, **50**, 5159–5169.

Rodríguez Cabello J C, Reguera J, Girotti A, Alonso M and Testera A M (2005) 'Developing functionality in elastin-like polymers by increasing their molecular complexity: the power of the genetic engineering approach', *Prog Polym Sci*, **30**, 1119–1145.

Rude R K and Gruber H E (2004) 'Magnesium deficiency and osteoporosis: animal and human observations', *J Nutr Biochem*, **15**, 710–716.

Russias J, Saiz E, Nalla R K, Gryn K, Ritchie R O and Tomsia A P (2006) 'Fabrication and mechanical properties of PLA/HA composites: A study of *in vitro* degradation', *Mater Sci Eng C*, **26**, 1289–1295.

Ryan G, Pandit A and Apatsidis D P (2006) 'Fabrication methods of porous metals for use in orthopaedic applications', *Biomaterials*, **27**(13), 2651–2670.

Salerno A, Iannace S and Netti P A (2008) 'Open-pore biodegradable foams prepared via gas foaming and microparticulate templating', *Macromol Biosci*, **8**(7), 655–664.

Seal B L, Otero T C and Panitch A (2001), 'Polymeric biomaterials for tissue and organ regeneration', *Mater Sci Eng*, **34**, 147–230.

Schepers E, de Clercq M, Ducheyne P and Kempeneers R (1991) 'Bioactive glass particulate material as a filler for bone lesions', *J Oral Rehabil*, **18**, 439–452.

Schinhammer M, Hanzi A C, Loffler J F and Uggowitzer P J (2010) 'Design strategy for biodegradable Fe-based alloys for medical applications'. *Acta Biomater*, **6**(5), 1705–1713.

Sepulveda P, Binner J P G, Rogero S O, Higa O Z and Bressiani J C (2000a) 'Production of porous hydroxyapatite by the gel-casting of foams and cytotoxic evaluation', *J Biomed Mater Res*, **50**(1), 27–34.

Sepulveda P, Ortega F S, Innocentini M D M and Pandolfelli V C (2000b) 'Properties of highly porous hydroxyapatite obtained by the gel casting of foams', *J Ceram Am Soc*, **83**(12), 3021–3024.

Shapiro L and Cohen S (1997) 'Novel alginate sponges for cell culture and transplantation', *Biomaterials*, **18**, 583–590.

Singh R and Dahotre N B (2007) 'Corrosion degradation and prevention by surface modification of biometallic materials', *J Mater Sci Mater Med*, **18**(5), 725–751.

Smidsrod O and Draget K I (1996) 'Chemistry and physical properties of alginates', *Carbohydr Eur*, **14**, 6–13.

Smith R (2005) *Biodegradable Polymers for Industrial Applications*, New York, Woodhead Publishing Limited.

Solchaga L A, Temenoff J S, Gao J, Mikos A G, Caplan A I and Goldberg V M (2005) 'Repair of osteochondral defects with hyaluronan- and polyester-based scaffold', *Osteoarthr Cartilage*, **13**, 297–309.

Spoerke E D, Murray N G, Li H, Brinson L C, Dunand D C and Stupp S I (2005) 'A bioactive titanium foam scaffold for bone repair', *Acta Biomater*, **1**, 523–533.

Staiger M P, Pietak A M, Huadmai J and Dias G (2006), 'Magnesium and its alloys as orthopedic biomaterials: A review', *Biomaterials*, **27**(9), 1728–1734.

Stanley H R, Hall M B, Clark A E, King C, Hench L L and Berte J J (1997) 'Using 45S5 bioglass cones as endosseous ridge maintenance implant to prevent alveolar ridge resorption: a 5 year evolution'. *Int J Maxillofac Implants*, **12**, 95–105.

Tamai N, Myoui A, Tomita T, Nakase T, Tanaka J, Ochi T and Yoshikawa H (2002) 'Novel hydroxyapatite ceramics with an interconnective porous structure exhibit superior osteoconduction *in vivo*', *J Biomed Mater Res*, **59**, 110–117.

Tampieri A, Celotti G, Sprio S, Delcogliano A and Franzese S (2001) 'Porosity-graded hydroxyapatite ceramics to replace natural bone', *Biomaterials*, **21**, 1365–1370.

Vaccaro A R (2002) 'The role of the osteoconductive scaffold in synthetic bone graft', *Orthopedics*, **25**(5), 571–578.

Vandiver J, Dean D, Patel N, Bonfield W and Ortiz C (2005) 'Nanoscale variation in surface charge of synthetic hydroxyapatite detected by chemically and spatially specific high-resolution force spectroscopy', *Biomaterials*, **26**, 271–283.

Vasconcellos L M, Oliveira M V, Graça M L, Vasconcellos L G, Cairo C A and Carvalho Y R (2008) 'Design of dental implants, influence on the osteogenesis and fixation', *J Mater Sci Mater Med*, **19**, 2851–2857.

Vert M (2005) 'Aliphatic polyesters: great degradable polymers that cannot do everything', *Biomacromolecules*, **6**, 538–546.

Vormann J (2003) 'Magnesium: nutrition and metabolism', *Mol Aspects Med*, **24**(1–3), 27–37.

Witte F, Kaese V, Haferkamp H, Switzer E, Meyer-Lindenberg A, Wirth C J and Windhagen H, (2005) '*In vivo* corrosion of four magnesium alloys and the associated bone response', *Biomaterials*, **26**(17), 3557–3563.

Woyansky J S, Scott C E and Minnear W P (1992) 'Processing of porous ceramics', *Am Cers Soc Bull*, **71**, 1674–1682.

Xynos I D, Edgar A J, Buttery L D K, Hench L L and Polak J M (2001) 'Gene-expression profiling of human osteoblasts following treatment with the ionic products of Bioglass (R) 45S5 dissolution', *J Biomed Mater Res*, **55**(2), 151–157.

Xiong J Y, Li Y C, Hodgson P D and Wen C E (2008a) 'Influence of porosity on shape memory behaviour of porous TiNi shape memory alloy', *Funct Mater Lett*, **1**(3), 215–219.

Xiong J Y, Li Y C, Wang X J, Hodgson P D and Wen C E (2008b) 'Titanium-nickel shape memory alloy foams for bone tissue engineering', *J Mech Behav Biomed Mater*, **1**(3), 269–273.

Yang S, Leong K F, Du Z and Chua C K (2001) 'The design of scaffolds for use in tissue engineering. Part I. Traditional factors', *Tissue Eng*, **7**, 679–689.

Yannas I V (2004) 'Classes of materials used in medicine: natural materials', in Ratner B D, Hoffman A S, Schoen F J and Lemons J, *Biomaterials Science—An Introduction to Materials in Medicine*, San Diego, Calif, USA, Elsevier Academic Press, 127–136.

Yu X and Bellamkonda R V (2003) 'Tissue-Engineered scaffolds are effective alternatives to autografts for bridging peripheral nerve gaps', *Tissue Eng*, **9**(3), 421–430.

Yuan B, Chung C Y and Zhu M (2004) Microstructure and martensitic transformation behavior of porous NiTi shape memory alloy prepared by hot isostatic pressing processing', *Mater Sci Eng A*, **382**, 181–187.

Zhang E and Yang L (2008) 'Microstructure, mechanical properties and biocorrosion properties of Mg–Zn–Mn–Ca alloy for biomedical application', *Mater Sci and Eng A*, **497**, 1–2, 111–118.

Zelazny M, Richardson R and Ackland G J (2011), 'Twinning hierarchy, shape memory, and superelasticity demonstrated by molecular dynamics', *Phys Rev B*, **84**, 144113–1–144113–7.

Zhao Y, Taya M, Kang Y and Kawasaki A (2005) 'Compression behavior of porous NiTi shape memory alloy', *Acta Mater*, **53**, 337–343.

Zhu S L, Yang X J, Chen M F, Li C Y and Cui Z D (2008) 'Effect of porous NiTi alloy on bone formation: a comparative investigation with bulk NiTi alloy for 15 weeks *in vivo*', *Mater Sci Eng C*, **8**, 1271–1275.

Zyman Z, Ivanov I, Glushko V, Dedukh N and Malyshkina S (1998) 'Inorganic phase composition of remineralisation in porous CaP ceramics', *Biomaterials*, **19**, 1269–1273.

3

Optimal design and manufacture of biomedical foam pore structure for tissue engineering applications

A. SALERNO, Center for Advanced Biomaterials for Health Care (IIT@CRIB), Istituto Italiano di Tecnologia, Italy and P. A. NETTI, Interdisciplinary Research Centre on Biomaterials (CRIB), University of Naples Federico II and Istituto Italiano di Tecnologia, Italy

DOI: 10.1533/9780857097033.1.71

Abstract: To date, the scaffold-based approach represents one of the most promising tissue engineering strategies for the repair/regeneration of damaged biological tissue. The goals of this chapter are (1) to provide the reader with an overview of current approaches to design and manufacture tissue engineering scaffolds with highly structured pore architectures; and (2) to illustrate experimental and theoretical evidence which should be taken into account in designing the pore structure of the scaffolds to trigger appropriate *in vitro* cell responses and promote *in vivo* new tissue regeneration.

Key words: biomimetic, cell colonization, pore structure, scaffold, vascularization.

3.1 Introduction

Tissue engineering (TE) is a challenging and increasingly growing research field holding the promise to develop novel therapeutic treatments for organ and tissue loss or failure, which represent two major human health problems. The approach of TE is highly multidisciplinary, as it requires the integration of emerging knowledge in the physical and life sciences with frontier engineering and clinical medicine to learn how to trigger the regeneration of failed human organs and tissues (Stupp, 2005).

One of the most promising approaches in TE involves the combination of cells (such as stem cells, osteoblasts, chondrocytes and fibroblasts), scaffolds and molecular cues (Yang *et al*., 2001; Lutolf and Hubbell, 2005; Ma, 2008). The underlying concept of this approach is the belief that cells isolated from a patient can be expanded in a cell culture system and seeded

within a scaffold for successful tissue regeneration. In particular, the scaffold must be characterized by biophysical and biochemical properties suitable to promote and guide cell adhesion, migration, proliferation and extracellular matrix (ECM) deposition in three dimensions. The new tissue development is induced by maintaining the cell-seeded scaffold in appropriate bioreactors (*in vitro* strategy) before implantation into the patient, or grafted back directly into the patient to function as the introduced replacement tissue (*in vivo* strategy) (Hutmacher, 2001).

In both approaches, the scaffold plays a pivotal role in the new tissue regeneration process, enhancing the ability of cells to induce appropriate *in vitro* tissue regeneration and *in vivo* restoration of a diseased tissue function by providing all of the functions of the native ECM. This is because, as observed in natural tissues, cells act in synergy with the ECM. The cells in natural tissues are connected to the ECM which provides, for instance, three-dimensionality, direct cell-to-cell communications and multiple biophysical and biochemical stimuli for cell adhesion, migration, proliferation and differentiation (Lutolf and Hubbell, 2005).

The principles of biomimetic and bioactive scaffold design and fabrication are derived from the natural processes which they intend to imitate. When biological tissue is injured, the normal healing response is initiated through a cascade of complex events that include acute inflammation, the formation of granulation tissue and eventual scar formation. Then, in a natural situation of regeneration and healing of damaged tissues, cells release a macromolecular network (mainly composed of proteins and polysaccharides) that serves as provisional three-dimensional matrix for the regeneration process. The ECM provides the necessary initial biophysical and biochemical milieu which regulates the cascade of events underlining the process of tissue repair/regeneration.

The design and development of biomimetic and bioactive scaffolds for regenerative medicine have to consider, consequently, the need to fabricate scaffolds that are able to provide all of the complex functions of native ECM, regulating the cell/ECM cross-talking and, ultimately, new tissue repair/regeneration (Lutolf and Hubbell, 2005; Stupp, 2005; Ma, 2008).

Since Langer and co-worker pioneered the concept of reconstructing biological tissues by using cells transplanted on synthetic scaffolds in the early 1990s, research in the field of scaffold design and fabrication has evolved greatly. Indeed, based on the extensive knowledge accumulated on materials design and processing, as well as characterization of scaffold/cell interactions, researchers have identified some important requirements for the *in vitro* cell culture and *in vivo* implantation as guidance for restoring tissue function (Hutmacher, 2001). These include:

1. providing a physically and chemically bioactive surface to promote cell–material interactions and the biological recognition by the host

2. supporting the development of a three-dimensional tissue by providing a pore structure suitable for cell adhesion, proliferation, migration, differentiation and ECM deposition
3. inducing functional construct vascularization and development via the correct presentation of topological and biochemical cues
4. providing a mechanical function stimulating cell differentiation and biosynthesis, as well as ensuring a temporary support for growing tissue development.

Apart from the properties of the materials, mainly in terms of biocompatibility, biodegradation and bioactivity, the 3D architecture of the scaffold is very important when attempting to mimic the structure and functions of native ECM. Controlling cell behaviour and tissue regeneration by tailoring the scaffold's pore structure is consequently a critical step in the development of the next generation of bioactive TE scaffolds.

Several fabrication processes have been developed to imprint 3D porous structures within biocompatible and biodegradable materials as scaffolds for TE. Most of these techniques have been implemented taking into account the parameters that have been identified as crucial in influencing cell organization and tissue regeneration. Examples of these properties are surface-to-volume ratio, pore size distribution, and pore geometry and interconnection (Yang *et al.*, 2001; Guarino *et al.*, 2008; Salerno *et al.*, 2009a).

The goal of this chapter is to provide the reader knowledge of the current approaches and technologies to design and fabricate porous scaffolds for TE. Furthermore, special emphasis is devoted to describing the basic aspects and experimental evidence regarding the optimal design of the scaffold pore structure to induce appropriate *in vitro* cell responses and to guide *in vivo* new tissue regeneration.

3.2 Micro-structure of biomedical foams and processing techniques

Scaffold design and manufacturing are key steps in defining scaffolds with prescribed mechanical, mass-transport and surface characteristics that can be used to test initial hypotheses regarding *in vitro* cells culture and *in vivo* tissue regeneration models. Furthermore, design and manufacturing techniques must be used to translate scaffold-based TE from concept to, ultimately, potential clinical applications.

In natural tissues, cells and ECM are organized into three-dimensional structures from the sub-cellular to the tissue level. Consequently, to engineer functional tissues and organs successfully, the scaffolds have to be designed with a micro-architecture able to facilitate cell distribution and guide tissue regeneration in three dimensions (Lutolf and Hubbell, 2005; Guarino *et al.*,

2008). Furthermore, recent development in nano-technology have demonstrated that the presence of controlled nano-structures on the surface of biomaterials and scaffolds is essential to promote and guide cellular processes involved in new tissue regeneration, such as cell adhesion, migration and differentiation (Lim and Donahue, 2007; Ma, 2008; Wang *et al*., 2011).

A number of fabrication technologies have been applied to process biocompatible and biodegradable materials into three-dimensional porous scaffolds with controlled nano- to micro-structures, and to ultimately tailor the final biological response. By considering the wide range of biomaterials and processing techniques for scaffold design, this section will discuss the most relevant aspects related to the processing-pore structure relationships of the scaffolds prepared by some of the most used techniques.

There are different techniques that can conceivably be used to process biomaterials for porous scaffold development. Traditional TE scaffold design strategies employ a 'top-down' approach to generate three-dimensional pore structures within biocompatible and biodegradable materials. The porogen leaching technique is one of the most investigated. This technique is based on the use of porogen agents, typically micro-particles of sodium chloride, sugar, paraffin or gelatin, which are dispersed within the biomaterial by melt or solution mixing. Once the setting of the mixture has been obtained, the particles are selectively extracted, leaving a porous network (Thomson *et al*., 1996; Capes *et al*., 2005; Zhang *et al*., 2005; Guarino *et al*., 2008). The main advantages of particulate leaching are that the porosity of the scaffolds is directly correlated to the porogen concentration, while the pore size distribution and pore shape are dependent on the size distribution and shape of the particles, respectively. Most importantly, pore interconnectivity, which is a key scaffold design and manufacturing parameter, depends on the contact points between adjacent porogen particles which, in turn, is dependent on concentration, size and shape (Zhang *et al*., 2005). Although scaffolds prepared via the particulate leaching technique are basically satisfactory and widely used for several applications, it is rather difficult to achieve by this technique an independent and precise control over porosity and interconnectivity. Furthermore, the achievement of a highly interconnected porosity requires high porogen concentration, leading to a drastic reduction of the mechanical properties of the final scaffold.

The selective polymer extraction from a co-continuous blend is a technique that belongs to the class of the porogen leaching and has been proposed as a suitable alternative to overcome the intrinsic limitations of particulate porogens. This technique involves the melt processing of two or more immiscible polymers, followed by the selective dissolution of one or more phases to create the porous network (Washburn *et al*., 2002; Salerno *et al*., 2009b; Virgilio *et al*., 2010). As a final achievement, the scaffolds obtained by this approach evidenced tube-like and highly interconnected

porous networks, overall porosity that can be lowered down to 30% and, consequently, mechanical response that may be tailored in a wide range, spanning from soft to hard tissue regeneration requirements (Washburn *et al*., 2002; Salerno *et al*., 2009b).

Thermodynamic-based processing of polymeric solutions, such as phase separation and gas foaming, are also widely used for scaffold fabrication.

The phase separation technique involves the preparation of a homogeneous solution of the polymeric biomaterial within an appropriate solvent, such as dioxane and tetrahydrofuran. The solution is then brought into a thermodynamically unstable state by exposure to a non-solvent or by the decrease of the temperature down to a binodal solubility curve or down the crystallization temperature of the solvent. This step leads to the formation of a heterogeneous morphology characterized by polymer-rich and polymer-lean phases. Later, the removal of the solvent within the polymer-lean phase by solvent evaporation, sublimation or solvent/non-solvent exchange, allows achieving an interconnected porous network within the crystallized polymer-rich phase (Nam and Park, 1999; Guarino *et al*., 2008; Ma, 2008). The main advantage of this technique is that the pore structure of the scaffold can be adequately modulated at the micro-metric and nano-metric scales by controlling the thermodynamic and kinetic of the phase separation process. An interesting example is the fabrication of nano-fibrous scaffolds resembling the fibre structure of the native collagen (Ma, 2008). On the other hand, the use of organic solvents, potentially harmful to cells and biological tissues, and the difficulty of creating interconnected macro-pores of the order of several hundreds of microns, represent the most limiting aspects of this technique (Guarino *et al*., 2008).

Gas foaming has been proposed as a suitable alternative to overcome the above mentioned limitations for scaffold design. This technique is based on the high pressure solubilization of a non-toxic blowing agent, mainly CO_2, N_2 or a mixture of these gases, within a polymeric biomaterial. The system is then brought into a supersaturated state either by increasing temperature or by reducing pressure, with the consequent nucleation and growth of gas bubbles. Finally, the decrease of the temperature and the vitrification of the polymeric matrix stabilize the pore structure (Montjovent *et al*., 2005; Salerno *et al*., 2009a, 2010a, 2011a). The gas foaming technique allows fine control over the extension of the porous network of the scaffolds by the selection of the proper operating conditions, mainly the blowing agent type and concentration, foaming temperature and pressure drop profile. Furthermore, the absence of organic solvents may also allow for the simultaneous processing of biomaterials, cells and growth factors, aiming to produce bioactive porous scaffolds in a one step process (Hile *et al*., 2000; Ginty *et al*., 2006). Such limitations of gas foaming are the presence of

closed pores entrapped within the scaffold, as well as the difficulty of processing polar molecules and highly crystalline polymers at low temperature (Salerno *et al.*, 2011a, 2011b).

Solid free form fabrication techniques have been developed holding the promise of allowing simultaneous and independent control over crucial scaffold micro-structural features, mainly pore size distribution, pore interconnectivity and mechanical functionality (Sachlos and Czernuszka, 2003; Hollister, 2005). Furthermore, as compared to previously cited techniques, solid free form fabrication approaches allow for a more predictable and precise control of scaffold consistency, design reproducibility and complex internal architecture and macro-scale morphological features (Sachlos and Czernuszka, 2003; Hollister, 2005).

Rapid prototyping is a solid free form fabrication process which creates a three-dimensional object through repetitive deposition and processing of material layers. Each layer is constructed based on 2D cross-sectional data obtained from slicing a computer-aided design model of the object. Among rapid prototyping strategies, three-dimensional printing and fused deposition modelling are the most used.

Three-dimensional printing produces porous scaffolds by ink-jet printing a binder into sequential powder layers (Seitz *et al.*, 2005; Williams *et al.*, 2005). Firstly, a thin distribution of powder is spread over the surface of a powder bed. From a computer model of the part, and by using a technology similar to ink-jet printing, a binder material is ejected onto the powder where the object is to be formed. A piston is then lowered so that the next layer of powder can be spread and selectively bonded. This layer-by-layer process repeats until the scaffold is completed. The packing density of the powder particles has a profound impact on the results of the adhesive bonding, which in turn affects the topography and mechanical properties of the scaffold (Seitz *et al.*, 2005; Williams *et al.*, 2005).

In the fused deposition modelling approach, a thermoplastic polymer is loaded within a temperature-controlled extrusion head, where it is heated to a semi-liquid state. The head extrudes and deposits precisely the material in ultra-thin layers onto a base. After a layer is completed, the height of the extrusion head is increased and the subsequent layers are built to construct the scaffold (Zein *et al.*, 2002; Shor *et al.*, 2007).

Because of the computer controlled processing, scaffold fabrication by these techniques is highly reproducible in terms of scaffold geometry and internal architecture. Furthermore, porous scaffolds obtained by these approaches are characterized by 100% pore interconnectivity. Finally, a wide range of mechanical properties, spanning from soft to load-bearing applications, may be achieved depending on both material and geometrical parameters selection. The advance of these techniques in controlling scaffold properties is directed toward developing high resolution fabrication

tools able to achieve tight control of the composition, nano-structure and drug releasing capability of the scaffolds.

3.3 Improving control of scaffold pore structure by combined approaches

To date, various methods have been used for the preparation of porous scaffolds for biomedical applications, such as porogen leaching, phase separation, gas foaming and solid free form fabrication. Although these techniques have demonstrated great advantages over the control of scaffold property, namely volume-to-surface ratio, pore size distribution and interconnectivity, each one is characterized by intrinsic limitations. More specifically, several investigations on particulate leaching techniques reported the fabrication of scaffolds with intact pore walls with few interconnection points, due to the contact between adjacent particles in the polymer network (Guarino *et al.*, 2008). This is also one of the most important drawbacks for gas foamed scaffolds, where the presence of closed pores along the inner and the outer surfaces is remarkable (Salerno *et al.*, 2009a). On the other hand, by using only one of these techniques, it is very difficult to fabricate scaffolds with spatially controlled and multi-scaled pore distribution and nano- and micrometric pore feature resolution.

Advances in TE have revealed that scaffolds characterized by multi-scaled pore structures are very promising for the regeneration of complex three-dimensional tissues, such as bone and cartilage (Silva *et al.*, 2006; Guarino *et al.*, 2008; Salerno *et al.*, 2009c). Indeed, different pore scale structures at the micro-metric size range are useful to (1) appropriately control the three-dimensional localization of cells and support the correct deposition of the ECM, (2) promote the development of a functional network of capillaries for tissue vascularization, and (3) ensure the transport of fluid and oxygen necessary for cell survival and new tissue synthesis in three dimensions. It is also important to point out that controlled topographies, at both micro- and nano-metric scales, on the pore surface of a biomaterial scaffold are essential to promote the adsorption of proteins, to guide specific cell/scaffold interaction, and to stimulate cell migration, differentiation, phenotypic expression and the deposition of ECM (Ma, 2008; Wang *et al.*, 2011).

One of the most efficient approaches to design and fabricate porous scaffolds with multi-scaled pore structures is based on the appropriate combination of different processing techniques, each characterized by different nano- and/or micro-metric resolution of pore features. As an example, Fig. 3.1 shows the processing scheme that is usually used for the fabrication of highly interconnected porous scaffolds with multi-scaled pore structure by the combination of gas foaming and porogen leaching techniques (Salerno *et al.*, 2009a, 2011c).

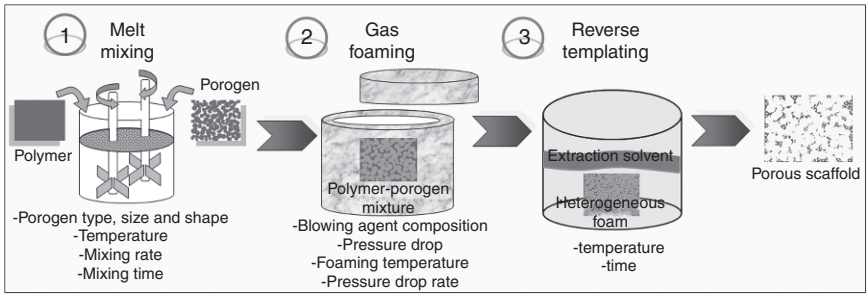

3.1 Scheme of the combined approach based on gas foaming and porogen leaching suitable for the design and fabrication of multi-scaled porous scaffolds for TE. (*Source*: From Salerno *et al.,* 2009a.)

The gas foaming/porogen leaching combined process involves the mixing of the biomaterial with the porogens, typically sodium chloride or gelatin particles (Step 1) followed by the foaming of the polymer/particles system (Step 2). Once the foaming step is completed, the selective removal of the porogen agent from the foamed matrix allows the achievement of the final multi-scaled pore structure.

The microstructure of the scaffolds that can be designed and fabricated with this combined technique strongly depends on several factors, related to the materials and the processes involved. For instance, in the case of the use of NaCl particles as porogens, the macro-porosity is controlled by selecting the NaCl concentration and size, usually in the range of 85–95 wt.% and 100–500 μm, respectively. Furthermore, the micro-porosity depends on the nucleation and growth of gas bubbles within the polymeric phase during the gas foaming process, in turn affected by the blowing agent composition and porogen concentration (Salerno *et al*., 2011c).

Figure 3.2a and 3.2b report scanning microscope images of porous polycaprolactone scaffolds prepared by using 90% of 300–500 μm size NaCl particles, with or without the foaming step. As shown in Fig. 3.2a, scaffolds prepared by using NaCl particles as templating agent are usually characterized by a mono-modal distribution of cubic-shaped pores and intact pore walls. On the other hand, by the foaming of the PCL/NaCl mixture before NaCl leaching, porous scaffolds with multi-scaled micro-metric pore size distributions and improved interconnectivity can be fabricated (Fig. 3.2b). These scaffolds are characterized by cubic-shaped macro-pores created by means of NaCl leaching, and rounded open micro-pores, of the order of ten microns, uniformly distributed through the macro-pore walls. Furthermore, depending on the desired application, by controlling the weight fraction of NaCl and the composition of the blowing agent mixture, different macro-porosity/micro-porosity fractions and micro-porosity dimensions may be

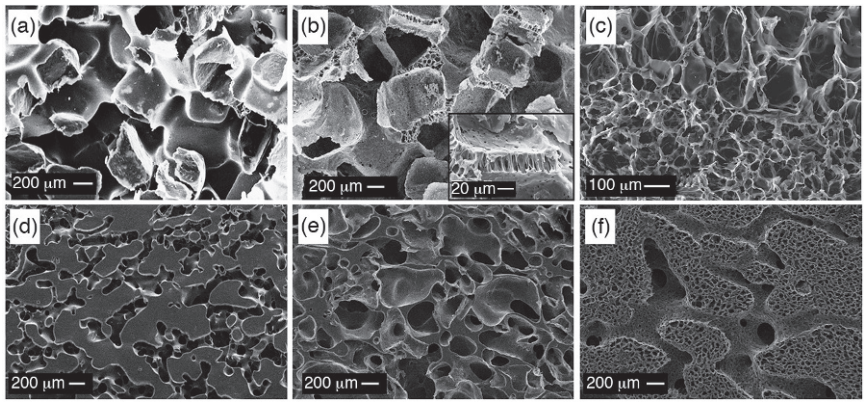

3.2 Morphology of porous polycaprolactone scaffolds fabricated by the combination of the techniques of gas foaming and porogen leaching: (a) mono-modal scaffold obtained by the selective dissolution of 300–500 μm NaCl particles from a 10/90 polymer/NaCl mixture; (b) bi-modal scaffold obtained by combining gas foaming and 300–500 μm NaCl particles leaching; (c) graded scaffold produced by foaming a polymeric composite with a stepwise gradient of micronized NaCl particles distribution; (d) mono-modal scaffold obtained by the selective polymer extraction from a co-continuous blend; (e) mono-modal and (f) bi-modal scaffolds obtained by combining gas foaming and selective polymer extraction. (*Source*: Adapted from Salerno *et al.*, 2008, 2009b, 2009c, 2010, 2012.)

acquired (Salerno *et al.*, 2011c). It is a matter of fact that the addition of micron-sized fillers to a polymer melt influences its flow properties. Several factors, such as particle size and shape, filler content and interactions between the phases, have complex influences on the viscoelastic behaviour of the composite. The foamability of a polymeric material is strongly affected by its flow behaviour, which then requires performing rheological investigations upon the polymer/filler composites in order to optimize the final scaffolds pore structure (Salerno *et al.*, 2008). Indeed, a decrease of the micro-porosity of the scaffolds is typically observed with increase of the NaCl concentration. This effect is ascribable to the decrease of the polymer amount and to the increase of the stiffness of the system with the NaCl concentration which, in turn, restricts the growth of the pores inside the polymeric matrix. As a direct consequence, high foaming temperatures and more plasticizing blowing agents are often required to produce appropriate micro-porosity fractions at high porogen concentrations (Salerno *et al.*, 2011c).

The possibility of preparing highly interconnected scaffolds with well-controlled anisotropic architectures is also highly desirable in designing TE scaffolds (Salerno *et al.*, 2008, 2012b; Harley *et al.*, 2010). Scaffolds

characterized by gradients of porosity and pore size offer the great advantage of reproducing the spatial organization of cells and extracellular matrix of highly complex three-dimensional tissues, such as bone and cartilage (Harley *et al*., 2010). The combination of gas foaming and NaCl leaching may also offer the possibility of designing and fabricating graded biomimetic scaffolds for osteochondral TE. Indeed, as previously discussed, the foaming behaviour of polymer/NaCl micro-composites is strictly correlated to the concentration of the inorganic filler; higher filler concentrations resulted in lower foaming. Consequently, by creation of a composite with a gradient of NaCl micro-particles concentration, it is possible to produce scaffolds with anisotropic pore structures. In Fig. 3.2c the morphology of a porous polycaprolactone scaffolds with a stepwise gradient of porosity 91–83% and pore size 71–24 μm (Salerno *et al*., 2008) is reported. This scaffold has been obtained by gas foaming of a PCL/NaCl composite with a 60/30% stepwise NaCl concentration gradient. To produce this type of scaffold, micronized 5 μm NaCl particles have been used as particulate porogen and CO_2 as blowing agent. The biomimetic character of this scaffold for osteochondral defect treatment may be also improved by the selective incorporation of bioactive fillers, such as hydroxyapatite particles, within the scaffold (Salerno *et al*., 2012b).

As shown in Fig. 3.2d–3.2f, completely different scaffold pore structures may be achieved by combining gas foaming and selective polymer extraction techniques. In particular, by using a continuous porogen agent, the formation of open macro-porous polymeric scaffolds, characterized by networks of elongated pores, is possible (Washburn *et al*., 2002; Salerno *et al*., 2009b). The scaffolds obtainable by this approach have shown low porosity fractions, in the range of 30–60%, mono-modal pore size distribution and full interconnectivity (Fig. 3.2d). Furthermore, as shown in Fig. 3.2e and 3.2f, by combining gas foaming and selective polymer extraction techniques, mono-modal or bi-modal porous scaffolds with completely different pore structures are achievable. These scaffolds have been fabricated by foaming a co-continuous blend of polycaprolactone and thermoplastic gelatin, a thermoplastic polymer prepared by mixing gelatin powder and glycerol, and selecting different foaming temperatures. In particular, by performing foaming at a temperature of 70°C, higher than polycaprolactone melting point, a mono-modal scaffold may be obtained because of the foaming and collapse of polycaprolactone at the interface with gelatin (Fig. 3.2e). Conversely, by performing the foaming step at 44°C, below the melting temperature of polycaprolactone, a homogeneous and highly open porosity is formed, because of the ability of the polymer to crystallize and stabilize its pore structure. As a direct consequence, after the leaching of the gelatin it was possible to fabricate polycaprolactone scaffolds with a bi-modal pore size distribution of

elongated macro-pores inside a micro-porous structure (Fig. 3.2f) (Salerno *et al.*, 2009b, 2009c, 2012). As described in the following paragraph, this multi-scaled pore structure may be very interesting in order to improve the three-dimensional colonization of cells and, concomitantly, ensure an adequate transport of fluids, as nutrients and metabolic wastes, through the entire cell/scaffold construct.

The ability of a porous scaffold to provide needed mechanical support is a critical issue. In general, proper tissue regeneration requires sufficient mechanical strength to maintain integrity until the new tissue regenerates. This biomechanical support is necessary *in vitro* to allow for adequate cell ingrowth and fluid transport, and to give the cells proper biomechanical cues they would normally receive in their native environment. Indeed, biomechanical cues are able to control the arrangement of cell cytoskeleton, affecting cell shape and structure and, ultimately, guiding important processes involved in new tissue morphogenesis, such as cell adhesion and migration. Furthermore, this crosstalk is mutual, as cells can also modify the mechanical properties of the biomaterial. It is important to consider that, when seeded within porous scaffolds with pore sizes larger than the cell size, the mechanical stimulus transmitted to the cell mainly depends on the individual scaffold strut where the cell is attached and not on the stiffness of the entire scaffold network. For example, Levy-Mishali and co-workers (2009) have recently demonstrated that, when cultured within 3D polylactic acid/polylactic-co-glycolic acid porous scaffolds of varied elasticity, myoblast cells evidenced different organization, myotube formation and cell viability. This effect was also dependent on the different scaffold shrinkage and pore area reduction by cell forces.

In the case of scaffolds for *in vivo* implantation, the biomechanical functionality must also provide a secure and stable fixation on or to the host tissue, and support physiological loadings which naturally occur in the body (Leong *et al.*, 2008). In designing the biomechanical properties of a porous scaffold, it must be also taken into account that scaffold degradation progressively induces a decrease of the mechanical functionality and, therefore, degradation must be tailored to match the rate of new tissue growth until the regenerated tissue provides sufficient load-bearing support and stress dissipation (Hutmacher, 2001).

The mechanical properties of porous scaffolds not only depend on the constituent material, but are also directly correlated to micro-structural features, mainly porosity and pore size distribution. In particular, a high porosity fraction, which is often desirable to facilitate cell infiltration and tissue ingrowths, results in a reduction in mechanical properties. A similar trend is also achieved with the increase of the mean pore size, because of the enhance tendency of pore wall bending and structure instability during compression.

Regarding multi-scale scaffold fabrication preparation, the optimal selection between micro-particulate porogens and continuous porogens is also related to the mechanical properties required for each specific application. Indeed, scaffolds prepared using particulate porogens are of high porosity, of the order of 90%, and then have limited capability to sustain mechanical stress during *in vivo* load-bearing applications. This aspect is very critical, especially when using soft polymeric biomaterials, because of their intrinsic low stiffness. Conversely, the lower porosity obtainable by using continuous porogens may result in scaffolds with a higher mechanical response. This aspect is clearly shown in Fig. 3.3, which shows the stress vs. strain curves obtained by static compression test performed on bi-modal scaffolds prepared by using different types of porogens. It can be observed that the scaffold prepared by using NaCl micro-particles is characterized by the typical stress vs. strain curve of highly porous materials, with a linear-elastic region followed by a plateau of roughly constant stress leading into a final region of steeply rising stress (Salerno *et al.*, 2009a). Conversely, the bi-modal scaffold prepared starting from a co-continuous blend of polycaprolactone and gelatin is characterized by higher stress values throughout the deformation range, with no evidence of the plateau region. As shown in the inset of Fig. 3.3, the enhanced mechanical properties of this scaffold may allow achieving one order of magnitude higher elastic modulus (E) values, from 1 to 11.4 MPa. The mechanical response of this scaffold, characterized by E values higher than 10 MPa, may ensure sufficient temporary mechanical

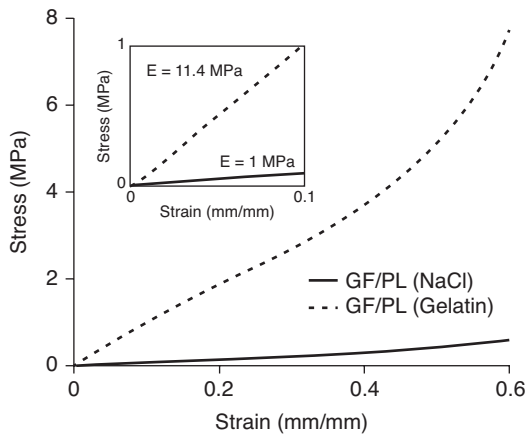

3.3 Comparison of the stress vs. strain curves obtained by static compressive tests of bi-modal porous polycaprolactone scaffolds prepared by using a micro-particulate (NaCl) or a continuous (gelatin) porogen. The inset shows the elastic region of the stress versus strain curves of the scaffolds and correspondent elastic compressive moduli. (*Source*: Adapted from Salerno *et al.,* 2009a.)

support to withstand *in vivo* stresses and loading and to avoid excessive new tissue deformation (Hollister, 2005).

The research in the field of the design and fabrication of porous scaffolds with complex multi-scaled pore structure is continuously growing, and numerous combinations of processing techniques have been reported. Such examples are the use of particulate leaching combined with solid free form fabrication to design polylactic-co-glycolic scaffolds with a highly ordered and orientated macro-porosity and micro-porous struts (Taboas *et al.*, 2003). Recent work has also investigated the fabrication of multi-scaled scaffolds with nano-structured pore surfaces, by combining phase separation with porogen leaching or gas foaming (Ma, 2008; Reverchon *et al.*, 2008; Wang *et al.*, 2011). Because of the simultaneous presence of a macro-porous network for cell colonization and a nano-fibrous pore wall topography which may mimic the collagen fibres of the native biological tissues, these scaffolds have been investigated for several applications, including bone and cartilage regeneration. Along the same research line, porous scaffolds with an interconnected macro-porosity to promote cell colonization and proliferation, and an interwoven nano-fibrous network to improve cell entrapment and differentiation, have been obtained by combining electrospinning with leaching of particulate porogens, such as NaCl and ice crystal templating, (Kim *et al.*, 2008; Leong *et al.*, 2009), or by integrating electrospinning and solid free form fabrication processes (Park *et al.*, 2008).

3.4 Pore structure versus *in vitro* cell culture

The *in vitro* culture of cells within porous scaffolds is an important step in the understanding of the cell/scaffold interaction and in characterizing the effect of the scaffold properties on its biological response *in vivo*. This approach involves the use of appropriate seeding and culture conditions to allow for cell/scaffold construct development and maturation. Concerning the actual techniques in cell culture, the stimulation of cellular proliferation and the formation of two-dimensional sheet tissues such as skin are widely performed and generally allow obtaining an implantable and functional tissue for clinical applications. The process becomes more complex for the formation of organized three-dimensional tissues for which it is necessary to culture cells within porous scaffolds. Indeed, in this case, the issues of cell distribution and ECM deposition in three dimensions, as well as nutrient transport within the cell/scaffold construct and during the entire new tissue development, are extremely important (Karande *et al.*, 2004).

Depending on the specific application, scaffolds can be fabricated from different materials; they must also possess some essential characteristics, including biocompatibility, and certain physical, mechanical, chemical and structural/architectural properties (Hollister, 2005). Architectural features,

namely pore size and shape, surface-to-volume ratio, pore wall morphology and pore interconnectivity are probably the most critical parameters, as these have been shown to directly impact cell seeding, cell migration, tissue differentiation, transport of oxygen, nutrients and wastes, and new tissue formation in three dimensions (Karande *et al*., 2004; Pamula *et al*., 2008; Lien *et al*., 2009; Jeong and Hollister, 2010; Salerno *et al*., 2010b).

The first important aspect in designing the architectural properties of porous scaffolds for *in vitro* cell culture is that the diameter of cells in suspension dictates the minimum scaffold pore size, which varies from one cell type to another (Ranucci *et al*., 2000; Yang *et al*., 2001).

As summarized in Table 3.1, the investigation of optimal scaffold microarchitecture for different *in vitro* culture models has also found a direct correlation between pore size distribution and cell adhesion, morphogenesis, proliferation and differentiation.

Regarding scaffolds for bone TE, Pamula and co-workers (2008) have studied the effect of the mean pore size of poly(L-lactide-co-glycolide) scaffolds, in the range from 40 to 600 μm, on the adhesion and colonization of osteoblast-like MG 63 cells in a conventional static culture system. The results of their study indicated that the higher surface of the 200 and 600 μm pores enhanced cell infiltration and allowed a more uniform cell distribution in the interior of the pore structure. Conversely, the scaffolds with 40 μm mean pore size allowed cell colonization prevalently on the seeding surface, therefore resulting in an inhomogeneous cell/scaffold construct.

Although several studies report static cell cultures within porous scaffolds, in this case transport issues in three dimensions are very difficult to achieve, especially at long culture times and when cell proliferation and ECM deposition start to occlude scaffold pores. Overcoming this limitation may be possible with a dynamic environment, which can be obtained by the use of a bioreactor (McCoy *et al*., 2012). The bioreactor (1) must provide control over the initial cell distribution, (2) must ensure efficient and continuous transport of fluid, such as oxygen, nutrient and metabolic waste, as well as regulatory factors to tissue-engineered constructs and, ultimately, (3) must expose the developing constructs to controlled mechanical stimuli. Bioreactors provide the ideal means to study in detail the effect of culture parameters, namely nutrient supply and mechanical stimuli, in combination with scaffold pore structure on tissue growth and development.

In dynamic culture conditions, optimal growth of a tissue *in vitro* not only depends on the appropriate scaffold pore structure, but is also correlated to the culture parameters. Then, in the design of TE scaffolds, parameters including pore size, shape and interconnectivity, mechanical and transport properties should be optimized concomitantly to perfusion conditions in order to maximize fluid diffusion and cell stimulation for a successful inducement of tissue ingrowth.

Table 3.1 Overview of the optimal scaffolds pore size for different TE applications

Application	Cell type	Pore size (μm)	Material scaffold	Fabrication technique	Comments	Reference
Cartilage	Chondrocytes	900	Polycaprolactone Polyglycerolsebacate Polyoctanediol-co-citrate	Solid free form	Polyoctanediol-co-citrate scaffold resulted in better results	Jeong and Hollister, 2010
	Chondrocytes	400	Collagen	Porogen leaching	Pore size tested: 180, 400 or 720 μm	Lu *et al.*, 2010
	Chondrocytes	70–120	Chitosan	Freeze-drying	Pore size tested: < 10 μm, 10–50 μm and 70–120 μm	Griffon *et al.*, 2006
	Chondrocytes	250–350; 350–500	Gelatin	Freeze-drying	Pore size tested: 50–150, 100–200, 250–350 and 350–500 μm	Lien *et al.*, 2009
	Chondrocytes	400	Hyaluronic acid coated chitosan	Woven fibres	Pore size tested: 100, 200 and 400 μm	Yamane *et al.*, 2007
	Adipose stem cells	370–400	Polycaprolactone	Centrifugation/ freeze-drying	Pore size tested: from 90 to 400 μm	Oh, 2010
	MC3T3-E1 mouse cells	95.9	Collagen-Glycosaminoglycans copolymer	Freeze-drying	Pore size tested: from 95.9 to 150.5 μm	O'Brien *et al.*, 2005
Bone	Mesenchymal stem cells	112–224; 400–500	Silk fibroin	Porogen leaching	Static and dynamic culture conditions	Hoffmann *et al.*, 2007
	Mesenchymal stem cells	200	Coralline hydroxyapatite	Hydrothermal treatment	Pore size tested: 200 and 500 μm	Mygind, 2007
	Human foetal osteoblasts	330	Polylactic-co-glycolic acid	Porogen leaching	Pore size tested: 100, 200 and 330 μm	Cuddihy and Kotov, 2008
	MG63 human osteoblasts	600	Polylactic-co-glycolic acid	Porogen leaching	Pore size tested: 40, 200 and 600 μm	Pamula, 2008

(*Continued*)

Table 3.1 (*Continued*)

Application	Cell type	Pore size (μm)	Material scaffold	Fabrication technique	Comments	Reference
	Calvarial osteoblasts	150–300; 500–710	Polylactic-co-glycolic acid	Porogen leaching	Similar results among the scaffolds tested	Ishaug-Riley *et al.*, 1998
	Primary rat osteoblasts	100	High internal phase emulsion polymer (PolyHIPE polymer)	Emulsion polymerization	Pore size tested: 40, 60 and 100 μm	Akay *et al.*, 2004
	Human primary osteoblasts	400	Polylactic acid Polylactic acid composites	Gas foaming	Improved response of composite scaffolds	Montjovent *et al.*, 2005
Liver	Hepatocytes	82	Collagen	Freeze-drying	Pore size tested: 10, 18 and 82 μm.	Ranucci *et al.*, 2000
	Hepatocytes	100	Chitosan-gelatin	Rapid prototyping	Freeze-dried scaffold was used as control	Jiankang *et al.*, 2009
Muscle	Myogenic cell line C2C12	20–50	Collagen	Freeze-drying	Parallel orientated pores to guide myotubes alignment	Koehne, 2008
	Cardiac cells	100	Alginate	Freeze-drying	Scaffolds functionalized with adhesion peptide and heparin	Sapir *et al.*, 2011
Blood vessel	Human smooth muscle cells	110	Poly(trimethylene carbonate)	Porogen leaching	Tubular scaffold with a central channel	Song *et al.*, 2010
	Vascular smooth muscle cells	50–100	Poly(L-lactide-co-caprolactone)	Porogen leaching	Tubular scaffold with a central channel	Park *et al.*, 2009

Mygind and co-workers (2007) cultured mesenchymal stem cells up to 21 days within coralline hydroxyapatite scaffolds with pore sizes of 200 and 500 μm, and compared cell colonization and osteogenic differentiation in static and dynamic culture conditions. As a result, these authors found that 200 μm pore scaffolds exhibited a faster rate of osteogenic differentiation. Conversely, the 500 μm pore scaffolds increased cell proliferation and accommodated a higher number of cells. Furthermore, compared to static cultures, dynamic culture conditions enhanced the proliferation, differentiation and distribution of cells in both scaffolds, finally indicating that scaffold pore structure act in synergy with culture conditions during cell culture and new tissue formation.

Over recent years, computational analysis has held great promise to allow finding the optimal scaffold and culture conditions for *in vitro* bone tissue regeneration, avoiding the use of highly expensive clinical experiments. Furthermore, this modelling approach may allow for a clearer interpretation and understanding of the biological mechanisms involved in new tissue genesis and growth aided by the scaffolds. Along this direction, Melchels and co-workers (2011) used computational fluid dynamic simulations to demonstrate the ability of the pore structure to transfer hydrodynamic forces during *in vitro* perfusion culture and to find the optimal flow rate conditions to improve cell adhesion and colonization. Two scaffold types, both with gyroid pore architectures, were designed and built by stereolithography: one with isotropic pore size (412 ± 13 μm) and porosity (62 ± 1%), and another with a gradient in pore size (250–500 μm) and porosity (35–85%). Computational fluid flow modelling showed the highest densities of cells correlated with regions of the scaffolds where the pores were larger, and the fluid velocities and wall shear rates were the highest. Under the applied perfusion conditions, cell deposition is mainly determined by local wall shear stress, which, in turn, is strongly influenced by the architecture of the pore network of the scaffold. Similar work has been also reported by Guarino and co-workers (2012), which compared experimental and theoretical mesenchymal stem cell culture parameters, aiming to find the optimal conditions to improve stem cell differentiation within porous polycaprolactone scaffolds. As predicted by computational simulation model, the authors verified that, when cultured within their scaffolds, a perfusion rate of 0.05 mL/min is the optimum to stimulate stem cell differentiation. Finally, all these results demonstrate the potential advantages of combining computational approaches and experimental culture models for optimal *in vitro* cell culture within porous scaffolds.

As reported in Table 3.1, great effort has been directed in the search for the optimal scaffold pore structure for a large variety of applications, such as the regeneration of bone, cartilage, liver, muscle and blood vessels. Regarding

scaffolds for cartilage regeneration, Lien and co-workers (2009) cultured chondrocytes within gelatin scaffolds with pores in the range of 50–600 μm, and observed that cells infiltrated and proliferated within the pore structure of all of the scaffolds up to 3 weeks of *in vitro* culture. However, as the pores became larger, the rate of cell growth and the amount of glycosaminoglycans as well as collagen Types I, II and X increased. Furthermore, the chondrocytes in the smaller pores often showed a dedifferentiated form, while the phenotype of the cells was maintained better in larger pores. The authors finally concluded that chondrocytes prefer the group of scaffolds with pore size between 250 and 500 μm for better proliferation and ECM production, demonstrating that the size of the space for cell growth is a key factor for cell metabolism. The results of Lien and co-workers have been also confirmed by those reported by Oh and co-workers (2010) for chondrocytes cultured within polycaprolactone scaffolds. In particular, in their work the authors fabricated polycaprolactone scaffolds characterized by gradually increasing pore size, from 90 to 400 μm, along the longitudinal direction by centrifugation and thermal fibril-bonding process. Although it could be expected that different scaffold biomaterials may require different pore size distribution for optimal chondrocytes culture, as previously reported for gelatin scaffold, the polycaprolactone scaffold section having a pore size range of 370–400 μm was found to be better for chondrogenic differentiation than other pore size groups.

Several reviews also indicate that, besides mean pore size, the pore size distribution and pore shape are also important architectural scaffold parameters in determining the *in vitro* biological outcomes (Silva *et al*., 2006; Koehne, 2008; Lu, 2010; Salerno *et al*., 2010b). Recent studies have reported the incorporation of aligned channels into the general porous structure of the scaffold enhanced cell, and subsequent tissue formation throughout the scaffold. This has been demonstrated using combined fabrication methods such as porogen templating and gas foaming (Silva *et al*., 2006; Salerno *et al*., 2010b), freeze-drying and ice particulate templating (Lu *et al*., 2010) as well as by unidirectional freezing process (Koehne, 2008). Indeed, compared to scaffolds with random porosity, those with the aligned pores evidenced improved cell colonization and infiltration as well as deposition of the ECM into the interior (Silva *et al*., 2006; Salerno *et al*., 2010b). This effect is related to the fact that, during seeding, the aligned pores improved the diffusion of cell suspension inside the interior of the scaffolds and, consequently, a more uniform cell adhesion and proliferation can be achieved. Confocal microscopic observation of the cell/scaffold construct allowed comparison of the colonization/infiltration of mesenchymal stem cells when statically seeded within polycaprolactone scaffolds with mono-modal or bi-modal pore size distribution. As shown in Fig. 3.4a, up to 90% of cells inoculated within the mono-modal scaffold adhered to the region close to the seeding

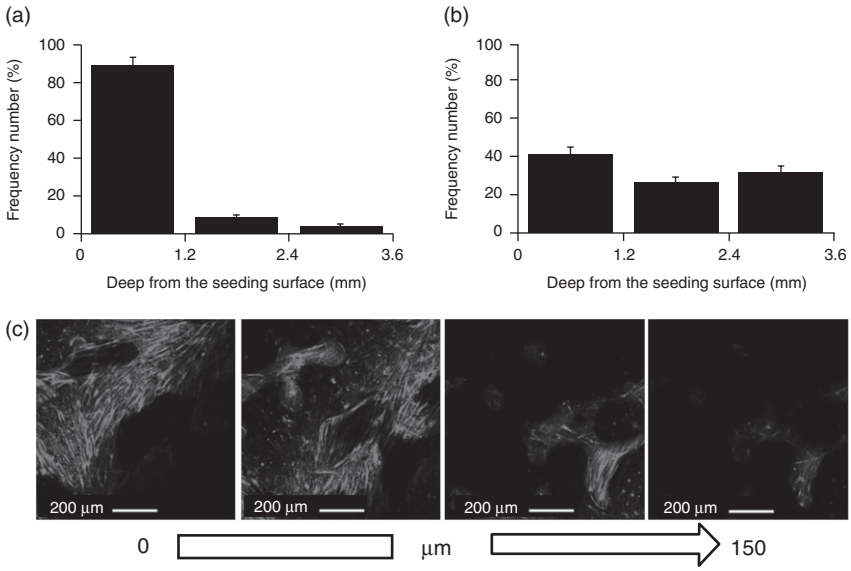

3.4 Effect of scaffold pore structure on mesenchymal stem cells adhesion and infiltration *in vitro*: cell infiltration at day 1 within (a) mono-modal and (b) bi-modal polycaprolactone scaffold; (c) cell distribution within the large, elongated macro-pores of the bi-modal polycaprolactone scaffold. (*Source*: Adapted from Salerno *et al.*, 2010b.)

surface. Conversely, an almost uniform cell infiltration was obtained along the depth of the scaffold when both random and elongated pores were present (Fig. 3.4b). As previously discussed, this effect can be explained by considering the ability of the elongated macro-pores to accommodate larger volumes of fluid compared to the rounded micro-pores and, therefore, allowing a faster drainage of the cell seeding suspension into the interior (Salerno *et al.*, 2010b). As a direct consequence, stem cell colonization and proliferation occurred preferentially within the macro-pores of the scaffolds (Fig. 3.4c).

The effect of the pore structure on cell adhesion and infiltration also had a direct impact on the rate of cell proliferation and osteogenic differentiation. In particular, it was observable that cells cultured within the mono-modal scaffold proliferated quickly in the first two weeks of culture (Fig. 3.5a), preferentially on the seeding surface. A marked decrease in the number of viable cells in the third week of culture was obtained for the mono-modal scaffold, because of the occlusion of the pores on the seeding surface and cell death and detachment at high culture times. Conversely, the number of viable cells within the bi-modal scaffold increased up to three times from day 1 to day 21, and cell proliferation occurred within the entire construct.

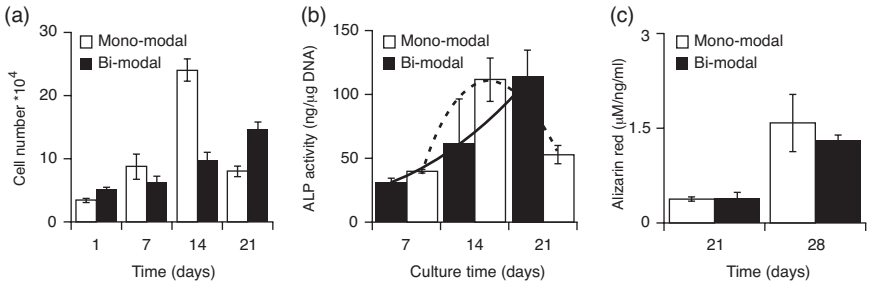

3.5 Effect of polycaprolactone scaffold pore structure on mesenchymal stem cells (a) proliferation, (b) differentiation and (c) calcium deposition.

The different pore structure of the mono-modal and bi-modal scaffolds also affected mesenchymal stem cell differentiation. In particular, the alkaline phosphatase activity, which is an early osteogenic differentiation marker, of cells cultured within mono-modal polycaprolactone scaffold, had a maximum at 14 days, followed by a decrease at later culture times (Fig. 3.5b). Conversely, the alkaline phosphatase activity of cells cultured within the bi-modal scaffold progressively increased up to four times from day 7 to 21 of culture. This is because cells on the seeding surface were exposed directly to the osteogenic medium and then, for the mono-modal scaffold cells, expressed earlier differentiation markers. A higher osteogenic differentiation was conversely obtained for cells cultured within the bi-modal scaffold. Similar amounts of deposited Ca^{2+} were quantified for both scaffold types up to 28 days (Fig. 3.5c), even if the more homogeneous cell organization within the bi-modal scaffold may allow us to speculate about its ability to induce a more homogeneous ECM deposition in three dimensions.

As discussed in the previous section, with the advent of solid free form fabrication techniques it has been also possible to design and fabricate porous scaffolds with highly sophisticated architectures and highly complex internal and external geometries. These scaffolds have been then used over recent years to test accurately the effect of parameters such as pore geometry and uniformity on cell behaviour.

The effect of pore size and channel geometry of 3D porous scaffolds on the osteogenic signal expression and subsequent differentiation of a transplanted cell population have been studied by Kim and co-workers (Kim *et al*., 2011). In particular, the authors cultured mesenchymal stem cells within porous photocrosslinked poly(propylene fumarate) scaffolds with random and highly ordered architectures fabricated by means of porogen leaching and stereolithography, respectively. Results showed that cells cultured within stereolithographic scaffolds with highly permeable and porous channels have significantly higher expression of fibroblast growth

factor, transforming growth factor and vascular endothelial growth factor than those cultured within the porogen leaching scaffold. Subsequent alkaline phosphatase activity expression and osteopontin secretion had also significantly increased in stereolithographic scaffolds, because of the continuous open channel geometry and a more favourable environment to facilitate early osteogenic signal expression and subsequent osteoblastic differentiation.

By means of solid free form fabrication Van Bael and co-workers (2012) fabricated titanium scaffolds with varying pore shape, more specifically triangular, hexagonal and rectangular, and two different pore sizes, 500 and 1000 μm, respectively. The scaffolds were obtained through selective laser melting and were used to test the effect of pore size and geometry on cell adhesion, growth and differentiation *in vitro*. Interestingly, it was observed that cell growth was affected by pore size but not pore shape. Conversely, the higher values of alkaline phosphatase activity of cell cultured within titanium scaffolds with 500 μm triangular pores demonstrated that cell differentiation was dependent on the synergistic effect of pore shape and size. In particular, as also previously discussed, the authors ascribed this effect to the dense cell distribution in the corners of the pores of this scaffold as induced by the different penetration of the seeding suspension.

Mimicking nano-scale topography of natural ECM is also advantageous for the successful *in vitro* cell culture. Indeed, most components of the natural ECM, such as collagen and hydroxyapatite, have structural features in the nano-metre dimensions, and the organization of cells and the corresponding tissue properties is highly dependent on the architecture of the ECM. Nano-fibrous polylactic acid scaffolds were fabricated to emulate the architecture of collagen fibres, demonstrating superior biological properties if compared to solid-wall scaffolds (Ma, 2008; Wang *et al*., 2011). For instance, Wang and co-workers (2011) optimized the phase separation of a polylactic acid solution in dioxane/methanol mixture solvent and containing gelatin micro-spheres, to fabricate macro-porous scaffolds with solid-walled or nano-fibrous architecture. Human dental pulp stem cells have then been cultured within the two scaffolds to investigate the role of pore wall structure on cell odontogenic differentiation. Compared to the solid-walled scaffold, the nano-fibrous scaffold enhanced the *in vitro* attachment and proliferation of stem cells and also improved alkaline phosphatase activity, calcium deposition and expression of genes such as collagen I, osteocalcin and dentin sialophosphoprotein. Among the factors that might explain the observed results, the greater adsorption of cell adhesion proteins, such as fibronectin, on the nano-fibrous scaffold has been indicated as the predominant one. Indeed, in dentin tissue, fibronectin enhances the differentiation of odontoblasts and dentine formation and, may also serve as a reservoir of growth factors, which participated in the differentiation of odontoblasts.

3.5 Pore structure vs. *in vivo* new tissue regeneration

Although many TE scaffold-based investigations currently focus on developing techniques appropriate for synthesis of tissues and organs *in vitro*, such scaffolds must eventually be implanted in the appropriate host site to promote tissue repair/regeneration.

In vivo regeneration of injured or excised tissue by a scaffold-based approach can be idealized as a process taking place within a bioreactor (the organism) with its complex biological mechanisms. The scaffold must be able to block wound contraction and scar tissue formation which occur after the surgical implantation procedure, while inducing regeneration of physiological tissue by the host.

To date, the goal of achieving *in vivo* scaffold-induced regeneration for a variety of tissues and organs, such as bone, cartilage and nerve, remains at the forefront of current TE investigations. In clinical settings, the nature of the wounds typically varies on a case-by-case basis, making it more difficult to understand the applicability of each treatment methodology to the range of injuries encountered, compared to *in vitro* evidence. This aspect, coupled with the wide range of materials and processing techniques for scaffold fabrication, is probably mainly responsible for the difficulty of defining the optimal pore structure properties for each specific tissue. It is therefore critical to standardize the wound site where *in vivo* studies are performed to ensure the presence of a consistent anatomical and physicochemical environment.

As discussed in the previous section, pore structure is an essential consideration for the design and fabrication of scaffolds for TE. As for *in vitro* cell culture, pores must be sufficiently interconnected to allow for cell growth, migration and nutrient flow *in vivo*. If pores are too small, cell migration and surrounding tissue infiltration are limited, resulting in the formation of a cellular capsule around the edges of the scaffold. This, in turn, can limit diffusion of nutrients and removal of waste, resulting in necrotic regions within the construct (Karande *et al*., 2004; Cao *et al*., 2006; Jones *et al*., 2009; Jeong *et al*., 2011). After implantation of tissue constructs, the transplanted cells' survival, as well as that of the native host cells that migrate into the scaffold, will depend on the transport of nutrients and waste products between cells and host tissue. Fluids transport in the first stage is exclusively carried out by diffusion processes that can supply the cells with nutrients only at a small distance, typically lower than 200 μm from the nearest capillary in the surrounding tissue. Consequently, the transplanted cells in central area of the scaffold frequently either fail to engraft, or die rapidly due to oxygen deficiency, lack of nutrient and inadequate removal of waste products. So, it is very important for implanted tissue-engineered constructs, especially larger implants, to develop sufficient vasculature rapidly *in vivo*.

To investigate the effect of the pore structure parameters on scaffold vascularization, Bai and co-workers (2010) fabricated b-tricalcium phosphate scaffolds with accurately controlled pore parameters by using assembled organic micro-spheres as templates combined with casting technique. Using this technique, the authors produced a series of scaffolds with variable pore sizes, in the range of 300–700 μm and variable interconnections, in the range of 70–200 μm, to evaluate the influence of the size and interconnection throat of the pores on the *in vivo* vascularization after implantation. The authors founded that both size and number of the blood vessels growing into the porous structure of the scaffolds when implanted in the rabbit model were strongly dependent on the pore structure parameters. In particular, the increase in pore size resulted in an increase in size of the growing blood vessels, while with the increase in size of interconnection, both the size and number of the blood vessels formed within the pore structure of the scaffold increased. On the other hand, there was no significant difference in scaffold vascularization with pores size above 400 μm, and there was no marked increase in the extent of vascularization with further increase in pore size above 400 μm, indicating that, in this case, the upper limit of pore size for vascularization is 400 μm.

In terms of pore interconnectivity and new tissue formation, bone tissue has been the most investigated. Various authors have suggested a minimum interconnection size, below which bone ingrowth cannot occur. Lu and co-workers (1999) reported that a minimum interconnection size of 50 μm is recommended for marked mineralized ingrowth.

The importance of scaffold pore size and interconnection on *in vivo* tissue formation has been also reported by Mastrogiacomo and co-workers (2006), which considered two hydroxyapatite bioceramics with identical microstructures but different surface areas, pore size distributions and pore interconnection pathways. These scaffolds had been fabricated by means of two different procedures, sponge matrix embedding and foaming. In the first case, the scaffold was characterized by surface area and pore interconnection pathway equal to 1.63 m^2/g and 100 μm, respectively, while in the second case these parameters were 0.87 m^2/g and 200 μm, respectively. Bone ingrowth within the two scaffolds was investigated using an established model of *in vivo* bone formation in mice by exogenously added osteoprogenitor cells. The histological analysis of specimens at different times after implantation revealed in both materials similar extents of bone matrix deposition, while different rates of bone formation and construct vascularization were observed. In particular, the presence of a more regular pore structure in the case of the foamed scaffold resulted in a faster occurrence of bone tissue, already after 4 weeks of implantation. Conversely, the wider and less tortuous pore interconnectivity of the scaffold prepared by the matrix embedding technique resulted in the formation of larger blood

vessels. These results clearly demonstrate that surface area and pore interconnection of osteoconductive scaffolds can influence the overall amount of bone deposition, the pattern of blood vessels invasion and, finally, the kinetics of the bone neo-formation process.

The continuous growth of 3D patterning technologies for developing scaffolds have allowed over the last years the systematic investigation of several micro-structural parameters of the scaffold, such as pore shape and geometry, on *in vivo* new tissue regeneration. Jeong and co-workers (2011) investigated the effect of three-dimensional poly(1,8-octanediol–co-citrate) scaffold pore shape on *in vivo* chondrogenesis using primary chondrocytes. Porous scaffolds with 900 μm interconnected spherical or cubical pores were designed using rapid prototyping technique. A significantly greater increase in cartilage matrix formation over 6 weeks *in vivo* implantation was observed for the scaffold with spherical pores, as evidenced by the higher ribonucleic acid expression for cartilage-specific proteins and matrix degradation proteins as well as glycosaminoglycans retained. The authors ascribed this effect to the lower permeability of the spherical-pore scaffold, which allowed keeping the ECM and maintaining a chondrocytic phenotype around pore necking areas better than the cubic-pore one.

In addition to the experimental techniques, computational simulation could be a helpful technique for evaluating the new tissue growth and the change in micro-structural properties of the scaffold during the regeneration process. Furthermore, the computationally predicted quantitative information may help to design an optimal scaffold microstructure to fulfil the desired conditions. For instance, Jones and co-workers (2009) compared computational approaches with *in vivo* implantation to assess the biocompatible properties of two types of hydroxyapatite scaffolds. One scaffold type has been fabricated via pressing and firing, and has a disordered pore structure, while the second scaffold type, based on fused depositional modelling, has a regular, lattice type architecture. The results of their work evidenced that the pore throat has a strong correlation with bone ingrowth. In particular, all pores with pore throat lower than 50 μm exhibit no bone ingrowth. Overall, a preference for bone ingrowths are based on the accessible pore radius with the cut-off radius around 100 μm for early implantation time points. Finally, a strong enhancement of bone ingrowth has been observed for pore diameters higher than 100 μm, while little difference in bone ingrowth has been measured with different scaffold design.

3.6 Conclusion

In this chapter we have provided an overview of the basic requirements of the pore structure of the scaffold for TE applications.

The processing techniques that are currently used for the fabrication of three-dimensional porous scaffolds are reviewed, with particular attention on the processing-pore structure–properties relationship. Furthermore, special emphasis is placed on design and fabrication of porous scaffolds with multi-scaled and highly complex pore structures by combined approaches.

Based on the wide literature investigation about porous scaffolds design and characterization of its biological performance *in vitro* and *in vivo*, the optimal design of scaffold pore structure is strongly required to trigger its biological response with precision. In particular, scaffold pore size, shape and interconnectivity have key roles in *in vitro* cell adhesion, proliferation and differentiation. Furthermore, multi-scaled pore structures provided by elongated macro-pores within a random micro-porosity may promote the formation of a homogeneous cell/scaffold construct and improve diffusion of oxygen and nutrients in three-dimension. Concomitantly, *in vivo* reports indicate that, along with pore size, new tissue ingrowth and vascularization are also modulated by pore interconnection pathway.

Finally, all of the results reported in this chapter evidence that the development of processing techniques able to improve the control of scaffold pore structure at both nano- and micro-metric size scales may represent the basis for the ultimate success of the *in vitro* and *in vivo* TE scaffold-based strategies.

3.7 References

Akay G, Birch M A and Bokhari M A (2004) 'Microcellular polyHIPE polymer supports osteoblast growth and bone formation in vitro', *Biomaterials*, **25**, 3991–4000.

Bai F, Wang Z, Lu J, Liu J, Chen G, Lv R, Wang J, Lin K, Zhang J and Huang X (2010) 'The correlation between the internal structure and vascularization of controllable porous bioceramic materials in vivo: a quantitative study', *Tissue Engineering Part A*, **16**, 3791–3803.

Cao Y, Mitchell G, Messina A, Price L, Thompson E, Penington A, Morrison W, O'Connor A, Stevens G and Copper-White J (2006) 'The influence of architecture on degradation and tissue ingrowth into three-dimensional poly(lactic-co-glycolic acid) scaffolds *in vitro* and *in vivo*', *Biomaterials*, **27**, 2854–2864.

Capes J S, Ando H Y and Cameron M E (2005) 'Fabrication of polymeric scaffolds with a controlled distribution of pores', *J Mater Sci Mater Med*, **16**, 1069–1075.

Cuddihy M J and Kotov N A (2008) 'Poly(lactic-co-glycolic acid) bone scaffolds with inverted colloidal crystal geometry', *Tissue Engineering Part A*, **14**, 1639–1649.

Ginty P J, Howard D, Rose F R A J, Whitaker M J, Barry J J A, Tighe P, Mutch S R, Serhatkulu G, Oreffo R O C, Howdle S M and Shakesheff K M (2006) 'Mammalian cell survival and processing in supercritical CO_2', *PNAS*, **9**, 7426–7431.

Griffon D J, Sedighi M R, Schaeffer D V, Eurell J A and Johnson A L (2006) 'Chitosan scaffolds: Interconnective pore size and cartilage engineering', *Acta Biomater*, **2**, 313–320.

Guarino V, Causa F, Salerno A, Ambrosio L and Netti P A (2008) 'Design and manufacture of microporous polymeric materials with hierarchal complex structure for biomedical application', *Mater Sci Tech*, **24**, 1111–1117.

Guarino V, Urciuolo F, Alvarez-Perez M, Mele B, Netti P A and Ambrosio L (2012) 'Osteogenic differentiation and mineralization in fibre-reinforced tubular scaffolds: theoretical study and experimental evidences', *J R Soc Interface*, DOI:10.1098/rsif.2011.0913.

Harley B A, Lynn A K, Wissner-Gross Z, Bonfield W, Yannas I V and Gibson L J (2010) 'Design of a multiphase osteochondral scaffold III: fabrication of layered scaffolds with continuous interfaces', *J Biomed Mater Res*, **92A**, 1078–1093.

Hile D D, Amirpour M L, Akgerman A and Pishko M V (2000) 'Active growth factor delivery from poly(D,L-lactide-coglycolide) foams prepared in supercritical CO_2', *J Control Release*, **66**, 177–185.

Hoffmann S, Hagenmuller H, Koch A M, Vunjak-Novakovic G, Kaplan D L, Merkle H P, Muller R and Meinel L (2007) 'Control of in vitro tissue-engineered bone-like structures using human mesenchymal stem cells and porous silk scaffolds', *Biomaterials*, **28**, 1152–1162.

Hollister S J (2005) 'Porous scaffold design for tissue engineering', *Nat Mater*, **4**, 518–524.

Hutmacher D W (2001) 'Scaffold design and fabrication technologies for engineering tissues-state of the art and future perspectives', *J Biomat Sci Polym E,* **12**, 107–124.

Ishaug-Riley S L, Crane-Kruger G M, Yaszemski M J and Mikos A G (1998) 'Three-dimensional culture of rat calvarial osteoblasts in porous biodegradable polymers', *Biomaterials*, **19**, 1405–1412.

Jeong C J and Hollister S J (2010) 'A comparison of the influence of material on in vitro cartilage tissue engineering with PCL, PGS, and POC 3D scaffold architecture seeded with Chondrocytes', *Biomaterials*, **31**, 4304–4312.

Jeong C J, Zhang H and Hollister S J (2011) 'Three-dimensional poly(1,8-octanediol–co-citrate) scaffold pore shape and permeability effects on sub-cutaneous in vivo chondrogenesis using primary chondrocytes', *Acta Biomater*, **7**, 505–514.

Jiankang H, Dichen L, Yaxiong L, Bo Y, Hanxiang Z, Qin L, Bingheng L and Yi L (2009) 'Preparation of chitosan–gelatin hybrid scaffolds with well-organized microstructures for hepatic tissue engineering', *Acta Biomater*, **5**, 453–461.

Jones A C, Arns C H, Hutmacher D W, Milthorpe B K, Sheppard A P and Knackstedt M A (2009) 'The correlation of pore morphology, interconnectivity and physical properties of 3D ceramic scaffolds with bone ingrowth', *Biomaterials*, **30**, 1440–1451.

Karande T S, Ong J L and Agrawal C M (2004) 'Diffusion in musculoskeletal tissue engineering scaffolds: Design issues related to porosity, permeability, architecture, and nutrient mixing', *Ann Biomed Eng*, **32**, 1728–1743.

Kim T G, Chung H J and Park T G (2008) 'Macroporous and nanofibrous hyaluronic acid/collagen hybrid scaffold fabricated by concurrent electrospinning and deposition/leaching of salt particles', *Acta Biomater*, **4**, 1611–1619.

Kim K, Dean D, Wallace J, Breithaupt R, Mikos A G and Fisher J P (2011) 'The influence of stereolithographic scaffold architecture and composition on

osteogenic signal expression with rat bone marrow stromal cells', *Biomaterials*, **32**, 3750–3763.

Koehne V, Heschel I, Scügner F, Lasrich D, Bartsch J W and Jockusch H (2008) 'Use of a novel collagen matrix with oriented pore structure for muscle cell differentiation in cell culture and in grafts', *J Cell Mol Med*, **12**, 1640–1648.

Leong K F, Chua C K, Sudarmadji N and Yeong W Y (2008) 'Engineering functionally graded tissue engineering scaffolds', *J Mech Behav Biomed*, **1**, 140–152.

Leong M F, Rasheed M Z, Lim T C and Chian K S (2009) 'In vitro cell infiltration and in vivo cell infiltration and vascularization in a fibrous, highly porous poly(D,L-lactide) scaffold fabricated by cryogenic electrospinning technique', *J Biomed Mater Res*, **91A**, 231–240.

Levy-Mishali M, Zoldan J and Levenberg S (2009) 'Effect of scaffold stiffness on myoblast differentiation', *Tissue Eng Pt A*, **15**, 935–944.

Lien S, Ko L and Huan T (2009) 'Effect of pore size on ECM secretion and cell growth in gelatin scaffold for articular cartilage tissue engineering', *Acta Biomater*, **5**, 670–679.

Lim J Y and Donahue H J (2007) 'Cell sensing and response to micro- and nanostructured surfaces produced by chemical and topographic patterning', *Tissue Eng*, **13**, 1879–1891.

Lu J, Flautre B, Anselme K, Hardouin P, Gallur M, Descamps M and Thierry B (1999) 'Role of interconnections in porous bioceramics on bone recolonization in vitro and in vivo', *J Mater Sci Mater M*, **10**, 111–120.

Lu H, Ko Y, Kawazoe N and Chen G (2010) 'Cartilage tissue engineering using funnel-like collagen sponges prepared with embossing ice particulate templates', *Biomaterials*, **31**, 5825–5835.

Lutolf M P and Hubbell J A (2005) 'Synthetic biomaterials as instructive extracellular microenvironments for morphogenesis in tissue engineering', *Nat Biotech*, **23**, 47–55.

Ma P X (2008) 'Biomimetic materials for tissue engineering', *Adv Drug Deliver Rev*, **60**, 184–198.

Mastrogiacomo M, Scaglione S, Martinetti R, Dolcini L, Beltrame F, Cancedda R and Quarto R (2006) 'Role of scaffold internal structure on in vivo bone formation in macroporous calcium phosphate bioceramics', *Biomaterials*, **27**, 3230–3237.

McCoy R J, Jungreuthmayer C and O'Brien F J (2012) 'Influence of flow rate and scaffold pore size on cell behavior during mechanical stimulation in a flow perfusion bioreactor', *Biotech Bioeng*, **109**, 1583–1594.

Melchels F P W, Tonnarelli B, Olivares A L, Martin I, Lacroix D, Feijen J, Wendt D J and Grijpma D W (2011) 'The influence of the scaffold design on the distribution of adhering cells after perfusion cell seeding', *Biomaterials*, **32**, 2878–2884.

Montjovent M, Mathieu L, Hinz B, Applegate L L, Bouban P, Zambelli P, Månson J and Pioletti D P (2005) 'Biocompatibility of bioresorbable poly(L-lactic acid) composite scaffolds obtained by supercritical gas foaming with human fetal bone cells', *Tissue Eng*, **11**, 1640–1649.

Mygind T, Stiehler M, Baatrup A, Li H, Zou X, Flyvbjerg A, Kassem M and Bünger C (2007) 'Mesenchymal stem cell ingrowth and differentiation on coralline hydroxyapatite scaffolds', *Biomaterials*, **28**, 1036–1047.

Nam Y S and Park T G (1999) 'Porous biodegradable polymeric scaffolds prepared by thermally induced phase separation', *J Biomed Mater Res*, **47**, 8–17.

O'Brien F J, Harley B A, Yannas I V and Gibson L J (2005) 'The effect of pore size on cell adhesion in collagen-GAG scaffolds', *Biomaterials*, **26**, 433–441.

Oh S H, Kim T H, Im G I and Lee J H (2010) 'Investigation of pore size effect on chondrogenic differentiation of adipose stem cells using a pore size gradient scaffold', *Biomacromolecules*, **11**, 1948–1955.

Pamula E, Bacakova L, Filova E, Buczynska J, Dobrzynski P, Noskova L and Grausov L (2008) 'The influence of pore size on colonization of poly(L-lactide-glycolide) scaffolds with human osteoblast-like MG 63 cells in vitro', *J Mater Sci Mater Med*, **19**, 425–435.

Park S H, Kim T G, Kim H C, Yang D and Park T G (2008) 'Development of dual scale scaffolds via direct polymer melt deposition and electrospinning for applications in tissue regeneration', *Acta Biomater*, **4**, 1198–1207.

Park I S, Kim S, Kim Y H, Kim I H and Kim S H (2009) 'A collagen/smooth muscle cell-incorporated elastic scaffold for tissue-engineered vascular grafts', *J Biomater Sci, Polym E*, **20**, 1645–1660.

Ranucci C S, Kumar A, Batra S P and Moghe P V (2000) 'Control of hepatocyte function on collagen foams: sizing matrix pores toward selective induction of 2-D and 3-D cellular morphogenesis', *Biomaterials*, **21**, 783–793.

Reverchon E, Cardea S and Rapuano C (2008) 'A new supercritical fluid-based process to produce scaffolds for tissue replacement', *J Supercrit Fluid*, **45**, 365–373.

Sachlos E and Czernuszka J T (2003) 'Making tissue engineering scaffolds work. Review on the application of solid free form fabrication technology to the production of tissue engineering scaffolds', *Eur Cells Mater*, **5**, 29–40.

Salerno A, Iannace S and Netti P A (2008) 'Open-pore biodegradable foams prepared via gas foaming and microparticulate templating', *Macromol Biosci*, **8**, 655–664.

Salerno A, Di Maio E and Iannace S and Netti P A (2009a) 'Engineering of foamed structures for biomedical application', *J Cell Plast*, **45**, 103–117.

Salerno A, Oliviero M, Di Maio E, Iannace S and Netti P A (2009b) 'Design of porous polymeric scaffolds by gas foaming of heterogeneous blends', *J Mat Sci Mater Med*, **20**, 2043–2051.

Salerno A, Guarnieri D, Iannone M, Zeppetelli S, Di Maio E, Iannace S and Netti P A (2009c) 'Engineered μ-bimodal poly(ε-caprolactone) porous scaffold for enhanced hMSC colonization and proliferation', *Acta Biomater*, **5**, 1082–1093.

Salerno A, Zeppetelli S, Di Maio E, Iannace S and Netti P A (2010a) 'Novel 3D porous multi-phase composite scaffolds based on PCL, thermoplastic zein and ha prepared via supercritical CO_2 foaming for bone regeneration', *Compos Sci Technol*, **70**, 1838–1846.

Salerno A, Guarnieri D, Iannone M, Zeppetelli S and Netti P A (2010b) 'Effect of micro- and macroporosity of bone tissue three-dimensional-poly(ε-Caprolactone) scaffold on human mesenchymal stem cells invasion, proliferation, and differentiation in vitro', *Tissue Eng Pt A*, **16**, 2661–2673.

Salerno A, Zeppetelli S, Di Maio E, Iannace S and Netti, P A (2011a) 'Design of bimodal PCL and PCL-HA nanocomposite scaffolds by two step depressurization during solid-state supercritical CO_2 foaming', *Macromol Rapid Comm*, **32**, 1150–1156.

Salerno A, Di Maio E, Iannace S and Netti P A (2011b) 'Solid-state supercritical CO_2 foaming of PCL and PCL-HA nano-composite: Effect of composition,

thermal history and foaming process on foam pore structure', *J Supercrit Fluid*, **58**, 158–167.

Salerno A, Zeppetelli S, Di Maio E, Iannace S and Netti P A (2011c) 'Processing/structure/property relationship of multi-scaled PCL and PCL–HA composite scaffolds prepared via gas foaming and NaCl reverse templating', *Biotech Bioeng*, **108**, 963–976.

Salerno A, Di Maio E, Iannace S and Netti P A (2012a) 'Tailoring the pore structure of PCL scaffolds for tissue engineering prepared via gas foaming of multiphase blends', *J Porous Mat*, **19**, 181–188.

Salerno A, Iannace S and Netti P A (2012b) 'Graded biomimetic osteochondral scaffold prepared via CO_2 foaming and micronized NaCl leaching', *Mater Lett*, **82**, 137–140.

Sapir Y, Kryukov O and Cohen S (2011) 'Integration of multiple cell-matrix interactions into alginate scaffolds for promoting cardiac tissue regeneration', *Biomaterials*, **32**, 1838–1847.

Seitz H, Rieder W, Irsen S, Leukers B and Tille C (2005) 'Three-dimensional printing of porous ceramic scaffolds for bone tissue engineering', *J Biomed Mater Res B: Appl Biomater*, **74B**: 782–788.

Shor L, Güçeri S, Wen X, Gandhi M and Sun W (2007) 'Fabrication of three-dimensional polycaprolactone/hydroxyapatite tissue scaffolds and osteoblast-scaffold interactions in vitro', *Biomaterials*, **28**, 5291–5297.

Silva M M C G, Cyster L A, Barry J J A, Yang X B, Oreffo R O C, Grant D M, Scotchford C A, Howdle S M, Shakesheff K M and Rose F R A J (2006) 'The effect of anisotropic architecture on cell and tissue infiltration into tissue engineering scaffolds', *Biomaterials*, **27**, 5909–5917.

Song Y, Wennink J W H, Kamphuis M M J, Vermes I, Poot A A, Feijen J and Grijpma D W (2010) 'Effective seeding of smooth muscle cells into tubular poly(trimethylene carbonate) scaffolds for vascular tissue engineering', *J Biomed Mater Res A*, **95A**, 440–446.

Stupp S I (2005) 'Biomaterials for regenerative medicine', *MRS Bulletin*, **30**, 546–553.

Taboas J M, Maddox R D, Krebsbach P H and Holliste S J (2003) 'Indirect solid free form fabrication of local and global porous, biomimetic and composite 3D polymer-ceramic scaffolds', Biomaterials, **24**, 181–194.

Thomson R C, Yaszemski M J, Powers J M and Mikos A G (1996) 'Fabrication of biodegradable polymer scaffolds to engineer trabecular bone', *J Biomat Sci Polym E*, **7**, 23–38.

Van Bael S, Chai Y C, Truscello S, Moesen M, Kerckhofs G, Van Oosterwyck H, Kruth J P and Schrooten J (2012) 'The effect of pore geometry on the in vitro biological behavior of human periosteum-derived cells seeded on selective laser-melted Ti6Al4V bone scaffolds', *Acta Biomater*, **8**, 2824–2834.

Virgilio N, Sarazin P and Favis B D (2010) 'Towards ultraporous poly(l-lactide) scaffolds from quaternary immiscible polymer blends', *Biomaterials*, **31**, 5719–5728.

Wang J, Ma H, Jin X, Hu J, Liu X, Ni L and Ma P X (2011) 'The effect of scaffold architecture on odontogenic differentiation of human dental pulp stem cells', *Biomaterials*, **32**, 7822–7830.

Washburn N R, Simon C G, Tona A, Elgendy H M, Karim A and Amis E J (2002) 'Co-extrusion of biocompatible polymers for scaffolds with co-continuous morphology', *J Biomed Mater Res*, **60**, 20–29.

Williams J M, Adewunmi A, Scheck R M, Flanagan C L, Krebsbach P H, Feinberg S E, Hollister S J and Das S (2005) 'Bone tissue engineering using polycaprolactone scaffolds fabricated via selective laser sintering', *Biomaterials*, **26**, 4817–4827.

Yamane S, Iwasaki N, Kasahara Y, Harada K, Majima T, Monde K, Nishimura S and Minami A (2007) 'Effect of pore size on in vitro cartilage formation using chitosan-based hyaluronic acid hybrid polymer fibers', *J Biomed Mater Res*, **81A**, 586–593.

Yang S, Leong K, Du Z and Chua C (2001) 'The design of scaffolds for use in tissue engineering. Part I. traditional factors', *Tissue Engineering*, **7**, 679–689.

Zein I, Hutmacher D W, Tan K C and Teoh S H (2002) 'Fused deposition modeling of novel scaffold architectures for tissue engineering applications', *Biomaterials*, **23**, 1169–1185.

Zhang J, Wu L, Jing D and Ding J (2005) 'A comparative study of porous scaffolds with cubic and spherical macropores', *Polymer*, **46**, 4979–4985.

4

Tailoring the pore structure of foam scaffolds for nerve regeneration

M. MADAGHIELE, L. SALVATORE and A. SANNINO, University of Salento, Italy

DOI: 10.1533/9780857097033.1.101

Abstract: Porosity is a key parameter in the design of tissue engineering scaffolds, as bioactivity can be controlled and tailored to the synthesis of the target tissue by finely tuning the porous structure of the scaffolding biomaterial. This chapter discusses the effect of structural parameters, such as pore volume fraction, pore size and distribution, pore shape, pore interconnectivity and pore orientation, on the performance of sponge-like scaffolds, with a special focus on those directed to nerve regeneration.

Key words: scaffold, porosity, nerve regeneration, pore orientation, nerve guidance conduits.

4.1 Introduction

Porous foam- or sponge-like scaffolds are essential in promoting and controlling the regeneration of adult human tissues in large defects. The scaffold itself is needed at the defect site, in order to provide both mechanical stability and an initial framework for cells to migrate within the lesion (and the latter is especially important for avascular tissues, where a fibrin scaffold/clot does not form in the wound bed). The bioactive role played by porosity is clearly multiple, as pores can potentially: (a) allow and control cell attachment, migration and infiltration; (b) provide improved nutrient and metabolite transport to and from the cells respectively, thus improving cell survival, especially in the centre of the defect (or device); (c) facilitate vascular infiltration; and (d) control the orientation of extracellular matrix (ECM) molecules produced and laid down by cells. The bioactive potential of porosity thus depends on how carefully pore size and shape, pore volume fraction, pore interconnectivity and pore orientation are designed, keeping in mind the 'gold standard' architecture of the native ECM of the target tissue or organ. In particular, assuming pore interconnectivity as a fundamental requirement, although difficult to measure (Li *et al.*, 2003; Karande *et al.*, 2004), size, volume fraction and orientation of pores are the key variables

to be tuned to adjust the bioactivity of the scaffold. The direct effect of pore shape on cell behaviour has not been completely elucidated yet, although recent studies suggest that pore shape plays an important role in controlling cell differentiation (Jeong *et al*., 2011; Van Bael *et al*., 2012). However, the effects of porosity (pore shape included) on both the mechanical properties and the biodegradation rate of the scaffold should be evaluated, as those properties might have a huge impact on the outcome of the scaffold implant.

Porous foam scaffolds are widely used for nerve regeneration, at least at a research level, both for peripheral nervous systems (PNS) and central nervous systems (CNS). Whereas for CNS a porous scaffold alone (i.e. without exogenous molecular regulators and/or cells) is not expected to induce a significant regeneration, due to the intrinsic complexity of CNS microenvironment, there is evidence suggesting that a porous scaffold alone in the PNS might be sufficient for at least partial regeneration and a certain functional recovery, following neurotmesis (i.e. nerve transection) (Yannas, 2001). The surgical insertion of a 'graft' between the nerve stumps (either a nerve autograft, when available, or an engineered porous scaffold) is needed to stimulate axonal regrowth and distal reinnervation. Nerve autograft is currently the 'gold standard' for nerve regeneration, although the functional recovery achievable with this technique is unfortunately far from optimal, probably due to the use of a sensory nerve to replace either a sensory or a motor nerve. When implanting a porous scaffold, for given defect size and location, the quality of nerve regeneration and the extent of functional recovery depend on the scaffold properties, i.e. surface/bulk chemistry, biodegradation rate, mechanical stiffness and porous structure.

It is worth noting that, in order to mimic the cylindrical and aligned arrangement of peripheral nerves, two types of scaffolds can be used for PNS regeneration: a tubular scaffold with a porous wall, also called a nerve guide or guidance conduit, and a cylindrical scaffold with longitudinally or axially orientated pores. Even though most studies report the use of conduits alone for PNS regeneration (the so-called entubulation strategy) (Yannas, 2001), the combined use of tubular and cylindrical scaffolds is likely the best operative option, since the two types of devices are expected to perform different but complementary functions, once implanted *in vivo* (Fig. 4.1).

The tubular device is envisaged to provide a chamber environment where a fibrin-based, longitudinally orientated matrix can form, in order to direct axons from the proximal to the distal stump, and where growth factors released by injured nerve cells can be retained at the defect site. The chamber is also expected to prevent the infiltration of surrounding soft tissue and to limit the contractile activity of myofibroblasts, which is responsible for scar formation (i.e. neuroma) in the physiological nerve response to injury. The design of the tubular scaffold wall should thus foresee specific

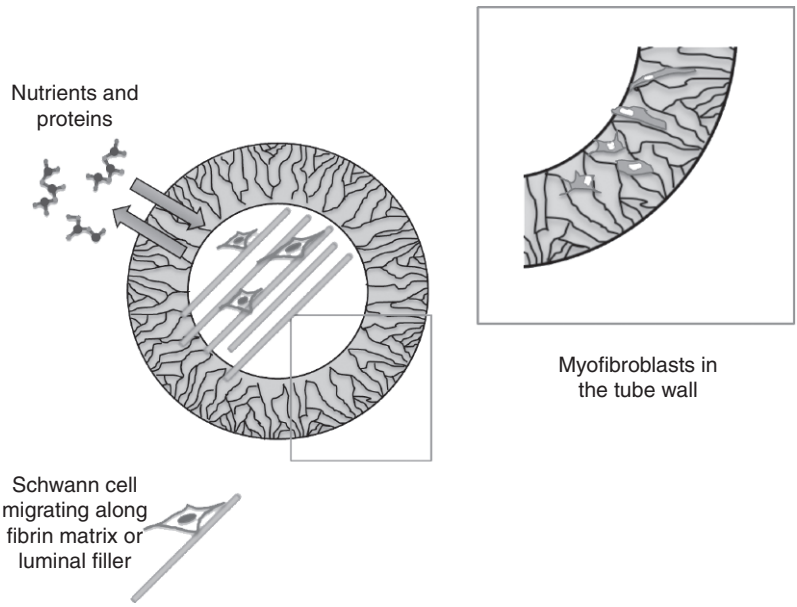

4.1 Role of conduit and luminal filler in PNS regeneration. The conduit is expected to provide a chamber permeable to nutrients and proteins, where an aligned fibrin-based matrix can form to allow Schwann cell migration. The conduit wall should also be able to host myofibroblasts. The luminal filler is expected to mimic the aligned fibrin cable, to accelerate the regenerative process in larger gaps.

microporous patterns which would allow the conduit to perform all of the above-mentioned functions.

Conversely, the cylindrical matrix is expected to possess axially orientated pores mimicking the structure of the fibrin cable formed between the nerve stumps and originating from the nerve exudate. The scaffold is thus meant to work as luminal filler of the chamber, providing an immediate support for the migration of Schwann cells and for elongating axons, in order to accelerate the reinnervation of the distal stump. Indeed, especially in the case of large defects (such as those found in clinical practice), the distal stump might undergo chronic degeneration before reinnervation occurs, i.e. the basement membrane making up the distal endoneurial tubes is disrupted, thus inhibiting Schwann cell migration and further reinnervation (Höke, 2006).

This chapter deals with the importance of scaffold porosity in peripheral nerve regeneration. Firstly, the most widely employed materials and techniques for the fabrication of porous scaffolds are presented, with focus on the specific design criteria needed for tubular and cylindrical scaffolds, respectively. The quality of nerve regeneration achieved by means of

foam- or sponge-like scaffolds (with pore sizes usually in the range 5–100 μm) is then briefly discussed, pointing out the difficulties of translating PNS regenerative medicine to clinical practice. With regard to hydrogel-based scaffolds, possessing pore sizes in the range 10–100 nm and obtained through chemical or physical crosslinking of aqueous solutions, and fibrous scaffolds, characterized by the assembly of nanometric fibres and usually produced by means of electrospinning, the readers are directed to further and recent reviews discussing their bioactivity in PNS regeneration (Jiang *et al*., 2010; Daly *et al*., 2012; Spivey *et al*., 2012).

4.2 Materials for foam scaffold fabrication

Although non-biodegradable scaffolds might be useful to induce a modest tissue regeneration, as demonstrated in PNS for silicone-based nerve guides (Lundborg *et al*., 1991, 1994), their sustained presence in the long term causes a foreign body reaction, which requires a second surgical intervention to remove the permanent scaffold (Mackinnon *et al*., 1984; Merle *et al*., 1989). A true regenerative medicine approach thus aims at using biodegradable polymers only, either synthetic or natural, for the scaffold fabrication. The scaffold performance is clearly affected by the nature of the degradation mechanism and the products that are released into the host site as resorption occurs, since those substances, even though not cytotoxic, might deeply change the local cell environment and have a negative effect on tissue regeneration.

Several biomaterials have been investigated for the production of nerve guides or axially orientated luminal fillers. The degradation rate and mechanical properties of synthetic polymers are more easily controllable, compared to those of naturally derived biomaterials, which, on the contrary, suffer from large batch-to-batch variations. However, those properties for natural polymers can be adjusted to a certain extent by means of several crosslinking methods (Lee *et al*., 2001; Itoh *et al*., 2002; Harley *et al*., 2004; Pek *et al*., 2004). Among the most widely employed synthetic polymers, several polyesters have been reported in the last two decades, including poly(lactic acid) (PLA), poly(glycolic acid) (PGA), poly-ε-caprolactone (PCL) and their copolymers (Dellon and Mackinnon, 1988; den Dunnen *et al*., 1993; Aldini *et al*., 1996; Bryan *et al*., 2000). Such polymers are degradable *in vivo* via hydrolysis of the ester linkage, and are approved by the US Food and Drug Administration (FDA) for use as sutures, surgical meshes and fixation components. Although their degradation rate can be easily adjusted and tailored to the specific application by changing their hydrophobicity and crystallinity degrees (Yang *et al*., 2001), their use as scaffolds in the clinical practice remains controversial, due to their unfavourable combination of degradation process (burst or 'bolus' degradation) and release products at

the implant site. Indeed, since the process of hydrolysis starts eroding the bulk polymer in a random manner, the total mass of the scaffold remains essentially the same for a relatively long time, until the molecular weight of the fragments formed is small enough to make them soluble. When this occurs, the bulk polymer is rapidly solubilized, causing a deep decrease in the local pH (Muschler *et al.*, 2004), before the degradation products can be further metabolized or excreted via normal physiological pathways (lactic and glycolic acids are eliminated from the body via Kreb's cycle as CO_2 and in urine as water (Sinha and Trehan, 2003)). However, for highly porous implants, the effects of the degradation products might not be pronounced, since the polymer is only a small amount of the total volume of the scaffold, and the released products might be readily cleared by extracellular fluids (Muschler *et al.*, 2004).

Intuitively porosity, i.e. the amount of void space within the volume of the scaffold is expected to lead not only to a higher rate of clearance of the degradation products from the graft site, but also to a higher degradation rate, since a larger surface of the bulk polymer comes into contact with biological fluids (Muschler *et al.*, 2004; Dellinger *et al.*, 2006). However, a few exceptions exist to this general rule, depending on the degradation products. Some studies have reported that scaffolds made up of poly(lactic-co-glycolic) acid (PLGA) degrade faster as their porosity decreases or their pore size increases, probably due to the slow diffusion and higher concentration of degradation products within the scaffold, which cause a stronger acid-catalysed hydrolysis (Agrawal *et al.*, 2000; Wu and Ding, 2005).

Polyphosphoesters and polyurethanes have also been used for the fabrication of nerve guidance conduits, but their fast degradation rate is unlikely to match the rate of tissue regeneration desired for therapeutic use (Borkenhagen *et al.*, 1998; Wang *et al.*, 2001).

Natural polymers used to produce porous scaffolds for nerve regeneration are mainly macromolecules derived from the mammalian ECM, which are easily recognized by cells and thus allow for cell–ECM interactions. Moreover, such polymers are susceptible to enzymatic digestion, which implies that the material or scaffold is locally resorbed, when specific enzymes secreted by cells meet its surface. Among ECM components, Type I collagen has been largely exploited to mimic the native ECM of peripheral nerve tissue. Other molecules which might be useful for stimulating PNS regeneration are laminin, fibrin, fibronectin and vitronectin (Martini, 1994; Fu and Gordon, 1997). It is important to note that the animal origin of such biopolymers, in addition to posing challenges in maintaining their activity during the extraction and processing, might raise questions about their immunogenicity and the risk of disease transmission. Collagen has been shown to be safe for clinical use, as its immunogenicity is particularly

Table 4.1 Main worldwide manufacturers/suppliers of Type I collagen derived from animal tissues

Manufacturer	Type I collagen form	Origin
Aesculap AG & Co. KG. (B. Braun) Tuttlingen, Germany	Solution	Bovine
Devro PTY Ltd Bathurst, NSW, Australia	Dry fibre, solution	Bovine
SYMATESE Biomateriaux Chaponost, France	Dry fibre	Bovine/porcine
INTEGRA lifesciences Co. Plainsboro, NJ, USA	Dry fibre	Bovine
Kensey-Nash Co. Exton, PA, USA	Dry flakes	Bovine
Collagen Matrix Oakland, NJ, USA	Powder/particles	Bovine
Innocoll (Syntacoll GmbH) Athlone, Ireland	Dry fibre, gel	Bovine/equine
Invitrogen Co. (Life technologies Co.) Carlsbad, CA, USA	Solution	Bovine/rodent
Advanced biomatrix Inc. San Diego, CA, USA	Dry fibre, solution	Bovine
SunMax biotechnology Co. Ltd. Taiwan, RC	Solution	Porcine
Collagen solutions LLC San Jose, CA, USA	Powder, gel	Bovine
KOKEN Co. Ltd. Tokyo, Japan	Solution	Bovine
Southern lights biomaterials Napier, New Zealand	Fibre/powder	Bovine
Orthovita Ltd. Malvern, PA, USA	Powder/solution	Bovine
EnColl Co. Newark, CA, USA	Powder/solution	Bovine
Angel biomedical Ltd. Cramlington, England	Powder/solution	Bovine

Note: The list was derived from keyword Web searches, and includes only manufacturers that supply medical-grade Type I collagen, not derived from marine sources.

low (Friess, 1998), and several medical-grade collagens of different origin are currently available on the market (Table 4.1).

Instead of processing ECM macromolecules to produce porous ECM-mimicking scaffolds, a relatively simple and alternative approach consists in borrowing ECMs from mammalian organs and using them as scaffolds for the synthesis of new tissues. Decellularized matrices, obtained from animal or human donor tissues, have been thus investigated as scaffolds for nerve regeneration (e.g. acellular muscle, vein and nerve grafts) (Kim *et al.*, 2004;

Stang *et al*. 2009; Barnes *et al*., 2011). Although concerns exist about their reproducibility and sterilization, and their regenerative potential seems to be lower than that of nerve autografts, some decellularized nerve allografts are available for clinical use (Kehoe *et al*., 2012).

Among other natural polymers investigated as porous templates for nerve regeneration, there are several polysaccharides, such as chitosan, alginate and agarose. Chitosan, a polymer, derived from crustacean shells, which can be digested *in vivo* by lysozyme, has been reported for the fabrication of nerve guides, often in combination with synthetic polymers, such as PLA (Xie *et al*., 2008). Sponges of alginate and agarose, two polymers derived from seaweed, have also been investigated as scaffolds for nerve regeneration (Kataoka *et al*., 2001; Zmora *et al*., 2002; Stokols and Tuszynski, 2006). Chitosan, alginate and agarose are also employed in the hydrogel form, either chemically or physically crosslinked. With regard to hydrogels, it is worth mentioning keratin, a protein derived from animal or human hair, which has the ability to self-assemble in hydrogel networks and has been recently proposed as a suitable substrate for Schwann cell migration (Apel *et al*., 2008; Sierpinski *et al*., 2008). Keratin-based sponges have been also proposed as scaffolds for tissue engineering (Katoh *et al*., 2004). For some physically crosslinked materials, such as alginate and agarose gels, dissolution is a possible mechanism of *in vivo* degradation. Dissolution is usually a slow, uncontrolled process, although the degree of physical crosslinking, to which the degradation rate is inversely proportional, can be modulated to some extent (Drury and Mooney, 2003).

4.3 Design and fabrication of foam scaffolds for nerve regeneration

A variety of fabrication techniques, and several combinations of them, have been developed to produce tubular and cylindrical scaffolds of given sizes and with well-defined porous structures. Once the 'bulking' biomaterial is chosen, the choice or development of a suitable fabrication method should take into account not only the specific material's processability (e.g. denaturing proteins such as collagen require low-temperature handling), but also the envisaged porous structure, which significantly affects the regenerative performance of the scaffold *in vivo*. In order to finely tune and/or optimize the final porosity, the current trend is to combine two or more pore-forming 'traditional' strategies. Furthermore, translational research requires the processing to be repeatable, susceptible of easy scale-up and biocompatible.

In the following, the design of porosity for both tubular and cylindrical scaffolds adopted in PNS regeneration is discussed. Hints as to traditional

and/or combined fabrication methods, useful to obtain the desired porosities, are also provided throughout the discussion.

4.3.1 Nerve guidance conduits

In addition to pursuing the optimization of the degradation rate and the mechanical properties of a nerve guide, the design of the conduit should include the tuning and the evaluation of the following properties affecting the quality of induced nerve regeneration: protein/cell permeability, surface area and contact guidance. It is clear that such properties are dependent on the macro- and micro-structure of the conduit, which in turn can be controlled by the processing method adopted.

With regard to protein/cell permeability, the tube wall is expected to be porous enough to allow an efficient transport of nutrients and oxygen from the surrounding environment, while preventing formation of fibrous tissue at the wound site (Fig. 4.1). Therefore, the tube wall should be at least protein-permeable (i.e. with pores larger than 50 nm, for large proteins) (Yannas, 2001). As for cell permeability (i.e. tube should possess a wall with pores approximately equal to or larger than 20 μm), a gradient of porosity along the tube wall appears a promising design criterion, in an attempt to meet two counter-acting requirements for the conduit: (a) the need to host myofibroblasts, in order to limit scar tissue formation at the wound site, as suggested for collagen conduits (Chamberlain *et al*., 1998a, 2000); and (b) the need to inhibit fibrous tissue infiltration from the surrounding environment. Whereas (a) requires cell-permeable pores, (b) can be met by designing cell-impermeable pores. Recent studies have thus focused on the development of fabrication techniques which lead to a gradient in pore size along the tube wall (Chang and Hsu, 2006; Harley *et al*., 2006; Oh and Lee, 2007). Two of these studies, in particular, have focused on the control of pore orientation, in addition to pore size.

Collagen-based tubes with radially aligned porosity, cell-permeable pores at the inner wall and cell-impermeable pores at the outer wall, show the potential to regulate myofibroblast attachment and migration, and have been synthesized by means of a spinning technique, combined with a freeze-drying process (Harley *et al*., 2006). The described spinning technique is a centrifugal casting process, in which a collagen slurry contained in a plastic tube is subjected to an ultra-centrifugation regime, which can be modelled to predict the collagen concentration profiles resulting from specific processing parameters (i.e. spinning time and velocity) (Sannino *et al*., 2010). Freeze-drying, also termed 'lyophilization', is a low-temperature, low-pressure process which consists of removing a liquid phase (usually water or aqueous solution) from a given suspension, via freezing and subsequent sublimation of ice. The removal

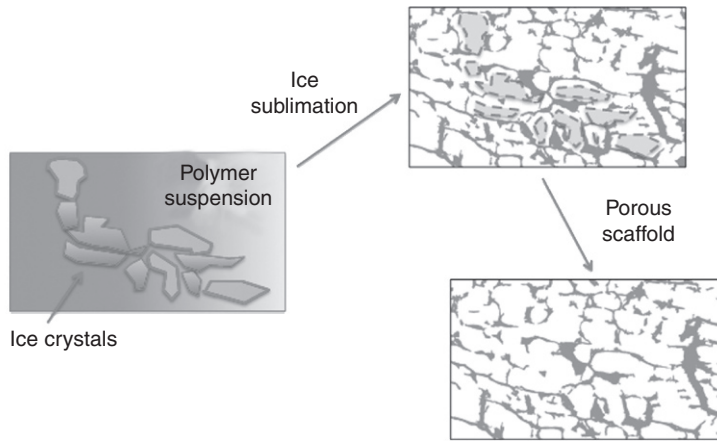

4.2 Schematization of the freeze-drying process. Ice crystals nucleate and grow by diffusion of water into a polymer suspension or solution (e.g. collagen slurry). The following sublimation of ice leaves the polymer struts or walls created during the solidification process, yielding a porous scaffold.

of ice via sublimation leaves behind a porous, sponge-like material, whose porosity is a negative replica of the ice crystal structure formed during the freezing (Fig. 4.2). Smaller pores are thus yielded by higher undercooling (i.e. lower temperatures of freezing) (O'Brien *et al.*, 2004), whereas orientated pores can be obtained by establishing a directional gradient of temperature during the solidification process (Kuberka *et al.*, 2001; Stokols and Tuszynski, 2004). The concentration of solid in the initial aqueous suspension might also affect the growth of ice crystals and the resulting pore size, with smaller pores obtained from suspensions with higher solid concentration (smaller pore volume fractions are also obtained). The combination of the spinning technique with rapid freezing of the spun collagen slurry (in liquid nitrogen) and subsequent freeze-drying thus yield porous tubular scaffolds, which show: (a) radially orientated pores, resulting from the radial freezing process; and (b) a gradient of pore sizes along the tube wall, with increasing pore sizes from the outer to the inner wall, resulting from the concentration profile of collagen established during the spinning.

Conversely, PLGA–pluronic composite tubes, possessing radial pores with a cell-impermeable inner wall and a cell-permeable outer wall, have been developed by means of a modified immersion precipitation method, to allow a good nutrient transport while isolating the defect from external fibrous tissues (Oh and Lee, 2007). The fabrication method described therein is one of the multitude of phase separation techniques,

either non-solvent or thermally induced, employed in the literature. In particular, the method involves a non-solvent induced phase separation (NIPS), which is based on contacting a polymer solution, previously cast into a mould, with a non-solvent. As the non-solvent penetrates the solution, the polymer precipitates, forming a solid phase. By evaporating the non-solvent, a porous scaffold is left behind. In that study, an alginate hydrogel rod was immersed in a PLGA–pluronic solution, and the diffusion of water (i.e. the non-solvent) from the rod to the solution caused the precipitation of a polymeric layer around the rod. Pluronic was used in addition to PLGA in order to increase the hydrophilic character of the device. The resulting polymeric tube showed a wall thickness dependent on the immersion time, whereas the gradient of pore sizes along the wall, with nanosized pores (50 nm) at the inner surface and cell-permeable pores at the outer one (50 μm), was related to the concentration profile of PLGA–pluronic generated by water diffusion. The pore volume fraction was also tunable, by changing the solvent/non-solvent ratio.

Regardless of the different biomaterials used, the implantation of conduits with micropatterned porosity in animal models could help in understanding the effect of tube wall porosity (in terms of both pore size and orientation) on the quality of nerve regeneration, which is still unclear.

In addition to the conduit permeability, findings from a number of independent investigations suggest that the surface area of the tube wall should be optimized, as better nerve regeneration is achievable with increased surface area (Chew *et al*., 2007; Vleggeert-Lankamp *et al*., 2007; Wang *et al*., 2007; Yang *et al*., 2007). The specific surface area of a scaffold, or surface area per unit volume (SAV), defines the area of the scaffold available for cell adhesion, and is strictly related to its porosity. The surface area can be assessed, at least approximately, if the pore volume fraction (P), pore size and pore shape are known (O'Brien *et al*., 2004), with SAV being inversely proportional to the pore diameter, and directly proportional to the solid volume fraction S (S = 1 – P) of the scaffold. The existence of an optimal pore size range for the regeneration of different tissue types (Yang *et al*., 2001; Yannas, 2001) suggests that an optimal surface area is needed for improved cell binding. For PCL tubes with a macroporous outer wall, a microporous inner wall (pore size 1–10 μm) was found to be more advantageous for nerve regeneration than non-porous and macroporous inner walls (Vleggeert-Lankamp *et al*., 2007), and this might be ascribed to the existence of an optimal surface area for nerve regeneration. However, it is worth stressing that the effective interaction of cells with the substrate should be considered for the estimation of the true surface area. For polymers that do not mimic the mammalian ECM, like synthetic ones, the effective SAV for a given porosity might be difficult to assess. Moreover, it should be considered that increased

porosity of the conduit wall might have a detrimental effect on its mechanical properties (Meek and den Dunnen, 2009), which are important for its protective chamber role as well as for proper handling and suturing.

Microfabrication by means of soft lithography is largely exploited for the production of microgrooved conduits, which possess increased surface area available for cell interaction and may also provide contact guidance to Schwann cells and axons (Hsu *et al*., 2009). Contact guidance is the ability of the matrix to provide cells with directional cues, in order to guide their migration along specific patterns. The orientation of the matrix pores (or fibres) has been shown to affect also the maturation of Schwann cells (Chew *et al*., 2008). In this perspective, it is clear that fibrous tubular scaffolds, produced, for example, by means of electrospinning (Subramanian *et al*., 2011), might be extremely advantageous compared to foam-like ones, as they intrinsically combine permeability, high surface area and increased contact guidance (Jiang *et al*., 2010).

Whether the surface area of the conduit is a more important design criterion than its contact guidance is still matter of investigation. A recent study shows that aligned poly(acrylonitrile-co-methacrylate) electrospun fibres deposited onto the inner wall of a polysulfone nerve conduit are fundamental to elicit nerve regeneration, compared to non-aligned ones (Kim *et al*., 2008). Conversely, an independent investigation on the effect of different electrospun fibres on the inner surface of synthetic conduits seems to suggest that increasing the surface area of the conduit may improve its regenerative capacity more significantly than the contact guidance, at least in the long term (Chew *et al*., 2007). Obviously, the quantitation of the true surface area available for cell interaction (which depends on the specific biomaterial used) would be helpful for a deeper understanding of its effects on nerve regeneration.

Considering the overall bioactive role played by the scaffold microstructure, the choice of a suitable fabrication method should be based on the processing variables that allow the modulation of porosity of the resulting scaffold, especially in terms of pore size, orientation and volume fraction. The larger the number of such variables, the higher is the potential of the fabrication method for the scaffold design. Among novel fabrication methods, it is worth mentioning rapid prototyping techniques as emerging tools to produce customized tissue engineering scaffolds, including nerve conduits. Unfortunately, to date only a limited number of materials can be processed, although recent investigations have shown the applicability of rapid prototyping techniques to collagen-based composites for nerve regeneration (Cui *et al*., 2009). Moreover, the spatial resolution of rapid prototyping methods is currently limited to tens of microns, which might represent a drawback for many tissue engineering applications.

4.3.2 Axially orientated cylindrical matrices

As discussed previously, luminal sponge-like fillers with axially orientated pores can improve PNS regeneration by providing prompt contact guidance to Schwann cells and axons, in an attempt to mimic what basement membrane endoneurial tubes physiologically do in response to axonotmesis. This is extremely important when bridging large defects, as accelerating axonal regrowth might impede distal denervation.

At this stage, it is worth highlighting what the expression 'large defects' in PNS regeneration stands for. Since the first studies on nerve entubulation, gap length has been considered the most limiting factor in regeneration. For gaps shorter than the critical length size, which is related to the animal species, the frequency of reinnervation obtained through the entubulation technique is usually high, regardless of the specific device used. This is why the regenerative potential of a nerve guide should be determined in gaps larger than the critical size (Yannas, 2001). However, it has been recently hypothesized that the overall volume of the nerve chamber, determined by length and diameter of the defect, is the true limiting factor in nerve regeneration (Moore *et al*., 2009). This assumption is based on the fact that, even when encouraging animal data have been provided for a given device, clinical studies on relatively large human nerves, such as the ulnar and median nerves (which have a diameter of approximately 3–4 mm), have mostly led to unsuccessful results (Stanec and Stanec, 1998; Weber *et al*., 2000; Meek and Coert, 2008). A possible explanation for a critical chamber volume lies in the inability of a larger chamber to provide a sufficient concentration of neurotrophic factors and/or a crossing fibrin cable. It is clear that, in such cases, the presence of a luminal filler with axially orientated pores within the chamber might be particularly helpful in promoting nerve regeneration, also considering that the porous matrix might serve as a delivery vehicle for exogenous cells (which are invaluable sources of growth factors) and/or growth factors.

As discussed above for nerve guidance conduits, surface area and contact guidance are key properties to consider when designing porous luminal fillers. As shown for different tissues, an optimal scaffold pore size exists for nerve regeneration. For instance, orientated collagen matrices, inserted into a collagen tube, provided results comparable to the ones achieved by the nerve autograft only with a pore size of 20 μm, in a 10 mm gap in the rat sciatic nerve model (Chang *et al*., 1988, 1990; Chamberlain *et al*., 1998b). In addition to the surface area, more recent studies seem to suggest that the contact guidance in the longitudinal direction is the key element for successful nerve regeneration (Yao *et al*., 2010), as non-orientated scaffolds might hamper nerve regeneration by obstructing axonal elongation (Evans *et al*., 2002; Stang *et al*., 2005).

Combined unidirectional freezing and freeze-drying are probably the most widely exploited techniques to produce orientated foam-like matrices, starting from natural biomaterials such as collagen (Chang *et al*., 1990; Schoof *et al*., 2000, 2001; Kuberka *et al*., 2002), agarose (Stokols *et al*., 2004) and alginate (Kataoka *et al*., 2001). Two different uniaxial freezing methods can be adopted to obtain orientated pores. An aligned porous structure can be obtained by freezing a polymer solution or suspension via slow immersion into a cooling bath, and subsequent freeze-drying. For a given polymer concentration, the velocity of immersion and the temperature of the freezing bath can significantly affect the pore size and the pore orientation of the resulting matrices, as shown for collagen-glycosaminoglycan scaffolds (Loree, 1996). For those matrices, only particular combinations of immersing velocity and freezing temperature were found to yield axially orientated pores for cylindrical scaffolds with diameters ranging from 1.5 to 3.8 mm (Loree, 1988; Louie, 1997; Chamberlain *et al*., 1998a; Spilker *et al*., 2001).

Alternatively, a solution or suspension of the selected biomaterial can be injected into a cylindrical mould, made of an insulating material, and the bottom of the mould can be placed in contact with a 'freezing' metal plate or shelf. Whereas pore orientation can be controlled by the longitudinal temperature gradient induced during the freezing, with ice crystals growing unidirectionally from the bottom to the top of the matrix, the pore size depends on polymer concentration and local freezing temperature (with the former affecting also the pore volume fraction). Indeed, the main limitation of the technique is that a pore size gradient is established throughout the length of the matrix, as a result of the longitudinal gradient of freezing temperature. This difference in pore size, which can be neglected for 'short' matrices, i.e. with lengths up to a few mm (Stokols *et al.,* 2004; Madaghiele *et al*., 2008), should be carefully evaluated when designing axially orientated matrices for bridging long nerve gaps, as pore size difference between the two sides of the matrix might be significant. Moreover, it might be also difficult to control the axial orientation of pores, considering that a certain radial freezing can be established near the wall of the mould, resulting from a minimal radial heat conduction (Madaghiele *et al*., 2008). Both pore size gradient and radial freezing might contribute to the non-continuity of pore channels along macroscopic lengths (Fig. 4.3).

Other fabrication techniques reported to date for the production of scaffolds with longitudinally orientated pores include fibre templating (Flynn *et al*., 2003), porogen leaching (Lin *et al*., 2003), injection moulding and solvent evaporation (Moore *et al*., 2006), microfilament alignment (Cai *et al*., 2005) and wire-heating (Huang *et al*., 2005). Most of these manufacturing methods are based on the use of additional chemicals and/or polymeric fibres or metal wires, which are incorporated into the scaffold architecture and then removed, e.g. through solvents or thermal separation processes, to

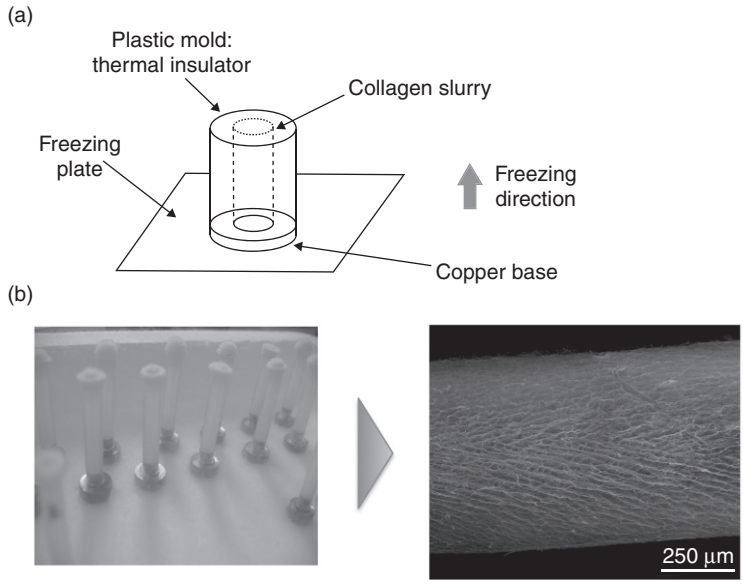

4.3 Synthesis of cylindrical collagen-based scaffolds with uniaxially orientated pores. (a) Schematization of the ideal uniaxial freezing process. (b) Real freezing process. A certain radial component of pore orientation can be obtained if the collagen slurry is not perfectly insulated along the radial direction, during the freezing (left: photograph of the non-ideal freezing process of a collagen slurry, by means of liquid nitrogen; right: resulting microstructure visualized by electron microscopy).

obtain the desired pore structure. However, the use of additional chemicals and/or complex fabrication methods is not recommended in terms of device safety and biocompatibility.

Aligned fibrous matrices, instead of foam-like ones, have also been investigated, based on collagen (Okamoto *et al.*, 2010), polyesters (Wang *et al.*, 2005; Hu, *et al.*, 2008) and silk (Yang *et al.*, 2007; Radtke *et al.*, 2011). With regard to collagen filaments used to bridge a rat sciatic nerve defect, a higher number of filaments was found to enhance the number of regenerated axons (Yoshii *et al.*, 2003), probably due to increased surface area and contact guidance. However, the packing density of fibres (i.e. the pore volume fraction of the fibrous filler), as well as their spatial distribution within the conduit, affects nerve regeneration (Ngo *et al.*, 2003). It has been recently argued that sponge-like matrices, with aligned microchannels over the entire length, might be more suitable for nerve regeneration than fibrous scaffolds (Spivey *et al.*, 2012). This hypothesis is based on the consideration that, regardless of fibre packing, fibres cannot be aligned over macroscale distances, thus do not provide continuous channels able to mimic the

morphology of the fibrin cable and/or the endoneurial tubes accommodating Schwann cells. A pioneering comparative study by Toba and colleagues (Toba *et al.*, 2001) attempted to analyse nerve regeneration achieved by either collagen fibres or an orientated collagen sponge, used as luminal fillers for PLA conduits along a 80 mm gap in a canine peroneal nerve. The study showed that there was no difference in regenerative efficacy between the two fillers, although in both cases axonal regeneration in the distal end was poor and functional recovery was not assessed.

4.4 Methods of assessing nerve regeneration and overview of porous scaffolds

As discussed above, the implant of a graft between the stumps of a transected nerve might suffice to induce a certain axonal regeneration. However, the quality of induced nerve regeneration is deeply affected by the following: (a) the properties of the graft, such as permeability, surface area, contact guidance, degradation rate and mechanical stiffness; and (b) the gap size (i.e. graft length and diameter), since, for a given animal model with critical defect length and for a selected device, the quality of nerve regeneration is found to decrease as the gap increases.

In order to analyse and compare the regenerative capability of different devices, a gap value equal to or larger than the critical size should be fixed, and nerve regeneration achievable in the distal end (if any) should be evaluated, together with reinnervation of the target muscle. In this section, after presenting the methods by which nerve regeneration can be assessed, we focus on the use of porous scaffolds in PNS regenerative medicine, stressing the reasons for the existing gap between experimental and clinical settings.

4.4.1 Evaluation methods

Nerve regeneration should be evaluated both morphologically and functionally, by comparing specific properties of the regenerated nerve graft with those of a normal or intact nerve. Some morphological and functional evaluation methods are briefly presented in the following, with the aim of providing a few basic elements for a correct interpretation of PNS regeneration data encountered in the literature.

Morphological analysis

Nerve histology is traditionally orientated to the assessment of nervous tissue regeneration. To this aim, key parameters to be evaluated are the number and diameter of myelinated axons, the thickness of the myelin sheath (expressed in terms of G-ratio, i.e. the ratio of the axon diameter to the

myelinated fibre diameter), and the ratio of the total myelinated fibre area to the total nerve tissue area (i.e. the so-called N-ratio). Experimental evidence suggests that axon remyelination during regeneration is impaired, leading to thinner myelinated axons (Dyck *et al.*, 2005), even though some myelinated tissue remodelling occurs in the long term (Archibald *et al.*, 1995; Chamberlain *et al.*, 2000). Values of G-ratio of about 0.7 are reported for normal rat nerves (Raimondo *et al.*, 2009), and G-ratios of regenerated nerves are usually far below the normal values (Dyck *et al.*, 2005). Even when normal values of G-ratios have been reported for the regenerated nerve trunk in the long term (den Dunnen *et al.*, 1993), functional recovery remains poor. This finding suggests that morphological analysis only of nerve tissue is not sufficient to demonstrate proper and full nerve regeneration, and functional analysis is thus additionally required.

From a morphological point of view, it is worth pointing out that regenerated and normal nerves differ also in their stromal tissues. Clear evidence of *in vivo* regeneration of physiological endoneurium and epineurium has not been shown (Yannas, 2001). The absence or improper formation of those tissues might explain, at least in part, the poor functional outcome of the regenerated nerve. Histology should thus be orientated to the assessment of regeneration of non-neuronal tissues as well.

Non-invasive magnetic resonance neurography can be implemented to evaluate nerve damage and/or regeneration, in addition to histology and electrophysiology (Cudlip *et al.*, 2002; Bendszus *et al.*, 2004; Hsu *et al.*, 2011).

Functional analysis

Electrophysiological measurements, which include sensory and motor nerve conduction, electromyography, spinal reflex tests, and motor and sensory evoked potentials (SEP), provide quantitative analysis of nerve function. Non-invasive methods, in particular, allow serial assessments of nerve regeneration and are directed to the evaluation of the compound muscle action potential (CMAP), which records the function of the target muscle following nerve stimulation, and the nerve conduction velocity (NCV). In the rat sciatic nerve model, the targets frequently used are the gastrocnemius, tibial or plantar muscles. Most studies show significant differences between the normal and regenerated nerves, with normal nerve usually having shorter latency and higher amplitude of CMAP (the latency and amplitude are often expressed as the ratio of the experimental side to the contralateral side) (Yannas, 2001). The NCV, measured along the nerve graft, is calculated as the ratio of the conducting distance and the latency time to the peak of the maximal action potential (Navarro and Udine, 2009). The NCV of a regenerated nerve is typically lower than that of normal nerves (Chamberlain

et al., 1998b). However, NCV values are strongly dependent on temperature and on evaluation time for the same animal, thus CMAP measurement is considered more meaningful than NCV one (Navarro and Udine, 2009).

Functional recovery can be evaluated also by kinematic gait analysis, which has been well established in the last decades, especially for the rat model. Sciatic functional index (SFI) calculation is based on the measurements of rat footprints in a walkway (de Medinaceli *et al*., 1982; Varejão *et al*., 2001). Video analysis and computerized technologies have been developed to allow for the measurement of dynamic and static gait parameters.

4.4.2 Current and 'next generation' porous scaffolds in peripheral nervous system (PNS) regenerative medicine

Although no tubular device has shown superior effectiveness compared to the nerve autograft, several guidance conduits, based either on natural or synthetic biomaterials, are currently available for clinical use (Kehoe *et al*., 2012), with inner diameters up to 10 mm and lengths up to 40 mm (with the longest size usually available for the smallest inner diameter). Conduits are indeed adopted for the treatment of small defects in small-diameter nerves (e.g. digital and radial sensory nerves). Good functional recovery has been reported so far for specific devices, at least in some treated patients (Bushnell *et al*. 2008; Farole and Jamal, 2008; Meek and Coert, 2008). A comprehensive review on the clinical applications and outcomes of available conduits for PNS regeneration has been recently published and is suggested for further reading (Kehoe *et al*., 2012). In this context, the focus is on the optimization of biomaterial-based scaffolds for an effective clinical outcome of nerve regenerative medicine. First, it is worth highlighting that no specific tube wall microstructure is reported for the 'first generation' devices that are currently available (Fig. 4.4). The Neuragen® tube, which is the one with the largest number of prospective and retrospective clinical studies, is a collagen-based device with a random, cell-impermeable porosity in the tube wall, which shows a comparable efficacy to autograft for gaps up to 20 mm. The choice of a tubular scaffold, among those currently available for clinical use, should thus be based on the reported clinical results, when these are available, and/or on the evaluation of their degradation rate and mechanical properties. Although being widely employed, the Neuragen® tube requires 36–48 months to fully degrade, which is probably too long a time for optimal nerve regeneration and can make other 'fast'-degrading tubular devices more appealing (other resorbable nerve guidance conduits, currently available, show residence times *in vivo* ranging from 3 to 16 months).

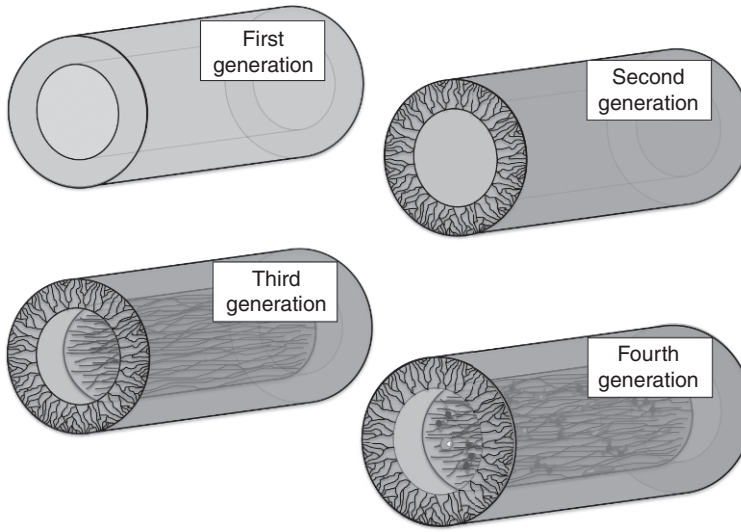

4.4 Scheme of current and next generation scaffolds for PNS regeneration. Second generation conduits differ from the current ones as they include specific porous patterns for optimized surface area and contact guidance. Third generation devices combine conduits and longitudinally orientated luminal fillers. Fourth generation devices include also exogenous molecules and/or cells.

As discussed above, relatively recent studies show that a more accurate design of conduit porosity and/or topography can potentially lead to improved nerve regeneration, in terms of axon remyelination and functional recovery, resulting from optimized surface area and contact guidance. Such 'second generation' devices are still matter of experimental investigation. Even when the positive effect of specific porous nano- and/or micropatterns in the tube walls has been demonstrated in animal models, further optimization of the fabrication methods is indeed required for translation to the clinical practice. In addition to the choice of a biocompatible material suitable for medical use, the fabrication method should be adjusted to fulfil the strict regulatory requirements concerning the production of implantable medical devices.

With specific regard to the design of conduits with luminal grooves for improved contact guidance, it is reasonable to hypothesize that orientated luminal fillers, instead of empty grooved conduits, are more capable of inducing nerve regeneration with functional recovery. Currently, no luminal fillers are used in clinical practice, in spite of the number of studies reporting their efficacy in enhancing nerve regeneration. In animal models, the bridgeable gap length has increased dramatically, when using a nerve conduit filled with either fibres or an aligned matrix, in the absence of any other exogenous

factor (i.e. cells and/or soluble molecular regulators). For example, a gap of 30 mm in the dog sciatic nerve has been bridged by using PGA filaments within a chitosan conduit, leading to a degree of functional recovery comparable to that of the autograft control (Wang *et al.*, 2005). Matsumoto and colleagues reported that a 8 cm long gap could be bridged in a dog model, with functional recovery, by using a PGA conduit filled with laminin coated collagen fibres (Matsumoto *et al.*, 2000). However, despite the encouraging animal results, the true evidence of the clinical efficacy of such 'third generation' devices seems hard to achieve.

First of all, translational research in PNS regeneration seems to be limited by the lack of standardization of experimental design. Very often, investigators choose arbitrarily the main variables of their experiments (i.e. animal species, gap length, time and location of observation along the regenerating nerve trunk). Moreover, many studies are performed without considering the presence of both a negative (i.e. silicone tube) and a positive (i.e. autograft) control, which can lead to erroneous or limited evaluations of the actual regenerative capability of a device. More importantly, in cases of complex device configurations (e.g. tubes with luminal fillers), the study of the efficacy of each part of the combined device is often missing, thus the evaluation of the effective contribution of a tube design or tube filling to regeneration cannot be performed. These limitations hinder the comprehension of the regenerative mechanisms induced by a specific device and make a comparison among different devices particularly challenging.

Finally, it is worth pointing out that the choice of the animal model seems to be extremely important and might explain, at least partially, the striking difference in PNS regeneration reported for animal and human nerves respectively, for given devices. The use of small animals (e.g. rat, mouse) for PNS injury is debatable, for both the much smaller gap sizes involved, compared to humans, and the superior neuroregeneration activity of rodents compared to higher mammals. Even if assuming that the speed of axonal growth in humans is comparable to that found in rodents, i.e. 1–4 mm/day (Williams *et al.*, 1983; Höke, 2006), such a speed would be unable to cover the entire gap length of the human nerve, before chronic denervation occurs in the distal stump (Höke, 2006). This observation confirms the importance of accelerating nerve regeneration along large gaps by means, for example, of porous luminal fillers inside a nerve guidance conduit, or by means of electrical stimulation (Gordon *et al.*, 2009).

4.5 Future trends

In spite of the conduits already available on the market for enhancing nerve regeneration, the poor clinical results suggest that there is yet a long way to go to achieve successful PNS regeneration with good functional recovery.

The intrinsic regenerative complexity of human nerves, which relates to the large gap volume to be bridged, highlights the need for an accurate design of both scaffolds and animal experiments.

The evolution from first generation guidance conduits to nano- or micro-patterned second generation ones appears feasible in the near future, if biocompatible fabrication methods are used and clear evidence of their safety and efficacy can be demonstrated in suitable animal models. With regard to the choice of the animal model, it has been recently suggested that rodent models would probably provide more reliable data for the development of novel therapies on humans if the evaluation of nerve regeneration was performed at relatively early time points, when differences between positive and negative control groups are still significant. Alternatively, the animal model could account for denervation of the distal segment before repair, i.e. a delayed repair (Shi *et al*., 2010). The timing of outcome measurement is thus an experimental variable that deeply affects the evaluation of PNS regeneration. This is why a standardization of observation times both in the short and in the long term, for given animal models, would be helpful for a deeper comprehension of nerve regeneration achieved by means of different devices. To the same aim, proteomic or genomic studies characterizing the response of PNS to the scaffold implant show promise for highlighting any key regenerative processes occurring within a given implant and/or undesired molecular patterns induced by the device (Jiménez *et al*., 2005; Bosse *et al*., 2006).

The experimental finding that no conduit has been so far superior to autograft seems to confirm that improvements in the scaffold design need to be addressed, including the possible use of biological stimuli, together with biomaterials, to restore nerve morphology and function. The use of orientated luminal fillers within guidance conduits, which would represent a third generation, assembled device for PNS regeneration, is probably a good strategy to follow and translate into the clinics especially for the treatment of large gaps, provided that the unique contribution of the filler to the regenerative capability of the entire device is clearly provided. The orientated matrix could also be used as a delivery vehicle for exogenous biological factors (i.e. cells and molecular regulators). As reported above, nerve conduits may indeed be unable to bridge large defects, due to a lower local concentration of soluble growth factors released by the nerve stumps. The delivery of exogenous molecules and/or cells to the injury site is thus expected to improve nerve regeneration and early functional outcome. According to the classification here presented, fourth generation devices for PNS regeneration are those that include exogenous bioactive agents in their design. Being very complex, the implementation in the clinical setting of such hybrid devices appears quite challenging and much more time consuming than that foreseen for biomaterial-only-based devices. Their clinical use for PNS regeneration thus seems unlikely in the near future.

4.6 Conclusion

PNS regeneration following nerve transection can be enhanced by implanting porous tubular scaffolds, either singularly or combined with cylindrical sponge-like or fibrous matrices with axially orientated pores. Although no device configuration has been found so far to lead to better regeneration compared to the nerve autograft, reported evidence suggests that an accurate design of scaffold porosity, aimed at optimizing surface area and contact guidance, can improve the functional outcome of next generation devices. Suitable animal models accounting for the larger defect size of human nerves might then help to predict a reliable clinical outcome, based on animal results.

4.7 References

Agrawal, C.M., McKinney, J.S., Lanctot, D. and Athanasiou, K.A. (2000). Effects of fluid flow on the *in vitro* degradation kinetics of biodegradable scaffolds for tissue engineering, *Biomaterials*, **21**(23), 2443–2452, DOI:10.1016/S0142-9612(00)00112-5.

Aldini, N.N., Perego, G., Cella, G.D., Maltarello, M.C., Fini, M., Rocca, M. and Giardino, R. (1996). Effectiveness of a bioresorbable conduit in the repair of peripheral nerves, *Biomaterials*, **17**, 959–962, DOI:10.1016/0142-9612(96)84669-2.

Apel, P.J., Garrett, J.P., Sierpinski, P., Ma, J., Atala, A., Smith, T.L., Koman, L.A. and Van Dyke, M.E. (2008). Peripheral nerve regeneration using a keratin-based scaffold: long-term functional and histological outcomes in a mouse model, *J Hand Surg*, **33**, 1541–1547, DOI:10.1016/j.jhsa.2008.05.034.

Archibald, S.J., Sheffner, J., Krarup, C. and Madison, R.D. (1995). Monkey median nerve repaired by nerve graft or collagen nerve guide tube, *J Neurosci*, **15**, 4109–4123.

Barnes, C.A., Brison, J., Michel R, Brown B.N., Castner D.G., Badylak S.F. and Ratner B.D. (2011). The surface molecular functionality of decellularized extracellular matrices, *Biomaterials*, **32**, 137–143, DOI: 10.1016/j.biomaterials.2010.09.007.

Bendszus, M., Wessig, C., Solymosi, L., Reiners, K. and Koltzenburg, M. (2004). MRI of peripheral nerve degeneration and regeneration: correlation with electrophysiology and histology, *Exp Neurol*, **188**, 171–177, DOI: 10.1016/j.expneurol.2004.03.025.

Borkenhagen, M., Stoll, R.C., Neuenschwander, P., Suter, U.W. and Aebischer, P. (1998). *In vivo* performance of a new biodegradable polyester urethane system used as a nerve guidance channel, *Biomaterials*, **19**, 2155–2165, DOI: 10.1016/S0142-9612(98)00122-7.

Bosse, F., Hasenpusch-Theil, K., Küry, P. and Müller, H.W. (2006). Gene expression profiling reveals that peripheral nerve regeneration is a consequence of both novel injury-dependent and reactivated developmental processes, *J Neurochem*, **96**, 1441–1457, DOI:10.1111/j. 1471-4159.2005.03635.x.

Bryan, D.J., Holway, A.H., Wang, K.K., Silva, A.E., Trantolo, D.J., Wise, D. and Summerhayes, I.C. (2000). Influence of glial growth factor and Schwann cells

in a bioresorbable guidance channel on peripheral nerve regeneration, *Tissue Eng*, **6**, 129–138, DOI:10.1089/107632700320757.

Bushnell, B.D., McWilliams, A.D., Whitener, G.B. and Messer, T.M. (2008). Early clinical experience with collagen nerve tubes in digital nerve repair, *J Hand Surg*, **33**, 1081–1087. DOI: 10.1016/j.jhsa.2008.03.015.

Cai, J., Peng, X., Nelson, K.D., Eberhart, R. and Smith, G.M. (2005). Permeable guidance channels containing microfilament scaffolds enhance axon growth and maturation, *J Biomed Mater Res A*, **75**, 374–386, DOI: 10.1002/jbm.a.30432.

Chamberlain, L.J., Yannas, I.V., Arrizabalaga, A., Hsu, H.-P., Norregaard, T.V. and Spector, M. (1998a). Early peripheral nerve healing in collagen and silicone tube implants: myofibroblasts and the cellular response, *Biomaterials*, **19**, 1393–1403. DOI: 10.1016/S0142-9612(98)00018-0.

Chamberlain, L.J., Yannas, I.V., Hsu, H.-P., Strichartz, G. and Spector M. (1998b). Collagen-GAG substrate enhances the quality of nerve regeneration through collagen tubes up to level of autograft, *Exp Neurol*, **154**, 315–329, DOI: 10.1006/exnr.1998.6955.

Chamberlain, L.J., Yannas, I.V., Hsu, H.-P. and Spector, M. (2000). Connective tissue response to tubular implants for peripheral nerve regeneration: the role of myofibroblasts, *J Comp Neurol*, **417**, 415–430, DOI: 10.1002/(SICI)1096-9861(20000221)417:4<415::AID-CNE3>3.0.CO;2–9.

Chang, A.S., Yannas, I.V., Krarup, C., Sethi, R.R., Norregaard, T.V. and Zervas, N.T. (1988). Polymeric templates for peripheral nerve regeneration. Electrophysiological study of functional recovery, *Proc ACS Div Polym Mater Sci Eng*, **59**, 906–910.

Chang, A.S., Yannas, I.V., Perutz, S., Loree, H., Sethi, R.R., Krarup, C., Norregaard, T.V., Zervas, N.T. and Silver, J. (1990). Electrophysiological study of recovery of peripheral nerves regenerated by a collagen-glycosaminoglycan copolymer matrix. In: Gebelein, C.G. (ed.), *Progress in Biomedical Polymers*. Plenum, New York.

Chang, C.J. and Hsu, S.H. (2006) The effect of high outflow permeability in asymmetric poly(D-L-lactic acid-co-glycolic acid) conduits for peripheral nerve regeneration, *Biomaterials*, **27**, 1035–1042, DOI: 10.1016/j.biomaterials.2005.07.003.

Chew, S.Y., Mi, R., Hoke, A. and Leong, K.W. (2007). Aligned protein-polymer composite fibers enhance nerve regeneration: a potential tissue-engineering platform, *Adv Funct Mater*, **17**, 1288–1296, DOI: 10.1002/adfm.200600441.

Chew, S.Y., Mi, R., Hoke, A. and Leong, K.W. (2008). The effect of the alignment of electrospun fibrous scaffolds on Schwann cell maturation, *Biomaterials*, **29**, 653–661, DOI: 10.1016/j.biomaterials.2007.10.025.

Cudlip, S.A., Howe, F.A., Griffiths, J.R. and Bell, B.A. (2002). Magnetic resonance neurography of peripheral nerve following experimental crush injury, and correlation with functional deficit, *J Neurosurg*, **96**, 755–775, DOI: 10.3171/jns.2002.96.4.0755.

Cui, T., Yan, Y., Zhang, R., Liu, L., Xu, W. and Wang, X. (2009). Rapid prototyping of a double-layer polyurethane-collagen conduit for peripheral nerve regeneration, *Tissue Eng Part C Methods*, **15**, 1–9, DOI:10.1089/ten.tec.2008.0354.

Daly, W., Yao, L., Zeugolis, D., Windebank, A. and Pandit, A. (2012). A biomaterials approach to peripheral nerve regeneration: bridging the peripheral nerve gap and enhancing functional recovery, *J R Soc Interface*, **9**, 202–221, DOI: 10.1098/rsif.2011.0438.

Dellinger, J.G., Wojtowicz, A.M. and Jamison, R.D. (2006). Effects of degradation and porosity on the load bearing properties of model hydroxyapatite bone scaffolds, *J Biomed Mater Res A*, **77**(3), 563–571, DOI: 10.1002/jbm.a.30658.

Dellon, A.L. and Mackinnon, S.E. (1988). Basic scientific and clinical applications of peripheral nerve regeneration, *Surg Ann*, **20**, 59–100.

de Medinaceli, L., Freed, W.J. and Wyatt, R.J. (1982). An index of the functional condition of rat sciatic nerve based on measurements made from walking tracks, *Exp Neurol*, **77**, 634–643, DOI: 10.1016/0014-4886(82)90234-5.

den Dunnen W.F.A., van der Lei, B., Schakenraad, J.M., Blaauw E.H., Stokroos, I., Pennings, A.J. and Robinson, P.H. (1993). Long-term evaluation of nerve regeneration in a biodegradable nerve guide, *Microsurg*, **14**, 508–515, DOI: 10.1002/micr.1920140808.

Drury, J.L. and Mooney, D.J. (2003). Hydrogels for tissue engineering: scaffold design variables and applications, *Biomaterials*, **24**(24), 4337–4351, DOI:10.1016/S0142-9612(03)00340-5.

Dyck, P.J., Dyck, P.J.B. and Engelstad, J.N. (2005). Pathological alterations of nerves. Schwann cell regulation of extracellular matrix biosynthesis and assembly. In: Dick, P.J. and Thomas, P.K. (eds.), *Peripheral Neuropathy*. 733–829. W.B Saunders, Philadelphia.

Evans, G.R.D., Brandt, K., Katz, S., Chauvin, P., Otto, L., Bogle, M., Wang, B., Meszlenyi R.K., Lu, L., Mikos, A.G. and Patrick C.W.Jr. (2002). Bioactive poly(l-lactic acid) conduits seeded with Schwann cells for peripheral nerve regeneration, *Biomaterials*, **23**, 841–848, DOI: 10.1016/S0142-9612(01)00190-9.

Farole, A. and Jamal, B.T. (2008). A bioabsorbable collagen nerve cuff (NeuraGen) for repair of lingual and inferior alveolar nerve injuries: a case series, *J Oral Maxil Surg*, **66**, 2058–2062, DOI: 10.1016/j.joms.2008.06.017.

Flynn, L., Dalton, P.D. and Shoichet, M.S. (2003). Fiber templating of poly (2-hydroxyethyl methacrylate) for neural tissue engineering, *Biomaterials*, **24**, 4265–4272, DOI:10.1016/S0142-9612(03)00334-X.

Friess, W. (1998). Collagen – biomaterial for drug delivery, *Eur J Pharm Biopharm*, **45**, 113–136, DOI: 10.1016/S0939-6411(98)00017-4.

Fu, S.Y. and Gordon, T. (1997). The cellular and molecular basis of peripheral nerve regeneration. *Mol Neurobiol*, **14**, 67e116, DOI: 10.1007/BF02740621.

Gordon, T., Chan, K.M., Sulaiman, O.A., Udina, E., Amirjani, N. and Brushart, T.M. (2009). Accelerating axon growth to overcome limitations in functional recovery after peripheral nerve injury, *Neurosurg*, **65**, A132–A144, DOI: 10.1227/01.NEU.0000335650.09473.D3.

Harley, B.A., Spilker, M.H., Wu, J.W., Asano, K., Hsu, H.-P., Spector, M. and Yannas, I.V. (2004). Optimal degradation rate for collagen chambers used for regeneration of peripheral nerves over long gaps, *Cells Tissues Organs*, **176**, 153–165, DOI: 10.1159/000075035.

Harley, B.A., Hastings, A.Z., Yannas, I.V. and Sannino, A. (2006). Fabricating tubular scaffolds with a radial pore size gradient by a spinning technique, *Biomaterials*, **27**, 866–874, DOI: 10.1016/j.biomaterials.2005.07.012.

Höke, A. (2006). Mechanisms of disease: what factors limit the success of peripheral nerve regeneration in humans?, *Nat Clin Pract Neuro*, **2**, 448–454, DOI:10.1038/ncpneuro0262.

Hsu, S.H., Su, C.H. and Chiu, I.M. (2009). A novel approach to align adult neural stem cells on micropatterned conduits for peripheral nerve regeneration: a feasibility study, *Artif Organs*, **33**, 26–35, DOI: 10.1111/j.1525-1594.2008.00671.x.

Hsu, S.H., Chan, S.H., Chiang, C.M., Chenand, C.C.C. and Jiang, C.F. (2011). Peripheral nerve regeneration using a microporous polylactic acid asymmetric conduit in a rabbit long-gap sciatic nerve transection model, *Biomaterials*, **32**, 3764–3775, DOI: 10.1016/j.biomaterials.2011.01.065.

Hu, W., Gu, J., Deng, A. and Gu, X. (2008). Polyglycolic acid filaments guide Schwann cell migration *in vitro* and *in vivo*, *Biotechnol Lett*, **30**, 1937–1942, DOI: 10.1007/s10529-008-9795-1.

Huang, Y.C., Huang, Y.Y., Huang, C.C. and Liu, H.C. (2005). Manufacture of porous polymer nerve conduits through a lyophilizing and wire-heating process, *J Biomed Mater Res B Appl Biomater*, **74**(1), 659–664, DOI: 10.1002/jbm.b.30267.

Itoh, S., Takakuda, K., Kawabata, S., Aso, Y., Kasai, K., Itoh, H. and Shinomiya, K. (2002). Evaluation of cross-linking procedures of collagen tubes used in peripheral nerve repair, *Biomaterials*, **23**, 4475–4481, DOI: 10.1016/S0142-9612(02)00166-7.

Jeong, C.G., Zhang, H. and Hollister S.J. (2011). Three-dimensional poly(1,8-octanediol–co-citrate) scaffold pore shape and permeability effects on sub-cutaneous *in vivo* chondrogenesis using primary chondrocytes, *Acta Biomater*, **7**, 505–514, DOI: 10.1016/j.actbio.2010.08.027.

Jiang, X., Lim, S.H., Mao, H.-Q. and Chew, S.Y. (2010). Current applications and future perspectives of artificial nerve conduits, *Exper Neurol*, **223**, 86–101, DOI: 10.1016/j.expneurol.2009.09.009.

Jiménez, C. R., Stam, F. J., Li, K. W., Gouwenberg, Y., Hornshaw, M. P., De Winter, F., Verhaagen, J. and Smit, A.B. (2005). Proteomics of the injured rat sciatic nerve reveals protein expression dynamics during regeneration, *Mol Cell Proteomics*, **4**, 120–132, DOI:10.1074/mcp. M400076-MCP200.

Karande, T.S., Ong, J.L. and Agrawal, C.M. (2004). Diffusion in musculoskeletal tissue engineering scaffolds: design issues related to porosity, permeability, architecture, and nutrient mixing, *Ann Biomed Eng*, **32**(12), 1728–1743, DOI: 10.1007/s10439-004-7825-2.

Kataoka, K., Suzuki, Y., Kitada, M., Ohnishi, K., Suzuki, K., Tanihara, M., Ide, C., Endo, K. and Nishimura, Y. (2001). Alginate, a bioresorbable material derived from brown seaweed, enhances elongation of amputated axons of spinal cord in infant rats. *J Biomed Mater Res*, **54**, 373–384, DOI: 10.1002/1097-4636(20010305)54:3<373::AID-JBM90>3.0.CO;2-Q.

Katoh, K., Tanabe, T. and Yamauchi, K. (2004). Novel approach to fabricate keratin sponge scaffolds with controlled pore size and porosity, *Biomaterials*, **25**, 4255–4262, DOI: 10.1016/j.biomaterials.2003.11.018.

Kehoe, S., Zhang, X.F. and Boyd, D. (2012). FDA approved guidance conduits and wraps for peripheral nerve injury: a review of materials and efficacy, *Injury Int J Care Injured*, **43**, 553–572, DOI:10.1016/j.injury.2010.12.030.

Kim, B.S., Yoo, J.J. and Atala, A. (2004). Peripheral nerve regeneration using acellular nerve grafts, *J Biomed Mater Res A*, **68**(2), 201–209, DOI: 10.1002/jbm.a.10045.

Kim, Y.T., Haftel, V.K., Kumar, S. and Bellamkonda, R.V. (2008). The role of aligned polymer fiber-based constructs in the bridging of long peripheral nerve gaps, *Biomaterials*, **29**, 3117–3127, DOI: 10.1016/j.biomaterials.2008.03.042.

Kuberka, M., Von Heimburg, D., Schoof, H., Heschel, I. and Rau, G. (2002). Magnification of the pore size in biodegradable collagen sponges, *Int J Artif Organs*, **25**(1), 67–73.

Li, S., de Wijn, J.R., Li, J., Layrolle, P. and de Groot, K. (2003). Macroporous biphasic calcium phosphate scaffold with high permeability/porosity ratio, *Tissue Eng*, **9**(3), 535–548, DOI:10.1089/107632703322066714.

Lin, A.S.P., Barrows, T.H., Cartmell, S.H. and Guldberg, R.E. (2003). Microarchitectural and mechanical characterization of oriented porous polymer scaffolds, *Biomaterials*, **24**, 481–489, DOI: 10.1016/S0142-9612(02)00361-7.

Louie, L.K. (1997). Effect of a porous collagen-glycosaminoglycan copolymer on early tendon healing in a novel animal model. Thesis Ph. D. – Massachusetts Institute of Technology Dept. of Materials Science and Engineering. 196 leaves p.

Loree, H.M. (1988). A freeze-drying process for fabrication of polymeric bridges for peripheral nerve regeneration. Thesis M.S. – Massachusetts Institute of Technology Dept. of Mechanical Engineering. 106 leaves p.

Lundborg, G., Dahlin, L.B. and Danielsen, N. (1991). Ulnar nerve repair by the silicone chamber technique, *Scand J Plast Reconstr Hand Surg*, **25**, 79–82, DOI: 10.3109/02844319109034927.

Lundborg, G., Rosén, B., Abrahamson, S.O., Dahlin, L. and Danielsen, N. (1994). Tubular repair of the median nerve in the human forearm, *J Hand Surg (Br Eur)*, **19B**, 273–276, DOI: 10.1016/0266-7681(94)90068-X.

Mackinnon, S.E., Dellon, A.N., Hudson, A.R. and Hunter, D.A. (1984). Chronic nerve compression – an experimental model in the rat, *Ann Plast Surg*, **13**, 112–120.

Madaghiele, M., Sannino, A., Yannas, I.V. and Spector, M. (2008). Collagen-based matrices with axially oriented pores, *J Biomed Mater Res*, **85A**, 757–767, DOI: 10.1002/jbm.a.31517.

Martini R. (1994). Expression and functional roles of neural cell surface molecules and extracellular matrix components during development and regeneration of peripheral nerves. *J Neurocytol*, **23**, 1–28, DOI: 10.1007/BF01189813.

Matsumoto, K., Ohnishi, K., Kiyotani, T., Sekine, T., Ueda, H., Nakamura, T., Endo, K. and Shimizu, Y. (2000). Peripheral nerve regeneration across an 80-mm gap bridged by a polyglycolic acid (PGA)-collagen tube filled with laminin-coated collagen fibers: a histological and electrophysiological evaluation of regenerated nerves, *Brain Res*, **868**, 315–328, DOI: 10.1016/S0006-8993(00)02207-1.

Meek, M.F. and Coert, J.H. (2008). US Food and Drug Administration/ Conformit Europe-approved absorbable nerve conduits for clinical repair of peripheral and cranial nerves, *Ann Plast Surg*, **60**, 466–472, DOI: 10.1097/SAP.0b013e31804d441c.

Meek, M.F. and den Dunnen, W.F. (2009). Porosity of the wall of a Neurolac nerve conduit hampers nerve regeneration, *Microsurg*, **29**, 473–478, DOI: 10.1002/micr.20642.

Merle, M., Dellon, A.N., Campbell, J.N. and Chang, P.S. (1989). Complications from silicone-polymer intubulation of nerves, *Microsurgery*, **10**, 130–133. DOI: 10.1002/micr.1920100213.

Moore, A.M., Kasukurthi, R., Magill, C.K., Farhadi, F., Borschel, G.H. and Mackinnon, S.E. (2009). Limitations of conduits in peripheral nerve repairs, *Hand*, **4**, 180–186, DOI: 10.1007/s11552-008-9158-3.

Moore, M.J., Friedman, J.A., Lewellyn, E.B., Mantila, S.M., Krych, A.J., Ameenuddin, S., Knight, A.M., Lu, L., Currier, B.L., Spinner, R.J., Marsh, R.W., Windebank, A.J. and Yaszemski, M.J. (2006). Multiple-channel scaffolds to promote spinal cord axon regeneration, *Biomaterials*, **27**(3), 419–429, DOI: 10.1016/j.biomaterials.2005.07.045.

Muschler, G.F., Nakamoto, C. and Griffith, L.G. (2004). Engineering principles of clinical cell-based tissue engineering, *J Bone Joint Surg Am*, **86-A**(7), 1541–1558.

Navarro, X. and Udine, E. (2009). Methods and protocols in peripheral nerve regeneration experimental research: Part III. Electrophysiological evaluation, *Int Rev Neurobiol*, **87**, 105–126, DOI: 10.1016/S0074-7742(09)87006-2.

Ngo, T.-T. B., Waggoner, P. J., Romero, A. A., Nelson, K. D., Eberhart, R. C. and Smith, G. M. (2003). Poly(L-lactide) microfilaments enhance peripheral nerve regeneration across extended nerve lesions, *J Neurosci Res*, **72**, 227–238, DOI:10.1002/jnr.10570.

O'Brien, F.J., Harley, B.A., Yannas, I.V. and Gibson L. (2004). Influence of freezing rate on pore structure in freeze-dried collagen-GAG scaffolds, *Biomaterials*, **25**(6), 1077–1086, DOI: 10.1016/S0142-9612(03)00630-6.

Oh, S.H. and Lee, J.H. (2007). Fabrication and characterization of hydrophilized porous PLGA nerve guide conduits by a modified immersion precipitation method, *J Biomed Mater Res*, **80A**, 530–538, DOI: 10.1002/jbm.a.30937.

Okamoto, H., Hata, K., Kagami, H., Okada, K., Ito, Y., Narita, Y., Hirata, H., Sekiya I., Otsuka, T. and Ueda, M. (2010). Recovery process of sciatic nerve defect with novel bioabsorbable collagen tubes packed with collagen filaments in dogs, *J Biomed Mater Res*, **92A**, 859–868, DOI: 10.1002/jbm.a.32421.

Pek, Y.S., Spector, M., Yannas, I.V. and Gibson, L.J. (2004). Degradation of a collagen-chondroitin-6-sulfate matrix by collagenase and by chondroitinase, *Biomaterials*, **25**, 473–482, DOI:10.1016/S0142-9612(03)00541-6.

Radtke, C., Allmeling, C., Waldmann, K.-H., Reimers, K., Thies, K., Schenk, H.C., Hillmer, A., Guggenheim, M., Brandes, G. and Vogt, P.M. (2011). Spider silk constructs enhance axonal regeneration and remyelination in long nerve defects in sheep, *PLOS ONE*, **6**(2), e16990, DOI:10.1371/journal.pone.0016990.

Raimondo, S., Fornaro, M., Di Scipio, F., Ronhi, G., Giacobini-Robecchi, M.G. and Geuna, S. (2009). Methods and protocols in peripheral nerve regeneration experimental research: Part II – morphological techniques, *Int Rev Neurobiol*, **87**, 81–103, DOI: 10.1016/S0074-7742(09)87005-0.

Sannino, A., Silvestri, L., Madaghiele, M., Harley, B.A. and Yannas, I.V. (2010). Modeling the fabrication process of micropatterned macromolecular scaffolds for peripheral nerve regeneration, *J Appl Polym Sci*, **116**, 1879–1888, DOI: 10.1002/app.31715.

Schoof, H., Bruns, L., Fischer, A., Heschel, I. and Rau, G. (2000). Dendritic ice morphology in unidirectionally solidified collagen suspensions, *J Crystal Growth*, **209**, 122–129, DOI: 10.1016/S0022-0248(99)00519-9.

Schoof, H., Apel, J., Heschel, I. and Rau, G. (2001). Control of pore structure and size in freeze-dried collagen sponges, *J Biomed Mater Res (Appl Biomater)*, **58**, 352–357, DOI: 10.1002/jbm.1028.

Shi, W., Yao, J., Chen, X., Lin, W., Gu, X. and Wang, X. (2010). The delayed repair of sciatic nerve defects with tissue engineered nerve grafts in rats, *Artif Cells Blood Substit Immobil Biotechnol*, **38**, 29–37, DOI:10.3109/10731190903495751.

Sierpinski, P., Garrett, J., Ma, J., Apel, P., Klorig, D., Smith, T., Koman, L.A., Atala, A. and Van Dyke, M. (2008). The use of keratin biomaterials derived from human hair for the promotion of rapid regeneration of peripheral nerves, *Biomaterials*, **29**, 118–128, DOI: 10.1016/j.biomaterials.2007.08.023.

Sinha, V.R. and Trehan, A. (2003). Biodegradable microspheres for protein delivery, *J Control Release*, **90**(3), 261–280, DOI: 10.1016/S0168-3659(03)00194-9.

Subramanian, A., Krishnan, U.M. and Sethuraman, S. (2011). Fabrication of uniaxially aligned 3D electrospun scaffolds for neural regeneration, *Biomed Mater*, **6**, 025044 (10 pp), DOI:10.1088/1748-6041/6/2/025004.

Spivey, E.C., Khaing, Z.Z., Shear, J.B. and Schmidt, C.E. (2012). The fundamental role of subcellular topography in peripheral nerve repair therapies, *Biomaterials*, **33**, 4264–4276, DOI:10.1016/j.biomaterials.2012.02.043.

Stang, F., Fansa, H., Wolf, G., Reppin, M. and Keilhoff, G. (2005). Structural parameters of collagen nerve grafts influence peripheral nerve regeneration, *Biomaterials*, **26**, 3083–3091, DOI:10.1016/j.biomaterials.2004.07.060.

Stang, F., Keilhoff, G. and Fansa, H. (2009). Biocompatibility of different nerve tubes, *Materials*, **2**, 1480–1507, DOI:10.3390/ma2041480.

Stanec, S. and Stanec, Z. (1998). Ulnar nerve reconstruction with an expanded polytetrafluoroethylene conduit, *Br J Plast Surg*, **51**, 637–639, DOI: 10.1054/bjps.1998.9996.

Stokols, S. and Tuszynski, M.H. (2004). The fabrication and characterization of linearly oriented nerve guidance scaffolds for spinal cord injury, *Biomaterials*, **25**(27), 5839–5846, DOI:10.1016/j.biomaterials.2004.01.041.

Stokols, S. and Tuszinsky, M.H. (2006). Freeze-dried agarose scaffolds with uniaxial channels stimulate and guide linear axonal growth following spinal cord injury, *Biomaterials*, **27**, 443–451, DOI:10.1016/j.biomaterials.2005.06.039.

Toba, T., Nakamura, T., Shimizu, Y., Matsumoto, K., Ohnishi, K., Fukuda, S., Yoshitani, M., Ueda, H., Hori, Y. and Endo, K. (2001). Regeneration of canine peroneal nerve with the use of a polyglycolic acid-collagen tube filled with laminin-soaked collagen sponge: a comparative study of collagen sponge and collagen fibers as filling materials for nerve conduits, *J Biomed Mater Res*, **58**, 622–630, DOI:10.1002/jbm.1061.

Van Bael, S., Chai, Y.C., Truscello, S., Moesen, M., Kerckhofs, G., Van Oosterwyck, H., Kruth, J.-P. and Schrooten J. (2012). The effect of pore geometry on the *in vitro* biological behavior of human periosteum-derived cells seeded on selective laser-melted Ti6Al4V bone scaffolds, *Acta Biomater*, **8**, 2824–2834, DOI:10.1016/j.actbio.2012.04.001.

Varejão, A.S.P., Meek, M.F., Ferreira, A.J.A., Patrício, J.A.B. and Cabrita, A.M. (2001). Functional evaluation of peripheral nerve regeneration in the rat: walking track analysis. *J Neurosci Methods*, **108**, 1–9, DOI: 10.1016/S0165-0270(01)00378-8.

Vleggeert-Lankamp, C.L.A.M., Ruiter, G.C.W., Wolfs, J.F.C., Pego, A.P., Berg, R.J. v.d., Feirabend, H.K.P., Malessy, M.J.A. and Lakke, E.A.J.F. (2007). Pores in synthetic nerve conduits are beneficial to regeneration, *J Biomed Mater Res*, **80A**, 965–982, DOI: 10.1002/jbm.a.30941.

Wang, S., Wan, A.C., Xu, X., Gao, S., Mao, H.Q., Leong, K.W. and Yu, H. (2001). A new nerve guide conduit material composed of a biodegradable poly(phosphoester), *Biomaterials*, **22**, 1157–1169, DOI: 10.1016/S0142-9612(00)00356-2.

Wang, W., Itoh, S., Matsuda, A., Ichinose, S., Shinomiya, K., Hata, Y. and Tanaka, J. (2007). Influences of mechanical properties and permeability on chitosan nano/microfiber mesh tubes as a scaffold for nerve regeneration, *J Biomed Mater Res*, **84A**, 557–566, DOI: 10.1002/jbm.a.31536.

Wang, X., Hu, W., Cao, Y., Yao, J., Wu, J. and Gu, X. (2005). Dog sciatic nerve regeneration across a 30-mm defect bridged by a chitosan/PGA artificial nerve graft, *Brain*, **128**, 1897–1910, DOI: 10.1093/brain/awh517.

Weber, R.A., Breidenbach, W.C., Brown, R.E., Jabaley, M.E. and Mass, D.P. (2000). A randomized prospective study of polyglycolic acid conduits for digital nerve reconstruction in humans, *Plast Reconstr Surg*, **106**, 1036–1045.

Williams, L.R., Longo F.M., Powell, H.C., Lundborg, G. and Varon, S (1983). Spatial-temporal progress of peripheral nerve regeneration within a silicone chamber: parameters for a bioassay, *J Comp Neurol*, **218**, 460–470, DOI: 10.1002/cne.902180409.

Wu, L. and Ding, J. (2005). Effects of porosity and pore size on *in vitro* degradation of three-dimensional porous poly(D,L-lactide-co-glycolide) scaffolds for tissue engineering, *J Biomed Mater Res A*, **75**(4), 767–777, DOI: 10.1002/jbm.a.30487.

Xie, F., Li, Q.F., Gu, B., Liu, K. and Shen, G.X. (2008). *In vitro* and *in vivo* evaluation of a biodegradable chitosan-PLA composite peripheral nerve guide conduit material, *Microsurg*, **28**, 471–479, DOI: 10.1002/micr.20514.

Yannas, I.V. (2001), *Tissue and Organ Regeneration in Adults*, Springer, New York.

Yang, S., Leong, K.F., Du, Z. and Chua, C.K. (2001). The design of scaffolds for use in tissue engineering. Part I. Traditional factors, *Tissue Eng*, **7**(6), 679–689, DOI: 10.1089/107632701753337645.

Yang, Y., Ding, F., Wu, J., Hu, W., Liu, W., Liu, J. and Gu, X. (2007). Development and evaluation of silk fibroin-based nerve grafts for use in peripheral nerve regeneration, *Biomaterials*, **28**, 5526–5535, DOI:10.1016/j.biomaterials.2007.09.001.

Yao, L., Billiar, K., Windebank, A.J. and Pandit, A. (2010). Multi-channelled collagen conduits for peripheral nerve regeneration: design, fabrication and characterization, *Tissue Eng Part C*, **16**(6), 1585–1596, DOI:10.1089/ten.tec.2010.0152.

Yoshii, S., Oka, M., Shima, M., Taniguchi, A. and Akagi, M. (2003). Bridging a 30-mm nerve defect using collagen filaments, *J Biomed Mater Res*, **67A**, 467–474, DOI: 10.1002/jbm.a.10103.

Zmora, S., Glicklis, R. and Cohen, S. (2002). Tailoring the pore architecture in 3-D alginate scaffolds by controlling the freezing regime during fabrication, *Biomaterials*, **23**, 4087–4094, DOI: 10.1016/S0142-9612(02)00146-1.

5

Tailoring properties of polymeric biomedical foams

E. M. PRIETO and S. A. GUELCHER,
Vanderbilt University, USA

DOI: 10.1533/9780857097033.1.129

Abstract: Synthetic polymers are versatile materials that can be processed into biomedical foams with a wide range of mechanical, thermal, and degradation properties. Tailoring of these properties can be achieved by using different polymeric families such as polyesters, polyurethanes, and tyrosine-derived polymers. Final properties also depend on the porous structure achieved. Foaming techniques such as porogen leaching, gas foaming, emulsion templating, and thermal induced phase separation each offer different ways to control pore structure. The current chapter focuses on polymeric biomedical foam formulations based on synthetic polymers with macropores and offers perspectives on future directions in the advancement of polymeric biomedical foam formulations.

Key words: synthetic polymer foams, macropores, polymer foaming, biomedical foams, foam characterization.

5.1 Introduction

As tissue engineering constructs evolved from inert materials that offered support to bioactive scaffolds that degrade as new tissue is developed, synthetic polymers have been widely studied as matrix materials for different biomedical applications. Resorbable polymers degrade in the body and can be processed using various techniques (Liu and Ma, 2004). In order to promote tissue regeneration, polymeric scaffolds must be biocompatible, degrade into nontoxic products at a rate matching that of new tissue deposition, have mechanical properties in the range of the surrounding host tissue, and allow the diffusion of nutrients to the interior of the scaffold to support cellular infiltration (Nair and Laurencin, 2007). Polymeric foams with interconnected pores provide continuous channels with increased surface area through which cells can migrate and infiltrate the material. According to the foaming technique used, different processing times and final porous structures can be obtained. This versatility has allowed polymeric foams to be developed for different biomedical applications such as skin, cartilage,

and bone scaffolds, each of which has different requirements. In addition, polymeric foams have also been used as delivery vehicles for growth factors or cells. The release mechanism of biologics can be controlled by encapsulation, tailored polymeric degradation, or attachment of signaling molecules to the polymer surface.

The scope of this chapter includes polymeric biomedical foam formulations based on synthetic polymers with macropores (pore size > 50 μm). A summary of polymers used extensively in foam formulation is presented, which discusses chemical compositions, synthesis routes, as well as thermal and degradation properties of the materials. The chapter continues with a review of current foaming and characterization techniques, a summary of applications in tissue engineering, and perspectives on future trends that will continue to advance the field.

5.2 Aliphatic polyesters used for porous scaffold fabrication

Polyesters are among the most studied biodegradable materials for biomedical applications (Agrawal and Ray, 2001; Liu and Ma, 2004; Nair and Laurencin, 2007; Pan and Ding, 2012). The degradation profiles and mechanical properties of polyesters can be tailored according to the final application by modifying the backbone composition. Due to this versatility, polyester foams have been developed as scaffolds for bone, cartilage, and meniscus, among other applications (Farng and Sherman, 2004; Nair and Laurencin, 2007).

Polylactic acid (PLA), polyglycolic acid (PGA), and PLA-PGA copolymer (PLGA) can be synthesized from the appropriate α-hydroxy acids through polycondensation, or from cyclic esters using ring opening polymerization (ROP) (Vaca-Garcia, 2008). ROP is often preferred since it generates higher molecular weights required to achieve target properties. Figure 5.1 shows cyclic monomers commonly used to synthesize PLA, PGA, and polycaprolactone (PCL) through ROP. Although there are several ROP catalysts that control the kinetics of the opening of cyclic esters, the most commonly used for biomedical applications are stannous octoate and stannous chloride, due to the minimal toxicity that they elicit at the doses found in biomaterials (Jamiolkowski and Dormier, 2006). ROP initiators usually contain hydroxyl active groups and can have different functionalities. The molecular weight of the final polymer is influenced by the amount of initiator used, not by its functionality, and higher concentrations of initiator generate lower molecular weight (Jamiolkowski and Dormier, 2006). Polyesters with increased branching are produced when an initiator with higher functionality is used.

The main degradation mechanism of polyesters is hydrolytic chain scission of the ester bonds in the backbone (Brannon-Peppas and Vert, 2000;

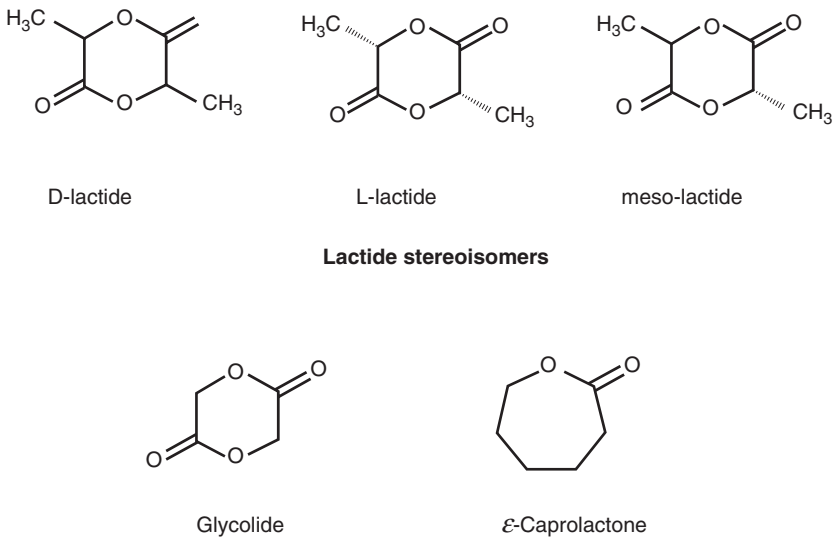

5.1 Cyclic monomers for the production of polyesters using ROP: Lactide (for PLA), Glycolide (for PGA), ε-Caprolactone (for PCL).

Agrawal and Ray, 2001; Nair and Laurencin, 2007; Vaca-Garcia, 2008). This process is a combination of diffusion–reaction–dissolution steps (Brannon-Peppas and Vert, 2000). As water diffuses into the scaffold it hydrolyzes accessible ester bonds. As a result, new carboxyl ends are generated, which in turn continue to catalyze the hydrolytic degradation. The molecular weight of the polymeric chains decreases until the fragments are capable of dissolving into the surrounding medium. Once dissolved, the fragments start diffusing toward the surface of the scaffold as they continue to degrade. At this stage the mechanical properties of the scaffold decrease and significant changes in weight loss are identified (Pan and Ding, 2012). The specific polyester formulation influences the rate of degradation by modifying the diffusion coefficient of water into the scaffold, the hydrolysis rate constant of the ester bonds, the diffusion coefficient of the polymeric fragments, and the solubility of the degradation products (Brannon-Peppas and Vert, 2000). Higher carboxylic acid concentration present in the interior of the scaffold accelerates the degradation rate of the bulk material compared to that of the surface. As a result, polyester foams have been reported to degrade more slowly than solid films (Pan and Ding, 2012).

5.2.1 Polyglycolide

PGA is a crystalline polymer (45–55%) with a glass transition temperature close to body temperature (35–40°C) and melting temperature between

225°C and 230°C depending on the molecular weight (Vaca-Garcia, 2008). Its high crystallinity provides PGA with excellent mechanical properties as well as low solubility in organic solvents (Nair and Laurencin, 2007; Vaca-Garcia, 2008). PGA has been processed into scaffolds for biomedical applications using extrusion, injection, compression molding, solvent casting, and specifically into foams using particulate leaching (Gunatillake *et al*., 2006) or fiber bonding (Mikos *et al*., 1993) techniques.

PGA is highly susceptible to the action of water and can also be degraded by esterases (Vaca-Garcia, 2008). Degradation studies have shown that the polymer loses its strength due to hydrolysis in 1–2 months, and loses mass within 6–12 months (Nair and Laurencin, 2007). Glycolic acid is the resulting degradation product, and it can be secreted in urine or as carbon dioxide and water after being processed in the tricarboxylic acid cycle (TCA) (Nair and Laurencin, 2007; Vaca-Garcia, 2008). Although glycolic acid is a natural metabolite, high acidic concentrations generated during PGA degradation can adversely affect the surrounding tissue.

5.2.2 Polylactide

Given the chirality of lactic acid, lactide monomer exists in three optically active forms: D-lactide, L-lactide, and meso-lactide (Fig. 5.1). Depending on the monomers used for polymerization, poly(L-lactic acid) (PLLA), poly(D-lactic acid) (PDLA), or poly(D,L-lactic acid) (PDLLA) are obtained with different crystalline structures and thermal properties. PLLA has a crystalline content of about 37% depending on molecular weight and processing parameters, a glass transition temperature in the range of 50°C to 80°C, and a melting temperature between 173°C and 178°C (Vaca-Garcia, 2008). On the other hand, the random distribution of D- and L-lactide units in PDLLA makes it an amorphous polymer with a glass transition temperature between 55°C and 60°C (Nair and Laurencin, 2007). Mainly due to the differences in crystallinity, PLLA exhibits higher mechanical properties than PDLLA. Porous PLA scaffolds have been developed using particulate leaching (Mikos *et al*., 1994), thermally induced phase separation (TIPS) (Nam and Park, 1999), and a combination of solvent casting and porogen leaching (Mikos and Temenoff, 2000; Ma and Choi, 2001) techniques.

In vivo, polylactides degrade into lactic acid, which can enter the TCA cycle and be subsequently secreted from the body as carbon dioxide (Agrawal and Ray, 2001). In comparison to PGA, the pendant methyl group in PLA increases the hydrophobicity of the material and shields the ester bonds from the effect of water (Jamiolkowski and Dormier, 2006). The resulting slower degradation rate of PLA makes it a more suitable material for orthopedic applications where healing times are longer than those required for

soft tissue (Jamiolkowski and Dormier, 2006). When hydrolyzed, PLLA has been reported to lose its strength after 6 months while PDLLA loses it after 1–2 months (Nair and Laurencin, 2007).

5.2.3 Poly(lactide-co-glycolide)

Polymers with intermediate properties can be obtained by copolymerizing glycolide and lactide monomers to obtain PLGA. By modifying the percentage of each monomer used, the final properties of the polymer can be tailored to specific applications. As a result, PLGA has been the most widely studied polyester for biomedical applications in the last 15 years. PLGA can be either semi-crystalline, with a melting temperature between 224°C and 226°C (Vaca-Garcia, 2008), or amorphous, depending on the ratio of lactide to glycolide monomers used during polymerization. Increasing the content of glycolide in the formulation has been shown to decrease the glass transition temperature and mechanical properties of the final PLGA (Pan and Ding, 2012). PLGA porous polymers have been obtained using solvent casting/porogen leaching (Mikos and Temenoff, 2000; Ma and Choi, 2001), gas foaming (Kim *et al*., 2006), super critical CO_2 foaming (Mooney *et al*., 1996; Nam and Park, 1999; Singh *et al*., 2004), phase separation (Zhang and Ma, 1999), thermal sintering/particle leaching (Amini *et al*., 2012), emulsion-freeze drying (Whang *et al*., 1995), three-dimensional printing (Zein *et al*., 2002), and electrospinning (Zeng *et al*., 2003) techniques.

Since PLGA contains both PLA and PGA, its degradation rate depends on the ratio of lactide to glycolide monomers, and can vary from months to years. The degradation rate also depends on the molecular weight, shape, structure, and porosity of the final product (Nair and Laurencin, 2007; Pan and Ding, 2012). PLGA 50/50 has been shown to be more hydrolytically unstable than its homopolymers, degrading in approximately 1–2 months (Nair and Laurencin, 2007). Increasing the amount of D,L-lactide monomer in the formulation slowed down the degradation time to 4–5 months when using a 75/25 formulation, or to 5–6 months when using an 85/15 PLA/PGA polymer ratio (Middleton and Tipton, 2000).

5.2.4 Polycaprolactone

PCL is a semi-crystalline polymer (up to 69% crystallinity (Labet and Thielemans, 2009)), with low glass transition and melting temperatures of about –60°C and 60°C, respectively (Vaca-Garcia, 2008). PCL has lower mechanical properties than the PLA or PGA polyesters, for example, with a tensile strength of 23 MPa (Gunatillake *et al*., 2006). It degrades into hexanoic

acid and is more stable under aqueous conditions than PLA or PGA polyesters. *In vivo*, it fully degrades in about 2–3 years (Nair and Laurencin, 2007). Due to its lower mechanical properties, PCL has not been widely studied for orthopedic applications. However, PCL is commonly copolymerized with PLA, PGA, or PLA-PLGA copolymers to lower the glass transition temperature and reduce the degradation rate of the resulting polymer. Processing techniques used to obtain PCL foams include supercritical CO_2 foaming (Liao *et al.*, 2012), and a combination of gas foaming and particulate leaching (Salerno *et al.*, 2008, 2012a, b).

5.2.5 Poly(propylene fumarate)

Poly(propylene fumarate) (PPF) is a linear, unsaturated, cross-linkable, and biodegradable polyester (Shi and Mikos, 2006; Wang *et al.*, 2006; Christenson *et al.*, 2007; Kasper *et al.*, 2009) used in bone scaffolds. Several synthetic procedures exist to obtain linear PPF (Peter *et al.*, 1997). A common synthesis protocol for linear biomedical-grade PPF with minimal generation of byproducts involves two steps (Kasper *et al.*, 2009) as shown in Fig. 5.2. The first step consists of the reaction of diethyl fumarate with excess propylene glycol in the presence of zinc chloride acid catalyst ($ZnCl_2$) and cross-linking inhibitor hydroquinone at a molar ratio of 1:3:0.01:0.002, respectively. Intermediate products from this initial step are bis(hydroxypropyl) fumarate and ethanol. After 90% of the ethanol has been collected as a distillate, the second step comprises transesterification of bis(hydroxypropyl fumarate) into PPF with the generation of propylene glycol as a byproduct. The molecular weight of PPF increases with reaction time and temperature. When the desired molecular weight of linear PPF is achieved (as measured by gel permeation chromatography), the product is purified by dissolution

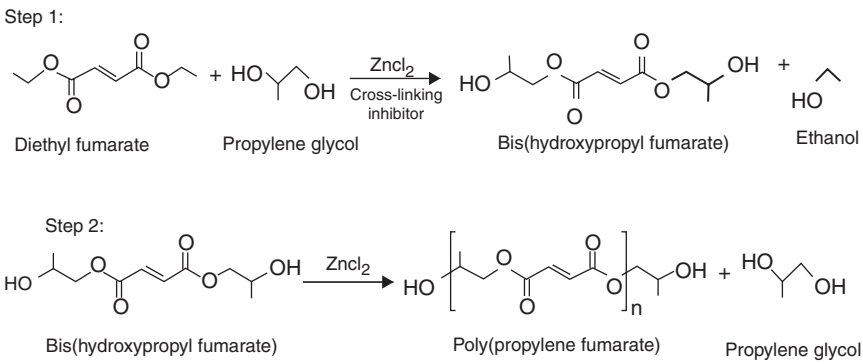

5.2 Two-step mechanism for the production of PPF. (*Source*: Adapted from Shi and Mikos, 2006.)

in methylene chloride followed by acid and water/brine washes, to remove the catalyst and rotary evaporation.

In order to obtain polymeric networks with higher mechanical properties, linear PPF can be cross-linked through the fumarate double bonds present in its backbone (Nair and Laurencin, 2007). Cross-linking can take place without the presence of cross-linking molecules, and it can be triggered either by thermal changes in the presence of free-radical initiators or by exposure to light in the presence of photoinitiators (Shi and Mikos, 2006). Biomedical formulations usually include cross-linking monomers that allow controlling the physical and curing properties of the materials. Poly(propylene fumarate)-diacrylate (PPF-DA), a derivative of PPF with terminal acrylate groups, is commonly used as a PPF cross-linker (Shi and Mikos, 2006).

Physical, mechanical, and degradation properties of PPF networks can be tuned by modifying one or several formulation parameters such as macromer molecular weight, cross-linking density, nature of the cross-linking agents, and porosity. Increased molecular weight of the linear PPF has been suggested to increase glass transition temperatures and viscosity (Wang *et al*., 2006). Increased viscosity allows PPF to be injected into irregular shaped defects to later be cross-linked *in situ*. PPF networks exhibit a wide range of mechanical properties that increase with higher cross-linking densities (Timmer *et al*., 2003). PPF degrades by hydrolysis of the ester bonds into propylene glycol and fumaric acid (Shi and Mikos, 2006). Fumaric acid is incorporated into the TCA cycle, while propylene glycol, which is a commonly used food additive, can be secreted by the body without generating any toxic reaction. Degradation products of networks that contain PPF-DA also include poly(acrylic acid-co-fumaric acid), and acrylic acid, both of which can be excreted by the kidneys (He *et al*., 2001). Degradation times can vary between 12 weeks, to degrade 50% of a weak thermal cross-linked PPF porous network with N-vinyl pyrrolidone (NVP) as the cross-linker, to more than 52 weeks to achieve the same mass loss with a solid network of PPF and PPF-DA (Shi and Mikos, 2006). Although porosity tends to reduce the mechanical properties of the materials, it enhances the biological response after implantation. Techniques to produce porous PPF-based scaffolds include cross-linking in combination with salt leaching (Fisher *et al*., 2002), emulsion templating (Christenson *et al*., 2007; Moglia *et al*., 2011), gas foaming (Kempen *et al*., 2006), and a combination of 3D printing and injection molding (Lee *et al*., 2006).

5.3 Polyurethanes for biomedical foam production

Since the 1960s when Biomer® was introduced to the biomedical field as an elastomeric material for cardiovascular applications (Lelah and Cooper,

1986), polyurethanes have been developed for a wide range of biomedical applications due to their versatility and biocompatibility. Both biostable and biodegradable polyurethanes with a variety of mechanical properties and porosities can be obtained by careful selection of raw materials and processing conditions. As a result, polyurethanes can be used as stable materials with low protein adhesion in blood-contact applications, or as tissue engineering scaffolds that support and promote cellular attachment and proliferation (Guelcher, 2006, 2008).

Polyurethanes are obtained from the reaction of isocyanates (-N=C=O functionality) with compounds containing active hydrogen atoms such as alcohols or amines. Extensive reviews of polyurethane chemistry are found in the literature (Woods, 1982; Hepburn, 1992; Oertel, 1994; Szycher, 1999; Reed, 2000), and relevant reactions involved in the production of biomedical polyurethanes are presented in Fig. 5.3. Urethane bonds are formed from the reaction of isocyanate and alcohol groups (Fig. 5.3a), while urea bonds result from the reaction of isocyanate with amine groups (Fig. 5.3b). In addition, the reaction of isocyanates with water generates unstable carbamic acid, which decomposes into an amine and carbon dioxide gas (Fig. 5.3c). The resulting amine produces urea bonds, while the carbon dioxide gas acts as an *in situ* blowing agent (Guelcher, 2006).

Polyisocyanates used in the synthesis of polyurethanes can be aliphatic or aromatic. Aromatic polyisocyanates include 4,4′-methylene diphenyl diisocyanate (MDI) and toluene diisocyanate (TDI), while aliphatic polyisocyanates include 1,6-diisocyanatohexanone (HDI), 1,4-diisocyanatobutane (BDI), and lysine methyl ester diisocyanate (LDI) (Nair and Laurencin, 2007). In comparison to aliphatic polyisocyanates, aromatic polyisocyanates have higher reactivity and generate polyurethanes with improved mechanical properties. However, aromatic isocyanates also have increased toxicity, which makes aliphatic polyisocyanates a preferred material for the formulation of biomedical polyurethanes. An important characteristic of polyisocyanates used to obtain polyurethanes is the free isocyanate (NCO) content, typically measured by titration:

$$\%\text{free NCO} = \frac{42}{w} = \frac{42f}{M} \qquad [5.1]$$

where w (Da eq^{-1}) corresponds to the equivalent weight, f is the functionality, and M is the molecular weight of the polyisocyanate (Guelcher, 2006).

Polyols that react with isocyanate to produce the urethane bonds have hydroxyl end groups and a backbone composed of polyesters, polyethers, polycarbonates, polydimethylsiloxane, or polybutadiene. Examples of commonly used polyols include poly(propylene oxide) (PPO), poly(ethylene

(a) Urethane production

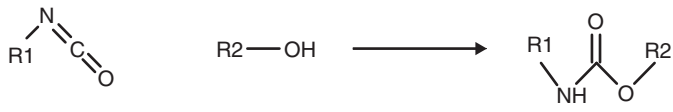

(b) Urea production

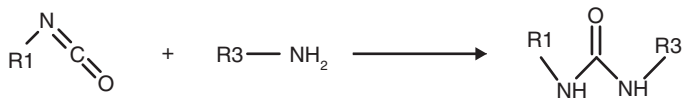

(c) Blowing reaction

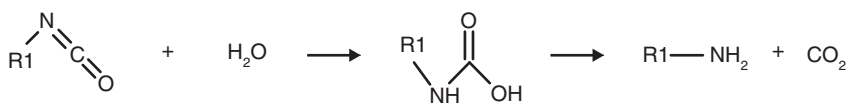

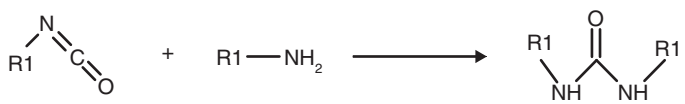

5.3 Reactions involved in the production of biomedical polyurethanes. (a) urethane production, (b) urea production, and (c) blowing reaction. (*Source*: Adapted from Guelcher, 2006.)

oxide) (PEO), and polyesters discussed in the previous section such as PDLA, PGA, and PCL. Polyol composition influences the processing, mechanical, and degradation properties of the polyurethane (Oertel, 1994; Herrington *et al.*, 2004). As a result, the design of the polyol backbone is dictated by the final application of the polyurethane. For example, for tissue engineering scaffolds, polyols synthesized by ROP of ε-caprolactone, glycolide, and D,L-lactide have been developed as polyurethane intermediates, due to their tunable hydrolytic degradation rates (Sawhney and Hubbell, 1990). Polyols are synthesized by reacting an initiator with appropriate types and amounts of monomers to achieve the target molecular weight. As discussed in the section on polyester synthesis, the initiator molecule defines the functionality (f) of the resulting polyol, while the ratio of monomers to initiator controls the final molecular weight. Common initiators include butanediol ($f = 2$), glycerol ($f = 3$), pentaerythritol ($f = 4$), or sucrose ($f = 8$). An important

characteristic of polyols used in the formulation of polyurethanes is the hydroxyl number, typically measured by titration (ASTM, 2008):

$$OH\,\text{number} = \frac{56.1 \times 10^3}{w} = 56.1 \times 10^3 \frac{f}{m} \qquad [5.2]$$

where w (Da eq^{-1}) corresponds to the hydroxyl equivalent weight, f is the polyol functionality, and m (Da) is the polyol molecular weight.

Prepolymers are intermediate compounds with either polyol or isocyanate functionality. They are obtained by reacting polyol with excess diisocyanate, or vice versa (Herrington *et al*., 2004). Even though obtaining polyurethanes using prepolymer intermediates is less cost effective than using isocyanates and polyols, advantages associated with this process include: increased viscosity, which favors better mixing, reduced vapor hazard due to higher molecular weight, improved control over the final properties of the product, and reduction of undesired side reactions (Herrington *et al*., 2004; Guelcher, 2008). Prepolymer properties (free NCO number and target molecular weight) can be tailored by modifying the NCO:OH ratio:

$$\text{NCO:OH ratio} = \frac{q_{\text{NCO},I}}{q_{\text{OH},P}} = \frac{m_I / w_I}{m_P / w_P} \qquad [5.3]$$

where q_i is the number of equivalents, m_I is the mass of component i, subscript I denotes isocyanate, and P the polyol (Guelcher, 2008). Addition of chain extenders to the prepolymer allows the production of higher molecular weight polyurethanes with hard (isocyanate) and soft (polyol) segments.

Another important parameter in the formulation of polyurethanes is the isocyanate index, defined as the ratio of NCO equivalents used in the formulation to the theoretical number of NCO equivalents required to react with the polyol and other active groups (total number of hydroxyl and amine equivalents in the formulation). It is calculated as (Herrington *et al*., 2004; Guelcher, 2006):

$$\text{Index} = \frac{\text{Actual amount of isocyanate used}}{\text{Theoretical amount of isocyanate used}} \times 100 = \frac{q_{\text{NCO},I}}{q_{\text{OH,P}} + q_{\text{NH}_2,A} + q_{\text{OH},C}} \times 10 \qquad [5.4]$$

Changes in the index of polyurethane formulations generate significant changes in hardness of the final product. Indexes in the range of 105–115

generate flexible foams, while increasing the index increases the hardness (up to a certain limit) and generates higher curing times. For biomedical applications, an additional consideration to take into account when increasing the index of polyurethane foams is the presence of unreacted isocyanate groups in the final foam.

Depending on the properties of the raw materials, polyurethanes can be polymerized either in solution or by reactive liquid molding, in which case the intermediates must be liquids at synthesis temperatures. Biomedical polyurethane foams have been developed using TIPS (Guan *et al*., 2005), salt leaching/freeze drying (Spaans *et al*., 1998; Gogolewski *et al*., 2006; Gogolewski and Gorna, 2007), wet fiber spinning (Gisselfaelt *et al*., 2002; Liljensten *et al*., 2002), electrospinning (Stankus *et al*., 2004; Stankus *et al*., 2007), emulsion templating (Moglia *et al*., 2011), and reactive liquid molding (Dumas *et al*., 2010; Adolph *et al*., 2012) techniques. In addition to the polyisocyanate and polyol components, polyurethane formulations can also include the addition of water, catalysts, surfactants, pore openers, plasticizers, and other additives (Herrington *et al*., 2004). In polyurethane foams, catalyst selection allows control of the curing time of the formulation according to the requirements of the specific application. Catalyst selection also influences the balance of the polymer formation rate (polyol–isocyanate reaction), and gas generation rate (isocyanate–water reaction). Although the catalytic activity of several classes of compounds has been studied, the most common polyurethane catalysts are tertiary amines and organometallic catalysts, which selectively catalyze the blowing and gelling reactions, respectively (Oertel, 1994; Herrington *et al*., 2004). The selection of additives must be done after a careful review of the literature, keeping in mind the final application of the product.

Degradation mechanisms of polyurethanes are dependent on the backbone composition of the intermediates. Lysine-derived poly(ester urethanes) have been reported to degrade via hydrolytic, enzymatic, and oxidative mechanisms (Hafeman *et al*., 2010). Biodegradable polyurethanes have also been developed containing enzymatically degradable chain extenders in the hard segment (Elliot *et al*., 2002; Guan and Wagner, 2005; Moglia *et al*., 2011). Strategies to reduce the degradation rate of polyurethane biomedical implants include the addition of antioxidants such as vitamin E (Anderson *et al*., 1998), the incorporation of ester- and ether-free soft segments (Mathur *et al*., 1997; Anderson *et al*., 1998; Coury, 2004), and the use of surface-modifying end groups (SME) (Ward *et al*., 1998) or surface-modifying macromolecules (SMM) (Santerre *et al*., 2000). The formulation of polyurethane scaffolds for biomedical applications requires careful design of the polymer backbone to ensure that the material remains in the defect as long as it is needed in each specific application to support healing.

5.4 Tyrosine-derived polymers

Tyrosine-derived polymers have been developed as materials with significant biological compatibility, due to the presence of naturally occurring building blocks and degradable bonds, as well as high mechanical properties provided by the aromatic rings in their backbone. The main building block of these polymers is the diphenolic monomer desaminotyrosyl-L-tyrosine alkyl ester (DTR, where R represents the alkyl pendant group), which is obtained from the carbodiimide-mediated reaction between L-tyrosine alkyl ester and desaminotyrosine (DAT) (Kohn and Schut, 2006). DTR can be polymerized with different reagents to create tyrosine-derived polymers with a range of mechanical properties and degradation profiles. Reaction with phosgene, dicarboxylic acids, or alkyl or aryl dichlorophosphates generates poly(DTR carbonates) (Magno *et al.*, 2010), poly(DTR arylates), or poly(DTR phosphate esters), respectively (Kohn and Schut, 2006). Tyrosine-derived polycarbonate foams have been prepared using a combination of solvent casting/porogen leaching techniques (Magno *et al.*, 2010).

The composition of the polymer backbone and the nature of the pendant alkyl group have great influence over the properties of DTR-derived polymers. By varying the composition of the alkyl chain, the glass transition temperature can be tuned to values ranging from 50 to 90 °C, strength can be adjusted from 50 to 70 MPa, and modulus from 1 to 2 GPa (Nair and Laurencin, 2007). Copolymerization with poly(ethylene glycol) (PEG) decreases the hydrophobicity of the material, thereby increasing water sorption, lowering wet mechanical properties, and accelerating hydrolytic degradation. The main product of hydrolytic degradation of tyrosine-derived polymers is desaminotyrosyl-tyrosine (DT) (Tangpasuthadol *et al.*, 2000a, 2000b), which *in vivo* undergoes additional enzymatic degradation to DAT and tyrosine (Nair and Laurencin, 2007). Similar to the effect of copolymerization with PEG, the inclusion of DT in the backbone of the polymer generates faster degradation rates, due to the free carboxylic acid group present (Johnson *et al.*, 2009; Magno *et al.*, 2010). Instead, incorporation of longer alkyl chains as the pendant groups reduces the hydrolytic degradation rate. The capability of modifying the properties of the polymer by varying the composition not only of the backbone but also of the pendant groups renders tyrosine-derived polymers a versatile platform for a wide range of biomedical applications. Specific formulations have been developed for bone tissue engineering where higher mechanical properties and longer degradation times than those of common α-polyesters are required (Ertel *et al.*, 1995; Magno *et al.*, 2010; Kim *et al.*, 2012).

5.5 Processing techniques for fabricating porous scaffolds

In addition to the material composition, the final porous structure of polymeric foams determines the mechanical properties and degradation rates of scaffolds. Different foaming techniques have been developed that offer control over pore size, shape, and interconnectivity. These techniques will be discussed next, highlighting the foaming mechanism used and relevant results presented in the literature.

5.5.1 Casting/porogen leaching

Polymer casting followed by porogen leaching is a simple technique to fabricate porous scaffolds and is one of the most widely used (Mikos and Temenoff, 2000; Liu and Ma, 2004). Casting can be carried out in solution or with reactive liquid intermediates, as is the case with some polyurethane formulations. When solvent casting is used, the polymer solution is mixed with porogen particles and cast into the desired mold. Afterwards, the polymeric solvent is removed (by evaporation or lyophilization) and the remaining composite is washed with a solvent capable of solubilizing the porogen particles. When using reactive liquid intermediates, the porogen particles are mixed with the reagents before the reaction proceeds (for example, before adding the catalyst). After the material has cured, the porogen is removed with an appropriate solvent. Advantages of using this processing technique are good control over scaffold porosity and pore size, which will depend on the porogen loading and size, respectively. However, the porogen content needs to be high enough to obtain sufficient pore interconnectivity. The major drawback of this technique is the use of solvents (for casting and/or removal of the porogen), the removal of which increases the processing time and precludes the loading of biologics into the material. Incomplete removal of the solvents can also affect cell viability after implantation, so this technique is mostly favorable for applications that can use pre-formed scaffolds.

Commonly used porogens include NaCl particles and paraffin beads. When using salt particles to prepare a porous PLLA or PLGA scaffolds for bone tissue engineering, porogen loadings above 70 wt.% are required to achieve high pore interconnectivity (Mikos *et al.*, 1994). The salt leaching technique has also been used to fabricate porous scaffolds using polyurethanes (Adhikari *et al.*, 2008) and PCL (Salerno *et al.*, 2008). Paraffin beads with controlled particle size have been used as porogens for PLLA and PLGA scaffolds (Ma and Choi, 2001). The beads were fused together using heat to form a three-dimensional array in a mold into which the polyesters were cast. The conditions of the heat treatment to bind the beads influenced

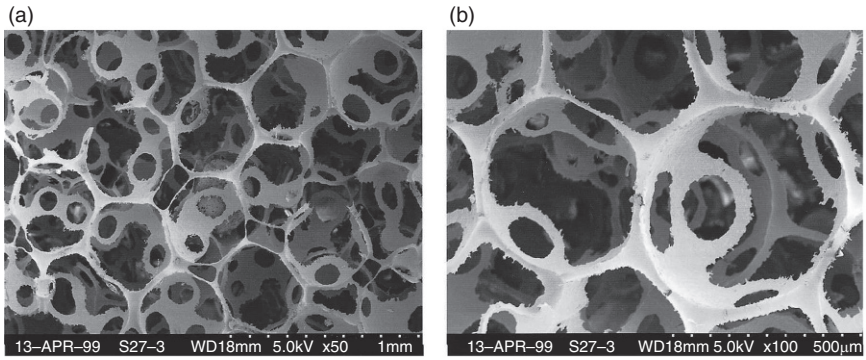

5.4 Scanning electron microscopy (SEM) images of PLGA foams after removal of the paraffin beads (420–500 μm) used as porogen. (a) ×50 (b) ×100. (*Source*: Ma and Choi, 2001.)

the size of the openings between pores. After leaching the porogen, scaffolds with high pore interconnectivity were obtained (Fig. 5.4).

5.5.2 Gas foaming

In contrast to the casting/porogen leaching technique, gas foaming does not require the use of organic solvents and the process can be carried on at low temperatures. Pores with various structures are generated, either by chemical or physical foaming (Christenson *et al*., 2007; Jacobs *et al*., 2008). Chemical foaming produces gaseous products (as a result of reactions or decomposition), which generate bubbles in the inside of the polymer. Pores created by carbon dioxide produced by isocyanates reacting with water are an example of chemical foaming in polyurethanes (Fig. 5.5a). On the other hand, physical foaming involves the removal of gas dissolved in the polymer at high pressures, a method known as supercritical gas foaming. In this technique, supercritical CO_2 ($scCO_2$) is used to generate pores in the material. A supercritical fluid is a dense phase that combines gas-like diffusivity with liquid-like density in a state above the critical temperature (T_c) and pressure (P_c). $scCO_2$ is a preferred foaming agent since, in addition to being nontoxic, nonflammable, noncorrosive, abundant, inexpensive, and commercially available, CO_2 has non-extreme critical properties (T_C = 31.1°C, P_C = 7.37 MPa) (Liao *et al*., 2012).

The first step in supercritical gas foaming is to saturate the non-porous, amorphous, or semi-crystalline polymer with $scCO_2$. At this stage the $scCO_2$ acts as a plasticizer and forms a single phase with the polymer (Mooney *et al*., 1996). Equilibrium conditions, such as concentration of dissolved CO_2, depend on the type of polymer, and operation temperature and pressure

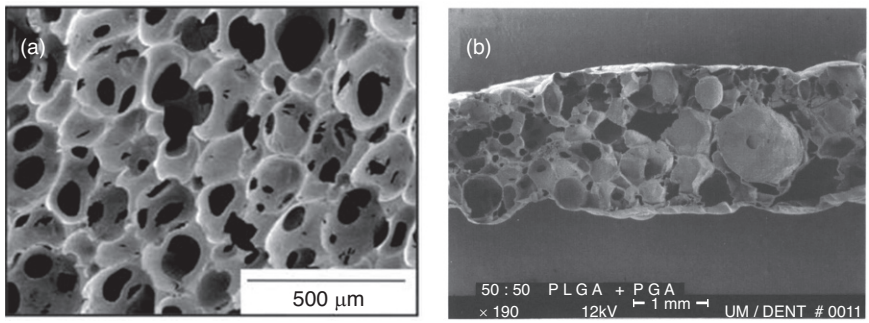

5.5 SEM images of foams produced using chemical and physical foaming. (a) Injectable polyurethane scaffold foamed with carbon dioxide gas produced by the blowing reaction. (*Source*: Adolph *et al.*, 2012.) (b) PLGA foamed with $scCO_2$. (*Source*: Mooney *et al.*, 1996.)

(Jacobs *et al.*, 2008). After equilibrium is reached, CO_2 is removed from the polymer, either by reducing the pressure (pressure quenching), increasing the temperature (temperature soaking), or both (Liao *et al.*, 2012). As a result, gas bubbles nucleate and grow inside the material. The rate at which nucleation takes place depends on the interactions of $scCO_2$ with the polymer, so different processing conditions are required for each system. Removal of the $scCO_2$ also increases the glass transition temperature of the polymer and the final porous structure is fixed in the glassy state (Fig. 5.5b).

$scCO_2$ gas foaming was first used to fabricate porous sponges of PLLA, PDLLA, and PLGA with pore diameters of 100 μm and porosities up to 93% (Mooney *et al.*, 1996). However, surfaces with low porosities were achieved and pore interconnectivity was low, which can directly affect nutrient transport inside the scaffold and hinder cellular viability. To overcome these limitations, several modifications to the original $scCO_2$ gas foaming technique have been developed. Open-pore PCL scaffolds were developed by combining $scCO_2$ gas foaming with thermoplastic gelatin (Salerno *et al.*, 2012b) or salt (Salerno *et al.*, 2008, 2012b) leaching. In this approach, the melt polymer was mixed with the porogen before the gas foaming step. Porosity, pore size and distribution, and interconnectivity were modified by optimizing the processing parameters (temperature, pressure, and porogen loading and distribution, Fig. 5.6). Increasing the porogen loading from 30 to 70 wt.% generated a scaffold with smaller pores and a narrower pore size distribution (Salerno *et al.*, 2008). Mooney *et al.* also used the combination of gas foaming and salt leaching to improve interconnectivity of PLGA scaffolds (Murphy *et al.*, 2002). In their approach, salt granules were fused under 95% humidity conditions before adding them to the polymer solution and proceeding with gas foaming. This led to solvent cast PLGA scaffolds

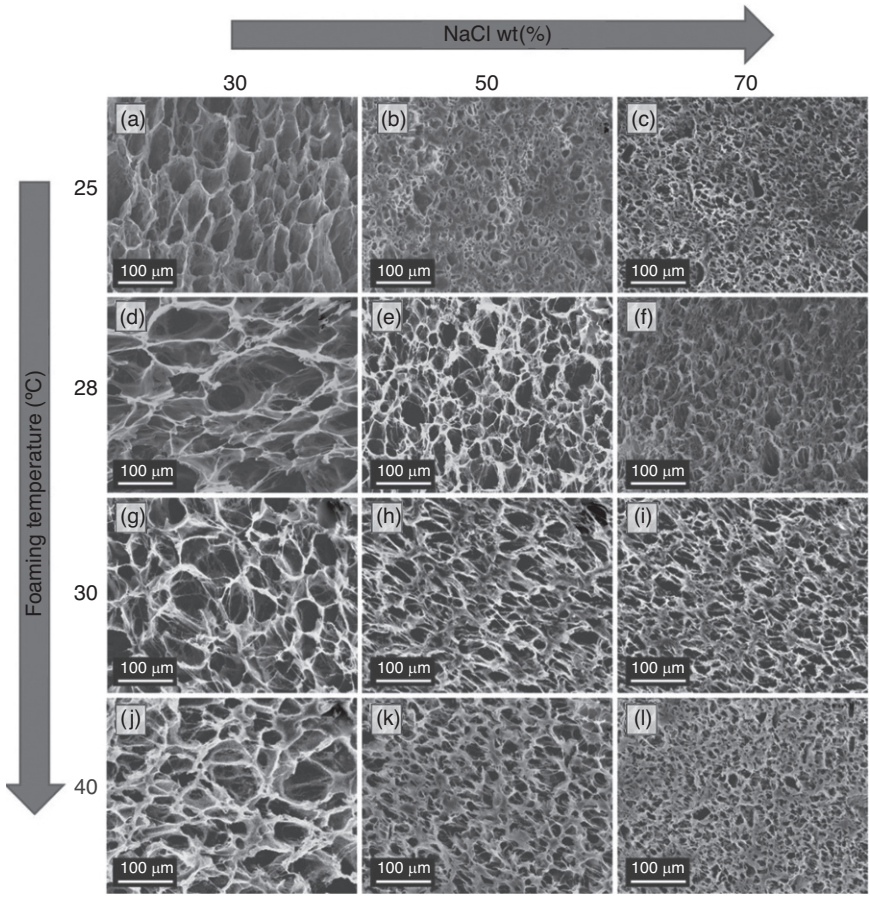

5.6 SEM images of PCL foams produced using a combination of CO_2 foaming and salt leaching techniques. The images show the dependence of morphology on salt concentration and foaming temperature. (*Source*: Salerno *et al.*, 2012.)

with open interconnected pores with two-fold higher mechanical properties than the gas-foamed PLGA controls. Even though porogen leaching in combination with $scCO_2$ has been shown to improve scaffold interconnectivity, its limitations include longer scaffold fabrication times and difficulties in removing the porogen material (Liao *et al.*, 2012). Additional process alternatives studied in the last decade include particle seeding (Collins *et al.*, 2010), ultrasound post-treatment (Wang *et al.*, 2006), and the use of cosolvents during gas foaming (Tsivintzelis *et al.*, 2007).

Detailed studies of the effect of processing parameters and polymer characteristics on the final porous morphology have also been completed in recent years. Depressurization rate (Barry *et al.*, 2006; Salerno *et al.*,

2008) and time (Jenkins *et al*., 2006) have been reported to influence the porosity and pore size and morphology of methacrylate and PCL foams. Regarding polymer characteristics, studies have suggested that crystallinity of the initial polymer (Fujiwara *et al*., 2005) and the addition of metal chromophores to the polymeric chains (Nawaby *et al*., 2005) can influence the pore size and distribution. Several reviews of the effects of these variables are extensively discussed in the literature (Jacobs *et al*., 2008; Salerno *et al*., 2008, 2012a; Liao *et al*., 2012; Tayton *et al*., 2012).

5.5.3 Emulsion-based methods

PLGA foams with porosities between 91% and 95% and median pore sizes in the range of 13–35 μm (with large pores greater than 200 μm) were first prepared by emulsion-freeze drying using methylene chloride as the solvent (Whang *et al*., 1995). In this study, the polymer solution was homogenized with distilled water, cast into a mold, and frozen in liquid nitrogen to preserve the emulsion structure. Solvent and water were removed using freeze drying. Parameters such as polymer solution to water ratio, and viscosity of the emulsion were modified to control the foam morphology. However, the use of organic solvents and the small pores obtained hindered the usefulness of these foams in tissue engineering.

Emulsion templating has emerged as a foam production technique with high control over pore size, morphology, and interconnectivity (Christenson *et al*., 2007; Moglia *et al*., 2011). Emulsions used as templates have a droplet volume >74% (Lissant, 1974) and are known as high internal phase emulsions (HIPEs). As shown in Fig. 5.7a, in emulsion templating a monomer (in solution or as a viscous liquid) is first homogenized with a diluent to create a HIPE. The HIPE is then cast into a mold at an appropriate temperature for monomer polymerization, and after droplet removal the resulting foams are known as polyHIPEs (Zhang and Cooper, 2005). Control over foam architecture is achieved by modifying parameters that influence the stability of the initial emulsion. Emulsion stability is determined by thermodynamics and it involves minimization of the free energy at the interface (Moglia *et al*., 2011). Emulsion stability studies have shown that surface tension is a more accurate predictor of emulsion stability (and thus morphology) than viscosity. Compared to non-emulsified components, the increase in surface energy of an emulsion is given by:

$$\Delta W = \sigma \Delta A \qquad [5.5]$$

where ΔW is the free energy of the interface, σ is the interfacial energy, and ΔA is the change in surface area (Moglia *et al*., 2011). The stability of the

emulsion increases when ΔA decreases and this translates into phase separation. Higher σ also translates into larger initial droplets (lower ΔA), and/or increased rate of droplet coalescence. According to these observations, modulation of the interfacial energy of the emulsion (for example using a surfactant) provides control over the final pore size of emulsion-templated foams. Interconnectivity of the foams is related to the thickness of the polymer film between droplets. During polymerization of the monomer into a higher density material, the film shrinks according to structural characteristics of the polymer. Shrinkage of thin films generates openings between pores in the final foam. Film thickness depends on the total droplet volume and individual droplet size. As a result, the pore size distribution and interconnectivity of emulsion-templated foams can be modified with variations of surfactant nature and concentration, polymer solution to aqueous phase ratio, and polymer composition, all of which affect initial emulsion stability (Williams *et al*., 1990; Christenson *et al*., 2007; Moglia *et al*., 2011).

Different polyHIPE formulations have been developed as potential materials for tissue engineering. Christenson *et al.* (2007) obtained PPF foams with pore sizes in the range of 10–300 μm, porosities of 80–89%, and open pores when the pores were smaller than 50 μm (Fig. 5.7b). PPF, PPF-DA (PPF)-diacrylate cross-linker, toluene, and sorbitan monooleate (surfactant) were premixed and then emulsified with an aqueous phase containing potassium persulfate and calcium chloride. Once the HIPE was uniform, it was transferred to a mold at 60°C and the polymer was allowed to cure for 48 h, locking the geometry of the HIPE. The remaining liquid was then removed in an oven at 60°C. Even though the proposed method allowed for controlling pore size and interconnectivity, the interconnected foams had pores smaller than those ideal for tissue engineering applications (> 100 μm (Nam and Park, 1999) and organic solvents were still employed. Aiming to overcome these limitations, an injectable propylene fumarate dimethacrylate (PFDMA)-based polyHIPE formulation was recently developed (Moglia *et al*., 2011). The biodegradable PFDMA macromer and the surfactant were premixed and then emulsified with an aqueous solution containing calcium chloride and ammonium persulfate (initiator). The emulsion was then injected into the mold and allowed to cross-link at 37°C for 12 h. The resulting foams had minimal residual solvent, closed pores with sizes in the range of 4–29 μm (Fig. 5.7c), porosity of 75%, and average compressive modulus and strength of 33 and 5 MPa, respectively. Even though none of the current foam formulations based on emulsion methods addresses all of the requirements for biomedical applications, the examples discussed above underscore the versatility of emulsion templating as a technique to develop porous materials with controlled morphology. Ongoing studies are being developed to obtain emulsion-templated foams with open interconnected pores with sizes > 100 μm (Moglia *et al*., 2011).

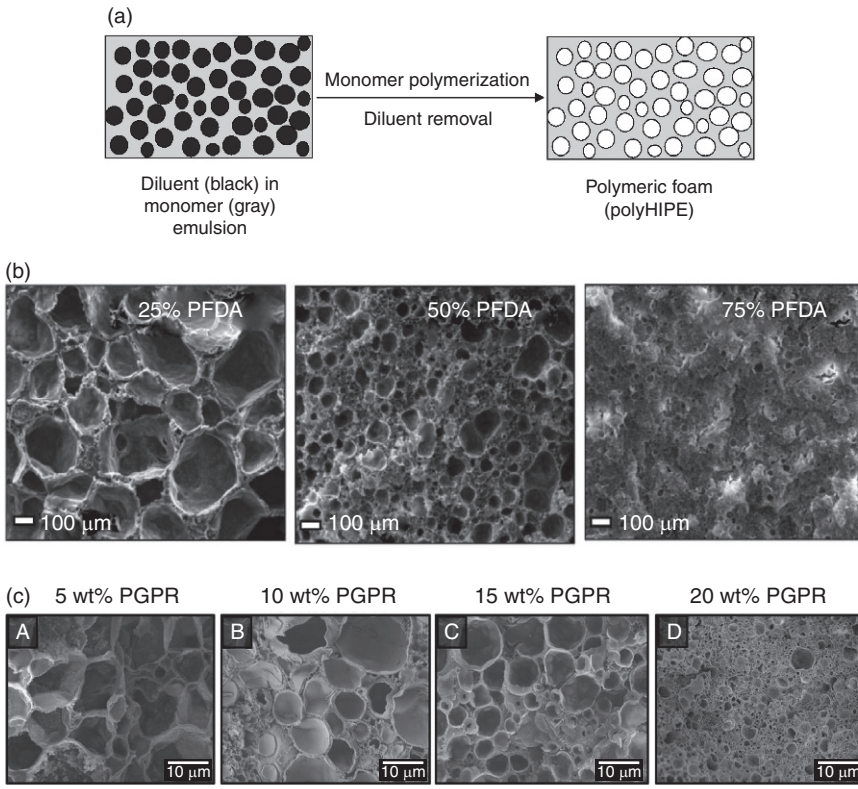

5.7 PolyHIPE foams. (a) Diagram illustrating the polymerization of a continuous monomer phase in a monomer/diluent emulsion followed by diluent removal to obtain a polymeric foam, (b) SEM images of PPF polyHIPES using toluene as the diluent and different concentrations of propylene fumarate diacrylate (PFDA) cross-linker. (*Source*: Christenson *et al.*, 2007.), and (c) SEM images of PFDMA injectable polyHIPES prepared with different concentrations of polyglycerol polyricinoleate (PGPR) surfactant. (*Source*: Moglia *et al.*, 2011.)

5.5.4 Thermally induced phase separation (TIPS)

Similar to emulsion-based methods, phase separation is the governing process controlling the creation of pores in TIPS. The phase distribution in polymer solutions depends on the composition and physical conditions (temperature and pressure) of the solution. A temperature-composition phase diagram describes the states of a specific solution at different conditions, and it is usually divided into three regions (Fig. 5.8a): (a) above the binodal curve where the solution exists as a single phase, (b) between the binodal and the spinodal curve in a metastable state, and (c) below the

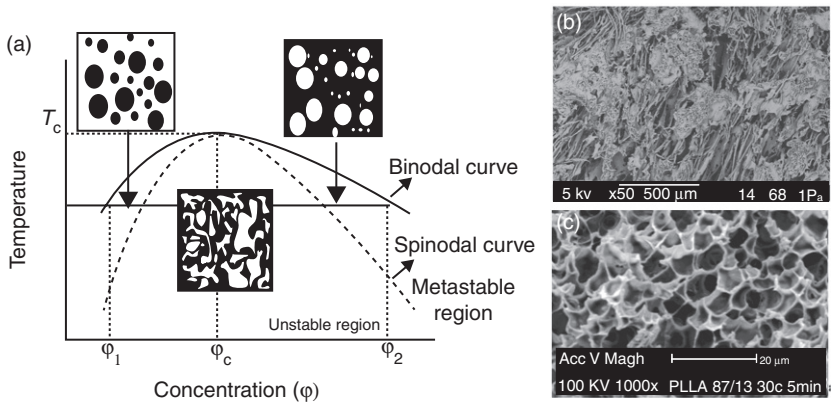

5.8 TIPS foaming. (a) Temperature vs concentration diagram with different states in a polymer solution. (*Source*: Nam and Park, 1999.) (b) SEM image of a PLGA/PUR (polyurethane) foam prepared using TIPS. (*Source*: Rowlands *et al.*, 2007.) (c) SEM image of a PLLA foam prepared via TIPS at 30°C. (*Source*: Carfi Pavia *et al.*, 2008.)

spinodal curve in an unstable state. Phase separation occurs both at the metastable and unstable states, and it is governed by different mechanisms in each region (Nam and Park, 1999; Rowlands *et al.*, 2007; Carfi Pavia *et al.*, 2008). When the temperature of the solution is lowered such that it exists in a metastable state, nucleation and growth dominate the phase separation process and result in an emulsion-like structure. Instead, if the temperature is lowered into an unstable state, phase separation is governed by a spinodal decomposition mechanism characterized by two continuous polymer-rich and solvent-rich phases.

Polymeric foams can be obtained using TIPS by removing the solvent after phase separation of a polymer solution. Increased interconnectivity is achieved when phase separation is promoted by spinodal decomposition in comparison to the nucleation-growth mechanism (Nam and Park, 1999). However, nucleation-growth mechanisms provide control over the pore size of the resulting foam (Carfi Pavia *et al.*, 2008). PLLA foams have been obtained by TIPS using protocols that include residence times at both of the states (metastable and unstable) (Carfi Pavia *et al.*, 2008). These studies showed that the resulting pore architecture depends on the specific thermal pathway selected for phase separation. In the metastable region, lower temperatures promoted faster nucleation and slower growth, while higher temperatures resulted in the opposite effect. Longer residence times at either of the states also increased the presence of micropores in the polymeric phase. TIPS has also been used to produce foams from combinations of dissimilar polymers such as MDI-polydimethylsiloxane (PDMS) based polyurethane

and PLGA (Rowlands *et al*., 2007). This technique achieved intimate mixing of the polymers in solution at 90°C, followed by phase separation at –5°C. The resulting foams had morphological, mechanical, and cell adhesion properties with values in between those of its homopolymers. These observations suggest that polymeric foams with varying porous architecture (Fig. 5.8b,c) and final properties can be obtained by varying the polymer and solvent nature and concentrations, as well as the cooling history of the material.

5.6 Characterization of polymeric foams

Independent of the processing technique used to obtain polymeric foams, parameters that influence their performance include, but are not limited to, polymer composition, porosity and pore size distribution, mechanical properties, and stability. This section provides a summary of the techniques and some protocols used to characterize the polymeric foams. A detailed discussion about how the techniques work is not provided, since this falls outside the scope of the chapter, but citations to previous work using the techniques have been included as reference.

Polymer composition and structure influence both its process ability as well as the foam's final performance. Molecular weight distribution is usually quantified using gas permeation chromatography (Lu *et al*., 2000; Kasper *et al*., 2009). Differential scanning calorimetry (DSC) is used to identify thermal transitions such as the glass transition and melting temperatures. Standard thermal analysis protocols include a combination of heat–cool–heat cycles with heating and cooling rates of 5–10°C min^{-1}, and identification of the thermal transitions from the second heating cycle (Rowlands *et al*., 2007; Magno *et al*., 2010). DSC can also be used to quantify the crystalline content of the polymeric phases (Lu *et al*., 2000; Ma and Choi, 2001), although more detailed information about crystallinity can be obtained using X-ray diffraction techniques (Carfi Pavia *et al*., 2008). For some processing techniques, such as those regulated by phase separation, the viscosity of the polymer solutions influences the morphology of the final foam. Rotational rheometers have been used to measure viscosity as well as the storage (G′) and loss (G″) moduli (Salerno *et al*., 2008). Additional protocols to measure viscosity include the use of more traditional Ubbelohde viscometers (ASTM, 1997; Christenson *et al*., 2007).

The porous architecture of polymeric foams has a direct impact on the mechanical properties, degradation rates, and cellular infiltration of the scaffolds. Although high porosity and interconnectivity are desired to support cellular infiltration, mechanical properties decrease with porosity squared, while the effect on degradation rates varies depending on the polymer. Pore size distribution and morphology can be evaluated using scanning electron microscopy (SEM). After foaming, a section of the material is gold sputter-

coated and imaged at different locations. The images are used to measure pore diameter, which is reported either as an average ($n > 100$) or after applying a statistical correction to account for non-ideal spherical pores (ASTM, 2004; Christenson *et al*., 2007; Salerno *et al*., 2008). Porosity is commonly determined gravimetrically by comparing dry foam density (ρ_F) with the density of bulk polymer (ρ_P) according to: Porosity $= 1 - (\rho_F / \rho_P)$ (Guelcher *et al*., 2006; Moglia *et al*., 2011). X-Ray microtomography (μCT) has also been used to accurately quantify porosity. In this case, dry foams are scanned in a μCT system at high resolution modes, and porosity values are obtained after thresholding the reconstructed image (Jacobs *et al*., 2008; McBane *et al*., 2011; Amini *et al*., 2012). Pore size distribution, total pore volume, surface area, and density can also be obtained using mercury intrusion porosimetry (MIP) (Nam and Park, 1999; Lu *et al*., 2000), although interconnected pores are required in order to obtain representative results using this technique.

In vitro degradation profiles of polymeric foams have been determined by incubating samples at 37°C in phosphate-buffered saline (PBS) at various pH levels, enzyme-containing media, or oxidative media (Lu *et al*., 2000; Carfi Pavia *et al*., 2008; Hafeman *et al*., 2010; McBane *et al*., 2011). At each time point, the media with degradation products is collected and the dry sample mass is measured and compared to the initial sample mass. In addition to reporting the mass loss in time, the media collected can be analyzed with techniques such as high-performance liquid chromatography (HPLC) to determine the nature and concentration of the degradation products.

Depending on the application of the polymeric foams, specific mechanical requirements must be achieved under tension, compression, and/or torsion. Mechanical testing of the samples resulting in stress–strain data is conducted with protocols modeled by standard methods (ASTM, 2001, 2002, 2010). Reported properties usually include compressive and tensile modulus and strength (Lu *et al*., 2000; Ma and Choi, 2001; Rowlands *et al*., 2007; Hafeman *et al*., 2010; Moglia *et al*., 2011).

5.7 *In vitro* and *in vivo* testing

The performance of biomedical polymeric foams is tested using both *in vitro* and *in vivo* models. *In vitro* testing provides preliminary information about cytotoxicity and cellular attachment, proliferation, and differentiation (Winn *et al*., 2006). Foam sterilization methods include ethanol treatment followed by washes with water or PBS, UV irradiation, or gamma irradiation. Cytotoxicity studies involve the contact of cells with leachates from the polymeric foams. Leachates can be collected before cell culture by incubating foams in appropriate solutions, which are then added to the cell culture media either directly or after dilution. Viability of the treated

Table 5.1 Examples of *in vivo* models used to test biomedical polymeric foams

Application	Animal (defect)	Polymer	Reference
Bone	Rabbit (calvaria)	PPF	Fisher *et al.*, 2002
		Tyrosine-derived	Kim *et al.*, 2012
	Rat (proximal tibia)	PPF	Yaszemski *et al.*, 1995
	Sheep (femoral cortical)	PUR	Adhikari *et al.*, 2008
	Rat (femoral plug)	PUR	Li *et al.*, 2009
Skin	Rat (excisional wounds)	PUR	Adolph *et al.*, 2012
Aneurysm	Dog (carotid artery aneurysms)	PUR	Metcalfe *et al.*, 2003

cells, measured using live/dead staining or metabolic activity based assays, is compared to that of cells treated only with media. As a variation of this method, well-plate inserts can be used to submerge the foams in the cell culture media without having direct contact with the cells. As an example, this insert method has been used to study the cytotoxicity of tyrosine-derived polycarbonate scaffolds containing DTR, DT, and low molecular weight blocks of PEG on MC3T3-E1 cells (Magno *et al.*, 2010). Cellular metabolic activity was above 98% for every group at all three time points tested (1, 7, 14 days), and cell numbers increased over time, which suggest that the tyrosine-derived polymers have minimal toxicity to the cells and support cellular proliferation. Direct contact *in vitro* models allow the study of cellular attachment, proliferation, and differentiation on the surface of the materials. Various cell types have been seeded on polymeric foams including 3T3 fibroblasts (Rowlands *et al.*, 2007; Moglia *et al.*, 2011) and RAW 264.7 macrophages (Hafeman *et al.*, 2010). After culture, cellular attachment is monitored by using a combination of fixation, staining, and imaging of the cells usually using optical, confocal fluorescent, or scanning electron microscopes. After lead-candidate polymeric foam formulations have been identified according to their performance *in vitro*, *in vivo* models are used to evaluate the biocompatibility and efficacy of the material to promote the desired healing outcome (Anderson, 2006). According to the target application, authors have used different animal models to test their developed materials. Examples of these models are summarized in Table 5.1.

5.8 Applications of polymeric foams in tissue engineering

The previous sections have discussed how the final performance of porous scaffolds strongly depends on several factors. Formulations with various degradation times, mechanical properties, and porosities, in addition to the

biocompatibility of the materials, position polymeric foams as materials with a wide range of applications in the field of tissue engineering. The following paragraphs contain examples of formulations that have shown high potential for their use in bone, cartilage, skin, and endovascular applications.

Scaffolds for bone tissue engineering must provide osteoconductivity, osteoinductivity, and biomechanical functionality in addition to being biocompatible and biodegradable (Amini *et al*., 2012; Kim *et al*., 2012). PPF foams prepared by solvent casting followed by salt leaching have been tested in calvarial defects *in vivo* and shown to be biocompatible and to support new bone formation after 8 weeks (Fisher *et al*., 2002). Polyurethane porous implants and injectable formulations with mechanical properties above those of trabecular bone (compressive modulus 50–800 MPa, compressive strength 1–10 MPa (Amini *et al*., 2012)) but lower than those of cortical bone (compressive modulus ~20 GPa, compressive strength ~200 MPa (An and Draughn, 1999)) were tested in femoral cortical defects in sheep (Adhikari *et al*., 2008). The implant and the injectable formulations were proven to be biocompatible and increased new bone formation was observed after 6 months. The incorporation of β-tricalcium phosphate (β-TCP) particles improved mechanical properties and reduced polymer degradation rates. Tyrosine-derived polycarbonates containing DTR, DT, and PEG, prepared using a combination of solvent casting, porogen leaching, and phase separation techniques have also been tested both *in vitro* and *in vivo*. The scaffolds had 85% porosity, a bimodal pore size distribution with macropores > 200 μm and micropores < 20 μm (Magno *et al*., 2010), and a compressive modulus > 0.5 MPa (minimal requirement for bone graft substitutes) after 6 weeks of incubation in PBS at 37°C (Kim *et al*., 2012). When tested *in vivo* using a critical size calvarial defect in New Zealand white rabbits, the materials generated minimal inflammatory response and degraded faster than under *in vitro* conditions. New bone formation was promoted when the scaffolds were loaded with 50 μg of recombinant human bone morphogenetic protein-2 (rhBMP-2) or coated with calcium phosphate (Kim *et al*., 2012).

Recently, PLGA porous scaffolds with pore sizes in the range of 200–600 μm were prepared via thermal sintering of PLGA spheres and porogen leaching (Amini *et al*., 2012). The scaffolds had initial mechanical properties in the range of human trabecular bone, and improved oxygen diffusion across the scaffold. This last property is of interest for the treatment of large-area bone defects to support cellular infiltration deep into the scaffolds. In general, the *in vivo* performance of polymeric foams in bone defects has shown to be improved with the incorporation of ceramic fillers or biologics which provide osteoinductive properties to the already biocompatible and osteoconductive scaffolds. Examples of ceramic fillers include calcium phosphates (Yaszemski *et al*., 1995; Bennett *et al*., 1996; Adhikari *et al*., 2008), allograft bone (Dumas *et al*., 2010), and bioactive glass (Lu

et al., 2003; Gentile *et al*., 2012), while biologics include rhBMP-2 (Li *et al*., 2009; Kim *et al*., 2012), lovastatin (Yoshii *et al*., 2010), and transforming growth factor beta (TGF-β) (Peter *et al*., 2000).

Scaffolds with graded porosity to treat osteochondral defects have recently been developed. A combination of supercritical gas foaming and salt leaching techniques was used to obtain PCL (Salerno *et al*., 2008) and PCL/ hydroxyapatite (HA) composite scaffolds (Salerno *et al*., 2012a) with porosities in the range of 75–93%. Controlled distribution of salt particles in the matrix generated a porosity gradient similar to that present in articular cartilage. *In vitro*, foams with graded porosity produced by three-dimensional fiber deposition have shown anisotropic cell distribution and glycosaminoglycan production similar to that observed in bovine articular cartilage (Woodfiled *et al*., 2005).

Scaffolds for skin wound healing protect the wound from infection and provide a pathway for cells to infiltrate and regenerate. Natural polymers such as collagen and chitosan have been extensively used as scaffolding materials for skin since they provide biological cues (Zhong *et al*., 2010). However, these polymers lack mechanical properties and are expensive to obtain. As an alternative, synthetic polymers used for skin wound treatment include polyurethanes as commercially available wound dressings (Tegaderm™), PLGA meshes (Chen *et al*., 2005), PLLA (Beumer *et al*., 1993), as well as composites of PCL and collagen which combine the advantages of both materials (Dai *et al*., 2004). Recently, an injectable polyurethane porous scaffold produced using chemical foaming was developed with positive net results *in vivo* (Adolph *et al*., 2012). The material had porosities between 86% and 91%, working times of 5–7 min, and curing times of 15–19 min. The mechanical properties of the scaffolds under wet conditions approached those of intact skin, with a compressive modulus between 30 and 60 kPa. When implanted in rat excisional wounds, the scaffolds promoted cellular proliferation and prevented wound contraction and scar formation.

Polyurethanes have also been used to formulate porous shape memory polymers (SMP) for embolic treatment of aneurysms using minimally invasive delivery techniques. In comparison to shape memory alloys (SMA), SMPs are lightweight, have high recovery strains and low recovery stresses, can be formulated with a wide range of glass transition temperatures (T_g), are easy to process, and have a lower cost (Sokolowski *et al*., 2007; Small *et al*., 2010). At temperatures near T_g, SMPs undergo drastic changes in elastic modulus (Sokolowski *et al*., 2007). As a result, SMPs can be processed and stored using cold hibernating elastic memory (CHEM) processing (Sokolowski, 2010). In CHEM processing, the SMP foam is heated and compacted above the T_g. Then the material is cooled for storage and/or delivery. The original shape of the SMP foam is recovered when the temperature is raised above the T_g. CHEM polyurethane foams with a density of 0.032 g/

cc have been tested in a dog aneurysm model and shown to support cellular infiltration and neointima formation (Metcalfe *et al*., 2003). For non-necked aneurysms, a device consisting of a light diffusing fiber covered by an SMP stent with an attached SMP foam was tested *in vitro* (Small *et al*., 2010). Upon thermal activation using the central fiber, the foam filled the aneurysm while the stent provided support to the artery. Recently, a highly chemically cross-linked polyurethane SMP foam was developed with improved shape memory behavior and increased expansion capacity due to reduced secondary-shape formation and ultra-low density (0.015–0.021 g/cc), respectively (Singhal *et al*., 2012). Additional characteristics of this foam included an activation temperature between 45°C and 70°C, mixed (closed and open) pore morphology, and *in vitro* biocompatibility.

5.9 Future trends

The previous sections have described currently available technologies for polymeric foam formulations with different degradation rates, mechanical properties, and pore size and shape distribution. Although control over these variables is achieved by modifying the starting materials and the foaming technique employed, future improvements will need to address challenges such as injectability, delivery of biologics, and polymer degradation in response to cellular activity. Injectable foams are capable of adapting to irregular defects and are delivered using minimally invasive techniques which favors faster healing progress. While solvents or high temperatures can be used to induce flow of solid polymers, these strategies present potential disadvantages of adverse effects on exogenous biologics or host tissue. Furthermore, polymers that set *in situ* in response to temperature or pH changes, or the action of low concentrations of a biocompatible catalyst, provide the opportunity to incorporate active molecules or cells that enhance the biological activity of the scaffold. Alternatively, the surface of implants can be modified to induce biological activity. Control of infection is required when implanting avascular foams in contaminated wounds. Thus, dual-purpose scaffolds that both promote healing and prevent infection are being developed to reduce the risk of infectious complications (Stewart *et al*., 2010; Zheng *et al*., 2010; Wenke and Guelcher, 2011; Sanchez Jr *et al*., 2013). In summary, future studies are required to identify materials and foaming techniques that result in injectable formulations under surgery room conditions, as well as scaffolds that can efficiently deliver biologics, such as cell, growth factors, and/or antimicrobial agents.

5.10 Sources of further information and advice

For further information, the reader is advised to consult the following references:

B. Ratner, A. Hoffman, F. Schoen and J. Lemons, eds. (2004) *Biomaterials Science: An Introduction to Materials in Medicine*. Boston: Elsevier Academic Press. A comprehensive textbook that provides an excellent reference on the basic science and clinical applications of biomaterials.

J. Hollinger, ed. (2012) *An Introduction to Biomaterials*, 2nd edition. Boca Raton, FL: Woodhead Publishing Limited. A textbook that reviews many classes of biomaterials, as well as their application in medicine.

B. Vernon, ed. (2012) *Injectable Biomaterials: Science and Applications*. Woodhead Publishing Limited. A textbook that reviews the composition and properties, technology, and clinical applications of injectable biomaterials.

5.11 References

Adhikari, R., Gunatillake, P., Griffiths, I., Tatai, L., Wickramaratna, M., Houshyar, S., Moore, T., Mayadunne, R., Field, J., McGee, M. and Carbone, T. (2008) 'Biodegradable injectable polyurethanes: Synthesis and evaluation for orthopaedic applications', *Biomaterials*, vol. **29**, pp. 3762–3770.

Adolph, E., Hafeman, A., Davidson, J., Nanney, L. and Guelcher, S. (2012) 'Injectable polyurethane composite scaffolds delay wound contraction and support cellular infiltration and remodeling in rat excisional wounds', *J Biomed Mater Res Part A*, vol. **100A**, pp. 450–461.

Adolph, E.J., Hafeman, A.E., Davidson, J.M., Nanney, L.B. and Guelcher, S.A. (2012) 'Injectable polyurethane composite scaffolds delay wound contraction and support cellular infiltration and remodeling in rat excisional wounds', *J Biomed Mater Res Part A*, vol. **100A**, no. 2, pp. 450–461.

Agrawal, C.M. and Ray, R.B. (2001) 'Biodegradable polymeric scaffolds for musculoskeletal tissue engineering', *J Biomed Mater Res*, vol. **55**, pp. 141–150.

Amini, A., Adams, D., Laurencin, C. and Nukavarapu, S. (2012) 'Optimally porous and biomechanically compatible scaffolds for large-area bone regeneration', *Tissue Eng: Part A*, vol. **18**, pp. 1376–1388.

An, Y. and Draughn, R. (1999) *Mechanical Testing of Bone and the Bone-Implant Interface*, Woodhead Publishing Limited, South Carolina, USA.

Anderson, J. (2006) 'Fundamental biological requirements of a biomaterial', in *An Introduction to Biomaterials*, eds S. Guelcher and J. Hollinger, Woodhead Publishing Limited, Boca Raton, pp. 3–13.

Anderson, J., Hiltner, A., Wiggins, M., Schubert, M., Collier, T., Kao, W. and Mathur, A. (1998) 'Recent advances in biomedical polyurethane biostability and biodegradation', *Polym Int*, vol. **46**, p. 163.

ASTM (1997) 'D445: Standard Test Method for Kinematic Viscosity of Transparent and Opaque Liquids (and Calculation of Dynamic Viscosity)'.

ASTM (2001) 'D-3574: Standard Test Methods for Flexible Cellular Materials- Slab, Bonded, and Molded Urethane Foams'.

ASTM (2002) 'D695: Standard Test Method for Compressive Properties of Rigid Plastics'.

ASTM (2004) 'D3576: Standard Test Method for Cell Size of Rigid Cellular Plastics'.

ASTM (2008) 'E1899: Standard Test Method for Hydroxyl Groups Using Reaction with p-Toluenesulfonyl Isocyanate (TSI) and Potentiometric Titration with Tetrabutylammonium Hydroxide'.

ASTM (2010) 'D-1621: Standard Test Method for Compressive Properties of Rigid Cellular Plastics'.

Barry, J., Silva, M., Popov, V., Shakesheff, K. and Howdle, S. (2006) 'Supercritical carbon dioxide: putting the fizz into biomaterials', *Philos Transact A Math Phys Eng Sci*, vol. **364**, pp. 249–261.

Bennett, S., Connolly, K., Lee, D., Jiang, Y., Buck, D., Hollinger, J. and Gruskin, E. (1996) 'Initial biocompatibility studies of a novel degradable polymeric bone substitute that hardens in situ', *Bone*, vol. **19**, p. 1015.

Beumer, G., van Blitterswijk, C., Bakker, D. and Ponec, M. (1993) 'Cell-seeding and in vitro biocompatibility evaluation of polymeric matrices of PEO/PBT copolymers and PLLA', *Biomaterials*, vol. **14**, pp. 598–604.

Brannon-Peppas, L. and Vert, M. (2000) 'polylactic and polyglycolic acids as drug delivery carriers', in *Handbook of Pharmaceutical Controlled Release Technology*, ed. D. Wise, Marcel Dekker, New York, pp. 99–130.

Carfi Pavia, F., La Carrubba, V., Piccarolo, S. and Brucato, V. (2008) 'Polymeric scaffolds prepared via thermally induced phase separation: Tuning of structure and morphology', *J Biomed Mater Res Part A*, vol. **86A**, no. 2, pp. 459–466.

Chen, G., Sato, T., Ohgushi, H., Ushida, T., Tateishi, T. and Tanaka, J. (2005) 'Culturing of skin fibroblasts in a thin PLGA-collagen hybrid mesh', *Biomaterials*, vol. **26**, pp. 2559–2566.

Christenson, E.M., Soofi, W., Holm, J. L., Cameron, N. R. and Mikos, A.G. (2007) 'Biodegradable fumarate-based polyHIPEs as tissue engineering scaffolds', *Biomacromolecules*, vol. **8**, pp. 3806–3814.

Collins, N.J., Bridson, R.H., Leeke, G.A. and Grover, L.M. (2010) 'Particle seeding enhances interconnectivity in polymeric scaffolds foamed using supercritical CO_2', *Acta Biomater*, vol. **6**, pp. 1055–1060.

Coury, A. (2004) 'Chemical and biochemical degradation of polymers', in *Biomaterials Science: An Introduction to Materials in Medicine*, eds B. Ratner, A. Hoffman, F. Schoen and J. Lemons, Elsevier Academic Press, Boston, p. 411.

Dai, N., Williamson, M., Khammo, N., Adams, E. and AGA, C. (2004) 'Composite cell support membranes based on collagen and polycaprolactone for tissue engineering of skin', *Biomaterials*, vol. **25**, pp. 4263–4271.

Dumas, J., Zienkiewicz, K., Tanner, S., Prieto, E., Battacharyya, S. and Guelcher, S. (2010) 'Synthesis and characterization of an injectable allograft bone/polymer composite bone void filler with tunable mechanical properties', *Tissue Eng: Part A*, vol. **16**, no. 8, pp. 2505–2518.

Elliot, S., Fromstein, J., Santerre, J. and Woodhouse, K. (2002) 'Identification of biodegradation products formed by L-phenylalanine based segmented polyurethaneureas', *J Biomater Sci Polym Ed*, vol. **13**, no. 6, pp. 691–711.

Ertel, S.I., Kohn, J., Zimmerman, M.C. and Parsons, J.R. (1995) 'Evaluation of poly(DTH carbonate), a tyrosine-derived degradable polymer, for orthopedic applications', *J Biomed Mater Res*, vol. **29**, no. 11, pp. 1337–1348.

Farng, E. and Sherman, O. (2004) 'Meniscal repair devices: a clinical and biomechanical literature review', *J Arthrosc Relat Surg*, vol. **20**, pp. 273–286.

Fisher, J., Vehof, J., Dean, D., van der Waerden, J., Holland, T., Mikos, A. and Jansen, J. (2002) 'Soft and hard tissue response to photocrosslinked poly(propylene fumarate) scaffolds in a rabbit model', *J Biomed Mater Res*, vol. **59**, no. 3, pp. 547–556.

Fujiwara, T., Yamaoka, T., Kimura, Y. and Wynne, K.J. (2005) 'Poly(lactide) swelling and melting behavior in supercritical carbon dioxide and post-venting porous material', *Biomacromolecules*, vol. **6**, pp. 2370–2373.

Gentile, P., Mattioli-Belmonte, M., Chiono, V., Ferretti, C., Baino, F., Tonda-Turo, C., Vitale-Brovarone, C., Pashkuleva, I., Reis, R. and Ciardelli, G. (2012) 'Bioactive glass/polymer composite scaffolds mimicking bone tissue', *J Biomed Mater Res Part A*, vol. **100A**, pp. 2654–2667.

Gisselfaelt, K., Edberg, B. and Flodin, P. (2002) 'Synthesis and properties of degradable poly(urethane urea)s to be used for ligament reconstructions', *Biomacromolecules*, vol. **3**, p. 951.

Gogolewski, S. and Gorna, K. (2007) 'Biodegradable polyurethane cancellous bone graft substitutes in the treatment of iliac crest defects', *J Biomed Mater Res*, vol. **80A**, p. 94.

Gogolewski, S., Gorna, K. and Turner, A. (2006) 'Regeneration of bicortical defects in the iliac crest of estrogen-deficient sheep, using new biodegradable polyurethane bone graft substitutes', *J Biomed Mater Res*, vol. **77A**, p. 802.

Guan, J., Fujimoto, K., Sacks, M. and Wagner, W. (2005) 'Preparation and characterization of highly porous, biodegradable polyurethane scaffolds for soft tissue applications', *Biomaterials*, vol. **26**, p. 3961.

Guan, J. and Wagner, W. (2005) 'Synthesis, characterization, and cytocompatibility of polyurethaneurea elastomers with designed elastase sensitivity', *Biomacromolecules*, vol. **6**, pp. 2833–2842.

Guelcher, S. (2006) 'Polyurethanes', in *An Introduction to Biomaterials*, eds S. Guelcher and J. Hollinger, Woodhead Publishing Limited, Boca Raton, pp. 161–183.

Guelcher, S. (2008) 'Biodegrabable polyurethanes: Synthesis and applications in regenerative medicine', *Tissue Eng: Part B*, vol. **14**, no. 1, pp. 3–17.

Guelcher, S., Patel, V., Gallagher, K., Connonlly, S., Didier, J., Doctor, J. and Hollinger, J. (2006) 'Synthesis and in vitro biocompatibility of injectable polyurethane foam scaffolds', *Tissue Eng*, vol. **12**, no. 5, pp. 1247–1259.

Gunatillake, P., Mayadunne, R. and Adhikari, R. (2006) 'Recent developments in biodegradable synthetic polymers', *Biotechnol Ann Rev*, vol. **12**, pp. 301–347.

Hafeman, A., Zienkiewicz, K., Zachman, A., Sung, H., Nanney, L., Davidson, J. and Guelcher, S. (2010) 'Characterization of the degradation mechanisms of lysine-derived aliphatic poly(ester urethane) scaffolds', *Biomaterials*, vol. **32**, no. 2, pp. 419–429.

He, S., Timmer, M., Yaszemski, M., Yasko, A., Engel, P. and Mikos, A. (2001) 'Synthesis of biodegradable poly(propylene fumarate) networks with poly(propylene fumarate)-diacrylate macromers as crosslinking agents and characterization of their degradation products', *Polymer*, vol. **42**, p. 1251.

Hepburn, C. (1992) *Polyurethane Elastomers*, Elsevier, London.

Herrington, R., Broos, R. and Knaub, P. (2004) 'Flexible polyurethane foams', in *Handbook of Polymeric Foams and Foam Technology*, eds D. Klemper and V. Sendijarevic, Hanser Gardner, Munich, pp. 55–119.

Jacobs, L.J.M., Kemmere, M.F. and Keurentjes, J.T.F. (2008) 'Sustainable polymer foaming using high pressure carbon dioxide: A review on fundamentals, processes and applications', *Green Chem*, vol. **10**, no. 7, pp. 731–738.

Jamiolkowski, D. and Dormier, E. (2006) 'The Poly a-esters', in *An Introduction to Biomaterials*, eds S. Guelcher and J. Hollinger, Woodhead Publishing Limited, Boca Raton, pp. 139–160.

Jenkins, M., Harrison, K., Silva, M., Whitaker, M., Shakesheff, K. and Howdle, S. (2006) 'Characterisation of microcellular foams produced from semi-crystalline PCL using supercritical carbon dioxide', *Eur Polym J*, vol. **42**, no. 11, pp. 3145–3151.

Johnson, P.A., Luk, A., Demtchouk, A., Hiral, P., Sung, H.-J., Treiser, M.D., Gordonov, S., Sheihet, L., Bolikal, D., Kohn, J. and Moghe, P.V. (2009) 'Interplay of anionic charge, poly(ethylene glycol), and iodinated tyrosine incorporation within tyrosine-derived polycarbonates: Effects on vascular smooth muscle cell adhesion, proliferation, and motility', *J Biomed Mater Res Part A*, vol. **93A**, pp. 505–514.

Kasper, F.K., Tanahashi, K., Risher, J.P. and Mikos, A.G. (2009) 'Synthesis of poly(propylene fumarate)', *Nat Protoc*, vol. **4**, no. 4, pp. 518–525.

Kempen, D.H., Lu, L., Kim, C., Zhu, X., Dhert, W.J.A., Currier, B.L. and Yaszemski, M.J. (2006) 'Controlled drug release from a novel injectable biodegradable microsphere/scaffold composite based on poly(propylene fumarate)', *J Biomed Mater Res A*, vol. **77**, pp. 103–111.

Kim, J., Magno, M., Waters, H., Doll, B., McBride, S., Alvarez, P., Darr, A., Vasanji, A., Kohn, J. and Hollinger, J. (2012) 'Bone regeneration in a rabbit critical-sized calvarial model using tyrosine-derived polycarbonate scaffolds', *Tissue Eng: Part A*, vol. **18**, no. 11/12, pp. 1132–1139.

Kim, T.K., Yoon, J.J., Lee, D.S. and Park, T.G. (2006) 'Gas foamed open porous biodegradable polymeric microspheres', *Biomaterials*, vol. **27**, pp. 152–159.

Kohn, J. and Schut, J. (2006) 'Polymers derived from L-Tyrosine', in *An Introduction to Biomaterials*, eds S. Guelcher and J. Hollinger, Woodhead Publishing Limited, Boca Raton, pp. 185–204.

Labet, M. and Thielemans, W. (2009) 'Synthesis of polycaprolactone: A review', *Chem Soc Rev*, vol. **38**, pp. 3484–3504.

Lee, K.W., Wang, S., Lu, L., Jabbari, E., Currier, B.L. and Yaszemski, M.J. (2006) 'Fabrication and characterization of poly(propylene fumarate) scaffolds with controlled pore structures using 3-Dimensional printing and injection molding', *Tissue Eng*, vol. **12**, pp. 2801–2811.

Lelah, M. and Cooper, J. (1986) *Polyurethanes in Medicine*, Woodhead Publishing Limited, Boca Raton.

Li, B., Yoshii, T., Hafeman, A., Nyman, J., Wenke, J. and Guelcher, S. (2009) 'The effects of rhBMP-2 released from biodegradable polyurethane/microsphere composite scaffolds on new bone formation in rat femora', *Biomaterials*, vol. **30**, pp. 6768–6779.

Liao, X., Zhang, H. and He, T. (2012) 'Preparation of porous biodegradable polymer and its nanocomposites by supercritical CO_2 foaming for tissue engineering', *J Nanomater*, vol. **2012**, pp. 1–12.

Liljensten, E., Gisselfaelt, K., Edberg, B., Bertilsson, H., Flodin, P., Nilsson, A., Lindhal, A. and Peterson, L. (2002) 'Studies of polyurethane urea bands for ACL reconstruction', *J Mater Sci Mater Med*, vol. **13**, p. 351.

Lissant, K. (1974) *Emulsions and Emulsion Technology Part 1*, Marcel Dekker Incl., New York.

Liu, X. and Ma, P.X. (2004) 'Polymeric scaffolds for bone tissue engineering', *Ann Biomed Eng*, vol. **32**, no. 3, pp. 477–486.

Lu, H., El-Amin, S., Scott, K. and Laurencin, C. (2003) 'Three-dimensional, bioactive, biodegradable, polymer-bioactive glass composite scaffolds with improved mechanical properties support collagen synthesis and mineralization of human osteoblast-like cells in vitro', *J Biomed Mater Res A*, vol. **64**, no. 3, pp. 465–474.

Lu, L., Peter, S.J., Lyman, M.D., Lai, H., Lin, Leite, S.M., Tamada, J.A., Vacanti, J., P., Langer, R. and Mikos, A.G. (2000) 'In vitro degradation of porous poly(L-lactic acid) foams', *Biomaterials*, vol. **21**, pp. 1595–1605.

Ma, P.X. and Choi, J.-W. (2001) 'Biodegradable polymer scaffolds with well-defined interconnected spherical pore network', *Tissue Eng*, vol. **7**, no. 1, pp. 23–49.

Magno, M., Kim, J., Srinivasan, A., McBride, S., Bolikal, D., Darr, A., Hollinger, J. and Kohn, J. (2010) 'Synthesis, degradation and biocompatibility of tyrosine-derived polycarbonate scaffolds', *J Mater Chem*, vol. **20**, pp. 8885–8893.

Mathur, A., Collier, T., Kao, W., Wiggins, M., Schubert, M. and Hiltner, A., Anderson, J.M. (1997) 'In vivo biocompatibility and biostability of modified polyurethanes', *J Biomed Mater Res*, vol. **36**, p. 246.

McBane, J.E., Sharifpoor, S., Kuihua, C., Labow, R.S. and Santerre, J.P. (2011) 'Biodegradation and in vivo biocompatibility of a degradable, polar/hydrophobic/ionic polyurethane for tissue engineering applications', *Biomaterials*, vol. **32**, pp. 6034–6044.

Metcalfe, A., Desfaits, A., Salazkin, I., Yahia, L., Sokolowski, W. and Raymond, J. (2003) 'Cold hibernated elastic memory foams for endovascular interventions', *Biomaterials*, vol. **24**, pp. 491–497.

Middleton, J. and Tipton, A. (2000) 'Synthetic biodegradable polymers as orthopedic devices', *Biomaterials*, vol. **21**, pp. 2335–2346.

Mikos, A., Bao, Y., Cima, L., Ingber, D., Vacanti, J. and Langer, R. (1993) 'Preparation of poly(glycolic acid) bonded fiber structures for cell attachment and transplantation', *J Biomed Mater Res*, vol. **27**, pp. 183–189.

Mikos, A. and Temenoff, J.S. (2000) 'Formation of highly porous biodegradable scaffolds for tissue engineering', *J Biotechnol*, vol. **3**, no. 2, pp. 1–6.

Mikos, A., Thorsen, A., Czerwonka, L., Bao, Y. and Langer, R. (1994) 'Preparation and characterization of poly(L-lactic acid) foams', *Polymer*, vol. **35**, no. 5, pp. 1068–1077.

Moglia, R.S., Holm, J.L., Sears, N.A., Wilson, C.J., Harrison, D. and Cosgriff-Hernandez (2011) 'Injectable polyHIPEs as high-porosity bone grafts', *Biomacromolecules*, vol. **12**, pp. 3621–3628.

Mooney, D.J., Baldwin, D.F., Suh, N.P., Vacanti, J. and Langer, R. (1996) 'Novel approach to fabricate porous sponges of poly(D,L-lactic-co-glycolic acid) without the use of organic solvents', *Biomaterials*, vol. **17**, pp. 1417–1422.

Murphy, W.L., Dennis, R., G., Kileny, J.L. and Mooney, D.J. (2002) 'Salt fusion: An approach to improve pore interconnectivity within tissue engineering scaffolds', *Tissue Eng*, vol. **8**, no. 1, pp. 43–52.

Nair, L.S. and Laurencin, C.T. (2007) 'Biodegradable polymers as biomaterials', *Prog Polym Sci*, vol. **32**, pp. 762–798.

Nam, Y.S. and Park, T.G. (1999) 'Porous biodegradable polymeric scaffolds prepared by thermally induced phase separation', *J Biomed Mater Res*, vol. **47**, pp. 8–17.

Nawaby, A.V., Farah, A., Liao, X., Pietro, W.J. and Day, M. (2005) 'Biodegradable open cell foams of telechelic poly(E-caprolactone) macroligand with Ruthenium (II) chromophoric subunits via sub-critical CO_2 processing', *Biomacromolecules*, vol. **6**, pp. 2458–2461.

Oertel, G. (1994) *Polyurethane Handbook*, Hanser Gardner Publications, Berlin.

Pan, Z. and Ding, J. (2012) 'Poly(lactide-co-glycolide) porous scaffolds for tissue engineering and regenerative medicine', *Interface Focus*, vol. **2**, pp. 366–377.

Peter, S., Lu, L., Kim, D., Stamatas, G., Miller, M., Yaszemski, M. and Mikos, A. (2000) 'Effects of transforming growth factor B1 released from biodegradable polymer microparticles on marrow stromal osteoblasts cultured on poly(propylene fumarate) substrates', *J Biomed Mater Res*, vol. **50**, no. 3, pp. 452–462.

Peter, S., Miller, M., MJ, Y. and Mikos, A. (1997) 'Poly(propylene fumarate)', in *Handbook of Biodegradable Polymers*, eds A. Domb, J. Kost and W. DM, Hardwood Academic, Amsterdam, pp. 87–97.

Reed, D. (2000) 'Polyester: Perfect when performance pays the price premium', *Urethanes Tech*, vol. **17**, no. 4, pp. 41–44.

Rowlands, A.S., Lim, S.A., Martin, D. and Cooper-White, J.J. (2007) 'Polyurethane/poly(lactic-co-glycolic) acid composite scaffolds fabricated by thermally induced phase separation', *Biomaterials*, vol. **28**, pp. 2109–2121.

Salerno, A., E., D.M., Iannace, S. and Netti, P.A. (2012b) 'Tailoring the pore structure of PCL scaffolds for tissue engineering prepared via gas foaming of multiphase blends', *J Porous Mater*, vol. **19**, pp. 181–188.

Salerno, A., Iannace, S. and Netti, P.A. (2008) 'Open-pore biodegradable foams prepared via gas foaming and microparticulate templating', *Macromol Biosci*, vol. **8**, pp. 655–664.

Salerno, A., Iannace, S. and Netti, P.A. (2012a) 'Graded biomimetic osteochondral scaffold prepared via CO_2 foaming and micronized NaCl leaching', *Mater Lett*, vol. **82**, pp. 137–140.

Sanchez Jr, C.J., Prieto, E.M., Krueger, C.A., Zienkiewicz, K.J., Romano, D.R., Ward, C.L., Akers, K.S., Guelcher, S.A. and Wenke, J.C. (2013) 'Effects of local delivery of d-amino acids from biofilm-dispersive scaffolds on infection in contaminated rat segmental defects', *Biomaterials*, vol. **34**, no. 30, pp. 7533–7543.

Santerre, J., Meek, E., Tang, Y. and Labow, R. (2000) 'Use of fluorinated surface modifying macromolecules to inhibit the degradation of polycarbonate-urethanes by human macrophages', in *Transactions of Sixth World Biomaterials Congress*, Hawaii, USA, p. 77.

Sawhney, A. and Hubbell, J. (1990) 'Rapidly degraded terpolymers of D,L-lactide, glycolide, and e-caprolactone with increased hydrophilicity by copolymerization with polyethers', *J Biomed Mater Res*, vol. **24**, p. 1397.

Shi, X. and Mikos, A. (2006) 'Poly(propylene fumarate)', in *An Introduction to Biomaterials*, eds S. Guelcher and J. Hollinger, Woodhead Publishing Limited, Boca Raton, pp. 205–218.

Singh, L., Kumar, V. and Ratner, B. (2004) 'Generation of porous microcellular 85/15 poly(dl-lactide-co-glycolide) foams for biomedical applications', *Biomaterials*, vol. **25**, pp. 2611–2617.

Singhal, P., Rodriguez, J., Small, W., Eagleston, S., Van de Water, J., Maitland, D. and Wilson, T. (2012) 'Ultra low density and highly crosslinked biocompatible shape memory polyurethane foams', *J Polym Sci Part B: Polym Phys*, vol. **50**, pp. 724–737.

Small, W., Singhal, P., Wilson, T. and Maitland, D. (2010) 'Biomedical applications of thermally activated shape memory polymers', *J Mater Chem*, vol. **20**, no. 17, pp. 3356–3366.

Sokolowski, W. (2010) 'Shape memory polymer foams for biomedical devices', *Open Med Devices J*, vol. **2**, pp. 20–23.

Sokolowski, W., Metcalfe, A., Hayashi, S., Yahia, L. and Raymond, J. (2007) 'Medical applications of shape memory polymers', *Biomed Mater*, vol. **2**, pp. S23–S27.

Spaans, C., de Groot, J., Dekens, F. and Pennings, A. (1998) 'High molecular weight polyurethanes and a polyurethane urea based on 1,4-butanediisocyanate', *Polym Bull*, vol. **41**, p. 131.

Stankus, J., Guan, J. and Wagner, W. (2004) 'Fabrication of biodegradable elastomeric scaffolds with sub-micron morphologies', *J Biomed Mater Res*, vol. **70A**, p. 603.

Stankus, J., Soletti, L., Fujimoto, K., Hong, Y., Vorp, D. and Wagner, W. (2007) 'Fabrication of cell microintegrated blood vessel constructs through electrohydrodynamic atomization', *Biomaterials*, vol. **28**, p. 2738.

Stewart, R.L., Cox, J.T., Volgas, D., Stannard, J., Duffy, L., Waites, K.B. and Chu, T. (2010) 'The use of a biodegradable, load-bearing scaffold as a carrier for antibiotics in an infected open fracture model', *J Orthop Trauma*, vol. **24**, no. 9, pp. 587–591.

Szycher, M. (1999) *Szycher's Handbook of Polyurethanes*, Woodhead Publishing Limited, Boca Raton.

Tangpasuthadol, V., Pendharkar, S.M. and Kohn, J. (2000a) 'Hydrolytic degradation of tyrosine-derived polycarbonates, a class of new biomaterials. Part I: Study of model compounds', *Biomaterials*, vol. **21**, pp. 2371–2378.

Tangpasuthadol, V., Pensharkar, S.M., Peterson, R.C. and Kohn, J. (2000b) 'Hydrolytic degradation of tyrosine-derived polycarbonates, a class of new biomaterials. Part II: 3-yr study of polymeric devices', *Biomaterials*, vol. **21**, pp. 2379–2387.

Tayton, E., Purcell, M., Aarvold, A., Smith, J.O., Kalra, S., Brisoce, A., Shakesheff, K., Howdle, S.M., Dunlop, D.G. and Oreffo, R.O.C. (2012) 'Supercritical CO_2 Fluid-foaming of polymers to increase porosity: A method to improve the mechanical and biocompatibility characteristics for use as a potential alternative to allografts in impaction bone grafting?', *Acta Biomater*, vol. **8**, pp. 1918–1927.

Timmer, M., Carter, C., Ambrose, C. and Mikos, A. (2003) 'Fabrication of poly(propylene fumarate)-based orthopaedic implants by photo-crosslinking through transparent silicone molds', *Biomaterials*, vol. **24**, p. 4707.

Tsivintzelis, I., Pavlidou, E. and Panayiotou, C. (2007) 'Biodegradable polymer foams prepared with supercritical CO_2-ethanol mixtures as blowing agents', *J Supercritic Fluids*, vol. **42**, no. 2, pp. 265–272.

Vaca-Garcia, C. (2008) 'Biomaterials', in *Introduction to Chemicals from Biomass*, eds J. Clark and F. Deswarte, Wiley, Chichester, pp. 103–142.

Wang, S., Lu, L. and Yaszemski, M.J. (2006) 'Bone tissue-engineering material poly(propylene fumarate): correlation between molecular weight, chain dimensions, and physical properties', *Biomacromolecules*, vol. **7**, no. 6, pp. 1976–1982.

Ward, R., Tian, Y. and White, K. (1998) 'Improved polymer biostability via oligomeric end groups incorporated during synthesis', *Polym Mater Sci Eng*, vol. **79**, p. 526.

Wenke, J. and Guelcher, S. (2011) 'Dual delivery of an antibiotic and a growth factor addresses both the microbiological and biological challenges of contaminated bone fractures', *Expert Opin Drug Deliv*, vol. **8**, no. 12, pp. 1555–1569.

Whang, K., Thomas, C., Healy, K. and Nuber, G. (1995) 'A novel method to fabricate bioabsorbable scaffolds', *Polymer*, vol. **36**, pp. 837–842.

Williams, J., Gray, A. and Wilkerson, M. (1990) 'Emulsion stability and rigid foams from styrene or divinylbenzene water-in-oil emulsions', *Langmuir*, vol. **6**, no. 2, pp. 437–444.

Winn, S., Mitchel, J. and Uludag, H. (2006) 'In vitro testing of biomaterials', in *An Introduction to Biomaterials*, eds S. Guelcher and J. Hollinger, Woodhead Publishing Limited, Boca Raton, pp. 63–80.

Woodfiled, T., Van Blitterswijk, C., De Wijn, J., Sims, T., Hollander, A. and Riesle, J. (2005) 'Polymer scaffolds fabricated with pore-size gradients as a model for studying the zonal organization within tissue-engineered cartilage constructs', *Tissue Eng*, vol. **11**, no. 9/10, pp. 1297–1311.

Woods, G. (1982) *Flexible Polyurethane Foams, Chemistry and Technology*, Applied Science, London.

Yaszemski, M., Payne, R., Hayes, W., Langer, R., Aufdemorte, T. and Mikos, A. (1995) 'The ingrowth of new bone tissue and initial mechanical properties of a degrading polymeric composite scaffold', *Tissue Eng*, vol. **1**, p. 41.

Yoshii, T., Hafeman, A., Nyman, J., Esparza, J., Shinomiya, K., Spengler, D., Mundy, G., Gutierrez, G. and Guelcher, S. (2010) 'A sustained release of lovastatin from biodegradable, elastomeric polyurethane scaffolds for enhanced bone regeneration', *Tissue Eng: Part A*, vol. **16**, no. 7, pp. 2379–2396.

Zein, I., Hutmacher, D., Tan, K. and Teoh, S. (2002) 'Fused deposition modeling of novel scaffold architectures for tissue engineering applications', *Biomaterials*, vol. **23**, pp. 1169–1185.

Zeng, J., Chen, X., Xu, X., Liang, Q., Bian, X., Yang, L. and Jing, X. (2003) 'Ultrafine fibers electrospun from biodegradable polymers', *J Appl Polym Sci*, vol. **89**, pp. 1085–1092.

Zhang, H. and Cooper, A.I. (2005) 'Synthesis and applications of emulsion-templated porous materials', *Soft Matter*, vol. **1**, pp. 107–113.

Zhang, R. and Ma, P. (1999) 'Poly(a-hydroxyl acids) hydroxyapatite porous composites for bone-tissue engineering. I. Preparation and morpohology', *J Biomed Mater Res*, vol. **44**, pp. 446–455.

Zheng, Z., Yin, W., Zara, J.N., Li, W., Kwak, J., Mamidi, R., Lee, M., Siu, R.K., Ngo, R., Wang, J., Carpenter, D., Zhang, X., Wu, B., Ting, K. and Soo, C. (2010) 'The use of BMP-2 coupled – Nanosilver-PLGA composite grafts to induce bone repair in grossly infected segmental defects', *Biomaterials*, vol. **31**, pp. 9293–9300.

Zhong, S., Zhang, Y. and Lim, C. (2010) 'Tissue scaffolds for skin wound healing and dermal reconstruction', *Wiley Interdiscip Rev Nanomed Nanobiotechnol*, vol. **2**, pp. 510–525.

6

Biodegradable biomedical foam scaffolds

S. IANNACE and L. SORRENTINO, National Research Council, Italy and E. DI MAIO, University of Naples Federico II, Italy

DOI: 10.1533/9780857097033.1.163

Abstract: This chapter discusses the theoretical and experimental aspects related to the techniques for the preparation of scaffold by gas foaming of biodegradable polymers, of both natural and synthetic origin. Properties of polymer/gas solutions controlling nucleation and growth of gas bubbles are analysed in the first part of this chapter. In the second part, specific preparation methodologies and morphologies of foams based on selected biodegradable polymers will be presented. These include polysaccharides (starch, chitosan, alginates), vegetal (zein) and animal (gelatin) proteins, and polyesters (poly(lactic acid) (PLA), poly(glycolic acid) (PGA), and their copolymers PLGA, and poly-ε-caprolactone (PCL)).

Key words: gas foaming, polysaccharides, proteins, polyesters, scaffolds.

6.1 Introduction

The design of scaffolds for tissue engineering (TE) strategies involves a number of criteria related to materials' properties and structure. The temporary 3D scaffolds, used as templates for cell interactions and the formation of the extracellular matrix, must be non-immunogenic, non-toxic, biocompatible and biodegradable. The architectural structure of the scaffold should be characterized by interconnected porosity with a well-defined pore-size distribution to allow not only cell adhesion, ingrowth and reorganization but also neovascularization *in vivo* (Puppi *et al.*, 2010). The selection of the biodegradable materials and the control of the distribution of pore size and interconnectivity must assure functional as well as structural requirements necessary for cells including: (i) diffusion of nutrients and gases to cells; (ii) removal of by-products from cells; (iii) mechanical compatibility with both growing cells and surrounding host tissue; (iv) cell adhesion and response to specific molecular signals; and (v) degradation and resorption rate compatible with the mechanical properties required by the newly grown tissue.

Many different polymeric materials have been used to develop 3D scaffolds. They can be categorized simply as naturally derived materials (e.g.

proteins and polysaccharides) and synthetic polymers (e.g. poly(lactic acid) (PLA), poly(glycolic acid) (PGA), and their copolymers PLGA, and poly(ε-caprolactone) (PCL)). Naturally derived materials have the potential advantage of biological recognition, which may positively support cell adhesion and function. However, there are a number of drawbacks related to some specific properties of natural polymers. They may exhibit immunogenicity, lower mechanical properties, be highly hydrophilic, have a high degradation rate, or, most of all, properties may vary among different production batches. For these reasons, synthetic polymers have often been preferred, due to their reproducible large-scale production, better control of strength, degradation rates and microstructures (Liu and Ma, 2004).

A variety of processing technologies have been developed to fabricate porous 3D polymeric scaffolds for tissue engineering (TE). These techniques mainly include solvent casting and particulate leaching, gas foaming, emulsion freeze-drying, electrospinning, rapid prototyping, thermally induced phase separation, or a combination of these (Ma, 2004; Puppi *et al.*, 2010).

In this chapter, we will focus on the theoretical and experimental aspects related to the preparation techniques of scaffolds based on gas foaming of biodegradable polymers, of both natural and synthetic origin. The strategies commonly employed when using the gas foaming technology to control the porous architecture in foams, such as number and size of pores and degree of pore interconnection, within a biodegradable polymeric phase will be described. Properties of biodegradable polymers/blowing agents solutions involved in nucleation and growth of gas bubbles are analysed in the first part of this chapter. Gas solubility and diffusivity, rheological, volumetric and thermal properties as well as interfacial tension of biodegradable polymer/gas systems are presented by taking into consideration both theoretical aspects and experimental data available in the scientific literature.

In the second part, specific preparation methodologies and morphologies of foams based on selected biodegradable polymers will be presented. These include polysaccharides (starch, chitosan, alginates), vegetal (zein) and animal (gelatin) proteins, and polyesters (PLA, PGLA, PCL).

6.2 Foaming techniques and properties of expanding polymer/gas solutions

Thermoplastic foams can be produced by using continuous or discontinuous technologies, such as extrusion, injection moulding and batch foaming. The basic principle of foam formation is similar in all techniques: the foamed structure is obtained through a nucleation and growth mechanism from a polymer/gas solution, induced by an abrupt pressure drop. The manufacture of foamed products requires a careful selection of the proper combination of

polymer/foaming agent systems, and careful coordination of the individual steps in the process. In particular, in extrusion foaming technologies there are several operations, each performed by a specific section of the screw profile, that need to be taken into account. These include: (i) polymer and additives feeding; (ii) melting and compounding; (iii) venting; (iv) dynamic sealing; (v) blowing agent injection; (vi) mixing and gas solubilization; (vii) cooling; (viii) pumping; (ix) homogenization; (x) die forming; and (xi) cooling of the extrudate and post processing.

In the batch process two methods are utilized. In the 'pressure quench method', foaming is obtained by a rapid pressure quench of the polymer/gas solution, stable at high blowing gas pressure. Fewer operations with respect to extrusion are performed: polymer melting, pressurization and solubilization, cooling and pressure quenching. In the 'temperature increase method', foaming occurs after an increase in temperature that produces a glassy to rubbery transition of the polymer/gas solution. Basic operations are: pressurization at ambient or low temperature, pressure release and heating.

In all these different methods, the optimization of the manufacturing processes involves the control of the physical as well as the rheological behaviour of macromolecular viscoelastic materials containing a dissolved gas at high concentration. In particular, nucleation and growth rates, which determine the final morphology of the foam, are related to the solubility and diffusivity of the gas into the polymer melt and to the surface tension, rheological, thermal and volumetric properties of the polymer/gas solution.

6.2.1 Sorption thermodynamics and mass transport properties

The first important step in foaming is the solubilization of low molecular weight blowing agents, such as water, nitrogen, carbon dioxide and hydrocarbons in the molten polymer. The blowing agent has to diffuse into the polymer and form a polymer/blowing agent solution prior to fast supersaturation. Two properties of the polymer/gas specific system contribute to the solubilization phase: solubility – determining the quantity of gas solubilized in the polymer at processing temperatures and pressures – and mutual diffusivity – determining the rate at which the solubilization occurs. Diffusivity defines the minimum residence time in the extruder, or the minimum duration of the saturation phase in the batch process and, in the case of biodegradable polymers, which are typically thermolabile (thermally decomposable), should be high enough to limit the residence time before degradation occurs. Furthermore, diffusivity has to be considered when designing cooling rates and pressure drop rates (processing) since it defines

foam morphology (in the competition between nucleation and growth) (Lin *et al*., 2010). Blowing agent solubility, conversely, determines the extent of plasticization (processing) and the final density of the foam.

The effects of sorption properties on the foamability of biodegradable polymers have been reported in the literature by a number of research groups. For instance, Di Maio *et al*. (2005) evidenced how CO_2 and N_2 solubility and diffusivity in PCL can be utilized for the optimization of both density and morphology of PCL foams by using specifically designed mixtures of the two blowing agents.

Similar results have been reported for PLA. Liu and Tomasko (2007) reported a rather good solubility of CO_2 which, in turn, is responsible for the achievement of PLA foam characterized by low density, as reported by, among others, Di *et al*. (2005), Mihai *et al*. (2007, 2010), Lee *et al*. (2008) and Zhai *et al*. (2009). Li *et al*. (2006), furthermore, reported solubility data of N_2 in PLA are almost one order of magnitude less than solubility of CO_2, at the same testing conditions. As expected, the very different solubilities gave foams characterized by different expansion ratios. In particular, Lee *et al*. (2008) reported PLA/CO_2 foams with densities as low as 0.03 g/cm^3, while, with N_2, the lowest reported density was 0.5 g/cm^3. It is worthy of note that the authors evidenced extensive differences in the foam morphology, with CO_2 giving pores with 100 μm mean diameter, while N_2 induced the formation of pores of sub-micron size.

Table 6.1 reports the sorption data for some biodegradable polymer of interest in foaming.

6.2.2 Rheological properties

The rheological properties of the expanding polymer are of great importance for their effect on the final foam density and morphology. For instance, an easily deformable polymeric matrix is required at the beginning of foaming, to allow the achievement of low-density foam and efficient use of the blowing agent; at the later stage of foam formation, conversely, strain hardening should occur, to avoid pore coalescence and foam collapse. Typically, strain hardening is a pure rheological property, as occurring in several strongly entangled polymers; however, alternative and/or concurrent mechanisms, such as crystallization and/or vitrification, may be also utilized.

A critical issue regarding the rheological properties of the expanding matter, in foaming, is the relevant effect of the blowing agent on the rheological properties of the polymer, typically leading to a reduction of the viscosity, commonly addressed to as the 'plasticization' effect. Furthermore, measurement of the rheological properties of polymer/gas mixture is relatively complex, mainly because of the need to keep the system as a solution,

Table 6.1 Sorption data for some biodegradable polymers

Polymer	Gas	Solubility (wt fraction)	Diffusivity (cm^2/s)	Temperature (°C)	Pressure (MPa)	References
Poly (lactic-co.glycolic acid), PLGA	CO_2	0.08		60	5	Liu and Tomasko, 2007
Poly (butylene succinate–co-adipate), PBSA	CO_2	0.11	2×10^{-5}	180	20	Sato *et al.*, 2000
Starch	CO_2	0.04		180	20	Mihai *et al.*, 2007
Poly (hydroxybutyrate), PHB	CO_2	0.025		35	2	Miguel *et al.*, 1999
Poly (ε-caprolactone), PCL	N_2	0.03	1×10^{-4}	75	10	Di Maio *et al.*, 2005
Poly (ε-caprolactone, PCL	CO_2	0.085	8×10^{-6}	75	6	Di Maio *et al.*, 2005
Poly (lactic acid), PLA	N_2	0.016	4×10^{-5}	200	28	Li *et al.*, 2006
Poly (lactic acid), PLA	CO_2	0.175	3×10^{-5}	200	28	Li *et al.*, 2006

and avoiding the formation of a biphasic flow during the experiment, to be conducted at high blowing agent pressure. This can be obtained with several techniques, but basically in-line (directly in the process stream) or on-line (a pressurized sampling stream) is taken from the process line and transferred to a measuring system (Gendron and Daigneault, 2000). In recent years, rheological data of polymer/blowing agent solutions have become available to the scientific community from a number of research groups (Dealy, 1982; Han and Ma, 1983; Macosko, 1994; Gerhardt *et al*., 1997; Elkovitch *et al*., 1999; Lee *et al*., 1999; Areerat *et al*., 2002). More recently, data on biodegradable polymers have been reported (Di Maio *et al*., 2006).

6.2.3 Volumetric, thermal and interfacial properties

When the polymer is exposed to a gaseous penetrant, its volume changes as a consequence of the compression of the gas saturated polymer melt by the mechanical action of pressure exerted by the external gas and of the gas solubilization. With the increase of external gas pressure, typically, both the volume and the mass monotonically increase. As a final balance, typically, at low gas concentration, mass increase is the dominant effect, and a reduction of the specific volume is observed, while at higher gas concentration, conversely, volume increase becomes the predominant effect, leading to a bell-shaped curve.

Another relevant effect of gas dissolution on the expanding polymer is the associated change of the characteristic thermal transitions. In foaming, this phenomenon is exploited in two ways: (i) melting point depression is desirable for lowering processing temperatures, to reduce energy consumption and thermal degradation; (ii) it allows foaming at lower temperatures and, hence, it helps in locking the newly formed porous structure by crystallization or vitrification, solely by the loss of the plasticizing effect when the blowing agent is released. Data on extrusion foaming die temperatures differ by several tens of degrees Celsius from those of neat polymer in numerous examples, as a result of the dependence on the amount and kind of blowing agent. Specific data on the depression of characteristic temperatures of biodegradable polymers by blowing agents absorption are available in the scientific literature, and the most relevant are reported in Table 6.2. Specific literature on non-biodegradable polymers and modelling attempts can be found in Quach and Simha (1972), Chiou *et al*. (1985), Wissinger and Paulaitis (1991) and Condo *et al*. (1992).

The interfacial tension of the separation surface between the molten polymer/blowing agent solutions and the surrounding blowing agent is another key parameter controlling the foam morphology. It can be measured by using the 'axisymmetric drop shape analysis' (ADSA), which is based on the evaluation of the shape of an axisymmetric pendant drop

Table 6.2 Effect of gas sorption on melting point of selected biodegradable polymers

Polymer	T_m (K)	Blowing agent (MPa)	ΔT (Lian *et al.*, 2006)
Poly (ε-caprolactone), PCL	332	CO_2 (9.0)	22
Poly (butylene succinate), PBS	388	CO_2 (14.5)	14
Poly (ethylene adipate), PEA	328	CO_2 (27.6)	22
Poly (L-lactic acid), PLLA	448	CO_2 (27.6)	55

(Wu, 1982) according to the Laplace equation. Typically, a depression of the interfacial tension is observed after blowing agent solubilization (Kiszka *et al*., 1998; Nalawade *et al*., 2008), reported, among others, by Harrison *et al*. (1996), Harrison *et al*. (1998), Li *et al*. (2004), Liu and Tomasko (2007) and Pastore Carbone *et al*. (2011, 2012). The plasticizing actions are generally attributed to two concurrent phenomena: (1) as pressure increases, the free energy density of the blowing agent becomes closer to that of the polymer phase and the interfacial tension decreases; (2) as gas pressure increases, the blowing agent concentration increases thus promoting a further decrease of interfacial tension since the two phases in contact become more similar.

6.3 Biofoams based on natural polymers

A great number of different natural materials have been studied and proposed for the preparation of scaffolds in tissue engineering. Natural materials, such as polysaccharides and proteins, offer several advantages such as biological signaling, cell adhesion, cell responsive degradation and remodelling. However, due to their inadequate physical properties they are often combined with other polymers. The most investigated polysaccharides for the preparation of porous scaffolds by using the gas foaming technique are starch, alginate and chitosan. Foams from proteins include zein and gelatine.

6.3.1 Polysaccharides

Polysaccharides are naturally occurring biomacromolecules derived from plants, animals and micro-organisms, characterized by monosaccharides linked together by O-glycosidic linkages. The composition of the monosaccharide units, the linkage types, the chain shape and the molecular weight dictate their physical properties, including solubility, surface and interfacial properties, and therefore their processability and biological response (Mano *et al*., 2007).

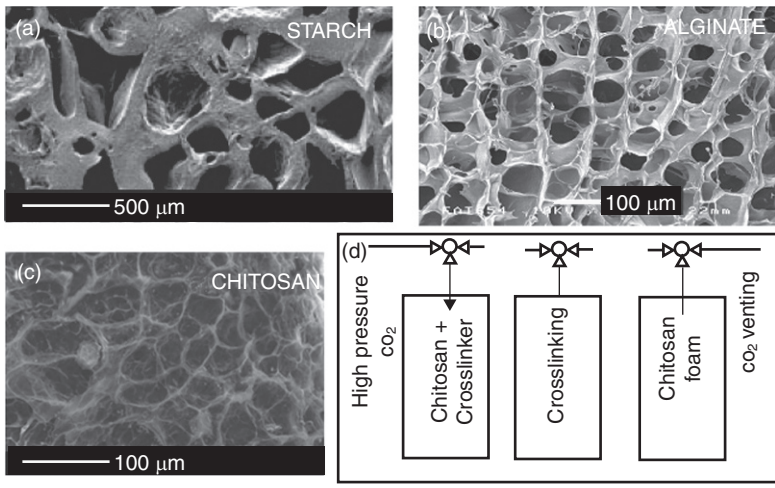

6.1 Polysaccharide foams prepared with different methods: (a) starch with the microwave foaming (Torres *et al.,* 2007), (b) alginate with the 'carbon dioxide in water' emulsion templating method (Partap *et al.,* 2006) and (c)-(d) chitosan with the CO_2 dense gas foaming (Ji *et al.,* 2011).

These polysaccharides have been utilized to develop porous structures by different methods. Starch-based scaffolds can be produced by using extrusion with blowing agents, *in situ* polymerization or by combining solvent casting and particulate leaching, compression moulding and particulate leaching (Gomes *et al*., 2002). Chitosan can be moulded in various forms with a fairly well-designed porous structure by means of techniques such as freeze-drying, rapid prototyping and internal bubbling process (Yannas, 1996; Di Martino *et al*., 2005; Ji *et al.,* 2011). Alginates have been used mainly in the form of hydrogels, since they can be easily prepared by crosslinking under very mild conditions, at low temperature, and in the absence of organic solvents (Puppi *et al*., 2010). Injectable gels based on pure alginate, and in combination with chitosan (Li *et al*., 2005; Park *et al*., 2005) or hyaluronic acid (Lindenhayn *et al*., 1999), have been used for TE.

Among polysaccharides employed as TE scaffold materials, only starch, alginate and chitosan have been used to develop porous structures based on the gas foaming technique. Examples of porous morphologies obtained from these biopolymers are shown in Fig. 6.1. More information on the processing and properties of such systems are given below.

Starch foams

Starch is a polysaccharide composed of a mixture of a linear polymer (amylose) and a highly branched macromolecule (amylopectin). In both

polymeric structures, the repeating unit is the glucose molecule (Daniel *et al*., 2000). This polysaccharide has been widely used to prepare plastic-like materials by mixing granular starch with water and/or non-volatile plasticizers, which decrease the glass transition and the melting temperature (Perry and Donald, 2000). Destructurized starch, also referred to as thermoplastic starch (TPS), is commonly processed with low molecular weight plasticizers such as glycerol, glycerol monostearate, glycol, xylitol, sorbitol, polyethylene glycol, sugars and oligosaccharides, fatty acids, lipids and derivatives.

Starch-based foams have been studied to develop food as well as lightweight biodegradable common products (Cotugno *et al*., 2005). The formation of porous structures in starch polymers was first studied for the preparation of food products. The oldest techniques to produce starch-based foams are the 'explosion puffing' (Hoseney *et al*., 1983) and the 'baking' techniques (Tiefenbacher, 1993; Haas and coworkers, 1996) where the steam generated by the moisture at high temperature in the sample acts as a blowing agent. More recently, continuous technologies based on both single and double screw extrusion processes have been used to produce extruded products for different applications, such as packaging, or for thermal/acoustic insulation (Willett and Shogren, 2002) with the aim of replacing oil-based polymers with bio-based, biodegradable polymeric materials. In these extrusion foaming technologies, bubbles nucleate at the die exit as a consequence of the pressure drop. Nuclei of water vapour bubbles are formed and grow in size as additional water vapour molecules diffuse into the nuclei, until the final structure of the extrudate is set. Starch-based products have also been produced by using a combination of supercritical carbon dioxide (Sc-CO_2) and water as blowing agent (Cho and Rizvi, 2008), and improved expansion porous structures were obtained.

In order to control the moisture resistance, the mechanical properties and the degradation rate, starch has been often mixed with other biodegradable thermoplastics (Shen *et al*., 2009). Blends of starch with PLA, ethylene vinyl alcohol (EVA), cellulose acetate (CA) and PCL were proposed as potential alternative biodegradable materials for a wide range of biomedical applications, including bone cements, hydrogels for drugs controlled delivery, and bone substitutes (Gomes *et al*., 2001, 2002; Salgado *et al*., 2002; Neves *et al*., 2005; Torres *et al*., 2007; Duarte *et al*., 2009).

Alginate foams

Alginates are linear unbranched polysaccharides constituted of varying amounts of (1- 4)-linked β-D-mannuronic acid and α-L-guluronic acid, and extracted primarily from brown algae (Smidsrød and Skjåk-Braek, 1990). Due to their biocompatibility, they have been widely investigated in biomedical applications, including TE scaffolds (Yasuda *et al*., 2006; Cheng *et al*.,

2008). The native alginates are mainly present as insoluble Ca^{2+} crosslinked gels, but they can form relatively stable hydrogels in the presence of other multivalent cations (e.g., Sr, Ba). These hydrogels are formed through interaction between the carboxylic acid group of the polymer and the chelating cation (Puppi *et al*., 2010).

Alginate porous structures have been successfully prepared by using a 'carbon dioxide in water' emulsion templating method by Partap *et al*. (2006). A highly porous alginate hydrogel was prepared by coupling a templating 'oil-in-water' emulsion reaction with an internal gelation reaction to 'lock in' the structure from the internal oil phase. In their work, both an organic solvent (isooctane) and dense-phase CO_2 (above the critical point of CO_2) have been used as the internal oil phases for the templating step. They found that the dense-phase CO_2 simultaneously acts both as a templating 'oil' phase as well as producing the acidity (carbonic acid, pH 3–4) that releases the calcium ions from their chelated form, crosslinking the alginate and forming a porous hydrogel. Due to the dual role of CO_2 as a reagent and a template, this process was named 'reactive emulsion templating' (RET). Highly porous alginate hydrogels with a narrow range of macropore sizes were obtained with the RET process. These hydrogels exhibit an open, well interconnected pore network with a narrow pore-size distribution suitable for tissue engineering applications.

Chitosan foams

Chitosan (CS) is a biodegradable cationic aminopolysaccharide derived from chitin (N-deacetylated derivative), the second most abundant polysaccharide after cellulose. Chitin is a structural biopolymer that provides structural integrity and protection to animals. While CS can be soluble in water, the dissolution of chitin is very difficult to achieve, due to the high intra- and inter-molecular hydrogen bonds. The main technologies utilized to process chitin are solvent-based, and they have been used to cast films or to make fibres by using the wet spinning process (Rinaudo, 2006; Pillai *et al*., 2009).

Solvent casting/salt leaching (Wan *et al.*, 2008) and freeze-drying have been used to generate porosity in chitosan and composite mixtures of chitosan and other polymers (Madihally and Matthew, 1999; Wu *et al*., 2008). However, there are, in general, several disadvantages when using these techniques due to the use of toxic solvents, the very slow removal of solvent by evaporation, the irregular shape of pores and the insufficient interconnectivity, a basic requirement necessary to enable the culture cells to diffuse throughout the scaffold.

The CO_2–water emulsion-template method, described above for alginate systems, was employed to produce highly porous structures in hydrophilic

poly(vinyl alcohol) (PVA) and chitosan (Lee *et al.*, 2007). Other CO_2-assisted methods based on solvent exchange/supercritical fluid drying (Tsioptsias and Panayiotou, 2008; Singh *et al.*, 2009; Ji *et al.*, 2010) were developed to produce porous hydrophilic polymers. However, these methods have limitations, such as the use of organic solvents and the inability to form microscale pores that are suitable for tissue engineering.

Ji *et al.* (2011) have used the CO_2 dense gas foaming method to generate gas bubbles in chitosan systems by rapid gas depressurization, as typically done in polymer foaming. Highly interconnected pores with an average pore diameter ranging from 30 to 40 μm able to support cell penetration and proliferation within the 3D structure were obtained with this technique.

6.3.2 Proteins

Many different proteins have been investigated to develop TE scaffolds. They are often preferred over carbohydrates and synthetic polymers for medical applications because proteins are a major part of the human body, they are bio- and cyto-compatible and, as scaffold materials, it is easier to maintain the functions of the extracellular matrix (ECM) with proteins than with synthetic polymers (Chan and Mooney, 2008). Proteins contain functional groups such as amino and carboxyl groups that can carry different charges depending on the pH. Therefore, proteins from animals and plants are good candidates to develop stimuli-responsive materials based on pH.

Proteins derived from animals, such as *collagen* and its denaturated derivatives *gelatin* and *silk* fibroin, have been widely studied. However, there are several drawbacks associated with these proteins. Collagen shows poor wet mechanical properties and potential immunogenicity, while silk is slowly biodegradable and it is difficult to process. Plant proteins are widely available, have low potential to be immunogenic, and can be made into fibres, films, hydrogels and micro- and nano-particles for medical applications (Reddy and Yang, 2011). Studies, mostly with zein, have demonstrated the potential of using plant proteins for tissue engineering and drug delivery. Other plant proteins that have also shown biocompatibility *in vitro* studies include wheat gluten and soy proteins.

Hydrogels, films, fibres, and nano- and micro-particles based on plant proteins have been developed for biomedical application by using solvent-based methods. In a similar way to TPS, addition of low molecular weight plasticizers allows the proteins to undergo glass transition, and facilitates deformation and processability. Agro-based proteins, such as wheat gluten, corn zein and soy protein, and whey proteins have been successfully formed into films using thermoplastic processes such as compression moulding and

extrusion (Wang and Padua, 2003; Pommet and coworkers, 2005; Selling, 2007; Hernandez-Izquierdo and Krotcha, 2008; Di Maio and coworkers, 2010; Oliviero and coworkers, 2010).

Very few works have reported on the thermo-plasticization and the foaming process of protein-based materials. As reported in the following, physical blowing agents, such as CO_2, N_2 and their mixtures have been used to prepare thermoplastic zein and thermoplastic gelatin foams using the batch foaming technique.

Zein-based foams

Thermoplastic zein (TPZ) can be obtained by applying heat and shear stresses in a mixer or in an extruder. Unfolding of the protein occurs in the presence of a suitable plasticizer. For example, Di Maio and coworkers (2010) have used several plasticizers (PEG400, lactic acid LA, lauric acid LAU and stearic acid ST) with different polarity characteristics and molecular weights to investigate the thermoplasticity of zein proteins. They have shown that the efficiency of the thermoplasticization process influences the mechanical properties of the final TPZ material and depends upon the initial temperature, the speed of rotation and time of mixing for each protein/plasticizer system.

TPZ samples were placed into the pressure vessel and kept with blowing agent mixture for 6 h at 70°C and at saturation pressure in the range 60–180 bar. After saturation, samples were rapidly cooled or heated to the desired foaming temperature with a controlled profile, and finally pressure was reduced to atmospheric pressure to allow foaming. To stabilize the porous structure, foams were immediately cooled down to ambient temperature and subsequently removed from the vessel. The authors have shown that the size and number of pores can be tuned by controlling the blowing agent composition, a mixture of N_2 and CO_2, the foaming temperature in the range 44–140°C and the pressure drop rate in the range 250–700 bar/s (Fig. 6.2).

Very different porous structures can be obtained with TPZ plasticized with 25% of polyethylene glycol (PEG 400, M.W. = 400) by changing the blowing agent composition (Fig. 6.2). The use of pure CO_2 resulted in poor porous morphologies characterized by few bubbles of larger size. Better morphologies, characterized by a high number of small pores, were obtained by using N_2. However, due to the lower solubility of N_2 in these materials, the density of these foams was high. The best blowing agent system was found to be a mixture of these two gases (80–20 of N_2–CO_2 vol.%) that allowed to prepare foams at temperatures in the range 70–90°C. Foams were characterized by pores of 20–40 μm in diameters and densities as low as 0.1 g/cm^3.

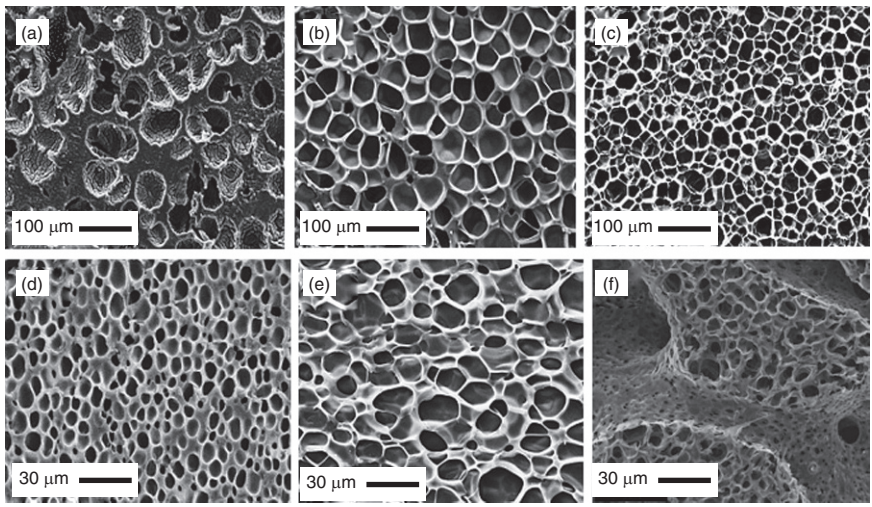

6.2 SEM micrographs of TPZ and TPG foams: (a) TPZ foamed with CO_2 at T_{foam} = 50°C; (b) TPZ foamed with N_2 at T_{foam} = 100°C; (c) TPZ foamed with a mixture 80–20 of CO_2–N_2 at T_{foam} = 79°C; (d) TPG foamed with a mixture 80–20 of CO_2–N_2 at T_{foam} = 44°C; (e) TPG foamed with a mixture 80–20 of CO_2–N_2 at T_{foam} = 120°C; (f) TPG/PCL, after removal of gelatin phase, foamed with a mixture 80–20 vol % of CO_2–N_2 at T_{foam} = 44°C. (*Source*: From Salerno *et al.* (2007a, 2007b.) (parts a to e only © Carl Hanser Verlag, Muenchen)

Gelatin-based foams

Gelatin is the result of the denaturation process of collagen, the major structural protein of most connective tissues (Bigi *et al.*, 2004). Due to its low cost and biodegradability, its use has been widely investigated in food, pharmaceutical and photographic industries.

Thermoplastic gelatin (TPG) can be produced by mixing gelatin powder and glycerol or lactic acid as plasticizer. Mixing temperature, speed of rotation, and mixing time need to be optimized to obtain plastic-like melts that can be foamed by using conventional gas foaming technologies. Salerno and coworkers (2007a) have shown that TPG can be foamed above its glass transition temperature (about 50°C) up to 140°C where severe thermal degradation starts to occur. Foaming experiments were carried out by using a batch process, with the same procedure as described above for TPZ foams. The TPG foams were mainly characterized by closed pores.

TPG can be easily blended with biodegradable polymers characterized by low melting temperatures. Blends of TPG and PCL can be foamed with the same methods described above. A selective extraction of the water soluble gelatin phase permits the development of porous network pathways characterized by multimodal porosities (Fig. 6.2) (Salerno *et al.*, 2007b).

6.4 Biofoams based on biodegradable polyesters

Many different types of polyesters have been employed to develop TE scaffolds. All polyesters are, in principle, hydrolytically degradable. Typically, (co)polyesters with short aliphatic chains between ester bonds degrade over the timeframe required for biomedical applications. The most investigated materials are the poly(hydroxycarboxylic acid), which are prepared by ring opening polymerization of lactones or cyclic diesters such as PLA, PGA, PLGA and PCL.

6.4.1 Polylactide-based foams

PLA can be synthesized by different routes starting from lactic acid, an α-hydroxy acid existing in either L(+) or D(−) stereoisomer. Its properties, namely the maximum crystallinity, melting temperature and glass transition temperature depend upon their molecular weight and stereochemistry. Both poly(L-lactic acid) (PLLA) and poly(D-lactic acid) (PDLA) are semicrystalline, while the presence of significant amounts of one form within a sequence of the other, giving poly(D,L-lactic acid), can result in an amorphous polymer (Steinbuchel and Doi, 2002). PLA can be processed by using conventional technologies such as extrusion, injection moulding, injection stretch blow moulding, casting, blown film thermoforming, foaming, blending, fibre spinning and compounding (Lim and coworkers, 2008).

The glass transition temperature (T_g) of amorphous PLA lies between 55 to 60°C and is a function of the PLA molecular weight and stereochemistry. In semicrystalline PLA, the T_g is higher (60–80°C) and depends on the crystallization conditions that determine both the morphology of the crystalline/amorphous phases and the degree of crystallinity. The amorphous phase in semicrystalline PLA is characterized by the presence of two phases, a mobile fraction and a rigid fraction characterized by lower mobility and higher T_g (Iannace and Nicolais, 1997). The amount of rigid fraction depends upon the crystallization conditions and it can reach values of about 25–30% when PLA is isothermally crystallized in the range of 90–110°C.

PLA crystallizes when cooled from melt (melt crystallization) or when heated above its T_g (cold crystallization) in the range 80–150°C, but its fastest rate of crystallization occurs between 95°C and 115°C. The melting temperature (T_m) of PLA occurs between 130°C and 180°C according to the L-lactide content and the type of crystals formed during the crystallization.

The selection of the processing window aimed at exploring foaming behaviour in the presence of blowing agents is based on the thermal properties of PLA. In particular, porous structures can be generated within a PLA matrix by promoting bubble nucleation and growth during a controlled cooling from the melt, typically in extrusion and injection-moulding-based

technologies, or in the 'solid state' above the T_g and below the T_m. In both methods, one must take into account that in presence of a physical blowing agent, the T_g, the crystallization temperatures, and the T_m will shift to lower values. Carbon dioxide has been used as an efficient plasticizer and foaming agent for the fabrication of 3D scaffolds based on PLA and poly(lactic acid-co-glycolic acid) (PLGA). CO_2 can be also used in combination with N_2 to improve the porous morphology of PLA and PLA-based nanocomposite matrices (Di *et al.*, 2005a, 2005b).

The effect of foaming conditions from the melt on foam architecture was investigated by Mathieu *et al.* (2005). Samples of PLA were placed in a pressure vessel and saturated at 100 and 250 bar at 195°C. Foam expansion was then achieved by sudden gas release, with additional water cooling. Neat PLA foams with interconnected pores with a diameter of 200–400 μm, and compressive moduli between 10 and 180 MPa for porosities from 78% to 92%, were obtained (Fig. 6.3a).

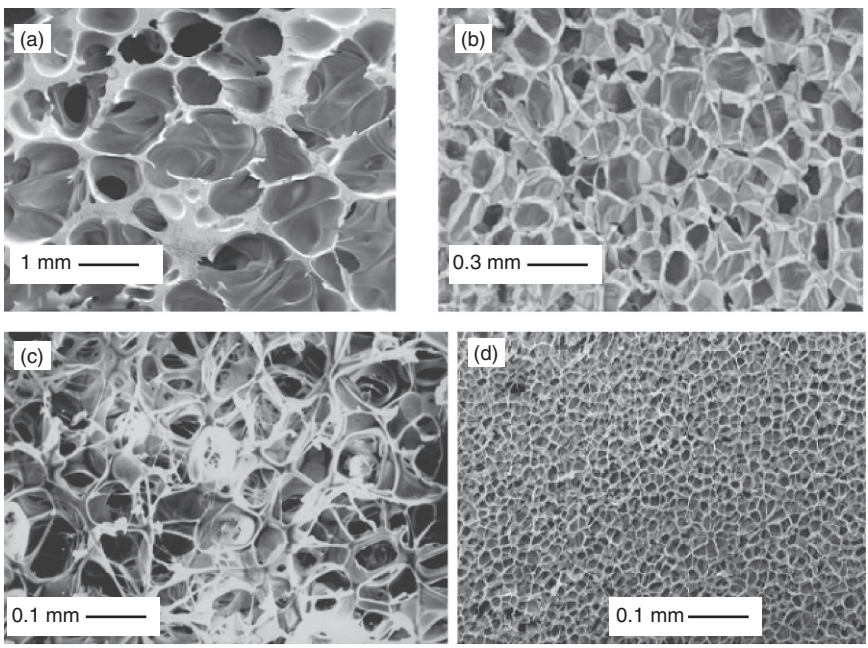

6.3 Porous morphologies of PLA foams prepared with different techniques and processing conditions: (a) PLA saturated with CO_2 at 195°C, 15 MPa, cooling at 5.1°C/s (Mathieu *et al.*, 2005); (b) PLA saturated with a mixture of CO_2 and N_2 (20:80) at 170°C, 16 MPa, T_{foam} = 110°C (Di *et al.*, 2005b); (c) PLA saturated with CO_2 at 100°C, 5 MPa, after ultrasound (Wang *et al.*, 2006); (d) PLA/nanoclay (1%) saturated with a mixture of CO_2 and N_2 (20:80) at 170°C, 16 MPa, T_{foam} = 110°C (Di *et al.*, 2005a).

Foaming from melt can be also used to develop composite scaffolds based on PLA matrix and ceramic fillers, hydroxyapatite (HA) or β-tricalcium phosphate (β-TCP) (Mathieu *et al*., 2006; Montjovent *et al*., 2007). The rate of cooling has a significant effect on the porous structure: cooling too rapidly will result in small closed pores, whereas a very slow cooling will not allow freezing of the structure, which will finally collapse. An intermediate cooling rate must be found which allows interconnections to be created, while still stabilizing the morphology before it collapses.

To control the morphology of supercritically foamed scaffolds, it is essential to study the interactions of polymers with CO_2 and the consequent solubility of CO_2 in the polymers, as well as the viscosity of the plasticized polymers. Tai *et al*. (2010) have shown that the viscosities of the CO_2-plasticized polymers at 35°C and 100 bar were comparable to the values for the polymer melts at 140°C. The PLA/gas solutions can therefore be foamed at relatively low temperature, and this allows the incorporation of biologically active guest species into polymer host with limited loss or change of activity.

Based on the above considerations, the solid-state foaming process has been studied to generate microporous foams (usually termed microcellular foams) for biomedical applications by using gases such as CO_2 and N_2. Singh *et al*. (2004) have used this method with an amorphous PLGA to generate microcellular structures with pore sizes ranging from submicrometres to a few hundred micrometres at 35°C. However, the disadvantage of the process is that the foams it produces are mostly close-pored and not suitable for tissue engineering applications. For this reason, solid-state gas foaming of PLA-based scaffolds is often coupled with particulate leaching to generate open-pore structures (Mooney *et al*., 1996; Harris *et al*., 1998; Nam *et al*., 2000).

Another method to break the pore walls of the solid-state foams is to use ultrasound. Wang *et al*. (2006) have used semicrystalline PLA. The samples were first foamed in the solid-state foaming process at temperature below the melting point (100–150°C) to achieve suitable pore sizes. Then the foamed samples were processed using ultrasound to enhance the inter-pore connectivity of the solid-state foams (Fig. 6.3c).

6.4.2 Poly(ε-caprolactone)-based foams

Poly(ε-caprolactone) is a semicrystalline aliphatic linear polyester with remarkable hydrophobicity. The hydrolytic degradation of PCL is very slow (years), and it is therefore indicated as base material for the development of long-term implants.

Poly(ε-caprolactone) (PCL) is obtained by ring opening polymerization of ε-caprolactone, and it has a very low T_g (–61°C) and a low melting point (65°C) (Chiellini and Solaro, 1996; Albertsson and Varma, 2002; Okada, 2002).

Due to the relatively low processing temperatures, and thanks to their good rheological properties, PCL foams are being widely investigated. In particular, their elongational viscosity is adequate for bearing the pore wall stretching during bubble growth. Nevertheless, improvement of the molecular weight has been pursued to reduce the mean pore size and to increase the nucleated bubbles as experienced by Di Maio and coworkers (2005a).

Microcellular structures can be easily prepared with batch foaming, by using the pressure quench (Xu *et al*., 2004; Jenkins *et al*., 2006) or the temperature increase (Liu, 2008) techniques. The porous structure can also be improved by carefully controlling the development of the crystalline phase during cooling from the melt state. Nucleated crystals can promote bubble nucleation in presence of supercritical CO_2 as blowing agent thus improving the microcellular morphology of the foam (Reignier and coworkers, 2007).

Combinations of different blowing agents have also been investigated. Di Maio and coworkers (2005b) tailored the porous morphology by changing the ratio between nitrogen and carbon dioxide contents. When using CO_2 alone, the plasticization of the PCL in presence of the blowing gas allowed the foaming of the polymer at temperatures in the range of 30–40°C. The lowest density (0.03 g/cm^3) was achieved at T_{foam} = 32°C, a saturation pressure of 59 bar, and pressure drop rate of 30 bar/s. In this case, the porous structure was characterized by pores with an average size of 250 μm. In the presence of pure nitrogen, the foaming temperatures were higher, in the range of 43–50°C. So-called microcellular foams were obtained at T_{foam} = 43°C, with a saturation pressure of 170 bar, and pressure drop rate of 80 bar/s, with a pore diameter of about 20 μm. However, due to the lower solubility of N_2 compared to CO_2, the densities of N_2-based foams were higher (0.2–0.6 g/cm^3). Low-density PCL foams characterized by lower pore size were obtained by using a mixture of CO_2 and N_2. In fact, CO_2 was found to be a good foaming agent, due to the high solubility and the high plasticizing effects, while N_2 led to a better morphology in terms of pore size and number of cells. Foams of different density and number of cells were obtained by using different compositions of CO_2/N_2 and different saturation pressures. In this case, a small amount of CO_2 was enough to inflate the high number of bubbles generated by N_2 and to achieve foams with a very fine morphology and low density (around 0.07 g/cm^3) at the same time. The foaming temperatures were intermediate between the foaming temperatures of the two pure gases, suggesting that the plasticizing effect could, in this gross evaluation,

be considered additive. SEM micrographs reported in Fig. 6.4a–6.4d show the porous structures of PCL foams prepared with different blowing agents and conditions.

Tsivitzelis and coworkers (2007) prepared PCL foams using CO_2–ethanol supercritical mixtures as blowing agents (Fig. 6.4e). The results revealed that difficulties in the foaming of polymers related to their crystalline structure could be overcome with the addition of small amounts of organic solvents. The structures that were obtained with the addition of small amounts of ethanol were more uniform with larger pore sizes with respect to pure CO_2.

Most of the PCL foams prepared by the gas foaming technique reported above are characterized by porous structures based on closed pores. The development of open-pore structures can be obtained by promoting the rupture of the pores during their growth, or by combining the gas foaming with

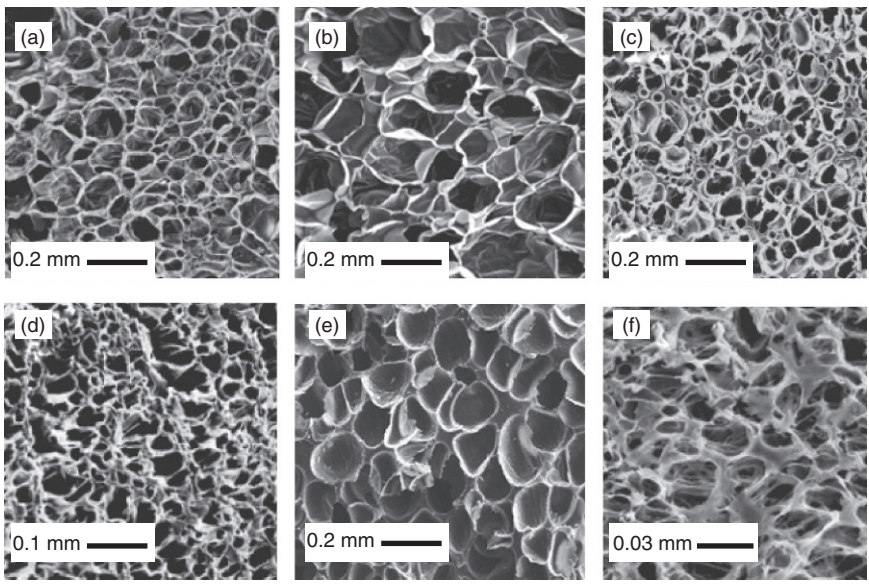

6.4 Porous morphologies of PCL foams prepared with different techniques and processing conditions: (a) PCL foamed with CO_2 at 29.4°C, Psat = 5 MPa, density = 0.099 g/cm^3 (Di Maio *et al.*, 2005b); (b) Crosslinked PCL foamed with chemical blowing agent (BA) in oil bath at 200°C, density = 0.044 g/cm^3 (Liu *et al.*, 2008); (c) PCL foamed with N_2 at 48.9°C, Psat = 17.2 MPa, density = 0.19 g/cm^3 (Di Maio *et al.*, 2005b); (d) PCL foamed with CO_2–N_2 mixture at 40.6°C, Psat(CO_2) = 1.7 MPa, Psat(N_2) = 12.1 MPa, density = 0.15 g/cm^3 (Di Maio *et al.*, 2005b); (e) PCL foamed with CO_2–ethanol mixture at 40°C, Psat = 14.7 MPa, density = 0.35 g/cm^3 (Tsivitzelis *et al.*, 2007); (f) Gas foaming combined with salt leaching from PCL/NaCl (50/50) microcomposites, T_{foam} = 34°C, Psat = 6.5 MPa at 70°C (Salerno *et al.*, 2008).

templating techniques. Microparticulate composites of PCL and micrometric sodium chloride particles (NaCl), in concentrations ranging from 70/30 to 20/80 wt.% of PCL/NaCl, were melt-mixed and gas-foamed using carbon dioxide as physical blowing agent by Salerno *et al.* (2008). After foaming, the microparticles were leached out, leading to a porous morphology characterized by an open-pore network (Fig. 6.4f). The control of porosity (in the range 78–93%) and pore size (from around 90 to 10 μm) was mainly achieved by varying microparticulate concentration and foaming temperatures.

6.5 References

Albertsson, A.-C. and Varma, I.K. (2002). 'Aliphatic polyesters: synthesis, properties and applications', *Advances in Polymer Science*, **157**, 1–40.

Areerat, S., Nagata, T. and Ohshima, M. (2002). 'Measurement and prediction of LDPE/CO_2 solution viscosity', *Polymer Engineering & Science*, **42**, 2234–2245.

Bigi, A., Panzavolta, S. and Rubini, K. (2004). 'Relationship between triple-helix content and mechanical properties of gelatin films', *Biomaterials,* **25**, 5675–5680.

Chan, G. and Mooney, D.J. (2008). 'New materials for tissue engineering: towards greater control over the biological response', *Trends Biotechnology*, **26**, 382–392.

Cheng, N., Wauthier, E. and Reid, L.M. (2008). 'Mature human hepatocytes from ex vivo differentiation of alginate-encapsulated hepatoblasts', *Tissue Engineering A*, **14**, 1–7.

Chiellini, E. and Solaro, R. (1996). 'Biodegradable polymeric materials', *Advanced Materials*, **8**(4), 305–313.

Chiou, J.S., Barlow, J.W. and Paul, D.R. (1985). 'Plasticization of glassy polymers by CO_2', *Journal of Applied Polymer Science*, **30**, 2633–2642.

Cho, K.Y. and Rizvi, S.S.H. (2008). 'The time-delayed expansion profile of supercritical fluid extrudates', *Food Research International*, **41**(1), 31–42.

Condo, P.D., Sanchez, I.C., Panayiotou, C.G. and Johnston, K.P. (1992). Glass transition behavior including retrograde vitrification of polymers with compressed fluid diluents, *Macromolecules*, **25**, 6119–6127.

Cotugno, S., Di Maio, E., Iannace, S., Mensitieri, G. and Nicolais, L. (2005). Biodegradable foams, in *Handbook of Biodegradable Polymeric Materials and Their Applications*, Ed. B. Narasimhan, E.S.K. Mallapragada, American Scientific Publishers: Iowa State University, Ames, USA, ISBN 1-58883-053-5.

Daniel, J.R., Whistler, R.L. and Röper, H. (2000). Starch. In: *Ullmann's Encyclopaedia of Industrial Chemistry* 2007. Wiley-VCH Verlag GmbH & Co. KGaA DOI: 10.1002/14356007.a25_001.

Dealy, J.M. (1982). In *Rheometers for Molten Plastics*, Dealy, J.M., Ed., Van Nostrand Reinhold Company: New York.

Di, Y., Iannace S., Di Maio, E. and Nicolais, L. (2005a). 'Poly(lactic acid)/organoclay nanocomposites: thermal, rheological properties and foam processing', *Journal of Polymer Science: Part B: Polymer Physics,* **43**, 689–698.

Di, Y., Iannace S., Di Maio, E. and Nicolais, L. (2005b). 'Reactively modified poly(lactic acid): properties and foam processing', *Macromolecular Materials and Engineering*, **290**, 1083–1090.

Di Maio, E., Iannace, S., Marrazzo C., Narkis, M. and Nicolais, L. (2005a). 'Effect of molecular modification on PCL foam formation and morphology of PCL', *Macromolecular Symposia*, **228**, 219–227.

Di Maio, E., Iannace, S., Mensitieri, G. and Nicolais, L. (2006). 'A predictive approach based on the Simha–Somcynsky free-volume theory for the effect of dissolved gas on viscosity and glass transition temperature of polymeric mixtures', *Journal of Polymer Science, Part B: Polymer Physics*, **44**, 1863–1873.

Di Maio, E., Mali, R. and Iannace, S. (2010). 'Investigation of thermoplasticity of zein and kafirin proteins: mixing process and mechanical properties', *Journal of Polymers & Environment*, **18**, 626–633.

Di Maio, E., Mensitieri, G., Iannace, S., Nicolais, L., Li, W. and Flumerfelt, R.W. (2005b). 'Structure optimization of polycaprolactone foams by using mixtures of CO_2 and N_2 as blowing agents', *Polymer Engineering & Science*, **45**, 432–441.

Di Martino, A., Sittinger, M. and Risbud, M.V. (2005). 'Chitosan: a versatile biopolymer for orthopaedic tissue-engineering', *Biomaterials*, **26**, 5983–5990.

Duarte, A.C., Mano, J.F. and Reis, R.L. (2009). 'Preparation of starch-based scaffolds for tissue engineering by supercritical immersion precipitation', *Journal of Supercritical Fluids*, **49**, 279–285.

Elkovitch, M. D., Tomasko, D. L. and Lee, L. (1999). 'Supercritical carbon dioxide assisted blending of polystyrene and poly(methyl methyacrylate)', *Polymer Engineering & Science*, **39**, 2075–2084.

Gendron R. and Daigneault L.E. (2000). Rheology of thermoplastic foam extrusion process. In *Foam Extrusion: Principle and Practice*, S.T. Lee Ed., Technomic Publ., Lancaster.

Gerhardt, L. J., Manke, C. W. and Gulari, E. (1997). 'Rheology of polydimethylsiloxane swollen with supercritical carbon dioxide', *Journal of Polymer Science: Part B: Polymer Physics*, **35**, 523–534.

Gomes, M.E., Ribeiro, A.S., Malafaya, P.B., Reis, R.L. and Cunha, A.M. (2001). 'A new approach based on injection moulding to produce biodegradable starch-based polymeric scaffolds: morphology, mechanical and degradation behaviour', *Biomaterials*, **22**, 883–889.

Gomes, M.E., Godinho, J.S., Tchalamov, D., Cunha, A.M. and Reis, R.L. (2002). 'Alternative tissue engineering scaffolds based on starch: processing methodologies, morphology, degradation and mechanical properties', *Materials Science and Engineering*, *C*, **20**, 19–26.

Haas, F., Haas, J. and Tiefenbacher, K.F. (1996). 'Process of manufacturing rottable thin-walled starch-based shaped elements', *US Patent*, 5,576,049.

Han, C.D. and Ma, C.Y. (1983). 'The effect of nucleating agents on the foam extrusion characteristics', *Journal of Applied Polymer Science*, **28**, 831–850.

Harris, L.D., Kim, B.S. and Mooney, D.J. (1998). 'Open pore biodegradable matrices formed with gas foaming', *Journal of Biomedical Material Research*, **42**, 396–402.

Harrison, K.L., da Rocha, S.R.P., Yates, M.Z., Johnston, K.P., Canelas, D. and De Simone, J.M. (1998). 'Interfacial activity of polymeric surfactants at the polystyrene–carbon dioxide interface', *Langmuir*, **14**, 6855–6863.

Harrison, K.L., Johnston, K.P. and Sanchez, I.C. (1996). 'Effect of surfactants on the interfacial tension between supercritical carbon dioxide and polyethylene glycol', *Langmuir*, **12**, 2637–2644.

Hernandez-Izquierdo, V.M. and Krotcha, J.M. (2008). 'Thermoplastic processing of proteins for film formation – A review', *Journal of Food Science*, **73**, 30–39.

Hoseney, R.C. and Zeleznak, K. A. (1983). 'A mechanism of popcorn poping', *Journal Cereal Science*, **1**, 43–52.

Iannace, S. and Nicolais, L. (1997). 'Isothermal crystallization and chain mobility of poly(L-lactide)', *Journal of Applied Polymer Science*, **64**, 911–919.

Jenkins, M.J., Harrison, K.L., Silva, M.M.C.G., Whitaker, M.J., Shakesheff, K.M. and Howdle, S.M. (2006). 'Characterisation of microcellular foams produced from semi-crystalline PCL using supercritical carbon dioxide', *European Polymer Journal*, **42**, 3145–3151.

Ji, C., Annabi, N., Khademhosseini, A. and Dehghani, F. (2011). 'Fabrication of porous chitosan scaffolds for soft tissue engineering using dense gas CO_2', *Acta Biomaterialia*, **7**, 1653–1664.

Ji, C., Barrett, A., Poole-Warren Laura, A., Foster, N.R. and Dehghani, F. (2010). 'The development of a dense gas solvent exchange process for the impregnation of pharmaceuticals into porous chitosan', *International Journal of Pharmacy*, **391**, 187–196.

Kiszka, M.B., Meilchen, M.A. and McHugh, M.A. (1998). 'Modeling high-pressure gas–polymer mixtures using the Sanchez–Lacombe equation of state', *Journal of Applied Polymer Science*, **36**, 583–597.

Lee, M., Park, C. B. and Tzoganakis, C. (1999). 'Measurements and modeling of PS/supercritical CO_2 solution viscosities', *Polymer Engineering & Science*, **39**, 99–109.

Lee, S.T., Kareko, L. and Jun, J. (2008). 'Study of thermoplastic PLA foam extrusion', *Journal of Cellular Plastics*, **44**, 293–305.

Lee, J.Y., Tan, B. and Cooper, A.I. (2007). 'CO_2-in-water emulsion-templated poly(vinyl alcohol) hydrogels using poly(vinyl acetate)-based surfactants', *Macromolecules*, **40**, 1955–1961.

Li, G., Li, H., Turng, T.S., Gong, S. and Zhang, C. (2006). 'Measurement of gas solubility and diffusivity in polylactide', *Fluid Phase Equilibria*, **246**, 158–166.

Li, Z., Ramay, H.R., Hauch, K.D., Xiao, D. and Zhang, M. (2005). 'Chitosan-alginate hybrid scaffolds for bone tissue engineering', *Biomaterials*, **26**, 3919–3928.

Lian, Z., Epstein, S.A., Blenk, C.W. and Shine, A.D. (2006). 'Carbon dioxide-induced melting point depression of biodegradable semicrystalline polymers', *Journal of Supercritical Fluids*, **39**, 107–117.

Lim, L.T., Auras, R. and Rubino, M. (2008). 'Processing Technologies for poly(lactic acid)', *Progress in Polymer Science*, **33**, 820–852.

Lin, S., Yang, J., Yan, J., Zhao, Y. and Yang, B. (2010). 'Sorption and diffusion of supercritical carbon dioxide in a biodegradable polymer', *Journal of Macromolecular Science, Part B: Physics*, **49**, 286–300.

Lindenhayn, K., Perka, C., Spitzer, R.S., Heilmann, H.H., Pommerening, K. and Mennicke, J, (1999). 'Retention of hyaluronic acid in alginate beads: aspects for in vitro cartilage engineering', *Journal of Biomedical Materials Research*, **44**, 149–155.

Liu, H., Han, C. and Dong, L. (2008). 'Study on the cell structure and compressive behavior of biodegradable poly(e-caprolactone) foam', *Polymer Engineering and Science*, **48**, 2432–2438.

Liu, X. and Ma, P.X. (2004). 'Polymeric scaffolds for bone tissue engineering', *Annals of Biomedical Engineering*, **32**, 477–486.

Liu, D. and Tomasko, D.L. (2007). 'Carbon dioxide sorption and dilation of poly(lactide-co-glycolide)', *Journal of Supercritical Fluids*, **39**, 416–425.

Ma, P.X. (2004). 'Scaffolds for tissue fabrication', *Materials Today*, May 2004, **7**, 30–40.

Macosko, C.H. (1994). In *Rheology: Principles, Measurements and Applications*, Macosko, C. H., Ed., Wiley-VCH, New York, p. 237.

Madihally, S.V. and Matthew, H.W.T. (1999). 'Porous chitosan scaffolds for tissue engineering', *Biomaterials*, **20**, 1133–1142.

Mano, J.F., Silva, G.A., Azevedo, H.S., Malafaya, P.B., Sousa, R.A., Silva, S.S., Boesel, L.F., Oliveira, J.M., Santos, T.C., Marques, A.P., Neves, N.M. and Reis, R.L. (2007). 'Natural origin biodegradable systems in tissue engineering and regenerative medicine: present status and some moving trends', *Journal of the Royal Society Interface*, **4**, 999–1030.

Mathieu, L.M., Montjovent, M.O., Bourban, P.E., Pioletti, D.P. and Manson, J.A.E. (2005). 'Bioresorbable composites prepared by supercritical fluid foaming', *Journal of Biomedical Materials Research A*, **75**, 89–97.

Mathieu, L.M., Mueller, T.L., Bourban, P.T., Pioletti, D.P., Muller, R. and Manson, J.E. (2006). 'Architecture and properties of anisotropic polymer composite scaffolds for bone tissue engineering', *Biomaterials*, **27**, 905–916.

Mihai, M., Huneault, M.A., Favis, B.D. and Li, H. (2007). 'Extrusion foaming of semi-crystalline PLA and PLA/thermoplastic starch blends', *Macromolecular Bioscience*, **7**, 907–920.

Mihai, M., Huneault, M.A. and Favis, B.D. (2010). 'Rheology and extrusion foaming of chain-branched poly (lactic acid)', *Polymer Engineering & Science*, **50**, 629–642.

Miguel, O., Barbari, T.A. and Iruin, J.J. (1999). 'Carbon dioxide sorption and diffusion in poly(3-hydroxybutyrate) and poly(3-hydroxybutyrate-CO-3-hydroxyvalerate)', *Journal of Applied Polymer Science*, **71**, 2391–2399.

Montjovent, M.O., Mathieu, L., Schmoekel, H., Mark, S., Bourban, P.E., Zambelli, P.Y., Laurent-Applegate, L.A. and Pioletti, D.P. (2007). 'Repair of critical size defects in the rat cranium using ceramic-reinforced PLA scaffolds obtained by supercritical gas foaming', *Journal of Biomedical Materials Research Part A*, **83A**, 41–51.

Mooney, D.J., Baldwin, D.F., Suh, N.P., Vacanti, J.P. and Langer, R. (1996). 'Novel approach to fabricate porous sponges of poly(D,L-lactic-co-glycolic acid) without the use of organic solvents'. *Biomaterials*, **17**, 1417–1422.

Nalawade, S.P., Picchioni, F., Janssen, L.P.B.M., Grijpma, D.W. and Feijen, J. (2008). 'Investigation of the interaction of CO_2 with poly (L-lactide), poly(DL-lactide) and poly(e-caprolactone) using FTIR spectroscopy', *Journal of Applied Polymer Science*, **109**, 3376–3381.

Nam, Y.S., Yoon, J.J. and Park, T.G. (2000). 'A novel fabrication method of macroporous biodegradable polymer scaffolds using gas foaming and salt as a porogen additive', *Journal of Biomedical Materials Research: Applied Biomaterials*, **53**, 1–7.

Neves, N.M., Kouyumdzhiev, A. and Reis, R.L. (2005). 'The morphology, mechanical properties and ageing behavior of porous injection molded starch-based blends for tissue engineering scaffolding', *Materials Science and Engineering C*, **25**, 195–200.

Oliviero, M., Di Maio, E. and Iannace, S. (2010). 'Effect of molecular structure on film blowing ability of thermoplastic zein', *Journal of Applied Polymer Science*, **115**, 277–287.

Okada, M. (2002). 'Chemical syntheses of biodegradable polymers', *Progress in Polymer Science*, **27**, 87–133.

Pastore Carbone, M.G., Di Maio, E., Iannace, S. and Mensitieri, G. (2011). 'Simultaneous experimental evaluation of solubility, diffusivity, interfacial tension and specific volume of polymer/gas solutions', *Polymer Testing*, **30**, 303–309.

Pastore Carbone, M.G., Di Maio, E., Scherillo, G., Mensitieri, G. and Iannace, S. (2012). 'Solubility, mutual diffusivity, specific volume and interfacial tension of molten PCL/CO_2 solutions by a fully experimental procedure: effect of pressure and temperature', *Journal of Supercritical Fluids*, **67**, 131–138.

Park, D.-J., Choi, B.-H., Zhu, S.-J., Huh, J.-Y., Kim, B.-Y. and Lee, S.-H. (2005). 'Injectable bone using chitosan-alginate gel/mesenchymal stem cells/BMP-2 composites', *Journal of Craniomaxillofac Surgery*, **33**, 50–54.

Partap, S., Rehman, I., Jones, J.R. and Darr, J.A. (2006). 'Supercritical carbon dioxide in water emulsion-templated synthesis of porous calcium alginate hydrogels', *Advanced Materials*, **18**, 501–504.

Perry, P.A. and Donald, A.M. (2000). 'The rule of plasticization in starch granule assembly', *Biomacromolecules*, **1**, 424–432.

Pillai, C.K.S., Paul W. and Sharma, C.P. (2009). 'Chitin and chitosan polymers: chemistry, solubility and fiber formation', *Progress in Polymer Science*, **34**, 641–678.

Pommet, M., Redl, A., Guilbert, S. and Morel M.-H. (2005). 'Intrinsic influence of various plasticizers on functional properties and reactivity of wheat gluten thermoplastic materials', *Journal of Cereal Science*, **42**, 81–91.

Puppi, D., Chiellini, F., Piras, A.M. and Chiellini, E. (2010). 'Polymeric materials for bone and cartilage repair', *Progress in Polymer Science*, **35**, 403–440.

Quach, A. and Simha, R. (1972). 'Statistical thermodynamics of the glass transition and the glassy state of polymers', *Journal of Physical Chemistry*, **76**, 416–421.

Reddy, N. and Yang, Y. (2011). 'Potential of plant proteins for medical applications', *Trends in Biotechnology*, **29**, 490–498.

Reignier, J., Gendron, R. and Champagne, M.F. (2007). 'Autoclave foaming of poly(ε-caprolactone) using carbon dioxide: impact of crystallization on cell structure', *Journal of Cellular Plastics*, **43**, 459.

Rinaudo, M. (2006). 'Chitin and chitosan: properties and applications', *Progress in Polymer Science,* **31**, 603–632.

Salerno, A., Iannace, S. and Netti, P.A. (2008). 'Open-pore biodegradable foams prepared via gas foaming and microparticulate templating', *Macromolecular Bioscience,* **8**, 655–664.

Salerno, A., Oliviero, M., Di Maio, E. and Iannace, S. (2007a) 'Thermoplastic foams from zein and gelatin', *International Polymer Processing*, **22**, 480–488.

Salerno, A., Oliviero, M., Di Maio, E., Iannace, S. and Netti, P.A. (2007b) 'Design and preparation of m-bimodal porous scaffold for tissue engineering', *Journal of Applied Polymer Science*, **106**, 3335–3342.

Salgado, A.J., Gomes, M.E., Chou, A., Coutinho, O.P., Reis, R.L. and Hutmacher, D.W. (2002). 'Preliminary study on the adhesion and proliferation of human osteoblasts on starch-based scaffolds', *Materials Science and Engineering C*, **20**, 27–33.

Sato, Y., Takikawa, T., Sorakubo, A., Takishima, S., Masuoka, H. and Imaizumi, M. (2000). 'Solubility and diffusion coefficient of carbon dioxide in biodegradable polymers', *Industrial & Engineering Chemistry Research*, **39**, 4813–4819.

Selling, G.W. (2007). 'Sample preparation and testing methods affect the physical properties and evaluation of plasticized zein', *Industrial Crops and Products*, **25**, 266–273.

Shen, L., Haufe, J. and Patel M.K., (2009). 'Product overview and market projection of emerging bio-based plastics', *PROEuropean Polymer Journal,* **42**, 3145–3151-BIP 2009 Final report, European Polysaccharide Network of Excellence (EPNOE, www.epnoe.eu).

Singh, J., Dutta, P.K., Dutta, J., Hunt, A.J., Macquarrie, D.J. and Clark, J.H. (2009). 'Preparation and properties of highly soluble chitosan-L-glutamic acid aerogel derivative', *Carbohydrate Polymers*, **76**, 188–195.

Singh, L., Kumar, V. and Ratner, B.D. (2004). 'Generation of porous microcellular 85/15 poly(D,L-lactide-co-glycolide) foams for biomedical applications', *Biomaterials*, **25**, 2611–2617.

Smidsrød, O. and Skjåk-Braek, G. (1990). 'Alginate as immobilization matrix for cells, *Trends in Biotechnology*, **8**, 71–78.

Steinbuchel, A. and Doi, Y. (2002). '*Biopolymers, Volume **4**: Polyesters III-Applications and Commercial Products*', Wiley-VCH: Weinheim (Germany).

Tai, H., Upton, C.E., White, L.J., Pini, R., Storti, G., Mazzotti, M., Shakesheff, K.M. and Howdle S.M. (2010). 'Studies on the interactions of CO_2 with biodegradable poly(DL-lactic acid) and poly(lactic acid-co-glycolic acid) copolymers using high pressure ATR-IR and high pressure rheology', *Polymer*, **51**, 1425–1431.

Tiefenbacher, K.F. (1993). 'Starch based foamed materials – use and degradation properties', *Pure Applied Chemistry*, **30**, 727–731.

Torres, F.G., Boccaccini, A.R. and Troncoso, O.P. (2007). 'Microwave processing of starch-based porous structures for tissue engineering scaffolds', *Journal of Applied Polymer Science*, **103**, 1332–1339.

Tsioptsias, C. and Panayiotou, C. (2008). 'Foaming of chitin hydrogels processed by supercritical carbon dioxide', *Journal of Supercritical Fluid*, **47**, 302–308.

Tsivintzelis, I., Pavlidou, E. and Panayiotou, C. (2007). 'Biodegradable polymer foams prepared with supercritical CO_2 –ethanol mixtures as blowing agents'. *Journal of Supercritical Fluids*, **42**, 265–272.

Wan, Y., Wu, H., Cao, X. and Dalai, S. (2008). 'Compressive mechanical properties and biodegradability of porous poly(caprolactone)/chitosan scaffolds', *Polymer Degradation and Stability*, **93**, 1736–1741.

Wang, X., Li, W. and Kumar, V (2006). 'A method for solvent-free fabrication of porous polymer using solid-state foaming and ultrasound for tissue engineering applications', *Biomaterials*, **27**, 1924–1929.

Wang, Y. and Padua, G.W. (2003). 'Tensile properties of extruded zein sheets and extrusion blown films', *Macromolecular Materials Engineering*, **288**, 886–893.

Willett, J.L. and Shogren, R.L. (2002). 'Processing and properties of extruded starch/polymer foams', *Polymer*, **43**, 5935–5947.

Wissinger, R.G. and Paulaitis, M.E. (1991). 'Molecular thermodynamic model for sorption and swelling in glassy polymer-carbon dioxide systems at elevated pressures', *Industrial & Engineering Chemistry Research*, **30**, 842–851.

Wu, S. (1982). *Polymer Interface and Adhesion*. Marcel Dekker, New York.

Wu, H., Wan, Y., Cao, X. and Wu, Q. (2008). 'Proliferation of chondrocytes on porous poly(DLlactide)/chitosan scaffolds', *Acta Biomaterialia*, **4**, 76–87.

Xu, Q., Ren, X., Chang, Y., Wang, J., Yu, L. and Dean, K. (2004). 'Generation of microcellular biodegradable polycaprolactone foams in supercritical carbon dioxide', *Journal of Applied Polymer Science*, **94**, 593–597.

Yannas, I.V. (1996). Natural materials. In: Ratner BD, HoffmanAS, Schoen FJ, Lemons JE, editors. *Biomaterials Science. An Introduction to Materials in Medicine*. Academic Press, California, pp. 84–94.

Yasuda, A., Kojima, K., Tinsley, K.W., Yoshioka, H., Mori, Y. and Vacanti, C.A. (2006). 'In vitro culture of chondrocytes in a novel thermoreversible gelation polymer scaffold containing growth factors', *Tissue Engineering*, **12**, 1237–1245.

Zhai, W., Ko, Y., Zhu, W., Wong, A. and Park, C.B. (2009). A study of the crystallization, melting, and foaming behaviors of polylactic acid in compressed CO_2, *International Journal of Molecular Sciences*, **10**, 5381–5397.

This page intentionally left blank

Part II

Tissue engineering applications of biomedical foams

This page intentionally left blank

7

Bioactive glass foams for tissue engineering applications

A. HOPPE and A. R. BOCCACCINI, University of Erlangen-Nuremberg, Germany

DOI: 10.1533/9780857097033.2.191

Abstract: Bioactive glasses have been widely used in the field of bone tissue engineering due to their appropriate biological and mechanical properties. In this chapter we will review recent developments in fabricating bioactive-glass-derived 3D foams (scaffolds), discussing also their structural and biological properties. The most common fabrication routes will be presented and discussed. Further key findings from *in vitro* and *in vivo* studies on bioactive glass scaffolds will be presented in order to support the concept of the use of bioactive glass in (bone) tissue engineering applications. In addition to the 'standard' silicate-based bioactive glass compositions, representative findings on novel glass compositions for biomedical use, e.g. containing therapeutic metal ions, will be highlighted.

Key words: bioactive glass, tissue engineering, scaffolds, osteogenesis, biomedical foams.

7.1 Introduction

During the last decades bioactive glasses (BG) and glass–ceramics have been widely used in biomedical applications, including as filler materials, tissue scaffolds and bioactive coatings (Hench, 1998, 2009). Several silicate-based compositions such as '45S5' (wt.%: 45 SiO_2, 24.5 Na_2O, 24.5 CaO, 6 P_2O_5) or '13–93' (wt.%: 53 SiO_2, 6 Na_2O, 12 K_2O; 5 MgO, 20 CaO, and 4 P_2O_5) have been shown to exhibit bioactive behavior by providing strong bonding to bone (Hench, 1991; Rahaman *et al*., 2011) and also inducing stimulatory effects on osteogenesis (Xynos *et al*., 2001; Jell and Stevens, 2006; Hench, 2009) and angiogenesis (Gorustovich *et al*., 2010). Since health issues related to the planet's aging population are increasing, the clinical demand for tissue and organ repair continues to grow (Palangkaraya and Yong, 2009). Therefore, tissue engineering (TE) is one

promising approach being developed to regenerate damaged hard and soft tissue (Hutmacher, 2000). In TE strategies, a 3D structure, the so-called scaffold, made from a suitable biomaterial and exhibiting interconnected pores with desired pore size and shape is used (Rezwan *et al.*, 2006; Gerhardt and Boccaccini, 2010). For bone TE these scaffolds should provide osteogenic and also (ideally) angiogenic properties, a surface which supports the adhesion, proliferation and differentiation of relevant cells (e.g. stem cells, osteoblast cells), and a sufficient mechanical integrity and adequate degradation kinetics that should correspond to the bone formation rate (Jones and Hench, 2003). Bioactive glass-derived foams (scaffolds) can be fabricated using several different techniques, including sol-gel foaming and foam replica (FR) methods, which are presented in Section 7.2 in more detail.

In addition, the incorporation of particular ions into the silicate network, such as silver (Bellantone *et al.*, 2002; Blaker *et al.*, 2004; Balamurugan *et al.*, 2008) and boron (Munukka *et al.*, 2008; Gorriti *et al.*, 2009), has been investigated in order to develop antibacterial and antimicrobial materials. BGs have been also suggested for use as carrier platforms for the delivery of metal ions with therapeutic effect and also for growth factors, hormones and drugs (Hoppe *et al.*, 2011; Hum and Boccaccini, 2012; Mouriño *et al.*, 2012). In addition, mesoporous BG microspheres have demonstrated enhanced hemostatic activity, as well as reduced clot detection times and increased coagulation rates compared to nonporous microspheres (Ostomel *et al.*, 2006). The present chapter focuses on bioactive glass foams being developed as scaffolds for bone TE applications, with emphasis on (i) fabrication routes for BGs (Section 7.2.1) (ii) the production of foam-like scaffolds (Section 7.2.2) and (iii) *in vitro* and *in vivo* studies on these scaffolds (Section 7.3). Beside standard silicate glass compositions such as '45S5,' recent studies on novel glass chemistries containing metal ions added for achieving specific cellular responses and to induce enhanced osteogenesis will be highlighted. Finally, Section 7.4 includes a summary of key developments and indications for future research.

7.2 Processing 'foam-like' bioactive glass-based scaffolds

In this section the glass fabrication and its further processing into 'foam-like' scaffolds is presented. The use of traditional melting route and sol-gel techniques for synthesis of bioactive glasses as two most common methods are described in detail. Furthermore, various techniques for processing bioactive glass derived foams and respective structural and mechanical properties are given.

7.2.1 Bioactive glass production

Melt-derived bioactive glass

BGs can be made by melting raw materials or by the sol-gel technique. In the melt-derived process conventional glass melting is used, whereby desired amounts of oxides, carbonates or phosphates are homogenized and melted in a platinum crucible at 1350–1500°C. The molten glass is then either poured into graphite molds, in order to obtain solid glass blocks, or quenched in water or oil, which results in a glass frit. Subsequent mechanical grinding (e.g. in a planetary mill) can be applied to obtain glass powder, which can be directly used as bone defect filler material, as an addition to polymer-BG composites, or can be further processed for fabrication of 3D scaffolds by sintering methods, as described in Section 7.2.2.

Melting is a flexible technique that allows the production of various different glass compositions, simply by varying the number and proportion ratio of the raw materials. Melting processes have been used in order to obtain metal oxide containing BG including Sr-containing glass (Fredholm *et al.*, 2010), boron-derived glasses (Brown *et al.*, 2009), Co-BG (Azevedo *et al.*, 2010) and F-containing glasses (Lusvardi *et al.*, 2009; Brauer *et al.*, 2010).

These novel compositions are being investigated for use in the biomedical field for bone TE applications, since several metallic ions, such as Cu and Sr, are known to stimulate bone formation and tissue vascularization (Hoppe *et al.*, 2011). Relevant studies on the *in vitro* and *in vivo* behavior of these glasses are summarized in Section 7.3.2.

The melt-derived route for processing BGs shows also some disadvantages. For example, it might be difficult to achieve high purity glasses due to the high melting temperatures involved (impurities from crucible material) and the subsequent use of grinding steps, which could lead to contamination with debris particles of the grinding media. Moreover, the standard 45S5 Bioglass® tends to crystallize during the sintering process forming a predominantly crystalline phase (combeite) (Boccaccini *et al.*, 2007), which may reduce the hydroxyapatite (HAp) conversion rate (Chen *et al.*, 2006; Breed and Hall, 2012) and thus affect the bioactivity of the material. Other modified bioactive glass compositions, such as '13–93,' have been developed that show enhanced viscous flow and can be densified without crystallization (Fu *et al.*, 2008).

Sol-gel-derived glass

Low-temperature techniques, such as the sol-gel route, offer another opportunity to produce BGs. Hereby the synthesis of an inorganic network is processed by mixing organic precursor (e.g. metal alkoxides) in solution, which

is followed by hydrolysis, gelation and low-temperature firing. Silicate glass alkoxide precursors, such as tetraethylorthosilicate (TEOS), undergo hydrolysis forming a colloidal solution (sol). After a polycondensation of silanol (Si–OH) groups, a silicate (–Si–O–Si–) network is formed. While the gel is forming, the viscosity of the system increases as the network connectivity raises. Afterwards the gel is dried and stabilized during a thermal process at around 600–800°C (Pereira *et al*., 2005; Jones, 2007). Sol-gel-derived glasses exhibit mesoporous characteristics and have larger surface area than melt-derived glasses, showing pores from 300 to 800 nm with total porosities of over 60% (Zhang *et al*., 2005). By choosing suitable precursor materials, novel bioactive glass compositions containing metal oxides can be produced. For instance, Zn containing sol-gel-derived glass (Du and Chang, 2004; Balamurugan *et al*., 2007), Sr (Hesaraki *et al*., 2010) and Mg-containing (Du and Chang, 2004) glasses for biomedical applications have been developed.

7.2.2 Scaffold fabrication

Various fabrication techniques have been described to produce 3D porous bioactive glass and ceramic foams (Deisinger, 2010) including FR (Chen *et al*., 2006), diverse rapid prototyping methods (Comesaña *et al*., 2011), freeze casting (Mallik, 2008) or freeze extrusion (Doiphode *et al*., 2011; Huang *et al*., 2011). Table 7.1 provides an overview of selected techniques currently used for fabrication of bioactive glass foams and corresponding structural and mechanical properties. A more comprehensive overview over fabrication methods of bioactive glass scaffolds and bioglass–polymer composite foams can be found elsewhere (Gerhardt and Boccaccini, 2010). Clearly, all these methods lead to different morphologies and structures of bioactive glass scaffolds, as given in Fig. 7.1.

The polymer FR method was introduced in 2006 (Chen *et al*., 2006) to fabricate 3D '45S5'-based scaffolds for bone TE and it has been widely used since then (Ramay and Zhang, 2003; Chen *et al*., 2006; Fu *et al*., 2008). Briefly, polyurethane (PU) foam, used as sacrificial template, is infiltrated with a glass powder containing slurry that adheres to the PU foam surface. Afterwards, the excess slurry is removed and the coated PU foam is dried and then densified in a sintering step. The PU template determines the macro-structure of the final glass or glass–ceramic foam-like scaffold. Typically, glass foams made by the FR method show total porosities of > 85 vol.% and pore sizes in the range 100–400 μm. The chemical composition and extent of crystallinity depends on the starting glass powder composition used. While 45S5 Bioglass®-derived scaffolds crystallize during sintering and form silicate and phosphorous rich phases (Chen *et al*., 2006; Boccaccini *et al*., 2007), more recently developed glasses such as '13–93', which contain larger amounts of

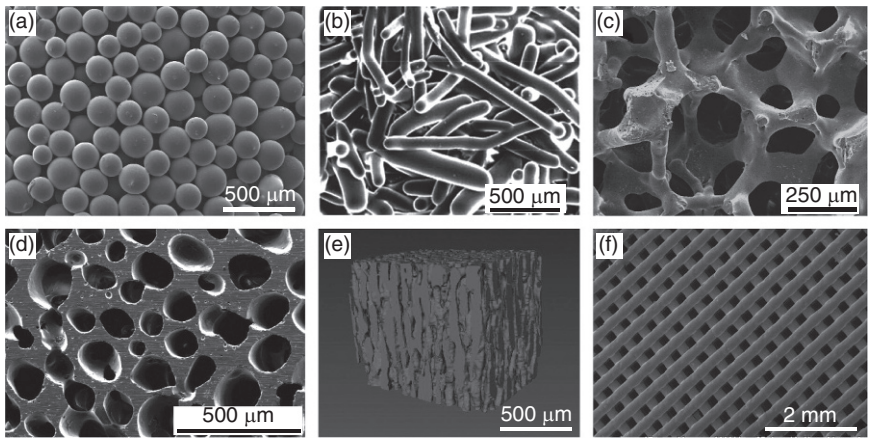

7.1 Different structures and morphologies for bioactive-glass-derived scaffolds made by a variety of methods: (a) thermal bonding (sintering) of particles (microspheres); (b) thermal bonding of short fibers; (c) 'trabecular' microstructure prepared by a polymer foam replication technique; (d) oriented microstructure prepared by unidirectional freezing of suspensions (plane perpendicular to the orientation direction); (e) X-ray microCT image of the oriented scaffold shown in (d); (f) grid-like microstructure prepared by robocasting. Glass composition: (a) 16CaO–21Li_2O–63B_2O_3; (b–e) 13–93; (f) 6P53B. (*Source*: Reprinted from Rahaman *et al.*, 2011.)

alkali oxides, remain amorphous without any crystallization during the densification heat treatment (Fu *et al.*, 2007, 2008). The structure and chemistry of the scaffold also determine the scaffold's *in vitro* bioactivity, mechanical properties and also has an effect on protein adsorption on scaffold surfaces. For example, dense highly crystalline 45S5 Bioglass®-derived scaffolds have compressive strength in the range of 0.25–0.4 MPa (see Table 7.1), lying even below the lowest compressive strength values reported for spongy bone. On the other hand, for amorphous 13–93 bioactive-glass-derived scaffolds, compressive strength values up to 11 MPa have been reported (Fu *et al.*, 2008). The different values for the strength of these scaffolds might be related to the processing conditions and the resulting structure of the scaffolds. 13–93 bioactive glass can be densified in a viscous flow process; this should lead to crack-free struts where sintering is not impaired by the crystallization process, which occurs in 45S5 type bioactive glass. Fu *et al.* (2008) reported pore size values of 100–500 μm and a compressive strength of 11 ± 1 MPa for 13–93-derived glass scaffolds made by FR technique. The influence of chemical composition, fabrication method and scaffold structure on the mechanical properties of bioactive-glass-derived foams has been discussed in the literature (Fu *et al.*, 2011a).

Table 7.1 Overview of selected available techniques for fabrication of bioactive-glass-derived foams and corresponding properties

Fabrication technique	Glass composition	Porosity (%)	Pore size (μm)	Strength (MPa)[a]	Reference
FR	'Fa-GC' (mol- %) 50 SiO_2, 18 CaO, 9 CaF_2, 7 Na_2O, 7 K_2O, 6 P_2O_5, 3 MgO	75	~100	2	Vitale-Brovarone *et al.*, 2008
	'13–93' (wt.%): 53 SiO_2, 6 Na_2O, 12 K_2O, 5 MgO, 20 CaO, 4 P_2O_5	85 ± 2	~100–500	11 ± 1	Fu *et al.*, 2008
	'45S5' (wt.%): 45 SiO_2, 24.5 Na_2O, 24.5 CaO, 6 P_2O_5	~90	510–720	0.3–0.4	Chen *et al.*, 2006
Gel casting	'ICIE'16 (mol-%): 49.46 SiO_2, 36.27 CaO, 6.6 Na_2O, 1.07 P_2O_5, 6.6 K_2O)	~80	~380	1.9	Wu *et al.*, 2011c
Freeze extrusion	'13–93'	~50	Pore width: 300 μm and struts diameter 300 μm	~140	Doiphode *et al.*, 2011; Huang *et al.*, 2011
	'45S5'	~53		–	Song *et al.*, 2006
	'13–93'	55–60%	90–110 (pore width, columnar) 20–30 (pore width, lamellar)	25 ± 3 MPa (columnar) 10 ± 2 (lamellar)	Fu *et al.*, 2010
Direct ink	'6P53B' (wt.%): 52.7 SiO_2, 10.3 Na_2O, 2.8 K_2O, 10.2 MgO, 18.0 CaO, 6 P_2O_5	60	500 μm (pores size), 100 μm (rod diameter)	136 ± 22	Fu *et al.*, 2011b
Lithography	'45S5'	–	–	0.33	Tesavibul *et al.*, 2012

[a]Compressive strength.

Related to *in vitro* bioactivity in simulated body fluid (SBF), early studies involving dense specimens indicated that crystallinity reduces the bioactivity of bioactive glass (Filho *et al*., 1996). However, later studies focusing on highly porous scaffolds have shown that the bioactive character remains for crystalline materials, and the formation of HAp is just delayed (Chen *et al*., 2006). Beside the now well-established FR method to make bioactive glass scaffolds, other techniques have been considered to fabricate 3D porous glass and glass–ceramic scaffolds. Organic molecules, starch from rice, potato, or corn grains for instance, can be used to introduce porosity by swelling these molecules in water (Vitale-Brovarone *et al*., 2005). After the sintering process and burn out of the organic fillers, a highly interconnected pore system remains, which contains pores of size 84 μm and a pore content of 40 vol.%, as reported for bioactive glass (Vitale-Brovarone *et al*., 2005).

Although not of a foam-like structure, for completeness fiber-derived scaffolds are also mentioned here, which are based on the assembly of bioactive glass fibers to produce porous structures. Melt-derived glass fibers are packed and bonded together in a ceramic mold using a continuous bead of silicone adhesive (Brown *et al*., 2008), or sintered together (Moimas *et al*., 2006). Typically, fiber-based scaffolds show porosities of 40–60 vol.% and compression strength values of 12–18 MPa, notably higher than values achieved by the FR method, albeit at lower porosities.

Other techniques for fabricating glass foams include freeze casting (Mallik, 2008) and freeze extrusion (Doiphode *et al*., 2011; Huang *et al*., 2011). Camphene, ice or water, and glycerol can be used as freezing vehicles (Song *et al*., 2006; Liu *et al*., 2011). After mixing the glass powder with the relevant vehicles, the slurries are cast and frozen at temperatures between −20°C and −70°C, followed by a sintering process.

Freeze-casted 13–93 scaffolds with oriented (lamellar and columnar) pores and equivalent porosity of 55–60% were shown to have a compressive strength of 25 ± 3 MPa, compressive modulus of 1.2 GPa and pore width of 90–110 μm for columnar scaffolds, compared to values of 10 ± 2 MPa, 0.4 GPa and 20–30 μm, respectively, obtained for the lamellar scaffolds (Fu *et al*., 2010).

Rapid prototyping techniques have also been described for fabricating porous bioactive glass-based scaffolds. Direct ink writing, for instance, was used to develop bioactive glass (6P53B composition) scaffolds exhibiting a compressive strength of 136 ± 22 MPa, which is comparable to the value for cortical bone (100–150 MPa) with porosity of 60% (Fu *et al*., 2011b). In a recent study, a method using lithography-based additive manufacturing technologies (AMT) was applied to create 45S5 bioactive glass scaffolds (Tesavibul *et al*., 2012), resulting in scaffolds showing biaxial strength and compressive strength of ~40 MPa and 0.33 MPa, respectively.

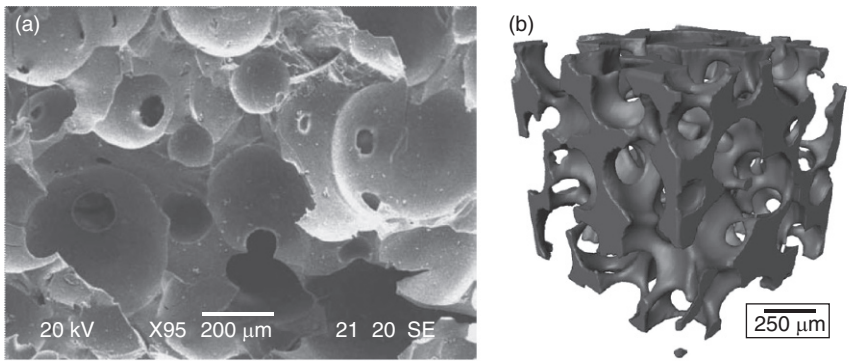

7.2 Microstructure of sol-gel-derived bioactive glass (70S30) scaffold shown by means of SEM (a) and X-ray micro-computed tomography (XMT) image (b). (*Source*: Reprinted from Jones *et al.*, 2006a.)

Using sol-gel-derived bioactive glass particles, direct foaming methods can be applied in order to fabricate porous scaffolds (Jones *et al.*, 2006b, 2010). Jones *et al.* (2006a) described sol-gel-derived BG foams where the scaffolds are obtained by direct foaming of the sol with Teepol as foaming agent. After a drying process, the gelled foams are aged at 60°C, dried at 130°C and stabilized at 600°C. In a further heat treatment process the foams are densified at 800°C. Figure 7.2 shows a typical structure of a sol-gel-derived bioactive glass scaffold. By varying the amount of foaming agent the pore size distribution and overall porosity can be tuned (Jones *et al.*, 2006a). The mechanical strength of sol-gel-derived bioactive glass scaffolds is usually in the range of 0.3–2.3 MPa (in compression), limiting their applications to non-load-bearing TE approaches. Another related technique involving sol-gel-derived glasses has been developed using sugar cane as a template (Qian *et al.*, 2009).

7.3 *In vitro* and *in vivo* studies of bioactive glass-based biomedical foams

Beside bioactive behavior, the ability to form a strong bonding to bone, bioactive glasses have been shown to upregulate several osteogenesis (and angiogenesis) related genes in relevant cell types resulting in enhanced tissue regeneration. Moreover, recent advances have been made in order to enhance the biocompatibility of bioactive glasses by introducing therapeutic metallic ions into the glass matrix which induce additional stimulating effects when released in physiological environment. In this section relevant studies on *in vitro* and *in vivo* behavior of traditional bioactive silicate glass compositions as well as novel metal ions containing bioactive glasses are summarized.

7.3.1 Basic silicate compositions

Since Hench *et al.* (1972) discovered the first bioactive silicate material (45S5 Bioglass®), with its ability to form a strong bond to bone, there has been extensive research work on bioactive silicate glasses for biomedical applications including bone TE (Hench *et al.*, 2004; Boccaccini *et al.*, 2005; Gorustovich, 2010; Hench and Thompson, 2010; Hoppe *et al.*, 2011). The relevant research has been extended from considerations of classical inorganic interactions between the materials interface and the physiological environment to the understanding of molecular interactions of ionic dissolution products of silicate glasses and human cells. It has been shown, for example, that ionic dissolution products released from silicate-based BGs can stimulate bone formation by expressing osteogenic genes in human stem cells (Xynos *et al.*, 2001). The evidence presented in the literature shows that ionic dissolution products released from BGs can stimulate specific genes of cells toward a path of bone regeneration and self-repair, resulting in stimulated and enhanced new bone formation. Key findings on gene stimulating potential of BGs were summarized elsewhere (Jell and Stevens, 2006; Hench, 2009; Hoppe *et al.*, 2011) describing the role of BGs as a so-called 'third generation biomaterial' (Hench and Polak, 2002). It is now well accepted that bioactive silicate glasses are able to stimulate osteogenesis, thus exhibiting unique properties relevant to bone TE applications.

In vitro studies on 45S5 glass-derived scaffolds have confirmed the potential of such 3D glass foams to support the attachment and growth of human osteoblast cells (HOB) (Chen *et al.*, 2008). Chen *et al.* (2008), for example, showed the attachment, infiltration and high level of proliferation of human osteosarcoma MG-63 cells when cultured for 6 days on a 45S5 Bioglass®-derived crystallized scaffold. Figure 7.3 shows the attachment and growth of MG-63 cells on a 45S5 derived scaffold according to experiments at our laboratory at the University of Erlangen-Nuremberg. Another study showed enhanced extra-cellular matrix (ECM) formation and development of mineralized nodules for osteoblast cells cultured in Bioglass® conditions medium (Tsigkou *et al.*, 2009). Fu *et al.* (2008) showed that FR derived 13–93 bioactive glass scaffolds support the attachment and subsequent proliferation of MC3T3-E1 preosteoblastic cells when cultured on the scaffold for 28 days.

In vitro studies on sol-gel-derived glass-based scaffolds have shown similar results. For example, osteoblast culture on sol-gel-derived foam (Gough *et al.*, 2004) revealed good attachment and proliferation of HOBs on the foams, as demonstrated by scanning electron microscopy (Fig. 7.4). Moreover, nodule formation and mineralization were observed in the pores. Jones *et al.* (2007) also observed the formation of mineralized bone nodules on 70S30 bioactive glass within 2 weeks of *in vitro* culture of primary HOBs without the presence of supplementary growth factors in the medium.

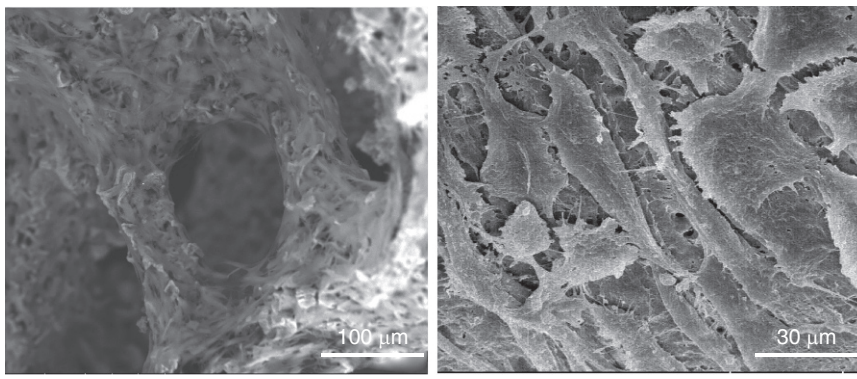

7.3 Osteosarcoma cells (MG-63) cultivated on a 45S5 Bioglass® - derived scaffold for 3 weeks at different magnifications. (*Source*: Micrograph courtesy of Dr Rainer Detsch, Institute of Biomaterials, University of Erlangen-Nuremberg.)

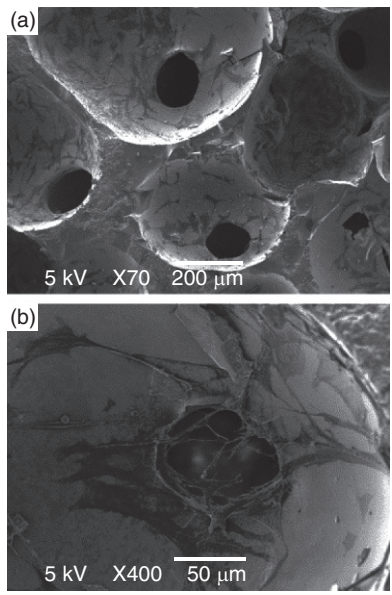

7.4 SEM micrographs of HOBs on a 70S30C derived scaffold after 2 weeks of cultured (a) cell distribution and (b) spreading over a pore interconnect. (*Source*: Reprinted from Jones *et al.*, 2007.)

Since it has become clear that successful application of an engineered tissue construct relies on highly vascularized structures, the angiogenic potential of biomaterials has moved into focus of researchers in the field of biomaterials for bone TE.

The angiogenic potential of BGs has been investigated in several *in vitro* studies (Day, 2005; Day and Boccaccini, 2005; Keshaw *et al.*, 2005; Leu

and Leach, 2008; Keshaw *et al*., 2009; Leu *et al*., 2009; Moosvi and Day, 2009; Gerhardt *et al*., 2011). It has been shown, for example, that bioactive glass (type 45S5 Bioglass®) stimulates the proliferation of endothelial cells (Leu and Leach, 2008; Gerhardt *et al*., 2011) and the formation of endothelial tubules (Leu and Leach, 2008). Further studies showed that Bioglass® stimulates the secretion of both vascular endothelial growth factor (VEGF) and basic fibroblast growth factor (bFGF), which are important angiogenic growth factors, from human fibroblasts cells (CCD-18Co), when the cells were cultivated in cell culture medium containing Bioglass® particles (Day, 2005). In addition, *in vivo* results confirmed that BG is able to stimulate and promote neovascularization (Mahmood *et al*., 2001; Day *et al*., 2004; Nandi *et al*., 2009; Vargas *et al*., 2009; Gorustovich *et al*., 2010). Day *et al*. (2004) for instance have shown the angiogenic effect of 45S5 Bioglass® indicated through neovascularization into BG-coated polymer meshes when implanted subcutaneously in rats.

Another study by Deb *et al*. (2010) investigated co-culturing of osteoblast and endothelial cells on Bioglass®-derived foams, which showed increased proliferation of both HOBs and human umbilical vein endothelial cells (HUVEC) compared to HAp scaffolds. Relevant studies on the angiogenic effects of BGs have been comprehensively reviewed elsewhere (Gorustovich *et al*., 2010) that have indicated the angiogenic potential of BGs. However, the specific role of BGs on angiogenic cellular and intermolecular mechanisms is still not fully understood. The influence of the shape, morphology and size of bioactive glass particles (which are for instance used as fillers in polymer–BG composites) should be taken into account and need further investigation. Moreover, the geometry and pore structure of the bioactive glass scaffold (pore size, pore orientation, interconnectivity, etc.) may affect the angiogenic properties of the construct.

For example, it has been described by Gerhard and Boccaccini (2010) that the angiogenic effect of bioactive glass seems to be more pronounced in bioactive glass-based scaffolds i.e. BG-loaded collagen sponges (Leu *et al*., 2009), disks (Andrade *et al*., 2006), meshes (Day *et al*., 2004), tubes (Ross *et al*., 2003) and porous glass–ceramic scaffolds (Mahmood *et al*., 2001; Nandi *et al*., 2009; Gorustovich *et al*., 2010) than in composite structures incorporating and fully embedding bioactive glass particles in polymer matrices such as microsphere composites (Keshaw *et al*., 2009) or foams (Day *et al*., 2005; Choi *et al*., 2006). Thus, the relationship between the structure, porosity, surface chemistry and ion release kinetics of bioactive glass scaffolds and possible angiogenic response of relevant human cells has to be investigated in more detail in order to gain further understanding of the mechanisms behind the angiogenic properties of BGs. This knowledge is important to be able to fabricate bioactive glass scaffolds with the tailored properties needed for their successful application in bone (Gerhardt and Boccaccini, 2010).

Recently, advances have been made in order to enhance the bioactivity of glasses and glass–ceramics by incorporating selected metal ions into silicate (or phosphate) glass matrices which are supposed to result in enhanced bone formation and angiogenesis using the therapeutic effects of metal trace elements or bioinorganics (Habibovic and Barralet, 2011; Hoppe *et al*., 2011). These effects were shown for various doped glasses and glass–ceramic materials including B-, Sr- and Cu-containing glasses (Hoppe *et al*., 2011). Selected studies are presented in the following section.

7.3.2 Silicate glass containing metal ions

Metallic ions are essential in human metabolism, and are also known to play a critical role in osteogenesis and angiogenesis (Beattie and Avenell, 1992; Habibovic and Barralet, 2011). They have long been considered highly promising for the field of biomedicine (Thompson, 2003). During the last decades, specific metallic ions such as copper, zinc, strontium, cobalt, silicon, and boron have emerged as potential therapeutic agents to be used in order to enhance bone formation due to their stimulating effects on osteogenesis as well as on angiogenesis (Habibovic and Barralet, 2011). Significant amounts of copper, for instance, are found in human endothelial cells when angiogenesis is taking place (Finney *et al*., 2009). Furthermore, there is evidence that Cu stimulates the proliferation of human endothelial cells (Hu, 1998) and induces differentiation of mesenchymal stem cells toward the osteogenic cell line (Rodríguez *et al*., 2002). Sr ions are also being considered as promising agents to be used in bone TE, since Sr is known for its bone stimulating ability (Marie *et al*., 2001; Marie, 2006), being also in use as therapeutic drug (Protelos) for osteoporosis treatment. Sr and Cu are just two examples from a wide range of metallic ions considered for use in bioactive glass matrices, as discussed in detail in the literature (Habibovic and Barralet, 2011; Hoppe *et al*., 2011; Mouriño *et al*., 2012). Metallic ions exhibit various advantages over organic molecules such as hormones or growth factors which are usually applied in TE and therapeutic approaches, since they can be processed at lower cost while maintaining high stability (Mouriño *et al*., 2012). Thereby, loading inorganic matrices with metallic ions offers a great opportunity to develop robust carrier systems with the ability to release specific metal ions in desired rates.

Both melt-derived and sol-gel-derived glasses can be considered as carriers of metallic ions with therapeutic function. For example, boron oxide (B_2O_3) was incorporated into a sol-gel-derived mesoporous silicate glass-based scaffold with the capability of controllable release of boron (Wu *et al*., 2011b). *In vitro* studies on these scaffolds revealed significantly enhanced proliferation and expression of osteogenesis-related genes (Col I and Runx2) in osteoblast cells (Wu *et al*., 2011b).

Another type of boron-containing glass scaffold made of sintered (irregular-shaped) glass particles and spherical particles (porosity of 25–40%) was investigated with mesenchymal stem cells (MSCs) revealing good adhesion and osteogenic differentiation of MSC-derived osteoblast cells (Liang *et al*., 2008). Of relevance for applications in bone TE, boron-containing silicate glasses have been shown to convert rapidly to biomimetic HAp, leading to enhanced formation of new bone tissue *in vivo* (Rahaman *et al*., 2011).

Recent investigations have shown that silicate glasses containing Sr enhance osteoblast differentiation, indicated through upregulation of several osteogenic genes (Gentleman *et al*., 2010). In these BGs the Sr concentration released can be tailored by adjusting the composition of the glass (Gentleman *et al*., 2010; Isaac *et al*., 2011). Zn releasing BG scaffolds have been described in another study (Haimi *et al*., 2009). It was observed that Zn addition had no significant effect on DNA content of human adipose derived stem cells (hASCs), but Zn ions inhibited the adhesion and proliferation of cells. The authors suggest that no stimulating effect of Zn ions has been measured, because the addition of Zn slowed down the overall degradation behavior and inhibited the HAp formation of the glass scaffold (Haimi *et al*., 2009).

Since a highly vascularized structure is essential for successful clinical application of engineered bone constructs, the use of angiogenic agents is being proposed in order to directly stimulate angiogenesis and vascularization. Besides angiogenic growth factors such as VEGF or IGF (insulin-like growth factor), copper ions have been known for decades to be able to stimulate angiogenesis and to promote formation (and maturation) of blood vessels (Xie and Kang, 2009). Indeed, there is evidence that addition of copper to a boron-containing glass (0.5 wt.%) resulted in increased blood vessel formation, as shown in an animal model (Rahaman *et al*., 2011).

Also Ag-containing BGs have been developed in order to obtain bioactive scaffolds with antibacterial potential (Vitale-Brovarone *et al*., 2008; Delben *et al*., 2009). Ag-doped bioactive glass scaffolds fabricated by the ion-exchange method, for instance, have been shown to exhibit antibacterial properties by inhibiting the growth of *Staphylococcus aureus*.

Beside bone TE, BGs have also been investigated in nerve regeneration approaches for use as nerve guidance conducts (NGCs) (Zhang *et al*., 2011a, b). For this application, BGs containing ZnO_2 and CeO_2, for instance, were proposed to be used as a component in bioactive glass/polymer composites for NGCs. These constructs have release capabilities of Ca^{2+} and Zn^{2+} (which are both known to be involved in peripheral nerve regeneration (Gomez and Spitzer, 1999; Frederickson *et al*., 2005)) and also provide appropriate mechanical performance when used as filler in a polymer matrix (Zhang *et al*., 2011b).

More recently, BGs have been considered as materials for cancer treatment (Cacaina *et al*., 2008; Shah *et al*., 2010, 2011; Jiang *et al*., 2011; Li *et al*., 2011; Wu *et al*., 2011a) where approaches have been put forward involving ferromagnetic (bioactive) glasses in hyperthermia treatment (Shah *et al*., 2010; Jiang *et al*., 2011; Li *et al*., 2011; Wu *et al*., 2011a). In a recent study, magnetic Fe-containing sol-gel-derived mesoporous glass scaffolds were proposed to be used for treatment of malignant bone disease using hyperthermia by inducing heat in the area of diseased bone leading to the killing of tumor cells (Wu *et al*., 2011a). Because of their osteoconductive properties, these scaffolds are also suggested to be used as templates for bone tissue regeneration at the same time, thus combining treatment of malignant bone and tissue regeneration in one procedure (Wu *et al*., 2011a).

Always considering risks related to possible toxic levels of metallic ions being released *in vivo,* the development of new metallic ion releasing bioactive glass scaffolds for applications in the field of TE is highly promising. In particular, the combined incorporation of osteogenic and angiogenic agents with additional antibacterial and wound healing potential will lead to the development of a new broad field of multifunctional biomaterials for regenerating large bone defects. However, more *in vitro* and *in vivo* data are needed to confirm the therapeutic action of metallic ions released from BGs and glass-derived foams. Furthermore, the exact mechanisms of the interactions between ionic dissolution products released from BGs and human cells and the role these ions play in related signaling pathways are still not fully understood.

7.4 Conclusions and future trends

Bioactive glass foams can be produced using different techniques that enable tailoring their micro structure, porosity, bioactivity and mechanical performance.

Classical techniques, such as the FR method, sol-gel direct foaming and new rapid prototyping techniques are being widely used to fabricate bioactive glass scaffolds with largely diverse properties and structure, e.g. exhibiting a wide range of porosity levels and mechanical properties.

In vitro and *in vivo* studies give evidence that bioactive glass-derived scaffolds support the adhesion and proliferation of human cells and can also provide stimulating effects related to osteogenesis and in some cases angiogenesis, which makes them highly promising materials for (bone) TE applications. Recent advances in developing novel bioactive glass compositions, including therapeutic metal ions that can act as matrices for delivery of inorganic therapeutics, were discussed. This new group of materials widens the application potential of bioactive glass foams for bone TE, enabling

the development of multifunctional bioactive scaffolds with improved biological response.

One of the challenges in developing such biomaterial platforms with ion delivery capability is to ensure local release of critical concentrations of the relevant metal ions and to avoid toxic levels being released into the physiological environment. Thus, in order to uncover the full therapeutic potential of metal ions, the remaining challenges are related to developing a family of bioactive glass foams with controlled microstructure (e.g. porosity, pore shape, pore interconnectivity) and well-defined and predictable ion release kinetics. Future research will have to consider systematic approaches and combination of *in vitro* and *in vivo* studies, including the use of bioreactors to assess the biological improvement of bioactive glass scaffolds incorporating metallic ions in comparison to 'standard' glass compositions such as '45S5' and '13–93.'

7.5 References

Andrade, A. L., Andrade, S. P. and Domingues, R. Z. (2006). In vivo performance of a sol-gel glass-coated collagen. *Journal of Biomedical Materials Research Part B: Applied Biomaterials,* **79b**, 122–128.

Azevedo, M. M., Jell, G., O'donnell, M. D., Law, R. V., Hill, R. G. and Stevens, M. M. (2010). Synthesis and characterization of hypoxia-mimicking bioactive glasses for skeletal regeneration. *Journal of Materials Chemistry,* **20**, 8854–8864.

Balamurugan, A., Balossier, G., Kannan, S., Michel, J., Rebelo, A. H. S. and Ferreira, J. M. F. (2007). Development and in vitro characterization of sol-gel derived CaO-P_2O_5-SiO_2-ZnO bioglass. *Acta Biomaterialia,* **3**, 255–262.

Balamurugan, A., Balossier, G., Laurent-Maquin, D., Pina, S., Rebelo, A. H. S., Faure, J. and Ferreira, J. M. F. (2008). An in vitro biological and anti-bacterial study on a sol-gel derived silver-incorporated bioglass system. *Dental Materials,* **24**, 1343–1351.

Beattie, J. H. and Avenell, A. (1992). Trace element nutrition and bone metabolism. *Nutrition Research Reviews,* **5**, 167–188.

Bellantone, M., Williams, H. D. and Hench, L. L. (2002). Broad-spectrum bactericidal activity of Ag_2O-doped bioactive glass. *Antimicrobial Agents and Chemotherapy,* **46**, 1940–1945.

Blaker, J. J., Nazhat, S. N. and Boccaccini, A. R. (2004). Development and characterisation of silver-doped bioactive glass-coated sutures for tissue engineering and wound healing applications. *Biomaterials,* **25**, 1319–1329.

Boccaccini, A. R., Blaker, J. J., Maquet, V., Jerome, R., Blacher, S. and Roether, J. A. (2005). Biodegradable and bioactive polymer/bioglass (R) composite foams for tissue engineering scaffolds. *In:* Uskokovic, D. P., Milonjic, S. K. and Rakovic, D. I. (eds) *Current Research in Advanced Materials and Processes*, **494**, 499–506.

Boccaccini, A. R., Chen, Q., Lefebvre, L., Gremillard, L. and Chevalier, J. (2007). Sintering, crystallisation and biodegradation behaviour of Bioglass-derived glass-ceramics. *Faraday Discussions,* **136**, 27–44.

Brauer, D. S., Karpukhina, N., O'donnell, M. D., Law, R. V. and Hill, R. G. (2010). Fluoride-containing bioactive glasses: Effect of glass design and structure on degradation, pH and apatite formation in simulated body fluid. *Acta Biomaterialia,* **6**, 3275–3282.

Breed, S. M. and Hall, M. M. (2012). Regression model for predicting selected thermal properties of next-generation bioactive glasses. *Acta Biomaterialia,* **8**, 2324–2330.

Brown, R. F., Day, D. E., Day, T. E., Jung, S., Rahaman, M. N. and Fu, Q. (2008). Growth and differentiation of osteoblastic cells on 13–93 bioactive glass fibers and scaffolds. *Acta Biomaterialia,* **4**, 387–396.

Brown, R. F., Rahaman, M. N., Dwilewicz, A. B., Huang, W., Day, D. E., Li, Y. and Bal, B. S. (2009). Effect of borate glass composition on its conversion to hydroxyapatite and on the proliferation of MC3T3-E1 cells. *Journal of Biomedical Materials Research. Part A,* **88a**, 392–400.

Cacaina, D., Ylanen, H., Simon, S. and Hupa, M. (2008). The behaviour of selected yttrium containing bioactive glass microspheres in simulated body environments. *Journal of Materials Science-Materials in Medicine,* **19**, 1225–1233.

Chen, Q. Z., Efthymiou, A., Salih, V. and Boccaccini, A. R. (2008). Bioglass®-derived glass-ceramic scaffolds: Study of cell proliferation and scaffold degradation in vitro. *Journal of Biomedical Materials Research. Part A,* **84a**, 1049–1060.

Chen, Q. Z., Thompson, I. D. and Boccaccini, A. R. (2006). 45S5 Bioglass®-derived glass-ceramic scaffolds for bone tissue engineering. *Biomaterials,* **27**, 2414–2425.

Choi, H. Y., Lee, J. E., Park, H. J. and Oum, B. S. (2006). Effect of synthetic bone glass particulate on the fibrovascularization of porous polyethylene orbital implants. *Ophthalmic Plastic and Reconstructive Surgery,* **22**, 121–125.

Comesaña, R., Lusquiños, F., Del Val, J., López-Álvarez, M., Quintero, F., Riveiro, A., Boutinguiza, M., De Carlos, A., Jones, J. R., Hill, R. G. and Pou, J. (2011). Three-dimensional bioactive glass implants fabricated by rapid prototyping based on CO_2 laser cladding. *Acta Biomaterialia,* **7**, 3476–3487.

Day, R. M. (2005). Bioactive glass stimulates the secretion of angiogenic growth factors and angiogenesis in vitro. *Tissue Engineering,* **11**, 768–777.

Day, R. M. and Boccaccini, A. R. (2005). Effect of particulate bioactive glasses on human macrophages and monocytes in vitro. *Journal of Biomedical Materials Research. Part A,* **73a**, 73–79.

Day, R. M., Boccaccini, A. R., Shurey, S., Roether, J. A., Forbes, A., Hench, L. L. and Gabe, S. M. (2004). Assessment of polyglycolic acid mesh and bioactive glass for soft-tissue engineering scaffolds. *Biomaterials,* **25**, 5857–5866.

Day, R. M., Maquet, V., Boccaccini, A. R., Jerome, R. and Forbes, A. (2005). In vitro and in vivo analysis of macroporous biodegradable poly(D,L-lactide-co-glycolide) scaffolds containing bioactive glass. *Journal of Biomedical Materials Research Part A,* **75**, 778–787.

Deb, S., Mandegaran, R. and Di Silvio, L. (2010). A porous scaffold for bone tissue engineering/45S5 Bioglass(A (R)) derived porous scaffolds for co-culturing osteoblasts and endothelial cells. *Journal of Materials Science-Materials in Medicine,* **21**, 893–905.

Deisinger, U. (2010). Generating porous ceramic scaffolds: Processing and properties. *Key Engineering Materials,* **441**, 155–179.

Delben, J. R. J., Pimentel, O. M., Coelho, M. B., Candelorio, P. D., Furini, L. N., Dos Santos, F. A., De Vicente, F. S. and Delben, A. (2009). Synthesis and thermal properties of nanoparticles of bioactive glasses containing silver. *Journal of Thermal Analysis and Calorimetry,* **97**, 433–436.

Doiphode, N. D., Huang, T. S., Leu, M. C., Rahaman, M. N. and Day, D. E. (2011). Freeze extrusion fabrication of 13–93 bioactive glass scaffolds for bone repair. *Journal of Materials Science-Materials in Medicine,* **22**, 515–523.

Du, R. L. and Chang, J. (2004). Preparation and characterization of Zn and Mg doped bioactive glasses. *Journal of Inorganic Materials,* **19**, 1353–1358.

Filho, O. P., La Torre, G. P. and Hench, L. L. (1996). Effect of crystallization on apatite-layer formation of bioactive glass 45S5. *Journal of Biomedical Materials Research,* **30**, 509–514.

Finney, L., Vogt, S., Fukai, T. and Glesne, D. (2009). Copper and angiogenesis: Unravelling a relationship key to cancer progression. *Clinical and Experimental Pharmacology and Physiology,* **36**, 88–94.

Frederickson, C. J., Koh, J.-Y. and Bush, A. I. (2005). The neurobiology of zinc in health and disease. *Nature Reviews. Neuroscience,* **6**, 449–462.

Fredholm, Y. C., Karpukhina, N., Law, R. V. and Hill, R. G. (2010). Strontium containing bioactive glasses: Glass structure and physical properties. *Journal of Non-Crystalline Solids,* **356**, 2546–2551.

Fu, Q., Rahaman, M. N., Bal, B. S. and Brown, R. F. (2010). Preparation and in vitro evaluation of bioactive glass (13–93) scaffolds with oriented microstructures for repair and regeneration of load-bearing bones. *Journal of Biomedical Materials Research Part A,* **93a**, 1380–1390.

Fu, Q., Rahaman, M. N., Bal, B. S., Brown, R. F. and Day, D. E. (2008). Mechanical and in vitro performance of 13–93 bioactive glass scaffolds prepared by a polymer foam replication technique. *Acta Biomaterialia,* **4**, 1854–1864.

Fu, Q., Rahaman, M. N., Bal, B. S., Huang, W. and Day, D. E. (2007). Preparation and bioactive characteristics of a porous 13–93 glass, and fabrication into the articulating surface of a proximal tibia. *Journal of Biomedical Materials Research Part A,* **82**, 222–229.

Fu, Q., Saiz, E., Rahaman, M. N. and Tomsia, A. P. (2011a). Bioactive glass scaffolds for bone tissue engineering: state of the art and future perspectives. *Materials Science and Engineering: C,* **31**, 1245–1256.

Fu, Q., Saiz, E. and Tomsia, A. P. (2011b). Direct ink writing of highly porous and strong glass scaffolds for load-bearing bone defects repair and regeneration. *Acta Biomaterialia,* **7**, 3547–3554.

Gentleman, E., Fredholm, Y. C., Jell, G., Lotfibakhshaiesh, N., O'donnell, M. D., Hill, R. G. and Stevens, M. M. (2010). The effects of strontium-substituted bioactive glasses on osteoblasts and osteoclasts in vitro. *Biomaterials,* **31**, 3949–3956.

Gerhardt, L. C. and Boccaccini, A. R. (2010). Bioactive glass and glass-ceramic scaffolds for bone tissue engineering. *Materials,* **3**, 3867–3910.

Gerhardt, L. C., Widdows, K. L., Erol, M. M., Burch, C. W., Sanz, J. A., Ochoa, I., Stämpfli, R., Roqan, I., Gabe, S., Ansari, A. and Boccaccini, A. R. (2011). The pro-angiogenic properties of multifunctional bioactive glass composite scaffolds. *Biomaterials,* **32**, 4096–4108.

Gomez, T. M. and Spitzer, N. C. (1999). In vivo regulation of axon extension and pathfinding by growth-cone calcium transients. *Nature,* **397**, 350–355.

Gorriti, M. F., Porto López, J., M., Boccaccini, A. R., Audisio, C. and Gorustovich, A. A. (2009). In vitro study of the antibacterial activity of bioactive glass-ceramic scaffolds. *Advanced Engineering Materials,* **11**, B67–B70.

Gorustovich, A., Roether, J. and Boccaccini, A. R. (2010). Effect of bioactive glasses on angiogenesis: *In-vitro* and *in-vivo* evidence. A review. *Tissue Engineering Part B: Reviews,* **16**, 199–207.

Gorustovich, A. A. (2010). Imaging resin-cast osteocyte lacuno-canalicular system at bone-bioactive glass interface by scanning electron microscopy. *Microscopy and Microanalysis,* **16**, 132–136.

Gough, J. E., Jones, J. R. and Hench, L. L. (2004). Nodule formation and mineralisation of human primary osteoblasts cultured on a porous bioactive glass scaffold. *Biomaterials,* **25**, 2039–2046.

Habibovic, P. and Barralet, J. E. (2011). Bioinorganics and biomaterials: Bone repair. *Acta Biomaterialia,* **7**, 3013–3026.

Haimi, S., Gorianc, G., Moimas, L., Lindroos, B., Huhtala, H., Räty, S., Kuokkanen, H., Sándor, G. K., Schmid, C., Miettinen, S. and Suuronen, R. (2009). Characterization of zinc-releasing three-dimensional bioactive glass scaffolds and their effect on human adipose stem cell proliferation and osteogenic differentiation. *Acta Biomaterialia,* **5**, 3122–3131.

Hench, L. L. (1991). Bioceramics: From concept to clinic. *Journal of the American Ceramic Society,* **74**, 1487–1510.

Hench, L. L. (1998). Bioceramics. *Journal of the American Ceramic Society,* **81**, 1705–1728.

Hench, L. L. (2009). Genetic design of bioactive glass. *Journal of the European Ceramic Society,* **29**, 1257–1265.

Hench, L. L. and Polak, J. M. (2002). Third-generation biomedical materials. *Science,* **295**, 1014–1017.

Hench, L. L., Splinter, R. J., Allen, W. C. and Greenlee, T. K. (1972). Bonding mechanism at the interface of ceramic prosthetic materials. *Journal of Biomedical Materials Research,* **2**, 117–141.

Hench, L. L. and Thompson, I. (2010). Twenty-first century challenges for biomaterials. *Journal of the Royal Society Interface,* **7**, S379–S391.

Hench, L. L., Xynos, I. D. and Polak, J. M. (2004). Bioactive glasses for in situ tissue regeneration. *Journal of Biomaterials Science, Polymer Edition,* **15**, 543–562.

Hesaraki, S., Alizadeh, M., Nazarian, H. and Sharifi, D. (2010). Physico-chemical and in vitro biological evaluation of strontium/calcium silicophosphate glass. *Journal of Materials Science-Materials in Medicine,* **21**, 695–705.

Hoppe, A., Güldal, N. S. and Boccaccini, A. R. (2011). A review of the biological response to ionic dissolution products from bioactive glasses and glass-ceramics. *Biomaterials,* **32**, 2757–2774.

Hu, G.-F. (1998). Copper stimulates proliferation of human endothelial cells under culture. *Journal of Cellular Biochemistry,* **69**, 326–335.

Huang, T. S., Rahaman, M. N., Doiphode, N. D., Leu, M. C., Bal, B. S., Day, D. E. and Liu, X. (2011). Porous and strong bioactive glass (13–93) scaffolds fabricated by freeze extrusion technique. *Materials Science and Engineering: C,* **31**, 1482–1489.

Hum, J. and Boccaccini, A. R. (2012). Bioactive glasses as carriers for bioactive molecules and therapeutic drugs: a review. *Journal of Materials Science: Materials in Medicine*, **23**, 1–17.

Hutmacher, D. W. (2000). Scaffolds in tissue engineering bone and cartilage. *Biomaterials,* **21**, 2529–2543.

Isaac, J., Nohra, J., Lao, J., Jallot, E., Nedelec, J. M., Berdal, A. and Sautier, J. M. (2011). Effects of strontium-doped bioactive glass on the differentiation of cultered osteogenic cells. *European Cells & Materials,* **21**, 130–143.

Jell, G. and Stevens, M. (2006). Gene activation by bioactive glasses. *Journal of Materials Science: Materials in Medicine,* **17**, 997–1002.

Jiang, Y. M. J. Y. M., Ou, J., Zhang, Z. H. and Qin, Q. H. (2011). Preparation of magnetic and bioactive calcium zinc iron silicon oxide composite for hyperthermia treatment of bone cancer and repair of bone defects. *Journal of Materials Science-Materials in Medicine,* **22**, 721–729.

Jones, J., Ehrenfried, L., Saravanapavan, P. and Hench, L. (2006a). Controlling ion release from bioactive glass foam scaffolds with antibacterial properties. *Journal of Materials Science: Materials in Medicine,* **17**, 989–996.

Jones, J. R. (2007). Bioactive ceramics and glasses. *In:* Boccaccini, A. R. and Gough, J. E. (eds.) *Tissue Engineering Using Ceramics and Polymers.* 1 edn. Cambridge, UK: Woodhead Publishing Limited.

Jones, J. R., Ehrenfried, L. M. and Hench, L. L. (2006b). Optimising bioactive glass scaffolds for bone tissue engineering. *Biomaterials,* **27**, 964–973.

Jones, J. R. and Hench, L. L. (2003). Regeneration of trabecular bone using porous ceramics. *Current Opinion in Solid State and Materials Science,* **7**, 301–307.

Jones, J. R., Lin, S., Yue, S., Lee, P. D., Hanna, J. V., Smith, M. E. and Newport, R. J. (2010). Bioactive glass scaffolds for bone regeneration and their hierarchical characterisation. *Proceedings of the Institution of Mechanical Engineers, Part H: Journal of Engineering in Medicine,* **224**, 1373–1387.

Jones, J. R., Tsigkou, O., Coates, E. E., Stevens, M. M., Polak, J. M. and Hench, L. L. (2007). Extracellular matrix formation and mineralization on a phosphate-free porous bioactive glass scaffold using primary human osteoblast (HOB) cells. *Biomaterials,* **28**, 1653–1663.

Keshaw, H., Forbes, A. and Day, R. M. (2005). Release of angiogenic growth factors from cells encapsulated in alginate beads with bioactive glass. *Biomaterials,* **26**, 4171–4179.

Keshaw, H., Georgiou, G., Blaker, J. J., Forbes, A., Knowles, J. C. and Day, R. M. (2009). Assessment of polymer/bioactive glass-composite microporous spheres for tissue regeneration applications. *Tissue Engineering Part A,* **15**, 1451–1461.

Leu, A. and Leach, J. (2008). Proangiogenic potential of a collagen/bioactive glass substrate. *Pharmaceutical Research,* **25**, 1222–1229.

Leu, A., Stieger, S. M., Dayton, P., Ferrara, K. W. and Leach, J. K. (2009). Angiogenic response to bioactive glass promotes bone healing in an irradiated calvarial defect. *Tissue Engineering Part A,* **15**, 877–885.

Li, G., Feng, S. and Zhou, D. (2011). Magnetic bioactive glass ceramic in the system CaO-P(2)O (5)-SiO (2)-MgO-CaF (2)-MnO (2)-Fe (2)O (3) for hyperthermia treatment of bone tumor. *Journal of Materials Science. Materials in Medicine,* **22**, 2197–2206.

Liang, W., Rahaman, M. N., Day, D. E., Marion, N. W., Riley, G. C. and Mao, J. J. (2008). Bioactive borate glass scaffold for bone tissue engineering. *Journal of Non-Crystalline Solids,* **354**, 1690–1696.

Liu, X., Ramahan, M. N. and Fu, Q. (2011). Oriented bioactive glass (13–93) scaffolds with controllable pore size by unidirectional freezing of camphene-based suspensions: Microstructure and mechanical response. *Acta Biomaterialia,* **7**, 406–416.

Lusvardi, G., Malavasi, G., Menabue, L., Aina, V. and Morterra, C. (2009). Fluoride-containing bioactive glasses: surface reactivity in simulated body fluids solutions. *Acta Biomaterialia,* **5**, 3548–3562.

Mahmood, J., Takita, H., Ojima, Y., Kobayashi, M., Kohgo, T. and Kuboki, Y. (2001). Geometric effect of matrix upon cell differentiation: BMP-induced osteogenesis using a new bioglass with a feasible structure. *Journal of Biochemistry,* **129,** 163–171.

Mallik, K. K. (2008). Freeze casting of porous bioactive glass and bioceramics. *Journal of the American Ceramic Society,* **92**, S85–S94.

Marie, P. J. (2006). Strontium ranelate: A physiological approach for optimizing bone formation and resorption. *Bone,* **38**, 10–14.

Marie, P. J., Ammann, P., Boivin, G. and Rey, C. (2001). Mechanisms of action and therapeutic potential of strontium in bone. *Calcified Tissue International,* **69**, 121–129.

Moimas, L., Biasotto, M., Di Lenarda, R., Olivo, A. and Schmid, C. (2006). Rabbit pilot study on the resorbability of three-dimensional bioactive glass fibre scaffolds. *Acta Biomaterialia,* **2**, 191–199.

Moosvi, S. R. and Day, R. M. (2009). Bioactive glass modulation of intestinal epithelial cell restitution. *Acta Biomaterialia,* **5**, 76–83.

Mouriño, V., Cattalini, J. P. and Boccaccini, A. R. (2012). Metallic ions as therapeutic agents in tissue engineering scaffolds: an overview of their biological applications and strategies for new developments. *Journal of the Royal Society Interface,* **9**, 401–419.

Munukka, E., Lepparanta, O., Korkeamaki, M., Vaahtio, M., Peltola, T., Zhang, D., Hupa, L., Ylanen, H., Salonen, J. I., Viljanen, M. K. and Eerola, E. (2008). Bactericidal effects of bioactive glasses on clinically important aerobic bacteria. *Journal of Materials Science: Materials in Medicine,* **19**, 27–32.

Nandi, S. K., Kundu, B., Datta, S., De, D. K. and Basu, D. (2009). The repair of segmental bone defects with porous bioglass: An experimental study in goat. *Research in Veterinary Science,* **86**, 162–173.

Ostomel, T. A., Shi, Q. H., Tsung, C. K., Liang, H. J. and Stucky, G. D. (2006). Spherical bioactive glass with enhanced rates of hydroxyapatite deposition and hemostatic activity. *Small,* **2**, 1261–1265.

Palangkaraya, A. and Yong, J. (2009). Population ageing and its implications on aggregate health care demand: empirical evidence from 22 OECD countries. *International Journal of Health Care Finance and Economics,* **9**, 391–402.

Pereira, M. M., Jones, J. R., Orefice, R. L. and Hench, L. L. (2005). Preparation of bioactive glass-polyvinyl alcohol hybrid foams by the sol-gel method. *Journal of Materials Science Materials in Medicine,* **16**, 1045–1050.

Qian, J., Kang, Y., Wei, Z. and Zhang, W. (2009). Fabrication and characterization of biomorphic 45S5 bioglass scaffold from sugarcane. *Materials Science and Engineering: C,* **29**, 1361–1364.

Rahaman, M. N., Day, D. E., Bal, B. S., Fu, Q., Jung, S. B., Bonewald, L. F. and Tomsia, A. P. (2011). Bioactive glass in tissue engineering. *Acta Biomaterialia,* **7**, 2355–2373.

Ramay, H. R. and Zhang, M. Q. (2003). Preparation of porous hydroxyapatite scaffolds by combination of the gel-casting and polymer sponge methods. *Biomaterials,* **24**, 3293–3302.

Rezwan, K., Chen, Q. Z., Blaker, J. J. and Boccaccini, A. R. (2006). Biodegradable and bioactive porous polymer/inorganic composite scaffolds for bone tissue engineering. *Biomaterials,* **27**, 3413–3431.

Rodríguez, J. P., Ríos, S. and González, M. (2002). Modulation of the proliferation and differentiation of human mesenchymal stem cells by copper. *Journal of Cellular Biochemistry,* **85**, 92–100.

Ross, E. A., Batich, C. D., Clapp, W. L., Sallustio, J. E. and Lee, N. C. (2003). Tissue adhesion to bioactive glass-coated silicone tubing in a rat model of peritoneal dialysis catheters and catheter tunnels. *Kidney International,* **63**, 702–708.

Shah, S. A., Hashmi, M. U. and Alam, S. (2011). Effect of aligning magnetic field on the magnetic and calorimetric properties of ferrimagnetic bioactive glass ceramics for the hyperthermia treatment of cancer. *Materials Science and Engineering: C,* **31**, 1010–1016.

Shah, S. A., Hashmi, M. U., Shamim, A. and Alam, S. (2010). Study of an anisotropic ferrimagnetic bioactive glass ceramic for cancer treatment. *Applied Physics A-Materials Science & Processing,* **100**, 273–280.

Song, J.-H., Koh, Y.-H., Kim, H.-E., Li, L.-H. and Bahn, H.-J. (2006). Fabrication of a porous bioactive glass–ceramic using room-temperature freeze casting. *Journal of the American Ceramic Society,* **89**, 2649–2653.

Tesavibul, P., Felzmann, R., Gruber, S., Liska, R., Thompson, I., Boccaccini, A. R. and Stampfl, J. (2012). Processing of 45S5 Bioglass® by lithography-based additive manufacturing. *Materials Letters,* **74**, 81–84.

Thompson, K. H. and Orvig C. (2003). Boon and bane of metal ions in medicine. *Science,* **300**, 936.

Tsigkou, O., Jones, J. R., Polak, J. M. and Stevens, M. M. (2009). Differentiation of fetal osteoblasts and formation of mineralized bone nodules by 45S5 Bioglass (R) conditioned medium in the absence of osteogenic supplements. *Biomaterials,* **30**, 3542–3550.

Vargas, G. E., Mesones, R. V., Bretcanu, O., López, J. M. P., Boccaccini, A. R. and Gorustovich, A. (2009). Biocompatibility and bone mineralization potential of 45S5 Bioglass®-derived glass-ceramic scaffolds in chick embryos. *Acta Biomaterialia,* **5**, 374–380.

Vitale-Brovarone, C., Miola, M., Balagna, C. and Verné, E. (2008). 3D-glass-ceramic scaffolds with antibacterial properties for bone grafting. *Chemical Engineering Journal,* **137**, 129–136.

Vitale-Brovarone, C., Verne, E., Bosetti, M., Appendino, P. and Cannas, M. (2005). Microstructural and in vitro characterization of SiO_2-Na_2O-CaO-MgO glass-ceramic bioactive scaffolds for bone substitutes. *Journal of Materials Science: Materials in Medicine,* **16**, 909–917.

Wu, C., Fan, W., Zhu, Y., Gelinsky, M., Chang, J., Cuniberti, G., Albrecht, V., Friis, T. and Xiao, Y. (2011a). Multifunctional magnetic mesoporous bioactive glass scaffolds with a hierarchical pore structure. *Acta Biomaterialia,* **7**, 3563–3572.

Wu, C., Miron, R., Sculean, A., Kaskel, S., Doert, T., Schulze, R. and Zhang, Y. (2011b). Proliferation, differentiation and gene expression of osteoblasts in boron-containing associated with dexamethasone deliver from mesoporous bioactive glass scaffolds. *Biomaterials,* **32**, 7068–7078.

Wu, Z. Y., Hill, R. G., Yue, S., Nightingale, D., Lee, P. D. and Jones, J. R. (2011c). Melt-derived bioactive glass scaffolds produced by a gel-cast foaming technique. *Acta Biomaterialia,* **7**, 1807–1816.

Xie, H. Q. and Kang, Y. J. (2009). Role of copper in angiogenesis and its medicinal implications. *Current Medicinal Chemistry,* **16**, 1304–1314.

Xynos, I. D., Edgar, A. J., Buttery, L. D. K., Hench, L. L. and Polak, J. M. (2001). Gene-expression profiling of human osteoblasts following treatment with the ionic products of Bioglass® 45S5 dissolution. *Journal of Biomedical Materials Research,* **55**, 151–157.

Zhang, K., Washburn, N. R. and Simon Jr, C. G. (2005). Cytotoxicity of three-dimensionally ordered macroporous sol–gel bioactive glass (3DOM-BG). *Biomaterials,* **26**, 4532–4539.

Zhang, X. F., Kehoe, S., Adhi, S. K., Ajithkumar, T. G., Moane, S., O'shea, H. and Boyd, D. (2011a). Composition-structure-property (Zn^{2+} and Ca^{2+} ion release) evaluation of Si-Na-Ca-Zn-Ce glasses: Potential components for nerve guidance conduits. *Materials Science and Engineering: C,* **31**, 669–676.

Zhang, X. F., O'shea, H., Kehoe, S. and Boyd, D. (2011b). Time-dependent evaluation of mechanical properties and in vitro cytocompatibility of experimental composite-based nerve guidance conduits. *Journal of the Mechanical Behavior of Biomedical Materials,* **4**, 1266–1274.

8

Bioactive glass and glass–ceramic foam scaffolds for bone tissue restoration

F. BAINO and C. VITALE-BROVARONE,
Politecnico di Torino, Italy

DOI: 10.1533/9780857097033.2.213

Abstract: One of the major goals of bone tissue engineering is the development of appropriate porous biomaterials (scaffolds) that can stimulate the body's own regenerative mechanism, to induce tissue healing and self-repair. Bioactive glasses are excellent candidates for producing 3-D scaffolds, as their properties can be finely tailored depending on the glass composition, and they can bond to bone, inducing osteogenesis at the defect site. This chapter is focused on glass/glass–ceramic scaffolds characterized by foam-like architecture closely mimicking that of natural cancellous bone. After giving an overview of the features and limitations of the biomedical glass foams investigated in the literature, future directions of research will be described, emphasizing the challenge to develop multifunctional foams able to combine bone regeneration with special therapeutic functionalities.

Key words: foam scaffold, glass, bioactivity, biocompatibility, bone tissue engineering.

8.1 Introduction

Natural materials are renowned for their exquisite designs that optimize function, as illustrated for instance by the elasticity of blood vessels, the toughness of bone and the protection offered by nacre (Kamat *et al.*, 2000; Gao *et al.*, 2003; Cranford *et al.*, 2012). Human cancellous bone is a highly porous natural material with high stiffness and strength (typically 2–20 MPa in compression (Hench, 1991; Boskey, 2007; Tassani *et al.*, 2010), and its remarkable mechanical properties are attributed to its anisotropic structure which has optimized strength-to-density and stiffness-to-density ratios over natural evolution (Boskey, 2007). One of the most important challenges of modern regenerative medicine, involving strong collaboration among biomedical/mechanical engineers, materials scientists, chemists, biologists and surgeons of various disciplines, is the development of bioactive three-dimensional (3-D) porous templates (scaffolds) able to mirror the efficiency

of natural materials from architectural and mechanical viewpoints, as well as to stimulate natural tissue regeneration *in situ*.

Scaffold properties depend primarily on the type of the biomaterial and the fabrication process, and should be carefully tailored depending on the intended application in tissue restoration. The nature of the biomaterial has been the topic of extensive studies including a wide range of materials such as ceramics, glasses, natural and chemically synthesized polymers, metals and combinations of these materials to obtain composites. The type of biomaterial, and the related application, influences the choice of fabrication method: different materials can be processed in different ways and, moreover, different applications in tissue engineering normally require special architectural and mechanical features of the scaffold.

In the field of bone tissue engineering, the preferred biomaterials for scaffolding are ceramics, glasses, polymers and composites of the above-mentioned materials, and many fabrication techniques have been investigated to produce suitable scaffolds for bone repair. This chapter is specifically focused on glass/glass–ceramic (GC) scaffolds characterized by a foam-like architecture that closely mimics that of natural trabecular bone; particular emphasis is devoted to their applications in bone tissue engineering and, finally, a forecast of the future challenges is presented.

8.1.1 Bone tissue repair: a short overview

Bone, often called osseous tissue, is a type of hard endoskeletal connective tissue found in many vertebrate animals, including man. Bones, collectively forming the skeleton, support body structures, protect internal organs, act for mineral storage (for instance, bones and teeth contain almost 99% of total body calcium) and, in conjunction with muscles and ligaments, allow and facilitate movement. From the material viewpoint, bone is a complex composite containing both an inorganic phase (mainly biological apatite) and organic compounds (mainly collagen). From a macroscopic viewpoint, bone is constituted of a dense outer layer (cortical or compact bone) covering an internal mesh-like core of cancellous bone (often called spongy or trabecular bone). Therefore, bone exhibits a hierarchical structure, wherein the pores size range within 1–100 μm in cortical bone and within 100–500 μm in cancellous bone, with the aim of optimizing its physico-mechanical performances. Furthermore, being a 'living' material, bone continuously undergoes a remodelling process, as it is resorbed by osteoclasts and re-deposited by osteoblasts in a delicate equilibrium. A comprehensive picture about the mineralization of bone and teeth was recently provided by Boskey (2007), while Dorozhkin (2007, 2009, 2010) has extensively reviewed the features and properties of biological bone apatite.

Bone loss can occur due to trauma, surgical removal (for instance, in the case of bone tumours) or relatively common age-related diseases such as osteoporosis and osteoarthritis. The gold standard in reconstructive surgery for damaged bone is the autograft, which involves harvesting the patient's own tissue from a donor site and transplanting it to the diseased region. Alternatives are homografts (transplantation from another living patient or from a cadaver) and xenografts (tissue from a different species, such as freeze-dried bovine bone). Both options, however, involve some limitations: autografts have limited availability, can induce infection or death of healthy tissue at the donor site, and need an extra-surgery operation for the patient; homografts, even though stored in large and controlled banks, can still carry the problem of disease transmission, as well as problems related to religion or ethics. Xenografts have higher risks of disease transmission, *in situ* degeneration, and too fast resorption as compared to the kinetics of the surrounding healing tissue.

The treatment of advanced-stage osteoarthritis at joint sites, such as hip or knee joint, involves the partial or total joint replacement by implantation of a prosthesis. However, orthopaedic implants generally have a limited life span as they unavoidably lack three of the most critical characteristics of living tissues: (i) the ability to self-repair, (ii) the ability to maintain a blood supply and (iii) the ability to modify in response to stimuli such as mechanical load, typical of bone remodelling.

As life expectancy increases and, accordingly, degenerative bone diseases become more common, the need for artificial alternatives to autografts will become ever more important and advantageous, as the so-called alloplastic materials are ideally available in an unlimited amount, and their properties can be finely tailored with respect to the nature of the used biomaterials and on the fabrication process.

8.1.2 Evolution of biomaterials and scaffolds for bone tissue engineering

During the last 70 years, the approach of materials scientists and clinicians to biomaterials for bone restoration has been deeply and repeatedly revolutionized; in fact, from the material researcher's viewpoint, at least three conceptual revolutions have occurred. Approximately up to the World War II (WWII), every (apparently) non-toxic material with adequate stiffness could be deemed – at least in principle – suitable for bone substitution: wood, animal- or cadaver-derived bone, metals and other natural or synthetic materials were subject to frequent experiment as bone fillers, since the primary goal was simply to fill the bone defect. After WWII, the first revolution took place: the search for bone substitutes was progressively

addressed to materials able to mimic bone mineral phase, such as hydroxyapatite (HA) and other calcium phosphates. Therefore, the criterion of biomaterial choice gained major specificity, evolving from a simple requirement of non-toxicity to the need for compositional bio-mimicry with bone inorganic matrix; however, biomaterials for bone substitution were still deemed to be mere defect fillers. The second revolution started in the early 1970s, with the discovery of biomedical glasses by Hench and co-workers, who first synthesized Bioglass® and coined the term 'bioactivity' to denote the peculiar ability of a selected subset of glasses to bond to bone, promoting its regeneration *in situ* (Hench *et al.*, 1972). Since then, biomaterials for bone substitution have been viewed as materials able to play an 'active role' in bone healing, regeneration and remodelling processes. The third revolution, that started about 15 years ago and still lingers on, is characterized by a further conceptual advance towards structural and functional bio-mimicry of bone substitutes: biomedical glasses are increasingly designed to act as porous templates (scaffolds) for new bone tissue growth in 3-D and to safely dissolve once they have performed their function, thereby leaving the body to remodel the tissue to its natural form.

An ideal scaffold for bone tissue engineering applications should fulfil a complex set of requisites (Hutmacher, 2000; Karageorgiou and Kaplan, 2005; Jones *et al.*, 2007a; Baino and Vitale-Brovarone, 2011); essentially, it should (i) be biocompatible, (ii) produce non-toxic degradation products, (iii) resorb (if the implant is temporary) at the same (or slower) rate as the bone is repaired, (iv) exhibit a 3-D porous skeleton of large macropores (above 50 vol.%, like in spongy bone) in the 100–600 μm range interconnected by pore windows, channels and canaliculi in the 1–100 μm range, (v) elicit a bioactive response, i.e. the formation of an HA layer on its surface in order to bond to the host bone (HA has a compositional and crystallographic similarity to bone mineral phase (Dorozhkin 2007, 2009, 2010)), (vi) promote cell adhesion, spreading, proliferation and differentiation, (vii) have mechanical properties matching those of the host bone, (viii) be easily produced and sterilized, and (ix) be made available on the market at a reasonable cost.

At present, such an ideal scaffold able to simultaneously fulfil all these criteria does not exist; however, much evidence suggests that biomedical glasses of appropriate composition are actually the most promising candidates to be used to achieve this goal, as demonstrated by the growing number of publications in the field (Fig. 8.1). In recent years, several studies have also demonstrated the feasibility to impart useful 'added value' to glass-derived scaffolds, such as *in situ* drug delivery ability, antibacterial properties, and an ever closer similarity to natural bone tissue in terms of macro-scale architecture (pore size, distribution and interconnection) and features at the micro-/nano-scale (surface roughness to promote cells adhesion).

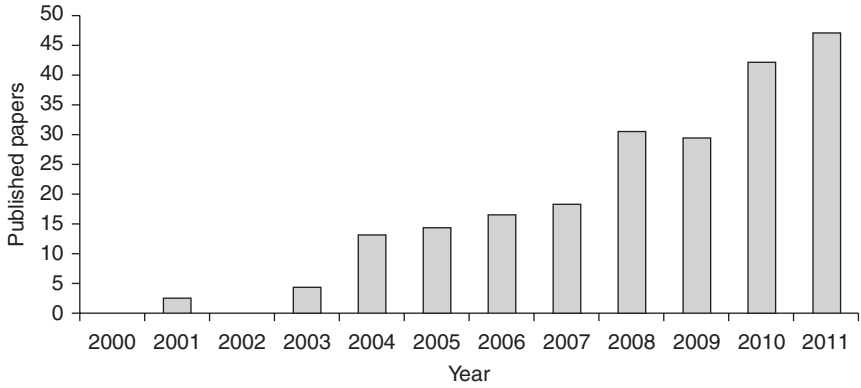

8.1 Number of scientific articles dealing with biomedical glass-based scaffolds published in the relevant literature over the last decade (the data is derived from SCOPUS; the article search was carried out by using the terms 'scaffold', 'glass', 'Bioglass', 'tissue engineering' as keywords, as well as appropriate combinations of these words).

8.2 The potential of bioactive glass and the bioactivity mechanism

The bone-bonding ability of bioactive glass can be attributed, as first hypothesized by Hench and co-workers in the early 1970s (Hench *et al.*, 1972) and subsequently confirmed by a lot of experimental work (Hench, 2006), to the formation of an HA layer on the glass surface in contact with biological fluids. Five reaction stages have been proposed to describe this process, commonly termed the 'bioactivity mechanism' in the scientific community: essentially, they involve the rapid release of soluble ionic species due to glass dissolution, ultimately leading to the formation of a hydrated silica and polycrystalline HA bilayer on the glass surface. The details of the bioactivity process are resuméd in Table 8.1.

With the initial formation of an apatitic layer, the biological mechanism of bonding to bone is believed to involve adsorption of growth factors, followed by attachment, proliferation and differentiation of osteoprogenitor cells. Osteoblasts then create extracellular matrix, which mineralizes to form a nanocrystalline mineral/collagen composite layer on the surface of the glass implant, while the degradation and conversion of the glass continues over time (Ducheyne and Qiu, 1999).

It is interesting to note that the nanocrystalline nature of the HA formed on bioactive glasses (globular agglomerates constituted by nano-sized needle-like crystals) closely mimics the features of the biological apatite of bones (Dorozhkin 2007, 2009, 2010), thereby promoting the cascade of biological events following Stage 5, whereas synthetic HA, commercialized

Table 8.1 Bioactive stages of a bioactive glass implant

Stage	Description
1	Rapid exchange of cations (e.g. Na^+ and Ca^{2+} belonging to glass modifier oxides) with H^+ or H_3O^+ from the surrounding solution, which leads to hydrolysis of silica groups and creation of silanols (Si–OH). The pH of the solution increases as H^+ in the biological fluids is gradually replaced by alkaline cations.
2	Attack of the silica network, loss of soluble silica in the form of $Si(OH)_4$ to the solution (resulting from the breaking of Si–O–Si bonds) and continued formation of silanols at the glass-solution interface.
3	Condensation and re-polymerization of the silanols, leading to the formation of a silica-rich layer depleted in alkalis and alkali-earth cations on the glass surface.
4	Migration of Ca^{2+} and PO_4^{3-} groups to the surface through the silica-rich layer and from the surrounding fluids, thereby forming an amorphous CaO/P_2O_5-rich (CaP) film on the top of the silica-rich layer.
5	Growth and crystallization of the CaP film to form a HA layer; actually, by incorporation of OH^-, CO_3^{2-} and F^- ions from the solution, a mixed apatitic layer constituted by HA, hydroxycarbonateapatite and fluoroapatite can develop

in the form of particles, granulates or even porous blocks, is characterized by larger grain size; this is the reason why HA is currently considered osteoconductive but not properly bioactive by most of the researchers.

Since the invention of 45S5 Bioglass® (Hench *et al.*, 1972), many glass formulations have been designed and tested for possible application in the field of bone repair. From a compositional viewpoint, biomedical glasses can be divided into three families, depending on the main former oxide present in the composition: (i) SiO_2-based (silicate), (ii) B_2O_3-based (borate) and (iii) P_2O_5-based (phosphate) glasses. The first group comprises the majority of biomedical glass formulations, including the original 45S5 Bioglass®. Borate glasses were first introduced by Andersson *et al.* (1990), who modified the 45S5 Hench's composition and implanted sixteen different glasses in the SiO_2-CaO-Na_2O-P_2O_5-Al_2O_3-B_2O_3 system into rabbit tibiae, demonstrating that bonding to bone occurred only for those glasses that could form an HA layer when tested in physiologically balanced ionic solution *in vitro*. Borate glasses have been, to this point, the least investigated, in spite of their very interesting bioactive properties, superior even to those of silicate glasses (Brink *et al.*, 1997; Huang *et al.*, 2006); this is essentially due to a concern associated with the potential toxicity of boron released in solution as borate ions, $(BO_3)^{3-}$. As far as phosphate glasses are concerned, it is interesting to underline that they may be, in principle, both bioactive and bioresorbable (Leonardi *et al.*, 2010) – and thus excellent candidates to

manufacture an ideal scaffold. The majority of studies on phosphate glasses have been addressed to investigating their suitability as carriers for releasing antimicrobial agents (metal ions) (Abou Neel *et al.*, 2009) or, thanks to their relative facility to be drawn in fibres, their possible application in soft tissue engineering (for instance, as guides for peripheral nerve regeneration (Abou Neel *et al.*, 2009; Vitale-Brovarone *et al.*, 2012a). The phosphate glass resorption kinetics, that can be modulated by adding proper metal oxides, generally remains quite fast, thereby representing a limitation for load-bearing applications in hard tissue engineering.

Table 8.2 Overview of the glasses used for producing the bone tissue engineering foam-like scaffolds described in the chapter

Composition family[a]	Glass name	Synthesis[b]	Oxide system and composition (mol.%)
Silicate, silica-phosphate	45S5 Bioglass®	M	$46.1SiO_2$-$26.9CaO$-$24.4Na_2O$-$2.7P_2O_5$
	58S	sg	$60SiO_2$-$36CaO$-$4P_2O_5$
	70S30C	sg	$70SiO_2$-$30CaO$
	70S26C	sg	$70SiO_2$-$26CaO$-$4P_2O_5$
	FaGC	M	$50SiO_2$-$18CaO$-$7Na_2O$-$6P_2O_5$-$7K_2O$-$3MgO$-$9CaF_2$
	CEL2	M	$45SiO_2$-$26CaO$-$15Na_2O$-$3P_2O_5$-$4K_2O$-$7MgO$
	13-93	M	$54.6SiO_2$-$6Na_2O$-$7.9K_2O$-$7.7MgO$-$22.1CaO$-$1.7P_2O_5$
	80S15C5P	EISA	$80SiO_2$-$15CaO$-$5P_2O_5$
	Fe-MBG	EISA	Like 80S15C5P + 5 or 10 mol.% of Fe
	SCNA	M	$57SiO_2$-$34CaO$-$6Na_2O$-$3Al_2O_3$
Borate, boro-silicate, boro-silica-phosphate	13-93B1	M	$6Na_2O$-$7.9K_2O$-$7.7MgO$-$22.1CaO$-$36.4B_2O_3$-$18.2SiO_2$-$1.7P_2O_5$
	13-93B2	M	$6Na_2O$-$8K_2O$-$8MgO$-$22CaO$-$36B_2O_3$-$18SiO_2$-$2P_2O_5$
	13-93B3	M	$6Na_2O$-$7.9K_2O$-$7.7MgO$-$22.1CaO$-$54.6B_2O_3$-$1.7P_2O_5$
Phosphate, phospho-silicate	TiGlass	M	$44.5P_2O_5$-$44.5CaO$-$6Na_2O$-$5TiO_2$
	CaP glass	M	CaO-CaF_2-P_2O_5-MgO-ZnO (unspecified composition)
	ICEL2	M	$45P_2O_5$-$26CaO$-$15Na_2O$-$3SiO_2$-$4K_2O$-$7MgO$
	PG1	M	$45P_2O_5$-$22CaO$-$25Na_2O$-$8MgO$

[a] Depending on the glass network former oxides.
[b] M = melt-derived, sg = sol-gel, EISA = evaporation-induced self-assembling (mesoporous glass).

The interested reader can find more details about the features of the different biomedical glass systems from some recent literature overviews (Gerhardt and Boccaccini, 2010; Baino and Vitale-Brovarone, 2011; Rahaman *et al.*, 2011).

Table 8.2, compiled on the basis of data available in the literature, reports a selection of biomedical glasses specifically used for fabricating bone tissue engineering foam-like glass/GC scaffolds. Scaffolds can be fabricated starting from glass powders obtained through the traditional melting–quenching route, or alternatively the glass synthesis can occur simultaneously with the scaffold manufacturing in sol-gel methods (scaffolds constituted by sol-gel glass or mesoporous glass are obtained).

8.3 Processing, 3-D architecture and mechanical properties of glass foams

A wide variety of synthesis methods has been proposed in the literature to produce glass-derived scaffolds for tissue engineering, including organic phase burning-out, sponge replication, solid free-form fabrication and techniques based on the sol-gel process and foaming (Baino and Vitale-Brovarone, 2011; Fu *et al.*, 2011). The main properties of the final scaffold, especially in terms of 3-D architecture, pore characteristics and mechanical strength, strongly depend on the particular processing method that has been chosen for the given application.

Organic additives such as starch from potato, rice or corn (Vitale-Brovarone *et al.*, 2005), polyethylene particles (Baino *et al.*, 2009) and rice husk (Wu *et al.*, 2009) were mixed with glass powders to act as thermally-removable pore formers; the resulting scaffolds generally exhibited high mechanical strength – even superior to that of cancellous bone – because of their thick struts but low pore content (well below 50 vol.%, which is the minimum threshold recommended for bone tissue engineering scaffolds) and low pore interconnectivity. Rapid prototyping techniques, such as selective laser sintering (Kolan *et al.*, 2011) and lithography-based manufacturing (Tesavibul *et al.*, 2012), have allowed accurate control of the internal scaffold architecture, but the necessary instrumentation is expensive and requires careful and often time-consuming programming and setting of the working parameters.

This chapter is particularly focused on porous glasses/GCs exhibiting foam-like structure and, therefore, only scaffolds fabricated by polymeric sponge replication and foaming techniques will be considered. Such scaffolds are particularly promising for bone tissue engineering since, as their basic architectural characteristics, they exhibit a 3-D network of open, large and highly interconnected macropores of sufficient size (100–800 μm) to

allow cells access and vascularization of the implant. In the following sections, the major characteristics of foam-like glass scaffolds proposed in the literature will be described and discussed; for sake of clarity, manufacturing techniques, pore content and mechanical strength are summarized in Table 8.3.

As a general comment, it is worth mentioning that all known methods for producing inorganic glass-derived scaffolds (polymer/glass porous composites do not belong to this category) require sintering treatment to ensure adequate structural integrity of the final porous body. Usually, the thermal treatment is applied above the crystallization onset temperature (T_x) of the glass, thereby leading to GC sintered scaffolds.

8.3.1 Macroporous foam-like scaffolds based on melt-derived glass

Silicate glass scaffolds

To the best of the authors' knowledge, the first study on bioactive glass scaffolds was reported by Yuan *et al.* (2001), who fabricated GC-Bioglass® scaffolds by H_2O_2 foaming followed by thermal treatment (5 μm-sized commercial 45S5 Bioglass® particles were used) and demonstrated the osteoinductive properties of the porous implants in dogs.

Chen *et al.* (2006a, 2006b) pioneered the fabrication of GC-Bioglass® scaffolds by polymeric sponge replication technique (also in this case, commercial 45S5 Bioglass® particles were used): the scaffolds had porous content (> 85 vol.%) and 3-D architecture closely mimicking those of cancellous bone, but their mechanical strength (0.3–0.4 MPa) was almost one order of magnitude lower than that of spongy bone (2–20 MPa (Hench, 1991)). Poor mechanical resistance was attributed to Bioglass® sintering behaviour that led to hollow struts in GC-Bioglass® final scaffolds.

Foam-like highly porous (~70 vol.%) scaffolds with mechanical strength (~2.5 MPa) actually comparable to that of cancellous bone were recently produced from commercial 45S5 Bioglass® powders by Baino *et al.* (2013): by carefully designing the sponge replication processing parameter and the sintering conditions, excellent densification of scaffold struts were achieved, which imparted high-strength properties to the final sintered scaffold.

Vitale-Brovarone and co-workers also spent a great effort in optimizing the mechanical properties of foam-like scaffolds based on an experimental highly bioactive glass named CEL2 (Fig. 8.2): starting from a compressive strength of 1 MPa for the first scaffold batches (Vitale-Brovarone *et al.*, 2007), the process parameters were successfully optimized to obtain

Table 8.3 Features of the glass/GC foam-like scaffolds described in the chapter

Scaffold material[a]	Fabrication method	Porosity (vol.%)	Compressive strength (MPa)	References
GC-Bioglass®	H_2O_2 foaming	–	–	Yuan *et al.* (2001)
	Polymeric sponge replication	~90.0	~0.4	Chen *et al.* (2006a, 2006b); Chen and Boccaccini (2006); Bretcanu *et al.* (2007)
	Polymeric sponge replication	~70.7	~1.3	Baino *et al.* (2013)
58S	Sol-gel foaming	–	–	Sepulveda *et al.* (2002); Jones and Hench (2003); Jones and Hench (2004)
70S30C	Sol-gel foaming	82–88[b]	0.3–2.2[b]	Jones *et al.* (2006, 2007a, b, 2009)
GC-70S26C	*In situ* foaming	~48	–	Rainer *et al.* (2008)
GC-FaGC	Polymeric sponge replication	~75	~2	Vitale-Brovarone *et al.* (2008)
GC-CEL2	Polymeric sponge replication	53.5–72.8[b]	1.0–5.4[b]	Vitale-Brovarone *et al.* (2007, 2009a, b); Renghini *et al.* (2009); Scheiner *et al.* (2009); Muzio *et al.* (2010); Baino *et al.* (2013)
13-93	Polymeric sponge replication	~85	~11	Fu *et al.* (2008, 2009, 2010a, 2010b, 2010c)
80S15C	EISA + polymer sponge replication	> 90	~60 × 10^{-3}	Yun *et al.*, 2007; Li *et al.*, 2007; Zhu *et al.*, 2008; Zhu and Kaskel, 2009; Wu *et al.*, 2010
Fe-MBG	EISA + polymer sponge replication	> 90	~50 × 10^{-3}	Wu *et al.* (2011a)
GC-SCNA	Polymeric sponge replication	~63.0	~12.5	Vitale-Brovarone *et al.* (2012b)
13-93B1	Polymeric sponge replication	~80	~7	Fu *et al.* (2010a, 2010b)
13-93B2	Polymeric sponge replication	~72.0	~6.4[b]	Fu *et al.* (2009)
13-93B3	Polymeric sponge replication	~80	~5	Fu *et al.*, (2010a, 2010b)
GC-TiGlass	H_2O_2 foaming	40–55	–	Navarro *et al.* (2004)
CaP glass	Polymeric sponge replication		0.6–1.5[b]	Park *et al.* (2006)
GC-ICEL2	Polymeric sponge replication	~85	~0.4	Vitale-Brovarone *et al.* (2009b, 2011)
β-TCP/GC-PG1	Polymeric sponge replication	60–85[b]	3.5–6[b]	Cai *et al.* (2009)

[a] If present, the notation 'GC-' followed by the name of the glass (see the Table 8.2) means that the material is a GC obtained from the parent glass by means of a thermal treatment above T_x.

[b] Different scaffolds batches were produced by varying the processing parameters in a controlled way (see the related references for details).

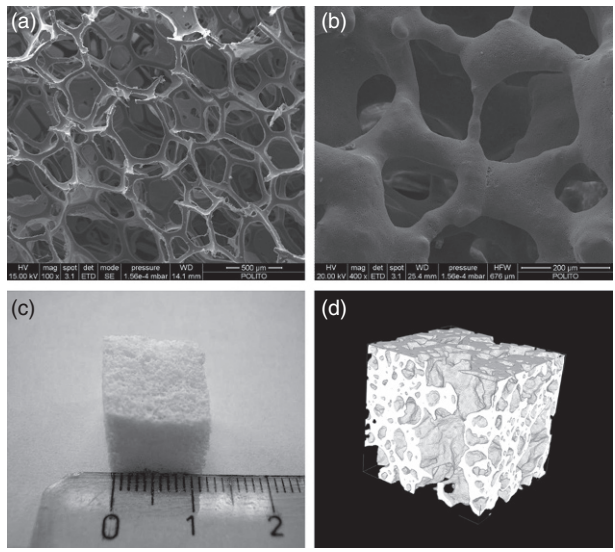

8.2 GC-CEL2 foam-like scaffolds produced by sponge replication method: (a) bare polyurethane foam used as scaffold template; (b) architecture of the sintered glass–ceramic foam (*Source*: adapted from Scheiner *et al.* (2009) © Elsevier); (c) typical cubic GC-CEL2 scaffold and (d) its 3-D reconstruction by X-ray micro-CT.

scaffolds with strength up to 6 MPa (Vitale-Brovarone *et al.*, 2009a, 2009b). This achievement can be mainly ascribable to the soundness of GC-CEL2 scaffolds trabeculae, that, differently from sponge-replicated GC-Bioglass® scaffolds (Chen *et al.*, 2006a), did not present inward cavities (hollow struts). GC-CEL2 foams were also non-destructively investigated by X-ray micro-computed tomography (micro-CT) (Fig. 8.2d) to acquire important information on the scaffold 3-D architecture (Renghini *et al.*, 2009), and their mechanical behaviour was modelled through an approach based on continuum micromechanics (Scheiner *et al.*, 2009).

It is known that the composition of the starting glass, being related to the softening–sintering behaviour as well as to the type and characteristics of the crystalline phases that can develop upon heating, plays a key role in affecting the mechanical properties of the final scaffold. A significant example of this effect is illustrated in Fig. 8.3, which reports a comparison of the compressive strengths of Bioglass®-, CEL2- and SCNA-derived scaffolds (see Table 8.3) produced exactly by the same method (optimized sponge replication technique described by Vitale-Brovarone *et al.* (2009a)) and by using a fixed powder size below 32 μm (non-commercial 45S5 Bioglass® particles were used). Relevant studies on this topic have been reported elsewhere (Vitale-Brovarone *et al.*, 2012b; Baino *et al.*, 2013).

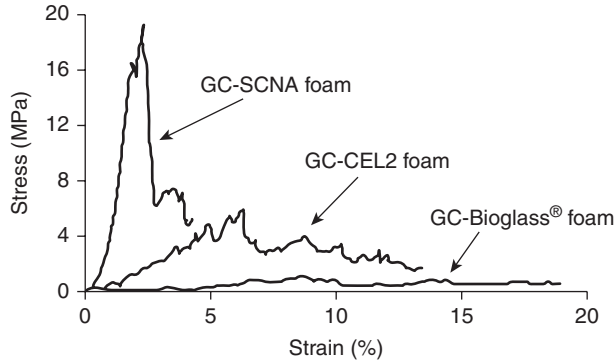

8.3 Comparison among the typical stress-strain curves (compressive test) of CG-Bioglass® (total porosity: 70.7 vol.%; major crystalline phase: $Na_2CaSi_2O_6$), GC-CEL2 (total porosity: 66.4 vol.%; major crystalline phase: $Na_4Ca_4(Si_6O_{18})$) and GC-SCNA (total porosity: 63.0 vol.%; crystalline phase: $CaSiO_3$) foam scaffolds produced by adopting the same processing parameters (optimized sponge replication method) and starting glass powders below 32 μm.

As previously mentioned, the final scaffold obtained by sponge replication is usually constituted by GC material, as a high-temperature thermal treatment (above T_x of the glass) for allowing glass particles sintering is applied. An interesting exception is represented by 3-D foam-like scaffolds based on the 13-93 glass: Fu *et al.* (2008) demonstrated by X-ray diffraction investigations that, after sintering, the scaffold material still remained amorphous (glass). This can occur thanks to the peculiar sintering behaviour of 13-93 glass: in comparison with 45S5 Bioglass®, for instance, 13-93 glass has more facile viscous flow behaviour, less tendency to crystallize – like CEL2 (Baino *et al.*, 2013) – and, therefore, a larger 'sinterability window'. It is also worth underlining that the porosity content and mechanical strength of 13-93 glass scaffolds are comparable to those of cancellous bone (Table 8.3); these features, associated with the good bioactivity and the initial results of *in vivo* studies (in animals), seem to suggest the potential suitability of 13-93 glass scaffolds for clinical use (13-93 glass is currently marketed for clinical use in Europe and USA in the form of bulk products and powder).

Borate glass scaffolds

At present, a quite limited number of B_2O_3-containing glass compositions have been used for producing foam-like scaffolds – and biomedical scaffolds in general. A systematic investigation of three types of borate/borosilicate scaffolds fabricated by polymeric sponge replication was recently carried out by Rahaman and co-workers who, in a series of studies (Fu

et al., 2009, 2010a, 2010b), produced bioactive glass scaffolds with controllable degradation and bioactivity by replacing various amounts of SiO_2 in silicate 13-93 glass with B_2O_3, thereby obtaining the so-called 13-93B1, 13-93B2 and 13-93B3 glasses. Upon soaking in simulated body fluid (SBF), the conversion rate of the scaffolds to HA increased markedly with increasing B_2O_3 content of the glass. The fully borate scaffolds, obtained by replacing all the SiO_2 in 13-93 with B_2O_3 (13-93 glass), converted completely to HA at a rate that was three to four times faster than silicate 13-93 scaffolds, whereas the 13-93B1 and 13-93B2 borosilicate scaffolds converted only partially to HA. The compressive strength of the as-prepared scaffolds decreased with the B_2O_3 content of the glass and, most importantly, also decreased markedly with the immersion time of the scaffolds in the SBF, which was related to the degradation and conversion of the scaffolds to HA; therefore, the authors concluded that such scaffolds might be suitable only for repairing small defects in non-bearing bone regions. Scaffold biocompatibility *in vitro* and *in vivo* was also assessed, as discussed in the Section 8.4.

Phosphate glass scaffolds

At present, a limited number of phosphate glasses (Tables 8.2 and 8.3) have been specifically used for fabricating 3-D glass-derived scaffolds for bone grafting. Navarro *et al.* (2004) successfully fabricated 3-D trabecular scaffolds from phosphate glass by H_2O_2 foaming. By varying the amount of incorporated H_2O_2 and the thermal treatment conditions, the total pore content and size, as well as the percentage of crystallinity, could be modulated.

Park *et al.* (2006) pioneered (simultaneously with Chen *et al.* (2006a)) the use of sponge replication in the biomedical field to obtain ZnO-containing phosphate glass scaffolds having 3-D foam-like architecture. This technique was more recently adopted by Vitale-Brovarone *et al.* (2009b, 2011) to manufacture GC scaffolds by using ICEL2 powders as glassy inorganic phase. ICEL2 composition was designed by modifying that of silicate CEL2 glass: specifically, the molar amounts of SiO_2 and P_2O_5 in ICEL2 composition are inverted in comparison with CEL2 one. GC-ICEL2 scaffolds were found to be resorbable as, after soaking in different media (water, Tris-HCl, SBF), they underwent a process of continuous dissolution whose rate was both medium-dependent and time-dependent. In addition, GC-ICEL2 scaffolds were also bioactive, as an HA layer formed on their trabeculae after soaking in SBF. Bone marrow stromal cells cultured on the scaffolds maintained their metabolic activity, proliferation ability and seemed to be stimulated towards differentiation. Cai *et al.* (2009) proposed the phosphate glass PG1 as reinforcing phase in β-tricalcium phosphate (β-TCP)-based scaffolds

(percentage weight ratio: β-TCP: PG1 = 80: 20). β-TCP/PG1 composite scaffolds exhibited enhanced mechanical properties (up to 6 MPa) with respect to pure β-TCP scaffolds (up to 2.3 MPa) as glass acted as viscous binder during sintering, thereby strengthening the final scaffold structure.

8.3.2 Foam-like glass scaffolds with multi-scale porosity

Glass-derived scaffolds produced by sponge replication or H_2O_2 foaming exhibit a foam-like architecture with all pores in the macro-range. Over the last decade, two approaches were carried out to synthesize scaffolds with hierarchical porosity, i.e. sol-gel glass scaffolds and mesoporous glass scaffolds.

Sol-gel scaffolds

Sol-gel bioactive glasses were synthesized for the first time in the early 1990s (Li *et al.*, 1991); in comparison to melt-derived 'traditional' glasses, sol-gel glasses can be prepared at relatively lower processing temperatures and exhibit higher bone-bonding rates, thanks to the high exposed surface (above 100 m^2/g vs. few m^2/g) due to their nanoporous texture (Avnir *et al.*, 2006). In the early 2000s, for the first time Sepulveda *et al.* (2002) combined the sol-gel route with foaming methods to obtain macro-/nano-porous hierarchical scaffolds: the sol was foamed by using a surfactant and, on gelation, the spherical bubbles formed in the sol after vigorous stirring became permanent in the gel, thereby leading to a 3-D foam-like highly porous structure mimicking the architecture of cancellous bone. Sol-gel glass scaffolds exhibited an excellent bioactive behaviour, due to the high surface area that is provided by the nanoporous network inherent to the sol-gel process and is then available for enhancing the ion-exchange phenomena with biological fluids. Sol-gel foaming led to scaffolds exhibiting a three-level porous organization, i.e. large pores up to 500 μm connected by pore windows (10–100 μm) (Fig. 8.4a) and a random-like nanoporous texture (10–20 nm). Jones and Hench demonstrated that many variables of sol-gel processing, such as surfactant agent and glass composition, can be used to control the final pore network structure of the scaffold (Jones and Hench, 2003, 2004). Sol-gel glass foams were also tested *in vitro* with osteoblast cultures and were found potentially suitable for bone repair (Valerio *et al.*, 2005). Some parameters of the sol-gel process, such as glass composition and type of surfactant, can be properly varied to tailor the scaffold pore network structure. Jones *et al.* (2006) showed that the compressive strength of sol-gel 70S30C glass scaffolds, that are in general dramatically brittle (about 0.3 MPa), can be improved up to 2.2 MPa by carefully adjusting the sintering temperature; however, this value is still far from the strength of spongy bone (2–20 MPa),

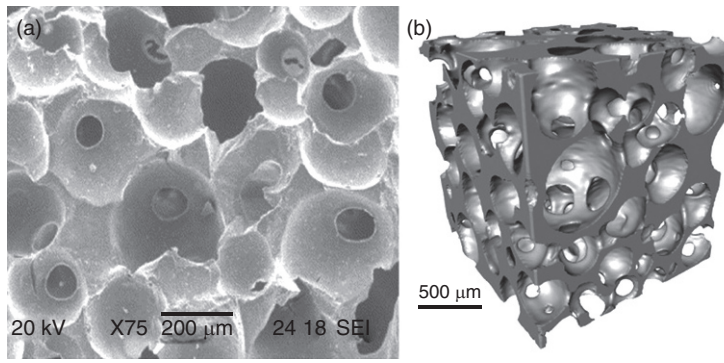

8.4 Typical architecture of sol-gel glass foam: (a) scanning electron microscope (SEM) micrograph (adapted from Jones and Hench (2006) © Elsevier) and (b) 3-D reconstruction of the whole cubic scaffold by X-ray micro-CT (*Source*: adapted from Jones (2009) © Elsevier).

as well as from the strength exhibited by other bone substitutes, such as clinically used HA (~6 MPa) (Hench, 1991).

Recently, Rainer *et al.* (2008) fabricated bioactive GC scaffolds by *in situ* foaming of sol-gel 70S26C glass powders. This technique involved the dispersion of sol-gel glass powders in an appropriate liquid monomer batch; after complete polymerization, glass-loaded polyurethane foams were obtained, and a final thermal treatment allowed the burning-out of the polymer and the sintering of the glass particles. The glass-loaded foams underwent severe shrinkage (> 75%) during sintering and, accordingly, exhibited a lower porosity content (48 vol.%) than that of spongy bone. This method of scaffolding appears to be suitable for producing patient-tailored grafts, but no indications of scaffold strength were presented by the authors.

The 3-D porous structure of sol-gel foamed scaffolds has been recently investigated in detail by micro-CT (Fig. 8.4b) and was found to be very similar to the trabecular 3-D architecture of cancellous bone (Jones *et al.*, 2007a, 2007b, 2009a; Jones, 2009b). However, the brittleness of sol-gel glass scaffolds remains an important issue that severely limits their potential range of application to bone defects in non-load-bearing regions of the skeleton.

Mesoporous glass scaffolds

The nanoporous texture of sol-gel glass scaffolds is not arranged according to a well-defined symmetry, but is randomly created in the course of the sol-gel process. In the last few years, significant effort has been dedicated to developing hierarchically porous scaffolds based on mesoporous bioactive glasses (MBG), characterized by an ordered arrangement of mesoporous channels

(pore diameter below 10 nm) according to a precise symmetry that can be properly tailored at the material synthesis stage. Almost all types of these hierarchical macro-/meso-porous scaffolds are based on SiO_2-CaO-P_2O_5 ternary MBGs and have been prepared by the simultaneous use of an appropriate block non-ionic copolymer (surfactant) as mesostructure template and a polymeric sponge as macropores former, as in the well-known sponge replication method (Li *et al.*, 2007; Yun *et al.*, 2007; Zhu *et al.*, 2008; Zhu and Kaskel, 2009). MBG scaffolds exhibited superior bioactivity as compared to bioactive non-mesoporous glass scaffolds of analogous composition, due to their higher pore volume and surface area available for ion-exchange in the biological fluids. The reported *in vitro* biological tests suggested that cell viability was not compromised by the presence of a porous nanotexture in the MBGs, but further studies are needed to better assess this crucial issue. Baino *et al.* (2012) observed that an increasing MBG amount seemed even to emphasize the viability of SAOS-2 cells: actually, this is not surprising as it was demonstrated that bioactive glasses can influence the cycle, metabolism and activity of cells (Hench 2009). It should be noted that MBGs are highly reactive because of their high specific surface area and, specifically, Si and Ca ions released from the glass can exert gene-control regulation emphasizing the activity of bone cells (Xynos *et al.*, 2000, 2001).

In general, MBG scaffolds have been developed as highly innovative, multifunctional systems for both bone grafting, thanks to their high bioactivity, and controlled release of drug molecules previously incorporated into the mesopores (see also Section 8.6.1). However, as for sol-gel glass scaffolds, MBG scaffolds also suffer from dramatic brittleness due to the intrinsic presence of a diffuse mesoporosity, which makes it very difficult to perform reproducible mechanical tests – this is probably the reason for the very few indications about the mechanical strength of these scaffolds reported in the literature. Wu *et al.* (2010) first tested as-such MBG scaffolds in compression reporting a strength value of 60 kPa, and one year later the same research group (Wu *et al.*, 2011a) synthesized Fe-doped MBG scaffolds assessing a compressive strength around 50 kPa.

From these few data, it appears clearly that the mechanical resistance of MBG-based foam-like scaffolds is almost two orders of magnitude lower than that of cancellous bone: this is a crucial drawback, dramatically affecting any actual clinical application, primarily due to obvious problems related to sample manipulation and safe implantation in the patient's bone. In order to overcome this drawback, again Wu *et al.* (2011b) proposed an alternative method for fabricating MBG scaffolds: 3-D printing allowed obtaining MBG scaffolds with a highly controllable inner architecture and exhibiting a mechanical strength about 200 times higher than that of traditional PU-foam templated MBG scaffolds. In such a context, it is worth mentioning also the study by Garcia *et al.* (2011) who reported the synthesis of 3-D hierarchical

macro-/meso-porous scaffolds in the $97.5SiO_2$.$2.5P_2O_5$ (mol.%) binary system by combining a single step sol-gel route, in the presence of a surfactant (meso-structure directing agent) and methylcellulose (macrostructure template) and a rapid prototyping technique (direct ink deposition); the mechanical properties of the samples, however, were not reported. These microfabrication techniques, although unable to lead to foam-like architectures, can be valuable resources to improve the mechanical strength of MBG scaffolds.

An interesting type of glass-based hierarchically porous system was also fabricated by incorporating mesoporous silica (SBA-15 and MCM-41) inside macroporous GC scaffolds produced through the polyethylene burning-out method (Cauda *et al.*, 2008; Mortera *et al.*, 2008, 2009, 2010; Vitale-Brovarone *et al.*, 2009c). These composite constructs showed an excellent mechanical resistance (compressive strength up to 20 MPa) thanks to the method adopted for fabricating the GC macroporous scaffold used as mesophase carrier, but their architecture could not be really considered as foam-like; these systems will be described in more detail in Section 8.6.1.

8.4 *In vitro* and *in vivo* behaviour

In vitro tests in acellular SBF mimicking the ionic composition of human plasma are commonly recognized as a standard procedure used for estimating the bioactive potential of biomaterials. On the basis of much experimental work carried out in the last three decades (Andersson *et al.*, 1990; Hench, 2006; Kokubo and Takadama, 2006; Hench, 2006), at present the majority of researchers agree that the formation of *in vitro* of an HA-like layer on the surface of biomedical glasses is a necessary pre-condition to reasonably predict the of *in vivo* bioactive behaviour (bone-bonding ability) of the implant. In recent years, however, the suitability of SBF has been called into question (Bohner and Lemaitre, 2009) and a recent work by Towler *et al.* (2009) indicates that forecasting a material ability to bond to bone based on SBF experiments may provide a false negative result. An interesting attempt to modify the Kokubo's standard SBF composition (Kokubo and Takadama, 2006) to enhance its similarity to biological fluids was reported by Dorozhkin and Dorozhkina (2007), who proposed a milk-based SBF incorporating albumin and other proteins. Therefore, the concept of bioactivity and the way adopted for its estimation maybe need to be re-discussed by the scientific community in the light of the recent advances.

In vitro tests with cells are aimed at investigating the biological compatibility of biomaterials and are essential to assess their clinical suitability. In the case of scaffolds, such tests are fundamental in assessing whether cells can colonize the inner structure of the implant and deposit new bone tissue within scaffold pores; furthermore, cellular tests can avoid unnecessary animal experiments.

In many research works carried out over the last 10 years it has been extensively demonstrated that the ions released by bioactive glasses, *e.g.* calcium and silicon (Xynos *et al.*, 2000, 2001; Hench, 2009), can exert gene-control regulation, influencing for instance osteoblast proliferation, differentiation and thus bone mineralization. The design of biomedical glasses at the genetic level is a fascinating and attractive field of research able to open new perspectives towards finely guided tissue regeneration; this challenge will be discussed in more detail in Section 8.6.2.

Another crucial issue is the influence of the topography of scaffold surface put in contact with cells, since cell–substrate interactions can be regarded as one of the major factors ultimately determining the long-term performance of a biomaterial/device *in situ*. The processes that mediate an altered cell response to micro- and nano-scale surface structure are still somewhat unclear, but it is known that they may be direct, as a result of the direct effect of surface topography on cells, or indirect, where surface features affect the composition, orientation or conformation of extracellular matrix (ECM) components (Biggs *et al.*, 2009; Mendonca *et al.*, 2009; Anselme *et al.*, 2010; Lamers *et al.*, 2010). In general, cells establish dynamic contacts with the underlying biomaterial termed points of focal adhesion, the regulation of which is highly complex and involves initial integrin binding to ECM components and the reinforcement of the adhesion plaque by further protein recruitment. Furthermore, integrins mediate bidirectional signalling between ECM and osteoblasts, thereby activating signalling pathways that regulate transcription factors activity, direct cells growth and promote cells differentiation.

As regards *in vivo* testing of biomedical glass foams, relatively few studies are available in the literature. Yuan *et al.* (2001) implanted GC-Bioglass® scaffolds in dogs without any preliminary *in vitro* test in order to investigate directly *in vivo* the osteoinductive properties of the implants. Since then, the ethical attention towards animals rapidly has grown and nowadays *in vivo* tests are recommended only after careful *in vitro* testing.

Rahaman and co-workers recently implanted 13-93, 13-93B1 and 13-93B3 glass scaffolds in subcutaneous pockets in rats, after performing *in vitro* cellular tests on the same porous biomaterials (Fu *et al.*, 2010b, 2010c). 13-93 and 13-93B1 glass scaffolds were found to support attachment and proliferation of bone marrow stromal and murine cells, whereas 13-93B3 was demonstrated to be toxic *in vitro*. However, all three groups of scaffolds showed the ability to support soft tissue infiltration *in vivo*; in the authors' opinion, the more favourable *in vivo* response of 13-93B3 scaffolds (that was toxic *in vitro*) was due to the more dynamic subcutaneous microenvironment with respect to the static *in vitro* conditions. These observations suggest that *in vivo* tests are unavoidable in reaching definite conclusions about the biocompatibility and bioactivity of potentially implantable materials.

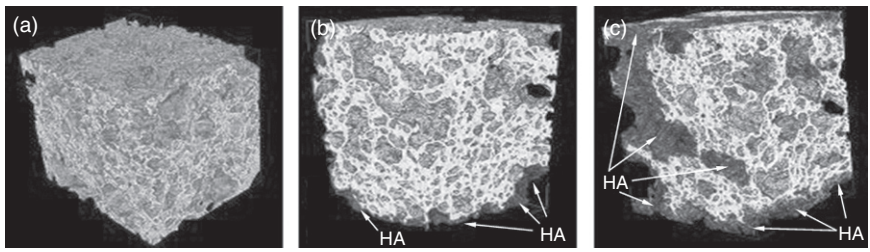

8.5 Micro-CT evaluation of HA formation on the struts of GC-CEL2 foams after *in vitro* tests in acellular SBF: (a) GC-CEL2 scaffold before soaking in SBF; (b) GC-CEL2 scaffold after soaking for 14 days in SBF (the growth of HA, visible as dark areas on scaffold struts, starts from the periphery) and (c) GC-CEL2 scaffold after soaking for 28 days in SBF (large zones coated by HA can be distinguished).

In this context, it is worth mentioning the investigation performed by Boccaccini and co-workers (Gorustovich *et al.*, 2008; Vargas *et al.*, 2009), who proposed an effective bioassay involving the assessment of biocompatibility and bone mineralization potential of GC-Bioglass® foam-like scaffolds using *ex ovo* (shell-less) chick embryos; this low-cost, original approach can be very useful in limiting animal experiments.

The knowledge of all the biological effects that can be potentially induced in the human body by biomaterials in generals and by scaffolds in particular is a complex issue; for instance, although there are standard guidelines to assess bone-bonding ability and osteoinductivity *in vivo* of glass implant, there is not yet a recognized protocol to investigate the systemic toxicity of implanted biomaterials. A recent, detailed study by Yun *et al.* (2011) could be considered as a starting point in this regard, which the scientific community is expected to debate in the near future.

As far as scaffold characterization is concerned after *in vitro* and *in vivo* testing, a powerful tool is represented by micro-CT, that allows non-destructive and non-invasive 3-D analysis of the constructs (Fig. 8.5). Renghini *et al.* (2009) used micro-CT for quantitative assessment of glass foams bioactivity *in vitro* by monitoring the kinetics of HA formation on scaffold struts (Fig. 8.5). The potential of micro-CT in characterizing tissue-engineered bone-scaffold constructs was recently highlighted by Belicchi *et al.* (2009), who showed how this technique can provide important information about mineral phase, organic compounds, newly formed tissue and stem cell homing, after appropriate cell labelling with metal nanoparticles.

8.5 Current clinical applications

In comparison to other bioceramic materials, such as HA and calcium orthophosphates that have been studied and tested since a longer period

of time (Dorozhkin, 2010), a quite limited number of biomedical glasses are available on the market, also due to the extensive procedures to gain definite clinical approval. 45S5 Bioglass® has been marketed worldwide since 1985, about 15 years before the first reported attempt at producing Bioglass®-derived scaffolds by Yuan *et al.* (2001). In the last 40 years, many glass formulations have been proposed for biomedical use; a selection of compositions, commercial forms and producers of bioactive glasses clinically approved and implanted in Europe and USA are collected in Table 8.4. The

Table 8.4 Overview of commercial BGs approved for clinical use

Commercial name	Composition	Form and use	Producer
Bioglass®	45SiO_2–24.5CaO–24.5Na_2O–6P_2O_5 (wt.%). It is the 45S5 Hench's glass.	NovaBone® Putty and NovaBone® Dental Putty: mouldable glass-based paste that can be also injected in the bone/dental defect site by a syringe NovaBone® Particulate (90–710 μm) for small graft areas NovaBone® Morsels: porous granulates PerioGlas®: fine particulate to be used in dental surgery and restoration NovaBone® porous blocks	Novabone (US); Mo-Sci Corp. (US)
TheraGlass®	70SiO_2–30CaO (mol.%)	Sol-gel powders	MedCell (UK)
S53P4 (BoneAlive®)	53SiO_2–20CaO–23Na_2O–4P_2O_5 (wt.%)	Powders, pieces of adjustable size and dimensions that can be custom-made processed	Abmin Technologies Ltd/Vivoxid (FI); Mo-Sci Corp. (US)
13-93	53SiO_2–6Na_2O–12K_2O–5MgO–20CaO–4P_2O_5 (wt.%)	Cast shapes, quenched frit, rods, fibres, discs, spheres and micro-sized powders	Mo-Sci Corp. (US)
S55F5	52SiO_2–11.7CaO–19.6Na_2O–5.8P_2O_5–10.9CaF_2 (wt.%)	Cast shapes, quenched frit, rods, fibres, discs, spheres and micro-sized powders	Mo-Sci Corp. (US)
StronBone®	SrO-containing silicate glass	Powders and porous granules	RepRegen (UK)

development of commercial products based on Bioglass® and other glass formulations has also been recently chronicled by Hench (2006, 2010).

All the reported biomedical commercial glasses exhibit an SiO_2-based composition containing modifier oxides in specific amounts with the aim to enhance the bioactive properties or to impart special characteristic (for instance, SrO is introduced in StronBone® to reduce bone resorption) to the material. In general, commercial biomedical glasses are used as bone fillers in orthopaedics, dentistry and maxillofacial/craniofacial surgery. To the best of the authors' knowledge, only 45S5 Bioglass® is commercially available in form of porous blocks (scaffolds).

8.6 Future trends

This section depicts eight 'hot' topics of research related to biomedical glass foams that, in the authors' opinion, will have a significant impact from technological, clinical and patient's life quality viewpoints in the next future. It is appropriate to introduce this final part of the chapter with an impressive statement by Prof. Larry L. Hench, the inventor of Bioglass®: 'Creative studies of novel glasses and GCs are needed more than ever to cope with the problems of a world that has finite resources but infinite desires' (Hench, 2011).

8.6.1 Drug release

Improvement of the biological activity and performance of bone-substitute biomaterials and scaffolds through the uptake and release of therapeutic agents is one of the most challenging fields of bone tissue engineering. Mourino and Boccaccini (2010) recently published a comprehensive overview on controlled drug delivery from 3-D scaffolds. In most cases, fully polymeric or ceramic (glass)/polymer composite scaffolds were proposed for drug delivery purposes, as the therapeutic agent can be incorporated in the polymer and subsequently delivered during the degradation of the organic phase.

Drug uptake is more difficult in the case of foam-like ceramics (porous monomaterials), but in recent years two interesting approaches based on the use of mesoporous materials, exhibiting a more or less ordered texture of nanopores in the 2–50 nm range, have been successfully proposed in the biomedical literature. The first approach was originally developed, by a group of researchers working at the Politecnico di Torino, in a series of publications dealing with the fabrication and characterization of glass-based multi-scale porous structures, constituted by GC macroporous scaffolds used as carriers for mesoporous silica spheres (Cauda *et al.*, 2008;

Mortera *et al.*, 2008, 2009, 2010; Vitale-Brovarone *et al.*, 2009c). The goal of these hierarchically porous composite scaffolds was the combination of the properties of glass-derived macroporous architectures, i.e. mechanical support in the defect zone, bone-bonding ability and bone tissue regeneration, with the drug adsorption/release ability of mesoporous materials. Thanks to host–guest physico-chemical interactions between drug molecule and mesopore surface, ibuprofen can be incorporated into the nanopores of the mesophase in order to impart an added value to the macroporous bioactive scaffold. At present, MCM-41 and SBA-15 have been loaded on bioactive GC scaffolds produced by polyethylene burning-out method (Baino *et al.*, 2009) and, accordingly, their 3-D architecture cannot be actually considered as foam-like; open direction of research could concern the mesophase incorporation into proper foam-like scaffolds, characterized by a higher degree of structural bio-mimicry with trabecular bone.

Even though interesting and innovative, this approach exhibits two potential weaknesses: (i) problems related to interfacial bonding between GC scaffold and silica mesophase, and (ii) lack of bioactivity of pure silica mesophases – even if a certain degree of bioactivity has been reported by some authors (Izquierdo-Barba *et al.*, 2005). In order to solve these problems, the second approach involves the fabrication of monomaterial (non-composite) bioactive scaffolds with multi-scale porosity by using MBGs. For instance, drug release studies of using gentamicin demonstrated that the drug uptake ability of MBG scaffolds was over two-fold higher than that of non-mesoporous bioactive glass scaffold; in addition, as far as drug delivery is concerned, during the whole release period in SBF, gentamicin was delivered from the MBG scaffold at a much lower release rate compared to that from non-mesoporous scaffolds (Zhu and Kaskel, 2009). Studies of ibuprofen incorporation and release from MBG membranes were also recently performed (Baino *et al.*, 2012). The interested reader is pointed towards a couple of comprehensive pictures on biomedical mesoporous materials (including MBGs) and related challenges (incorporation and release of therapeutic agents) that were recently provided by Vallet-Regi and co-workers (Arcos and Vallet-Regi, 2010; Izquierdo-Barba and Vallet-Regi, 2011). However, the fabrication of MBG foams or constructs with adequate mechanical strength allowing safe manipulation and implantation still remains an open issue (Wu *et al.*, 2010, 2011a; Baino *et al.*, 2012) that should contextually deserve future experimental work.

8.6.2 Metal ion incorporation and release for targeted therapy

Biomaterials scientists often find that some crucial aspects involved in tissue engineering scaffold design are in conflict with each other. For instance,

some very convenient methods used for fabricating scaffolds are incompatible with the incorporation and stability of organic drugs (Mourino and Boccaccini, 2010). Therefore, it is fascinating to explore the use of specific – usually metallic – ions as therapeutic and/or regenerative agents. Hench and co-workers (Xynos *et al.*, 2000, 2001; Hench, 2009) demonstrated that ionic dissolution products released by bioactive glasses (mainly Si and Ca ions) can stimulate the genes of cells towards a path of regeneration and self-repair. Very recently, Gerhardt *et al.* (2011) demonstrated that the ions released by 45S5 Bioglass® have a stimulatory effect on angiogenesis, which is a significant added value for biomaterials to be used in bone tissue engineering.

Metal ions for incorporation in scaffold biomaterials usually belong to the group comprising essential enzymatic cofactors; an extensive picture of this topic was recently provided in a couple of very comprehensive reviews (Hoppe *et. al.*, 2011; Mourino *et al.*, 2012). The use of metallic ions allows overcoming the risk of decomposition or instability, which is intrinsic to organic molecules. Each metal ion can have a specific therapeutic significance and can alter cell functions and metabolism by binding to biological macromolecules such as enzymes or nucleic acids and/or activating ion channels and secondary signalling. Incorporation of metal ions exhibiting magnetic properties, such as iron, can be also useful for *in situ* cancer treatment trough hyperthermia, as discussed in the Section 8.6.6.

From a technological viewpoint, introduction of metal ions is usually economic and compatible with the typical processes used for fabricating both polymeric and ceramic scaffolds.

At present, the literature covering the incorporation of metal ions in glass or GC foams is still extremely scarce (polymeric foams or calcium phosphate scaffolds were mainly studied in this regard). For instance, Zn- and Ti-containing foam-like phosphate glass scaffolds were produced by using appropriate reagents as sources of ZnO and TiO_2 to be introduced in the glass formulations (Navarro *et al.*, 2004; Park *et al.*, 2006). Vitale-Brovarone *et al.* (2008) followed a different approach, proposing the ion-exchange technique for the surface Ag-doping of GC-FaGC scaffolds (Table 8.3) able to exert local antibacterial activity.

It is interesting to underline that perhaps the most promising group of glasses suitable to be used for targeted therapy via metal ion release comprises phosphate glasses. Their solubility is strongly dependent on their composition, therefore their degradation rate can be tailored by proper addition of metal oxides, such as TiO_2, CuO and Fe_2O_3, that, when released, are also able to induce specific biological responses (Abou Neel *et al.*, 2009). In general, the existing studies demonstrated that these metal ions are able to exert antibacterial properties.

This field of research is extremely challenging and opens new perspectives for tissue engineering, but the potential toxicity of released metallic

ions (for instance, local accumulation, unwanted interactions with other ions and phenomena of systemic toxicity) is a complex, crucial and still often partially unknown issue that must be carefully taken into account in the development of such smart biomaterials and scaffolds.

8.6.3 Surface functionalization

Protein adsorption on the surfaces of biomaterials and medical devices is an essential aspect of the cascade of chemico-biological reactions that take place at the interface between a synthetic material and the biological environment. A great challenge of modern biomedical sciences is to design biomaterials as vehicles to incorporate and, if necessary, locally release various molecules involved in protein signalling, including both growth factors and peptide sequences mimicking the whole protein. Incorporation of biomolecules in biodegradable polymeric matrices able to release them over time has been widely investigated, but there has been much less research work on designing strategies to load inorganic substrates, such as bioactive glasses (Verné *et al.*, 2009, 2010), with analogous biomolecules. Protein grafting on the surface of biomedical glasses, commonly referred to as surface functionalization, typically involves three major steps: (i) hydroxyl exposure (for instance by means of a cleaning treatment), (ii) introduction of a specific functional group (for instance by means of silanization with an appropriate sol-gel precursor) to promote and stabilize bonding between the material and the organic molecule, and (iii) biomolecule anchoring (for instance by soaking the samples in a protein-rich solution). As for the functionalization of foam-like glass scaffolds, a very limited number of reports have been documented in the literature. Protein-release kinetics studies for sol-gel 58S and 70S30C glass scaffolds were carried out by Lenza *et al.* (2003), but organic solvents were used for silanization, which are not ideal from the viewpoint of biocompatibility. Chen *et al.* (2006b) functionalized highly porous 45S5 Bioglass®-derived GC scaffolds by silanization followed by glutaraldehyde grafting without using toxic organic solvent, and found that aqueous heat treatment involved in the functionalization process accelerated the structural transition of the crystalline phase of the sintered Bioglass® to an amorphous one during soaking in SBF, thereby promoting hydroxyapatite formation *in vitro* (bioactivity).

Loading of ceramic scaffolds without using coupling agents has been also experimented for ceramic scaffolds (Rosengren *et al.*, 2003), but conformational changes of the native biomolecule structure, due to remarkable electrostatic and hydrophobic interactions, should be taken into account.

8.6.4 Polymeric coatings

Polymer-coated glass scaffolds belong to the group of composite biomaterials, which are discussed in Chapter 9 of the present volume. However, the two major added values carried by the use of polymeric coatings on porous glass substrates are briefly mentioned here, as promising fields for future research.

From a mechanical viewpoint, polymeric coatings have been recently proposed to reduce the intrinsic brittleness and to increase the toughness of 45S5 Bioglass®-derived GC foams. Chen and Boccaccini (2006) performed a comparative investigation on the mechanical properties and *in vitro* bioactivity of Bioglass®-based foams before and after applying a poly(D,L-lactic acid) (PDLLA) coating on the scaffold struts. In comparison to bare Bioglass®-derived foams, the bioactivity upon soaking in SBF was maintained, although the kinetics of HA formation were delayed by the presence of the polymeric coating, the compressive (0.9 MPa vs. 0.3 MPa) and 3-point bending strengths were slightly improved, and the work of fracture was considerably enhanced, thereby increasing the scaffold toughness.

One year later, Bretcanu *et al.* (2007) fabricated porous composites by coating foam-like GC-Bioglass® scaffolds with poly(3-hydroxybutyrate): the polymer strengthened the inorganic porous matrix acting as a glue and holding the GC particles together when the scaffold struts began to fail. The results were encouraging: the values of compressive strength obtained (up to 1.5 MPa) were still far from the typical range of cancellous bone, but superior to those of uncoated scaffolds (up to 0.4 MPa) (Chen *et al.*, 2006a). In the near future, it will be necessary to act on (i) the sintering conditions of the glass foam (Baino *et al.*, 2013), (ii) the type of polymer used for the coating, and (iii) the technique to coat the original glass foam, in order to really obtain scaffold suitable for clinical use.

An approach similar to that followed by Chen and Boccaccini (2006) and Bretcanu *et al.* (2007) was also followed by Wu *et al.* (2010) to improve the mechanical strength of MBG scaffolds that were soaked in silk solution; the authors found that silk-induced modification improved the uniformity and continuity of scaffold pore network, maintained high porosity (~94 vol.%) as well as large pore size (200–400 μm), and increased the mechanical strength up to 250 kPa (with respect to 60 kPa of the uncoated ones).

The use of polymeric coatings on biomedical glass (ceramic) foams can also provide additional extra-functionalities to the biomaterial: from pharmaceutical and therapeutic viewpoints, biodegradable polymeric coatings can be used as matrices for incorporating biomolecules, drugs or specific moieties for local treatment of various diseases; a valuable picture on this topic was provided in a recent review by Mourino and Boccaccini (2010).

8.6.5 Carbon nanotube coatings

Carbon nanotubes (CNT), first developed and characterized in the early 1990s (Iijima, 1991), exhibit attractive properties, such as high mechanical strength, flexibility, high aspect ratio, excellent thermal and electrical conductivity. The effect of interaction between cells and CNTs is a crucial issue from the biocompatibility viewpoint: recent studies have been particularly focused on this topic (Zanello *et al.*, 2006), but definite conclusions have not yet been reached. It is generally recognized that scaffold enrichment by the integration of CNTs can potentially carry a significant added value for tissue engineering applications from various perspectives. First, CNTs can provide enhanced structural reinforcement, either embedded in a ceramic or polymeric matrix or deposited on the surface of scaffold struts. From a manufacturing viewpoint, Boccaccini *et al.* (2007) demonstrated that electrophoretic deposition (EPD) is a versatile and effective technique to coat Bioglass®-derived foams with a CNT layer. As a general rule, CNTs should be incorporated in very small concentration as they are non-degradable and possible cytotoxic effects could occur, as mentioned above. Another key reason for incorporating CNTs into scaffolds is the ability to tailor the scaffold surface at the nanoscale, by modulating the biomaterial nano-roughness and nano-topography to enhance cells adhesion and proliferation. Furthermore, the enrichment with CNTs is expected to provide functional added values to the construct, such as cell tracking, radio-tracking functions for living tissues discrimination, sensing functions of microenvironments by exploiting CNTs electrical conductivity and biomolecule release. It was also demonstrated in the literature that external electrical stimulation can influence cell life cycles, maximizing tissue regeneration in comparison with non-stimulated biomaterials; in a pilot study, Meng *et al.* (2011) coated Bioglass®-derived foams with CNT by electrophoretic deposition and cultured mesenchymal stem cells on the constructs with and without electrical stimulation, demonstrating that the electrical conductivity associated to the CNTs can promote the proliferation and differentiation of the cells attached onto the scaffold.

8.6.6 Magnetic properties and hyperthermia for cancer therapy

Bone tumours are one of the main non-traumatic causes leading to the need for bone surgical resection. The treatment of such bone diseases typically comprises two surgical stages: (i) removal of the diseased bone portion, which results in a bone defect, and (ii) implantation of a graft biomaterial at the defect site. Therefore, the clinical challenge is two-fold: it is necessary not only to successfully repair the – often quite large – bone defect,

but also to avoid the re-development of the tumour. Hyperthermia therapy using biocompatible magnetic materials has emerged as a promising option for the treatment of malignant bone tumours; an excellent overview of this topic was recently provided by Vallet-Regi and Ruiz-Hernandez (2011). These smart biomaterials are designed to be magnetic, and when exposed to an external magnetic field, they can produce heat within the diseased tissue region. It is known that cancer cells are killed if exposed at temperatures above 43°C, whereas normal cells can survive in such conditions: since the vascular system is poorly developed in the diseased tissue, the heat cannot be dissipated and results in a higher temperature than in the surrounding health tissues; therefore, hyperthermia therapy is virtually considered as an effective option for *in situ* treatment without adverse side effects.

A number of biomaterials, including calcium phosphates (Hou *et al.*, 2009), glasses/GCs (Bretcanu *et al.*, 2005; Bretcanu *et al.*, 2006; Li *et al.*, 2010), mesoporous silica (Martin-Saavedra *et al.*, 2010) and composites (Bock *et al.*, 2010) have been considered and properly processed for possible application in hyperthermia. These materials, however, are usually prepared in form of bulk, thermoseeds, particles or powder; studies of magnetic scaffolds are extremely scarce (Bock *et al.*, 2010; Wu *et al.*, 2011a), and only one report on magnetic glass foams has been documented in the literature (Wu *et al.*, 2011a). In this study, the authors proposed an innovative approach to bone tumour treatment by combining hyperthermia therapy and local drug delivery in a multifunctional Fe-containing MBG scaffold prepared through co-templating method: large macropores were useful to allow cells colonization and subsequent tissue regeneration, mesopores allowed sustained drug release and the magnetic properties of the Fe-containing glass were exploited for *in situ* treatment by hyperthermia. Although this approach is highly fascinating, one of the major limitations of these Fe-MBG scaffolds is their dramatic brittleness (compressive strength results around 50 kPa), that compromise any real clinical application; improvement of the scaffold strength by using polymeric coating could be a valuable option to be considered in future investigations.

8.6.7 Pore-graded foams for high-strength applications

As recently reviewed by Miao and Sun (2010), calcium phosphate bioceramics, as well as their composites with biocompatible polymers, have been widely adopted for fabricating pore-graded scaffolds mimicking the hierarchical porous organization of bone. Among bioactive glasses, however, to the best of the authors' knowledge only Bioglass® and CEL2 have been proposed for this purpose. Bretcanu *et al.* (2008) used pre-formed polyurethane sponges with tailored gradient of porosity as sacrificial templates for

manufacturing highly porous (> 80 vol.%) foam-like GC-Bioglass® scaffolds through the replication technique. The pore-graded architecture could contribute to improve the mechanical strength of GC-Bioglass® foams, but no data in this regard have been reported in the literature up to now.

Vitale-Brovarone *et al.* (2010) used CEL2 particles to fabricate graded GC scaffolds by means of different processing methods, i.e. sponge replication, polyethylene (PE) burning-out and enamelling together with various combinations of such techniques. GC-CEL2 scaffolds able to mimic the porosity gradient of cancellous bone or to reproduce the trabecular/cortical bone system were successfully obtained, with significant increase of compressive strength. This approach can be useful to fulfil specific criteria depending on the end use, such as high-strength properties required for the substitution of load-bearing bone portions.

Very recently, Bellucci *et al.* (2010, 2012) fabricated GC-Bioglass® scaffolds by using a modified sponge replication method involving the incorporation of polyethylene particles in the slurry used for sponge impregnation and the slurry removal under rotation in air flux. These scaffolds had a highly porous internal structure together with an external resistant surface similar to a shell; the compressive strength was found to be below 1 MPa, which demonstrates that, although being interesting, this method still needs careful optimization.

8.6.8 Trabecular coatings on prosthetic devices

As previously underlined, glass-based bone tissue engineering scaffolds are purposely designed to act as foam-like templates allowing and promoting the growth of new bone tissue in order to repair osseous defects. An innovative application of GC scaffolds, intended to act not only as bone defect fillers, was disclosed in a recent patent by Verné *et al.* (2008), who merged the concepts of bioactive glass coating and foam scaffold to propose the use of trabecular coatings on ceramic prosthetic devices. Referring specifically to the context of hip joint prosthesis, the authors proposed a monoblock acetabular cup that could be anchored to the patient's bone without using either cement or metal-back, but by means of a bioactive trabecular GC coating (foam scaffold), mimicking the architecture of cancellous bone and able to promote implant osteointegration. The use of bioactive high-strength glass-derived foam scaffolds as key components of implantable devices to promote their osteointegration is highly innovative and could lead to the birth of a new generation of prostheses with relevant impacts from clinical, commercial and patient's life quality viewpoints.

The same group of research tested and successfully demonstrated the feasibility of such an innovative device in a simplified, flat geometry: GC

scaffolds, prepared by polymeric sponge replication, were joined to alumina square substrates by a dense glass coating (interlayer), and the devices thereby obtained were demonstrated to have good bioactive properties and adequate mechanical resistance to be safely handled and potentially implanted (Vitale-Brovarone *et al.*, 2012b). Indeed, the majority of medical implants are characterized by complex, often curved shapes, such as the semi-spherical one that is typical of the acetabular component of hip joint prostheses; extension of the promising results achieved in this pilot work to curved geometry, which involves optimization of glass composition, scaffold shaping and coating techniques, is currently in progress in the framework of an European Project (MATCh – Monoblock Acetabular cup with Trabecular-like Coating').

8.7 References

Abou Neel, E. A., Pickup, D. M., Valappil, S. P., Newport, R. J. and Knowles, J. C. (2009) 'Bioactive functional materials: a perspective on phosphate-based glasses', *J Mater Chem*, **19**, 690–701.

Andersson, O. H., Liu, G., Karlsson, K. H. and Juhanoja, J. (1990) '*In vivo* behaviour of glasses in the SiO_2-Na_2O-CaO-P_2O_5-Al_2O_3-B_2O_3 system', *J Mater Sci: Mater Med*, **1**, 219–227.

Anselme, K., Davidson, P., Popa, A. M., Giazzon, M., Liley, M. and Ploux, L. (2010) 'The interactions of cells and bacteria with surfaces structured at the nanometre scale', *Acta Biomater*, **6**, 3824–2846.

Arcos, D. and Vallet-Regi, M. (2010) 'Sol-gel silica-based biomaterials and bone tissue regeneration', *Acta Biomater*, **6**, 2874–2888.

Avnir, D., Coradin, T., Lev, O. and Livage, J. (2006) 'Recent bio-applications of sol-gel materials', *J Mater Chem*, **16**, 1013–1030.

Baino, F., Verné, E. and Vitale-Brovarone, C. (2009) '3-D high strength glass-ceramic scaffolds containing fluoroapatite for load-bearing bone portions replacement', *Mater Sci Eng C*, **29**, 2055–2062.

Baino, F. and Vitale-Brovarone, C. (2011) 'Three-dimensional glass-derived scaffolds for bone tissue engineering: current trends and forecasts for the future', *J Biomed Mater Res A*, **97**, 514–535.

Baino, F., Fiorilli, S., Mortera, R., Onida, B., Saino, E., Visai, L., Verné, E. and Vitale-Brovarone, C. (2012) 'Mesoporous bioactive glass as a multifunctional system for bone regeneration and controlled drug release', *J Appl Biomater Funct Mater*, **10**, 12–21.

Baino, F., Ferraris, M., Bretcanu, O., Verné, E. and Vitale-Brovarone, C. (2013) 'Optimization of composition, structure and mechanical strength of bioactive 3-D glass-ceramic scaffolds for bone substitution', *J Appl Biomater*, **27**, 872–890.

Belicchi, M., Cancedda, R., Cedola, A., Fiori, F., Gavina, M., Giuliani, A., Komlev, V. S., Lagomarsino, S., Mastrogiacomo, M., Renghini, C., Rustichelli, F., Sykova, E. and Torrente, Y. (2009) 'Some applications of nanotechnologies in stem cells research', *Mater Sci Eng B*, **165**, 139–147.

Bellucci, D., Cannillo, V. and Sola, A. (2010) 'Shell scaffolds: a new approach towards high strength bioceramic scaffolds for bone regeneration', *Mater Lett*, **64**, 203–206.

Bellucci, D., Chiellini, F., Ciardelli, G., Gazzarri, M., Gentile, P., Sola, A. and Cannillo, V. (2012) 'Processing and characterization of innovative scaffold for bone tissue engineering', *J Mater Sci: Mater Med*, **23**, 1397–1409.

Biggs, M. J. P., Richards, R. G., Gadegaard, N., Wilkinson, C. D. W., Oreffo, R. O. C. and Dalby, M. J. (2009) 'The use of nanoscale topography to modulate the dynamics of adhesion formation in primary osteoblast and ERK/MAPK signalling in STRO-1+ enriched skeletal stem cells', *Biomaterials*, **30**, 5094–5113.

Boccaccini, A. R., Chicatun, F., Cho, J., Bretcanu, O., Roether, J. A., Novak, S. and Chen, Q. Z. (2007) 'Carbon nanotube coatings on bioglass-based tissue engineering scaffolds', *Adv Funct Mater*, **17**, 2815–2822.

Bock, N., Riminucci, A., Dionigi, C., Russo, A., Tampieri, A., Landi E., Goranov, V. A., Marcacci, M. and Dediu, V. (2010) 'A novel route in bone tissue engineering: magnetic biomimetic scaffolds', *Acta Biomater*, **6**, 786–796.

Bohner, M. and Lemaitre, J. (2009) 'Can bioactivity be tested *in vitro* with SBF solution?', *Biomaterials*, **20**, 2175–2179.

Boskey, A. L. (2007) 'Mineralization of bone and teeth', *Elements*, **3**, 385–391.

Bretcanu, O., Spriano S., Verné, E., Coisson, M., Tiberto P. and Allia, P. (2005) 'The influence of crystallised Fe_3O_4 on the magnetic properties of coprecipitation-derived ferrimagnetic glass-ceramics', *Acta Biomater*, **1**, 421–429.

Bretcanu, O., Spriano S., Verné, E., Coisson, M., Tiberto P. and Allia, P. (2006) 'Magnetic properties of the ferrimagnetic glass-ceramics for hyperthermia', *J Magn Magn Mater*, **305**, 529–533.

Bretcanu, O., Chen, Q., Misra, S. K., Boccaccini, A. R., Verné, E. and Vitale-Brovarone, C. (2007) 'Biodegradable polymer coated 45S5 Bioglass-derived glass-ceramic scaffolds for bone tissue engineering', *Glass Tech Eur.: Glass Sci Tech A*, **48**, 227–234.

Bretcanu, O., Samaille, C. and Boccaccini, A. R. (2008) 'Simple methods to fabricate Bioglass®-derived glass-ceramic scaffolds exhibiting porosity gradient', *J Mater Sci*, **43**, 4127–4134.

Brink, M., Turunen, T., Happonen, R. P. and Yli-Urpo, A. (1997) 'Compositional dependence of bioactivity of glasses in the system Na_2O-K_2O-MgO-CaO-B_2O_3-P_2O_5-SiO_2,' *J Biomed Mater Res*, **37**, 114–121.

Cai, S., Xu, G. H., Yu, X. Z., Zhang, W. J., Xiao, Z. Y. and Yao, K. D. (2009) 'Fabrication and biological characteristics of β-tricalcium phosphate porous ceramic scaffolds reinforced with calcium phosphate glass', *J Mater Sci: Mater Med*, **20**, 351–358.

Cauda, V., Fiorilli, S., Onida, B., Verné, E., Vitale-Brovarone, C., Viterbo, D., Croce, G., Milanesio, M. and Garrone, E. (2008) 'SBA-15 ordered mesoporous silica inside a bioactive glass-ceramic scaffold for local drug delivery', *J Mater Sci: Mater Med*, **19**, 3303–3310.

Chen, Q. Z., Thompson, I. D. and Boccaccini, A. R. (2006a) '45S5 Bioglass®-derived glass-ceramic scaffolds for bone tissue engineering', *Biomaterials*, **27**, 2414–2425.

Chen, Q. Z., Rezwan, K., Armitage, D., Nazhat, S. N. and Boccaccini, A. R. (2006b) 'The surface functionalization of 45S6 Bioglass®-based glass-ceramic scaffolds and its impact on bioactivity', *J Mater Sci: Mater Med*, **17**, 979–987.

Chen, Q. Z. and Boccaccini, A. R. (2006) 'Poly(D,L-lactic acid) coated 45S5 Bioglass®-based scaffolds: processing and characterization', *J Biomed Mater Res A*, **77**, 445–457.

Cranford, S. W., Tarakanova, A., Pugno, N. M. and Buehler, M. J. (2012) 'Nonlinear material behaviour of spider silk yields robust webs', *Nature*, **482**, 72–76.

Dorozhkin, S. V. and Dorozhkina, W. I. (2007) 'Crystallization from a milk-based revised simulated body fluid', *Biomed Mater*, **2**, 87–92.

Dorozhkin, S. V. (2007) 'Calcium orthophosphates', *J Mater Sci*, **42**, 1061–1095.

Dorozhkin, S. V. (2009) 'Calcium orthophosphates in nature, biology and medicine', *Materials*, **2**, 399–498.

Dorozhkin, S.V. (2010) 'Bioceramics of calcium orthophosphates', *Biomaterials*, **31**, 1465–1485.

Ducheyne, P. and Qiu, Q. (1999) 'Bioactive ceramics: the effect of surface reactivity on bone formation and bone cell function', *Biomaterials*, **20**, 2287–2303.

Fu, Q., Rahaman, M. N., Bal, B. S., Brown, R. F. and Day, D. E. (2008) 'Mechanical and *in vitro* performance of 13-93 bioactive glass scaffolds prepared by a polymer foam replication technique', *Acta Biomater*, **4**, 1854–1864.

Fu, H., Fu, Q., Zhou, N., Huang, W., Rahaman, M. N., Wang, D. and Liu, X. (2009) '*In vitro* evaluation of borate-based bioactive glass scaffolds prepared by a polymer foam replication method', *Mater Sci Eng C*, **29**, 2275–2281.

Fu, Q., Rahaman, M. N., Fu, H. and Liu, X. (2010a) 'Silicate, borosilicate, and borate bioactive glass scaffolds with controllable degradation rate for bone tissue engineering applications. I. Preparation and *in vitro* degradation', *J Biomed Mater Res A*, **95**, 164–171.

Fu, Q., Rahaman, M. N., Sonny Bal, S., Bonewald, L. F., Kuroki, K. and Brown, R. F. (2010b) 'Silicate, borosilicate, and borate bioactive glass scaffolds with controllable degradation rate for bone tissue engineering applications. II. *In vitro* and *in vivo* biological applications', *J Biomed Mater Res A*, **95**, 172–179.

Fu, Q., Rahaman, M. N., Sonny Bal, S., Kuroki, K. and Brown, R. F. (2010c) '*In vivo* evaluation of 13-93 bioactive glass scaffolds with trabecular and oriented microstructures in a subcutaneous rat implantation model', *J Biomed Mater Res A*, **95**, 235–244.

Fu, Q., Saiz, E., Rahaman, M. N. and Tomsia, A. P. (2011) 'Bioactive glass scaffolds for bone tissue engineering: state of the art and future perspectives', *Mater Sci Eng C*, **31**, 1245–1256.

Gao, H., Ji, B., Jager, I. L., Arzt, E. and Fratzl, P. (2003) 'Materials become insensitive to flaws at nanoscale: lessons from nature', *Proc Natl Acad Sci USA*, **100**, 5597–5600.

Garcia, A., Izquierdo-Barba, I., Colilla, M., Lopez de Laorden, C. and Vallet-Regi, M. (2011) 'Preparation of 3-D scaffolds in the SiO_2-P_2O_5 with tailored hierarchical meso-macroporosity', *Acta Biomater*, **7**, 1265–1273.

Gerhardt, L. C. and Boccaccini, A. R. (2010) 'Bioactive glass and glass-ceramic scaffolds for bone tissue engineering', *Materials*, **3**, 3867–3910.

Gerhardt L. C., Widdows, K. L., Erol, M. M., Burch, C. V., Sanz-Herrera, J, A, Ochoa, I., Stampfli, R., Roqan, I. S., Gabe, S., Ansari, T. and Boccaccini, A. R. (2011) 'The pro-angiogenic properties of multi-functional bioactive glass composite scaffolds', *Biomaterials*, **32**, 4096–4108.

Gorustovich, A. A., Vargas, G. E., Bretcanu, O., Vera Mesones, E., Porto Lopez, J. M. and Boccaccini, A. R. (2008) 'Novel bioassay to evaluate biocompatibility

of bioactive glass scasffolds for tissue engineering', *Adv Appl Ceram*, **107**, 274–276.

Hench, L. L., Splinter, R. J., Allen, W. C. and Greenlee, T. K. (1972) 'Bonding mechanisms at the interface of ceramic prosthetic materials', *J Biomed Mater Res*, **2**, 117–141.

Hench, L. L. (1991) 'Bioceramics: from concept to clinic', *J Am Ceram Soc*, **74**, 1487–1510.

Hench, L. L. (2006) 'The story of Bioglass®', *J Mater Sci: Mater Med*, **17**, 967–978.

Hench, L. L. (2009) 'Genetic design of bioactive glass', *J Eur Ceram Soc*, **29**, 1257–1265.

Hench, L. L. (2010) 'Glass and medicine', *Int J Appl Glass Sci*, **1**, 104–117.

Hench, L. L. (2011) 'Glass and glass-ceramic technologies to transform the world', *Int J Appl Glass Sci*, **2**, 162–176.

Hoppe, A., Guldal, N. S. and Boccaccini, A. R. (2011) 'A review of the biological response to ionic dissolution products from bioactive glasses and glass-ceramics', *Biomaterials*, **32**, 2757–2774.

Hou, C. H., Hou, S. M., Hsueh Y. S., Lin, J., Wu, H. C and Lin, F. H. (2009) 'The *in vivo* performance of biomagnetic hydroxyapatite nanoparticles in cancer hyperthermia therapy', *Biomaterials*, **30**, 3956–3960.

Huang, W., Day, D. E., Kittiratanapiboon, K. and Rahaman, M. N. (2006) 'Kinetics and mechanism of the conversion of silicate (45S5), borate and borosilicate glasses to hydroxyapatite in dilute phosphate solutions', *J Mater Sci: Mater Med*, **17**, 583–596.

Hutmacher, D. W. (2000) 'Scaffolds in tissue engineering bone and cartilage', *Biomaterials*, **21**, 2529–2543.

Iijima, S. (1991) 'Helical microtubules of graphitic carbon', *Nature*, **354**, 56–58.

Izquierdo-Barba, I., Ruiz-Gonzalez, L., Doadrio, J. C., Gonzalez-Calbet, J. and Vallet-Regi, M. (2005) 'Tissue regeneration: a new property of mesoporous materials', *Solid State Sci*, **7**, 983–989.

Izquierdo-Barba, I. and Vallet-Regi, M. (2011) 'Fascinating properties of bioactive templated glasses: a new generation of nanostructured bioceramics', *Solid State Sci*, **13**, 773–783.

Jones, J. R. and Hench, L. L. (2003) 'Effect of surfactant concentration and composition on the structure and properties of sol-gel-derived bioactive glass scaffolds for tissue engineering', *J Mater Sci*, **38**, 1–8.

Jones, J. R. and Hench, L. L. (2004) 'The effect of processing variables on the properties of bioactive glass foams', *J Biomed Mater Res B*, **68**, 36–44.

Jones, J. R., Ehrenfried, L. M. and Hench, L. L. (2006) 'Optimising bioactive glass scaffolds for bone tissue engineering', *Biomaterials*, **27**, 964–973

Jones, J. R., Gentleman E. and Polak, J. (2007a) 'Bioactive glass scaffolds for bone regeneration', *Elements*, **3**, 393–399.

Jones, J. R., Poologasundarampillai, G., Atwood, R. C., Bernard, D. and Lee, P. D. (2007b) 'Non-destructive quantitative 3D analysis for the optimisation of tissue scaffolds', *Biomaterials*, **28**, 1404–1413.

Jones, J. R., Atwood, R. C., Poologasundarampillai, G., Yue, S. and Lee, P. D. (2009a) 'Quantifying the 3D macrostructure of tissue scaffolds', *J Mater Sci: Mater Med*, **20**, 463–471.

Jones, J. R. (2009b) 'New trends in bioactive scaffolds: the importance of nanostructure', *J Eur Ceram Soc*, **29**, 1275–1281.

Kamat, S., Su, X., Ballarini, R. and Heuer, A. H. (2000) 'Structural basis for the fracture toughness of the shell of the conch Strombus gigas', *Nature*, **405**, 1036–1040.

Karageorgiou, V. and Kaplan, D. (2005) 'Porosity of 3D biomaterial scaffolds and osteogenesis', *Biomaterials*, **26**, 5474–5491.

Kokubo, T. and Takadama, H. (2006) 'How useful is SBF in predicting *in vivo* bone bioactivity?', *Biomaterials*, **27**, 2907–2915.

Kolan, K. C. R., Leu, M. C., Hilmas, G. E., Brown, R. F. and Velez, M. (2011) 'Fabrication of 13-93 bioactive glass scaffolds for bone tissue engineering using indirect selective laser sintering', *Biofabrication*, **3**, 025004.

Lamers, E., Walboomenrs, X. F., Domanski, M., Te Riet, J., Van Delft, F., Luttge, R., Winnbust, L., Gardeniers, H. and Jansen, J. A. (2010) 'The influence of nanoscale grooved substrates on osteoblast behaviour and extracellular matrix deposition', *Biomaterials*, **31**, 3307–3316.

Lenza, R. F. S., Jones, J. R., Wasconcelos W. L. and Hench L. L. (2003) '*In vitro* release kinetics of proteins from bioactive foams', *J Biomed Mater Res A*, **57**, 121–129.

Leonardi, E., Ciapetti, G., Baldini, N., Novajra, G., Verné, E., Baino, F. and Vitale-Brovarone, C. (2010) 'Response of human bone marrow stromal cells to a resorbable P_2O_5-SiO_2-CaO-MgO-Na_2O-K_2O phosphate glass-ceramic for tissue engineering applications', *Acta Biomater*, **6**, 598–606.

Li, L., Clark, A. E. and Hench, L. L. (1991) 'An investigation of bioactive glass powders by sol-gel processing', *J Biomed Mater Res (Appl Biomater)*, **2**, 231–239.

Li, X., Wang, X., Chen, H., Jiang, P., Dong, X. and Shi, J. (2007) 'Hierarchically porous bioactive glass scaffolds synthesized with a PUF and P123 cotemplated approach', *Chem Mater*, **19**, 4322–4326

Li, G., Zhou, D., Lin, Y., Pan, T., Chen, G. and Yin, Q. (2010) 'Synthesis and characterization of magnetic bioactive glass–ceramics containing Mg ferrite for hyperthermia', *Mater Sci Eng C*, **30**, 148–153.

Martin-Saavedra, F. M., Ruiz-Hernandez, E., Bore, A., Arcos, D., Vallet-Regi, M. and Vilaboa, N. (2010) 'Magnetic mesoporous silica spheres for hyperthermia therapy', *Acta Biomater*, **6**, 4522–4531.

Mendonca, G., Mendonca, D. B. S., Simoes, L. G. P., Araujo, A. L., Leite, E. R., Duarte, W. R., Aragao, F. J. L. and Cooper, L. F. (2009) 'The effects of implant surface nanoscale features on osteoblast-specific gene expression', *Biomaterials*, **30**, 4053–4062.

Meng, D., Narayan Rath, S., Mordan, N., Salih, V., Kneser, U. and Boccaccini, A. R. (2011) '*In vitro* evaluation of 45S5 Bioglass®-derived glass-ceramic scaffolds coated with carbon nanotubes', *J Bioamed Mater Res A*, **99**, 435–444.

Miao, X. and Sun, D. (2010) 'Graded/gradient porous biomaterials', *Materials*, **3**, 26–47.

Mortera, R., Onida, B., Fiorilli, S., Cauda, V., Vitale-Brovarone, C., Baino, F., Verné, E. and Garrone, E. (2008) 'Synthesis of MCM-41 spheres inside bioactive glass-ceramic scaffold', *Chem Eng J*, **137**, 54–61.

Mortera, R., Baino, F., Croce, G., Fiorilli, S., Vitale-Brovarone, C., Verné, E. and Onida, B. (2010) 'Monodisperse mesoporous silica spheres inside a bioactive macroporous glass-ceramic scaffold', *Adv Eng Mater*, **12**, B256–B259.

Mourino, V. and Boccaccini, A. R. (2010) 'Bone tissue engineering therapeutics: controlled drug delivery in three dimensional scaffolds', *J R Soc Interface*, **7**, 209–227.

Mourino, V., Cattalini, J. P. and Boccaccini A. R. (2012) 'Metallic ions as therapeutic agents in tissue engineering scaffolds: an overview of their biological applications and strategies for new developments', *J R Soc Interface*, **9**, 401–419.

Muzio, G., Verné, E., Canuto, R. A., Martinasso, G., Saracino, S., Baino, F., Mola, M., Berta, L., Frairia, R. and Vitale-Brovarone, C. (2010) 'Shock waves induce activity of human osteoblast-like cells in bioactive scaffolds', *J Trauma Inj Infect Crit Care*, **68**, 1439–1444.

Navarro, M., Del Valle, S., Martínez, S., Zeppetelli, S., Ambrosio, L., Planell, J. A. and Ginebra, M. P. (2004) 'New macroporous calcium phosphate glass ceramic for guided bone regeneration', *Biomaterials*, **25**, 4233–4241.

Park, Y. S., Kim, K. N., Kim, K. M., Choi, S. H., Kim, C. K., Legeros, R. Z. and Lee, Y. K. (2006) 'Feasibility of three-dimensional macroporous scaffold using calcium phosphate glass and polyurethane sponge', *J Mater Sci*, **41**, 4357–4364.

Rahaman, M. N., Day, D. E., Bal, B. S., Fu, Q., Jung, S. B., Bonewald, L. F. and Tomsia, A. P. (2011) 'Bioactive glass in tissue engineering', *Acta Biomater*, **7**, 2355–2373.

Rainer, A., Giannitelli, S., Abbruzzese, F., Licoccia, S., Traversa, E. and Trombetta, M. (2008) 'Fabrication of bioactive glass-ceramic foams mimicking human bone portions for regenerative medicine', *Acta Biomater*, **4**, 362–369.

Renghini, C., Komlev, V., Fiori, F., Verné, E., Baino, F. and Vitale-Brovarone, C. (2009) 'Micro-CT studies on 3-D bioactive glass-ceramic scaffolds for bone regeneration', *Acta Biomater*, **5**, 1328–1337.

Rosengren, A., Oscarsson, S., Mazzocchi, M., Krajewski, A. and Ravaglioli, A. (2003) 'Protein adsorption onto two bioactive glass-ceramics', *Biomaterials*, **24**, 147–155.

Scheiner, S., Sinibaldi, R., Pichler, B., Komlev, V., Renghini, C., Vitale-Brovarone, C., Rustichelli, F. and Hellmich, C. (2009) 'Micromechanics of bone tissue-engineering scaffolds, based on resolution error-cleared computer tomography', *Biomaterials*, **30**, 2411–2419.

Sepulveda, P., Jones, J. R. and Hench, L. L. (2002) '*In vitro* dissolution of melt-derived 45S5 and sol-gel derived 58S bioactive glasses', *J Biomed Mater Res*, **61**, 301–311.

Tassani, S., Ohman, C., Baleani, M., Baruffaldi, F. and Viceconti, M. (2010) 'Anisotropy and inhomogeneity of the trabecular structure can describe the mechanical strength of osteoarthritic cancellous bone', *J Biomech*, **43**, 1160–1166.

Tesavibul, P., Felzmann, R., Gruber, S., Liska, R., Thompson, I., Boccaccini, A. R. and Stampfl, J. (2012) 'Processing of 45S5 Bioglass® by lithography-based additive manufacturing', *Mater Lett*, **74**, 81–84.

Towler, M. R., Boyd, D., Freeman, C., Brook, I. M. and Farthing, P. (2009) 'Comparison of *in vitro and in vivo* bioactivity of SrO-CaO-ZnO-SiO_2 glass grafts', *J Biomater Appl*, **23**, 561–572.

Valerio, P., Guimaraes, M. H. R., Pereira, M. M., Leite, M. F. and Goes, A. M. (2005) 'Primary osteoblast cell response to sol-gel derived bioactive glass foams', *J Mater Sci: Mater Med*, **16**, 851–856.

Vallet-Regi, M. and Ruiz-Hernandez, E. (2011) 'Bioceramics: from bone regeneration to cancer therapy', *Adv Mater*, **23**, 5177–5218.

Vargas, G. E., Vera Mesones, R., Bretcanu, O., Porto Lopez, J. M., Boccaccini, A. R. and Gorustovich, A. (2009) 'Biocompatibility and bone mineralization potential of 45S5 Bioglass®-derived glass-ceramic scaffolds in chick embryos', *Acta Biomater*, **5**, 374–380.

Verné, E., Vitale-Brovarone, C., Bui, E. and Boccaccini, A. R. (2009) 'Surface functionalization of bioactive glasses', *J Biomed Mater Res A*, **90**, 981–992.

Verné, E., Ferraris, S., Vitale-Brovarone, C., Spriano, S., Bianchi, C. L., Naldoni, A., Morra, M. and Cassinelli, C. (2010) 'Alkaline phosphatase grafting on bioactive glasses and glass-ceramics', *Acta Biomater*, **6**, 229–240.

Verné, E., Vitale-Brovarone, C., Robiglio, L. and Baino, F., (Politecnico di Torino) (2008) *Single-piece ceramic prosthesis elements*. WO 2008/146322 A2.

Vitale-Brovarone, C., Verné, E., Bosetti, M., Appendino, P. and Cannas, M. (2005) 'Microstructural and *in vitro* characterization of SiO_2-Na_2O-CaO-MgO glass-ceramic bioactive scaffolds for bone substitutes', *J Mater Sci: Mater Med*, **16**, 909–917.

Vitale-Brovarone, C., Verné, E., Robiglio, L., Appendino, P., Bassi, F., Martinasso, G., Muzio and G., Canuto, R. (2007) 'Development of glass-ceramic scaffolds for bone tissue engineering: characterisation, proliferation of human osteoblasts and nodule formation', *Acta Biomater*, **3**, 199–208.

Vitale-Brovarone, C., Miola, M., Balagna, C. and Verné, E. (2008) '3D-glass-ceramic scaffolds with antibacterial properties for bone grafting', *Chem Eng J*, **137**, 129–136.

Vitale-Brovarone, C., Baino, F. and Verné, E. (2009a) 'High strength bioactive glass-ceramic scaffolds for bone regeneration', *J Mater Sci: Mater Med*, **20**, 643–653.

Vitale-Brovarone, C., Baino, F., Bretcanu, O. and Verné, E. (2009b) 'Foam-like scaffolds for bone tissue engineering based on a novel couple of silicate-phosphate specular glasses: synthesis and properties', *J Mater Sci: Mater Med*, **20**, 2197–2205.

Vitale-Brovarone, C., Baino, F., Miola, M., Mortera, R., Onida, B. and Verné, E. (2009c) 'Glass-ceramic scaffolds containing silica mesophases for bone grafting and drug delivery', *J Mater Sci: Mater Med*, **20**, 809–820.

Vitale-Brovarone, C., Baino, F. and Verné, E. (2010) 'Feasibility and tailoring of bioactive glass-ceramic scaffolds with gradient of porosity for bone grafting', *J Biomater Appl*, **24**, 693–712.

Vitale-Brovarone, C., Ciapetti, G., Leonardi, E., Baldini, N., Bretcanu, O., Verné, E. and Baino, F. (2011) 'Resorbable glass-ceramic phosphate-based scaffolds for bone tissue engineering: synthesis, properties and *in vitro* effects on human marrow stromal cells', *J Biomater Appl*, **26**, 465–489.

Vitale-Brovarone, C., Novajra, G., Lousteau, J., Milanese, D., Raimondo, S. and Fornaro, M. (2012a) 'Phosphate glass fibres and their role in neuronal polarization and axonal growth direction', *Acta Biomater*, **8**, 1125–1136.

Vitale-Brovarone, C., Baino, F., Tallia, F., Gervasio, C and Verné, E. (2012b) 'Bioactive glass-derived trabecular coating: a smart solution for enhancing osteointegration of prosthetic elements', *J Mater Sci: Mater Med*, **23**, 2369–2380.

Wu, C., Zhang, Y., Zhu, Y., Friis, T. and Xiao, Y. (2010) 'Structure-property relationships of silk-modified mesoporous bioglass scaffolds', *Biomaterials*, **31**, 3429–3438.

Wu, C., Fan, W., Zhu, Y., Gelinsky, M., Chang, J., Cuniberti, G., Albrecht, V., Friis, T. and Xiao, Y. (2011a) 'Multifunctional magnetic mesoporous bioactive glass scaffolds with a hierarchical pore structure', *Acta Biomater*, **7**, 3563–3572.

Wu, C., Luo, Y., Cuniberti, G., Xiao, Y. and Gelinky, M. (2011b) 'Three-dimensional printing of hierarchical and tough mesoporous bioactive glass scaffolds with a

controllable pore architecture, excellent mechanical strength and mineralization ability', *Acta Biomater*, **7**, 2644–2650.

Wu, S. C., Hsu, H. C., Hsiao, S. H. and Ho, W. F. (2009) 'Preparation of porous 45S5 Bioglass®-derived glass-ceramic scaffolds by using rice husk as a porogen additive', *J Mater Sci: Mater Med*, **20**, 1229–1236.

Xynos, I. D., Hukkanen, M. V., Batten, J. J., Buttery, L. D., Hench, L. L. and Polak, J. M. (2000) 'Bioglass 45S5 stimulates osteoblast turnover and enhances bone formation *in vitro*: implications and applications for bone tissue engineering', *Calcif Tissue Int*, **67**, 321–329.

Xynos, I. D., Edgar, A. J., Buttery, L. D., Hench, L. L. and Polak, J. M. (2001) 'Gene-expression profiling of human osteoblasts following treatment with the ionic products of Bioglass 45S5 dissolution', *J Biomed Mater Res*, **55**, 151–157.

Yuan, H., De Buijin, J. D., Zhang, X., Van Blitterswijk, C. A. and De Groot, K. (2001) 'Bone induction by porous glass ceramic made from Bioglass® (45S5)', *J Biomed Mater Res (Appl Biomater)*, **58**, 270–276.

Yun, H. S., Kim, S. E. and Hyeon, Y. T. (2007) 'Design and preparation of bioactive glasses with hierarchical pore networks', *Chem Comm*, 2139–2141.

Yun, H. S., Park, J. W., Kim, S. H., Kim, Y. J. and Jang, J. H. (2011) 'Effect of the pore structure of bioactive glassballs on biocompatibility *in vitro* and *in vivo*', *Acta Biomater*, **7**, 2651–2660.

Zanello, L. P., Zhao, B., Hu, H. and Haddon, R. C. (2006) 'Bone cell proliferation on carbon nanotubes', *Nano Lett*, **6**, 562–567.

Zhu, Y., Wu, C., Ramaswamy, Y., Kockrick, E., Simon, P., Kaskel, S. and Zreiqat, H. (2008) 'Preparation, characterization and *in vitro* bioactivity of mesoporous bioactive glasses (MBGs) scaffolds for bone tissue engineering', *Microporous Mesoporous Mater*, **112**, 494–503.

Zhu, Y. and Kaskel, S. (2009) 'Comparison of the *in vitro* bioactivity and drug release property of mesoporous bioactive glasses (MBGs) and bioactive glasses (BG) scaffolds', *Microporous Mesoporous Mater*, **118**, 176–182.

9

Composite biomedical foams for engineering bone tissue

S. SPRIO, M. SANDRI, M. IAFISCO and S. PANSERI, Institute of Science and Technology for Ceramics, National Research Council, Italy, G. FILARDO, E. KON and M. MARCACCI, Rizzoli Orthopaedic Institute, Italy and A. TAMPIERI, Institute of Science and Technology for Ceramics, National Research Council, Italy

DOI: 10.1533/9780857097033.2.249

Abstract: The regeneration of extended bone defects is a serious concern and the number of patients affected by bone diseases is ever increasing. The continuous progress in materials science and nanotechnology is providing novel approaches to developing new porous materials with structures that are able to mimic the morphological and mechanical features of bone, thus achieving improved assistance to the regenerative processes. This chapter provides an overview of the technologies that have recently been developed for use in manufacturing porous ceramics and composites for bone scaffolding, including the new biomorphic processes that, by transforming ligneous sources into hierarchically organized hydroxyapatite, may provide solutions to assist the regeneration of long segmental bones.

Key words: biomimesis, bone regeneration, porous scaffolds, hydroxyapatite, hierarchical organization.

9.1 Introduction

In recent decades, scientific research into the development of biomaterials for bone grafting has continuously progressed and bio-devices with improved performances have been designed and manufactured. The increasing knowledge of the biological processes and mechanisms yielding the formation and structural rearrangement (remodeling) of new bone tissue has provided an awareness of the importance of physico-chemical and structural biomimicry that bone implants should possess in order to activate tissue regeneration. For this reason, designs have moved from dense, bioinert implants to new implants that contain bioactive phases such as biomimetic calcium phosphate phases and porous, osteoconducting structures that have the ability to

host human cells. Therefore, inert dense or microporous implants have now evolved into macroporous scaffolds designed to sustain and assist extensive cell colonization and anchorage to the existing bone, finally leading to osteointegration and progressive resorption, which allows the new bone to replace the scaffold and restore full functionality. Hydroxyapatite was soon recognized as the ideal material to be developed into porous scaffolds for bone repair, since it is the main inorganic component of bone and can easily induce cell adhesion and proliferation. Upon recognition of the true nature of the inorganic bone, i.e. a multi-substituted, poorly crystalline hydroxyapatite, and of the relevant function of the various ions contained in the apatite structure, biomaterial synthesis became focused on reproducing the complex chemical composition of bone. In the attempt to find a balance between composition, structure, porosity, and mechanical strength, material scientists developed many different approaches to create structures with open and interconnected pores by imposing different geometries or by allowing the formation of complex structures by using natural templates. In this respect, features such as the quality of the newly formed bone became increasingly important; accordingly, the establishment of angiogenesis soon became one of the key features of synthetic bone grafts.

This chapter covers all these aspects, exploring the main features that may enhance the *in vivo* behavior of bone scaffolds, i.e. the surface chemistry, morphology, and porosity extent. These characteristics will be described in relation to bone scaffolds of different natures, including ceramic and ceramic/polymeric composites, new biologically inspired hybrid composites that mimic the features of newly formed bones, and finally the recently developed hierarchically organized scaffolds that are obtained by wood transformation.

9.2 Chemical and morphological biomimesis: the key for osteointegration

The ideal device for bone regeneration must exhibit good biocompatibility without inducing inflammation or toxic reactions. Moreover, it has to promote strong bonding with the host bone and extensive bone ingrowth into the graft, as well as allowing bio-resorption. To do this, regenerative bone scaffolds must exchange suitable chemical signals with the surrounding extra-cellular matrix (ECM) in order to activate and promote the series of events at cell level, thus triggering the formation and organization of new bone tissue. In this respect, the first interactions between the cells and the scaffold surface define the quality of the tissue implant interface, which is a key issue for the regenerative ability of the bio-device. The interactions between ECM and the implant's surface are mediated by early adsorption

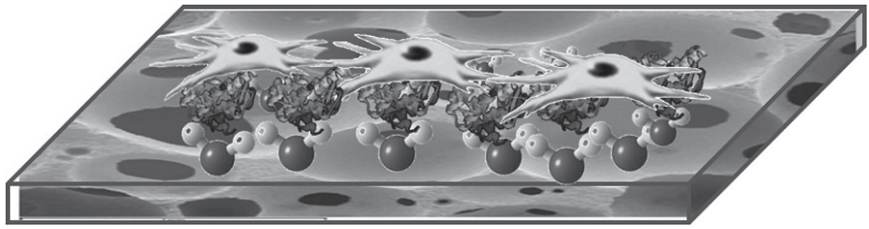

9.1 Schematic draw of the sequence of events leading to cell attachment on scaffolds.

of water molecules and the subsequent adsorption of proteins from the biological fluid, which in turn transcribe the surface characteristics into information for cells (Boyan *et al*., 1996) (Fig. 9.1). Therefore, the performances of implanted materials are strictly related to a variety of features, such as chemistry and topography, at the macro-, micro-, and nano-scale.

In this respect, a close biomimicry to natural tissues enables cells to attach, proliferate, and differentiate, following a quasi-physiological bone generation/remodeling path. From a chemical–physical perspective, the mineral part of bone is a poorly crystalline apatite containing ions such as CO_3^{2-}, Mg^{2+}, SiO_4^{4-}, Sr^{2+}, HPO_4^{2-}, Na^+, and K^+, which have specific functions in the formation, stabilization, and maturation of bone (LeGeros and LeGeros, 1984; LeGeros, 1991). The nano-size of the biologic apatite, the bio-availability of these ions, and the presence of acidic and alkaline surface sites at defined crystal planes (i.e. the so-called C and P sites, respectively) provide the potential for protein and cell adhesion as well as proliferation (Webster *et al*., 1999, 2000, 2001; Kandori *et al*., 2002; Capriotti *et al*., 2007; Corno *et al*., 2010). For several decades synthetic hydroxyapatite (HA) has been considered the best biomaterial for bone scaffolding. The development of preparation techniques has led to methods for obtaining HA in nanosized forms that mimic those naturally occurring in bone (Robinson, 1952; Lowenstam and Weiner, 1989; Iafisco *et al*., 2010; Sakhno *et al*., 2010). Moreover, it is now possible to change bulk structures from highly crystalline to poorly crystalline or disordered by changing the preparation conditions (such as the temperature, presence of anionic and/or cationic substituents, and nucleation on collagen fibers) (Landi *et al*., 2000; Tampieri *et al*., 2003; Celotti *et al*., 2006).

Indeed, in its stoichiometric composition $[Ca_{10}(PO_4)_6(OH)_2]$, hydroxyapatite (HA) is virtually insoluble in physiological conditions and thus has low bio-availability. The bioactivity and bio-solubility of bone is induced by the incorporation of several foreign ions (namely calcium, phosphorus, and hydroxyl) into the HA lattice, which disturbs the crystallographic order of the apatite structure itself and thus reduces its stability in the physiological environment (Fig. 9.2). In particular, CO_3^{2-} ions in the phosphate site

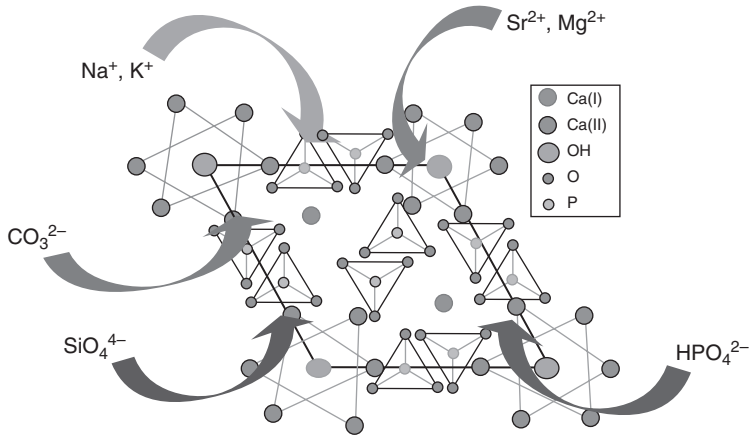

9.2 Scheme of some possible ionic substitution in the hydroxyapatite lattice.

(i.e. B position) are the major source of structural disorder in bone, as they increase the chemical reactivity and enhance the apatite solubility without changing the surface polar property and the affinity of the osteoblast cells. As bone matures, carbonate ions are more likely to be located in place of hydroxyl (i.e. A position). Particularly in young bone, CO_3^{2-} ions are also present in non-apatitic domains, mainly located in a hydrated layer surrounding the apatite crystals and thus representing a group of ions that promote the remodeling processes (Boskey, 2006). The increased solubility of synthetic HA containing carbonates was proved in ion release tests, which were carried out in simulated body fluid at 37°C (Sprio *et al.*, 2008; Landi *et al.*, 2008a). The ability to be bio-resorbed is a key feature for osteoclastogenesis, as this can regulate the physiological bone turnover and enhance osteoblast proliferation and osteogenesis (Spence *et al.*, 2009, 2010).

Divalent ions that replace calcium (such as magnesium and strontium) are particularly active during the first stages of the regenerative and remodeling processes (Driessens, 1980; Bigi *et al.*, 1997). In particular, magnesium is associated with the first stages of the bone formation and enhances skeletal metabolism and bone growth. Like carbonate, magnesium decreases with increasing calcification and with the aging of the bone (Bigi *et al.*, 1992). In synthetic HA, the controlled substitution of calcium ions with magnesium increases the chemical–physical mimesis of the mineral bone. In fact, magnesium increases the kinetic of HA nucleation on collagen and retards its crystallization, affecting the size and shape of mineral nuclei. The incorporation of Mg^{2+} into the HA structure induces a disordered state on the HA surface where ions are continuously exchanged from the outer hydrated layer to the well-crystallized apatite lattice. Moreover, the replacement

of calcium by magnesium in surface crystal sites increases the number of molecular layers of coordinated water (Bertinetti *et al*., 2006); all of these phenomena favor protein adsorption and the adhesion of cells to the scaffold (Cazalbou *et al*., 2005). The increase of osteogenic activity in the presence of magnesium-substituted HA was shown in *in vivo* studies: a greater osteoconductivity over time and higher material resorption, compared to stoichiometric HA, were detected in granulated Mg-HA powders that were implanted in a rabbit's femur (Landi *et al*., 2008b). Additionally, studies of osteoblast gene expression profiles from Mg-HA grafts revealed a higher expression of specific markers of osteoblast differentiation and bone formation, which are associated with a lower osteoclastogenic potential (Crespi *et al*., 2009).

Strontium is also considered to be a relevant trace ion that enhances osteogenesis while reducing bone resorption; this effect provides enhanced collagen synthesis and improved physical stabilization of the new bone matrix, as shown in *in vitro* and *in vivo* studies (Dahl *et al*., 2001; Marie *et al*., 2001). Due to its potential as an anti-osteoporotic agent, the incorporation of strontium ions into the HA lattice has been practiced in recent years (Bigi *et al*., 2007; Landi *et al*., 2007), and increasing effort is being dedicated to the development of strontium-containing bone cements (Guo *et al*., 2005; Boanini *et al*., 2010; Pina *et al*., 2010; Tadier *et al*., 2012).

Like strontium, silicon is an essential trace element for the formation and stabilization of bones and connective tissues (Carlisle, 1970, 1988; Jugdaohsingh, 2007). Aqueous silicon in the form of orthosilicic acid ($Si(OH)_4$) has been shown to enhance osteoblast proliferation, differentiation, and collagen production and to have dose-dependent effects on osteoclast cells under *in vitro* conditions (Xynos *et al*., 2001). The synthesis of silicon-substituted HA was performed, showing that silicon yields tetrahedral distortion and disorder at the hydroxyl site of the HA lattice, which can potentially decrease the stability of the apatite structure and enhance apatite solubility and bio-availability of silicon (Vallet-Regì and Arcos, 2005; Thian *et al*., 2006; Pietak *et al*., 2007; Sprio *et al*., 2008). An increase of the osteoblast activity induced by silicon was also detected *in vivo* (Porter *et al*., 2003), where the migration of Ca, P, and Si ions to the bone–HA interface, consequent to apatite dissolution, accelerated the precipitation of biological apatite and induced bone apposition at the surface of the ceramic. Metal ions such as zinc, copper, iron, and manganese are also essential factors that enhance the functions of enzymes involved in the synthesis of the constituents of the bone matrix (Saltman and Strause, 1993; Reid and New, 1997) (Table 9.1).

To achieve a synergistic effect, the synthesis of a multi-substituted HA phase is obtained in biomimetic conditions by carrying out the nucleation of the apatite phase in simulated body fluid (SBF) that has been enriched with

Table 9.1 Indicative ions content in human bone mineral

Ion	(mol.%)	(wt.%)
Ca^{2+}	8.7	34.8
PO_4^{3-}	4.9	46.6
Na^{+}	0.4	0.9
K^{+}	0.01	0.03
Mg^{2+}	0.2–0.5	0.5–1.3
CO_3^{2-}	0.5–1.3	3–8
F^{-}	0.02	0.03
SiO_4^{4-}	0.15–0.30	1.4–2.7
Cl^{-}	0.04	0.13
Ba^{2+}	trace	trace
Sr^{2+}	trace	trace

biomimetic ions at 37°C. This procedure mimics the physiological conditions of bone formation and allows synthetic HA to incorporate various ions (Na^{+}, K^{+}, HPO_4^{2-}, Mg^{2+}, SiO_4^{4-}, Sr^{2+}, CO_3^{2-}), which are present in the physiological environment (Landi *et al.*, 2005; Sprio *et al.*, 2008). In particular, co-substitution with carbonate favored higher bio-availability of osteogenic chemical agents, thus increasing solubility in physiological conditions (Sprio *et al.*, 2008) and yielding improved *in vitro* results compared to silicon-free carbonated HA (Landi *et al.*, 2010).

Biomimetic HA powders can be synthesized and used as granules to fill bone defects of limited size. However, the lack of specific morphology and mechanical stability of granulated bio-devices does not enable regeneration of extended bone parts; in this case the implantation of a 3D porous scaffold is required, with characteristics of bioactivity and osteoconductivity associated to bio-mechanic performance suitable for the specific implant site (Babis and Soucacos, 2005; Sprio *et al.*, 2011). More specifically, scaffolds have to provide the space for new bone formation and the necessary support for cells to proliferate and maintain their differential function. Moreover, they should exhibit suitable architectures for inducing the formation and maturation of well-organized tissue (Daculsi, 1998; Kessler *et al.*, 2003). Osteoconductivity ensures physical and mechanical integration with the surrounding bone, which in turn prevents micro-movements and the possibility of early mechanical loading *in vivo*; this process can be facilitated by the use of bioactive scaffolds that permit osteoclastic resorption.

Porosity in bone scaffolds is essential because it allows the transmission of changes in hydrodynamic pressure, thus activating mechanotransduction processes. It has been reported that around 80% of total porosity is the critical point for ensuring both pore interconnectivity and sufficient mechanical properties of scaffolds (Burdick *et al.*, 2002, 2003). Pore volume and size, both

at the macroscopic and the microscopic level, are important morphological properties of a scaffold for bone regeneration (Karageorgiou and Kaplan, 2005). Although no precise measurements can be provided for optimal void volumes and pore sizes due to the wide range of bone features in different anatomical districts, some general indications can be provided. Firstly, there is general consensus on the key effect of high porosity and large pores for the activation and enhancement of bone ingrowth and osseointegration of the implant after surgery. However, the extent of the porosity and the pore size should be associated with mechanical properties suitable for the specific implant site. The minimum pore size for cell colonization and substantial bone ingrowth was reported as 100 μm (Hulbert *et al.*, 1970), whereas smaller pores can result in the growth of unmineralized osteoid tissue or fibrous tissue. However, there is wide consensus that the mean pore size should be approximately 300 μm to achieve better osteogenesis, as this size provides improved vascularization and oxygenation (Tsuruga *et al.*, 1997; Kuboki *et al.*, 2001; Gotz *et al.*, 2004). Macroscopic porosity (i.e. several hundreds of μm) should also be interconnected with channel-like microporosity that enables fluid exchange throughout the whole scaffold, thus providing a supply of nutrients and the elimination of metabolic waste products.

Besides these general guidelines, the pore size of bone scaffolds should be designed with consideration of the features of the specific bone tissue to be repaired. In this respect, cortical bone is characterized by reduced porosity and activity and higher compression strength, compared to spongy bone, which exhibits a complex pore organization that allows physical stability and resistance against complex biomechanical stimuli. Hence, the design of bone scaffolds in a graded form allows for the reproduction of both parts of bone (Tampieri *et al.*, 2001) that may improve the scaffold performance, thus enabling application in long-bone regeneration. The architecture of the scaffold is relevant since the bone ingrowth is guided by the scaffold voids and may be interrupted by lack of pore interconnection, thus creating spatially discontinuous ingrowth with the formation of bone islands throughout the whole scaffold. The formation of new bone in the inner part of the scaffold is a key feature for ensuring optimal osseointegration and reduced physical mismatch at the bone–scaffold interface.

9.3 Foaming: an approach to fabricate highly porous bioactive scaffolds

In the last two decades, different technological approaches have been developed to manufacture biomimetic 3D foams with specifically designed phase composition and porosity (Cooke, 1992). Due to intrinsic brittleness, porous scaffolds made of HA can only exhibit limited fracture strength, which limit

their use to non-load-bearing sites. For this reason, recent designs have aimed at bone scaffolds made of HA with anisotropic and a more organized structure in order to achieve improved bone-mimicking.

Generally, techniques aimed at forming porous ceramics are based on aqueous suspensions of pulverized raw materials (also known as slurries), opportunely dispersed and processed to form a porous structure that is then consolidated by using thermal processes (Sprio *et al.*, 2011). The forming process can be subdivided into template-assisted and template-free techniques. In both cases, as the process should generate green ceramic bodies with high particle packing and homogeneous pore distribution, the rheological properties of the suspension are a key feature. The control of the slurry's properties is less critical when using sacrificial phases that are uniformly dispersed into a ceramic matrix and then eliminated by controlled processes so as to produce defined porosity distribution. The method of sacrificial template has been successful for obtaining porous bodies in a variety of compositions (e.g. alumina, zirconia, hydroxyapatite, tricalcium-phosphate, titania, silica, and mullite). Polymeric components are the most commonly used pore-forming agents and include polyethylene, polystyrene, polyvinylchloride, and polymethylmethacrylate. However, natural sources (e.g. gelatin, textile fibers) and inorganic soluble salts (NaCl, $BaSO_4$, K_2SO_4) are also employed. The organic components are usually removed by processes of thermal decomposition, whereas inorganic agents are extracted through chemical processes, such as solubilization in water or other solvents.

The replica method is a template-assisted process that makes use of polymeric templates with defined pore size and 3D arrangement that can be repeatedly soaked into ceramic suspensions to allow the loading of the matrix. Green ceramic bodies formed by the imbibition of synthetic polymeric matrices (e.g. polyurethane) reproduce the 'negative' shape of the matrix. Therefore, when subjected to firing, the decomposition of the polymer leaves equally spaced voids that retain the original shape of the matrix (Studart *et al.*, 2006).

In the case of using a support made of natural polymers (e.g. cellulose), their fibrous nature creates micron-sized voids, which permit the imbibition of the matrix at a smaller scale due to the increased hydrophilic character. Therefore, repeated imbibition can provide green bodies that reproduce the 'positive' shape of the template (Tampieri *et al.*, 2001). To achieve this, the suspension must exhibit thixotropic properties, i.e. they must be able to permeate the micro-struts of the organic template without filling its pores and allowing water to flow away. To achieve this, several parameters should be well defined and optimized, including the specific surface area (SSA), particle size distribution, and the surface activity of the powder. Surface activity is a key factor governing particle agglomeration, which in turn can alter the homogeneity of the ceramic green body. Hence, the surface activity of HA can be reduced by thermal treatments aimed at allowing partial particle

coalescence and increasing the crystal order while reducing the SSA (Landi *et al*., 2000; Sprio *et al*., 2012; Cunha *et al*., 2013). Suitable dispersion of the HA powder can be achieved by using deflocculating agents (Pretto *et al*., 2003). Thermal consolidation processes include a step where the organic template is slowly eliminated; this is a crucial stage of the process, since mechanical micro-damage can occur due to inappropriate heating rates and/or lack of suitable procedures for the elimination of the combustion products. The use of cellulose sponges and the fine set-up of slurries based on HA powders enable the fabrication of bone scaffolds with irregularly arranged, interconnected porosity that is similar to that of bone (Tampieri *et al*., 2001). Due to the different rheological behaviors of HA powders with different degrees of crystal order (Landi *et al*., 2000), forming techniques based on template imbibition were designed to produce scaffolds with graded morphology that mimicked spongy and cortical bones (Tampieri *et al*., 2001).

Template-free approaches have the advantage of avoiding the use of solid structures that need to be eliminated during the manufacturing of the scaffold; among these techniques, forming processes based on foaming effects are of particular interest (Studart *et al*., 2006; Sprio *et al*., 2011). The pore-forming agents are usually organic-based components that are able to induce the formation of bubbles through nucleation, coalescence, and growth phenomena. The composition of the suspension, the use of suitable stabilizing agents, and careful homogenization enable control of these phenomena, thus achieving the formation of bubbles of controlled size. The rheological properties of the slurry should include high powder concentration and thus high viscosity, which helps to achieve the early stabilization of the slurry and the immobilization of the bubbles. Upon slow evaporation of the residual water, the green body is then fired by thermal routes, ensuring the elimination of the organic components and the sintering of the ceramic matrix while also retaining the spherical voids left by the bubbles (Sprio *et al*., 2011; Cunha *et al*., 2013). The high porosity and osteoconductivity of HA porous scaffolds obtained by a foaming method are illustrated in Fig. 9.3, where MG63 osteoblast-like cells covered the entire scaffold's surface after 14 days of incubation and also penetrated the inner parts of the scaffold. This technique enables the design of ceramic compositions that are suitable for developing composites with improved features, such as mechanical strength or osteogenic character (Cunha *et al*., 2013; Sprio *et al*., 2013). The absence of any templates allows the establishment of stable suspensions, yielding porous scaffolds with improved properties.

Freeze-casting techniques have recently been investigated. They can be considered as a development of foaming processes and can be designed to produce bone scaffolds with defined pore orientation. The technique is based on the controlled freezing of ceramic slurries, which induces the formation of structures oriented along the cold propagation front. Both the

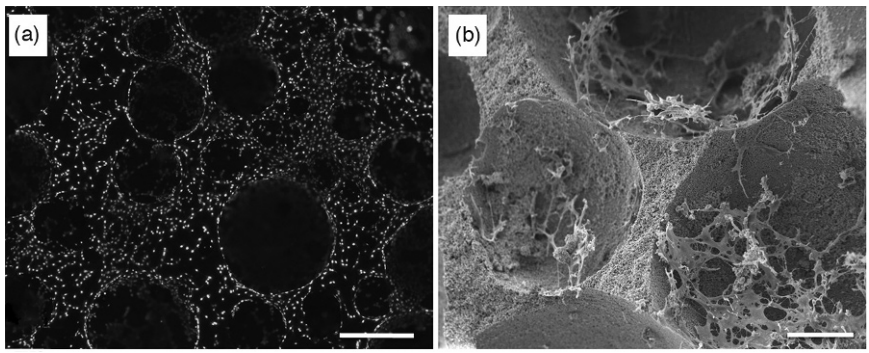

9.3 HA porous scaffold cell colonization. (a) DAPI stains cell nuclei. (b) Detailed analysis of cell morphology assessed by scanning electron microscopy. Scale bars: (a) 200 μm. (b) 150 μm.

kinetics and the freezing have an effect on the shape and orientation of the scaffold's porosity upon sublimation of the liquid medium (Lu *et al.*, 1998; Deville, 2008). The key parameters related to the process are the characteristics of the additives (e.g. dispersants, plasticizers), the solvent used, the solid/liquid ratio (hence, the slurry viscosity), and the freezing kinetics, which strongly influences the distribution of the frozen solvent crystals, in turn affecting the pores of the final device upon sublimation (Landi *et al.*, 2008c) (Fig. 9.4). Such features also influence the porosity distribution and the mechanical strength of the final construct (Deville, 2008). The uni-directional orientation of pores induced by freeze-drying techniques mimics the structural organization of long bones and promotes higher cell conductivity and faster vascularization (Deville *et al.*, 2006). Like bone, the mechanical properties of freeze-dried scaffolds with lamellar porosity are strongly anisotropic, which is a good feature for load-bearing applications.

9.3.1 Foams as net-shaped scaffolds

Although the features of bioactive, osteoconductive ceramics have several advantages for tissue regeneration, certain properties are drawbacks, e.g. brittleness. In the past 20 years, polymeric, or ceramic–polymer composite, scaffolds have been developed and increased elasticity and the potential for bio-degradation of polymeric phases has been considered. The versatility of polymers enables the implementation of various manufacturing technologies, including freeform fabrication, phase separation, emulsion-solvent diffusion, porogen leaching (Taboas *et al.*, 2003; Karageorgiou and Kaplan, 2005), as well as electrospinning (Li *et al.*, 2002), which is able to generate pure and composite scaffolds with controlled pore size, geometry, orientation, and interconnectivity.

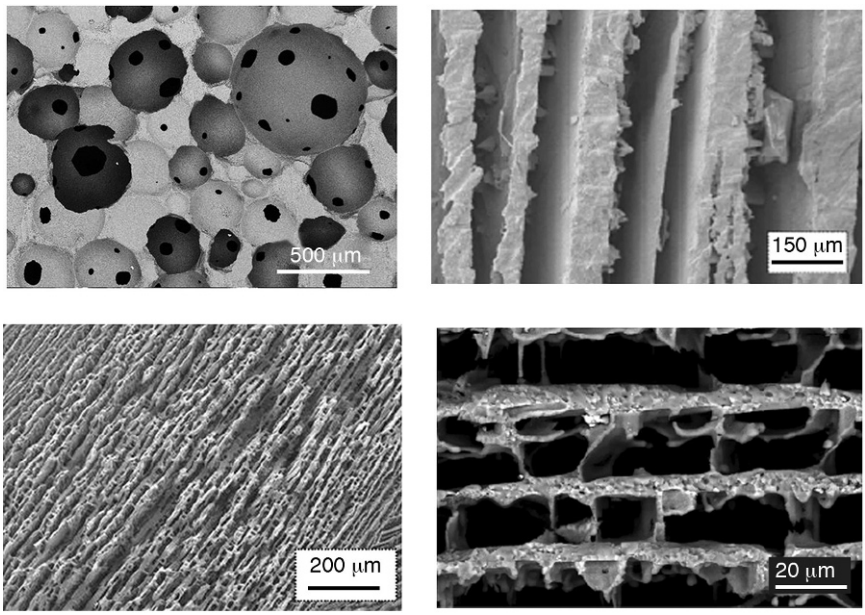

9.4 Different microstructures achievable by foaming/freeze-casting techniques.

The versatility of chemically synthesized polymers enables the fabrication of scaffolds with different features (shape, porosities and pore sizes, rates of degradation, mechanical properties) to match tissue specific applications. Among the polymers suitable for bone scaffolding, poly(D,L-lactide), poly(ethylene glycol), poly(lactide-co-glycolide), and poly (ε-caprolactone) are particularly suitable, due to their biocompatibility and ability to trigger and sustain cell proliferation and differentiation (An *et al*., 2000; Schaefer *et al*., 2000; Yang *et al*., 2001; Hu *et al*., 2002; Oh *et al*., 2003; Taboas *et al*., 2003; Gloria *et al*., 2013). Polymeric phases are also suitable as beads to be incorporated into ceramic scaffolds to produce porosity of defined extent with thermal consolidation processes. Alternatively, composites can be developed by loading porous polymeric matrices with functional, bioactive inorganic phases (Bañobre-Lopez *et al*., 2011; Iafisco *et al*., 2012; Gloria *et al*., 2013). This approach is suitable for providing mechanical reinforcement and for tailoring the hydrophilic character of the scaffold, which is a key feature affecting the capability of cell attachment. Moreover, in the case of scaffold loading with apatite nanoparticles, the reinforcing phase also provides chemical signals to cells to promote osteogenic differentiation. Recently, experiments were done with new approaches that were designed to improve tissue regeneration. They used localized magnetic fields to assist tissue regeneration by both cell stimulation and delivery of growth factors

(Bañobre-Lopez *et al*., 2011; Tampieri *et al*., 2012; Panseri *et al*., 2012a, b). The use of bioactive scaffolds endowed with superparamagnetic properties may represent a new concept of scaffold that provides controlled delivery of osteogenic and angiogenic growth factors, thus aiding the regeneration of extended bone parts, also including long bones. In particular, the recent discovery of a bioactive superparamagnetic apatite phase, obtained by controlled ion substitution of Ca^{2+} with $Fe^{2+/3+}$ ions in the HA lattice (Tampieri *et al*., 2012), promises new advances in tissue regeneration. This is because this new phase may replace superparamagnetic iron oxides such as magnetite and maghemite, which are cytotoxic (Tampieri *et al*., 2011a).

9.4 Freeze-dried hybrid gels for bone and osteochondral regeneration

Despite the continuous progress in material science and technology to develop bone scaffolds with complex structures, conventional approaches are still far from developing inorganic matrices that really mimic natural tissues. In the last decade, increasing efforts were dedicated to creating fabrication methods that could reproduce biological processes thus generating complex devices with features similar to natural materials. Also, the use of natural polymers for the fabrication of bio-devices is gradually being increased. Natural polymers have the advantage of biocompatibility and biodegradability as they are the structural components of living tissues (i.e. collagen and glycosaminoglycans). In spite of the intrinsically low mechanical strength of their components, biological structures exhibit outstanding physical and mechanical properties, such as high resistance, lightness, and the ability to continuously adapt to constantly changing external stimuli; the establishment of these properties is due to the complexity and hierarchical organization of the natural structures (e.g. shells, plants, exoskeletons) from the nano- to the macro-scale. The complex arrangement of nanosized organic and inorganic elements is obtained due to information exchanged at the molecular level between the organic structure, which acts as a template, and the inorganic phases that heterogeneously nucleate on it (Fratzl and Weinkamer, 2007; Meyers *et al*., 2008).

In particular, the hard tissues in mammals are generated by a biomineralization process (Mann, 2001), where collagen-based components self-assemble and organize, thus acting as templates for the heterogeneous nucleation of ion-substituted apatites by mediation of chemical, physical, morphological, and structural control mechanisms. In other words, the exposed functional groups of collagen in specific regions, represented and delimited by insoluble macromolecules, act as sites of heterogeneous nucleation for the mineral phase upon precipitation of the ions present in the surrounding ECM (e.g. Ca^{2+}, PO_4^{3-}, Na^+, K^+, Mg^{2+}). The apatite nuclei subsequently grow under the physical constraints of the complex macromolecular

organic structures and assume specific morphologies and crystal orientations, which results in the exposure of crystal planes that specifically enable the adhesion of proteins that promote focal adhesions. The structural organization of the newly formed bone proceeds from the nanometer to the macroscopic scale, where the mineral phase exhibits a complex architecture that is strictly dependent on the combination of the various phenomena that are described above (Tampieri *et al*., 2011a).

Due to the large amount of information relating to the complexity of these constructs, as well as the reduced size of their elemental components, it is not possible to build a similar structure with conventional manufacturing methods. In this respect, over the past decade, the establishment of assembling processes guided by control mechanisms similar to those existing in nature is increasingly being viewed as a feasible way of creating bio-devices with smart multi-functionality. In the early 2000s, a new concept for bone scaffolding was developed, involving a biologically inspired fabrication process with the purpose of obtaining 3D constructs that strongly mimic the chemico-physical, morphological, and structural features of hard human tissues (Tampieri *et al*., 2003). By this process, type I collagen fibrils, dispersed in quasi-physiological aqueous solutions containing ions involved in bone formation, are assembled and organized by pH variation, thus yielding hybrid fibrous mineralized constructs that mimic the composition and structure of the newly formed bone (Fig. 9.5, left). These scaffolds exhibit biomimetic chemico-physical features (i.e. a collagen fibrous matrix) formed by the spontaneous assembling and hierarchical organization of nano-fibrils that are embedded in the nano-nuclei of biomimetic apatite (HA/Collagen), the heterogeneous nucleation of which took place in specific sites corresponding to the periodic gaps of the collagen bands (Sprio *et al*., 2012). The devices that were obtained exhibited very high open surface and macroscopic porosity that could easily be tailored by different approaches (Fig 9.5, right). The soft nature of the bio-inspired hybrid HA/collagen composite allows for specific pore sizes and orientations during the synthesis process through the use of chemical cross-linking or freeze-casting/drying processes (Tampieri *et al*., 2011a). The controlled cross-linking enables the improvement of the physical stability of the scaffold against early enzymatic resorption as well as the tailoring of the pore size. In turn, pore size affects the local oxygen tension and this can influence cell differentiation; hence, a reduced pore size can promote cell differentiation in chondrocytes rather than osteoblasts. This is of particular interest in the view of developing scaffolds for the regeneration of multi-functional tissues, such as the osteochondral or periodontal regions. Moreover, the bio-inspired synthesis process allows for the control of the mineralization extent (i.e. the amount of mineral phase heterogeneously nucleated onto the collagen fibers), which can range from zero to bone-mimicking composition (i.e. ≈70%). Hence, graded hybrid

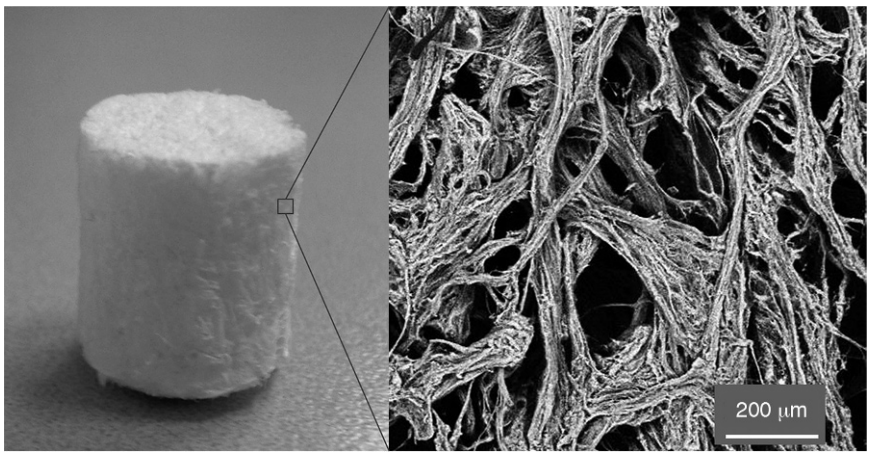

9.5 Bone scaffold obtained by bio-inspired mineralization process (left: macroscopic view; right: microscopic detail).

composites were developed, which mimic the composition and structure of the subchondral bone and mineralized cartilage (Tampieri *et al*., 2008). Mineral-free layers, enriched with hyaluronic acid, were also produced to mimic the cartilaginous region: processes of controlled freeze-drying allowed for the suitable orientation of the fibers of the cartilage-like layer into a columnar-like structure (Schoof *et al*., 2001), converging toward the external surface into horizontal flat ribbons, thus resembling the morphology of the lamina splendens (Fig. 9.6).

The morphological and compositional gradients exhibited by the multilayered osteochondral scaffold offer spatially-defined environmental cues that are able to guide specific cell differentiation and fast tissue regeneration (Kon *et al*., 2010). This shows the importance of biomimicry in the design of scaffolds for tissue regeneration (Sprio *et al*., 2012). Moreover, the possibility of controlling the processes of scaffold formation by soft chemistry offers high flexibility of production and functionalization. In this respect, due to the high exposed surface area and the presence of many different active surface sites (e.g. COO- and $–NH_2$ groups), bio-inspired hybrid composites offer the possibility to associate suitable signaling molecules to improve the biological response in terms of the amount and quality of the newly formed tissue (Hench and Polak, 2002; Schulz-Ekloff *et al*., 2002; Brown and Puleo, 2008).

Relevant bio-triggers can be proteins or short peptide epitopes; for bone regeneration, the most commonly used peptide for surface modification is Arg-Gly-Asp (RGD) (Durrieu *et al*., 2004; Zurlinden *et al*., 2005; Balasundaram *et al*., 2006), which is a signaling domain derived from fibronectin and laminin (Hersel *et al*., 2003). Moreover, the high surface activity of natural polymers allows the possibility of biomimetic composite scaffolds

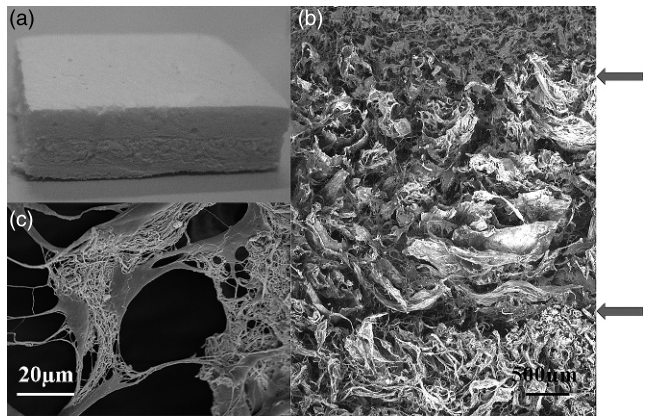

9.6 Graded osteochondral scaffold obtained by bio-inspired mineralization process. (a) Macroscopic view (upper part: cartilage-like layer, lower part: bone-like layer); (b) microscopic details (upper part: cartilage-like layer, lower part: bone-like layer); (c) scanning electron microscope (SEM) image showing adhesion of mesenchymal stem cells (MSCs) on mineralized collagen fibers.

with improved mechanical properties (i.e. strength, elasticity, stiffness) by association of collagen with other natural sources that are able to mediate bio-inspired mineralization processes (Li *et al.*, 2005; Svensson *et al.*, 2005; Mano *et al.*, 2007; Wang *et al.*, 2009; Venkatesan and Kim, 2010). The potential to tailor the features of multi-functional hybrid scaffolds will pave the way to the development of scaffolds with wider applications in the field of regenerative medicine. For instance, with reference to dental tissue, the alveolar bone and cementum form upon processes of assembling and mineralization similar to those involved in the formation of bones and their main cells follow similar behavior (Linde and Goldberg, 1993). Dental pulp and dentinal tissue are collagen-based constructs where the degree of assembling, mineralization, and organization progressively increase from the pulp to the predentin and the dentin, therein reaching a very high mineralization extent, organized in micron-sized tubules. The application of controlled processes of casting/drying, which are able to yield channel-like morphologies, may enable the future development of scaffolds for dental regeneration, which would be a breakthrough in medicine with huge socio-economic impacts.

9.5 *In vivo* performances of bioactive foams with defined morphology and microstructure

The scaffold morphology and pore size have a key effect on the amount and quality of the newly formed bone *in vivo*. As a result, several studies have

investigated the key features that improve bone regeneration. In particular, systematic studies were carried out on *in vivo* implanted HA scaffolds that had been specifically manufactured with defined porosity, pore size, and pore organization/interconnection, thus confirming that these factors are all key issues in influencing cell colonization, osteointegration, and the quality of the newly formed tissue.

Among the various animal models, sheep are of particular interest from a biomechanical point of view, since they have patterns of bone remodeling similar to humans; in particular, they exhibit chewing forces similar to those of humans and, due to daily mastication, the articular tubercles and eminences are thin and similar to human temporomandibular joints (TMJ). In the case of mandibular sheep defects filled with HA scaffolds with defined macro-porosity, those with homogeneous, interconnected pores favored the formation of interpenetrating matrices of newly formed bone, thus leading to better integration and functionality of the construct (Chu *et al*., 2002). With respect to the quality and 3D penetration of the newly formed bone, the development of substantial angiogenesis is a key feature for cell colonization and new bone formation in the inner parts of the scaffolds. It was observed that, by increasing pore size from 100 to 300–400 μm, the extent of bone formation increased, also evidenced by the expression of osteocalcin and alkaline phosphatase. Moreover, bone scaffolds with porosity in the 300–400 μm range were the minimum requirement for achieving capillary development (Tsuruga *et al*., 1997; Kuboki *et al*., 2001). The positive effect of angiogenesis was also highlighted in further studies and a correlation was shown between the pore size and the cell phenotype expressed in contact with the HA scaffold. In particular, smaller sizes induce chondrogenesis and then osteogenesis via further mineralization. In contrast, larger pores induce direct osteogenesis; this result was correlated with the extensive angiogenesis that was detected, which was promoted by increased oxygen tension and supply of nutrients (Jin *et al*., 2000; Kuboki *et al*., 2001, 2002). The pore morphology also had an effect on direct bone formation; pore tortuosity and restraints in the pore lumen hindered the penetration of cells and the development of angiogenesis, thus resulting in the formation of new bone only in the outer part of the scaffold (Kuboki *et al*., 2002). As a result of the ordered porosity, a channel-like orientation of pores was found to promote the synthesis of osteon structures, whereas randomly-oriented porosity was more likely to favor the formation of woven new bone (Chang *et al*., 2000). In this respect, when specific orientation is present and pore tortuosity is reduced, the development of blood vessels can be achieved in cases where the pore size was lowered to ~50 μm.

The repair/regeneration of large bone defects is still a concern due to several factors, including the reduced mechanical strength of bioactive materials and the insufficient cell conductivity in the scaffold core. Over

the last two decades, the strategies to repair large bone defects have been increasingly oriented toward the use of scaffolds associated with tissue-engineering strategies. In particular, cell seeding on bone scaffolds can greatly enhance the extent of cell colonization, which has a positive impact on tissue regeneration (Kon *et al*., 2000; Petite *et al*., 2000; Schliephake *et al*., 2001; Annaz *et al*., 2004; Bensaïd *et al*., 2005; Marcacci *et al*., 2007; Yuan *et al*., 2007). However, in this case the use of scaffolds with highly exposed and interconnected macro-porosity is mandatory. In fact, many of the current tissue-engineering scaffold-based strategies have suffered from limited cell-depth viability when cultured *in vitro*, with viable cells only existing within the outer 250–500 μm from the fluid–scaffold interface (Freed *et al*., 1994; Dunn *et al*., 2006). This is believed to be due to a lack of nutrient delivery and of waste removal from the inner regions of the scaffold (Ishaug-Riley *et al*., 1998; Galban and Locke, 1999). Bone substitutes have been used in combination with osteogenic cells for use in the prefabrication of bioartificial bone grafts in several studies with animals (Ellisseef *et al*., 2000; Nuttelman *et al*., 2006; Tampieri *et al*., 2011). The use of multipotent mesenchymal stem cells (MSC) has opened up new therapeutic options for bone substitution (Ohgushi *et al*., 1989). The scaffold can be implanted into the patient to function as replacement tissue after *in vitro* MSC colonization, or it may be seeded with MSCs during surgery. From a clinical perspective, the establishment of channel-like porosity may increase cell seeding efficiency and the distribution of viable cells in the inner part of the scaffolds by improving fluid conductivity and permeability. This feature helps to prevent the formation of necrotic regions (Conor and O'Kelly, 2010) and also creates anisotropic mechanical strength, i.e. increased resistance along the direction of the channels, which can promote the development of new bone with tailored textures and is thus particularly suitable for segmental bone regeneration (see the next section). The primary fixation and the absence of micro-movements, in particular during the early stages after *in vivo* implantation, are also key factors that ensure cell colonization and osteointegration. A recent study developed bone scaffolds made of hydroxyapatite via a foaming method that were used in the replacement of sheep TMJ condyles (Ciocca *et al*., 2012). CAD/CAM techniques were used extensively for the virtual creation of mandibular bone defects and subsequent 3D scaffold prototyping and machining, in order to achieve precise adaptation to the bone defect. Also, fixation media were suitably designed and produced for optimal scaffold fixation. The scaffold porosity was designed to have 150–500 μm pores, interconnected by 70–120 μm pores; smaller size micropores (10 μm) were also present, which played a primary role in the first stages of cell anchorage and attachment. This approach enabled firm stabilization of the scaffold upon implantation and the formation of new bone throughout the whole scaffold.

In spite of the ever-increasing potential offered by current manufacturing approaches, there are limitations in achieving high biomimicry of the target tissues and controlled bio-resorption behavior. Hybrid scaffolds manufactured by biologically inspired assembling/organization/mineralization processes represent a new concept in tissue regeneration (see also previous section). *In vivo* studies on sheep have demonstrated that the chemical–physical and morpho-structural characteristics of the biologically inspired graded composites functioned as biomimetic cues that were able to differentially support and direct the formation of different tissues (i.e. bone and cartilage) in the different histological layers, as occurring in the native healthy tissues (Kon *et al.*, 2010). The formation of newly hyaline-like tissue and orderly patterns of tissue could also take place in the case of implantation without any seeded cells, with a strong proteoglycan staining and columnar rearrangement of chondrocytes, as well as an underlying well-structured sub-chondral trabecular bone. Moreover, the biological-like features of the scaffolds allowed complete resorption and replacement with new healthy tissue, which was detected after only six months from implantation. The high elasticity of these scaffolds provided good shape memory that allowed easy deformation and adaptation to bone cavities by press-fit. These properties are of great relevance in orthopedic surgery, since ease of handling in the implantation of scaffolds is a feature that helps greatly to increase the level of reliability and confidence.

9.6 Future trends

The new concept of fabrication based on the reproduction of biological processes may pave the way to a new generation of smart devices with multiple functionalities. However, the low mechanical properties of the hybrid tissue-mimicking devices are described in the previous section, as a result of their soft nature, pose some limitations in their use. In particular, the regeneration of segmental long bones is still an unmet clinical need. Presently, the healing of load-bearing bone segments still relies on bioinert dense implants based on alumina, titanium, etc., due to the inability of the current manufacturing technologies to form mechanically strong porous inorganic structures with a hierarchic pore organization and complex morphological details in the sub-micron scale. The main goal is the implantation of osteoinducting, osteoconducting scaffolds with spatially organized macroporosity and mechanical strength sufficient for early *in vivo* loading upon implantation and elastic properties close to those of bone. This may enable scaffolds to actively respond to the complex biomechanical loads and activate the mechano-transduction processes, yielding formation and remodeling of new functional bone (Ingber, 1993; Sikavitsas, 2001; Bilezikian *et al.*, 2002; Pavalko *et al.*, 2003). The outstanding mechanical performances of

bones are mostly due to their complex structure, hierarchically organized from the nano- to the macro-scale, and to the interaction taking place across all levels of organization. For this reason, long-bone regeneration should be assisted by scaffolds endowed with bone-like composition and similar structural complexity; however, the conventional manufacturing methods do not produce inorganic, mechanically resistant scaffolds with the required bioactivity and hierarchical pore organization. The expression of chemical biomimesis in scaffolds for long-bone regeneration is made difficult by the reduced mechanical strength of HA-based materials. Several solutions based on composite materials have been studied, making use of strong bioinert or bioactive phases (Abdelrazek *et al*., 2007; Heilmann *et al*., 2007; Sung *et al*., 2007; Encinas-Romero *et al*., 2008; Sprio *et al*., 2009) that were dispersed in a calcium phosphate matrix. However, the limitation in the achievement of hierarchically organized structures still remains.

To address this problem, the attention of scientists has been dedicated to investigating and reproducing complex morphologies that exist in nature, particularly among ligneous structures that strongly resemble bones in their morphology, structural organization, and mechanical performances (Wegst and Ashby, 2004; Fratzl and Weinkamer, 2007).

Like bone, wood can be regarded as a cellular material at the scale of hundred micrometers to centimeters. At the cell level, the mechanical properties are governed by the diameter and shape of the cell cross-section, as well as by the thickness of the cell wall. In particular, the ratio of cell-wall thickness to cell diameter is directly related to the apparent density of wood, which in turn is a determining factor for the performance of lightweight structures (Fengel and Wegener, 1989). The unique hierarchical architecture of the cellular microstructure gives wood a remarkable combination of high strength, stiffness, and toughness at low density (Gibson, 1992; Lucas *et al*., 1995). The alternation of fiber bundles and channel-like porous areas makes the wood an elective material to be used as a template in the preparation of a new bone substitute that is characterized by a biomimetic hierarchical structure.

The transformation of wood into inorganic, hierarchically organized materials (e.g. oxidic ceramics such as Al_2O_3, ZrO_2, TiO_2, MnO and non-oxidic ceramics such as SiC, TiC, ZrC) was the subject of investigation in the late 1990s (Greil *et al*., 1998a, 1998b; Binghe *et al*., 2004; de Arellano-Lopez *et al*., 2004; Singh and Yee, 2004; Cao *et al*., 2004a, 2004b; Rambo and Sieber, 2005; Rambo *et al*., 2005; Li *et al*., 2006). This approach was addressed to the synthesis of hierarchically organized bone scaffolds made of SiC (de Arellano-Lopez *et al*., 2004), which have the advantage of offering very high fracture strength and bio-tolerated surfaces. More recently, these kinds of biomorphic transformations were also used to manufacture hierarchically organized scaffolds made of hydroxyapatite (Tampieri *et al*. 2009).

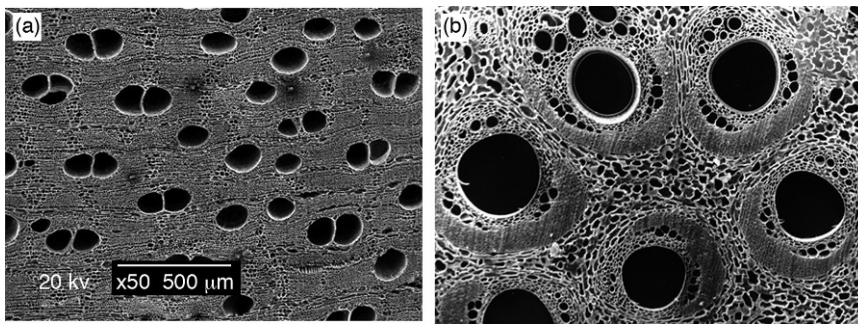

9.7 Microstructure of pyrolyzed woods. (a) sipo wood; (b) rattan wood.

The complexity of the apatite phase, in comparison with oxides, carbides, and nitrides, required the settling of a multi-step transformation route, where the native wood was sequentially transformed into pure carbon, calcium carbide, calcium oxide, calcium carbonate, and finally hydroxyapatite. Due to their bone-mimicking composition, microstructure, and hierarchical organization, these newly conceived bioceramics promise to offer enhanced osteogenesis, integration and biomechanical behavior when implanted *in vivo*.

Woods such as rattan and sipo have strong morphological similarities to spongy and cortical bones, respectively (Fig. 9.7). Rattan is characterized by channel-like pores (simulating the Haversian system in bone), interconnected with a network of smaller channels (such as the Volkmann system) (Tampieri *et al.*, 2009). Sipo is a tougher, denser wood that has a microporosity that can promote cell adhesion and anchorage.

The multi-step transformation process (Fig. 9.8) allowed precise control of the phase composition, crystallinity, and microstructure, since the different reactions occurred between a gas and the solid template, where calcium, oxygen, carbonate, and phosphate ions were progressively added while building the HA molecules. The control of the kinetic reaction throughout the different steps of the transformation process enabled precise control of the scaffold composition, microstructure, and bioactivity (Ruffini *et al.*, 2013). Importantly, the maintenance of the original wood microstructure allowed scaffolds to exhibit mechanical strengths comparable to those of spongy bone (~4 MPa) when measured along the channel direction, even in the absence of thermal consolidation treatments. The bioactivity of the rattan-derived HA scaffolds was assessed by *in vitro* investigation of MG63 osteoblast-like cells' adhesion and morphology in contact with the scaffold, revealing a nearly complete covering of the scaffold surface after only 7 days (Fig. 9.9) and a good morphology of the attached cells, which were well distributed on the scaffold trabeculae. The cells appeared to interact

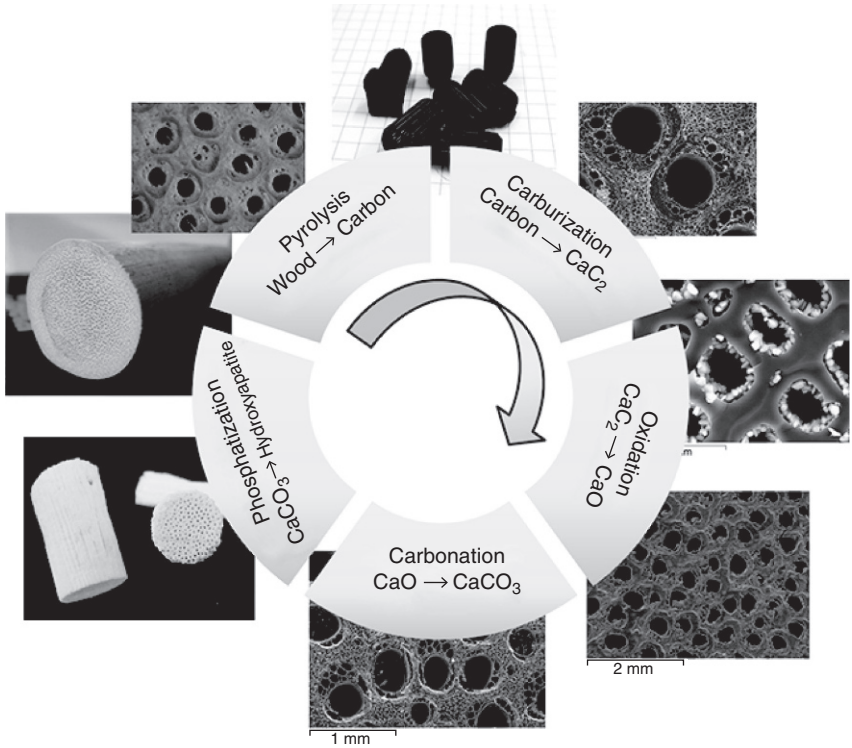

9.8 Scheme illustrating the multi-step transformation process of natural wood into biomorphic HA scaffold.

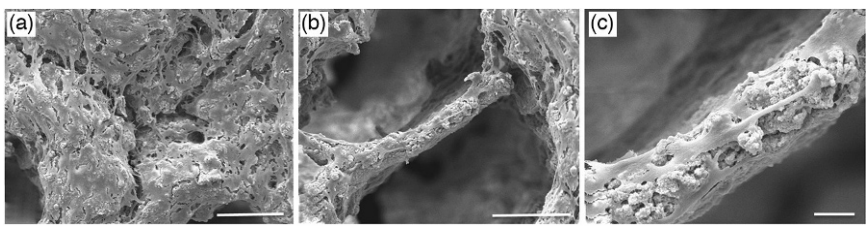

9.9 SEM image of human osteoblast-like cells seeded on rattan-derived HA scaffold. Scale bars: (a, b) 150 μm. (c) 20 μm.

closely with the scaffold surface, which is evidence of good material biocompatibility. The implantation of rattan-derived scaffolds in critical defects created in the femoral distal epiphysis of skeletally mature, adult, disease-free, New Zealand White rabbits confirmed the *in vivo* bioactivity and osteoconductivity after 1 month follow-up. Extensive bone formation inside the scaffold channels with a regular architectural pattern was detected, without any

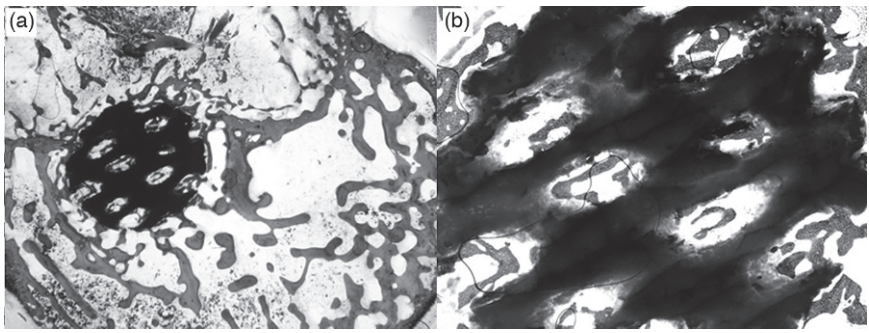

9.10 (a) Histomorphometry of a biomorphic bone implant made of rattan-derived HA, inserted into a diaphyseal defect in rabbit. Follow-up time: one month.; (b) a detail evidencing osteointegration.

inflammatory or toxic reaction against the scaffolds, nor connective capsules or bone gaps (Fig. 9.10).

The establishment of biomorphic transformations that are able to transform woods into biomimetic bone scaffolds can provide solutions for long-bone regeneration and can be designed in a custom-made fashion. The association of a mechanically resistant cortical-like shell and a highly biomimetic sponge-like core may enable the substitution of segmental bone parts (Tampieri *et al*., 2011b). Selected wood structures could reproduce different bone portions that are characterized by different porosities and pore distributions, as occurring in cortical and spongy bones. Such structures can enable complete regeneration of bones, in particular long bones, provided that: (i) the core exhibits a structure with bone-like composition and is highly permeable to cells and physiological fluids to allow cell colonization and proliferation as well as extensive angiogenesis; and (ii) the external shell exhibits porosity sufficient for cell anchorage and mechanical strength that is able to withstand biomechanical stimuli, so as to load the scaffold soon after implantation.

Such devices may enable the establishment of a biological chamber that encloses a suitable environment that is conditioned to promote and enhance bone formation and remodeling. The implant will function as an *in vivo* bioreactor, thus facing an unsolved clinical problem related to the vanishing of the regenerative process at distances far from the bone–implant interface.

9.7 Conclusion

With the continuous advances in material science and nanotechnology, great progress has been made in the development of biomedical devices for bone regeneration. However, some serious limitations still exist that are related

to the development of bio-devices that mimic the structure and composition of biological tissues with high complexity and load-bearing properties, such as extended bone and osteochondral parts or segmental bones. For this reason, in the absence of well-established regenerative devices for such applications, the related clinical needs remain unmet and their socio-economic impact is large and continuously increasing due to the progressive aging of the population and the new lifestyles that expose younger people to serious injuries and traumas. The recent advances in materials science offer many possibilities for solving these concerns in the coming decades; the new fabrication approaches that draw inspiration from nature and from the multitude of outstanding biological structures and phenomena will enable a new generation of smart and multi-functional devices. Moreover, the recent discovery of superparamagnetism in bioactive Fe-substituted apatite will pave the way for new biomedical devices endowed with a number of smart functionalities that can be switched on and off by exposure to magnetic fields. Bio-inspiration and remote activation are thus two new concepts that will allow material science and knowledge of biomaterials to progress well beyond the current state of the art and will give an outstanding contribution to the biomedical field. The preliminary steps that have already been taken in this direction are very promising and, although the development of bio-inspired materials is still in its infancy, it is rapidly becoming a priority for the development of new smart materials. It is expected that, in the years to come, a number of unmet clinical needs will benefit from a new generation of biologically inspired smart devices.

9.8 References

Abdelrazek, K.K., Won, K.S. and Yong, K.H. (2007). Consolidation and mechanical properties of nanostructured hydroxyapatite.(ZrO_2 C 3 mol% Y_2O_3) bioceramics by highfrequency induction heat sintering. *Mater. Sci. Eng. A*, **456**(1.2), 368–372.

An, Y.H., Woolf, S.K. and Friedman, R.J. (2000). Pre-clinical in vivo evaluation of orthopaedic bioabsorbable devices. *Biomaterials*, **21**(24), 2635–2652.

Annaz, B., Hing, K.A., Kayser, M., Buckland, T. and Di Silvio, L. (2004). Porosity variation in hydroxyapatite and osteoblast morphology: a scanning electron microscopy study. *J. Micr.*, **215**(1), 100–110.

Babis, G.C. and Soucacos, P.N. (2005). Bone scaffolds: The role of mechanical stability and instrumentation. *Int. J. Care Injured*, **36S**, S38–S44.

Balasundaram, G., Sato, M. and Webster, T.J. (2006). Using hydroxyapatite nanoparticles and decreased crystallinity to promote osteoblast adhesion similar to functionalizing with RGD. *Biomaterials*, **27**, 2798–2805.

Bañobre-Lopez, M., Pineiro-Redondo, Y., De Santis, R., Gloria, A., Ambrosio, L., Tampieri, A., Dediu, V. and Rivas, J. (2011). Poly(caprolactone) based magnetic scaffolds for bone tissue engineering. *J. Appl. Phys.*, **109**(7), 07B313.

Bensaïd, W., Oudina, K., Viateau, V., Poitier, E., Bousson, V., Blanchat, C., Sedel, L., Guillemin, G. and Petite, H. (2005). De novo reconstruction of functional bone by tissue engineering in the metatarsal sheep model. *Tissue Eng*., **5–6**, 814–824.

Bertinetti, L., Tampieri, A., Landi, E., Martra, G. and Coluccia, S. (2006). Punctual investigation of surface sites of HA and magnesium-HA. *J. Eur. Ceram. Soc.*, **26** (6), 987–991.

Bigi, A., Foresti, E., Gregorini, R., Ripamonti, A., Roveri, N. and Shah, J.S. (1992). The role of magnesium on the structure of biological apatite. *Calcif. Tissue Int.*, **50**, 439–444.

Bigi, A., Cojazzi, G., Panzavolta, S., Ripamonti, A., Roveri, N., Romanello, M., Noris Suarez, K. and Moro, L. (1997). Chemical and structural characterization of the mineral phase from cortical and trabecular bone. *J. Inorg. Biochem.*, **68**, 45–51.

Bigi, A., Boanini, E., Cappuccini, C. and Gazzano, M. (2007). Strontium-substituted hydroxyapatite nanocrystals. *Inorg. Chim. Acta*, **360**, 1009–1016.

Bilezikian, J.P., Raisz, L.G. and Rodan, G.A. (2002). Principles of bone biology, vol. **1**, Academic Press, San Diego.

Binghe, S., Tongxiang, F., Di, Z. and Okabe, T. (2004). The synthesis and microstructure of morph-genetic TiC/C ceramics. *Carbon*, **42**, 177–182.

Boanini, E., Gazzano, M. and Bigi, A. (2010). Ionic substitutions in calcium phosphates synthesized at low temperature. *Acta Biomater*., **6**, 1882–1894.

Boskey, A.L. (2006). Mineralization, structure and function of bone, in: Seibel, M.J., Robins, S.P. and Bilezikian, J.P. (Eds.), *Dynamics of Bone and Cartilage Metabolism*. Academic Press, San Diego.

Boyan, B.D., Hummert, T.W., Dean, D.D. and Schwartz, Z. (1996). Role of material surfaces in regulating bone and cartilage cell response. *Biomaterials*, **17**, 137–146.

Brown, M.E. and Puleo, D.A. (2008). Protein binding to peptide-imprinted porous silica scaffolds. *Chem. Eng. J.*, **137**, 97–101.

Burdick, J.A., Padera, R.F., Huang, J.V. and Anseth, K.S. (2002). An investigation of the cytotoxicity and histocompatibility of in situ forming lactic acid based orthopedic biomaterials. *J. Biomed. Mater. Res*., **63**(5), 484–491.

Burdick, J.A., Frankel, D., Dernell, W.S. and Anseth, K.S. (2003). An initial investigation of photocurable three-dimensional lactic acid based scaffolds in a critical-sized cranial defect. *Biomaterials*, **24**(9), 1613–1620.

Cao, J., Rambo, C. R. and Sieber, H. (2004a). Preparation of porous Al_2O_3-ceramics by biotemplating of wood. *J. Por. Mater*., **11**, 163–172.

Cao, J., Rusina O. and Sieber, H. (2004b). Processing of porous TiO2-ceramics from biological preforms. *Ceram. Int*., **30**, 1971–1974.

Capriotti, L.A., Beebe, T.P., Jr. and Schneider, J.P. (2007). Hydroxyapatite surface-induced peptide folding. *J. Am. Chem. Soc*., **129**, 5281–5287.

Carlisle, E.M. (1970). Silicon: a possible factor in bone calcification. *Science*, **167**, 279–280.

Carlisle, E.M. (1988). Silicon as a trace nutrient. *Sci. Total Environ*., **73**, 95–106.

Cazalbou, S., Eichert, D., Ranz, X., Drouet, C., Combes, C., Harmand, M.F. and Rey, C. (2005). Ion exchanges in apatites for biomedical applications. *J. Mater. Sci: Mater. Med*., **16**, 405–409.

Celotti, G., Tampieri, A., Sprio, S., Landi, E., Bertinetti, L., Martra, G. and Ducati, C. (2006). Crystallinity in apatites: what is the disordered fraction made of?. *J. Mater. Sci: Mater. Med*., **17**, 1079–1087.

Chang, B.-S., Lee, C.-K., Hong, K.-S., Youn, H.-J., Ryu, H.-S., Chung, S.-S. and Park, K.-W. (2000). Osteoconduction at porous hydroxyapatite with various pore configurations. *Biomaterials*, **21**, 1291–1298.

Chu, T.M., Orton, D.G., Hollister, S.J., Feinberg, S.E. and Halloran, J.W. (2002). Mechanical and in vivo performance of hydroxyapatite implants with controlled architectures. *Biomaterials*, **23**(5), 1283–1293.

Ciocca, L., Donati, D., Fantini, M., Landi, E., Piattelli, A., Iezzi, G., Tampieri, A., Spadari, A., Romagnoli, N. and Scotti, R. (2012). CAD-CAM-generated hydroxyapatite scaffold to replace the mandibular condyle in sheep: Preliminary results. *J Biomater Appl.*, 5 April 2012, 22492196.

Conor, T.B. and O'Kelly, K.U. (2010). Fabrication and characterization of a porous multidomain hydroxyapatite scaffold for bone tissue engineering investigations. *J Biomed Mater Res Part B: Appl Biomater*, **93B**, 459–467.

Cooke, F.W. (1992). Ceramics in orthopedic surgery. *Clin. Orthop*., **276**, 135–146.

Corno, M., Rimola, A., Bolis, V. and Ugliengo, P. (2010). Hydroxyapatite as a key biomaterial: quantum-mechanical simulation of its surfaces in interaction with biomolecules. *Phys. Chem. Chem. Phys*., **12**, 6309–6329.

Crespi, R., Mariani, E., Benasciutti, E., Capparè, P., Cenci, S. and Gherlone, E. (2009). Magnesium-enriched hydroxyapatite versus autologous bone in maxillary sinus grafting: combining histomorphometry with osteoblast gene expression profiles ex vivo. *J. Periodontol*., **80**(4), 586–593.

Cunha, C., Sprio, S., Panseri, S., Dapporto, M., Marcacci, M. and Tampieri, A. (2013). High biocompatibility and improved osteogenic potential of novel Ca-P/titania composite scaffolds designed for regeneration of load-bearing segmental bone defects. *J. Biomed. Mater. Res.: Part A*., 101A(6), 1612-1619.

Daculsi, G., (1998). Biphasic calcium phosphate concept applied to artificial bone, implant coating and injectable bone substitute. *Biomaterials*, **19**, 1473–1478.

Dahl, S.G., Allain, P., Marie, P.J., Mauras, Y., Boivin, G., Ammann, P., Tsouderos, Y., Delmas, P.D. and Christiansen, C. (2001). Incorporation and distribution of strontium in bone. *Bone*, **28**(4), 446–453.

de Arellano-Lopez, A. R., Martinez-Fernandez, J., Gonzalez, P., Dominguez, C., Fernandez-Quero, V. and Singh, M. (2004). Biomorphic SiC: A new engineering ceramic material. *Int. J. Appl. Ceram. Technol*., **1** (1), 56–67.

Deville, S., Saiz, E. and Tomsia, A.P. (2006). Freeze casting of hydroxyapatite scaffolds for bone tissue engineering. *Biomaterials*, **27**, 5480–5489.

Deville, S. (2008). Freeze-casting of porous ceramics: A review of current achievements and issues. *Adv. Eng. Mater*., **10**, 155–169.

Driessens, F.C.M. (1980). The mineral in bone, dentin and tooth enamel. *Bull. Soc. Chim. Belg*., **89**, 663–689.

Dunn, J.C., Chan, W.Y., Cristini, V., Kim, J.S., Lowengrub, J., Singh, S. and Wu, B.M. (2006). Analysis of cell growth in three-dimensional scaffolds. *Tissue Eng*., **12**, 705–716.

Durrieu, M.C., Pallu, S., Guillemot, F., Bareille, R., Amédée, J., Baquey, C., Labrugère, C. and Dard, M., (2004). Grafting RGD containing peptides onto hydroxyapatite to promote osteoblastic cells adhesion. *J. Mater. Sci.: Mater. Med*., **15**, 779–786.

Ellisseef, J., McIntosh, W., Anseth, K., Riley, S., Ragan, P. and Langer, R., (2000). Photoencapsulation of chondrocytes in poly(ethylene oxide)-based semi-interpenentrating networks. *J. Biomed. Mater. Res. A*., **51**(2), 164–171.

Encinas-Romero, M.A., Aguayo-Salinas, S., Castillo, S.J., Castillón-Barraza, F.F. and Castano, V.M. (2008). Synthesis and characterization of hydroxyapatite–wollastonite composite powders by sol–gel processing. *Int. J. Appl. Ceram. Technol*., **5**(4), 401–411.

Fengel, D. and Wegener, G. (1989). *Wood: Chemistry, Ultrastructure, Reactions*, de Gruyter, Berlin.

Fratzl, P. and Weinkamer, R. (2007). Nature's hierarchical materials. *Progr. Mater. Sci*., **52**, 1263–1334.

Freed, L.E., Marquis, J.C., Langer, R. and Vunjak-Novakovic, G. (1994). Kinetics of chondrocyte growth in cell-polymer implants. *Biotechnol. Bioeng*., **43**, 597–604.

Galban, C.J. and Locke, B.R. (1999). Analysis of cell growth kinetics and substrate diffusion in a polymer scaffold. *Biotechnol. Bioeng*., **65**, 121–132.

Gibson, E.J. (1992). Wood: a natural fibre reinforced composite. *Met. Mater*., **6**, 333–336.

Gloria, A., Russo, T., D'Amora, U., Zeppetelli, S., D'Alessandro, T., Sandri, M., Bañobre-López, M., Piñeiro-Redondo, Y., Uhlarz, M., Tampieri, A., Rivas, J., Herrmannsdörfer, T., Dediu, V.A., Ambrosio, L. and De Santis, R. (2013). Magnetic poly(e-caprolactone)/iron-doped hydroxyapatite nanocomposite substrates for advanced bone tissue engineering. *J. R. Soc. Interf*, **10**, 20120833.

Gotz, H.E., Muller, M., Emmel, A., Holzwarth, U., Erben, R.G. and Stangl, R. (2004). Effect of surface finish on the osseointegration of laser-treated titanium alloy implants. *Biomaterials*, **25**(18), 4057–4064.

Greil, P., Lifka, T. and Kaindl, A. (1998a). Biomorphic cellular silicon carbide ceramics from wood: I. processing and microstructure. *J. Eu. Ceram. Soc*., **18**, 1961–1973.

Greil, P., Lifka, T. and Kaindl, A. (1998b). Biomorphic cellular silicon carbide ceramics from wood: II. mechanical properties. *J. Eu. Ceram. Soc*., **18**, 1975–1983.

Guo, D., Xu, K., Zhao, X. and Han, Y. (2005). Development of a strontium-containing hydroxyapatite bone cement. *Biomaterials*, **26**(19), 4073–4083.

Heilmann, F., Standard, O.C., Müller, F.A. and Hoffmann, M. (2007). Development of graded hydroxyapatite/CaCO3 composite structures for bone ingrowth. *J. Mater. Sci. Mater. Med*., **18**(9), 1817–1824.

Hench, L.L. and Polak, J.M. (2002). Third-generation biomedical materials. *Science*, **295**, 1014–1017.

Hersel, U., Dahmen, C. and Kessler, H. (2003). RGD modified polymers: biomaterials for stimulated cell adhesion and beyond. *Biomaterials*, **24**, 4385–4415.

Hu, Y., Grainger, D.W., Winn, S.R. and Hollinger, J.O. (2002). Fabrication of poly(alpha-hydroxy acid) foam scaffolds using multiple solvent systems. *J. Biomed. Mater. Res*., **59**(3), 563–572.

Hulbert, S.F., Young, F.A., Mathews, R.S., Klawitter, J.J., Talbert, C.D. and Stelling, F.H. (1970). Potential of ceramic materials as permanently implantable skeletal prostheses. *J. Biomed. Mater. Res*., **4**(3), 433–456.

Iafisco, M., Morales, J.G., Hernandez-Hernandez, M.A., Garcia-Ruiz, J.M. and Roveri, N. (2010). Biomimetic carbonate hydroxyapatite nanocrystals prepared by vapour diffusion. *Adv. Eng. Mater*., **12**(7), B218–B233.

Iafisco, M., Palazzo, B., Ito, T., Otsuka, M., Senna, M., Delgado-Lopez, J.M., Gomez-Morales, J., Tampieri, A., Prat, M. and Rimondini, L. (2012). Preparation of core-shell poly(L-lactic) acid-nanocrystalline apatite hollow microspheres for bone repairing applications. *J. Mater Sci.: Mater. Med*., **23**(11), 2659–2669.

Ingber, D.E. (1993). Cellular tensegrity: defining new rules of biological design that govern the cytoskeleton. *J. Cell. Sci*., **104**, 613–627.

Ishaug-Riley, S.L., Crane-Kruger, G.M., Yaszemski, M.J. and Mikos, A.G. (1998). Three-dimensional culture of rat calvarial osteoblasts in porous biodegradable polymers. *Biomaterials*, **19**, 1405–1412.

Jin, Q.M., Takita, H., Kohgo, T., Atsumi, K., Itoh, H. and Kuboki, Y. (2000). Effects of geometry of hydroxyapatite as a cell substratum in BMP-induced ectopic bone formation. *J. Biomed. Mater. Res*., **51**(3), 491–499.

Jugdaohsingh, R. (2007). Silicon and bone health. *J. Nutr. Health Aging*, **11**(2), 99–110.

Kandori, K., Fudo, A. and Ishikawa, T. (2002). Study on the particle texture dependence of protein adsorption by using synthetic micrometer-sized calcium hydroxyapatite particles. *Colloids Surf., B*. **24**, 145–153.

Karageorgiou, V. and Kaplan, D. (2005). Porosity of 3D biomaterial scaffolds and osteogenesis. *Biomaterials*, **26**, 5474–5481.

Kessler, S., Mayr-Wohlfart, U., Ignatius, A., Puhl, W., Claes, L. and Günther, K.P. (2003). Der Einfluss von Bone Morphogenetic Protein-2 (BMP-2), Vascular Endothelial Growth Factor (VEGF) und basischem Fibroblastenwachstumsfaktor (b-FGF) auf Osteointegration, Degradation und biomechanische Eigenschaften eines synthetischen Knochenersatzstoffes. *Z. Orthop*., **141**, 472–480

Kon, E., Muraglia, A., Corsi, A., Bianco, P., Marcacci, M., Martin, I., Boyde, A., Ruspantini, I., Chistolini, P., Rocca, M., Giardino, R., Cancedda, R. and Quarto, R. (2000). Autologous bone marrow stromal cells loaded onto porous hydroxyapatite ceramic accelerate bone repair in critical-size defects of sheep long bones. *J. Biomed. Mater. Res*., **3**, 328–337.

Kon, E., Delcogliano, M., Filardo, G., Fini, M., Giavaresi, G., Francioli, S., Martin, I., Pressato, D., Arcangeli, E., Quarto, R., Sandri, M. and Marcacci, M. (2010) Orderly osteochondral regeneration in a sheep model using a novel nano-composite multilayered biomaterial, *J. Orthop. Res.*, **28**, 116–124.

Kuboki, Y., Jin, Q. and Takita, H. (2001). Geometry of carriers controlling phenotypic expression in BMP-induced osteogenesis and chondrogenesis. *J. Bone Joint Surg. Am*., **83A** (1.2), S105–115.

Kuboki, Y., Jin, Q., Kikuchi, M., Mamood, J. and Takita, H. (2002). Geometry of artificial ECM: sizes of pores controlling phenotype expression in BMP-induced osteogenesis and chondrogenesis. *Connect. Tissue Res*., **43**(2–3), 529–534.

Landi, E., Tampieri, A., Celotti, G. and Sprio, S. (2000). Densification behaviour and mechanisms of synthetic hydroxyapatites. *J. Eu. Ceram. Soc*., **20**, 2377–2387.

Landi, E., Tampieri, A., Celotti, G., Langenati, R., Sandri, M. and Sprio, S. (2005). Nucleation of biomimetic apatite in synthetic body fluids: dense and porous scaffold development. *Biomaterials*, **26**, 2835–2845.

Landi, E. Tampieri, A., Celotti, G., Sprio, S., Sandri, M. and Logroscino, G. (2007). Sr-substituted hydroxyapatites for osteoporotic bone replacement. *Acta Biomater*., **3**, 961–969.

Landi, E., Sprio, S., Sandri, M., Tampieri, A., Bertinetti, L. and Martra, G. (2008a). Development of multisubstituted apatites for bone reconstruction. *Key Eng. Mat*., **361–363**, 171–174.

Landi, E. Logroscino, G., Proietti, L., Tampieri, A., Sandri, M. and Sprio, S. (2008b). Biomimetic Mg-substituted Hydroxyapatite: from synthesis to in vivo behaviour. *J. Mater. Sci: Mater. Med*., **19**, 239–247.

Landi, E., Valentini, F. and Tampieri, A. (2008c). Porous hydroxyapatite/gelatine scaffolds with ice designed channel-like porosity for biomedical applications. *Acta Biomater*., **4**, 1620–1626.

Landi, E., Uggeri, J., Sprio, S., Tampieri, A. and Guizzardi, S. (2010). Human osteoblast behavior on as-synthesized SiO_4 and B-CO_3 co-substituted apatite. *J. Biomed. Mater. Res. A*, **94**, 59–70.

LeGeros, R.Z. and LeGeros, J.P. (1984). Phosphate minerals in human tissues, in: Nriagu J.O. and Moore P.B., (Eds), *Phosphate minerals*. Springer-Verlag, New York.

LeGeros, R.Z. (1991). Calcium phosphates in oral biology and medicine, *Monogr. Oral Sci.*, **15**, 1–201.

Li, W.J., Laurencin, C.T., Caterson, E.J., Tuan, R.S. and Ko, F.K. (2002). Electrospun nanofibrous structure: a novel scaffold for tissue engineering. *J. Biomed. Mater. Res*., **60**(4), 613–621.

Li, X., Feng, Q., Jiao, Y. and Cui, F. (2005). Collagen-based scaffolds reinforced by chitosan fibres for bone tissue engineering. *Pol. Int*., **54**, 1034–1040.

Li, X., Fan, T., Liu, Z., Ding, J., Guo, Q. and Zhang, D. (2006). Synthesis and hierarchical pore structure of biomorphic manganese oxide derived from woods. *J. Eu. Ceram. Soc*., **26**, 3657–3664.

Linde, A. and Goldberg, M. (1993). Dentinogenesis. *Crit. Rev. Oral Biol. Med*., **4**(5), 679–728.

Lowenstam, H.A. and Weiner, S. (1989). *On Biomineralization*. Oxford University Press: New York.

Lu, H., Qu, Z. and Zhou, Y. (1998). Preparation and mechanical properties of dense polycrystalline hydroxyapatite through freeze-drying. *J. Mater. Sci.: Mater. Med*., **9**, 583–587.

Lucas, P.W., Darvell, B.W., Lee, P.K.D., Yuen, T.D.B. and Choong, M.F. (1995). The toughness of plant cell walls. *Phil. Trans. Roy. Soc. B*, **348**, 363–372.

Mann, S. (Ed.) (2001) *Bio-Mineralization: Principles and Concepts in Bioinorganic Materials Chemistry*, Oxford University Press: Oxford.

Mano, J.F., Silva, G.A., Azevedo, H.S., Malafaya, P.B., Sousa, R.A., Silva, S.S., Boesel, L.F., Oliveira, J.M., Santos, T.C., Marques, A.P., Neves, N.M. and Reis, R.L. (2007). Natural origin biodegradable systems in tissue engineering and regenerative medicine: Present status and some moving trends. *J. Royal Soc. Interf*., **4**, 999–1030.

Marcacci, M., Kon, E., Moukhachev, V., Lavroukov, A., Kutepov, S., Quarto, R., Mastrogiacomo, M. and Cancedda, R. (May 2007) Stem cells associated with macroporous bioceramics for long bone repair: 6- to 7-year outcome of a pilot clinical study. *Tissue Eng*., **13**(5), 947– 955.

Marie, J.P., Ammann, P., Boivin, G. and Rey, C. (2001). Mechanisms of action and therapeutic potential of strontium in bone. *Calcif. Tissue Int*., **69**, 121–129.

Meyers, M.A., Chen, P.-Y., Yu-Min Lin, A. and Seki, Y. (2008). Biological materials: Structure and mechanical properties. *Progr. Mater. Sci*., **53**, 1–206.

Nuttelman, C.R., Benoit, D.S.W., Tripodi, M.C. and Anseth, K.S. (2006). The effect of ethylene glycol methacrylate phosphate in PEG hydrogels on mineralization and viability of encapsulated hMSCs. *Biomaterials*, **27**(8), 1377–1386.

Oh, S.H., Kang, S.G., Kim, E.S., Cho, S.H. and Lee, J.H. (2003). Fabrication and characterization of hydrophilic poly(lactic-co-glycolic acid)/poly(vinyl alcohol) blend cell scaffolds by melt-molding particulate-leaching method. *Biomaterials*, **24**(22), 4011–4021.

Ohgushi, H., Goldberg, V.M. and Caplan, A.I. (1989). Heterotopic osteogenesis in porous ceramics induced by marrow cells. *J. Orthop. Res*., **7**, 568–578.

Panseri, S., Russo, A., Giavaresi, G., Sartori, M., veronesi, F., Fini, M., Salter, D.M., Ortolani, A., Strazzari, A., Visani, A., Dionigi, C., Bock, N., Sandri, M., Tampieri, A. and Marcacci, M. (2012a). Innovative magnetic scaffolds for orthopaedic tissue engineering. *J. Biomed. Mater. Res. A*, **100A**(9), 2278–2286.

Panseri, S., Cunha, C., D'Alessandro, T., Sandri, M., Russo, A., Giavaresi, G., Marcacci, M., Hung, C.T. and Tampieri, A. (2012b). Magnetic hydroxyapatite bone substitutes to enhance tissue regeneration: Evaluation in vitro using osteoblast-like cells and in vivo in a bone defect. *PLOS ONE*, **7**(6), e38710.

Pavalko F.M., Norvell, S.M., Burr, D.B., Turner, C.H., Duncan, R.L. and Bidwell, J.P. (2003). A model for mechanotransduction in bone cells: The load-bearing mechanosomes. *J. Cell. Biochem*., **88**, 104–112.

Petite, H., Viateau, V., Bensaïd, W., Meunier, A., de Pollak, C., Bourguignon, M., Oudina, K., Sedel, L. and Guillemin, G. (2000). Tissue-engineered bone regeneration. *Nature Biotech*., **18**, 959–963.

Pietak, A.M., Reid, J.W., Stott, M.J. and Sayer, M. (2007). Silicon substitution in the calcium phosphate bioceramics. *Biomaterials*, **28**, 4023–4032.

Pina, S., Torres, P.M., Goetz-Neunhoeffer, F., Neubauer, J. and Ferreira, J.M.F. (2010). Newly developed Sr-substituted a-TCP bone cements. *Acta Biomater*., **6**, 928–935.

Porter, A. E., Patel, N., Skepper, J.N., Best, S.M. and Bonfield, W. (2003). Comparison of in vivo dissolution processes in hydroxyapatite and silicon-substituted hydroxyapatite bioceramics. *Biomaterials*, **24**, 4609–4620.

Pretto, M., Costa, A.L., Landi, E., Tampieri, A. and Galassi C. (2003). Dispersing behavior of hydroxyapatite powders produced by wet-chemical synthesis. *J. Amer. Ceram. Soc*., **86**(9), 1534–1539.

Rambo, C.R. and Sieber, H. (2005). Novel synthetic route to biomorphic Al_2O_3 ceramics. *Adv. Mater*., **17**(8), 1088–1091.

Rambo, C.R., Cao, J., Rusina, O. and Sieber, H. (2005). Manufacturing of biomorphic (Si, Ti, Zr)-carbide ceramics by sol–gel processing. *Carbon*, **43**, 1174–1183.

Reid, D.M. and New, S.A. (1997). Nutritional influences on bone mass. *Proc. Nutr. Soc*., **56**, 977–987.

Robinson, R.A. (1952). An electronic microscopic study of the crystalline inorganic component of bone and its relationship to the organic matrix. *J. Bone Jt. Surg*., **34A**, 389–434.

Ruffini, A., Sprio, S. and Tampieri, A. (2013). Study of the hydrothermal transformation of wood-derived calcium carbonate into 3D hierarchically organized hydroxyapatite. *Chem. Eng. J*., **217**, 150–158.

Sakhno, Y., Bertinetti, L., Iafisco, M., Tampieri, A., Roveri, N. and Martra, G. (2010). Surface hydration and cationic sites of nanohydroxyapatites with amorphous or crystalline surfaces: A comparative study. *J. Phys. Chem. C*, **114**, 16640–16648.

Saltman, P.D. and Strause, L.G. (1993). The role of trace minerals in osteoporosis. *J. Amer. Coll. Nutr*., **12**(4), 384–389.

Schaefer, D., Martin, I., Shastri, P., Padera, R.F., Langer, R., Freed, L.E. and Vunjak-Novakovic, G. (2000). In vitro generation of osteochondral composites. *Biomaterials*, **21**(24), 2599–2606.

Schliephake, H., Knebel, J.W., Aufderheide, M. and Tauscher, M. (2001). Use of cultivated osteoprogenitor cells to increase bone formation in segmental mandibular defect: an experimental pilot study in sheep. *Int. J. Oral Maxillofac. Surg*., **30**, 531–537.

Schoof, H., Apel, J., Heschel, I. and Rau, G. (2001). Control of pore structure and size in freeze-dried collagen sponges, *J. Biomed. Mater. Res. (Appl. Biomater.)*, **58**, 352–357.

Schulz-Ekloff, G., Wöhrle, D., Van Duffel, B. and Schoonheydt, R.A. (2002). Chromophores in porous silicas and minerals: preparation and optical properties. *Micropor. Mesopor. Mater*., **51**, 91–138.

Sikavitsas V.I. (2001). Biomaterials and bone mechanotransduction. *Biomaterials*, **22**, 2581–2593.

Singh, M. and Yee, B.M. (2004). Reactive processing of environmentally conscious, biomorphic ceramics from natural wood precursors. *J. Eu. Ceram. Soc*., **24**, 209–217.

Spence, G., Patel, N., Brooks, R. and Rushton, N. (2009). Carbonate substituted hydroxyapatite: resorption by osteoclasts modifies the osteoblastic response. *J. Biomed. Mater. Res*., **90A**, 217–224.

Spence, G., Patel, N., Brooks, R., Bonfield, W. and Rushton, N. (2010). Osteoclastogenesis on hydroxyapatite ceramics: The effect of carbonate substitution. *J. Biomed. Mater. Res*., **92A**, 1292–1300.

Sprio, S., Tampieri, A., Landi, E., Sandri, M., Martorana, S., Celotti, G. and Logroscino, G. (2008). Physico-chemical properties and solubility behaviour of multi-substituted hydroxyapatite powders containing silicon. *Mater. Sci. Eng. C*, **28**, 179–187.

Sprio, S., Tampieri, A., Celotti, G. and Landi, E. (2009). Development of Hydroxyapatite/calcium silicate composites addressed to the design of load-bearing bone scaffolds. *J. Mech. Behav. Biomed. Mater*., **2**(2), 147–155.

Sprio, S., Ruffini, A., Valentini, F., D'Alessandro, T., Sandri, M., Panseri, S. and Tampieri, A. (2011). Biomimesis and biomorphic transformations: new concepts applied to bone regeneration. *J. Biotechnol*., **156**(4), 347–355.

Sprio, S., Sandri, M., Panseri, S., Cunha, C. and Tampieri, A. (2012). Hybrid scaffolds for tissue regeneration: chemotaxis and physical confinement as sources of biomimesis. *J. Nanomater*, **2012**(2012), Article ID 418281, 10 pages.

Sprio, S., Guicciardi, S., Dapporto, M., Melandri, C. and Tampieri, A. (2013). Synthesis and mechanical behavior of beta-tricalcium phosphate/titania composites addressed to regeneration of long bone segments. *J. Mech. Behav. Biomed. Mater*., **17**, 1–10.

Studart, A.R., Gonzenbach, U.T., Tervoort, E. and Gauckler, L.J. (2006). Processing routes to macroporous ceramics: a review. *J. Am. Ceram. Soc*., **89**(6), 1771–1789.

Sung, Y.M., Shin, Y.K. and Ryu, J.J. (2007). Preparation of hydroxyapatite/zirconia bioceramic nanocomposites for orthopaedic and dental prosthesis applications. *Nanotechnology*, **18**(6), 065602–065607.

Svensson, A., Nicklasson, E., Harrah, T., Panilaitis, B., Kaplan, D.L., Brittberg, M. and Gatenholm, P. (2005). Bacterial cellulose as a potential scaffold for tissue engineering of cartilage. *Biomaterials*, **26**, 419–431.

Taboas, J.M., Maddox, R.D., Krebsbach, P.H. and Hollister, S.J. (2003). Indirect solid-free form fabrication of local and global porous, biomimetic and composite 3D polymer-ceramic scaffolds. *Biomaterials*, **24**(1), 181–194.

Tadier, S., Bareille, R., Siadous, R., Marsan, O., Charvillat, C., Cazalbou, S., Amédée, J., Rey, C. and Combes, C. (2012). Strontium-loaded mineral bone cements as sustained release systems: Compositions, release properties, and effects on human osteoprogenitor cells. *J. Biomed. Mater. Res. Part B: Appl. Biomater*., **100B**(2), 378–390.

Tampieri, A., Celotti, G., Sprio, S., Delcogliano, A. and Franzese, S. (2001). Porosity-graded hydroxyapatite ceramics to simulate natural bone. *Biomaterials*, **22**, 1365–1370.

Tampieri, A., Celotti, G., Landi, E., Sandri, M., Roveri, N. and Falini, G. (2003). Biologically inspired synthesis of bone like composite: self-assembled collagen fibers/hydroxyapatite nanocrystals. *J. Biomed. Mater. Res. A*., **67**(2), 618–625.

Tampieri, A., Sandri, M., Landi, E., Pressato, D., Francioli, S., Quarto, R. and Martin, I. (2008). Design of graded biomimetic osteochondral composite scaffolds. *Biomaterials*, **29**(26), 3539–3546.

Tampieri, A., Sprio, S., Ruffini, A., Celotti, G., Lesci, I.G. and Roveri, N. (2009). From wood to bone: multi-step process to convert wood hierarchical structures into biomimetic hydroxyapatite scaffolds for bone tissue engineering. *J. Mater. Chem*., **19**(28), 4973–4980.

Tampieri, A., Sprio, S., Sandri, M. and Valentini, F. (2011a). Mimicking natural bio-mineralization processes: a new tool for osteochondral scaffold development. *Trends in Biotech*., **29**(10), 526–535.

Tampieri, A., Sprio, S., Ruffini, A., Martínez-Fernández, J., Torres Raya, C., Varela Feria, F.M., Ramírez Rico, J. and Harmand, M-F. (2011b). WO2013063201, Implants for 'load-bearing' bone substitutions having hierarchical organized architecture deriving from transformation of vegetal structures. PCT/IB2011/054980.

Tampieri, A., D'Alessandro, T., Sandri, M., Sprio, S., Landi, E., Bertinetti, L., Panseri, S., Pepponi, G., Goettlicher, J., Bañobre-López, M. and Rivas, J. (2012). Intrinsic magnetism and hyperthermia in bioactive Fe-doped hydroxyapatite. *Acta Biomater*., **8**, 843–851.

Thian, E.S., Huang, J., Vickers, M.E., Best, S.M., Barber, Z.H. and Bonfield, W. (2006). Silicon-substituted hydroxyapatite (SiHA): A novel calcium phosphate coating for biomedical applications. *J. Mater. Sci*., **41**, 709–717.

Tsuruga, E., Takita, H., Itoh, H., Wakisaka, Y. and Kuboki, Y. (1997). Pore size of porous hydroxyapatite as the cell-substratum controls BMP-induced osteogenesis. *J. Biochem. (Tokyo)*, **121**(2), 317–324.

Vallet-Regì, M. and Arcos, D. (2005). Silicon substituted hydroxyapatites. A method to upgrade calcium phosphate based implants. *J. Mater. Chem*., **15**, 1509–1516.

Venkatesan, J. and Kim, S.K. (2010). Chitosan composites for bone tissue engineering – An overview. *Mar Drugs*, **8**, 2252–2266.

Wang, X., Tan, Y., Zhang, B., Gu, Z. and Li, X. (2009). Synthesis and evaluation of collagen-chitosan- hydroxyapatite nanocomposites for bone grafting. *J. Biomed. Mater. Res. – Part A*, **89**, 1079–1087.

Webster, T., Siegel, R. and Bizios, R. (1999). Osteoblast adhesion on nanophase ceramics. *Biomaterials*, **20**, 1221–1227.

Webster, T., Ergun, C., Doremus, R., Siegel, R. and Bizios, R. (2000). Enhanced functions of osteoblasts on nanophase ceramics. *Biomaterials*, **21**, 1803–1810.

Webster, T., Ergun, C., Doremus, R., Siegel, R. and Bizios, R. (2001). Enhanced osteoclast-like cell functions on nanophase ceramics. *Biomaterials*, **22**, 1327–1333.

Wegst, U.G.K. and Ashby, M.F. (2004). The mechanical efficiency of natural materials. *Philos. Mag*., **84**, 2167–2181.

Xynos, I.D., Edgar, A.J., Buttery, L.D., Hench, L.L. and Polak, J.M. (2001). Gene-expression profiling of human osteoblasts following treatment with the ionic products of Bioglass 45S5. *J. Biomed. Mater. Res*., **55**, 151–157.

Yang, X.B., Roach, H.I., Clarke, N.M., Howdle, S.M., Quirk, R., Shakesheff, K.M. and Oreffo, R.O. (2001). Human osteoprogenitor growth and differentiation on synthetic biodegradable structures after surface modification. *Bone*, **29**(6), 523–531.

Yuan, J., Cui, L., Zhang, W.J., Liu, W. and Cao, Y. (2007). Repair of canine mandibular bone defects with bone marrow stromal cells and porous beta-tricalcium phosphate. *Biomaterials*, **6**, 1005–1013.

Zurlinden, K., Laub, M. and Jennissen, H.P. (2005). Chemical functionalization of a hydroxyapatite based bone replacement material for the immobilization of proteins. *Materialwissenschaft und Werkstofftechnik*, **36**, 820–827.

10

Injectable biomedical foams for bone regeneration

M. P. GINEBRA and E. B. MONTUFAR,
Technical University of Catalonia, Spain

DOI: 10.1533/9780857097033.2.281

Abstract: The growing clinical need for synthetic bone grafting materials has given rise to the development of injectable and *in situ* self-setting calcium phosphate foams. The present chapter aims at providing an overview of the state of the art of the processing and characterization of these low temperature macroporous ceramics, suitable for bone grafting applications via minimally invasive surgery. Based on their low temperature processing, multimodal porosity, ranging from the nano- to the macro-scale, biocompatibility, bioactivity, and osteoconductivity, these foams can also be used as scaffolds for bone tissue engineering or as controlled drug delivery systems for the treatment of bone pathologies.

Key words: calcium phosphates, hydroxyapatite, injectable material, calcium phosphate cement, bone regeneration.

10.1 Introduction

Bone is among the most transplanted tissues. Although autologous bone grafts are still the gold standard in bone regeneration, they have some disadvantages, such as the need for a second surgery, morbidity, and limited availability. Grafts from the bone bank or other animals are also not free of such problems as immune responses or disease transmission. For these reasons, the development of synthetic materials has emerged as an alternative strategy to overcome the limitations associated with these problems. This chapter provides an overview of a specific type of synthetic bone graft, namely injectable calcium phosphate foams. The chapter reviews the state of the art in the processing and characterization of calcium phosphate foams suitable for bone grafting applications. First, the concept of self-setting calcium phosphate foams and the requirements they should comply with are introduced. Second, the structural and mechanical characteristics of the foams, together with their behavior during injection are presented, followed by an overview of their biological interactions both *in vitro* and *in vivo*. Third, specific applications of these calcium phosphate foams are discussed.

10.1.1 Biomaterials for bone regeneration

Bone and teeth are the only mineralized connective tissues in the human body.

Bone is a nanocomposite material formed by a matrix of type I collagen fibers reinforced with hydroxyapatite nanocrystals. Collagen is the most abundant protein in the body. It assembles in an organized pattern, providing bone calcification sites. The mineral phase represents approximately 65% by weight of bone tissue.

Moreover, bone is a self-repairing structural material; it is capable of adapting its mass, shape, and properties to the changes in mechanical and physiological requirements, and to regenerate small bone defects. This capacity stems from the fact that bone is in fact alive, and contains cells that work continuously to regenerate and repair it.

The regeneration mechanism, however, fails in some situations. This applies, for example, to large bone defects caused by trauma, or open resection of tumors. Moreover, sometimes it is necessary to increase the amount of bone prior to implant placement or in some pathologies. In these situations it is necessary to have materials that act as a bridge, leading to bone growth and, if possible, encouraging it. Among the different synthetic biomaterials, the best alternatives to regenerate bone are those that are able to bond directly with bone tissue, without the formation of a fibrous layer. The materials that fulfill this requirement are named bioactive materials (Cao and Hench, 1996). Bioactivity is defined as the property of materials to develop a direct, adherent, and strong bonding with the bone tissue. From a cellular perspective, bioactivity reflects the attachment and differentiation of osteogenic cells on ceramic surfaces. The concept of bioactive materials, as opposed to the inert biomaterials, was born in the 1970s. It was a feature of those materials that, instead of eliciting the formation of a fibrous capsule that isolated them from the surrounding tissue, they allowed bone growth on the surface. Besides the bioactive glass developed by Hench (Hench, 1998), calcium phosphates such as hydroxyapatite (HA), beta tricalcium phosphate (β-TCP) and the biphasic ceramics (BCP, a combination of HA and β-TCP) belong to the group of bioactive materials (LeGeros, 2008). These ceramics now comprise most of the market for synthetic bone substitutes.

HA is the calcium orthophosphate most similar to bone mineral, which in fact can be defined as a low-crystallinity, non-stoichiometric carbonated hydroxyapatite, also known as biological hydroxyapatite (Dorozhkin and Epple, 2002). Synthetic HA can be obtained either through high temperature ceramic routes or by low temperature precipitation processes, in the form of biomimetic coatings, or as calcium phosphate cements. Low temperature

processes that get biomimetic hydroxyapatite closer to the bone mineral phase, result in a material with lower crystallinity, ionic substitutions, higher surface area and, therefore, higher reactivity and resorption rate (Ginebra, 2008). Furthermore, they allow the incorporation of drugs, bioactive molecules, or even cells to promote bone formation or to combat infections or other pathologies (Ginebra *et al.*, 2012).

10.1.2 The relevance of porosity and injectability in bone tissue engineering and regenerative medicine

In addition to allowing bone formation on its surface, the structure of a bioactive material should foster cell migration from the surface to the bulk of the structure. For this reason porosity has emerged as one of the key requirements for the materials designed to act as substrates for bone regeneration (Hutmacher, 2000). In fact, it is known that porous materials can guide the growth direction of blood vessels, muscle, and nerve tissue (Stokols and Tuszynski, 2004). In bone, osseointegration has been improved using porous materials (Hutmacher, 2000; Jones, 2013). Porosity provides higher surface area for cell adhesion, proliferation, and differentiation, thereby increasing the probability of bone regeneration. Last but not least, open porosity improves the diffusion of oxygen, nutrients, and waste cellular products, enabling the survival of the cells in the bulk of the material (Annabi *et al.*, 2010). Furthermore, to allow the complete regeneration of the bone tissue, it is necessary that the bioactive material disappears over time, and porosity enhances material resorption (Bohner and Baumgart, 2004). Hence, structural characteristics of bioactive materials that should be tuned to improve bone healing include porosity, defined as the volumetric percentage of empty spaces in the material, pore size, pore shape, pore volume/pore area ratio, and pore interconnectivity.

In the biomaterials field, pores are usually classified in two different categories according to their size: micropores (pores smaller than 100 μm) and macropores (pores larger than 100 μm). Both microporosity and macroporosity are important for the bone regeneration potential of the material; on the one hand, macroporosity plays an important role in guiding new tissue ingrowth within the material, so that cell colonization and angiogenesis events can take place along with the progressive bioresorption of the substrate. On the other hand, microporosity results in larger surface area, which is believed to contribute to higher bone-inducing protein adsorption as well as to ionic exchange and bone-like apatite formation by dissolution and reprecipitation. Despite there being no universal rule applicable to all tissues, the following trends are in general accepted (Green *et al.*, 2002; Yang *et al.*, 2001).

- Pores smaller than 40 μm favor the growth of fibroblasts.
- Pores between 40 and 100 μm favor the formation of non-mineralized bone.
- Pores larger than 100 μm favor the formation of mineralized bone.

Nowadays, the use of minimally invasive surgical techniques represents a major achievement in orthopedic surgery for different applications. In contrast to traditional open surgery, minimally invasive surgery uses laparoscopic devices, inserted through small incisions, to carry out the intervention (Assaker, 2004; Park *et al.*, 2007). This new approach reduces damage to the patient, the risk and cost of intervention, but requires injectable materials that after implantation remain in place. Therefore, injectability followed by *in vivo* self-setting ability is a new requirement for the next generation bioactive materials for bone regeneration.

10.2 Injectable calcium phosphate foams

Injectable and self-setting calcium phosphate foams can be obtained by applying a foaming process to calcium phosphate cements (CPC). CPCs are osteoconductive hydraulic cements that harden *in vivo* through a setting reaction. As shown in Fig. 10.1, CPCs are formed by one or more calcium phosphate powders, which upon mixing with a liquid, usually water or an aqueous solution, form a moldable paste that can be injected through a cannula. Due to its mouldability, the cement paste can easily adapt to complex shaped bone cavities, ensuring a perfect contact that encourages a good osteointegration of the cement. CPCs can be classified according to the end product of the setting reaction, and despite the large number of possible formulations, up to now only two different end products have been obtained, hydroxyapatite (apatite cements) or brushite (brushite cements) (Bohner *et al.*, 2005c).

CPCs are intrinsically porous materials, with total porosities ranging between 30 and 50 vol.%. However, the pore size falls within the nano/micrometer range and therefore is too small to allow for cell colonization or angiogenesis (Espanol *et al.*, 2009). The absence of macropores limits the *in vivo* active resorption of the cement, mediated by cell activity, which is especially needed in the case of apatite CPCs, given their low solubility.

Different strategies have been adopted over the last decade to introduce macroporosity in CPCs, as summarized in Table 10.1. Macroporosity can be created by the dissolution of sacrificial particles after the cement sets. The porogenic agents can be added within the cement paste that, after setting, degrade faster than the cement itself, giving rise to the macroporosity. Different porogenic agents have been suggested, such as mannitol (Markovic, *et al.*, 2001), sucrose (Takagi and Chow, 2002), PLA fibers or particles (Ruhé

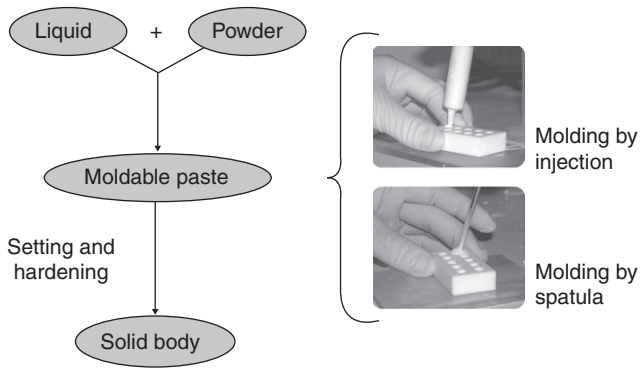

10.1 CPCs consist of a liquid and a powder phase. The liquid phase is water or an aqueous solution that can contain phosphate salts and/or polymers as additives. The powder phase consists of one or several calcium phosphate powders. When the liquid and powder phases are mixed, they produce a paste that can be molded either by injection or by spatula. After some minutes the paste sets and finally, after some hours, it becomes a solid body through dissolution/precipitation chemical reactions. The composition of the end product (normally either apatite or brushite) depends on the starting powder, and the properties of the cement such as workability, setting time, porosity, and mechanical strength depend also on other parameters such as the L/P ratio of the mixture, usually expressed in milliliters per gram (mL/g).

et al., 2005; Xu and Quinn, 2002), or frozen sodium phosphate solution particles (Barralet *et al.*, 2002). However, one of the drawbacks of this approach is that it is necessary to add a large amount of porogenic agent to guarantee interconnectivity of the porosity.

In a different approach, macroporosity can be introduced in the cement paste before it sets, while it has a viscous consistency. After setting, a solid macroporous construct is obtained. Macroporosity can be produced by the addition of some gas-generating compounds, such as hydrogen peroxide (Almirall *et al.*, 2004) or sodium bicarbonate (del Real *et al.*, 2002; Georgescu *et al.*, 2004). However, the risk of gas embolism associated with gas bubbles being released from the material after implantation compromises this strategy. An attractive alternative is the fabrication of self-setting calcium phosphate foams by the incorporation of a foaming agent in the cement formulation. The selection of the foaming agent is of paramount relevance in the development of successful implantable calcium phosphate foams. The most important requirements of the foaming agent are the following: (1) it must be soluble in water; (2) it must be biocompatible; and (3) it should not hinder the setting reaction of the cement. The candidates can be selected from either among synthetic surfactants approved for parenteral administration, or among macromolecular surfactants, namely, some

Table 10.1 Different processing techniques for the preparation of CPC-based macroporous scaffolds

Approach	Process	Category	Additive	Macroporosity (%)	Macropore size (μm)	References
After setting	Leaching	Particles	Mannitol, sucrose, sodium carbonate, or sodium phosphate	17–65	125–270	Cama *et al.*, 2009; Markovic *et al.*, 2001; Takagi and Chow, 2002; Xu and Simon 2005
			Frozen sodium phosphate solution	29–41	1000	Barralet *et al.*, 2002
			Calcium sulfate dehydrate			Fernández *et al.*, 2005
		Fibers	Polyglactin 910 (Vicril®)	25–35	322	Xu and Quinn, 2002; Xu *et al.*, 2006, 2008
			Aramid, carbon, E-glass, or polyglactin	2–9	8–200	Xu *et al.*, 2000, 2001
			Poly (ε-polycaprolactone) or poly (L-Lactic acid)	5–30	180–210	Zuo *et al.*, 2010
		Meshes	Polyglactin 910 (Vicril®) mesh		140	Xu and Simon, 2004a; Xu *et al.*, 2004b
		Microspheres	Poly(DL-lactic-co-glycolic acid) (PLGA)	30–69	17–66	Habraken *et al.*, 2006
			Gelatin	45–57	20–37	Habraken *et al.*, 2009; Link *et al.*, 2008

	Emulsion	Oil/water	High viscous paraffin with sorbitan monooleate as dispersed phase	52–64	100–900	Bohner, 2001; Bohner *et al.*, 2005b
	Templates	Positive and negative replica	Polyurethane template		700–1000	Miao *et al.*, 2004, 2005
			Negative resin	20–50	300–1000	Charriere *et al.*, 2003; Li *et al.*, 2005; Guo *et al.*, 2009; Li *et al.*, 2007
Before setting	Foaming	Gas generation	Decomposition of $NaHCO_3$	13–20	100–170	Del Real *et al.*, 2002, 2003; Hesaraki and Sharifi, 2007; Hesaraki *et al.*, 2008
			Decomposition of H_2O_2	11–36	200	Almirall *et al.*, 2004
	Freeze drying		Alginate or gelatin water solutions		100–380	Panzavolta *et al.*, 2009; Qi *et al.*, 2009
	Rapid proto-typing	3D printing			12–27	Gbureck *et al.*, 2007a, 2007b; Habibovic *et al.*, 2008
		Robocasting	Alginate			Lee *et al.*, 2011
			Gelatin			Maazouz *et al.*, 2012
			Miglyol-Tween 80-Amphisol			Lode *et al.*, 2012

proteins and polysaccharides with amphiphilic character, able to form and stabilize colloidal systems.

10.2.1 Foams and surfactant theory

Foams are a particular case of colloidal systems. In general, colloidal systems consist of a disperse phase, also called an internal phase, in the form of particles, drops, or bubbles, and a continuous phase, also called an external phase, which can be either gas, liquid, or solid. Foams can be liquid or solid depending on the physical state of the continuous phase, while the dispersed phase is always a gas, usually air (Schramm, 2005). Liquid foams are not thermodynamically stable systems, with a lifetime that can range from seconds until days. During the life of a liquid foam the following stages can be distinguished (Weaire and Hutzler, 1999): (1) foam formation, through turbulent flow of gases or liquids, or the destabilization of a gas previously dissolved in a liquid; (2) foam maturation, by the progressive disruption of the foam due to two mechanisms acting in parallel, namely gravitational separation of the liquid (drainage) leading to the thinning of the walls of the bubbles until they are in direct contact; and coarsening of the bubbles due to pressure differences between the cells (Ostwald ripening), which leads to the coalescence and disappearance of the smaller bubbles – these mechanisms are relevant in the period prior to the setting of the cement paste; and (3) the foam collapse would be the final stage, corresponding to the extinction of the foam at the end of the maturation period. However, the setting of the cement paste hinders this last phase, leading to the formation of a solid foam.

Relatively stable foams can be obtained by the incorporation of a surfactant in the liquid phase of the CPC. Surfactants are amphiphilic molecules that are absorbed in the liquid/gas interphase, reducing the interfacial energy and therefore stabilizing the bubbles inside the liquid (Porter, 1994). A greater interfacial area can be stabilized when more quantity of surfactant is incorporated, generating more bubbles with lower size. Furthermore, the incorporation of the surfactant can also increase the viscosity of the continuous phase of the foam, resulting in the reduction of the drainage, or in other words increasing foam stability. Alternatively, drainage can be further reduced with the incorporation of soluble polymers or particles in the continuous phase of the foam (Porter, 1994; Schramm, 2005).

10.2.2 Foaming agents

Foaming agents can be divided in two main categories, namely low and high molecular weight surfactants (Bos and van Vliet, 2001). Basically, synthetic

surfactants correspond to the low molecular weight category. Their main disadvantage is that most of them are toxic. Some of them are known to interfere with the homeostasis of the physiological fluids, or to disrupt the cell membrane. Only few non-ionic surfactants are considered biocompatible, such as Polysorbate 80 and Poloxamer 407 (Aulton, 2002). They are used in biomedical applications as additives in drugs for parenteral administration. They are efficient foaming agents, produce foams with good stability, and are not known to have any immunogenic response. Polysorbate 80 has been proven to be a very efficient synthetic surfactant for the fabrication of calcium phosphate foams (Montufar *et al.*, 2009). It is a non-ionic surfactant with critical micelle concentration in water between 13 and 15 mg/L (Hillgren *et al.*, 2002). It is approved by the food and drug administration as carrier of drugs for parenteral administration in a maximum dose of 4 mg/mL (Floyd, 1999).

An alternative approach is based on the good emulsifying and foaming properties of some proteins or polysaccharides, which are natural surfactants. The foaming properties of proteins depend on their ability to adsorb and unfold at the surface, forming a flexible, elastic interfacial film that is capable of entrapping and retaining air. For instance, it is well known that albumen, the protein mixture derived from egg white, has an excellent foaming capacity (Zayas, 1997). Native albumen contains as many as 40 different proteins (Powrie, 1973) and some of them are water-soluble surface-active proteins that can migrate to the air/water interphase. In particular, foaming properties of albumen are related to surface denaturation of the globulin fraction of albumen. Albumen has been proven to be an efficient foaming agent for CPCs (del Valle *et al.*, 2007; Ginebra *et al.*, 2007b).

Gelatin, denaturated collagen, is another example of an amphiphilic protein with good foaming capacity. In fact, calcium phosphate foams have been produced with gelatin that show enhanced injectability and cohesion (Montufar *et al.*, 2010). Moreover, in addition to their foaming ability, proteins can endow the material with other interesting bioactive functionalities. For instance, in the case of gelatin, it can improve cell recruitment due to adhesive peptide sequences naturally present in its composition. Moreover, since gelatin is partially hydrolyzed collagen, in combination with calcium phosphates, it mimics the composite structure of bone. Nonetheless, it should be kept in mind that the use of heterogenic proteins can increase the probability of immunogenic responses (De Groot and Scott, 2007).

Soybean-derived proteins have also been studied as foaming agents for CPCs (Perut *et al.*, 2011). Rather than being a pure protein, the soybean extract consists of a mixture of proteins, carbohydrates, and natural oils. The attraction of soybean extract resides in that it contains isoflavones, which are similar to estrogens and can thus prevent bone decalcification, due to

Table 10.2 Summary of the foaming agents reported for the fabrication of injectable calcium phosphate foams

Category	Foaming agent	Type of solid foam	Reference
Low molecular weight	Polysorbate 80	CDHA	Montufar *et al.*, 2009
High molecular weight	Albumen	CDHA	Ginebra *et al.*, 2007b
	Gelatin	CDHA	Montufar *et al.*, 2010
	Soybean extract	CDHA	Perut *et al.*, 2011

CDHA: calcium-deficient hydroxyapatite.

the depression of the osteoclast activity, and can also stimulate osteoblast differentiation (Morris *et al.*, 2006; Santin *et al.*, 2007).

The various foaming agents reported in the literature for the preparation of apatite foams are summarized in Table 10.2.

10.2.3 Calcium phosphate foam processing

Few years ago Ginebra *et al.* (2007a) proposed a method to obtain injectable self-setting calcium phosphate foams. It consists in mixing the powder phase of a CPC with a previously foamed liquid. The mixing must be performed with caution, to avoid the breakdown of the bubbles (Montufar *et al.*, 2009). Alternatively, the liquid foam can be mixed with a previously prepared cement paste (Ginebra *et al.*, 2007b). In the two cases, the liquid foam acts as a template for the cement paste. The difference between the first and the second method lies in the shear stress produced during mixing, which is lower when the liquid foam is mixed with a previously prepared paste than when it is mixed with a dry powder. The two alternative methods are summarized in Fig. 10.2.

The continuous phase in the foamed CPCs is a suspension of reactive cement particles. As a consequence, the foamed paste is very stable because the high viscosity of the suspension prevents drainage and Ostwald ripening. The high elasticity of this viscous foam tolerates high deformation levels during the injection of the paste without bubble breakdown. Moreover, due to the cement setting reaction taking place, the continuous phase is transformed over time from liquid into solid. In contrast to liquid foams, solid foams are stable systems. Therefore, once the CPC is set, the calcium phosphate foam retains its shape permanently. This allows the implantation of the calcium phosphate foam using a minimally invasive surgical technique. The foam will perfectly adapt to the shape of the bone cavity, being able to harden afterwards under physiological conditions.

In principle, any CPC formulation can be used to prepare calcium phosphate foams, in combination with the previously mentioned foaming agents.

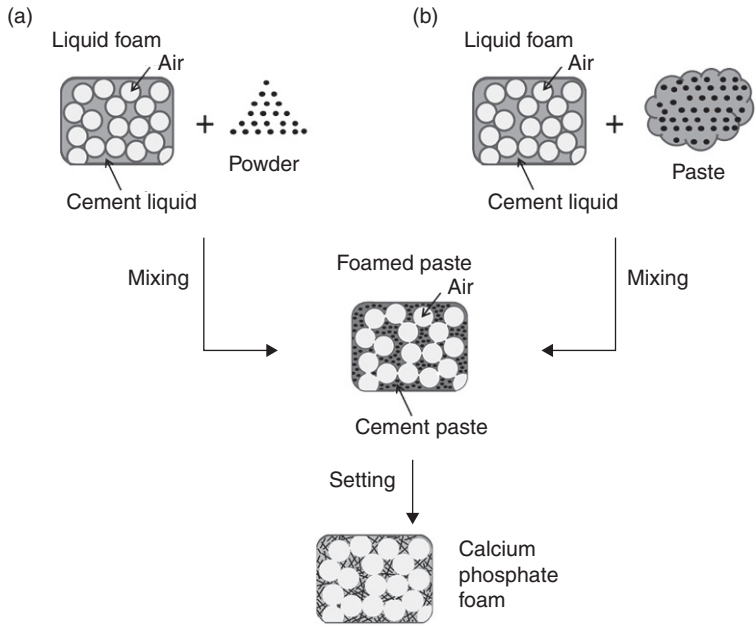

10.2 CPCs can be used to fabricate calcium phosphate foams following two different routes: (a) mixing the cement powder with a liquid foam, or (b) mixing the cement paste with a liquid foam. In both cases, the liquid foam acts as a template for the formation of macropores in the cement. After mixing, the foamed cement paste replicates the liquid foam and progressively transforms into a stable solid foam due to the setting and hardening reactions.

However, most studies have used monocomponent apatite CPCs, based on α-tricalcium phosphate (α-TCP). This phosphate is hydrolyzed in contact with water, resulting in calcium-deficient hydroxyapatite through a dissolution/precipitation process according to the following chemical reaction (Ginebra *et al.*, 1997).

$$3\alpha\text{-}Ca_3(PO_4)_{2(s)} + H_2O_{(l)} \rightarrow Ca_9(HPO_4)(PO_4)_5OH_{(s)} \qquad [10.1]$$

10.3 Porosity and mechanical performance of calcium phosphate foams

While porosity and mechanical properties of the calcium phosphate foams evolve along the setting process, the final values reached are the most

relevant for clinic applications. In this section, after a brief description of the techniques available for the characterization of porous materials, the porous structure and mechanical properties of the solid calcium phosphate foams obtained after setting are described.

10.3.1 Porosity characterization

Various techniques are available for the study of porous systems, with distinct advantages and disadvantages. There is not a single technique that describes comprehensively the porous systems. Therefore, the characterization of the calcium phosphate foams requires the combination of several techniques, the most relevant being described below.

Microscopy gives information about pore morphology, homogeneity, and pore size. Quantitative estimations can be derived by image analysis techniques. However, the extrapolation to three dimensions of the lengths observed in the bidimensional images must be carried out carefully to avoid erroneous estimations. The resolution of the microscope determines the degree of accuracy for the analysis of the porosity. In general, conventional optical microscopes have resolutions around 1–5 μm. For smaller pore sizes scanning electron microscopy (SEM) is the best alternative. Moreover, SEM has larger depth of field, allowing better panoramic images of macropores.

Mercury pycnometry is the simplest and cheaper way to quantify the total porosity. However, it does not give any information about pore size or morphology. The technique is based on the Archimedes' principle using mercury as immersion medium, which allows the characterization of permeable and hydrophilic materials.

Mercury intrusion porosimetry (MIP) is a technique that determines the percentage of open pores between 0.006 and 360 μm together with the pore entrance size distribution, and also gives information on pore shape and tortuosity. In contrast to mercury pycnometry, MIP forces the intrusion of mercury in the material by gradual increments of pressure. The pressure required for mercury intrusion is related through the Washburn model to the size of the channels that connect the pores (Webb and Orr, 1997). Thus, strictly speaking this technique does not determine the pore size but the size of pore interconnections. Furthermore, the volume of mercury used to fill the pores corresponds to the volume of free spaces in the material (porosity). Note that pores detected by this technique should be accessible for mercury from the surface of the material. Therefore, isolated pores, also called closed pores, do not contribute to the quantification of the porosity. This is not a drawback for the characterization of the calcium phosphate foams, since open porosity or the pores accessible for the cells are those that are relevant for bone ingrowth. Indeed, despite the presence of a large

number of macropores, without macro-connections cell colonization and vascularization would not be possible.

Microcomputed tomography is an alternative method to determine porosity, pore morphology, and pore size. The advantages of this technique over MIP are that it is a non-destructive method, and it can quantify pores larger than 360 μm. Besides, images acquired with this technique can be used to obtain three dimensional reconstructions of porous materials, very useful for the analysis and finite element modeling of the pore structure and behavior. The disadvantages are the high computational power required to manage the images of a representative volume of the sample, and the limited resolution. In this respect, it has to be mentioned that significant advances have been made in recent years, leading to resolution up to 500 nm, with even higher resolution expected to be achievable shortly.

10.3.2 Micro- and macro-structure of calcium phosphate foams

After this brief summary of the techniques for the analysis of porous materials, the structure of the calcium phosphate foams will be described from the nano- to the macro-scale. As shown in Fig. 10.3, the multimodal porosity of calcium phosphate foams results from the overlapping of the macropores generated by the foaming process with the intrinsic porosity of CPCs.

It is well known that the intrinsic porosity of CPCs increases when the volume of liquid used to prepare the paste increases or, in other words, when the liquid to powder (L/P) ratio increases (Espanol *et al.*, 2009). As an example, Fig. 10.4a shows the dependence of the total porosity of an apatitic α-TCP cement on the L/P ratio. Interestingly, the information provided by MIP shows that not only the total porosity, but also the pore size distribution is affected by the L/P ratio. As shown in Fig. 10.4b, at an L/P ratio of 0.35 mL/g, the cement has a broad pore size distribution in the submicrometric region, with a main peak centered at the lowest size range. When the L/P ratio increases to 0.55 mL/g, a bimodal pore size distribution is found. The left hand peak (1) shifts to slightly larger sizes with respect to the main peak observed with the L/P ratio of 0.35 mL/g. Moreover, a new sharp peak is found (2). As represented in Fig. 10.4b, the smaller-size peak corresponds to the porosity between the individual entangled crystals formed during the setting of the cement, while the right hand peak corresponds to the porosity between crystal aggregates, and reflects the crystal organization in the cement matrix, which precipitates surrounding the original α-TCP particles (Espanol *et al.*, 2009).

Similarly, the L/P ratio is a relevant parameter to control the total porosity of the calcium phosphate foams. In this case, the global increment in

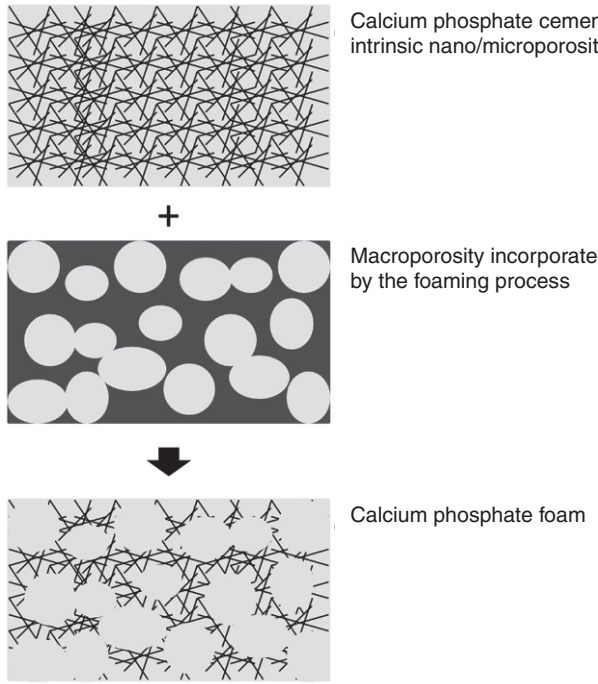

10.3 The total porosity of a calcium phosphate foam, represented in light gray, results from the intrinsic porosity of the calcium phosphate cement used to fabricate the foam and the macroporosity incorporated by the liquid foam template. Note that in the calcium phosphate foam the intrinsic porosity of the cement is located in the walls of the macropores.

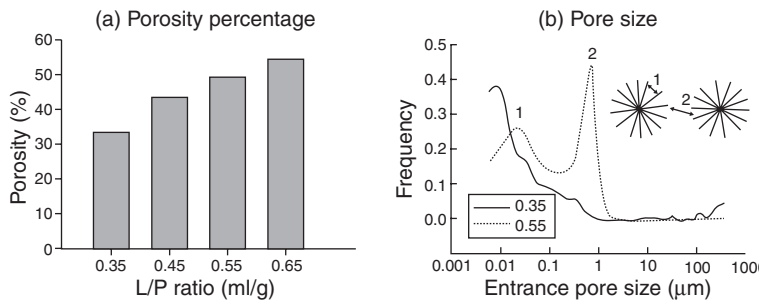

10.4 (a) Total porosity and (b) pore entrance size distribution, determined by MIP, for a cement based on α-TCP prepared with several liquid to powder (L/P) ratios. The inset in (b) represents the pores between the crystals precipitated during the hardening reaction (1), and the pores between crystal aggregates (2). The latter are more evident at higher L/P ratio because as the amount of liquid increases, the distance between the original particles of the cement powder also increases.

porosity results from the higher intrinsic porosity of the foam walls (continuous phase) together with the higher number of macropores formed during the foaming process due to the lower viscosity of the paste. This is illustrated in the SEM micrographs of two calcium phosphate foams with different L/P ratios shown in Fig. 10.5, where it is clear that the number of macropores incorporated by the foaming process increases with the L/P ratio. There are two reasons for this. First, since the surfactant is incorporated in the liquid phase of the CPC, the higher the L/P ratio the higher the number of surface-active molecules, allowing the formation of higher number of macropores. Second, the smaller amount of powder incorporated in the foam produces less viscous cement pastes, which can be foamed more easily than thick pastes. It is interesting to note that there is a critical L/P ratio for the formation of connections between macropores. In fact, the connections between macropores are formed before setting, by partial breakage of the pore walls. As shown in Fig. 10.5, the thickness of the pore walls is inversely proportional to the number of macropores. When few macropores are produced, they are connected only by the microporosity of the walls. In contrast, if macropore density increases, the walls become thinner and the probability of wall breakage to form macroscale connections increases. Therefore, using L/P ratios above the critical L/P ratio is a requirement to obtain interconnected macroporosity.

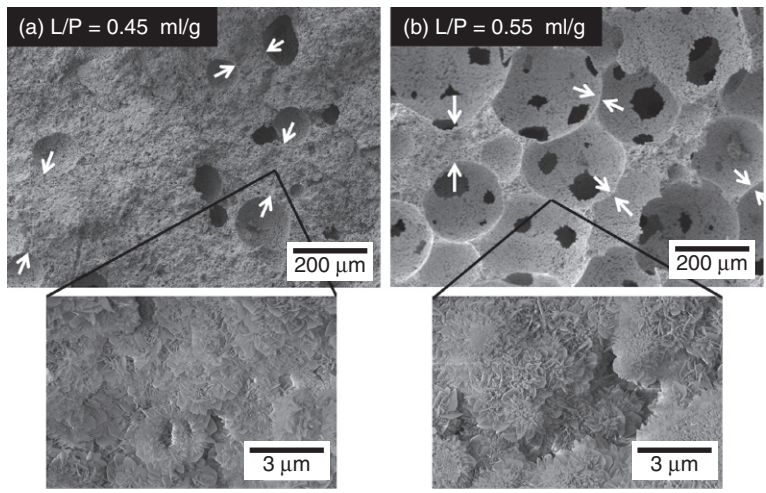

10.5 SEM micrographs for two calcium-deficient hydroxyapatite foams fabricated with two different L/P ratios, (a) 0.45 and (b) 0.55 mL/g. The space between white arrows highlights the thickness of the walls of the macropores. The insets in the bottom show the intrinsic porosity of the walls, which interconnects the macropores in the nano/micro scale range. Note that only at 0.55 mL/g circular interconnections between macropores are observed.

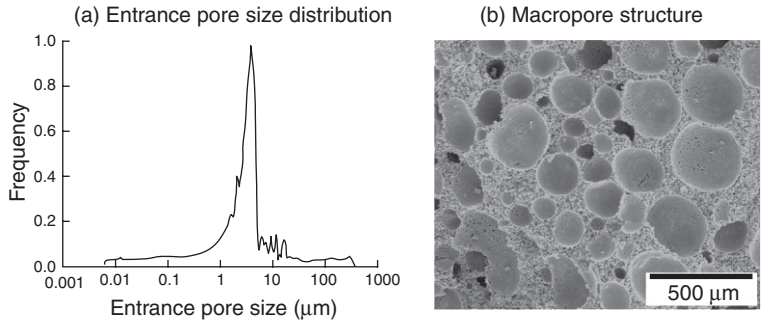

10.6 (a) Pore entrance size distribution determined by MIP and (b) macropore structure observed by SEM, of a calcium-deficient hydroxyapatite/gelatin foam obtained with an L/P ratio of 0.80 mL/g. Note that although the spherical macropores are near to each other, no interconnections are formed between them. This fact is reflected in the pore size distribution, where no pore entrances larger than 10 μm are found.

In addition to the L/P ratio, also the properties of the surfactant used, and more specifically the stability and elasticity of the liquid foams, determine the final interconnectivity of the solid foam. In fact, even if the macropores can be separated by very thin walls, if the stability of the foam is high the walls will not break before setting, and consequently the macropores will be connected only by the intrinsic porosity of the cement. For example, Fig. 10.6 shows the pore entrance size distribution and the macropore structure of an apatitic foam prepared with gelatin as foaming agent. Gelatin is a temperature-sensitive polymer that presents a gelling process below 37–40°C. At room temperature, below its gelling temperature, the stability of the foam is high (Montufar *et al.*, 2010). This is consistent with the pore size distribution determined by MIP, where no pore entrances larger than 10 μm are found, as an indication that no windows are formed in the pore walls. The main peak of the MIP pore entrance size distribution shown in Fig. 10.6, centered at 2 μm, is relatively high as a consequence of the method of determining the porosity by MIP. According to this technique, the size of the pores is estimated through the pressure needed by the mercury to enter them. When big macropores with microporous walls are found, the total volume of the macropore is ascribed to their entrance size, in this case in the micrometric range. Thus, when carefully interpreted, MIP results are in agreement with the structure observed by SEM, clearly showing spherical macropores without connections at the macroscale, which according to mercury pycnometry corresponds to nearby 15% porosity. Note that the stability of the foamed paste depends on the capacity of the foaming agent to form stable gels, and on its concentration. In general, higher concentrations

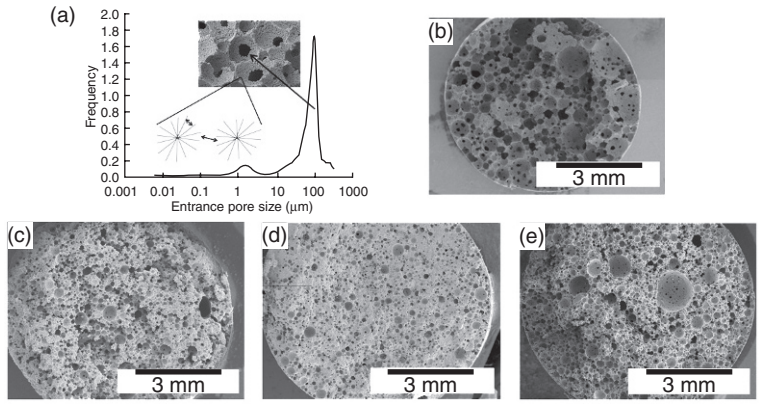

10.7 (a) Pore entrance size distribution determined by MIP for a calcium-deficient hydroxyapatite foam obtained with 1 wt.% of low molecular weight foaming agent (L/P = 0.65 mL/g). The inset in figure (a) shows the relationship between the peaks in the distribution and the pore interconnections observed by SEM. SEM micrographs for different calcium-deficient hydroxyapatite foams obtained with different foaming agents: (b) 1 wt.% polysorbate 80 (L/P = 0.55 mL/g), (c) 20 wt.% gelatin (L/P = 0.80 mL/g), (d) 20 wt.% soybean extract (L/P = 0.40 mL/g) and (e) 5 wt.% gelatin plus 20 wt.% soybean extract (L/P = 0.60 mL/g).

result in higher stability of the pore walls. Furthermore, foam stability also tends to increase with the molecular weight of the foaming agent.

An MIP diagram showing the pore size distribution of an apatite foam with open macroporosity is presented in Fig. 10.7a. In this example, the peaks that correspond to the intrinsic nano-/micro-porosity of the cement are hardly visible due to the large volume associated to the macropores, since most of them are connected by apertures larger than 10 μm, and only the walls of the pores contribute with some nano/micropores. Figure 10.7 also shows SEM images of various foams obtained with different foaming agents (Table 10.2). In general, all foams present spherical macropore structure, with several circular connections between them.

As shown in Fig. 10.8, open macropores are also present on the surface of the foam. This is important to facilitate surrounding cells and blood vessels to enter the foam. Once inside, the interconnections provide a way to fully colonize it.

10.3.3 Mechanical properties of calcium phosphate foams

Mechanical properties of ceramic materials are strongly dependent on their porosity.

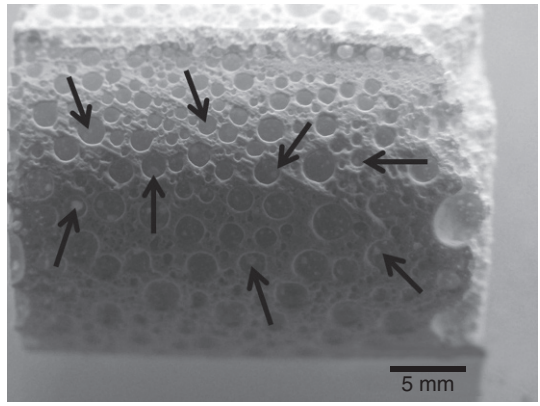

10.8 Optical image of the surface of a calcium-deficient hydroxyapatite foam obtained with 0.5 wt.% of polysorbate 80 (L/P = 0.55 mL/g). The arrows indicate the presence of open macropores at the surface of the foam, which in fact are connected with the internal macropores through macroscopic connections.

The compressive strength of the calcium phosphate foams can be mathematically modeled by the critical size defect theory, considering the compressive strength of the continuous phase of the foam as the strength of the CPC used to prepare the foam (see Equation [10.2]) (Ginebra *et al.*, 2007b). Thus, the model considers both the intrinsic porosity of the CPCs and the macroporosity incorporated during the foaming process, to estimate the compressive strength.

$$\sigma = \sigma_0 \left(\rho^*/\rho\right)^m \exp\left(-bP\right) \qquad [10.2]$$

where σ is the compressive strength for the set calcium phosphate foam; σ_0 is the theoretic compressive strength of the continuous phase of the foam without porosity (for the monocomponent apatitic cement based on α-TCP this strength corresponds to 112.36 MPa (Ginebra *et al.*, 2007b)); ρ^*/ρ_0 is the relative density of the cement; P is the macroporosity incorporated by the foaming process, expressed as volumetric fraction; and m and b are constants that depend on the material (for the α-TCP cement are 2.64 and 6.56, respectively (Ginebra *et al.*, 2007b)).

As shown in Fig. 10.9, the experimental data obtained for an apatitic foam fit well with this theoretical model. Its main limitation is that it does not take into account the possible binding forces that some agglutinant additives can have on the crystals that compose the foam.

The low mechanical strength of the foams, and the poor toughness associated with their ceramic nature, limit their use to non-load-bearing

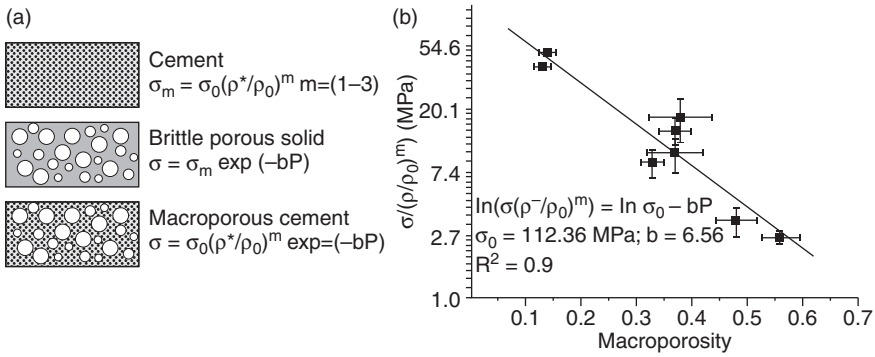

10.9 (a) schematic diagram showing the model proposed for the mathematical determination of the compressive strength of the foamed cements through the critical size defect theory; (b) semilog plot of the experimental results obtained for $\sigma/(\rho^*/\rho_0)^m$ versus macroporosity for a calcium-deficient hydroxyapatite foams obtained with 7–10 wt.% of albumen. (*Source*: Image reproduced with permission (Ginebra *et al.*, 2007b).)

applications. When used in load-bearing zones, they must be combined with orthopedic fixation systems that can withstand the external load. It is important to highlight that the main benefits of the calcium phosphate foams are not associated with their mechanical performance, but rather to the possibility of using them via minimally invasive surgery, generating *in situ* a bioactive ceramic with macropore structure that can promote the regeneration of bone tissue.

10.4 Injectability and cohesion of calcium phosphate foams

Injectability allows implantation of calcium phosphate foams via minimally invasive surgery. However, there is another property that is crucial to ensure that the foam stays in place during setting, keeping its dimensions and geometrical structure, and this is cohesion.

Injectability of a paste is defined as its ability to be extruded through an aperture without the separation of the liquid and the powder that compose it (Bohner and Baroud, 2005a). This definition can be extrapolated into the calcium phosphate foams as the additional ability of the foam to be extruded without breaking of the bubbles and disruption of the foamed structure. The injectability of calcium phosphate foams increases when the L/P ratio increases (Montufar *et al.*, 2009). Furthermore, the use of high molecular weight foaming agents also improves the injectability of calcium phosphate foams (Montufar *et al.*, 2011). Although increasing the L/P ratio

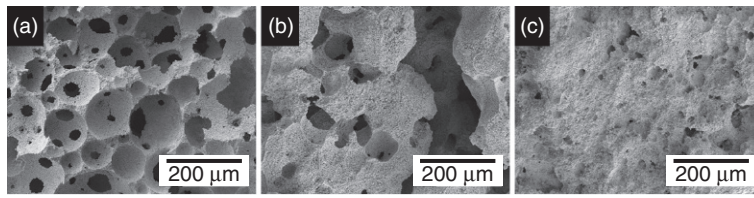

10.10 Differences in the macropore morphology when the calcium-deficient hydroxyapatite foam (1 wt.% of polysorbate 80 and L/P = 0.55 mL/g) was injected at different post mixing times, (a) just after mixing (2 min), (b) after 6 min and (c) after 16 min.

compromises the mechanical strength of the foam, it improves the open macroporosity and injectability. The preservation of the geometry of the macropores during injection depends on the time elapsed since the foaming process. As shown in Fig. 10.10, if injection is performed soon after foaming, the spherical macropore structure is maintained; otherwise the macropores are distorted, resulting in irregular shapes with random connections, which disappear when the injection is considerably delayed. This behavior can be attributed to the advance of the setting reaction, which decreases the elasticity of the paste. Shear stresses produced during injection overcome the yield stress of the foam, leading to plastic deformation and eventually collapse of the macropores.

The cohesion of the foamed paste determines if the foam can be used or not as an injectable bone grafting material. Cohesion can be defined as the ability of the foamed paste to maintain its shape until setting when in contact with body fluids. Indeed, if the injected foam is not able to support the blood pressure and the perfusion of physiological fluids after implantation, the foam structure will collapse, leaving behind the bone defect unfilled. Moreover, the release of particles can trigger the inflammatory response against foreign body (Velard *et al.*, 2013), which can compromise the clinical success of the treatment.

It is generally accepted that the cohesion of CPCs depends on different parameters, such as the particle size of the powder, pH and ionic strength of the liquid phase, L/P ratio, incorporation of polymeric admixtures, rate of cement setting, and osmotic pressure between the cement paste and the surrounding liquid (Bohner *et al.*, 2006). In the case of foams, cohesion in addition depends on total porosity, and as a general rule cohesion decreases with increasing macroporosity and pore interconnectivity. The nature of the foaming agent also affects the cohesion of the foam. Thus, while the foams containing gelatin have good cohesion (Montufar *et al.*, 2010; Perut *et al.*, 2011), those obtained with low molecular weight non-ionic surfactants tend to have poor cohesion (Montufar *et al.*, 2009, 2011).

The further improvement of cohesion remains a challenge for the optimal use of low molecular weight foaming agents in injectable calcium phosphate foams.

While the selection of the foam composition to maximize simultaneously porosity and cohesion is mandatory for the correct performance of injectable calcium phosphate foams, cohesion is not a requirement for the fabrication of preset foams, since in this case the foams can be set in controlled moisture atmospheres. Despite the preset foams not being injectable, they retain other advantages related to their low temperature processing. Moreover, complex shapes can be processed, due to the malleability of the foam before setting, enabling the fabrication of customized foams for bone grafting and tissue engineering applications.

10.5 *In vitro* and *in vivo* response to injectable calcium phosphate foams

Calcium phosphate foams obtained with different foaming agents are able to support osteoblastic-like cell adhesion, proliferation, and differentiation. In comparison with non-ionic surfactants, the use of gelatin as foaming agent has been shown to improve the attachment of osteoblastic cells, which was attributed to the presence of the RGD (Arginine-glycine-aspartate) sequence as a signaling cue in the inorganic structure of the foam (Montufar *et al.*, 2011).

Another example of the synergistic effect of the foaming agent was found when defatted soybean extract was used together with gelatin as foaming agent. The intrinsic bioactivity of soybean and gelatin was shown to favor osteoblast adhesion and growth. Moreover, the osteoblastic phenotype of cells seeded on apatite foams was promoted as revealed by the higher production of collagen and alkaline phosphatase (Perut *et al.*, 2011).

The calcium phosphate-based foams can find application also as scaffolds for *in vitro* tissue engineering. As an example, a perfusion bioreactor is shown in Fig. 10.11a, together with a calcium phosphate foam used as a scaffold for the dynamic culture of mesenchymal stem cells (Fig. 10.11b). The cells were able to attach and penetrate inside the macroporous structure when seeded under dynamic conditions. Figure 10.11c and 10.11d demonstrate the good permeability of the foam due to macropore interconnectivity, allowing the cells to homogeneously colonize the bulk of the scaffold.

Despite the good *in vitro* performance, there are still few *in vivo* studies on the application of calcium phosphate foams for bone regeneration. Del Valle *et al.* (2007) showed that albumen-based apatitic foams were resorbed significantly faster than their unfoamed counterparts and were progressively replaced by new bone, proving a good biocompatibility,

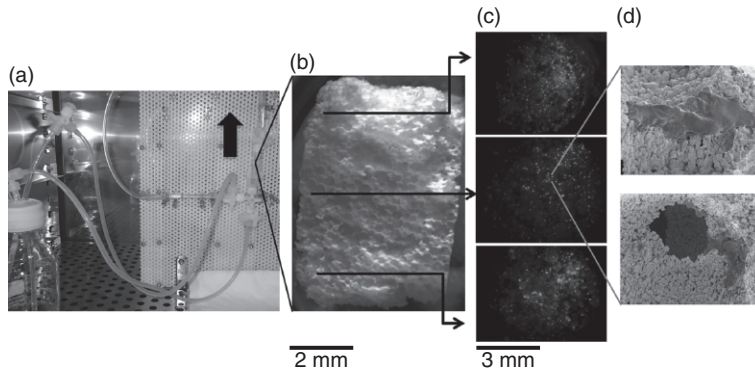

10.11 Dynamic culture of rat mesenchymal stem cells in direct contact with a calcium-deficient-hydroxyapatite foam (1 wt.% of polysorbate 80 and L/P = 0.55 mL/g) in a perfusion bioreactor system. (a) Image of the perfusion system showing the medium reservoir, the scaffold chamber and the flow direction. (b) Optical image of the macroporous foam placed in the chamber (6 mm in diameter and 10 mm in length). (c) Cell distribution observed at three different transversal sections of the scaffold after 3 h seeding. Images were obtained with a fluorescent stereoscope using calcein-AM as vital cell staining. (d) Morphology of the cells inside the foam observed by SEM.

osteoconductivity, and enhanced resorption in a femoral diaphyseal defect model in rabbits.

Calcium phosphate foams prepared with other high molecular weight foaming agents such as gelatin and soybean-derived polymers have also been tested as injectable bone grafts in a femoral diaphyseal critical size defect model in rabbits (Göckelmann, 2010; Göckelmann *et al.*, 2009). As shown in Fig. 10.12a, the foams were implanted by injection in cylindrical drilled cavities of 5 mm diameter and 10 mm depth. The injected paste adopted the shape of the cavity, filling it completely. Furthermore, as can be observed in Fig. 10.12b, the freshly injected foam had enough cohesion to resist the blood pressure without collapsing. The presence of homogeneously distributed macropores can be observed in a representative transversal section of the foam (see Fig. 10.12c). The setting of the foams was confirmed after one month of implantation by X-ray diffraction, showing the presence of hydroxyapatite as the main phase with very small traces of unreacted α-TCP. The histological analysis of the implants after 5 months of implantation showed the partial resorption of the foam, together with the formation of new trabecular bone (see Fig. 10.12d), with no signs of inflammation or immunological response. This confirmed that the self-setting hydroxyapatite foams are suitable for bone grafting applications via minimally invasive surgery.

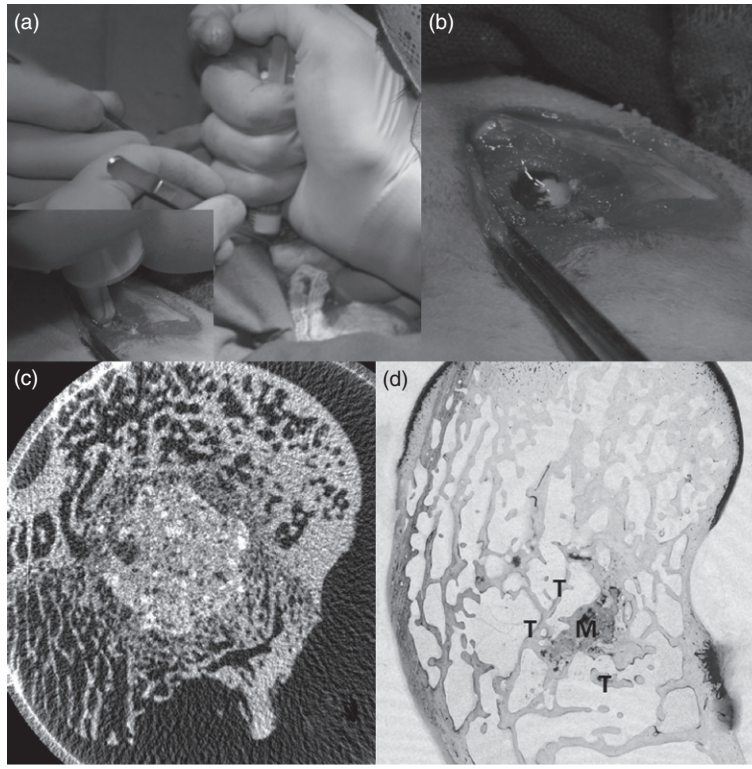

10.12 Preclinical study of a calcium-deficient hydroxyapatite foam (20 wt.% soybean extract plus 5 wt.% gelatin and L/P = 0.55 mL/g). (a) The foam was implanted by injection in a critical size defect at the femoral diaphysis of New Zealand white rabbits. (b) Foam placed in the bone defect. Good cohesion was observed after injection, with no collapse or disintegration. (c) Micro tomography of the site of implantation after 1 month of surgery. The bright zone corresponds to the implanted foam that perfectly adapts to the shape of the defect. Macropores can be observed in the material. (d) Histology of the site of implantation after 5 months of surgery (Paragon One staining), where T indicates the growing bone trabecula and M the remaining material.

10.6 Applications of injectable calcium phosphate foams

In the previous sections the processing routes and the properties of injectable calcium phosphate foams have been presented. In this section the advantages of this family of materials for different applications, like bone grafting, tissue engineering, and drug delivery are reviewed.

10.6.1 Bone grafting

The main field of application of calcium phosphate foams is bone regeneration in clinical areas such as orthopedic, craniofacial, and dental surgery. In general terms, calcium phosphate foams are designed to be used as substitutes of bone autografts, which nowadays represent the gold standard in bone regenerative medicine. Depending on the porosity and cohesion, these synthetic bone grafts can be used as: (1) injectable bone grafting material through minimally invasive surgery procedures; (2) preset bone grafting material used in traditional surgery; or (3) macroporous scaffold for tissue engineering applications. Possible orthopedic applications include reconstruction of bones after simple or comminuted fractures, bone filler materials after removing previous implanted materials, or resections of tumor or cysts, treatment of nonunion fractures, arthrodesis, and osteotomies. In dentistry they can be used for nasal sinus lift, filling cavities caused by dental extractions, periodontal disease or traumas, or the augmentation of alveolar ridge before placing a dental implant. In any case, the application should be restricted to non-load-bearing situations. Otherwise calcium phosphate foams should be used in combination with an external fixation device. The clinical approval of the calcium phosphate foams for the treatment of any of the preceding applications requires further specific preclinical studies that validate their efficacy.

10.6.2 Tissue engineering

Tissue engineering is based on the combination of progenitor cells, signaling molecules, and scaffolds for the development of cell/material constructs to regenerate damaged tissues in the human body (Place *et al.,* 2009). In particular, bone tissue engineering requires the successful *in vitro* interaction of these factors to direct mesenchymal stem cells extracted from the own patient into the osteoblastic phenotype, to further use the obtained constructs to repair the bone lesion. The correct selection of the scaffold is of paramount importance, since it must support the cells, direct its differentiation and provide the appropriate biomechanical environment and fluid flow dynamics.

Due to the bioactivity and cytocompatibility of apatites, calcium phosphate foams are promising scaffold materials for bone tissue engineering. In fact, as mentioned in Section 10.5, calcium phosphate foams fabricated with different foaming agents sustain the adhesion, proliferation, and differentiation of osteoblastic-like cells cultured in static conditions (Montufar *et al.*, 2009, 2011; Perut *et al.*, 2011).

Furthermore, as show in Fig. 10.11, mesenchymal stem cells are able to grow and colonize the bulk of calcium phosphate foams when seeded and

cultured under dynamic conditions in a perfusion bioreactor system. While cell infiltration into the calcium phosphate foams was possible due to the open macropores connected by windows of around 100 μm in diameter (see Fig. 10.7a), the space for cell proliferation was provided by the surface of the spherical macropores (see Fig. 10.5b). Cell intrusion was further improved by the dynamic seeding protocol, reaching cell seeding efficiencies of around 80%. Dynamic culture also improved cell proliferation, doubling the number of cells after three days of culture with respect to static conditions.

10.6.3 Drug delivery

A controlled drug delivery system is aimed at releasing the correct dose of a therapeutic directly in the desired zone and during the required period of time. This allows maximizing the efficacy of the therapeutic and minimizing the possible side effects. The incidence of musculoskeletal diseases (i.e. osteoporosis and osteoarthritis) has increased continuously in the last decades, driven by the aging of the population. This requires a renewed effort to develop new strategies for the regeneration of functional bone tissues. In this context, the discovery of factors that induce bone growth, such as bone morphogenic proteins (BMP) has generated great expectations in their local application associated with biomaterials (Mehta *et al*., 2012). The local delivery of other active principles or drugs, such antibiotics, antiosteoporotic, or anticancer drugs, has also been shown to be a promising strategy to combat these pathologies (Arkfield and Rubenstein, 2005). An ideal drug carrier for the treatment of skeletal disorders should be bioactive, which would ensure the ability of the material to bond to bone tissue, and resorbable to allow its progressive substitution by newly formed bone. In fact, much attention has been given to the development of bioactive drug delivery matrices that combine bone-bonding ability and drug release capacity, i.e. bioactive glasses or CPCs (Baino *et al*., 2012; Ginebra *et al*., 2006). In this respect, the control of the kinetics of the two ongoing processes, namely, bone bonding and drug release, is a key issue.

Calcium phosphate foams add to the advantages of other bioactive materials their injectability (Ginebra *et al.,* 2006) and macroporosity. Moreover, they can be resorbable, with a resorption rate that depends on their composition and microstructural features. In contrast to calcium phosphate granules or beads where pharmacological agents do only absorb on the surface, self-setting CPCs and foams can incorporate pharmacological agents throughout their entire structure. In fact, drugs or active principles can be incorporated either in the liquid or in the powder phase of the foam. Alternatively, the drug can also be loaded in preset foams by droplet addition or immersion of the foam in the drug solution (Ginebra *et al.*, 2012).

The presence of open macropores has been shown to facilitate fluid flow within the carrier, enhancing diffusion and drug release in comparison to the unfoamed counterparts (Pastorino *et al.*, 2012).

Calcium phosphate foams have been tested as delivery systems for BMPs with the aim of inducing *de novo* bone formation. BMP-2 was adsorbed in preset apatite foams. The release patterns showed a burst release during the first 2 h, followed by a sustained release, reaching a maximum release of 4.6% after 15 days. Furthermore, the released BMP-2 was shown to trigger mesenchymal stem cell differentiation into the osteoblastic phenotype *in vitro* and the formation of new bone when subcutaneously implanted in athymic nude mice (Montufar *et al.*, 2012). In another study, an antibiotic, doxycycline hyclate, was incorporated into the powder phase of an apatitic foam before the foaming process. The *in vitro* release assay performed in phosphate buffer solution showed that the calcium phosphate foam released a higher percentage of doxycycline than CPCs. This was attributed to the macroporosity and interconnectivity introduced by foaming, which enhanced fluid circulation within the CPC. No burst release was observed. Moreover, the concentration of doxycycline in the medium was in the adequate range for the local treatment of bone infections such as periodontitis (Pastorino *et al.*, 2012).

10.7 Conclusion and future trends

Calcium phosphate foams are promising materials for bone grafting applications, compatible with minimally invasive surgery techniques. Unlike CPCs, calcium phosphate foams are macroporous materials, with open pores suitable for cell infiltration and angiogenesis, and enhanced properties for *in vivo* bone ingrowth and the local release of drugs. In general, low molecular weight foaming agents, such as non-ionic surfactants, present a higher foamability than high molecular weight protein-based foaming agents, such as gelatin or albumen. Nevertheless, the use of proteins provides signaling cues that enhance the material's biological performance. Two challenges still remain open in the design of injectable calcium phosphate foams with a very high interconnectivity, namely the improvement of cohesion and the enhancement of their mechanical properties.

Several applications are envisaged for these materials in the skeletal system, such as their use as synthetic bone grafts, as drug delivery systems for the treatment of infections, tumors, or other pathologies, or as porous bioactive scaffolds. The design of preclinical studies that validate the efficacy of the calcium phosphate foams in such fields represents the next frontier in the study of these smart materials. These studies can provide us further insight into the mechanisms underlying bone tissue formation.

10.8 Sources of further information and advice

Further information on the processing and properties of calcium phosphate foams can be found in the references listed in Table 10.2. Alternative low temperature processing routes for CPC-based porous materials can be found in the article 'New processing approaches in calcium phosphate cements and their applications in regenerative medicine' (Ginebra *et al.*, 2010) and in the references listed in Table 10.1. For more information on CPC chemistry and properties the reader is referred to 'Calcium orthophosphate cements for biomedical applications' (Dorozhkin, 2008). Their application as drug delivery systems is reviewed in the article 'Calcium phosphate cements as drug delivery materials' (Ginebra *et al.*, 2012). A general overview of bone tissue engineering can be found in the article 'Tissue engineering strategies for bone regeneration' (Mistry and Mikos, 2005).

10.9 Acknowledgments

Authors acknowledge *J Biomed Mater Res A* (Wiley) for the permission for the reproduction of Fig. 10.9, and the financial support of the Spanish Ministry of Science and Innovation (MAT 2009–13547 project), and of the European Commission Seventh Framework Programme (FP7/2007–2013, Grant agreement no. 241879, REBORNE project). Support for the research of MPG was received through the prize 'ICREA Academia' for excellence in research, funded by the Generalitat de Catalunya.

10.10 References

Almirall, A., Larrecq, G., Delgado, J.A., Martinez, S., Planell, J.A. and Ginebra, M.P. (2004), 'Fabrication of low temperature macroporous hydroxyapatite scaffolds by foaming and hydrolysis of an α-TCP paste', *Biomaterials*, **25**, 3671–3680.

Annabi, N., Nichol, J.W., Zhong, X., Ji, C., Koshy, S., Khademhosseini, A. and Dehghani, F. (2010), 'Controlling the porosity and microarchitecture of hydrogels for tissue engineering', *Tissue Eng Part B: Rev*, **16**, 371–383.

Arkfield, D.G. and Rubenstein, E. (2005), 'Quest for the holy grail to cure arthritis and osteoporosis: emphasis on bone drug delivery systems', *Adv Drug Deliv Rev,* **57**, 934–944.

Assaker, R. (2004), 'Minimal access spinal technologies: state of the art, indications, and techniques', *Joint Bone Spine*, **71**, 459–469.

Aulton, M.E. (2002), *Pharmaceutics. The Science of Dosage Form Design*, London: Churchill Livingstone.

Baino, F., Fiorilli, S., Mortera, R., Onida, B., Saino, E., Visai, L., Verné, E. and Vitale-Brovarone C. (2012), 'Mesoporous bioactive glass as a multifunctional system for bone regeneration and controlled drug release', *J Appl Biomater Funct Mater*, **10**, 12–21.

Barralet, J.E., Grover, L., Gaunt, T., Wright, A.J. and Gibson, I.R. (2002), 'Preparation of macroporous calcium phosphate cement tissue engineering scaffold', *Biomaterials*, **23**, 3063–3072.

Bohner, M. (2001), 'Calcium phosphate emulsions: possible applications', *Key Eng Mater*, **765–768**, 192–195.

Bohner, M. and Baumgart, F. (2004), 'Theoretical model to determine the effects of geometrical factors on the resorption of calcium phosphate bone substitutes', *Biomaterials*, **25**, 3569–3582.

Bohner, M. and Baroud, G. (2005a), 'Injectability of calcium phosphate pastes', *Biomaterials*, **26**, 1553–1563.

Bohner, M., van Lenthe, G.H., Grünenfelder, S., Hirsiger, W., Evison, R. and Müller, R. (2005b), 'Synthesis and characterization of porous β-tricalcium phosphate blocks', *Biomaterials*, **26**, 6099–6105.

Bohner, M., Gbureck, U. and Barralet, J.E. (2005c), 'Technological issues for the development of more efficient calcium phosphate bone cements: A critical assessment', *Biomaterials*, **26**, 6423–6429.

Bohner, M., Doebelin, N. and Baroud, G. (2006), 'Theoretical and experimental approach to test the cohesion of calcium phosphate pastes', *Eur Cells Mater*, **12**, 26–35.

Bos, M.A. and van Vliet, T. (2001), 'Interfacial rheological properties of adsorbed protein layers and surfactants: a review', *Adv Colloid Interf Sci*, **91**, 437–471.

Cama, G., Barberis, F., Botter, R., Cirillo, P., Capurro, M., Quarto, R., Scaglione, S., Finocchio, E., Mussi, V. and Valbusa, U. (2009), 'Preparation and properties of macroporous brushite bone cements', *Acta Biomater*, **5**, 2161–2168.

Cao, W. and Hench, L. L. (1996), 'Bioactive materials', *Ceramics Int*, **22**, 493–507.

Charriere, E., Lemaitre, J. and Zysset, P. (2003), 'Hydroxyapatite cement scaffolds with controlled macroporosity: fabrication protocol and mechanical properties', *Biomaterials*, **24**, 809–817.

De Groot, A.S. and Scott, D.W. (2007), 'Immunogenicity of protein therapeutics', *Trends Immunol*, **28**, 482–490.

Del Real, R.P., Wolke, J.G.C., Vallet-Regi, M. and Jansen, J.A. (2002), 'A new method to produce macropores in calcium phosphate cements', *Biomaterials*, **23**, 3673–3680.

Del Real, R.P., Ooms, E., Wolke, J.G.C., Vallet-regí, M. and Jansen, J.A. (2003), '*In vivo* bone response to porous calcium phosphate cement', *J Biomed Mater Res A*, **65**, 30–36.

Del Valle, S., Miño, N., Muñoz, F., González, A., Planell, J.A. and Ginebra M.P. (2007), '*In vivo* evaluation of an injectable macroporous calcium phosphate cement', *J Mater Sci Mater Med*, **18**, 353–361.

Dorozhkin, S.V. and Epple, M. (2002), 'Biological and medical significance of calcium phosphates', *Angew Chem Int Ed*, **41**, 3130–3146.

Dorozhkin, S.V. (2008), 'Calcium orthophosphate cements for biomedical applications', *J Mater Sci*, **43**, 3028–3057.

Espanol, M., Perez, R.A., Montufar, E.B., Marichal, C., Sacco, A. and Ginebra, M.P. (2009), 'Intrinsic porosity of calcium phosphate cements and its significance for drug delivery and tissue engineering applications', *Acta Biomater*, **5**, 2752–2762.

Fernandez, E., Vlad, M.D., Gel, M.M., Lopez, J., Torres, R., Cauich, J.V. and Bohner, M. (2005), 'Modulation of porosity in apatitic cements by the use of α-tricalcium phosphate-calcium sulphate dihydrate mixtures', *Biomaterials*, **26**, 3395–3404.

Floyd, A.G. (1999), 'Top ten considerations in the development of parenteral emulsions', *Pharm Sci Tech Today*, **4**, 134–143.

Gbureck, U., Hölzel, T., Doillon, C.J., Müller, F.A. and Barralet, J.E. (2007a), 'Direct printing of bioceramic implants with spatially localized angiogenic factors', *Adv Mater*, **19**, 795–800.

Gbureck, U., Hölzel, T., Klammert, U., Würzler, K., Müller, F. A. and Barralet, J. E. (2007b), 'Resorbable dicalcium phosphate bone substitutes prepared by 3D powder printing', *Adv Funct Mater*, **17**, 3940–3945.

Georgescu, G., Lacout, J.L. and Frèche, M. (2004), 'A new porous osteointegrative bone cement material', *Key Eng Mater*, **201–204**, 254–256.

Ginebra, M.P., Fernandez, E., DeMaeyer, E. A.P., Verbeeck, R.M. H., Boltong, M.G., Ginebra, J., Driessens, F.C.M. and Planell, J.A. (1997), 'Setting reaction and hardening of an apatitic calcium phosphate cement', *J Dental Res*, **76**, 905–912.

Ginebra, M.P., Traykova, T. and Planell, J.A. (2006), 'Calcium phosphate cements as bone drug delivery systems: A review', *J Control Release* **113**, 102–110.

Ginebra, M.P., Planell, J.A. and Gil, F.J. (Technical University of Catalonia) (2007a), Injectable, self-setting calcium phosphate foam. European patent application EP1787626A1. 23 May 2007.

Ginebra, M.P., Delgado, J.A., Harr, I., Almirall, A., Del Valle, S. and Planell, J.A. (2007b), Factors affecting the structure and properties of an injectable self-setting calcium phosphate foam, *J Biomed Mater Res A*, **80**, 351–361.

Ginebra, M.P. (2008), 'Calcium phosphate bone cements', in Deb, S. (ed.), *Orthopaedic Bone Cements*, Cambridge, Woodhead Publishing Limited, 206–230.

Ginebra, M.P., Espanol, M., Montufar, E.B., Perez, R.A. and Mestres, G. (2010), 'New processing approaches in calcium phosphate cements and their applications in regenerative medicine', *Acta Biomater*, **6**, 2863–2873.

Ginebra, M.P., Canal, C., Espanol, M., Pastorino, D. and Montufar, E.B. (2012), 'Calcium phosphate cements as drug delivery materials', *Adv Drug Deliv Rev*, **64**, 1090–1110.

Göckelmann, M., Niclas, A., Bausewein, C., Friemert, B., Salvage, J.P., Santin, M., Montufar, E.B., Traykova, T., Ginebra, M.P., Planell, J.A. and Ignatius, A. (2009), '*In vivo* untersuchung poröser zemente aus kalziumphosphat, gelatine und sojabohnenextrakt als knochenersatzstoff', *Jahrestagung Deutsch gesellschaft für biomaterialien*, Tübingen-Duchland, 10 October 2009.

Göckelmann, M. (2010), *Untersuchung von neuen injizierbaren makroporösen knochenzementen im tiermodell*, Ulm, Ulm Universität.

Green, D., Walsh, D., Mann, S. and Oreffo, R.O.C. (2002), 'The potential of biomimesis in bone tissue engineering: lessons from the design and synthesis of invertebrate skeletons', *Bone*, **30**, 810–815.

Guo, D., Xu, K. and Han, Y. (2009), 'The *in situ* synthesis of biphasic calcium phosphate scaffolds with controllable compositions, structures, and adjustable properties', *J Biomed Mater Res A*, **88**, 43–52.

Habibovic, P., Gbureck, U., Doillon, C.J., Bassett, D.C., Van Blitterswijk, C.A. and Barralet, J.E. (2008), 'Osteoconduction and osteoinduction of low-temperature 3D printed bioceramic implants', *Biomaterials*, **29**, 944–953.

Habraken, W.J.E.M., Wolke, J.G.C., Mikos, A.G. and Jansen, J.A. (2006), 'Injectable PLGA microsphere/calcium phosphate cements: physical properties and degradation characteristics', *J Biomater Sci Polym E*, **17**, 1057–1074.

Habraken, W.J.E.M., Wolke, J.G.C., Mikos, A.G. and Jansen, J.A. (2009), 'Porcine gelatin microsphere/calcium phosphate cement composites: An *in vitro* degradation study', *J Biomed Mater Res B*, **91**, 555–561.

Hench, L.L. (1998), 'Bioceramics', *J Am Ceram Soc*, **81**, 1705–1728.

Hesaraki, S. and Sharifi, D. (2007), 'Investigation of an effervescent additive as porogenic agent for bone cement macroporosity', *Biomed Mater Eng*, **17**, 29–38.

Hesaraki, S., Zamanian, A. and Moztarzadeh, F. (2008), 'The influence of the acidic component of the gas-foaming porogen used in preparing an injectable porous calcium phosphate cement on its properties: acetic acid versus citric acid', *J Biomed Mater Res B*, **86**, 208–216.

Hillgren, A., Lindgren, J. and Aldqn, M. (2002), 'Protection mechanism of Tween 80 during freeze-thawing of a model protein, LDH', *Int J Pharm*, **237**, 57–69.

Hutmacher, D.W. (2000), 'Scaffolds in tissue engineering bone and cartilage', *Biomaterials*, **21**, 2529–2543.

Jones, J.R. (2013). 'Review of bioactive glass: From hench to hybrids', *Acta Biomater*, **9**, 4457–4486.

Lee, G. S., Park, J.H., Shin, U.S. and Kim, H.W. (2011), 'Direct deposited porous scaffolds of calcium phosphate cement with alginate for drug delivery and bone tissue engineering', *Acta Biomater*, **7**, 3178–3186.

LeGeros, R.Z. (2008), 'Calcium-phosphate based osteoinductive materials', *Chem Rev,* **108**, 4742–4753.

Li, X., Li, D., Lu, B., Tang, Y. and Wang, L. (2005), 'Design and fabrication of CAP scaffolds by indirect solid free form fabrication', *Rapid Prototyping J*, **11**, 312–318.

Li, X., Li, D., Lu, B., Wang, L. and Wang, Z. (2007), 'Fabrication and evaluation of calcium phosphate cement scaffold with controlled internal channel architecture and complex shape', *Proc Inst Mech Eng H*, **221**, 951–958.

Link, D. P., van den Dolder, J., van den Beucken, J. J., Wolke, J. G., Mikos, A. G. and Jansen, J. A. (2008), 'Bone response and mechanical strength of rabbit femoral defects filled with injectable CaP cements containing TGF-β1 loaded gelatin microparticles', *Biomaterials*, **29**, 675–682.

Lode, A., Meissner, K., Luo, Y., Sonntag, F., Glorius, S., Nies, B., Vater, C., Despang, F., Hanke, T. and Gelinsky, M. (2012), 'Fabrication of porous scaffolds by three-dimensional plotting of a pasty calcium phosphate bone cement under mild conditions', *J Tissue Eng Regen Med*, DOI: 10.1002/term.1563.

Maazouz, Y., Montufar, E.B., Fernandez, F. and Ginebra, M.P. (2012), 'Low temperature hydroxyapatite/gelatine robocasted scaffolds for bone tissue engineering', *J Tissue Eng Regen Med*, **6**, 212.

Markovic, M., Takagi, S. and Chow, L.C. (2001), 'Formation of macropores in calcium phosphate cement through the use of mannitol crystals', *Key Eng Mater*, **773–776**, 192–195.

Mehta, M., Schmidt-Bleek, K., Duda, G.N. and Mooney, D.J. (2012), 'Biomaterial delivery of morphogens to mimic the natural healing cascade in bone', *Adv Drug Deliv Rev*, **64**, 1257–1276.

Miao, X., Hu, Y., Liu, J. and Wong, A.P. (2004), 'Porous calcium phosphate ceramics prepared by coating polyurethane foams with calcium phosphate cements', *Mater Lett*, **58**, 397–402.

Miao, X., Lim, W.K., Huang, X. and Chen, Y. (2005), 'Preparation and characterization of interpenetrating phased TCP/HA/PLGA composites', *Mater Lett*, **59**, 4000–4005.

Mistry, A.S. and Mikos, A.G. (2005), 'Tissue engineering strategies for bone regeneration', *Adv Biochem Eng/Biotechnol*, **94**, 1–22.

Montufar, E.B., Traykova, T., Gil, C., Harr, I., Almirall, A., Aguirre, A., Engel, E., Planell, J.A. and Ginebra, M.P. (2009), 'Foamed surfactant solution as a template for self-setting injectable hydroxyapatite scaffolds for bone regeneration', *Acta Biomater*, **6**, 876–885.

Montufar, E.B., Traykova, T., Schacht, E., Ambrosio, L., Santin, M., Planell, J.A. and Ginebra, M.P. (2010), 'Self-hardening calcium deficient hydroxyapatite/gelatine foams for bone regeneration', *J Mater Sci Mater Med*, **21**, 863–869.

Montufar, E.B., Traykova, T., Planell, J.A. and Ginebra, M.P. (2011), 'Comparison of a low molecular weight and a macromolecular surfactant as foaming agents for injectable self setting hydroxyapatite foams: Polysorbate 80 versus gelatine', *Mater Sci Eng: C*, **31**, 1498–1504.

Montufar, E.B., Ben-David, D., Espanol, M., Livne, E. and Ginebra, M.P. (2012), 'BMP-2 release from low-temperature processed calcium phosphate foams', *J Tissue Eng Regen Med*, **6**, 328.

Morris, C., Thorpe, J., Ambrosio, L. and Santin, M. (2006), 'The soybean isoflavone genistein induces differentiation of MG63 human osteosarcoma osteoblasts', *J Nutr*, **136**, 1166–1170.

Panzavolta, S., Fini, M., Nicoletti, A., Bracci, B., Rubini, K., Giardino, R. and Bigi, A. (2009), 'Porous composite scaffolds based on gelatin and partially hydrolyzed α-tricalcium phosphate', *Acta Biomater*, **5**, 636–643.

Park, A., Kavic, S.M., Lee, T.H. and Heniford, B.T. (2007), 'Minimally invasive surgery: The evolution of fellowship', *Surgery*, **142**, 505–513.

Pastorino, D., Canal, C. and Ginebra, M.P. (2012), 'Antibiotic-eluting calcium phosphate foams for bone regeneration', *J Tissue Eng Regen Med*, **6**, 327.

Perut, F., Montufar, E.B., Ciapetti, G., Santin, M., Salvage, J., Traykova, T., Planell, J.A., Ginebra, M.P. and Baldini, N. (2011), 'Novel soybean/gelatine-based bioactive and injectable hydroxyapatite foam: Material properties and cell response', *Acta Biomater*, **7**, 1780–1787.

Place, E.S., Evans, N.D. and Stevens, M.M. (2009), Complexity in biomaterials for tissue engineering, *Nat Mater*, **8**, 457–470.

Porter, M.R. (1994), *Handbook of Surfactants*, UK, Blackie Academic and Professional.

Powrie, W. (1973), 'Chemistry of eggs and egg products', in Stadelman, W. and Cotterill, O. (eds.), *Egg Science and Technology*, Conneticut, AVI, 61–90.

Qi, X., Ye, J. and Wang, Y. (2009), 'Alginate/poly (lactic-co-glycolic acid)/calcium phosphate cement scaffold with oriented pore structure for bone tissue engineering', *J Biomed Mater Res A*, **89**, 980–987.

Ruhé, P.Q., Hedberg, E.L., Padron, N.T., Spauwen, P.H.M., Jansen, J.A. and Mikos, A.G. (2005), 'Biocompatibility and degradation of poly(DL-lactic-co-glycolic acid)/calcium phosphate cement composites', *J Biomed Mater Res A*, **74**, 533–544.

Santin, M., Morris, C., Standen, G., Nicolais, L. and Ambrosio, L. (2007), 'A new class of bioactive and biodegradable soybean-based bone fillers', *Biomacromolecules*, **8**, 2706–2711.

Schramm, L.L. (2005), *Emulsions, Foams and Suspensions*, Weinheim, Wiley-VCH.
Stokols, S. and Tuszynski, M.H. (2004), 'The fabrication and characterization of linearly oriented nerve guidance scaffolds for spinal cord injury', *Biomaterials*, **25**, 5839–5846.
Takagi, S. and Chow, L.C. (2002), 'Formation of macropores in calcium phosphate cement implants', *J Mater Sci Mater Med*, **12**, 135–139.
Velard F., Braux J., Amedee J. and Laquerriere P. (2013), 'Inflammatory cell response to calcium phosphate biomaterial particles: An overview', *Acta Biomater*, **9**, 4956–4963.
Weaire, D.L. and Hutzler, S. (1999), *The Physics of Foams*, New York, Oxford University Press.
Webb, P.A. and Orr, C. (1997), *Analytical Methods in Fine Particle Technology*, Atlanta, Micromeritics Instrument Corporation.
Xu, H.H.K., Eichmiller, F.C. and Giuseppetti, A.A. (2000), 'Reinforcement of a self-setting calcium phosphate cement with different fibers', *J Biomed Mater Res A*, **52**, 107–114.
Xu, H.H.K., Eichmiller, F.C. and Barndt, F.C. (2001), 'Effects of fiber length and volume fraction on the reinforcement of calcium phosphate cement', *J Mater Sci Mater Med*, **12**, 57–65.
Xu, H.H.K. and Quinn, J.B. (2002), 'Calcium phosphate cement containing resorbable fibers for short-term reinforcement and macroporosity', *Biomaterials*, **23**, 193–202.
Xu, H.H.K. and Simon, C.G. (2004a), 'Self-hardening calcium phosphate cement-mesh composite: reinforcement, macropores, and cell response', *J Biomed Mater Res A*, **69**, 267–278.
Xu, H.H.K., Quinn, J.B., Takagi, S. and Chow, L.C. (2004b), 'Synergistic reinforcement of *in situ* hardening calcium phosphate composite scaffold for bone tissue engineering', *Biomaterials*, **25**, 1029–1037.
Xu, H.H.K. and Simon, C.G. (2005), 'Fast setting calcium phosphate-chitosan scaffold: mechanical properties and biocompatibility', *Biomaterials*, **26**, 1337–1348.
Xu, H.H., Weir, M.D., Burguera, E.F. and Fraser, A.M. (2006), 'Injectable and macroporous calcium phosphate cement scaffold', *Biomaterials*, **27**, 4279–4287.
Xu, H.H.K., Weir, M.D. and Simon, C.G. (2008), 'Injectable and strong nano-apatite scaffolds for cell/growth factor delivery and bone regeneration', *Dent Mater*, **24**, 1212–1222.
Yang, S., Leong, K., Du, Z. and Chua, C. (2001), 'The design of scaffolds for use in tissue engineering. Part I: traditional factors', *Tissue Eng*, **7**, 679–689.
Zayas, J.F. (1997), *Functionality of Proteins in Food*, Berlin, Springer.
Zuo, Y., Yang, F., Wolke, J.G.C., Li, Y. and Jansen, J.A. (2010), 'Incorporation of biodegradable electrospun fibers into calcium phosphate cement for bone regeneration', *Acta Biomater*, **6**, 1238–1247.

11

Polylactic acid (PLA) biomedical foams for tissue engineering

M. SHAH MOHAMMADI, McGill University, Canada, M. N. BUREAU, National Research Council of Canada, Canada and S. N. NAZHAT, McGill University, Canada

DOI: 10.1533/9780857097033.2.313

Abstract: Porous scaffolds based on polylactic acid (PLA) and its copolymers have been extensively used as templates for potential tissue regeneration applications. This chapter discusses the techniques involved in creating PLA-based foams, focusing on gas foaming. It also covers the structure, physical and mechanical properties of the scaffolds. It then reviews some of the applications of PLA-based foams for the engineering of soft and hard tissues. It also provides an insight into future trends in the design of PLA foams for biomedical applications.

Key words: polylactic acid, PLA, foam, biomedical, tissue engineering, porous scaffolds.

11.1 Introduction

Porous scaffolds based on biodegradable polymers have been extensively used as templates for tissue regeneration applications. Highly porous polymer matrices are required to provide a homogenously distributed cell seeding density and effective oxygen and nutrient supply to maintain cell viability.[1] A critical challenge in tissue engineering (TE) is the material from which the scaffolds are fabricated, as these should provide physical, mechanical, and chemical cues to direct various cell growth and differentiation programs.[2–4] In addition, modulation of cellular function and neotissue formation significantly depends on the engineering design of the three dimensional (3D) scaffolds.[5,6] For example, the size, orientation, and surface chemistry of the pores in a scaffold can considerably manipulate tissue ingrowth and the transmission of biomechanical signals within the scaffold.[7,8] Moreover, the regeneration process may be impacted as a consequence of the lack of oxygen and nutrient transportation, since any potential for new blood vessel formation takes several days post implantation.[9] In

bone tissue engineering (BTE), for example, along with design issues there is also a challenge regarding the fabrication of reproducible biodegradable 3D scaffolds that are able to function for a certain period of time under load-bearing conditions.[10]

Polylactic acid (PLA) and its copolymer with poly(glycolic acid) ((poly(lactide-co-glycolide) (PLGA)) are among the most widely used synthetic polymers in TE, due to their versatile biodegradability and biocompatibility.[11,12] PLA-based composites have also been investigated for TE applications by incorporating bioactive ceramics (e.g. hydroxyapatite (HA) and other calcium phosphates)[13–15] and glasses (silicate-based glass (SG) and phosphate-based glass (PG))[16–18] into the matrix in an attempt to improve the bioactivity, degradation, mechanical properties, and ultimately the potential clinical performance of the scaffolds.[16,18,19]

This chapter will focus on PLA foams for TE applications. It begins with an introduction on PLA as a biomaterial, followed by the fabrication of PLA-based foams and their specific TE applications, and will end with conclusions and future trends of these foams as potential substrates for tissue repair and regeneration.

11.2 Polylactic acid (PLA)

Polylactic acid ($[\text{-O-CH}(\text{CH}_3)\text{-CO-}]_n$), belonging to the family of aliphatic polyesters commonly made from α-hydroxy acids, is biodegradable and compostable.[20,21] Since lactic acid is a chiral molecule, PLA exists in two stereo-isomeric forms, D-PLA (PDLA) and L-PLA (PLLA), and a mixture of D- and L-lactic acid also exists as D,L-PLA (PDLLA).[22] The polymers, which are derived from optically active D and L monomers, are semi-crystalline while the optically inactive D,L-PLA is amorphous. Generally, L-PLA is preferred in applications where high mechanical strength and toughness are required, e.g. sutures and orthopedic devices.[22,23] In contrast, due to the amorphous nature of D,L-PLA, it is usually considered for applications such as drug delivery systems, as it is important to have a homogeneous dispersion of the active species within a monophasic matrix.

PLA degrades through hydrolysis of the ester bond, negating the need for enzymes. The degradation rate depends on the shape and size of the article, the isomer ratio, time and temperature of the hydrolysis, low-molecular-weight impurities, and catalyst concentration.[20] It is well known that the degradation rate of PLA is greatly influenced by the stereo-isomeric L/D ratio of the lactate units. In general, the crystallinity decreases with increased stereo-isomeric ratio.[24,25] The degradation of PLA has also been demonstrated to be considerably decreased when the crystallinity increased.[26] Therefore, the polymer blend of PLLA and PDLLA is an effective approach for tuning the polymer crystallization and morphology, and hence its physico-mechanical

properties as well as hydrolysis behavior.[27] This is of utmost importance, particularly in TE scaffolds where a tailored degradation rate is required alongside adequate mechanical properties. For the aforementioned purpose, Carfi Pavia *et al.*[24] produced PLLA/PLA foams in different proportions in order to tune scaffold morphology, as well as mechanical properties and degradation kinetics up to 4 weeks. They showed that, while the crystallinity of pure PLLA and 95/5 (wt/wt) foams did not increase, that of the 90/10 foams increased from 40% to 70% after the first week. Consequently, it was indicated that pure PLLA and 95/5 PLLA/PLA do not exhibit significant differences in terms of degradation rate; however, 90/10 PLLA/PLA foams display a faster degradation rate as a result of higher amorphous phase content. The data confirmed that the characteristic time of degradation of the scaffolds can be tuned by blending different PLA typologies.

The degradation of PLA-based polymers is considered to be a collective process of bulk and surface diffusion, as well as bulk and surface erosion.[28] However, since the water penetration into the matrix is higher than the rate of polymer degradation for these polymers, the degradation is dominated by uniform bulk degradation of the matrix. In addition, the process is autocatalyzed with the increase of carboxylic end groups as a result of biodegradation.[28] It has also been demonstrated that when producing PLA-based composite materials under certain conditions (e.g. high temperature), the addition of a second phase would change the degradation behavior of PLA. For example, the incorporation of SG and PG particles into PLA has been shown to significantly accelerate the degradation of PLA.[29,30] Semicrystalline PLA has glass transition (T_g) and melting temperatures (T_m) of approximately 55°C and 175°C, respectively,[31] and at temperatures above 200°C it undergoes thermal degradation due to hydrolysis, oxidative main chain scission, lactide formation, and inter- and intra-molecular transesterification reactions.[32]

11.3 Fabrication of PLA foams

Numerous techniques have been used to produce TE scaffolds,[33] which include textile technologies, solvent casting, phase separation, gas foaming, freeze drying, electrospinning, UV and laser radiation, salt leaching, and 3D pore architecture designs (CAD/CAM and rapid prototyping). The selection of scaffolding technique can have a critical effect on the properties of the scaffold and its *in vivo* performance. Despite the progress made in the fabrication of 3D scaffolds, there are still some challenges that need to be overcome, which include accurate and consistent techniques and minimal variation in the properties in different scaffold batches.[34] It is worth mentioning that some techniques (e.g. electrospinning) may form porosity in the material; however, they do not allow the production of 3D structures,

namely foams. Therefore, in this section, the techniques that result in the creation of 3D porous structures (properly called foams) will be addressed.

Solvent casting with particulate leaching is the most widely used and one of the simplest methods to prepare the scaffold, first described by Mikos *et al.* in 1994.[35] This technique involves the dissolution of the polymer in an organic solvent followed by mixing with ceramic granules and dispersing calibrated minerals, such as sodium chloride, sodium tartrate, and sodium citrate, or organic (e.g. saccharose) particles in the polymer solution. The salt particles are leached out by selective dissolution to create a porous polymer matrix.[34,36,37] Ease of manufacturing and the ability to incorporate drugs and chemicals into the scaffold are the main advantages of this technique, but there are several limitations, e.g. only simple shapes can be formed.[38] Furthermore, the very low pore interconnectivity usually makes it unsuitable for TE applications. In addition, highly toxic solvents are used[10] and residual solvent may remain trapped, which would reduce the activity of bioinductive molecules, e.g. incorporated proteins.[36] Moreover, the mechanical properties of these scaffolds are inferior to those of trabecular bone.[39]

The thermally induced phase separation (TIPS) approach rapidly lowers the temperature of a homogenous solution of polymer to solidify the solvent and induce solid–liquid phase separation. The solidified solvent forces the polymer into the interstitial spaces. Using a freeze-dryer, the frozen mixture is lyophilized to remove the solvent and create the foam structure.[40,41] Highly porous PLA and Bioglass® incorporated PLA scaffolds with anisotropic tubular morphology and extensive pore interconnectivity can be produced with this fabrication technique.[16,40,42] However, sensitivity of the technique regarding its processing parameters, use of toxic solvents, low mechanical stability, and pore size in the range of 10–100 μm are main disadvantages.[38,43] Nevertheless, the TIPS technique has been demonstrated to produce microspheres of PLGA–bioactive glass composites, which have been investigated for potential tissue regeneration and drug delivery applications.[44,45] In order to produce fully degradable micro/macro-spheres, Blaker *et al.*[45] incorporated PG particulates (3, 5, and 20 wt.%) into PLGA. TIPS technique was used to enable the rapid formation of monodisperse porous macro-spheres. Macro-spheres (up to 2 mm in diameter) with isotropic pore morphology (interconnected spherical pores of 30–70 μm) were produced. PLA and blends of PLLA/PLA foams have also been prepared through the TIPS process for TE scaffold applications by La Carrubba *et al.*[25] Dioxane and water were used as the solvent and non-solvent, respectively. Results demonstrated that morphology and mechanical properties of the foams depended upon a combination of the operating conditions, such as solvent/non-solvent ratio, polymer concentration, and demixing time and temperature. It was found that by blending PLLA with PLA, the biodegradability of the foam could be tuned for various soft TE applications. Chen *et al.*[46] also

investigated the production of PLA scaffolds from a ternary PLA–dioxane–water system using the TIPS technique. The presence of water non-solvent was found to be essential for a liquid–liquid phase separation according to the phase diagram of this system. While the binary PLA-dioxane system shows only a solid–liquid phase separation resulting in a highly anisotropic tubular morphology with an internal ladder-like structure, the ternary PLA–dioxane–water system resulted in liquid–liquid phase separation leading to the formation of scaffolds with isotropic morphology.

Solid free form (SFF) fabrication refers to techniques, including selective laser sintering, 3D printing, and fused deposition modeling (FDM), that are based on computer-aided design/manufacture (CAD/CAM) methodologies.[36,41] These methods have been developed to manufacture scaffolds for BTE with specific designed properties[47–50] and has been used for polymer composites containing calcium phosphate as the bioactive phase. For example, PLLA–tricalcium phosphate (TCP) composites have been fabricated by Xiong *et al.*[15] with up to 90% porosity by a layer-by-layer manufacturing method. PLA scaffolds with computationally designed pores (wide channels) in the range of 500–800 μm and solvent-derived local pores of 50–100 μm were also produced by Taboas *et al.*[51] Complex equipment requirement and increased fabrication time compared to other direct techniques are shortcomings of this method.[36] There are also specific disadvantages associated with each SFF technique: e.g. use of organic solvents as binders, and lack of mechanical properties due to the combination of several stack up powdered layers in 3D printing.[52] While FDM does not use organic solvents, the non-incorporation of growth factors and range of polymers that can be used due to the processing requirements and temperatures are the main disadvantages of this method.[52]

Gas foaming technique was developed for producing highly porous foams without the use of organic solvents. Carbon dioxide (CO_2) can be used as a porogen to create 3D polymeric structures to be used as scaffolds. There are different approaches in using CO_2 such as supercritical fluids or high pressure to process polymers into 3D TE scaffolds.[53]

11.4 Gas foaming using supercritical CO_2 ($scCO_2$)

CO_2 exists at supercritical condition above a critical temperature (T_c = 304.1 K) and pressure (P_c = 73.8 bar). It has the properties of both a gas and a liquid in this state. By changing the temperature and pressure, the phase changes from solid to liquid and then to gas. However, at the intersection of T_c and P_c, the liquid and gas phases cannot be distinguished, and the single fluid phase CO_2 is said to be supercritical carbon dioxide ($scCO_2$).[53] $ScCO_2$ is inexpensive, non-flammable, non-toxic, and its properties can be tuned through its density.[54] In addition, there is a high level of control over

porosity and morphology of scaffolds by applying $scCO_2$ and tuning the parameters of the process.[55]

$ScCO_2$ has been found to be soluble in some polymers.[56] Plasticization occurs when $scCO_2$ diffuses into the polymer matrix and separates the polymer chains resulting in lower resistance to chain rotation resulting in a reduction of the polymer T_g. By reducing the CO_2 pressure, the solubility of the gas in the polymer decreases,[57] generating nuclei (or bubbles) that then grow to form the pores in the foam. The T_g begins to increase once the CO_2 vacates the polymer making it glassy, and the pores cannot grow further, fixing the porous structure.[56–58] Control of the nucleation and diffusion of the gas are very important in creating suitable scaffolds for TE. The nucleation is rapid, leading to a large number of nucleation sites if the venting rate is high and the structure will have a uniform and homogenous pore size distribution.

In contrast, the pores that nucleate initially will be significantly larger than others because of greater diffusion of gas from the surrounding matrix. Therefore, a wide dispersion in pore size would be present in the resultant structure.[59] The effect of changing the molecular weight of the polymer, pressure, and venting rate on pore structure has been demonstrated using different gases (CO_2, N_2, and He).[57,58,60–63] Sheridan *et al*.[62] compared CO_2, N_2, and He gas foaming by fabricating 3D porous matrices from bioabsorbable materials (e.g. PLA-based polymers). It was demonstrated that the choice of gas and polymer has a large influence on the final scaffold structure. While highly porous PLGA matrices were produced using CO_2, use of N_2 and He led to no measurable pore formation. While the mechanism is not known, the greater degree of foaming with CO_2 compared to N_2 and He may be due to a specific interaction between CO_2 and carbonyl groups of PLGA. It has been demonstrated that specific interactions with CO_2 occur in polymers with electron donating functional groups, as in the case of the carbonyl groups, most probably because of Lewis acid–base nature. In this case, the electron lone pairs of the carbonyl oxygen interact with the carbon atom of the CO_2 molecule.[64] The effect of gas type on porosity and a micrograph of typical scaffold by foaming PLGA are presented in Fig. 11.1.[62]

A critical challenge in fabricating TE scaffolds certainly concerns the pore interconnectivity to assure appropriate colonization of cells. In gas foaming technique, pore interconnectivity still remains a challenge, especially based on the crystallinity and molecular weight of the polymer to be foamed. Amorphous polymers have the ability to foam more easily than the crystalline polymers due to increased gas dissolution in less organized morphologies.[65] Therefore, gas foaming technique would be more difficult for semi-crystalline polymers (e.g. semi-crystalline PLA[18] or polycaprolactone)[66] than amorphous polymers (e.g. PDLLA).[67] In addition, scaffolds made of a high molecular weight polymer have less porosity and interconnectivity

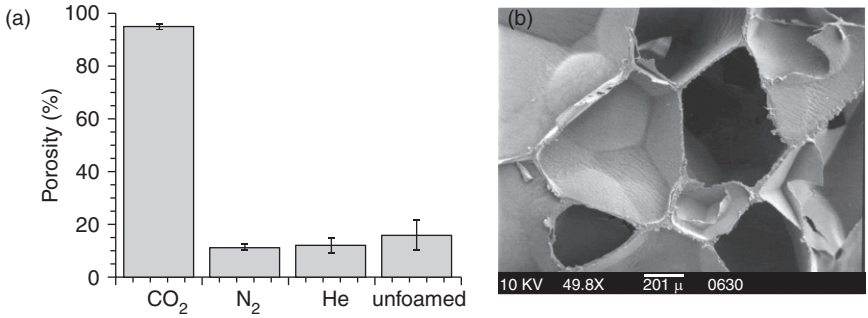

11.1 (a) The influence of gas type on porosity. (b) Photomicrograph of typical PLGA scaffold foamed for 24 h in 850 psi CO_2. PLGA (85:15) discs were equilibrated for 1 h in 850 psi gas prior to pressure release (340 psi/min).[62]

compared to the same polymer with lower molecular weight. Longer polymer chains in high molecular weight polymers are likely to be entangled to a greater extent, which provides a stronger resistance to expansion during the phase separation step compared to shorter polymer chains. Tai *et al.*[67] demonstrated that the pore size and structure of PDLLA and PLGA scaffolds produced by $scCO_2$ can be modified by altering the processing conditions. A longer soaking time and higher pressure resulted in a higher nucleation density due to more CO_2 molecules diffusion into the polymer matrix leading to a structure with smaller pores. Foams with larger pores were produced when higher temperatures were applied because increased diffusion rates facilitated pore growth. Moreover, a reduction in the depressurization rate led to larger pores, since it allowed for longer period of pore growth. Increasing the amount of glycolic acid content in the PLGA copolymer decreased the pore size of the scaffold. Mathieu *et al.*[13,14] investigated supercritical fluid foaming of PLA and PLA-ceramic (HA and β-TCP). Neat PLA foams with 78–92% porosities and interconnected pores (200–400 μm) were prepared. The addition of fillers reduced the foam porosity, and a higher density of smaller and more closed pores was achieved as a consequence of increased matrix viscosity due to the presence of fillers. The compressive strength and modulus were increased up to 6 and 250 MPa, respectively, with fillers for a given porosity.

The application of $scCO_2$ for producing PLA-based nanocomposite foams has also been investigated. For example, Blaker *et al.*[68] have used $scCO_2$ technology to simultaneously disperse a nano-clay in PLA and fabricate a porous structure for load-bearing applications. The incorporation of nanoclay into PLA resulted in significant improvement in mechanical properties (2.5-fold increase in compressive strength compared to neat PLA), and biocompatibility of the foams. The pore size of these porous nanocomposites

was about 200 μm which also suggested that they can support neovascularization. Despite the advantages of this technique for preparation of polymer/nanocomposites scaffolds, designing a porous polymer nanocomposite with adequate interconnected pores through $scCO_2$ remains a challenge.[55]

11.5 Solid-state foaming with high pressure CO_2

Gas foaming can also be performed with high pressure CO_2 at low temperatures (solid-state foaming). In this CO_2-based foaming process, the polymer is initially saturated with CO_2, and then followed by an expansion step.[69] The polymer is plasticized during the saturation step since the T_g of the polymer decreases to a value below the saturation temperature. In addition, the polymer matrix swells, and the reduced viscosity allows the polymer–CO_2 mixture to be processed at lower temperatures. Once the polymer matrix is saturated with CO_2, a rapid decrease in pressure provokes a shift in the thermodynamic equilibrium. Consequently, an oversaturation of CO_2 occurs in the polymer. However, foaming (nucleation and cell growth) will not occur below the T_g because the polymer matrix can still be in the glassy state, e.g. if the saturation temperature is relatively low, and T_g has not been adequately depressed by CO_2 sorption. Therefore, phase separation and nucleation will only occur when the saturated specimen is heated to a temperature above T_g. It should be noted that the foaming will take place instantaneously if the saturation temperature is high enough, and the polymer is in the rubbery state due to sufficient decrease in T_g. When the polymer returns to the glassy state, either by a decrease in temperature or a decrease in the CO_2 concentration, cell growth will stop.[69]

Mooney *et al.*[70] developed this technique by foaming poly(D,L-lactic-co-glycolic acid) that was exposed to high pressure CO_2 (5.5 MPa) for 72 h at room temperature. By reducing the CO_2 pressure to atmospheric levels, the solubility of the gas in the polymer matrix decreased rapidly, resulting in thermodynamic instability of the dissolved CO_2 and leading to the nucleation and growth of gas cells within the polymer matrix. Large pores (~100 μm) and up to 93% porosity could be produced using this technique. The porosity and pore structure depend on the amount of gas dissolved in the polymer and the rate and type of nucleation, as well as the diffusion rate of gas molecules through the polymer to the pore nuclei.[61,65] By changing the gas pressure and temperature, the amount of dissolved gas can be controlled. Homo/heterogeneous nucleation and the diffusion rate of dissolved gas can be regulated by the processing temperature and the rate at which the gas pressure is changed. By increasing the amount of dissolved gas in the polymer matrix, or increasing the gas diffusion rate after thermodynamic instability, a more interconnected pore structure could be created.[70] Singh *et al.*[71] investigated the fabrication of PLGA foams for biomedical

applications. Porosity of 89% with a pore size ranging from 30 to 100 μm was achieved at CO_2 pressures of 100–200 bar and temperatures up to 40°C. Hu *et al.*[72] suggested that the foamability of the PLA depends on solubility, diffusion coefficient of CO_2 into the material, and the polymer degree of crystallinity. It was found that the presence of CO_2 induced crystallinity in PLA, and the degree of crystallinity increased with increasing saturation pressure. Foaming was performed by saturating the polymer for 2 days with CO_2 at different pressures and at room temperature. The pressure was rapidly released and samples were subsequently allowed to foam at a range of temperatures from 25°C to 160°C for 5, 10, 30, and 90 s. A more uniform cellular structure was obtained when PLA samples were saturated at 2.8 MPa and room temperature followed by foaming at 100°C.

Matuana *et al.*[73] investigated the effect of gas (CO_2) saturation conditions on the expansion ratio of microcellular PLA through a batch foaming process. Various gas saturation times and pressures were applied at room temperature to produce PLA foams with a high expansion ratio. A high expansion ratio (10-fold) was achieved at a gas saturation pressure up to 2.76 MPa corresponding to a critical gas concentration of approximately 9.4%. There was a significant reduction in foam expansion beyond this critical processing condition.

It is worth pointing out that CO_2 has also been used as a foaming agent to create porous structures of PLA blended with other polymers. For example, the gas foaming technique using supercritical and subcritical CO_2 has been shown to be efficient in creating porosity in poly(D,L-lactide)/polyethylene glycol (PDLLA/PEG) blends.[74] PDLLA/PEG blend with 70/30 weight ratio was found to demonstrate the optimum properties. This foaming technique allowed for the production of 3D porous scaffolds whereby the pore size could be tailored by adjusting the process variables. While the average pore diameter was reported to be in the range of 15–150 μm, the pore size was larger at subcritical conditions. The pore size had a considerable influence on the mechanical properties, as well as medium up-take and degradation. The pore size of the produced scaffolds could be modified for various TE applications.

11.6 Tissue engineering applications of PLA and PLA-based foams

PLA-based materials have extensively been investigated for different TE applications such as skin, nerve, liver, vascular, intestine, cartilage, and bone regeneration.

PLA and PLA-blend foams alone have been a major focus of studies as TE biodegradable scaffolds; however, in order to improve the load-bearing

capacity, bioactivity, and biological response of the scaffolds for certain applications, composite foams based on PLA have widely been also developed. For this purpose, several fillers have been incorporated into PLA, which include SGs (e.g. Bioglass®),[75] PGs,[18] HA,[14] TCP[14], and silk.[76] Incorporation of these fillers has been shown to successfully improve the mechanical properties of the foams, as well as induce bioactive functions (e.g. bone bonding ability through the formation of a HA-like surface layer).[77,78] Furthermore, the addition of HA and β-TCP to PLA foams, processed by supercritical gas foaming, has been shown to increase alkaline phosphatase activity for fetal bone cells, and a stronger production of Gla-osteocalcin for adult bone cells.[79] In addition, the addition of fillers can negatively or positively affect the foam morphology, which should be taken into account in the design of composite foams. For example, although the fillers can act as nucleating agents, resulting in increased pore formation, higher volume fractions may lead to very small pore size impeding suitability for TE applications. Moreover, while increased amounts of filler can hinder the foamability of PLA by altering its viscoelasticity, the presence of fillers can contribute to increased open pore morphology, and interconnectivity. Because of the aforementioned reasons, TE applications of both PLA and PLA-based composites will be addressed in this section.

Dense and porous PLLA membranes with different pore size (< 45 μm, between 180 and 250 μm, and between 250 and 350 μm) were investigated by Santos *et al.*[80] for potential applications as substrates for skin regeneration. A fibroblastic cell line, attached to the PLLA membranes, was found to proliferate, and produce extracellular matrix molecules such as collagen IV and fibronectin, which suggested that PLLA membranes could have the potential to be used as substrates in skin injuries. PLA copolymers have also gained attention as skin dressing in wound healing applications, due to their mechanical properties and controlled degradation rate, such as PLLA/PHBV (polyhydroxybutyrate-co-hydroxyvalerate).[81]

Neural TE targets nerve regeneration by using scaffolds, neuronal support cells, and growth factors.[82] Reconnection of the proximal and distal ends of injured nerves is the route for the peripheral nerve regeneration of transacted nerves that is conducted by using autografts or tubular polymeric nerve guides. Non-degradable silicon tubes were initially used as nerve guidance channels for nerve regeneration. However, silicon tubes are being replaced by biodegradable polymers such as PLLA and PLGA, as these polymers negate the need for second surgery.[83]

Liver replacement using isolated hepatocytes is a potential alternative to orthotropic liver transplantation that has serious limitations, such as rapid progression of the disease and donor shortages. Culturing the hepatocytes in suspensions and encapsulating them in polymeric microcapsules have been investigated for this purpose. Among the biodegradable

synthetic polymers, PLA and PLGA have been considered as substrates for hepatocyte culture in liver TE.

Cardiovascular disease has been a major cause of mortality in the western world, particularly coronary artery disease.[84] TE approaches have been investigated to overcome the problems associated with surgical techniques using arterial grafts (e.g. acute thrombogenicity of the graft, anastomotic intimal hyperplasia, aneurysm formation, infection, and progression of atherosclerotic disease).[85] TE approaches rely on using tubular porous structures, which should be biocompatible, flexible, elastic, and biodegradable, are being seeded by autologous vascular cells, and subsequently cultured *in vitro* or immediately implanted.[86] Carfi Pavia *et al.*[87] have developed and characterized tubular scaffolds of PLLA/PLA blends (100/0, 90/10, 75/25 wt/wt) for vascular tissue engineering (VTE) applications. A diffusion-induced phase separation (DIPS) process, after dip coating around a nylon fiber with a diameter of about 700 μm, was performed to produce the vessel-like scaffolds. The fiber was initially immersed in a PLA/dioxane or PLLA/PLA blend/dioxane solution (dip coating bath) at 35°C, followed by immersion in a second bath (DIPS bath) containing pure water at the same temperature once it was pulled out at different constant rates. The as-produced scaffolds exhibited an open pore structure with interconnectivity along the wall. It was also demonstrated that the thickness of the wall could be changed by altering the rate at which the fiber was extracted from the polymer/dioxane bath. Preliminary biological assessment of the scaffolds using endothelial cells (ECV304 continuous human endothelial cell) showed a good level of adhesion and proliferation with a development of a homogenous vessel-like monolayer. The results indicated promising applications of PLA scaffolds in VTE.

Lee *et al.*[88] have used PLGA to produce macroporous foams for intestine TE. In order to improve the hydrophobicity of PLGA, and also introduce bioactive functionality, small intestine submucosa (SIS) was added as a natural source to produce SIS-powder-impregnated PLGA (SIS/PLGA) hybrid scaffolds. These macroporous foams were 90% porous, and had a relatively homogeneous pore structure, and good interconnected pores with an average pore size ranging between 69 and 106 μm. After implanting the PLGA and SIS/PLGA scaffolds subcutaneously under the dorsal skin of an athymic nude mouse, SIS/PLGA scaffolds were found to be osteoconductive to allow remodeling and replacement by osseous tissue.

PLA, its copolymers and blends, have also been studied as scaffolds for cartilage TE. Freed *et al.*[89] investigated the use of porous PDLLA membranes as scaffolds for neocartilage formation. PDLLA scaffolds were produced using solvent casting particulate leaching technique. PDLLA sponges were $1 \times 0.5 \times 0.3$ cm^3 with a porosity of 91%, and pores with diameters less than 308 μm. Chondrocytes cultured on porous PLLA membranes showed

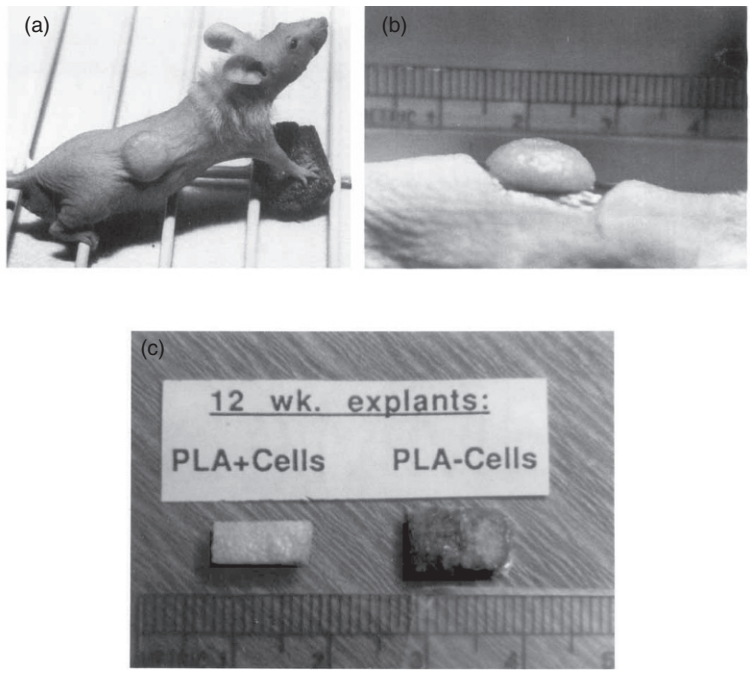

11.2 (a, b) Nude mice with a subcutaneous implant of human rib chondrocytes cultured on a PLLA scaffold. (c) Explants with and without cultured bovine chondrocytes.[89]

neocartilage formation, comparable to that observed for chondrocytes cultured on collagen substrates prepared from articular cartilage. Chondrocytes grew on these substrates for up to 6 months, and maintained the shape of the initial apparatus, and a tissue with characteristics similar to those of cartilage was formed, i.e., the synthesis of glycosaminoglycans and collagen type I and II. A subcutaneous implant of human rib chondrocytes cultured on PLLA scaffolds in a nude mouse is shown in Fig. 11.2. The dimensions of the original polymer scaffold were maintained, and appeared glistening white macroscopically (Fig. 11.2b). PLLA scaffolds without seeded cells remained intact for up to 6 months, and explants appeared to be macroscopically red (Fig. 11.2c). In this case, the polymers appeared to be infiltrated by red blood cells in new blood vessels, lymphocytes, multinucleated giant cells, and fibroblasts. It should be mentioned that subcutaneous injection of isolated bovine chondrocytes resulted in irregular cartilaginous nodules in the absence of a polymer scaffold.

Bone repair has been considered to be a major application of TE. The general concept of BTE includes the use of a construct to promote the regeneration of the damaged tissue.[90] This construct is composed of a scaffold, viable

cells, and biologically active agents (e.g. growth factors).[90,91] An ideal scaffold for BTE applications should have biodegradability, biocompatibility, interconnected porosity with appropriate pore size, and appropriate mechanical properties to be able to stand the applied forces.[5,34,43,92] While current scaffolds in BTE are made either of polymers or ceramics, the inherent properties of these base materials, such as brittleness when made of ceramics and/or relatively low mechanical strength when made of polymers, limit their use. To overcome this issue, porous structures based on composites have been developed for bone repair applications. In these, the mechanical properties of the polymer matrix are improved through particle reinforcement. Attributable to their bioactivity, bioceramics have been shown to improve the overall biological response of the construct.[93,94] PLA and PLGA have been extensively considered as degradable synthetic polymers for matrices of BTE scaffolds.[16] Osteoblastic cell adhesion, spreading, as well as ability to grow and proliferate on PLLA and PLGA films, have been demonstrated. In addition, increased alkaline phosphatase activity and synthesis of collagen I have been reported for cells grown on these polymers.[95] Bone marrow cells cultured on porous PLGA scaffolds were also found to be able to initiate ectopic bone formation when implanted into the rat mesentery.[96] Porous materials present a better integration with the recipient tissue when implanted *in vivo*. It has been reported by Salgado *et al.*[34] that an optimal pore size for BTE should be between 200 and 900 μm. However, according to Karageorgiou and Kaplan,[97] it is not possible to suggest an optimal pore size due to the large number of bone features *in vivo*, and the diversity of biomaterials and cells used *in vitro* and *in vivo*. They also reported that, although there is no optimal pore size, larger pore size favors osteogenesis as it allows sufficient nutrient supplies and exchange of metabolic products. However, there is also an upper limit for the pore size, due to reduction in the mechanical stability of the scaffolds and surface area available for cell attachment. In contrast, pore occlusion by cells will prevent cellular diffusion within the scaffold if the pores are excessively small.

Gugala *et al.*[98] showed that porous PDLLA membrane provided a suitable scaffold for BTE since osteoblasts attached proliferated and expressed osteoblastic phenotype. Scanning electron microscopy micrographs of the PDLLA membranes are shown in Figs. 11.3a and 11.3b that reveal interconnected open pores with a diameter in the range of 50–70 μm. The osteoblasts, harvested from the calvariae of 8-day old OFA strain rats, attached to the PDLLA membrane grew into the pores while maintaining the phenotype and morphology (Fig. 11.3c). It was demonstrated that the cell number, DNA amount, alkaline phosphatase activity, and total protein amount were higher for the porous membranes as compared to those that were nonporous. Therefore, the beneficial effects of porous membranes in the regeneration of bone could be attributed to the superior surface characteristics of

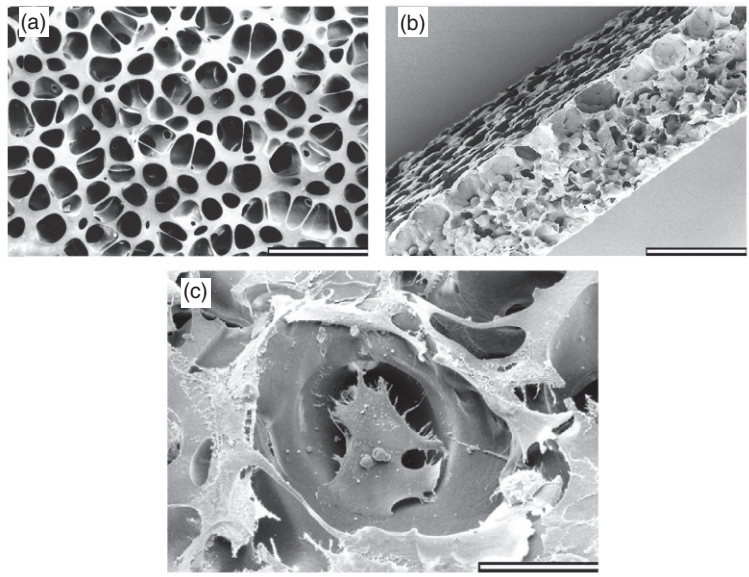

11.3 Scanning electron microscope (SEM) micrographs of the porous PLA membranes; (a) surface and (b) cross-section (scale bars represent 200 μm). (c) SEM micrograph of osteoblasts on the porous PLA membrane: the cells attached to the membrane surface and grew into the pores (scale bar represents 50 μm).[98]

the porous membranes. It was also stated that such membranes seeded with autogenous osteoblasts have the potential to be used as tissue-engineered implants for the treatment of critical sized bone defects.

Although highly porous polymer matrices have a great potential for serving as TE scaffolds, they may be associated with poor mechanical properties (e.g. low strength), especially in BTE. Therefore, the incorporation of bioactive ceramics (e.g. calcium phosphates), or glasses (e.g. bioactive SGs and PGs) into biodegradable polymers has been of interest. In addition to improving the mechanical properties, such incorporation could also lead to increased osteoconductivity of the scaffolds.[47] Ma *et al.*[99] produced highly porous PLLA and PLLA-HA scaffolds using TIPS technique. The fabricated foams have revealed interconnected porosity (approximately 93% for PLLA and 89% for PLLA-HA composite) with pore size in the range of tens to hundreds of microns (Fig. 11.4). It was found that the PLLA-HA foams were mechanically strong, with architectures suitable for seeding and growth of osteoblast. The compressive modulus and yield strength of the PLLA-HA composite foam were significantly greater compared to those for neat PLLA foam. PLLA-HA foams were demonstrated to possess higher osteoblast survival rate. In addition, cell distribution

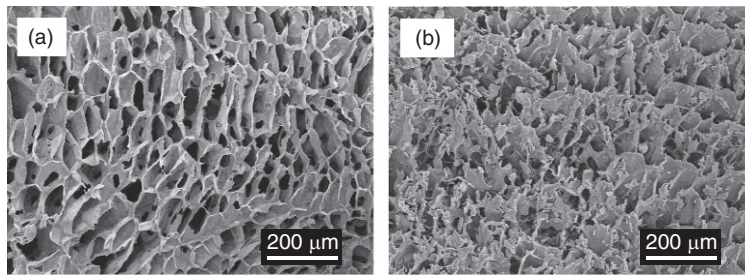

11.4 SEM micrographs of (a) PLLA and (b) PLLA-HA foams.[99]

and growth was more uniform, and improved new tissue formation was observed. PLLA-HA composite foams revealed enhanced bone specific gene expression *in vitro* compared to neat PLLA foams. These findings suggested that the PDLLA-HA scaffolds were superior to the pure PDLLA scaffolds for osseous TE.[99]

Phosphate glass incorporated PLA (PLA-PG) composite foams have also been produced and studied for BTE by Georgiou *et al.*[18] using $scCO_2$. The glass content was shown to affect the foam morphology. Smaller pores were created with increasing amounts of glass content and the foaming of PLA-20 (wt.%) PG was found not to be efficient. The addition of fillers increased the foam densities; nevertheless, the required level of porosity for BTE remained above 75%. Direct contact of PLA-PG foams with human fetal bone cells and their proliferation have shown similar results compared to foams of PLA with HA or β-TCP.

11.7 Conclusion and future trends

PLA and PLA-based foams have been extensively considered as scaffolds for TE applications as a consequence of their biodegradability, biocompatibility, and ease of fabrication with desired morphologies. Several fabrication techniques have been used to create PLA foams, including solvent casting-salt leaching, phase separation, gas foaming, and freeze drying, among which gas foaming using CO_2 has been of interest since it negates the need for organic solvents. Although PLA satisfies some of the required properties for TE applications, it lacks some important requirements, such as bioactive functionality and adequate mechanical properties for certain applications (e.g. load-bearing applications). Therefore, the incorporation of bioactive ceramics or glasses, and biofactors (e.g. proteins, genes and growth factors) into PLA scaffolds has been the focus of recent studies. For example, Ginty *et al.*[100] developed composite scaffolds of alginate and PLA using $scCO_2$ and alginate entrapment technique to allow several degradation rates and release of selected biofactors. The encapsulation of vascular

endothelial growth factor (VEGF) in the alginate fibers, and bone morphogenetic protein (BMP) in PDLLA resulted in accelerated release of VEGF and slower release of BMP which play a prominent role in bone regeneration. Kanczler *et al.*[101] investigated the delivery of human bone marrow stromal cells (HBMSC) onto the similar composite scaffold to enhance the bone regenerative capacity of the scaffold. It was demonstrated that a combination of HBMSC and release of angiogenic and osteogenic factors from the alginate-VEGF/PDLLA-BMP scaffold improved the repair and regeneration of bone critical sized defects. Therefore, since the biodegradability, biocompatibility, and morphologies of PLA foams have been approved for TE applications, current and future research should be more focused on the enhancement of the biological response of these synthetic polymeric foams to improve the cell-scaffold interaction.

11.8 References

1. Lee JH, Oh JH, Lee JH, Kim MR and Min CK (2011). Evaluation of *in vitro* spermatogenesis using poly(D,L-lactic-co-glycolic acid) (PLGA)-based macroporous biodegradable scaffolds. *J Tissue Eng Regen M*. **5**(2):130–7.
2. Griffith LG (2000). Polymeric biomaterials. *Acta Mater*. **48**(1):263–77.
3. Shoichet MS (2010). Polymer scaffolds for biomaterials applications. *Macromolecules*. **43**(2):581–91.
4. Park JB and Lakes RS (2007). *Biomaterials: An Introduction*. New York, NY: Springer.
5. Chen GP, Ushida T and Tateishi T (2002). Scaffold design for tissue engineering. *Macromol Biosci*. **2**(2):67–77.
6. Hollister SJ (2005). Porous scaffold design for tissue engineering. *Nat Mater*. **4**(7):518–24.
7. Griffith LG and Naughton G (2002). Tissue engineering – Current challenges and expanding opportunities. *Science*. **295**(5557):1009–14.
8. Liu C, Xia Z and Czernuszka JT (2007). Design and development of three-dimensional scaffolds for tissue engineering. *Chem Eng Res Des*. **85**(A7):1051–64.
9. Howard D, Buttery LD, Shakesheff KM and Roberts SJ (2008). Tissue engineering: strategies, stem cells and scaffolds. *J Anat*. **213**(1):66–72.
10. Hutmacher DW (2000). Scaffolds in tissue engineering bone and cartilage. *Biomaterials*. **21**(24):2529–43.
11. Hollinger JO and Battistone GC (1986). Biodegradable bone repair materials – Synthetic-polymers and ceramics. *Clin Orthop Relat R*. **207**:290–305.
12. Pan Z and Ding JD (2012). Poly(lactide-co-glycolide) porous scaffolds for tissue engineering and regenerative medicine. *Interface Focus*. [Review]. **2**(3):366–77.
13. Mathieu LM, Montjovent MO, Bourban PE, Pioletti DP and Manson JAE (2005). Bioresorbable composites prepared by supercritical fluid foaming. *J Biomed Mater Res A*. **75**A(1):89–97.
14. Mathieu LM, Mueller TL, Bourban PE, Pioletti DP, Muller R and Manson JAE (2006). Architecture and properties of anisotropic polymer composite scaffolds for bone tissue engineering. *Biomaterials*. **27**(6):905–16.

15. Xiong Z YY, Wang SG and Zhang RJ (2002). Fabrication of porous scaffolds for bone tissue engineering via low temperature deposition. *Sci Mater*. **46**:771–6.
16. Blaker JJ, Maquet V, Jerome R, Boccaccini AR and Nazhat SN (2005). Mechanical properties of highly porous PDLLA/Bioglass (R) composite foams as scaffolds for bone tissue engineering. *Acta Biomaterialia*. **1**(6):643–52.
17. Blaker JJ, Gough JE, Maquet V, Notingher I and Boccaccini AR (2003). *In vitro* evaluation of novel bioactive composites based on Bioglass (R)-filled polylactide foams for bone tissue engineering scaffolds. *J Biomed Mater Res A*. **67A**(4):1401–11.
18. Georgiou G, Mathieu L, Pioletti DP, Bourban PE, Manson JAE, Knowles JC and Nazhat SN (2007). Polylactic acid-phosphate glass composite foams as scaffolds for bone tissue engineering. *J Biomed Mater Res B*. **80B**(2):322–31.
19. Mohammadi MS, Ahmed I, Muja N, Rudd CD, Bureau MN and Nazhat SN (2011). Effect of phosphate-based glass fibre surface properties on thermally produced poly(lactic acid) matrix composites. *J Mater Sci-Mater M*. **22**(12):2659–72.
20. Hartmann MH (1998). *Biopolymers from Renewable Resources*. Berlin: Springer-Verlag. p. 367–411.
21. Garlotta D (2001). A literature review of poly(lactic acid). *J Polym Environ*. **9**(2):63–84.
22. Kohn J and Engelberg I (1990). Physico-mechanical properties of degradable polyesters used in medical applications: a comparative study. *Biomaterials*. **12**:292–303.
23. Christel P, Chabot F, Leray JL, Morin C and Vert M (1980). Biodegradable composites for internal fixation. In: G.D. Winter DFG and Plenk H, (eds.) *Biomaterilas*. New York: Wiley and Sons. p. 271–80.
24. Pavia FC, La Carrubba V and Brucato V (2009). Tuning of biodegradation rate of PLLA scaffolds via blending with PLA. *Int J Mater Form*. [Article]. **2**:713–6.
25. La Carrubba V, Carfi Pavia F, Brucato V and Piccarolo S (2008). PLLA/PLA scaffolds prepared via thermally induced phase separation (TIPS): Tuning of properties and biodegradability. *Int J Mater Foaming*. **1**(1):619–22.
26. Cai H DV, Gross RA and McCarthy SP (1996). Effect of physical aging, crystallinity, and orientation on the enzymatic degradation of poly(lactic acid) *J Polym Sci B: Polym Phys*. **34**:2701–8.
27. Tsuji H and Ikarashi K (2004). *In vitro* hydrolysis of poly(L-lactide) crystalline residues as extended-chain crystallites. Part I: long-term hydrolysis in phosphate-buffered solution at 37°C. *Biomaterials*. [Article]. **25**(24):5449–55.
28. Makadia HK and Siegel SJ (2011). Poly lactic-co-glycolic acid (PLGA) as biodegradable controlled drug delivery carrier. *Polymers*. **3**:1377–97.
29. Navarro M, Ginebra MP, Planell JA, Barrias CC and Barbosa MA (2005). *In vitro* degradation behavior of a novel bioresorbable composite material based on PLA and a soluble CaP glass. *Acta Biomaterialia*. **1**(4):411–9.
30. Blaker JJ, Bismarck A, Boccaccini AR, Young AM and Nazhat SN (2010). Premature degradation of poly(alpha-hydroxyesters) during thermal processing of Bioglass (R)-containing composites. *Acta Biomaterialia*. **6**(3):756–62.
31. Spinu M, Jackson C, Keating MY and Gardner KH (1996). Material design in poly(lactic acid) systems: Block copolymers, star homo- and copolymers, and stereocomplexes. *J Macromol Sci Pure*. **A33**(10):1497–530.

32. Hyon SH, Jamshidi K and Ikada Y (1998). Effects of residual monomer on the degradation of DL-lactide polymer. *Polym Int*. **46**(3):196–202.
33. Eisenbarth E (2007). Biomaterials for tissue engineering. *Adv Eng Mater*. **9**(12):1051–60.
34. Salgado AJ, Coutinho OP and Reis RL (2004). Bone tissue engineering: state of the art and future trends. *Macromol Biosci*. **4**(8):743–65.
35. Mikos AG, Thorsen AJ, Czerwonka LA, Bao Y, Langer R, Winslow DN and Vacanti JP (1994). preparation and characterization of poly(L-Lactic acid) foams. *Polymer*. **35**(5):1068–77.
36. Misra SK and boccaccini AR (2007). Biodegradable and bioactive polymer/ceramic composite scaffolds. In: AR Boccaccini and J Gough, (eds.) *Tissue Engineering using Ceramics and Polymers*. Cambridge: Woodhead Publishing Limited.
37. LeBlon CE, Pai R, Fodor CR, Golding AS, Coulter JP and Jedlicka SS (2013). *In vitro* comparative biodegradation analysis of salt-leached porous polymer scaffolds. *J Appl Polym Sci*. [Article]. **128**(5):2701–12.
38. Yang SF, Leong KF, Du ZH and Chua CK (2001). The design of scaffolds for use in tissue engineering. Part 1. Traditional factors. *Tissue Eng*. **7**(6):679–89.
39. Gomes ME and Salgado AJ (2002). *Polymer Based Systems on Tissue Engineering, Replacement and Regeneration*. 1st edn. The Netherlands: Kluwer, Dordrecht.
40. Boccaccini AR and Maquet V (2003). Bioresorbable and bioactive polymer/Bioglass (R) composites with tailored pore structure for tissue engineering applications. *Compos Sci Technol*. **63**(16):2417–29.
41. Chen Q, Roether JA and Boccaccini AR (2008). Tissue engineering scaffolds from bioactive glass and composite materials. In: N Ashammakhi, R Reis and F Chiellini (eds.) *Topics in Tissue Engineering*, Vol. **4**. Available at: http://www.oulu.fi/spareparts/ebook_topics_in_t_e/list_of_contr.html
42. Boccaccini AR and Blaker JJ (2005). Bioactive composite materials for tissue engineering scaffolds. *Expert Rev Med Devic*. **2**(3):303–17.
43. Hutmacher DW (2001). Scaffold design and fabrication technologies for engineering tissues – state of the art and future perspectives. *J Biomat Sci-Polym E*. **12**(1):107–24.
44. Keshaw H, Georgiou G, Blaker JJ, Forbes A, Knowles JC and Day RM (2009). Assessment of polymer/bioactive glass-composite microporous spheres for tissue regeneration applications. *Tissue Eng Pt A*. **15**(7):1451–61.
45. Blaker JJ, Knowles JC and Day RM (2008). Novel fabrication techniques to produce microspheres by thermally induced phase separation for tissue engineering and drug delivery. *Acta Biomaterialia*. **4**(2):264–72.
46. Chen JS, Tu S-L and Tsay R-Y (2010). A morphological study of porous polylactide scaffolds prepared by thermally induced phase separation. *J Taiwan Inst Chem Eng*. **41**:229–38.
47. Hutmacher DW, Schantz JT, Lam CXF, Tan KC and Lim TC (2007). State of the art and future directions of scaffold-based bone engineering from a biomaterials perspective. *J Tissue Eng Regen M*. **1**(4):245–60.
48. Pang L, Hu YY, Yan YN, Liu L, Xiong Z, Wei YY and Bai JP (2007). Surface modification of PLGA/beta-TCP scaffold for bone tissue engineering: Hybridization with collagen and apatite. *Surf Coat Tech*. **201**(24):9549–57.

49. Shor L, Guceri S, Wen XJ, Gandhi M and Sun W (2007). Fabrication of three-dimensional polycaprolactone/hydroxyapatite tissue scaffolds and osteoblast-scaffold interactions *in vitro*. *Biomaterials*. **28**(35):5291–7.
50. Hutmacher DW and Cool S (2007). Concepts of scaffold-based tissue engineering-the rationale to use solid free-form fabrication techniques. *J Cell Mol Med*. **11**(4):654–69.
51. Taboas JM, Maddox RD, Krebsbach PH and Hollister SJ (2003). Indirect solid free form fabrication of local and global porous, biomimetic and composite 3D polymer-ceramic scaffolds. *Biomaterials*. **24**(1):181–94.
52. Leong KF, Cheah CM and Chua CK (2003). Solid freeform fabrication of three-dimensional scaffolds for engineering replacement tissues and organs. *Biomaterials*. **24**(13):2363–78.
53. Barry JJA, Silva MMCG, Popov VK, Shakesheff KM and Howdle SM (2006). Supercritical carbon dioxide: putting the fizz into biomaterials. *Philos T Roy Soc A*. **364**(1838):249–61.
54. Woods HM, Silva MMCG, Nouvel C, Shakesheff KM and Howdle SM (2004). Materials processing in supercritical carbon dioxide: surfactants, polymers and biomaterials. *J Mater Chem*. **14**(11):1663–78.
55. Liao X, Zhang HC and He T (2012). Preparation of porous biodegradable polymer and its nanocomposites by supercritical CO_2 foaming for tissue engineering. *J Nanomater*. **2012**:1–12, Article ID 836394. doi:10.1155/2012/836394.
56. Cooper AI (2000). Polymer synthesis and processing using supercritical carbon dioxide. *J Mater Chem*. **10**(2):207–34.
57. Goel SK and Beckman EJ (1994). Generation of microcellular polymeric foams using supercritical carbon-dioxide.1. Effect of pressure and temperature on nucleation. *Polym Eng Sci*. **34**(14):1137–47.
58. Arora KA, Lesser AJ and McCarthy TJ (1998). Preparation and characterization of microcellular polystyrene foams processed in supercritical carbon dioxide. *Macromolecules*. **31**(14):4614–20.
59. Alavi SH, Gogoi BK, Khan M, Bowman BJ and Rizvi SSH (1999). Structural properties of protein-stabilized starch-based supercritical fluid extrudates. *Food Res Int*. **32**(2):107–18.
60. Goel SK and Beckman EJ (1994). Generation of microcellular polymeric foams using supercritical carbon-dioxide.2. Cell-growth and skin formation. *Polym Eng Sci*. **34**(14):1148–56.
61. Park CB, Baldwin DF and Suh NP (1995). Effect of the pressure drip rate on cell nucleation in continuous processing of microcellular polymers. *Polym Eng Sci*. **35**(5):432–40.
62. Sheridan MH, Shea LD, Peters MC and Mooney DJ (2000). Bioadsorbable polymer scaffolds for tissue engineering capable of sustained growth factor delivery. *J Control Release*. **64**(1–3):91–102.
63. Howdle SM, Watson MS, Whitaker MJ, Popov VK, Davies MC, Mandel FS, Wang JD and Shakesheff KM (2001). Supercritical fluid mixing: preparation of thermally sensitive polymer composites containing bioactive materials. *Chem Commun*. (1):109–10.
64. Kazarian SG, Vincent MF, Bright FV, Liotta CL and Eckert CA (1996). Specific intermolecular interaction of carbon dioxide with polymers. *J Am Chem Soc*. **118**(7):1729–36.

65. Baldwin DF, Shimbo M and Suh NP (1995). The role of gas dissolution and induced crystallization during microcellular polymer processing – A study of poly(ethylene-terephthalate) and carbon-dioxide systems. *J Eng Mater-T Asme*. **117**(1):62–74.
66. Di Maio E, Mensitieri G, Iannace S, Nicolais L, Li W and Flumerfelt RW (2005). Structure optimization of polycaprolactone foams by using mixtures of CO_2 and N-2 as blowing agents. *Polym Eng Sci*. [Article]. **45**(3):432–41.
67. Tai HY, Mather ML, Howard D, Wang WX, White LJ, Crowe JA, Morgan SP, Chandra A, Williams DJ, Howdle SM and Shakesheff KM (2007). Control of pore size and structure of tissue engineering scaffolds produced by supercritical fluid processing. *Eur Cells Mater*. **14**:64–76.
68. Baker KC, Manitiu M, Bellair R, Gratopp CA, Herkowitz HN and Kannan RM (2011). Supercritical carbon dioxide processed resorbable polymer nanocomposite bone graft substitutes. *Acta Biomaterialia*. [Article]. **7**(9):3382–9.
69. Jacobs LJM, Kemmere MF and Keurentjes JTF (2008). Sustainable polymer foaming using high pressure carbon dioxide: a review on fundamentals, processes and applications. *Green Chem*. **10**(7):731–8.
70. Mooney DJ, Baldwin DF, Suh NP, Vacanti LP and Langer R (1996). Novel approach to fabricate porous sponges of poly(D,L-lactic-co-glycolic acid) without the use of organic solvents. *Biomaterials*. **17**(14):1417–22.
71. Singh L, Kumar V and Ratner BD (2004). Generation of porous microcellular 85/15 poly ((DL)-lactide-co-glycolide) foams for biomedical applications. *Biomaterials*. **25**(13):2611–7.
72. Hu X, Nawaby AV, Naguib HE, Day M, Ueada K and Liao X (2005). Ploylactic acid (PLA)-CO_2 foams at sub-critical conditions. In *SPE ANTEC Technical Papers*, Boston, USA, p. 2670–3.
73. Matuana LM and Faruk O (2010). Effect of gas saturation conditions on the expansion ratio of microcellular poly(lactic acid)/woof flour composites. *Exp Polym Lett*. **4**(10):621–31.
74. Ji CD, Annabi N, Hosseinkhani M, Sivaloganathan S and Dehghani F (2012). Fabrication of poly-(DL)-lactide/polyethylene glycol scaffolds using the gas foaming technique. *Acta Biomaterialia*. [Article]. **8**(2):570–8.
75. Caridade SG, Merino EG, Martins GV, Luz GM, Alves NM and Mano JF (2012). Membranes of poly(DL-lactic acid)/Bioglass (R) with asymmetric bioactivity for biomedical applications. *J Bioact Compat Pol*. [Article]. **27**(5):429–40.
76. Kang DJ, Xu D, Zhang ZX, Pal K, Bang DS and Kim JK (2009). Well-controlled microcellular biodegradable PLA/silk composite foams using supercritical CO_2. *Macromol Mater Eng*. [Article]. **294**(9):620–4.
77. Hench LL, Splinter RJ, Allen WC and Greenlee TK (1972). Bonding mechanisms at the interface of ceramic prosthetic materials. *J Biomed Mater Res.* **5**(6):117–41.
78. Jones JR (2013). Review of bioactive glass: From Hench to hybrids. *Acta Biomaterialia*. [Review]. **9**(1):4457–86.
79. Montjovent MO, Mathieu L, Hinz B, Applegate LL, Bourban PE, Zambelli PY, Manson JA and Pioletti DP (2005). Biocompatibility of bioresorbable poly(L-lactic acid) composite scaffolds obtained by supercritical gas foaming with human fetal bone cells. *Tissue Eng*. [Article]. **11**(11–12):1640–9.

80. Santos AR, Barbanti SH, Duek EAR, Dolder H, Wada RS and Wada MLF (2001). Vero cell growth and differentiation on poly(L-lactic acid) membranes of different pore diameters. *Artif Organs*. **25**(1):7–13.
81. Santos AR, Ferreira BMP, Duek EAR, Dolder H, Wada RS and Wada MLF (2004). Differentiation pattern of Vero cells cultured on poly(L-lactic acid)/poly(hydroxybutyrate-co-hydroxyvalerate) blends. *Artif Organs*. **28**(4):381–9.
82. Lanza RP, Langer R and Vacanti J (2000). *Principles of Tissue Engineering*. New York: Academic.
83. Nair LS and Laurencin CT (2006). Polymers as biomaterials for tissue engineering and controlled drug delivery. *Adv Biochem Eng Biot*. **102**:47–90.
84. Soletti L, Hong Y, Guan JJ, Stankus JJ, El-Kurdi MS, Wagner WR and Vorp DA. A bilayered elastomeric scaffold for tissue engineering of small diameter vascular grafts. *Acta Biomaterialia*. [Article]. **6**(1):110–22.
85. Conte MS (1998). The ideal small arterial substitute: a search for the Holy Grail?. *FASEB J*. [Editorial Material]. **12**(1):43–5.
86. Song Y, Wennink JWH, Kamphuis MMJ, Vermes I, Poot AA, Feijen J and Grijpma DW (2010). Effective seeding of smooth muscle cells into tubular poly(trimethylene carbonate) scaffolds for vascular tissue engineering. *J Biomed Mater Res A*. [Article]. **95A**(2):440–6.
87. Carfi Pavia F, Rigogliuso S, La Carrubba V, Mannella GA, Ghersi G and Brucato V (2012). Poly lactic acid based scaffolds for vascular tissue engineering. *Chem Eng Trans*. **27**:409–14.
88. Lee SJ, Lee IW, Lee YM, Lee HB and Khang G (2004). Macroporous biodegradable natural/synthetic hybrid scaffolds as small intestine submucosa impregnated poly(D,L-lactide-co-glycolide) for tissue-engineered bone. *J Biomat Sci-Polym E*. **15**(8):1003–17.
89. Freed LE, Marquis JC, Nohria A, Emmanual J, Mikos AG and Langer R (1993). Neocartilage formation *in vitro* and *in vivo* using cells cultured on synthetic biodegradable polymers. *J Biomed Mater Res*. **27**(1):11–23.
90. Hutmacher DW and Garcia AJ (2005). Scaffold-based bone engineering by using genetically modified cells. *Gene*. **347**(1):1–10.
91. Langer R and Vacanti JP (1993). Tissue engineering. *Science*. **260**(5110):920–6.
92. Ma PX (2004). Scaffolds for tissue fabrication. *Mater Today*. **7**(5):30–40.
93. Laurencin CT and Lu HL (2000). Polymer-ceramic composites for bone tissue engineering. In: J Davies (ed.) *Bone Engineering*. p. 462–72.
94. Wang M (2003). Developing bioactive composite materials for tissue replacement. *Biomaterials*. **24**(13):2133–51.
95. Ishaug SL, Yaszemski MJ, Bizios R and Mikos AG (1994). Osteoblast function on synthetic biodegradable polymers. *J Biomed Mater Res*. **28**(12):1445–53.
96. IshaugRiley SL, Crane GM, Gurlek A, Miller MJ, Yasko AW, Yaszemski MJ and Mikos AG (1997). Ectopic bone formation by marrow stromal osteoblast transplantation using poly(DL-lactic-co-glycolic acid) foams implanted into the rat mesentery. *J Biomed Mater Res*. **36**(1):1–8.
97. Karageorgiou V and Kaplan D (2005). Porosity of 3D bimaterial scaffolds and osteogenesis. *Biomaterials*. **26**(27):5474–91.
98. Gugala Z and Gogolewski S (2004). Protein adsorption, attachment, growth and activity of primary rat osteoblasts on polylactide membranes with defined surface characteristics. *Biomaterials*. **25**(12):2341–51.

99. Ma PX, Zhang RY, Xiao GZ and Franceschi R (2001). Engineering new bone tissue *in vitro* on highly porous poly(alpha-hydroxyl acids)/hydroxyapatite composite scaffolds. *J Biomed Mater Res*. **54**(2):284–93.
100. Ginty PJ, Barry JJA, White LJ, Howdle SM and Shakesheff KM (2008). Controlling protein release from scaffolds using polymer blends and composites. *Eur J Pharm Biopharm*. **68**(1):82–9.
101. Kanczler JM, Ginty PJ, White L, Clarke NMP, Howdle SM, Shakesheff KM and Oreffo RO (2010). The effect of the delivery of vascular endothelial growth factor and bone morphogenic protein-2 to osteoprogenitor cell populations on bone formation. *Biomaterials*. **31**(6):1242–50.

12

Porous hydrogel biomedical foam scaffolds for tissue repair

S. VAN VLIERBERGHE, G.-J. GRAULUS, S. KESHARI SAMAL, I. VAN NIEUWENHOVE and P. DUBRUEL, Ghent University, Belgium

DOI: 10.1533/9780857097033.2.335

Abstract: In the present chapter, the state-of-the-art of porous hydrogel foams will be described and emphasis will be made on their relevance for biomedical applications and, more specifically, tissue repair. The description aims at emphasizing both some novel aspects as well as the versatility of hydrogel foams. In addition, an overview of some general hydrogel aspects will be given. Next, a section will deal with natural polymers commonly used and suitable for hydrogel foam development and their respective tissue regeneration applications, followed by a description on advanced technologies applied to design and characterize novel hydrogel foams.

Key words: porous hydrogel scaffolds, surface modification, tissue engineering, processing techniques, characterization tools.

12.1 Introduction

Mankind has always been looking for new ways to prevent or treat diseases and injuries. In infectious diseases, large steps forward have been taken with the introduction of antibiotics, vaccines, anti-virals, anti-fungals, etc. (Andre *et al.*, 2008; Jayachandran *et al.*, 2010). When it comes to injured or failing tissues, however, patients often end up on waiting lists for organ or tissue transplantation (Langer and Vacanti, 1993; Risbud, 2001; The Organ Procurement and Transplantation Network, 2012). Interestingly, the relatively new research domain of regenerative medicine may offer new ways to treat patients with tissues that are failing due to trauma or disease. Regenerative medicine can be seen as an emerging interdisciplinary field of research and clinical applications focused on the repair, replacement or regeneration of cells, tissues or organs to restore impaired function resulting from any cause, but including congenital defects, disease and trauma

(Greenwood *et al.*, 2006). However, a more practical definition was proposed by Mason and Dunnill (2008):

> '*Regenerative medicine replaces or regenerates human cells, tissues or organs, to restore or establish normal function*.'

Because the aim of regenerative medicine is the restoration of normal function, it can be distinguished from organ transplantation, since patients receiving donor organs often require immunosuppressant drugs. This dependence on pharmaceuticals cannot be considered 'normal function' (Yannas, 2001; Mason and Dunnill, 2008).

One can distinguish four different strategies towards regenerative medicine (Yannas, 2001). The first strategy uses the patient's own proteins, antibodies or genes to restore tissue function (Go *et al.*, 2011; Rios *et al.*, 2011). The second is based on mature cells which are grown into functional tissues; this method is more commonly known as 'tissue engineering' (Langer and Vacanti, 1993; Risbud, 2001; Griffith and Naughton, 2002; Tabata, 2009; Gojo *et al.*, 2011; van Vlierberghe *et al.*, 2011a). The third is the use of (embryonic) stem cells (Gojo *et al.*, 2011). Finally, prosthetic devices can be used to replace the failing tissue's function (Chehade and Elder, 1997).

Tissue engineering has been defined by Langer and Vacanti as an interdisciplinary field that applies the principles of engineering and life sciences toward the development of biological substitutes that restore, maintain or improve tissue function (Langer and Vacanti, 1993).

One can distinguish four main strategies for engineering new tissues (Langer and Vacanti, 1993; Peter, 2004). The first is the delivery of biologically active molecules, including growth factors, therapeutic genes and drugs, that can act as cues to induce new tissue formation (Langer and Vacanti, 1993; Risbud, 2001; Dang and Leong, 2006; Go *et al.*, 2011; Ladewig, 2011). In the second, isolated cells or cell substitutes can be applied. The third is the combination of donor cells with semi-permeable membranes, which are subsequently implanted; these biomedical devices are able to perform some biochemical tasks, which healthy tissue should perform, but without the risk of tissue rejection by the patient's immune system (Langer and Vacanti, 1993). The use of porous hydrogel foams where cells can be seeded onto, offers a fourth possibility.

Ideal scaffolds share a number of characteristics, as reported by Ma (Peter, 2004):

1. Ideal cell supports should possess a high porosity and a suitable pore size fine-tuned to the cell type applied.
2. They should have a large surface area.
3. The materials should show adequate mechanical strength.

4. Both the scaffolds and their metabolites should be non-toxic and biocompatible.
5. The scaffolds should positively interact with cells.
6. Biodegradability is often required, and the degradation rate should ideally match the rate of new tissue formation.

Interestingly, tissue engineering is not limited to medical applications. The possibility of growing tissues *in vitro* in such a manner that they mimic their *in vivo* counterparts could also have a great impact on drug development and physiological and biological research (Dutta and Dutta, 2009).

In the present chapter, the fourth strategy of tissue engineering will be described. Porous three-dimensional scaffolds can be designed and developed that resemble the natural extracellular environment. Therefore, the biomaterials which are often selected show similar physico-chemical properties to the extracellular matrix (ECM). One example includes the development of porous scaffolds containing bioactive compounds such as glycosaminoglycans and/or growth factors (Ellis and Yannas, 1996; Freyman *et al.*, 2001; Pek *et al.*, 2004; Zaleskas *et al.*, 2004). Subsequently, autologous or allogenic cells can be seeded and cultured on these materials, resulting in newly formed tissue *in vitro* (Nehrer *et al.*, 1997) or *in vivo* (Nehrer *et al.*, 1997; Lee *et al.*, 2003).

12.2 Hydrogel foam materials

In the past, a large number of materials, both synthetic and natural, have been proposed as cell carriers, including hydrogels. Hydrogels are hydrophilic polymer networks able to absorb large quantities of water, ranging from ten up to thousands of times their dry weight (Hoffman, 2002). When it comes to biomedical applications, hydrogels are in general biocompatible (Hennink and van Nostrum, 2002). Because of their high water content and rubbery nature, hydrogels resemble the aqueous environment cells reside in (van Vlierberghe *et al.*, 2011a). Their hydrophilic nature will also result in a low tendency for proteins and cells to adhere to their surface (Hennink and van Nostrum, 2002). In tissue engineering, however, cell adherence is often desired. This implies that, in some cases, specific functional groups should be introduced enabling cell attachment. To this end, arginylglycylaspartic acid (RGD) sequences are frequently applied. These RGD motives can bind to cell surface integrins thus facilitating cell adhesion (Barczyk *et al.*, 2010). Hydrogels are also by definition porous and therefore enable the homogeneous penetration of cells through the interconnected pores and the subsequent formation of three-dimensional tissues (Park *et al.*, 2011). In addition, a steady supply of nutrients towards, and removal of waste products away from the cells will be ensured (Park *et al.*, 2011).

A disadvantage of hydrogels, however, is their limited mechanical stability and challenging sterilization (Hoffman, 2002). To improve the mechanical properties, the inclusion of synthetic or natural fibres, inorganic clay particles and carbon nanotubes have already been suggested (Zhou and Wu, 2011). Interestingly, the formation of (semi-) interpenetrating polymer networks (IPN) or double networks have also been proposed to improve the mechanical strength of hydrogel materials.

12.2.1 Physical hydrogels

A hydrogel is defined as 'physical' or 'reversible' when the polymer network is held together by molecular entanglements and/or secondary forces (Hennink and van Nostrum, 2002).

A first class of physical hydrogels is formed via ionic interactions (Hennink and van Nostrum, 2002). This includes polyions which form a hydrogel by the addition of oppositely charged ions. A typical example includes alginates. Interestingly, uncharged polymers can also be crosslinked using ions. Dextran, which lacks ionic binding sites for cations, forms hydrogels in the presence of potassium ions, although these gels are unstable in water. Finally, ionic crosslinking can also be observed between polycations and polyanions. This is the case upon formation of chitosan hydrogels by complexation with dextran sulphate, polyphosphoric acid or alginate (Hennink and van Nostrum, 2002; George and Abraham, 2006).

Crystallization of polymer chains can also result in the formation of physical gels (e.g. poly(vinyl alcohol) (PVA)) (Hennink and van Nostrum, 2002). Aqueous PVA solutions stored at room temperature will gradually form gels with a low mechanical strength. When the same solution is subjected to a freeze–thaw process, a highly elastic gel is formed. The latter can be attributed to the formation of crystalline PVA domains upon cooling, which act as physical junction zones.

Crosslinking due to stereocomplex formation is an alternative, also enabling physical hydrogel formation (Ikada *et al.*, 1987; Hennink and van Nostrum, 2002). For example, for blends of poly(L-lactic acid) (PLLA) and poly(D-lactic acid) (PDLA), a melting temperature (T_m) of 230°C has been observed, while the homopolymers of both stereoisomers show a T_m of 170°C (Ikada *et al.*, 1987). This increase was attributed to the formation of stereocomplexes. As a result, PLLA–PDLA has already been applied frequently to physically crosslink a series of (bio)polymers, including poly(ethylene glycol) (PEG), dextran and poly(hydroxyethylmethacrylate) (pHEMA) (Lim *et al.*, 2000; Hennink *et al.*, 2004; Nouailhas *et al.*, 2011).

A fourth strategy is based on the amphiphilic nature of block or graft copolymers (Hennink and van Nostrum, 2002). Hydrophobic regions will

aggregate due to hydrophobic interactions. When a polymer chain contains only two blocks, this will result in micelle formation. In order to obtain a hydrogel network, multiblock copolymers or graft copolymers should be applied.

In some cases, graft copolymers can also be crosslinked by the formation of inclusion complexes. Choi *et al*. applied PEG grafts to physically crosslink dextran chains in the presence of β-cyclodextrin (Choi *et al.*, 2002).

In another strategy, the secondary interactions responsible for gelation are hydrogen bonds. The base pairing in DNA which results in the well-known double helix is probably the best example of this principle. This concept has already been applied to crosslink polymers onto which oligodeoxyribonucleotides were grafted (Nagahara and Matsuda, 1996; Hennink and van Nostrum, 2002). Another example is the complexation of poly((meth) acrylic acid) (P(M)AA) with PEG. The oxygen of PEG will act as a hydrogen bond acceptor for the (meth)acrylic acid hydrogen bond donors. Since the (meth)acrylic acid pendant groups need to be protonated to form hydrogen bonds, the gel formation will be strongly pH dependent (Eagland *et al.*, 1994; Hennink and van Nostrum, 2002).

A final method of enabling physical hydrogel formation is crosslinking via protein interactions. This method can be considered as a special case of hydrogen bonding or crystallization, but with much tighter control of the complexation via the proper design of the genetic code in synthetic DNA sequences. Some proteins form so-called coiled coils (i.e. left-handed superhelices of right-handed α-helices), of which the collagen superhelix is an example. The same effect can be achieved via synthetic polypeptides that contain the so-called 'leucine zipper' motif (Petka *et al.*, 1998; Hennink and van Nostrum, 2002). Because peptide conformations are strongly pH and temperature sensitive, gel formation can be induced or inhibited via external stimuli (Petka *et al.*, 1998; Hennink and van Nostrum, 2002).

12.2.2 Chemical hydrogels

A polymer network is permanent when the polymer chains are crosslinked via covalent bonds (Hennink and van Nostrum, 2002). Depending on the chemical bonds introduced, they may be biodegradable or not.

A first method to develop chemical hydrogels is crosslinking of polymers using radical polymerization. This strategy often implies the introduction of vinyl moieties. These vinyl groups can be introduced as end-groups or as pendant moieties along the polymer backbone. When adding vinyl (macro) monomers, radical polymerization enables the bridging of the different polymer chains. This method has already been applied for the development of a large variety of hydrogels. Hutson *et al*. used this method to develop

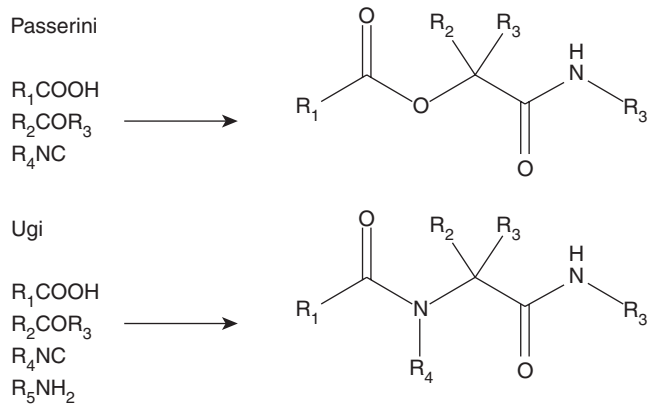

12.1 Overview of Passerini (top) and Ugi (bottom) reactions.

gelatin–PEG composite hydrogels (Hutson *et al.*, 2011). Lee *et al*. applied PEG–diacrylate as crosslinker for the polymerization of N-methacrylated L-3,4-dihydroxyphenylalanine (L-DOPA) monomers (Lee *et al.*, 2004a).

In a second strategy, reactions between complementary chemical moieties are applied. The coupling of amines and carboxylic acids using carbodiimide chemistry is a straightforward example of this strategy (Tillet *et al.*, 2011). Other examples include the reaction of hydroxyl- or amine-containing polymers with dialdehydes (Balakrishnan and Jayakrishnan, 2005; Manju *et al.*, 2011; Tillet *et al.*, 2011) or condensation reactions including the Ugi or Passerini reactions (de Nooy *et al.*, 1999; Hennink and van Nostrum, 2002). In the Passerini reaction, a carboxylic acid and an aldehyde or a ketone are condensed with an isocyanide, resulting in the formation of an α-(acryloxy) amide. In the Ugi reaction, an amine is added to the reaction mixture, which then yields an α-(acylamino)amide. Both reaction schemes are shown in Fig. 12.1.

A third possibility is crosslinking via high-energy irradiation. This method can be used to form networks starting from water-soluble polymers. Gamma or electron beam irradiation is applied to generate radicals along the polymer backbone by homolytic scission of C–H bonds. In addition, radiolysis of water results in the formation of hydroxyl radicals which can attack the polymer chains, resulting in additional radical centres. Recombination of the formed macroradicals results in a crosslinked network. This strategy has the advantage that it can be performed in water under mild conditions. Interestingly, the use of a potentially toxic crosslinker is avoided and sterilization and crosslinking can be performed simultaneously (van Vlierberghe *et al.*, 2011a).

Covalent links can also be introduced by enzymatic processes. Several successful enzymatic crosslinking strategies have already been reported in

literature (Sperinde and Griffith, 1997; Sperinde and Griffith, 2000; Ogushi *et al.*, 2007; Sakai *et al.*, 2009; Davis *et al.*, 2010; Jin *et al.*, 2010).

Interestingly, in recent years, various research groups have also described the potential of 'click chemistry' to develop chemical hydrogels (Hu *et al.*, 2011; Koschella *et al.*, 2011). 'Click chemistry' is a term used to indicate a set of powerful and selective reactions able to form heteroatom links (Kolb *et al.*, 2001; Bock *et al.*, 2006). Click reactions to be applied for the modification of macromolecules should meet certain conditions (Nandivada *et al.*, 2007; Barner-Kowollik *et al.*, 2011):

1. Resulting in the formation of stable bonds
2. Tolerating other functional groups
3. Reacting in a quantitative manner
4. Producing few or no side products
5. Occurring under mild conditions
6. Easy work-up and purification possible.

A material to be applied as scaffold should fulfil certain requirements. First, high porosity is required in order to support diffusion of oxygen and nutrients towards the cells and drainage of waste products from the matrix. In addition, pore interconnectivity is important to promote phenomena such as cell migration and angiogenesis. Secondly, the porous biomaterials should be biocompatible and in some cases also biodegradable (Kang *et al.*, 1999; O'Brien *et al.*, 2004).

The pore size required for cellular ingrowth depends on the cell type seeded on the matrix (Whang *et al.*, 1995). For porous silicon nitride scaffolds, for example, endothelial cells bind preferentially to scaffolds with pores smaller than 80 μm, while fibroblasts preferentially bind to larger pores (> 90 μm) (O'Brien *et al.*, 2005). A pore size gradient through the scaffold could be favourable in some cases to mimic the complex architectures of tissues. Porous scaffolds with spatially variable pore size can influence the location and mechanical properties required by tissue interfaces. Pore size gradients can also impact cell migration *in vitro* and *in vivo*, which is a significant advantage for generating the complex tissue interfaces required for functional tissue regeneration (Wang *et al.*, 2006).

The most frequently used porous synthetic polymeric hydrogels include poly(hydroxyethylmethacrylate) (pHEMA) (Dragusin *et al.*, 2012), poly(sodium acrylate) (Pourjavadi *et al.*, 2008) and poly(vinylalcohol) (PVA) (Lee *et al.*, 2009). Common natural cell matrices include chitosan (Lee *et al.*, 2004b; O'Brien *et al.*, 2005), collagen (Schoof *et al.*, 2001; O'Brien *et al.*, 2005) and gelatin (Kang *et al.*, 1999; Ren *et al.*, 2001; Ulubayram *et al.*, 2002). Gelatin has also often been selected, since it is a self-assembling, non-toxic, biodegradable, inexpensive and non-immunogenic material (Ulubayram

et al., 2002). It has been widely applied in medicine as a wound dressing and as an adhesive and absorbent pad for surgical use (Choi *et al.*, 2001). Moreover, several studies on gelatin-based sponges have already indicated that acellular sponges composed of gelatin have potential application in the field of tissue engineering (Lee *et al.*, 2003).

12.3 Equilibrium swelling theory and rubber elasticity theory

The upcoming subsections will give insight in the background of the equilibrium swelling theory and the rubber elasticity theory. In addition, various examples will be given to indicate the applicability of both theories with respect to hydrogel characterization.

12.3.1 Equilibrium swelling theory

Different theoretical models exist to determine the number-average molecular weight between crosslinks (M_c), among which the model of Flory and Rehner is the most important (Peppas *et al.*, 2000). This model is based on two assumptions:

1. The polymer chains follow a Gaussian distribution. This implies that the end-to-end distance between the chain ends is much smaller than the contour length of the chain.
2. The crosslinks are tetrafunctional.

During swelling, the polymer chains of a hydrogel network are subject to two opposing forces, the thermodynamic force of mixing and the retractive force of the polymer chains (Peppas *et al.*, 2000). At equilibrium swelling, both forces are equal. The corresponding change in free energy during swelling can be described according to the following equation:

$$\Delta G = \Delta G_{mix} + \Delta G_{el} \qquad [12.1]$$

ΔG_{mix} = free energy of mixing (i.e. indication of the compatibility between polymer and solvent, expressed by polymer–solvent interaction parameter χ_1),
ΔG_{el} = elastic free energy.

Differentiation of Equation [12.1] with respect to the number of solvent molecules at a constant temperature and pressure, results in the chemical potential of the solvent in a swollen hydrogel:

$$\mu_1 - \mu_{1,0} = \underbrace{N(\partial \Delta G_{mix}/\partial n_1)_{T,P}}_{\mathbf{A}} + \underbrace{N(\partial \Delta G_{el}/\partial \alpha_s)_{T,P}(\partial \alpha_s/\partial n_1)_{T,P}}_{\mathbf{B}} \quad [12.2]$$

μ_1 = chemical potential of the solvent in the hydrogel,
$\mu_{1,0}$ = chemical potential of the pure solvent,
N = Avogadro's number,
n_1 = number of moles of solvent,
α_s = expansion factor which expresses the linear deformation of the network structure due to isotropic swelling.

In Equation [12.2], the terms A and B rule out at equilibrium swelling. Upon equating these two contributions and substituting the free energies G_{mix} and G_{el}, an expression is obtained for the average molecular weight between two neighbouring junctions for a neutral hydrogel prepared in the absence of a solvent (Brannonpeppas and Peppas, 1991).

$$\frac{1}{\overline{M_c}} = \frac{2}{\overline{M_n}} - \frac{(\bar{v}/V_1)\left[\ln(1-v_{2,s}) + v_{2,s} + \chi v_{2,s}^2\right]}{v_{2,s}^{1/3} - \frac{v_{2,s}}{2}} \quad [12.3]$$

$\overline{M_c}$ = average molecular weight between crosslinks,
$\overline{M_n}$ = number-average molecular weight of the polymer before crosslinking,
$\bar{v}$ = specific volume of the polymer,
V_1 = molar volume of water,
$v_{2,s}$ = polymer volume fraction of the hydrogel at equilibrium swelling,
χ_1 = polymer–solvent interaction parameter.

The original Flory-Rehner theory was extended by Peppas and Merrill to be applied for hydrogels prepared in the presence of water. This led to the following equation (Peppas and Merrill, 1977):

$$\frac{1}{\overline{M_c}} = \frac{2}{\overline{M_n}} - \frac{(\bar{v}/V_1)\left[\ln(1-v_{2,s}) + v_{2,s} + \chi_1 v_{2,s}^2\right]}{v_{2,r}\left[\frac{v_{2,s}^{1/3}}{v_{2,r}^{1/3}} - \frac{v_{2,s}}{2v_{2,r}}\right]} \quad [12.4]$$

$v_{2,r}$ = polymer volume fraction in the relaxed state (i.e. state of the polymer after crosslinking but before swelling).

This equation thus takes into account the polymer volume fraction in the relaxed state.

Further theoretical descriptions for hydrogels containing ionic moieties will not be discussed in the present work, but can be found in the literature (Peppas *et al.*, 2000).

Looking at Equation [12.4], $\overline{M_c}$ can only be obtained when the values of the number-average molecular weight of the polymer before crosslinking ($\overline{M_n}$), the specific volume of the polymer ($\bar{v}$), the polymer–solvent interaction parameter (χ_1) and the polymer volume fractions $v_{2,r}$ and $v_{2,s}$ are known. The number-average molecular weight can be obtained from size exclusion chromatography using universal calibration. The polymer volume fraction in the relaxed state can be determined from density measurements via pycnometry. The polymer volume fraction in the swollen state and the specific volume of the polymer can be derived from a combination of pycnometry and swelling studies. The polymer–solvent interaction parameter can be determined from equilibrium swelling measurements (Bahar *et al.*, 1987).

12.3.2 Rubber elasticity theory

A second theory which is often applied to obtain a variety of hydrogel properties is the rubber elasticity theory, which can be applied to hydrogels since they respond like rubber (i.e. elastically) to externally applied stresses. The rubber elasticity theory was originally developed for vulcanized rubbers by Treloar and Flory (Flory, 1944; Treloar, 1944). Later, it was extended to a larger class of polymers by Flory (Peppas *et al.*, 2000). Since hydrogels are water-swollen networks, the rubber elasticity theory was further modified by Silliman, Peppas and Merrill, enabling structure analysis of hydrogels prepared in the presence of a solvent (Peppas *et al.*, 2000). Excellent reviews describing the various rubber elasticity theories developed can be found in literature (Gent, 1974; Boyce and Arruda, 2000; Kloczkowski, 2002).

Summarizing the main outcome of the rubber elasticity theory for hydrogels prepared in the presence of a solvent, the following equation gives the relation between a series of hydrogel parameters (Peppas *et al.*, 2000):

$$\tau_s = \frac{\rho RT}{\overline{M}_c}\left(1-\frac{2\overline{M}_c}{\overline{M}_n}\right)\left(\alpha-\frac{1}{\alpha^2}\right)\left(\frac{v_{2,s}}{v_{2,r}}\right)^{1/3} \qquad [12.5]$$

τ_s = stress applied to the polymer sample,
ρ = density of the polymer,
R = universal gas constant,
T = absolute experimental temperature,
$<\alpha>$ = isotropic dilation factor ($\sim v_{2,r}^{1/3}$),

The rubber elasticity theory has already been frequently applied to characterize various hydrogel systems (Anseth *et al.*, 1996); Lee *et al.* have studied the degradation profile of poly(aldehyde guluronate) hydrogels by monitoring the change of the crosslink density during degradation (Lee *et al.*, 2004c). Alternatively, the influence of the selected crosslinker on the crosslink density of poly(methyl methacrylate) beads was examined (Ding *et al.*, 1991). Chiu *et al.* have determined the effective network density of temperature and pH-sensitive hydrogels, prepared by copolymerization of N-isopropylacrylamide, N-t-butylacrylamide, acrylic acid and methacryloylglycylglycine p-nitrophenylester, using cystamine as crosslinker (Chiu and Yang, 2000). Finally, our research group has previously evaluated the effect of applying a cryogenic treatment on the crosslink densities of gelatin-based scaffolds using the rubber elasticity theory (VanVlierberghe *et al.*, 2009).

Looking at the various examples given, the rubber elasticity theory has shown to be a valuable tool to study the crosslink density of hydrogels, by applying straightforward experimental set-ups (Ding *et al.*, 1991).

12.4 Overview of hydrogel properties

In the upcoming sections, an overview of a series of important hydrogel properties including the hydrogel crosslinking efficiency and mechanical and swelling properties is presented. In addition, specific examples are given to highlight their relevance for several applications, together with a straightforward procedure on how to determine the hydrogel properties.

12.4.1 Hydrogel crosslinking efficiency

Since UV curing of hydrogels results in water-insoluble polymer networks, these hydrogels cannot be characterized using conventional ^{1}H-NMR spectroscopy due to considerable line broadening. These broad signals can be attributed to the presence of dipolar interactions, chemical shift anisotropy and magnetic susceptibility (Shapiro and Gounarides, 2000; Li, 2006; Roy *et al.*, 2008).

Interestingly, the observed line broadening can be strongly reduced by rapidly rotating the sample at an angle of 54.7° relative to the static magnetic field (Li, 2006). At this magic angle θ, the $(3\cos^2\theta - 1)/2$ contribution of the Hamiltonian disappears, effectively removing the line broadening effects. Magic angle spinning-nuclear magnetic resonance (MAS-NMR) spectroscopy therefore allows the recording of NMR spectra of solids, with narrower signals. The applied spinning rates are generally in the order of a few kilohertz.

An additional improvement can be achieved for hydrogel samples which can be swollen in a deuterated solvent (e.g. deuterium oxide, D_2O). As a

result, the polymer gains translational movement, enabling the chains to more closely resemble the conditions they would experience in solution. The latter results in a further decrease in line width in the recorded spectra (Rueda *et al.*, 2005). As a consequence, hydrogel materials with a high crosslinking degree will show broader peaks than less crosslinked materials because of their reduced chain mobility (Rueda *et al.*, 2003a).

The combination of the above-mentioned effects thus enables the application of ^{1}H-NMR spectroscopy to semi-solid samples. Because of this, HR-MAS NMR spectroscopy is increasing in importance as a characterization tool in solid-state synthesis (Shapiro and Gounarides, 2000; Ramadhar *et al.*, 2008), polymer chemistry (Capitani *et al.*, 2001; Rueda *et al.*, 2003a, 2003b, 2005; Kimoto *et al.*, 2005; Annunziata *et al.*, 2007; Cuggino *et al.*, 2008; van Vlierberghe *et al.*, 2010), food science (Castejon *et al.*, 2010; Perez *et al.*, 2011; Valentini *et al.*, 2011), analytical chemistry (Simpson *et al.*, 2001; Bradley and McLaughlin, 2007), heterogeneous catalysis (Roy *et al.*, 2008) and in the biomedical field (Birkefeld *et al.*, 2003; Chen *et al.*, 2004; Mancuso and Glickson, 2004; Cheng *et al.*, 2006; Li, 2006).

As an example in the field of hydrogel foams, HR-MAS ^{1}H-NMR spectroscopy has already been applied to determine the crosslinking degree of porous gelatin-based hydrogels. By comparing the integration of the signal corresponding to the double bonds present in methacrylamide-modified gelatin with the integration of a signal that remains chemically inert during the crosslinking procedure, the crosslinking efficiency can be determined (van Vlierberghe *et al.*, 2010).

12.4.2 Mechanical properties

The first technique which is applied to determine the mechanical properties of hydrogels is rheology. Rheology is the study of the deformation and flow of matter under the influence of an applied stress. The term was introduced in 1920 by Bingham, based on 'panta rhei' (i.e. 'everything flows') initiated by Heraclitus. Rheology is extending the conventional principles of elasticity and Newtonian fluid mechanics to materials whose mechanical properties cannot be described using classical theories. Rheological behaviour is particularly observed in polymeric hydrogels (Lohse, 2005; Seema and Kutty, 2005).

In general, oscillatory tests are used to examine all kinds of viscoelastic materials including low-viscosity liquids (Nijenhuis and Winter, 1989; Schurz, 1996), polymer solutions (Chambon *et al.*, 1986; Bindal *et al.*, 2003), melts (Li *et al.*, 2005), pastes (Rasteiro and Antunes, 2005), gels (Ramakrishnan *et al.*, 2004), elastomers (Shin *et al.*, 1991) and even rigid solids (Telis *et al.*, 2005). This mode of testing is also referred to as 'dynamic mechanical analysis' (Wolfe *et al.*, 1989). The measurements

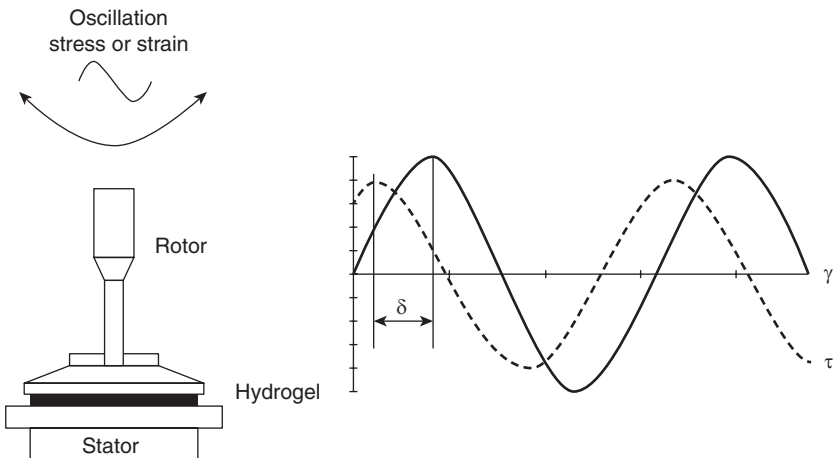

12.2 Preset shear strain function γ(t), and resulting shear stress function τ(t), applied during a rheological experiment.

can be performed by means of a rheometer, consisting of two basic components separated by the sample (Fig. 12.2). Tests with controlled shear strain are applied on visco-elastic materials in the form of oscillatory sine functions according to:

$$\gamma(t) = \gamma_0 \sin \omega t \qquad [12.6]$$

with γ_0 = amplitude,
ω = frequency.

The shear stress corresponding to this deformation is a phase-shifted sine function:

$$\tau(t) = \tau_0 \sin(\omega t + \delta) \qquad [12.7]$$

with the phase shift angle δ between the preset and the resulting curve, as illustrated in Fig. 12.2. The phase shift angle is always in the range from 0° to 90°. For ideal elastic behaviour $\delta = 0°$, for ideal viscous behaviour $\delta = 90°$ and for visco-elastic behaviour $0° < \delta < 90°$.

Two important parameters exist enabling the characterization of visco-elastic materials, namely the storage modulus (G') and the loss modulus (G'').

The G'-value is a measure of the deformation energy stored by the sample during the shear process. After the load is removed, this energy is

completely available, now acting as the driving force for the reformation process, which partially or completely compensates the previously applied deformation of the structure. Materials which store the whole deformation energy show completely reversible deformation behaviour, since they resume an unchanged shape after a load cycle. Thus, G' represents the elastic behaviour of a test material:

$$G'(\omega) = \frac{\tau_0 \cos \delta}{\gamma_0} \qquad [12.8]$$

The G''-value is a measure of the deformation energy consumed by the sample during the shear process and thereafter lost. This energy is spent during the process of changing the material's structure, e.g. when the sample is flowing. There exists relative motion between the molecules inducing frictional forces between these components, causing frictional heat. Energy is dissipated during this process. Part of this energy heats up the test material, and another part may be lost to the surrounding environment. Energy losing materials are characterized by irreversible deformation behaviour, since their final shape is changed after a load cycle. Thus, G'' represents the viscous behaviour of a test material:

$$G'(\omega) = \tau_0 / \gamma_0 \sin \delta \qquad [12.9]$$

In contrast to dynamic oscillation measurements, measuring at small deformations (Osaki, 1993), large deformations are also applied in order to gain an idea of the mechanical properties of a material (Nunes *et al.*, 2006). Usually tensile tests are performed (Stern *et al.*, 2007). However, these are less suitable for hydrogels since cracks can occur at the fixation points. Consequently, the majority of publications about large-deformation experiments on hydrogels are concerned with compression tests (Bartkowiak and Brylak, 2006; Iritani *et al.*, 2006). In general, large-deformation experiments can be performed by means of a texturometer, enabling fast and simple determination of the hydrogel properties.

Texturometry analysis is mainly used in the food industry (Soeda, 1995; Alasalvar *et al.*, 2001). However, nowadays it has also proven its use in the pharmaceutical industry (Johnson *et al.*, 1997; Pillay and Fassihi, 1999) and cosmetics (Jachowicz and Yao, 1996; Smewing, 1998).

By means of a plunger or probe (cylindrical, sphere-shaped, etc.), which compresses the sample at a constant rate, a compression force is applied to the testing material. Hydrogel samples can be positioned on a round opening in the bottom plate and fixed by the upper plate (Fig. 12.3).

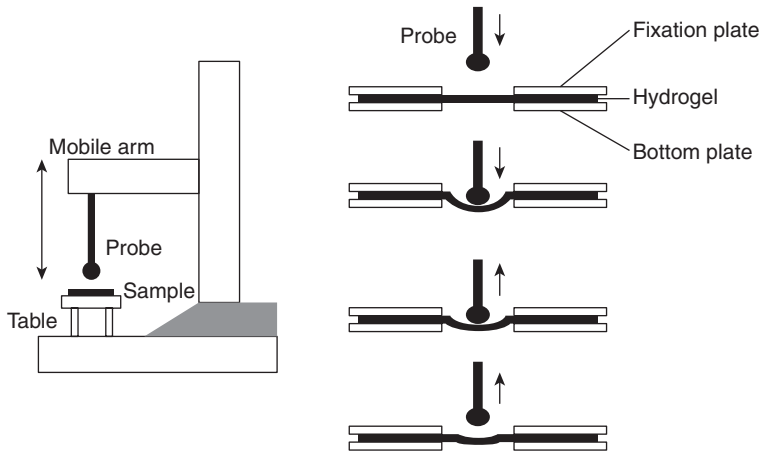

12.3 Scheme of a texturometer apparatus and the TPA-test procedure.

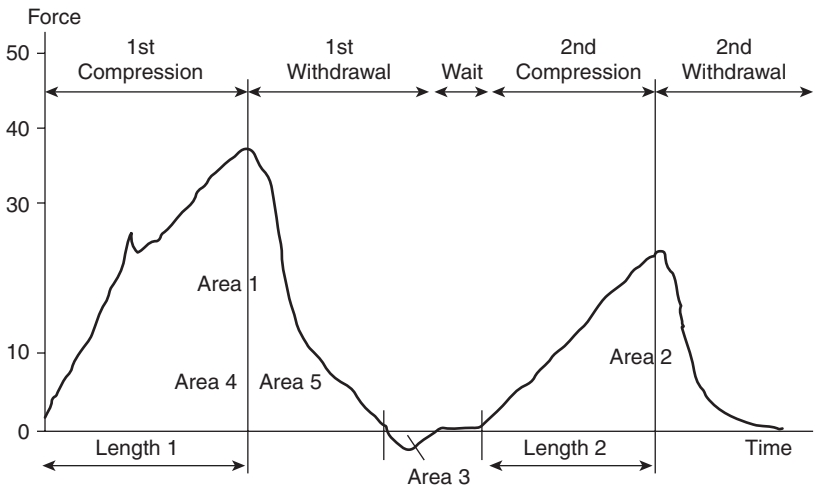

12.4 Overview of conventional texture profile analysis test.

Different testing procedures can be applied when using texturometry. A 'texture profile analysis test' (TPA-test) can be performed in order to examine the 'recovery'-properties of the hydrogels developed after compression. Fatigue and fracture tests give additional information on polymeric hydrogel samples (Tanahashi *et al.*, 2006).

When performing the TPA-test, the sample is compressed twice by the plunger moving with the same speed. The theoretical curve, depicted in Fig. 12.4, always represents force as a function of time. From the surface

Table 12.1 Texturometrical parameters that can be obtained from a TPA-experiment

Parameter	Unit	Definition
Hardness	N	The hardness value is the peak force of the first compression of the product.
Fracturability	N	When a product fractures, the fracturability point occurs where the plot has its first significant peak (where the force falls off) during the probe's first compression of the product.
Cohesiveness	–	Cohesiveness is how well the product withstands a second deformation relative to how it behaved under the first deformation. It is measured as the area of work during the second compression divided by the area of work during the first compression. (i.e. Area 2/Area 1)
Springiness	–	Springiness is how well a product physically springs back after it has been deformed during the first compression. Springiness is typically measured by the distance of the detected height of the product after the second compression (i.e. Length 2), divided by the original compression distance (i.e. Length 1). The original definition of springiness used Length 2 only, however, comparison could then only be made among products which were identical in their original shape and height.
Chewiness	N	Chewiness only applies for solid products and is calculated as Gumminess x Springiness.
Gumminess	N	Gumminess only applies for semi-solid products and is Hardness × Cohesiveness.
Resilience	–	Resilience is how well a product 'fights to regain its original position'. You can think of it as instant springiness, since resilience is measured on the withdrawal of the first penetration, before the waiting period is started. (i.e. Area 5/Area 4)

areas below the curves and from the measured forces, different parameters can be calculated, as shown in Table 12.1.

Fatigue tests are similar to TPA-tests. In contrast to TPA, where only two compression cycles are applied, hydrogel films then undergo a large number of cycles in order to test for a possible change in mechanical properties after repeated loading (Cheng and Hwu, 2006).

In fracture experiments, only one compression cycle is applied until the hydrogel breaks. Parameters such as fracture force and fracture deformation are obtained after performing these tests (see Fig. 12.5) (Van Vlierberghe *et al.*, 2011b). Elastic materials will break fast and suddenly. Plastic materials, however, will break slowly (Bastun *et al.*, 2006).

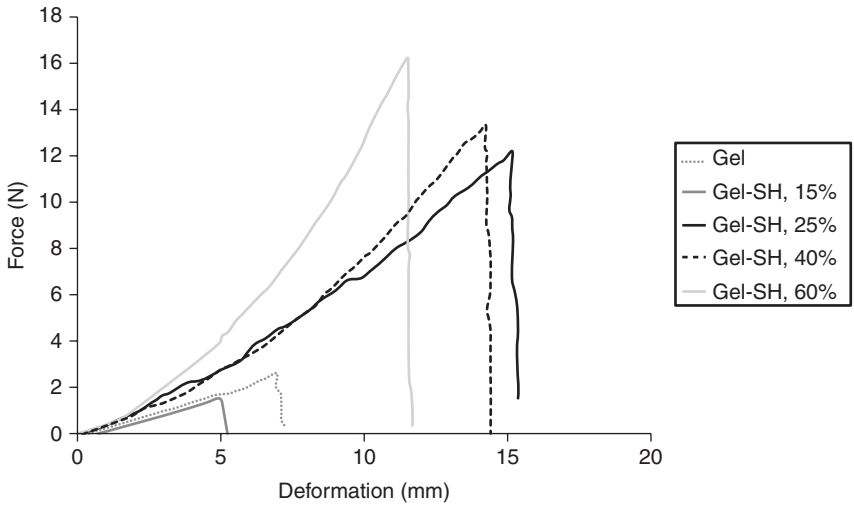

12.5 Force-deformation curve of disulphide-crosslinked gelatin hydrogels with increasing degree of substitution (15–60% DS) (test rate = 20 mm/min, $T = 21°C$). (*Source*: Republished with permission of Pergamon, from *European Polymer Journal*, Van Vlierberghe S *et al.*, **47**, 5, 2013; permission conveyed through Copyright Clearance Center, Inc.)

12.4.3 Swelling properties

For some applications, not only the swelling capacity is important, the swelling rate can also influence the applicability of materials. For certain *in vivo* applications, knowledge of the swelling rate is important since it provides information on how quick a certain defect can be filled during or after a surgical procedure (Boelen *et al.*, 2006). Therefore, the swelling kinetics of hydrogels foams can also be relevant.

An interesting alternative, if the experimental data obtained cannot be fitted using simple power law expressions, was provided by the Voigt model, which consists of a spring and a dashpot in parallel (Omidian *et al.*, 1998; Pourjavadi *et al.*, 2006; Pourjavadi and Kurdtabar, 2007). The spring and dashpot respectively provide the immediate elastic and delayed viscous strain responses to an externally applied stress. Any number of arrangements of these elements can be applied to simulate a particular kind of time dependence. In molecular terms, the elastic responses are the fast, reversible changes in bond length, shape and orientation which occur when stress is applied to a polymer chain. The viscous responses are the slower, irreversible energy dissipating processes, which occur as a result of the molecular movements.

In case of hydrogel swelling, there is no externally applied stress. Instead, stress is exerted on the hydrogel network by the interaction with water.

When a stress σ_0 is applied at time t_0, the strain response ε of the model with Young's modulus E is given at time t by the following expression:

$$\varepsilon(t) = \sigma_0 / E\left[1 - \exp\{(t_0 - t)/\tau_0\}\right] \quad [12.10]$$

where τ_0 is known as the retardation time and determines the influence of the dashpot (Omidian *et al.*, 1998). The system differs fundamentally from the stretching of a dry rubber, in that the volume drastically increases and the number of chain entanglements decreases with time. Consequently, the modulus in the equation mentioned above cannot have the same significance for absorbents, although Flory referred to an inverse relationship between the equilibrium swelling of a rubber by a solvent and the modulus of the rubber. However, the time dependence of swelling was not discussed (Omidian *et al.*, 1998).

The experimental swelling data follow a typical exponential relationship which has two characteristic constants, i.e. σ_0/E and τ_0. The quantitative value of the former can be estimated from the values of the steady state swelling of the individual samples, since the water transport is diffusion-controlled (Pourjavadi and Kurdtabar, 2007). For the latter, minus the reciprocal value of the slope of the plot of $\ln[1\text{-}S_t/S_\infty]$ against time can be used (S_∞ is equilibrium or steady state swelling). Since such a plot possesses a typical first-order relationship, the slope is a measure of the characteristic time (τ_0) for the individual scaffolds (Fig. 12.6). The Voigt-based equation can thus be rewritten as follows (Pourjavadi *et al.*, 2006):

$$S_t = S_e(1 - e^{-t/\tau}) \quad [12.11]$$

where S_t is swelling at time t, S_e is equilibrium swelling and τ stands for the rate parameter.

Starting from this model, the rate parameter τ for a hydrogel matrix, which is a measure for the swelling rate, can be determined.

12.5 Natural hydrogel materials

Cells, being components of tissues or organs, never exist in isolation. They are always embedded in a structural support (i.e. the ECM). The ECM can be considered as a crosslinked hydrogel network, containing both polysaccharides as well as structural, signalling and cell-adhesive proteins (West,

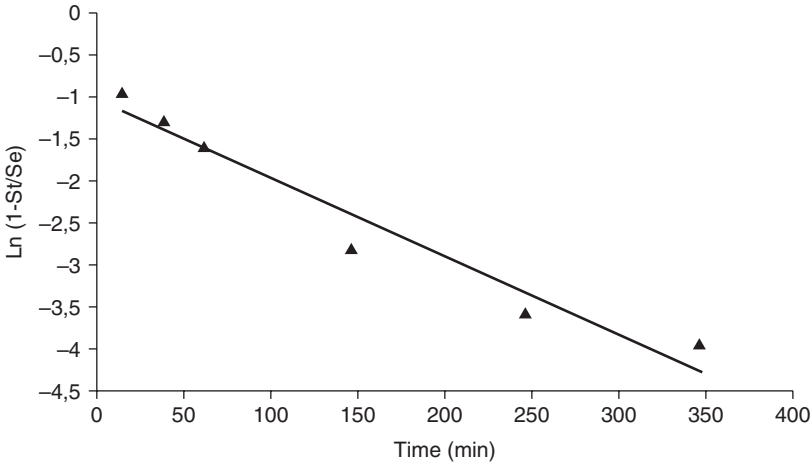

12.6 Determination of τ as derived from the linear relationship between $\ln[1-S_t/S_\infty]$ and time for type gelatin-based hydrogel foams.

2011). These biopolymers control the biochemical and biophysical interactions which cells experience in tissues. They thus play a vital role in cell viability and function.

The ECM is composed of a variety of biopolymers including collagens, elastin fibres, glycosaminoglycans (GAG), proteoglycans and adhesive glycoproteins (Rosso *et al.*, 2004). Different combinations or spatial arrangements of the above-mentioned components result in a series of different scaffold types that characterize tissues and organs.

In the following subsections, the most important ECM components will be discussed.

12.5.1 Collagen

Collagen is one of the most important constituents of the ECM and is responsible for the structural integrity and tensile strength of tissues (Sell *et al.*, 2009; van Vlierberghe *et al.*, 2011a). The protein consists of three mutually interacting polymer chains. These α-chains are arranged into a repeating motif which forms a triple helical structure.

The collagen family consists of at least 12 different collagen types, which can be either homotrimeric or heterotrimeric (Sell *et al.*, 2009; van Vlierberghe *et al.*, 2011a). Collagen types I, II and III occur most frequently, and they form fibrous structures (Rosso *et al.*, 2004). Other collagens, including types IV, VII, IX, X and XII, are associated with collagen fibrils or are involved in the formation of basement membranes.

Because of its presence in the ECM, collagen has already been frequently applied to develop biomaterials and hydrogels (Adhirajan *et al.*, 2009; Sell *et al.*, 2009). Kew *et al.* recently reviewed the application of collagen for the regeneration of tendons and ligaments (Kew *et al.*, 2011).

An inherent drawback related to the application of collagen is the general concern of immunogenicity and disease transfer (Hubbell, 2003; Huang and Fu, 2010). Although most of the immunogenic character in collagen type I can be removed via enzymatic treatment, not all of the non-human proteins can be effectively cleaved from collagen. The use of exclusive human proteins might circumvent this issue, but even when applying human collagen, the risk of disease transfer remains. Recombinant collagen type I has already been developed to completely rule out the risk of disease transfer (Toman *et al.*, 2000). Interestingly, recombinant collagen types I and III are already commercially available (Hubbell, 2003).

12.5.2 Elastin

Another fibrous protein present in the ECM is elastin. Its name is derived from the elastic properties which it introduces in the ECM (Stevens and Lowe, 1997; Rosso *et al.*, 2004). Elastin is thus a key component of the ECM found within skin, the bladder, tendons, blood vessels, the lungs and elastic cartilage (Mithieux *et al.*, 2004; van Vlierberghe *et al.*, 2011a).

Elastin is assembled extracellularly and consists of tropoelastin molecules (Mithieux *et al.*, 2004), which are synthesized and secreted by smooth muscle cells and fibroblasts. In a subsequent step, the enzyme lysyl oxidase converts the ε-amines on the occasional lysine residues in adipic semi-aldehydes, which can act as cross-linkers.

Elastin is present in the ECM as a highly crosslinked biopolymer and forms strong associations with other (glyco)proteins present in the extracellular environment (Stevens and Lowe, 1997; Mithieux *et al.*, 2004; van Vlierberghe *et al.*, 2011a). Because of its high crosslinking degree and the formation of supramolecular associations, elastin is highly stable in healthy tissue, with an estimated half-life of 70 years, rendering it the most persistent protein in the human body (Mithieux *et al.*, 2004).

Native elastin is not frequently applied for tissue engineering purposes, due to its substantial insolubility and the occurrence of associations with other biopolymers (Mithieux *et al.*, 2004; Rosso *et al.*, 2004). To circumvent this difficulty, research has already been performed on the development of recombinant elastin and elastin-mimetic polymers (Mithieux *et al.*, 2004; van Vlierberghe *et al.*, 2011a).

12.5.3 Laminin

Laminin is a major component of basal laminae. This protein can occur in different forms, resulting from closely related gene translation (Rosso *et al.*, 2004). Laminin shows a high binding affinity for cell surfaces as well as for heparin and collagen type IV. Cell adhesion results from the presence of specific binding motives including RGD (Arg-Gly-Asp), PDSGR (Pro-Asp-Ser-Gly-Arg), YIGSR (Tyr-Ile-Gly-Ser-Arg) and IKVAV (Ile-Lys-Val-Ala-Val) that can interact with cell-specific surface receptors. Because of these cell binding capabilities, laminin is often applied to coat cell culture dishes and tissue plates to facilitate cell attachment and spreading (Rosso *et al.*, 2004).

12.5.4 Gelatin

Gelatin is single-stranded protein obtained from collagen by hydrolytic degradation (van Vlierberghe *et al.*, 2011a). Gelatin has already been used in a large variety of applications, including food industry, pharmaceutical formulations, photographic and other technical products.

Interestingly, gelatin solutions form gel-like structures upon cooling. This renders gelatin an interesting biopolymer for tissue engineering applications. The gelation is thought to be driven by hydrogen bonding and van der Waals interactions, resulting in the aggregation of certain gelatin domains into collagen-like triple helices separated by peptide residues in the disordered conformation (Djagny *et al.*, 2001; Chatterjee and Bohidar, 2005; van Vlierberghe *et al.*, 2011b). These junction zones, however, melt at temperatures around 30°C (van Vlierberghe *et al.*, 2011a). This implies that chemical crosslinking is required to avoid dissolution at body temperature. Since gelatin is only soluble in water and some alcohols, only water-soluble reagents can be used to achieve this goal (2011).

Gelatin can be obtained from collagen via an acid or basic hydrolysis (Djagny *et al.*, 2001). An acidic treatment results in the production of gelatin type A, while basic treatments yield gelatin type B. In addition to the difference between both gelatin types, the collagen type applied and its animal origin also influence the composition and physical properties of the gelatin developed (see Table 12.2).

The preparation methodology of gelatin differs depending on the collagen source applied and the chemical reagents used, while the overall principle remains the same (Djagny *et al.*, 2001). Collagen (usually derived from skin or bone) is first cut into smaller pieces, which can be handled more easily (Stacey and Blachford, 2002). The material is then washed and subsequently transferred into hot water to reduce the fat content to about 2%. The

Table 12.2 Amino acid composition of different gelatin types

Amino acids	Gelatin A	Gelatin B		
	Porcine skin (g/100 g)	Bovine (g/100 g)	Bovine hides (g/100 g)	Bovine bones (g/100 g)
Aspartate	4.4 ± 0.12	4.95 ± 0.18	5.01 ± 0.14	4.20 ± 0.17
Glutamate	8.14 ± 0.34	9.31 ± 0.35	9.20 ± 0.20	7.99 ± 0.37
Serine	3.12 ± 0.09	2.66 ± 0.07	2.76 ± 0.05	2.84 ± 0.06
Histidine	0.69 ± 0.02	0.56 ± 0.03	0.61 ± 0.01	0.53 ± 0.01
Glycine	21.63 ± 0.71	21.99 ± 0.89	22.12 ± 0.59	21.88 ± 0.61
Threonine	1.77 ± 0.03	2.24 ± 0.07	2.18 ± 0.05	1.77 ± 0.08
Arginine	7.32 ± 0.22	7.37 ± 0.25	6.74± 0.14	6.95 ± 0.24
Alanine	8.18 ± 0.24	9.06 ± 0.32	8.76 ± 0.18	8.69 ± 0.31
Tyrosine	0.64 ± 0.01	0.18 ± 0.01	0.21 ± 0.01	0.17 ± 0.02
Valine	2.49 ± 0.13	2.69 ± 0.11	2.63 ± 0.08	2.59 ± 0.10
Methionine	0.95 ± 0.03	0.76 ± 0.02	0.86 ± 0.02	0.68 ± 0.02
Hydroxylysine	1.24 ± 0.03	1.17 ± 0.05	1.26 ± 0.03	1.21 ± 0.04
Phenylalanine	1.92 ± 0.07	1.81 ± 0.06	1.76 ± 0.04	1.75 ± 0.04
Isoleucine	1.42 ± 0.05	1.67 ± 0.06	1.68 ± 0.04	1.62 ± 0.04
Ornithine	–	0.55 ± 0.05	0.97 ± 0.04	0.93 ± 0.07
Leucine	3.42 ± 0.12	3.41 ± 0.09	3.24± 0.07	3.47 ± 0.06
Lysine	3.85 ± 0.11	3.75 ± 0.09	3.49 ± 0.08	3.99 ± 0.09
Proline	13.57 ± 0.23	13.49 ± 0.43	14.35 ± 0.40	12.54 ± 0.39

degreased bone and skin is then dried and subsequently treated with either acid or alkaline solution. The reagents commonly applied are hydrochloric acid and sodium hydroxide for the acid and basic treatments, respectively (Djagny *et al.*, 2001). Next, gelatin is extracted at elevated temperatures. The raw gelatin solution is subsequently purified using classical techniques including filtration, centrifugation, etc., to obtain the end product. Finally, the gelatin is pressed into sheets or ground into a powder, depending on its final application.

As a result of the different preparation methods, gelatin type A and B also differ in their physico-chemical properties. It has been reported that gelatin type A possesses an isoelectric point (IP) of 7–9, while gelatin type B is characterized by an IP ranging from 4.8 to 5.1 (Djagny *et al.*, 2001). This difference can be attributed to the conversion of asparagine and glutamine into aspartic acid and glutamic acid, respectively, during the basic reaction conditions (Veis, 1964). The IP determines the charges present along the gelatin backbone at physiological pH and could thus affect its biocompatibility. Gelatin type A will be positively charged at physiological pH, while gelatin type B will possess negative charges. It has been reported that gelatin B shows a better biocompatibility compared to gelatin type A. This can be attributed to the more severe basic treatment as compared to the softer acidic route. Another difference between the gelatin types is the intrinsic

viscosity of their solutions. Gelatin A results in slightly more viscous solutions, although there is no difference in the melting temperatures of the resulting gels (Djagny *et al.*, 2001).

12.5.5 Alginate

Alginates are a class of salts derived from alginic acid (i.e. a polysaccharide derived from brown algae). They are unbranched copolymers of D-mannuronic acid (i.e. M block) and L-guluronic acid (i.e. G block) units arranged in an irregular, blockwise pattern of varying proportions of GG, MM and MG blocks (Yang *et al.*, 2011). Mannuronic acid forms β (1 → 4) linkages, while guluronic acid forms α (1 → 4) bonds resulting in sterical hindrance around the carboxylic acid groups. As a result, M blocks form linear domains while G blocks introduce folded regions responsible for a more rigid structure (Qin, 2008; Yang *et al.*, 2011). The structure of sodium alginate is shown in Fig. 12.7.

Alginates can be obtained from a series of seaweeds, including ascophyllum, durvillaea, ecklonia, laminaria, lessonia, macrocystis, sargassum and turbinaria (Qin, 2008). However, laminaria, macrocystis and ascophyllum are the most important sources, with alginate contents ranging from 17% to 44 %. Alginates can be extracted from raw seaweeds by an alkaline treatment, often using NaOH. The basic conditions transform the alginic acid in water-soluble sodium alginate. After filtration, the alginate can be precipitated using Ca^{2+} ions. Further purification and conversion finally yields commercially available sodium alginate.

Alginate is an interesting biopolymer for biomedical applications because of its ability to rapidly form gels upon addition of multivalent ions (Ahmad and Khuller, 2008; van Vlierberghe *et al.*, 2011a). This gelation mechanism is, however, hard to control and does not result in a uniform structure (Peter, 2004). A method to fine-tune the gelation kinetics using D-glucono-δ-lactone (GDL) was proposed by Ma *et al.* (Kuo and Ma, 2001). Interestingly, polyols

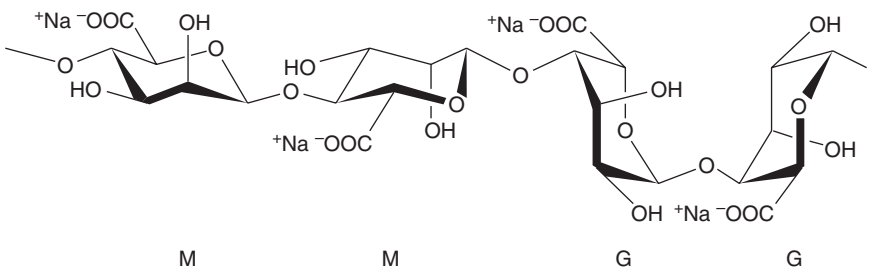

12.7 Structure of sodium alginate.

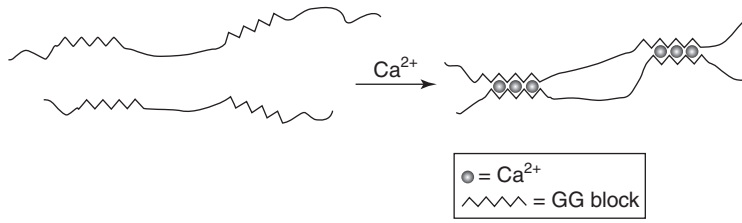

12.8 Egg box model for physical crosslinking of alginate. (*Source*: Reprinted from Febs Letters, **32**, Grant *et al.*, Biological Interactions between polysaccharides and divalent cations – egg box model, 195–198, Copyright (2013), with permission from Elsevier.)

have also been reported to reduce the gelation rate enabling the injection and subsequent gelation of calcium alginate *in vivo* (van Vlierberghe *et al.*, 2011a).

The formation of an ionotropic hydrogel starting from alginate upon Ca^{2+} addition mainly involves the GG blocks along the polymer backbone (Qin, 2008). Grant *et al*. proposed a model in which the GG blocks were thought to combine with the Ca^{2+} ions forming structures resembling an egg box (Grant *et al.*, 1973) (see Fig. 12.8). Since different algae species result in alginates possessing different M and G contents, the physico-chemical properties of alginates from different sources can vary greatly. Alginates with a higher GG concentration result in the formation of stronger gels (d'Ayala *et al.*, 2008; Qin, 2008).

In addition to its potential to form hydrogels in the presence of multivalent ions, alginate is mucoadhesive, biocompatible and non-immunogenic, making it very suitable for biomedical applications (d'Ayala *et al.*, 2008). Alginate is particularly interesting when combined with stem cells, since alginate has been reported to reduce stem cell dedifferentiation (Abbah *et al.*, 2006, Evangelista *et al.*, 2007; Barminko *et al.*, 2011). Although alginate is not cell-interactive as such, this drawback can easily be circumvented by the incorporation of cell-interactive peptides (e.g. RGD motives) or growth factors (e.g. VEGF) along the polymer backbone (Chan and Mooney, 2008; Hunt and Grover, 2010; van Vlierberghe *et al.*, 2011a). Alginate has already been applied frequently both *in vitro* as well as *in vivo* to induce the repair of cartilage, bone, blood vessels, neuronal tissue and hepatocytes (Drury and Mooney, 2003; Dvir-Ginzberg *et al.*, 2003; Awad *et al.*, 2004; Abbah *et al.*, 2006; Cho *et al.*, 2006).

12.5.6 Glycosaminoglycans

Another important class of biopolymers present in the ECM are glycosaminoglycans (GAG). GAGs are linear polysaccharides consisting of repeating

disaccharide units which contain sulphate groups. The most important GAGs include heparin, heparan sulphate, dermatan sulphate, chondroitin sulphate (4 and 6 derivative), keratan sulphate and hyaluronan (Rosso *et al.*, 2004).

GAGs, with the exception of hyaluronan, are generally part of a larger biopolymer – proteoglycan. The molecules consist of a small protein core covalently linked to a large molecular weight glycosaminoglycan (i.e. up to 95% by mass) (Campbell and Reece, 2005).

An important function of GAGs and proteoglycans is their ability to form larger aggregates which can absorb large amounts of water (Rosso *et al.*, 2004). The pressure generated by their swelling ability ensures tissues can withstand compression during joint movement. When associated with other ECM components, GAGs and proteoglycans play a vital role in the hydration and spatial organization of the ECM.

GAGs, including chondroitin sulphate and hyaluronan, can be applied for a variety of tissue engineering purposes, as reported in a review by van Vlierberghe *et al.* (van Vlierberghe *et al.*, 2011a). For example, hyaluronic acid (HA) was modified with crosslinkable moieties using glycidyl methacrylate by Leach *et al.* (Leach and Schmidt, 2004, 2005; Leach *et al.*, 2004). As anticipated, the degradation profile of covalently crosslinked HA could be fine-tuned by varying the amount of incorporated double bonds. The hydrogels developed were evaluated for their potential to support revascularization upon subcutaneous implantation in rats. The results indicated that the materials did not evoke a severe inflammatory response. In addition, it was anticipated that the hydrogels developed possessed the potential to be applied for wound repair.

12.5.7 Fibronectin

Fibronectin is a multifunctional glycoprotein that can exist in different forms which are the result of alternative splicing of its mRNA precursor (Rosso *et al.*, 2004; Huang and Fu, 2010). Fibronectin plays a vital role in cell attachment to a substrate, cell movement and cell differentiation (Rosso *et al.*, 2004). Along the protein backbone, a variety of binding motives can be distinguished, including RGD (Arg-Gly-Asp), RGDS (Arg-Gly-Asp-Ser), LDV (Leu-Asp-Val) and REDV (Arg-Glu-Asp-Val) sequences. These peptides function as important cell attachment sites. In this regard, RGD and LDV are particularly interesting, since they are able to bind to cell surface integrins (Barczyk *et al.*, 2010). Other binding domains are able to associate with other ECM components including collagen, heparan sulphate and fibrin (Rosso *et al.*, 2004).

Integrins are a class of transmembrane proteins connecting the ECM to the cytoskeleton (Barczyk *et al.*, 2010). This allows them to pass on mechan-

ical cues from the ECM to the cell's interior and vice versa (Stevens and Lowe, 1997).

Because fibronectin contains a large number of binding motives, it is widely used in cell culture systems to promote cell adhesion and spreading (Rosso *et al.*, 2004).

12.6 Hydrogel foam processing technologies

After hydrogel synthesis and/or modification, the materials developed have to be processed into functional devices. In addition to the chemical composition, the microstructure, 3D porosity and surface roughness of the hydrogel scaffolds developed are also important parameters affecting cell adhesion (Meng *et al.*, 2010). Although cellular dimensions are in general within the micrometre range, cells closely interact with the ECM, which is characterized by topographical and structural features in the nanometre range. The influence of surface topography has not been studied in depth up to now, but the available data indicate that the obtained results strongly depend on the cell type applied (Bacakova *et al.*, 2011).

At present, different techniques exist to fabricate porous scaffolds including porogen leaching (Kang *et al.*, 1999; Kawanishi *et al.*, 2004), phase separation, emulsion freeze-drying (Whang *et al.*, 1995; Hou *et al.*, 2003b), solvent evaporation (Laurencin *et al.*, 1998), gas foaming (Mooney *et al.*, 1996a), fibre bonding (Mooney *et al.*, 1996b), electrospinning and rapid prototyping.

One of the most common and straightforward techniques to prepare porous scaffolds is the particulate leaching method, which involves the selective leaching of a mineral, usually NaCl, or of an organic compound such as saccharose to generate the pores (van Tienen *et al.*, 2002; Horak *et al.*, 2004).

Phase separation can result in scaffolds with porosities up to 95% (Ma and Zhang, 2001). Basically, the polymer is dissolved in a solvent, and phase separation is induced by lowering the solution temperature or by adding a non-solvent to the solution. The presence of polymer solvent or non-solvent residues in the scaffolds can, however, represent a limitation of phase separation techniques (Reignier and Huneault, 2006). However, several papers have already reported on the use of water as solvent, excluding the possible disadvantage of residual (toxic) solvents (Dubruel *et al.*, 2007; van Vlierberghe *et al.*, 2007; van Vlierberghe *et al.*, 2008).

An alternative, proposed for the fabrication of porous polymer scaffolds, is emulsion freeze-drying (Mu *et al.*, 2006). Poly(DL-lactic-co-glycolic acid), for example, is dissolved in methylene chloride and then distilled water is added to form an emulsion. The polymer/water mixture is cast into a mould and quenched by placing it in liquid nitrogen. After quenching, the scaffolds are freeze-dried at –55°C, resulting in the removal of the dispersed

water and polymer solvents. Scaffolds with large porosities (up to 95%), but small pore sizes (13–35 μm) have been fabricated using this technique. Porous nano-hydroxyapatite (n-HA) /PVA hydrogel composites have also been prepared using an *in situ* hydrothermal treatment in combination with emulsion freeze-drying. The pores exhibited full interconnectivity with a narrow pore size distribution and a high porosity because of the injection of air bubbles and the emulsifier removal. Interestingly, both the pore size and the size distribution could be influenced by the weight of the emulsifier added. The emulsion foam freeze-drying method can be used to prepare porous (protein-based) hydrogel scaffolds for tissue engineering purposes since the operating procedure occurs at a low temperature. Moreover, scaffolds with large porosities (up to 95%) but with small pore sizes (13–35 μm) have already been fabricated using this technique. The above-mentioned pore-related parameters are very dependent on several factors, including the polymer concentration applied and the emulsion viscosity because of their effect on the stability of the emulsion prior to quenching. It is therefore anticipated that the pore size could be further increased in the future upon applying the optimized parameters. However, although this technique could be interesting because the additional leaching step is not required, the use of organic solvents remains a concern for the inclusion of cells and bioactive molecules (Mikos and Temenoff, 2000).

Solvent casting/particulate leaching involves the casting of a polymer solution and dispersed porogen particulates in a mould, the removal of the polymer solvent, followed by leaching out of the porogen (Mikos *et al.*, 1994; Hou *et al.*, 2003a). Because of the casting and the solvent evaporation step, this technique is only suitable for thin scaffolds. A drawback of this technique again is the application of organic solvents, which can be hard to completely remove from the scaffolds during the drying process.

In order to circumvent this problem, several authors proposed replacing solvent casting by melt-moulding, resulting in the melt-moulding/particulate leaching method. Briefly, the melt-moulding step consists of premixing polymer powder and solid porogen particulates and hot-pressing them together. The samples are then subjected to the same solid porogen leaching step as for the solvent-cast samples (Iannace *et al.*, 2001; Oh *et al.*, 2003).

Gas foaming is another alternative for the fabrication of porous polymer scaffolds. It is carried out by dissolving a gas at elevated pressure (i.e. physical blowing agent) or by incorporating a chemical that yields gaseous decomposition products (i.e. chemical blowing agent). The foaming technique generally leads to pore structures that are not fully interconnective (Reignier and Huneault, 2006). The application of supercritical carbon dioxide ($scCO_2$) can also result in the formation of hydrogel foams (Lee *et al.*, 2007; Ji *et al.*, 2011; Tsioptsias *et al.*, 2011). Different approaches can be used to realize this, including gas foaming, phase inversion, emulsion formation,

critical point drying, etc. The driving force behind this strategy is the polymer plasticization upon CO_2 sorption since pore formation occurs when the polymer is in the rubbery state. Upon cooling below the T_g, the porous structure developed is fixed because of the solidification. Tsioptsias *et al*. have applied supercritical fluids to develop porous hydrogel foams starting from gelatin, chitosan and blends thereof (Tsioptsias *et al.*, 2011). Porous chitosan foams were also produced in a similar fashion by Ji *et al*. (Ji *et al.*, 2011). The subsequent covalent crosslinking occurred using genipin or glutaraldehyde. The materials developed enabled fibroblast adhesion and subsequent proliferation over 7 days. Starch-based foams have also already been developed using a gas-blowing approach. For example, Kuang *et al*. applied Pluronic F127 and acetic acid as foam stabilizer and foaming aid, respectively (Kuang *et al.*, 2011). The starch foams produced possessed superabsorbent properties and were proposed to be applied for pharmaceutical and biomedical purposes.

Fibre bonding typically requires high temperatures (above the transition temperature of the polymer) and is not applicable for the processing of amorphous polymers. The high temperatures used in this process are also likely to denature any biologically active molecules one might wish to incorporate into the matrix (Harris *et al.*, 1998).

Unlike the conventional fabrication techniques, solid freeform fabrication has no restriction on shape control. The latter is a computerized fabrication technique that can rapidly produce highly complex three-dimensional objects using data from computer medical imaging equipment such as MRI and CT scans. The prototyping material is deposited to build the final structure in a layer-by-layer process, as discussed in Section 12.4.2 (Hutmacher *et al.*, 2003; Khalil *et al.*, 2005).

Finally, combinations of the above-mentioned techniques can also be applied. For example, a combination of phase separation and freeze-drying has already been used to successfully induce pore formation within gelatin-based hydrogels (Dubruel *et al.*, 2007; van Vlierberghe *et al.*, 2007, 2009; Fassina *et al.*, 2010). When an aqueous gelatin solution is solidified (i.e. frozen), phase separation occurs between the growing ice crystals and the concentrated gelatin solution (non-frozen liquid micro-phase) (Lozinsky, 2002; Lozinsky *et al.*, 2001). After sublimation of the ice crystals (freeze-drying), a porous scaffold originates (Fig. 12.9).

Using a novel cryo-set-up (Fig. 12.10), the cooling rate, the temperature gradient and the final freezing temperature during the cryogenic treatment can be varied in a controlled manner. Under the bottom of the mould, a Peltier element (also known as thermoelectric cooler, TEC) can be positioned (see Fig. 12.10). Thermoelectric modules are solid-state heat pumps that operate on the Peltier effect. A thermoelectric module consists of an

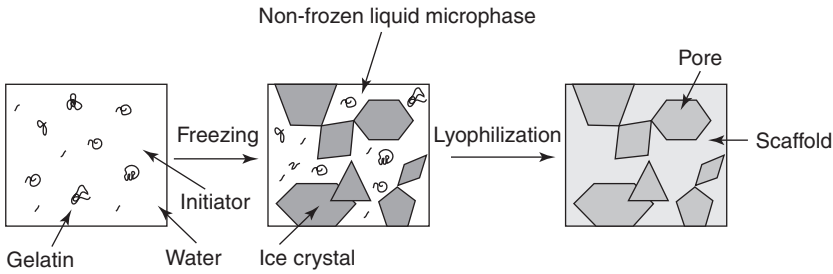

12.9 Cryogenic treatment of a gelatin-based hydrogel, followed by Lyophilization.

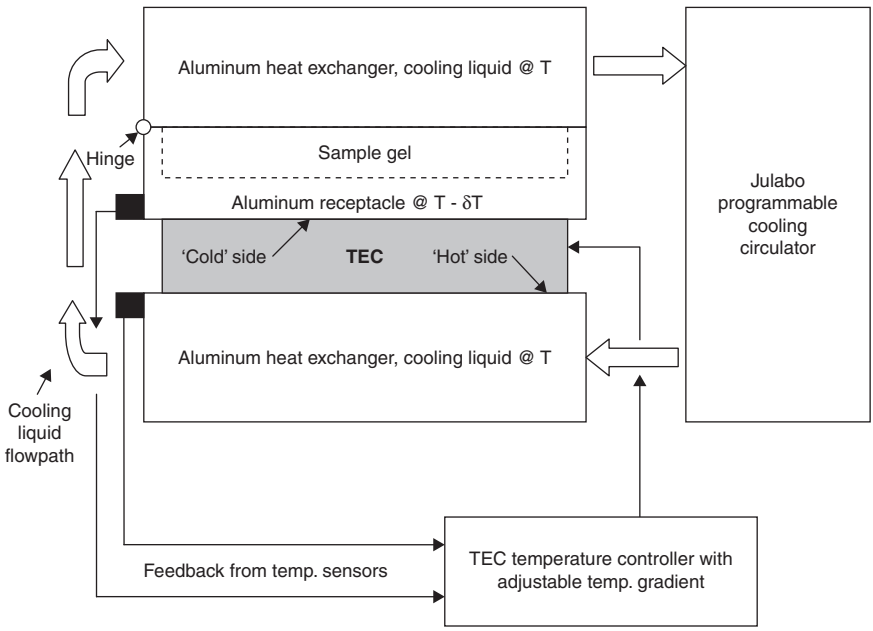

12.10 Schematic overview of a programmable cryo-unit. (*Source*: Reprinted with permission from (Van Vlierberghe *et al*. Porous gelatin hydrogels: 1. Cryogenic formation and structure analysis (2007) *Biomacromolecules*, **8**(2),331–337). Copyright (2013) American Chemical Society.)

array of p- and n-type semiconductor elements, heavily doped with electrical carriers. The array of elements is electrically connected in series and thermally connected in parallel. This array is then attached to two ceramic substrates, one on each side of the elements (Fig. 12.11). Heat transfer occurs as electrons flow through one pair of n- and p-type elements (often referred to

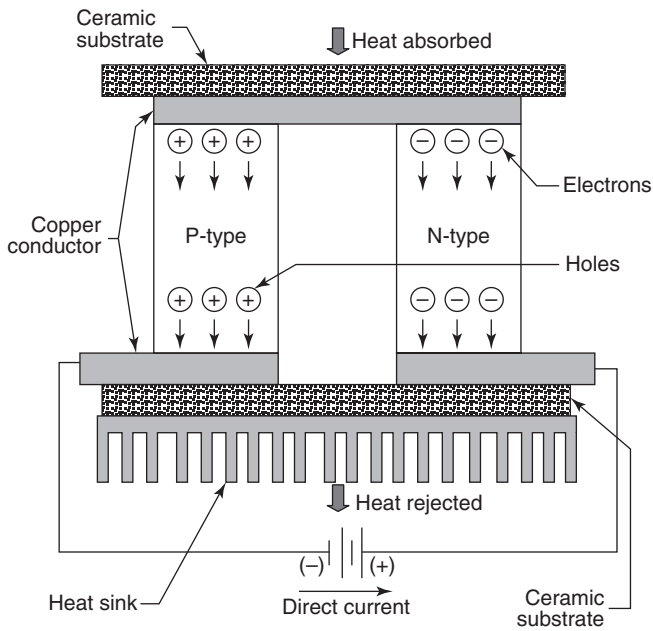

12.11 Working principle of thermoelectric coolers (i.e. Peltier elements).

as a 'couple') within the thermoelectric module. More specifically, electrons can travel freely in the copper conductors but not so freely in the semiconductor. As the electrons leave the copper conductor and enter the hot side of the p-type, they must fill a 'hole' in order to move through the p-type. When the electrons fill a hole, they drop down to a lower energy level and release heat in the process. Essentially the holes in the p-type are moving from the cold side to the hot side. Then, as the electrons move from the p-type into the copper conductor on the cold side, the electrons are bumped back to a higher energy level and absorb heat in the process. Next, the electrons move freely through the copper until they reach the cold side of the n-type semiconductor. When the electrons move into the n-type, they must bump up an energy level in order to move through the semiconductor. Heat is absorbed when this occurs. Finally, when the electrons leave the hot side of the n-type, they can move freely in the copper. They drop down to a lower energy level and release heat in the process.

In summary, heat is always absorbed at the cold side of the n- and p- type elements. The electrical charge carriers (holes in the p-type and electrons in the n-type) always travel from the cold side to the hot side, and heat is always released at the hot side of thermoelectric element. The heat pumping capacity of a module is proportional to the current and is dependent on the element geometry, number of couples and material properties.

The Peltier element applied by van Vlierberghe *et al*. enabled a temperature gradient of maximum 30°C to be established between the top and the bottom of the mould. For the samples obtained by applying a temperature gradient, the temperature at the top of the mould was the highest. The temperature gradient was applied to create porous scaffolds with predetermined pore morphologies (Van Vlierberghe *et al.*, 2007).

However, nowadays, the most commonly applied techniques for polymer processing are electrospinning and rapid prototyping. These methodologies will be explained in depth in the following section.

12.7 Electrospinning and rapid prototyping

The following subsections are dealing with two hydrogel processing techniques gaining increasing attention, including electrospinning and rapid prototyping. The techniques are explained in detail, together with their advantages and disadvantages. In addition, examples are given on hydrogel types which have been processed to date using either of both techniques.

12.7.1 Electrospinning

In order to perform electrostatic spinning or electrospinning, a high-voltage electric field (typically 10–20 kV) is applied to form micro- and even nanoscale fibres from a suspended droplet of polymer melt or solution (Meng *et al.*, 2010). A high voltage is applied at the end of a capillary tube where the polymer is suspended. When the repulsive electrostatic interactions overcome the droplet's surface tension, a Taylor cone is formed and a polymer jet is ejected from the tip of this Taylor cone (Park *et al.*, 2008). The polymer jet is then accelerated towards a grounded collector screen. As the jet moves through the air, a stretching process occurs and the solvent evaporates, which results in a non-woven polymer fabric or *polymer mat* (Peter, 2004). The set-up of the electrospinning process is shown in Fig. 12.12.

Electrospinning has already been applied for both synthetic and natural polymers (Baji *et al.*, 2010; Chang *et al.*, 2012; Dasari *et al.*, 2012). Rnjak-Kovacina *et al*. have electrospun elastin scaffolds for dermal tissue engineering applications (Rnjak-Kovacina *et al.*, 2011).

Despite the interesting applications of electrospinning, the technique is limited to the formation of two-dimensional polymer mats (Holzwarth and Ma, 2011). Although the structures developed often show excellent cell adhesion, cell colonization is frequently problematic since the dense polymer mats generally do not allow cell permeation (Mironov *et al.*, 2009; Holzwarth and Ma, 2011). Another problem with electrospun matrices can be their inferior mechanical properties.

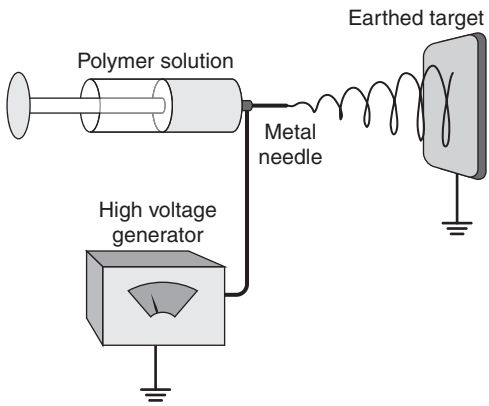

12.12 Schematic overview of the electrospinning process. (Copyright permission obtained from Neotherix Ltd – www.neotherix.com)

In order to mimic the three-dimensional extracellular environment, electrospinning should be combined with other polymer processing techniques. An example has been described by Park *et al.*, applying microfibers as spacers between polymer mats deposited subsequently (Park *et al.*, 2008). An excellent review from Dalton *et al.* describes the combination of electrospinning and additive manufacturing for a broad application range (Brown *et al.*, 2011; Dalton *et al.*, 2013). They anticipate that these converging technologies will also show great promise in the development of tissue engineering scaffolds. Another possibility includes the rolling of cell-seeded polymer mats into tubular constructs as proposed by Hashi *et al.* (2007).

12.7.2 Rapid prototyping

When designing and manufacturing three-dimensional scaffolds, solid free-form fabrication (SFF) offers many possibilities to control both the pore size and the pore geometry (Park *et al.*, 2011). SFF techniques, also known as rapid prototyping techniques, include 3D printing, stereolithography, fused deposition modelling, phase change jet printing and 3D plotting. SFF has already been applied to produce scaffolds for hard tissue engineering (e.g. bone), but it is also applicable for soft tissue applications (Park *et al.*, 2011).

The Bioscaffolder™ technology was first proposed by Landers *et al.* to process hydrogels for soft tissue engineering applications (Landers and Mulhaupt, 2000; Billiet *et al.*, 2012). Polymer solutions are transferred to an air driven pneumatic syringe which is mounted on a three-axis robotic dispenser. Moreover, the syringe is placed inside a heating element enabling

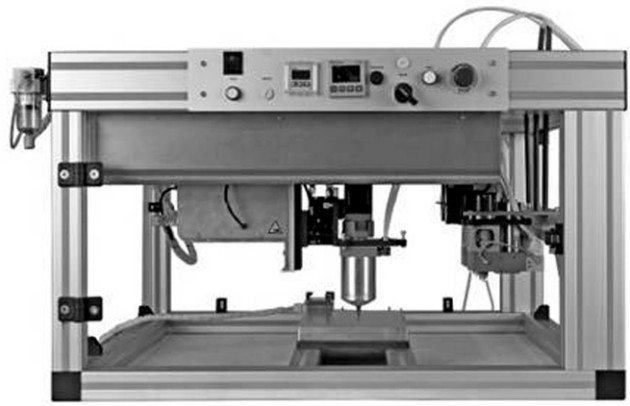

12.13 Bioscaffolder™ set-up applied for scaffold preparation.

precise temperature control. The experimental set-up is depicted in Fig. 12.13.

In order to control the pore size and the pore geometry, computer aided design and manufacture (CAD/CAM) software is applied (Peter, 2004). Using the appropriate CAD software, cross-sections of the scaffold are designed, which are then deposited layer by layer in a sequential build-up process (Peter, 2004; Nie and Kumacheva, 2008; Park *et al.*, 2011). Alternatively, a scan from a medical imaging technique can also be used as starting point. As the dispensing head moves, a polymer strand is ejected from the syringe onto a collecting plate where the material sets. The deposition of subsequent layers, enables the formation of complex three-dimensional structures (see Fig. 12.14).

Material deposition can also be performed in a medium with matching density (Landers and Mulhaupt, 2000; Pfister *et al.*, 2004; Peltola *et al.*, 2008). The latter results in a buoyancy effect which prevents the deposited material to collapse under its own weight, thus eliminating the need for temporary support structures.

The quality of the scaffolds developed strongly depends on the processing parameters applied. A brief overview of the most relevant processing parameters is described in the upcoming section.

A first variable is the needle mounted on the syringe. As the internal needle diameter decreases, the amount of ejected material per time unit will also decrease. Ideally, this would enable the deposition of very thin fibres increasing the scaffold porosity. For very thin needles, however, the pressure drop across the needle increases dramatically, resulting in the need for a higher pressure to be applied. Since the experimental set-up is limited to a specific pressure, the needle diameter to be applied is also limited.

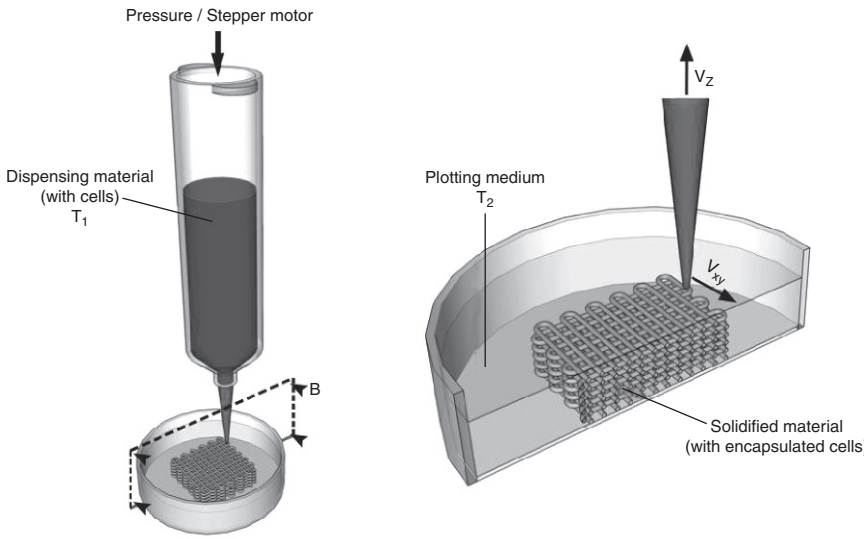

12.14 Image showing the principle of 3D-bioplotting. (*Source*: Republished with permission of Pergamon, from Biomaterials, Billiet *et al.*, **33**, 26, 2013; permission conveyed through Copyright Clearance Center, Inc.)

In addition to the needle diameter, the applied pressure also has a great impact on the strand diameter obtained. As the pressure is increased, more material will be ejected per time unit. In order to obtain thin fibres, the applied pressure should thus be kept as low as possible.

Another important parameter affecting the scaffold obtained, is the polymer concentration.

Higher polymer concentrations yield more viscous solutions that require higher pressures to plot. Too dilute solutions will not be able to gel upon cooling or heating for upper critical solution temperature (UCST) or lower critical solution temperature (LCST) polymers, respectively. A certain minimal concentration, i.e. the critical gel concentration, is thus required to enable gelation.

The speed of the dispensing head in the XY-plane is another important parameter when considering the strand diameter. As the dispensing head moves more quickly, the ejected material will be spread out over a longer distance, resulting in thinner fibres. Slower deposition on the other hand, gives the material more time to solidify, since it will take the device longer to start plotting the next layer. The dispensing speed can thus be seen as an interesting tool to fine-tune the scaffold properties.

A final parameter that will be discussed is the temperature. In order to obtain a polymer solution that can be ejected from the nozzle, the temperature is generally brought above or below the gel point of the material for UCST or LCST polymers, respectively. At this temperature, however, material droplets are often ejected, since the solution lacks the viscosity required to enable the ejection of polymer strands.

Despite the huge potential of the Bioscaffolder™ technology, the technique also shows some very important shortcomings (Peter, 2004; Ovsianikov *et al.*, 2011). A first drawback is its limited resolution, which is mainly influenced by the needle diameter and the rate at which the printing head operates (Billiet *et al.*, 2012). The Bioscaffolder™ technology can also be very time consuming since the processing parameters have to be optimized for each new polymer (and even each new polymer derivative). Another issue is orthogonality with the (bio)polymers applied: polymers to be applied in combination with the Bioscaffolder™ technology should show a well-defined visco-elastic response allowing them to quickly set (Billiet *et al.*, 2012). In addition, the deposited material should contain a high colloid-volume ratio to prevent shrinkage by solvent evaporation. Despite these restrictions, a variety of polymers including poly(L-lactic acid) (PLLA), poly(ε-caprolactone) (PCL), agarose, gelatin, chitosan and polyelectrolytes have already been applied as starting materials to develop porous scaffolds using the bioplotter technology (Peter, 2004; Nie and Kumacheva, 2008).

In order to circumvent the drawback of the limited resolution, novel techniques are also being developed. An interesting processing technique is two-photon polymerization (2PP) (Engelhardt *et al.*, 2011; Ovsianikov *et al.*, 2011). Using 2PP, a photocurable material is subjected to spatially well-defined laser irradiation. The microscope objective used to focus the laser beam, can be moved relative to the sample, thus allowing the formation of scaffolds via direct laser writing (Ovsianikov *et al.*, 2011; West, 2011).

The wavelength applied is double that of the λ_{max} of the photoinitiator used to initiate the photopolymerization. As a result, two photons are required to provide the energy needed. This explains the more precise control over the polymerization, since the curing will only take place in the focal point of the laser beam (West, 2011).

12.8 Characterization of hydrogel foams

In this section, some relevant characterization techniques will be described, enabling the characterization of produced hydrogel foams including micro-computed tomography, helium pycnometry, scanning electron microscopy (SEM) and dynamic vapour sorption (DVS) analysis.

12.8.1 Scanning electron microscopy (SEM)

SEM is a technique used to visualize surfaces with nanometre resolution (2004). SEM provides easily interpretable, 3D-like, topological information.

In SEM analysis, a beam of high-energy electrons is applied to a sample's surface. When these electrons interact with the material, secondary electrons are generated, which are detected. In addition to the generation of secondary electrons (SE), elastic scattering can also take place resulting in backscattered electrons (BSE). BSEs are more energetic compared to SEs and are thus able to penetrate the sample and re-emerge as much as 1 μm from their point of entry. Along their path, they may give rise to additional SEs, which will reach the detector as well and will lead to a decrease in the attainable resolution.

A scanning electron microscope generally consists of a series of fixed components (see Fig. 12.15). First, a tungsten filament generates a narrow beam of electrons. This can be achieved by simply heating the filament (traditional set-up) or, in more recent field emission guns, by drawing electrons from a very sharp tungsten tip using high electric fields. Next, the electron beam is focused via one or two electromagnetic lenses. The entire system has to be kept at high vacuum to prevent collisions of the electrons generated with air molecules present within the device. Finally, scanning coils are applied to slightly deflect the electron beam, enabling the operator to scan the entire surface. The detector is generally an Everhart-Thornley detector, located on the chamber wall. Electrons (BSEs and SEs) are attracted toward a positively charged scintillator, where they generate photons. These photons are

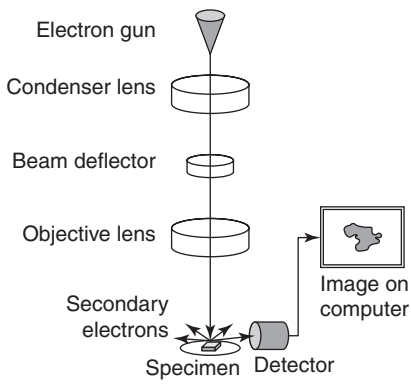

12.15 Schematic drawing of the electron column in a SEM showing the various components. (*Source*: Republished with permission of John/Wiley and Sons, Inc., from Microscopy Research and Technique, Jin S. E. *et al.*, **73**, 2013; permission conveyed through Copyright Clearance Center, Inc.)

transferred through a light guide toward a photomultiplier tube, where they are counted.

The electrons used to scan the sample's surface are removed from the device by grounding the sample to the device. This implies that the sample has to be (semi)conductive. Otherwise charges would build up on the sample, greatly deteriorating system performance. In general, non-conductive samples are therefore coated with a thin metal layer (Au/Pd).

12.8.2 Micro-computed tomography (μCT)

Radiography is the recording of a shadow image of an optically opaque object, using penetrating radiation and a recording medium (Dierick, 2005). Tomography is an extension of radiography. In general terms, it is a non-destructive technique to investigate the inner structure of an object in 3D. Basically, the 3D object is reconstructed, based on a set of 2D projections (or radiographies), taken from different angles by rotating the sample around a defined axis (Fig. 12.16) (Cnudde, 2005). The original mathematical framework was developed by Radon in 1917. It provided the solution for the reconstruction of a distribution of a given parameter based on its projections, taken with a parallel beam of penetrating radiation (Dierick, 2005). More recently, X-ray tomography has become an important technique for non-destructive testing in various research fields, such as biology, geology, archaeology, industry, etc (Cnudde *et al.*, 2006). Over the years, the resolution of CT imaging systems has steadily improved. Modern medical scanners now have a resolution of a few hundred microns. The reason for this limitation is the fact that for medical purposes the radiation dose has to be

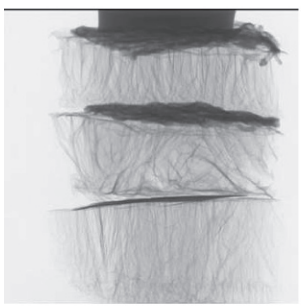

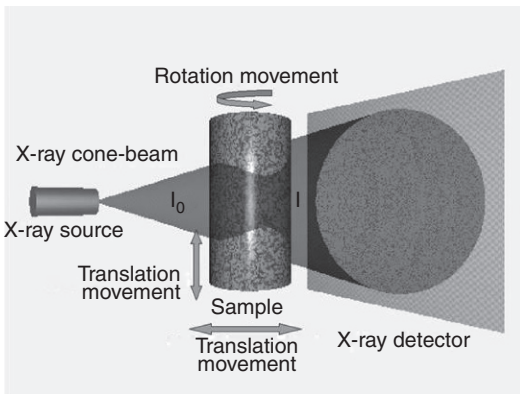

12.16 Radiography depicting three porous polymeric scaffolds stacked on top of each other (left); overview of μ-CT set-up in which radiographies are taken from different angles by rotating the sample around a defined axis (right).

as low as possible and the radiation energy is generally limited to about 100 keV, resulting in relatively large detector elements. Non-medical devices do not suffer from dose or energy restrictions. Resolving powers below 1 micron have already been achieved (Dierick, 2005).

In several studies, a 'Skyscan 1072' X-ray micro-tomograph has already been used. This compact desktop system, consisting of an X-ray shadow microscopic system and a computer with tomographic reconstruction software, generates high-resolution images for small samples (7 mm diameter). During a measurement, both the X-ray source and the detector are fixed while the sample rotates around a stable vertical axis (Fig. 12.16). Random movement and multiple-frame averaging were used to minimize the Poisson noise in the images. The spot size of the Hamamatsu microfocus tube limits the spatial resolution of the reconstructed slices to 10 μm in the X, Y and Z directions. During acquisition, X-ray radiographs are recorded at different angles during step-wise rotation between 0° and 180° around the vertical axis. The attenuation of the X-rays passing through a sample when scanning is performed, depends on the atomic number of the material and its density. These two features are crucial in the resulting contrast of the images.

After reconstruction of the 2D cross-sections, several software packages can be applied, including 3D software μCTanalySIS, in order to segment the images and determine their 3D porosity and pore size distribution (Steppe *et al.*, 2004; De Graef *et al.*, 2005). For the determination of the pore size distribution, each pore is filled with the largest sphere possible (the so-called 'maximum opening'). The total volume filled by this maximum sphere is determined during the analysis. Subsequently, the software fills the total volume of each pore with a smaller sphere while its total filling volume is determined. This process continues until the total volume of each pore is contained within the smallest inscribed sphere, with a size of one voxel (Fig. 12.17). From this analysis, data of all pores can be acquired.

Another software program (Octopus) can also be used to analyse certain images and to show the similarity with micrographs generated using SEM (Dierick *et al.*, 2004; vanVlierberghe *et al.*, 2007). Octopus is a server/client tomography reconstruction package for parallel and cone beam geometry.

12.8.3 Helium pycnometry

A pycnometer allows measuring the volume and the density of solid objects in a non-destructive manner. The latter is accomplished by employing Archimedes' principle of fluid displacement and Boyle's law of volume–pressure relationships, respectively, for liquid and gas pycnometers (Tamari and Aguilar-Chavez, 2005). Archimedes' principle is that an object totally

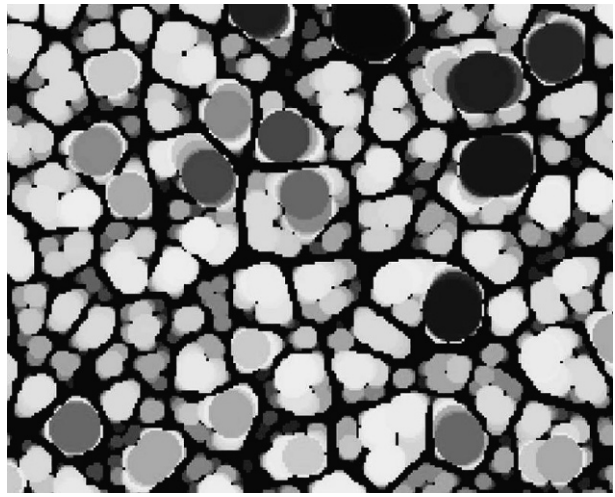

12.17 Principle of the pore analysis performed by μCTanalySIS. (*Source*: Reprinted with permission from (van Vlierberghe *et al*. Porous gelatin hydrogels: 1. Cryogenic formation and structure analysis (2007) *Biomacromolecules,* **8**(2),331–337). Copyright (2013) American Chemical Society.)

or partially immersed in a fluid is lifted up by a force equal to the weight of the fluid that is displaced.

Ideally, a gas is used as the displacing fluid since it penetrates the finest pores, allowing maximum accuracy. That is why helium is used preferentially, since its small atomic dimension enables entry into pores approaching one Ängström (10^{-10} m). Its behaviour as an ideal gas is also desirable. Other gases, such as nitrogen, could also be used, often with no measurable differences.

In general, a 'constant-volume' gas pycnometer is applied (Fig. 12.18) (Tamari, 2004). The latter is composed of a sample chamber, a tank and an absolute pressure transducer, which is positioned in a thermostatically controlled environment.

In order to determine the volume of a sample, the following procedure should be applied:

1. the sample is positioned in the sample chamber,
2. valves 'Z' and 'M' are opened and the pycnometer is filled with gas,
3. valve 'M' is closed and the absolute pressure transducer is used to measure the initial gas pressure in the pycnometer (P_i),
4. valve 'Z' is closed to isolate the sample chamber,
5. valve 'M' is opened and some gas is introduced into the tank (or removed from it),

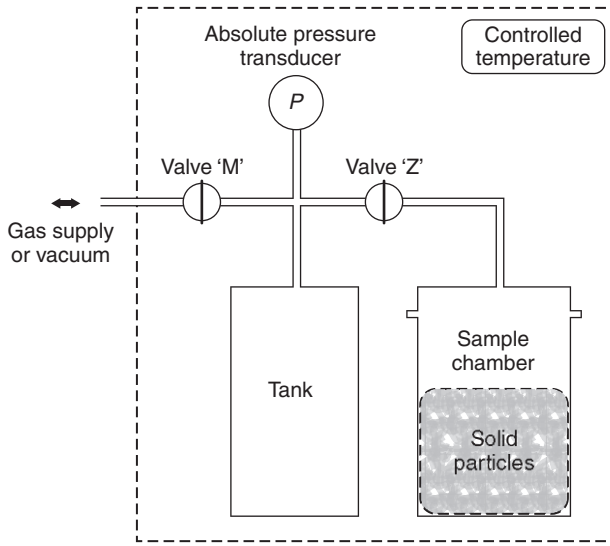

12.18 Diagram of a constant-volume gas pycnometer. (*Source*: © IOP Publishing. Reproduced by permission of IOP Publishing from Tamari, S., Optimum design of the constant-volume gas pycnometer for determining the volume of solid particles. *Measurement Science and Technology* 2004, **15** (3), 549–558. All rights reserved.)

6. valve 'M' is closed again and the gas pressure into the tank is measured (P_j),
7. valve 'Z' is opened so that the gas can expand from the tank to the sample chamber (or vice versa),
8. the final gas pressure is measured (P_f) when the gas expansion is finished.

Based on the hypotheses that the gas behaves ideally and that the expanding gas quickly reaches equilibrium, the following equation can be deduced:

$$V_s = V_c + V_t \left(P_f - P_j\right) / \left(P_f - P_i\right) \qquad [12.12]$$

with V_s = sample volume
V_c = sample chamber volume
V_t = tank (i.e. reservoir) volume

Pycnometers are used for research and quality control in a broad application field, such as ceramics, petrochemicals, fibres, pharmaceuticals, cosmetics, etc. (Cilli *et al.*, 2002; Amore *et al.*, 2003).

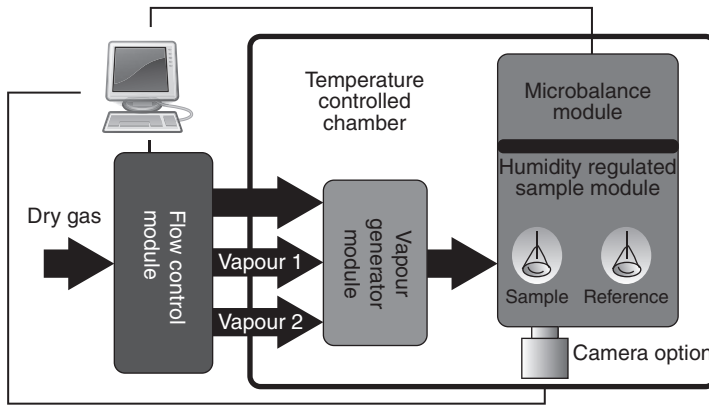

12.19 Overview of the DVS apparatus. (*Source*: Republished with permission of Surface Measurement Systems – The Total Sorption Solution (United Kingdom), 2013.)

12.8.4 Dynamic vapour sorption analysis

A DVS apparatus regulates the temperature and humidity of the environment surrounding a sample, allowing any weight change in a sample due to sorption or desorption of water vapour to be accurately measured (Fig. 12.19).

The DVS utilizes a dry carrier gas (i.e. nitrogen). Precise control of the ratio of saturated and dry carrier gas flows is enabled with mass flow control. Samples can be subjected to a controlled cycle of changing relative humidity, beginning with an initial drying phase at 0% relative humidity. Mass changes can be measured by means of a recording ultra-microbalance, which measures the weight change caused by sorption or desorption of the vapour molecule.

A DVS is a valuable tool to measure sorption/desorption isotherms and kinetics, surface energies, diffusion coefficients, amorphous content in polymers, etc. It is often used for the analysis of pharmaceuticals (McInnes *et al.*, 2005), food components (Czepirski *et al.*, 2002) and polymers (Tesch *et al.*, 1999; Cross *et al.*, 2000).

12.9 Future trends

Hydrogel foams for tissue engineering purposes can be developed using a large panel of (state-of-the-art) polymer processing techniques of which each is concomitant with its specific advantages and disadvantages. In general, a superior resolution corresponds with a time-consuming technology. Future developments will mainly focus on optimizing existing techniques

both time-wise as well as resolution-related. In addition, it can be anticipated that existing methodologies will merge into converging technologies. For example, when considering rapid prototyping techniques including the bioplotter technology, they result in the production of highly regular porous materials. However, when considering the irregularity of the extracellular matrix, bioplotted hydrogels might insufficiently mimic the complexity of the cellular environment. As a result, the convergence of electrospinning with rapid prototyping technologies could be a promising approach to merge the strengths of both methodologies and minimizing their weaknesses.

In addition to equipment-related perspectives, novel cell-biomaterial approaches should also be considered, as a recent trend includes material processing taking place in the presence of (autologous stem) cells. Up to recently, hydrogel foams were designed and produced in the absence of cells, followed by sterilizing the materials prior to cell seeding. Recent work, however, has clearly indicated the potential of cell encapsulation and biomaterial processing in the presence of cells. The main challenges herein reside in two different aspects. A first important issue includes the possibility to perform hydrogel development under sterile conditions. A second aspect to be considered is the incompatibility of cells with a large number of hydrogel processing technologies.

In conclusion, the ideal strategy should aim at a 'cell-friendly' production process which should ideally take place in a sterile environment. The development of biocompatible (photo)initiators enabling hydrogel polymerization will therefore also gain increasing interest in the future.

12.10 References

Abbah, S. A., Lu, W. W., Chan, D., Cheung, K. M. C., Liu, W. G., Zhao, F., Li, Z. Y., Leong, J. C. Y. and Luk, K. D. K. (2006) *In vitro* evaluation of alginate encapsulated adipose-tissue stromal cells for use as injectable bone graft substitute, *Biochemical and Biophysical Research Communications*, **347,** 185–191.

Adhirajan, N., Shanmugasundaram, N., Shanmuganathan, S. and Babu, M. (2009) Functionally modified gelatin microspheres impregnated collagen scaffold as novel wound dressing to attenuate the proteases and bacterial growth, *European Journal of Pharmaceutical Sciences*, **36,** 235–245.

Ahmad, Z. and Khuller, G. K. (2008) Alginate-based sustained release drug delivery systems for tuberculosis, *Expert Opinion on Drug Delivery,* **5,** 1323–1334.

Alasalvar, C., Taylor, K. D. A., Oksuz, A., Garthwaite, T., Alexis, M. N. and Grigorakis, K. (2001) Freshness assessment of cultured sea bream (Sparus aurata) by chemical, physical and sensory methods, *Food Chemistry,* **72**, 33–40.

Amore, R., Pagani, C., Youssef, M. N., Netto, C. A. and Lewgoy, H. R. (2003) Polymerization shrinkage of packable resins varying the light source distance, measured by gas pycnometer, *Journal of Dental Research,* **82,** 213–213.

Andre, F. E., Booy, R., Bock, H. L., Clemens, J., Datta, S. K., John, T. J., Lee, B. W., Lolekha, S., Peltola, H., Ruff, T. A., Santosham, M. and Schmitt, H. J. (2008)

Vaccination greatly reduces disease, disability, death and inequity worldwide, *Bulletin of the World Health Organization,* **86**, 140–146.

Annunziata, R., Franchini, J., Ranucci, E. and Ferruti, P. (2007) Structural characterisation of poly(amidoamine) networks via high-resolution magic angle spinning NMR, *Magnetic Resonance in Chemistry,* **45,** 51–58.

Anseth, K. S., Bowman, C. N. and Brannon-Peppas, L. (1996) Mechanical properties of hydrogels and their experimental determination, *Biomaterials,* **17,** 1647–1657.

Awad, H. A., Wickham, M. Q., Leddy, H. A., Gimble, J. M. and Guilak, F. (2004) Chondrogenic differentiation of adipose-derived adult stem cells in agarose, alginate, and gelatin scaffolds, *Biomaterials,* **25,** 3211–3222.

Bacakova, L., Filova, E., Parizek, M., Ruml, T. and Svorcik, V. (2011) Modulation of cell adhesion, proliferation and differentiation on materials designed for body implants, *Biotechnology Advances,* **29,** 739–767.

Bahar, I., Erbil, H. Y., Baysal, B. M. and Erman, B. (1987) Determination of Polymer Solvent Interaction Parameter from Swelling of Networks – the System Poly(2-Hydroxyethyl Methacrylate)-Diethylene Glycol, *Macromolecules,* **20,** 1353–1356.

Baji, A., Mai, Y.-W., Wong, S.-C., Abtahi, M. and Chen, P. (2010) Electrospinning of polymer nanofibers: Effects on oriented morphology, structures and tensile properties, *Composites Science and Technology,* **70,** 703–718.

Balakrishnan, B. and Jayakrishnan, A. (2005) Self-cross-linking biopolymers as injectable in situ forming biodegradable scaffolds, *Biomaterials,* **26,** 3941–3951.

Barczyk, M., Carracedo, S. and Gullberg, D. (2010) Integrins, *Cell and Tissue Research,* **339,** 269–280.

Barminko, J., Kim, J. H., Otsuka, S., Gray, A., Schloss, R., Grumet, M. and Yarmush, M. L. (2011) Encapsulated mesenchymal stromal cells for *in vivo* transplantation, *Biotechnology and Bioengineering,* **108,** 2747–2758.

Barner-Kowollik, C., Du Prez, F. E., Espeel, P., Hawker, C. J., Junkers, T., Schlaad, H. and Van Camp, W. (2011) 'Clicking' polymers or just efficient linking: what is the difference?, *Angewandte Chemie-International Edition,* **50,** 60–62.

Bartkowiak, A. and Brylak, W. (2006) Hydrogel microcapsules containing natural and chemically modified oligochitosan – Mechanical properties and porosity, *Polimery,* **51,** 547–554.

Bastun, V. N., Nizhnik, S. B. and Usikova, G. I. (2006) Structural approach to enhance the fracture resistance of high-strength metallic materials, *International Applied Mechanics,* **42,** 904–912.

Billiet, T., Vandenhaute, M., Schelfhout, J., Van Vlierberghe, S. and Dubruel, P. (2012) A review of trends and limitations in hydrogel-rapid prototyping for tissue engineering, *Biomaterials*, **33**(26), 6020–6041.

Bindal, A., Narsimhan, G., Hem, S. L. and Kulshreshtha, A. (2003) Effect of steam sterilization on the rheology of polymer solutions, *Pharmaceutical Development and Technology,* **8,** 219–228.

Birkefeld, A. B., Bertermann, R., Eckert, H. and Pfleiderer, B. (2003) Liquid- and solid-state high-resolution NMR methods for the investigation of aging processes of silicone breast implants, *Biomaterials,* **24,** 35–46.

Bock, V. D., Hiemstra, H. and Van Maarseveen, J. H. (2006) Cu-I-catalyzed alkyne-azide 'click' cycloadditions from a mechanistic and synthetic perspective, *European Journal of Organic Chemistry*, 51–68.

Boelen, E. J. H., Van Hooy-Corstjens, C. S. J., Gijbels, M. J. J., Bulstra, S. K., Van Ooij, A., Van Rhijn, L. W. and Koole, L. H. (2006) Preliminary evaluation of new intrinsically radiopaque hydrogels for replacing the nucleus pulposus, *Journal of Materials Chemistry,* **16,** 824–828.

Boyce, M. C. and Arruda, E. M. (2000) Constitutive models of rubber elasticity: A review, *Rubber Chemistry and Technology,* **73,** 504–523.

Bradley, S. A. and Mclaughlin, R. L. (2007) High-resolution magic-angle spinning NMR for the identification of reaction products directly from thin-layer chromatography spots, *Magnetic Resonance in Chemistry,* **45,** 814–818.

Brannonpeppas, L. and Peppas, N. A. (1991) Equilibrium swelling behavior of ph-sensitive hydrogels, *Chemical Engineering Science,* **46,** 715–722.

Brown, T. D., Dalton, P. D. and Hutmacher, D. W. (2011) Direct writing by way of melt electrospinning, *Advanced Materials,* **23,** 5651–5657.

Campbell, N. and Reece, J. (2005) Extracellular components and connections between cells help coordinate cellular activities. *Biology.* 7th ed. UK: Pearson Benjamin Cummings.

Capitani, D., De Angelis, A. A., Crescenzi, V., Masci, G. and Segre, A. L. (2001) NMR study of a novel chitosan-based hydrogel, *Carbohydrate Polymers,* **45,** 245–252.

Castejon, D., Villa, P., Calvo, M. M., Santa-Maria, G., Herraiz, M. and Herrera, A. (2010) (1)H-HRMAS NMR study of smoked Atlantic salmon (Salmo salar), *Magnetic Resonance in Chemistry,* **48**, 693–703.

Chambon, F., Petrovic, Z. S., Macknight, W. J. and Winter, H. H. (1986) Rheology of model polyurethanes at the gel point, *Macromolecules,* **19**, 2146–2149.

Chan, G. and Mooney, D. J. (2008) New materials for tissue engineering: towards greater control over the biological response, *Trends in Biotechnology,* **26**, 382–392.

Chang, J.-J., Lee, Y.-H., Wu, M.-H., Yang, M.-C. and Chien, C.-T. (2012) Preparation of electrospun alginate fibers with chitosan sheath, *Carbohydrate Polymers,* **87**, 2357–2361.

Chatterjee, S. and Bohidar, H. B. (2005) Effect of cationic size on gelation temperature and properties of gelatin hydrogels, *International Journal of Biological Macromolecules,* **35**, 81–88.

Chehade, M. and Elder, M. J. (1997) Intraocular lens materials and styles: A review, *Australian and New Zealand Journal of Ophthalmology,* **25**, 255–263.

Chen, J. H., Sambol, E. B., Kennealey, P. T., O'connor, R. B., Decarolis, P. L., Cory, D. G. and Singer, S. (2004) Water suppression without signal loss in HR-MAS H-1 NMR of cells and tissues, *Journal of Magnetic Resonance,* **171**, 143–150.

Cheng, H. C. and Hwu, F. S. (2006) Fatigue reliability analysis of composites based on residual strength, *Advanced Composite Materials,* **15**, 385–402.

Cheng, L. L., Burns, M. A. and Lean, C. L. (2006) High resolution magic angle spinning (HRMAS) proton MRS of surgical specimens. In*:* Webb, G. A. (ed.), *Modern Magnetic Resonance*, Springer Netherlands.

Chiu, H. C. and Yang, C. H. (2000) Synthesis of temperature/pH-sensitive hydrogels containing disulfide linkages as cross-links and their characterization, *Polymer Journal,* **32**, 574–582.

Cho, C. S., Seo, S. J., Park, I. K., Kim, S. H., Kim, T. H., Hoshiba, T., Harada, I. and Akaike, T. (2006) Galactose-carrying polymers as extracellular matrices for liver tissue engineering, *Biomaterials,* **27**, 576–585.

Choi, H. S., Kontani, K., Huh, K. M., Sasaki, S., Ooya, T., Lee, W. K. and Yui, N. (2002) Rapid induction of thermoreversible hydrogel formation based on poly(propylene glycol)-grafted dextran inclusion complexes, *Macromolecular Bioscience,* **2**, 298–303.

Choi, Y. S., Lee, S. B., Hong, S. R., Lee, Y. M., Song, K. W. and Park, M. H. (2001) Studies on gelatin-based sponges. Part III: A comparative study of cross-linked gelatin/alginate, gelatin/hyaluronate and chitosan/hyaluronate sponges and their application as a wound dressing in full-thickness skin defect of rat, *Journal of Materials Science-Materials in Medicine,* **12**, 67–73.

Cilli, R., Prakki, A. and Araujo, M. A. J. (2002) Utilizing gas pycnometer for measuring polymerization contraction of composite resins, *Journal of Dental Research,* **81**, A259–A259.

Cnudde, V. (2005) Exploring the potential of x-ray tomography as a new non-destructive research tool in conservation studies of natural building stones. *PhD Thesis.* Ghent University.

Cnudde, V., Masschaele, B., Dierick, M., Vlassenbroeck, J., Van Hoorebeke, L. and Jacobs, P. (2006) Recent progress in X-ray CT as a geosciences tool, *Applied Geochemistry,* **21**, 826–832.

Cross, G. H., Ren, Y. T. and Swann, M. J. (2000) Refractometric discrimination of void-space filling and swelling during vapour sorption in polymer films, *Analyst,* **125**, 2173–2175.

Cuggino, J. C., Alvarez Igarzabal, C. I., Rueda, J. C., Quinzani, L. M., Komber, H. and Strumia, M. C. (2008) Synthesis and characterization of new hydrogels through copolymerization of N-acryloyl-tris-(hydroxymethyl) aminomethane and different crosslinking agents, *European Polymer Journal,* **44**, 3548–3555.

Czepirski, L., Komorowska-Czepirska, E. and Szymonska, J. (2002) Fitting of different models for water vapour sorption on potato starch granules, *Applied Surface Science,* **196**, 150–153.

D'ayala, G. G., Malinconico, M. and Laurienzo, P. (2008) Marine derived polysaccharides for biomedical applications: Chemical modification approaches, *Molecules,* **13**, 2069–2106.

Dalton, P. D., Vaquette, C., Farrugia, B. L., Dargaville, T. R., Brown, T. D. and Hutmacher, D. W. (2013) Electrospinning and additive manufacturing: converging technologies, *Biomaterials Science*, **1**, 171–185.

Dang, J. M. and Leong, K. W. (2006) Natural polymers for gene delivery and tissue engineering, *Advanced Drug Delivery Reviews,* **58**, 487–499.

Dasari, A., Quirós, J., Herrero, B., Boltes, K., García-Calvo, E. and Rosal, R. (2012) Antifouling membranes prepared by electrospinning polylactic acid containing biocidal nanoparticles, *Journal of Membrane Science,* **405–406**, 134–140.

Davis, N. E., Ding, S., Forster, R. E., Pinkas, D. M. and Barron, A. E. (2010) Modular enzymatically crosslinked protein polymer hydrogels for in situ gelation, *Biomaterials,* **31**, 7288–7297.

De Graef, B., Cnudde, V., Dick, J., De Belie, N., Jacobs, P. and Verstraete, W. (2005) A sensitivity study for the visualisation of bacterial weathering of concrete and stone with computerised X-ray microtomography, *Science of the Total Environment,* **341**, 173–183.

De Nooy, A. E. J., Masci, G. and Crescenzi, V. (1999) Versatile synthesis of polysaccharide hydrogels using the Passerini and Ugi multicomponent condensations, *Macromolecules,* **32**, 1318–1320.

Dierick, M. (2005). *Tomographic Imaging Techniques Using Cold and Thermal Neutron Beams.* PhD Dissertation, Ghent University.

Dierick, M., Masschaele, B. and Van Hoorebeke, L. (2004) Octopus, a fast and user-friendly tomographic reconstruction package developed in LabView (R), *Measurement Science and Technology,* **15**, 1366–1370.

Ding, Z. Y., Aklonis, J. J. and Salovey, R. (1991) Model filled polymers.6. determination of the cross-link density of polymeric beads by Swelling, *Journal of Polymer Science Part B-Polymer Physics,* **29**, 1035–1038.

Djagny, K. B., Wang, Z. and Xu, S. (2001) Gelatin: A valuable protein for food and pharmaceutical industries: review, *Critical Reviews in Food Science and Nutrition,* **41**, 481–492.

Dragusin, D.-M., Van Vlierberghe, S., Dubruel, P., Dierick, M., Van Hoorebeke, L., Declercq, H. A., Cornelissen, M. M. and Stancu, I.-C. (2012) Novel gelatin-PHEMA porous scaffolds for tissue engineering applications, *Soft Matter,* **8**, 9589–9602.

Drury, J. L. and Mooney, D. J. (2003) Hydrogels for tissue engineering: scaffold design variables and applications, *Biomaterials,* **24**, 4337–4351.

Dubruel, P., Unger, R., Van Vlierberghe, S., Cnudde, V., Jacobs, P. J. S., Schacht, E. and Kirkpatrick, C. J. (2007) Porous gelatin hydrogels: 2. *In vitro* cell interaction study, *Biomacromolecules,* **8**, 338–344.

Dutta, R. C. and Dutta, A. K. (2009) Cell-interactive 3D-scaffold; advances and applications, *Biotechnology Advances,* **27**, 334–339.

Dvir-Ginzberg, M., Gamlieli-Bonshtein, I., Agbaria, R. and Cohen, S. (2003) Liver tissue engineering within alginate scaffolds: Effects of cell-seeding density on hepatocyte viability, morphology, and function, *Tissue Engineering,* **9**, 757–766.

Eagland, D., Crowther, N. J. and Butler, C. J. (1994) Complexation between polyoxyethylene and polymethacrylic acid – the importance of the molar-mass of polyoxyethylene, *European Polymer Journal,* **30**, 767–773.

Ellis, D. L. and Yannas, I. V. (1996) Recent advances in tissue synthesis *in vivo* by use of collagen-glycosaminoglycan copolymers, *Biomaterials,* **17**, 291–299.

Engelhardt, S., Hoch, E., Borchers, K., Meyer, W., Krueger, H., Tovar, G. E. M. and Gillner, A. (2011) Fabrication of 2D protein microstructures and 3D polymer-protein hybrid microstructures by two-photon polymerization, *Biofabrication,* 3.

Evangelista, M. B., Hsiong, S. X., Fernandes, R., Sampaio, P., Kong, H. J., Barrias, C. C., Salema, R., Barbosa, M. A., Mooney, D. J. and Granja, P. L. (2007) Upregulation of bone cell differentiation through immobilization within a synthetic extracellular matrix, *Biomaterials,* **28**, 3644–3655.

Fassina, L., Saino, E., Visai, L., Avanzini, M. A., De Angelis, M. G. C., Benazzo, F., Van Vlierberghe, S., Dubruel, P., Magenes, G. and IEEE (2010) Use of a gelatin cryogel as biomaterial scaffold in the differentiation process of human bone marrow stromal cells. *2010 Annual International Conference of the IEEE Engineering in Medicine and Biology Society*, 31 Aug–4 Sept, Buenos Aires.

Flory, P. (1944) Network structure and the elastic properties of vulcanized rubber, *Chemical Reviews,* **35**, 51–75.

Freyman, T. M., Yannas, I. V., Yokoo, R. and Gibson, L. J. (2001) Fibroblast contraction of a collagen-GAG matrix, *Biomaterials,* **22**, 2883–2891.

Gent, A. N. (1974) Rubber and rubber elasticity – Review, *Journal of Polymer Science Part C-Polymer Symposium*, **48**(1), 1–17.

George, M. and Abraham, T. E. (2006) Polyionic hydrocolloids for the intestinal delivery of protein drugs: Alginate and chitosan – a review, *Journal of Controlled Release,* **114**, 1–14.

Go, D. P., Gras, S. L., Mitra, D., Nguyen, T. H., Stevens, G. W., Cooper-White, J. J. and O'connor, A. J. (2011) Multilayered microspheres for the controlled release of growth factors in tissue engineering, *Biomacromolecules,* **12**, 1494–1503.

Gojo, S., Toyoda, M. and Umezawa, A. (2011) Tissue engineering and cell-based therapy toward integrated strategy with artificial organs, *Journal of Artificial Organs,* **14**, 171–177.

Grant, G. T., Morris, E. R., Rees, D. A., Smith, P. J. C. and Thom, D. (1973) Biological interactions between polysaccharides and divalent cations – EGG-box model, *Febs Letters,* **32**, 195–198.

Greenwood, H. L., Singer, P. A., Downey, G. P., Martin, D. K., Thorsteinsdottir, H. and Daar, A. S. (2006) Regenerative medicine and the developing world, *PLOS Medicine,* **3**, 1496–1500.

Griffith, L. G. and Naughton, G. (2002) Tissue engineering–current challenges and expanding opportunities, *Science,* **295**, 1009–1014.

Harris, L. D., Kim, B. S. and Mooney, D. J. (1998) Open pore biodegradable matrices formed with gas foaming, *Journal of Biomedical Materials Research,* **42**, 396–402.

Hashi, C. K., Zhu, Y., Yang, G.-Y., Young, W. L., Hsiao, B. S., Wang, K., Chu, B. and Li, S. (2007) Antithrombogenic property of bone marrow mesenchymal stem cells in nanofibrous vascular grafts, *Proceedings of the National Academy of Sciences of the United States of America,* **104**, 11915–11920.

Hennink, W. E., De Jong, S. J., Bos, G. W., Veldhuis, T. F. J. and Van Nostrum, C. F. (2004) Biodegradable dextran hydrogels crosslinked by stereocomplex formation for the controlled release of pharmaceutical proteins, *International Journal of Pharmaceutics,* **277**, 99–104.

Hennink, W. E. and Van Nostrum, C. F. (2002) Novel crosslinking methods to design hydrogels, *Advanced Drug Delivery Reviews,* **54**, 13–36.

Hoffman, A. S. (2002) Hydrogels for biomedical applications, *Advanced Drug Delivery Reviews,* **54**, 3–12.

Holzwarth, J. M. and Ma, P. X. (2011) Biomimetic nanofibrous scaffolds for bone tissue engineering, *Biomaterials,* **32**, 9622–9629.

Horak, D., Kroupava, J., Slouf, M. and Dvorak, P. (2004) Poly(2-hydroxyethyl methacrylate)-based slabs as a mouse embryonic stem cell support, *Biomaterials,* **25**, 5249–5260.

Hou, Q. P., Grijpma, D. W. and Feijen, J. (2003a) Porous polymeric structures for tissue engineering prepared by a coagulation, compression moulding and salt leaching technique, *Biomaterials,* **24**, 1937–1947.

Hou, Q. P., Grijpma, D. W. and Feijen, J. (2003b) Preparation of interconnected highly porous polymeric structures by a replication and freeze-drying process, *Journal of Biomedical Materials Research Part B-Applied Biomaterials,* **67B,** 732–740.

Hu, X., Li, D., Zhou, F. and Gao, C. (2011) Biological hydrogel synthesized from hyaluronic acid, gelatin and chondroitin sulfate by click chemistry, *Acta Biomaterialia,* **7**, 1618–1626.

Huang, S. and Fu, X. (2010) Naturally derived materials-based cell and drug delivery systems in skin regeneration, *Journal of Controlled Release,* **142**, 149–159.

Hubbell, J. A. (2003) Materials as morphogenetic guides in tissue engineering, *Current Opinion in Biotechnology,* **14**, 551–558.

Hunt, N. C. and Grover, L. M. (2010) Cell encapsulation using biopolymer gels for regenerative medicine, *Biotechnology Letters,* **32**, 733–742.

Hutmacher, D. W., Ng, K. W., Kaps, C., Sittinger, M. and Klaring, S. (2003) Elastic cartilage engineering using novel scaffold architectures in combination with a biomimetic cell carrier, *Biomaterials,* **24**, 4445–4458.

Hutson, C. B., Nichol, J. W., Aubin, H., Bae, H., Yamanlar, S., Al-Haque, S., Koshy, S. T. and Khademhosseini, A. (2011) Synthesis and characterization of tunable poly(ethylene glycol): gelatin methacrylate composite hydrogels, *Tissue Engineering Part A,* **17**, 1713–1723.

Iannace, S., Di Maio, E. and Nicolais, L. (2001) Preparation and characterization of polyurethane porous membranes by particulate-leaching method, *Cellular Polymers,* **20**, 321–338.

Ikada, Y., Jamshidi, K., Tsuji, H. and Hyon, S. H. (1987) Stereocomplex formation between enantiomeric poly(lactides), *Macromolecules,* **20**, 904–906.

Iritani, E., Katagiri, N., Yamaguchi, K. and Cho, J. H. (2006) Compression-permeability properties of compressed bed of superabsorbent hydrogel particles, *Drying Technology,* **24**, 1243–1249.

Jachowicz, J. and Yao, K. (1996) Dynamic hairspray analysis. I. Instrumentation and preliminary results *Journal of the Society of Cosmetic Chemists,* **47**, 73–84.

Jayachandran, S., Lleras-Muney, A. and Smith, K. V. (2010) Modern medicine and the twentieth century decline in mortality: evidence on the impact of sulfa drugs, *American Economic Journal-Applied Economics,* **2**, 118–146.

Ji, C. D., Annabi, N., Khademhosseini, A. and Dehghani, F. (2011) Fabrication of porous chitosan scaffolds for soft tissue engineering using dense gas CO_2, *Acta Biomaterialia,* **7**, 1653–1664.

Jin, R., Teixeira, L. S. M., Dijkstra, P. J., Zhong, Z. Y., Van Blitterswijk, C. A., Karperien, M. and Feijen, J. (2010) Enzymatically crosslinked dextran-tyramine hydrogels as injectable scaffolds for cartilage tissue engineering, *Tissue Engineering Part A,* **16**, 2429–2440.

Johnson, F. A., Craig, D. Q. M., Mercer, A. D. and Chauhan, S. (1997) The effects of alginate molecular structure and formulation variables on the physical characteristics of alginate raft systems, *International Journal of Pharmaceutics,* **159**, 35–42.

Kang, H. W., Tabata, Y. and Ikada, Y. (1999) Fabrication of porous gelatin scaffolds for tissue engineering, *Biomaterials,* **20**, 1339–1344.

Kawanishi, M., Ushida, T., Kaneko, T., Niwa, H., Fukubayashi, T., Nakamura, K., Oda, H., Tanaka, S. and Tateishi, T. (2004) New type of biodegradable porous scaffolds for tissue-engineered articular cartilage, *Materials Science and Engineering C-Biomimetic and Supramolecular Systems,* **24**, 431–435.

Kew, S. J., Gwynne, J. H., Enea, D., Abu-Rub, M., Pandit, A., Zeugolis, D., Brooks, R. A., Rushton, N., Best, S. M. and Cameron, R. E. (2011) Regeneration and repair of tendon and ligament tissue using collagen fibre biomaterials, *Acta Biomaterialia,* **7**, 3237–3247.

Khalil, S., Nam, J. and Sun, W. (2005) Multi-nozzle deposition for construction of 3D biopolymer tissue scaffolds, *Rapid Prototyping Journal,* **11**, 9–17.

Kimoto, H., Fukuda, A., Asano, A. and Kurotsu, T. (2005) Pulsed NMR study of network formation in the course of bulk polymerization of methyl acrylate, *Analytical Sciences,* **21**, 315–319.

Kloczkowski, A. (2002) Application of statistical mechanics to the analysis of various physical properties of elastomeric networks – a review, *Polymer,* **43**, 1503–1525.

Kolb, H. C., Finn, M. G. and Sharpless, K. B. (2001) Click chemistry: diverse chemical function from a few good reactions, *Angewandte Chemie International Edition,* **40**, 2004–2021.

Koschella, A., Hartlieb, M. and Heinze, T. (2011) A 'click-chemistry' approach to cellulose-based hydrogels, *Carbohydrate Polymers,* **86**, 154–161.

Kuang, J., Yuk, K. Y. and Huh, K. M. (2011) Polysaccharide-based superporous hydrogels with fast swelling and superabsorbent properties, *Carbohydrate Polymers,* **83**, 284–290.

Kuo, C. K. and Ma, P. X. (2001) Ionically crosslinked alginate hydrogels as scaffolds for tissue engineering: Part 1. Structure, gelation rate and mechanical properties, *Biomaterials,* **22**, 511–521.

Ladewig, K. (2011) Drug delivery in soft tissue engineering, *Expert Opinion on Drug Delivery,* **8**, 1175–1188.

Landers, R. and Mulhaupt, R. (2000) Desktop manufacturing of complex objects, prototypes and biomedical scaffolds by means of computer-assisted design combined with computer-guided 3D plotting of polymers and reactive oligomers, *Macromolecular Materials and Engineering,* **282**, 17–21.

Langer, R. and Vacanti, J. (1993) Tissue engineering, *Science,* **260**, 920–926.

Laurencin, C. T., Ko, F. K., Attawia, M. A. and Borden, M. D. (1998) Studies on the development of a tissue engineered matrix for bone regeration, *Cells and materials,* **8**, 175–181.

Leach, J. B., Bivens, K. A., Collins, C. N. and Schmidt, C. E. (2004) Development of photocrosslinkable hyaluronic acid-polyethylene glycol-peptide composite hydrogels for soft tissue engineering, *Journal of Biomedical Materials Research Part A,* **70A,** 74–82.

Leach, J. B. and Schmidt, C. E. (2004) Photocrosslinkable hyaluronic acid hydrogels for tissue engineering. In: Wong, J. Y., Plant, A. L., Schmidt, C. E., Shea, L., Coury, A. J., Chen, C. S., Barron, A. E., Klok, H. A., Saltzman, W. M., Chilkoti, A., Luo, D. and Uhrich, K. (eds.), *Architecture and Application of Biomaterials and Biomolecular Materials*, Materials Research Society.

Leach, J. B. and Schmidt, C. E. (2005) Characterization of protein release from photocrosslinkable hyaluronic acid-polyethylene glycol hydrogel tissue engineering scaffolds, *Biomaterials,* **26**, 125–135.

Lee, B. P., Huang, K., Nunalee, F. N., Shull, K. R. and Messersmith, P. B. (2004a) Synthesis of 3, 4-dihydroxyphenylalanine (DOPA) containing monomers and their co-polymerization with PEG-diacrylate to form hydrogels, *Journal of Biomaterials Science-Polymer Edition,* **15**, 449–464.

Lee, J. E., Kim, S. E., Kwon, I. C., Ahn, H. J., Cho, H., Lee, S. H., Kim, H. J., Seong, S. C. and Lee, M. C. (2004b) Effects of a chitosan scaffold containing TGF-beta 1 encapsulated chitosan microspheres on *in vitro* chondrocyte culture, *Artificial Organs,* **28**, 829–839.

Lee, J. Y., Tan, B. and Cooper, A. I. (2007) CO_2-in-water emulsion-templated poly(vinyl alcohol) hydrogels using poly(vinyl acetate)-based surfactants, *Macromolecules,* **40**, 1955–1961.

Lee, K. Y., Bouhadir, K. H. and Mooney, D. J. (2004c) Controlled degradation of hydrogels using multi-functional cross-linking molecules, *Biomaterials,* **25**, 2461–2466.

Lee, S. B., Jeon, H. W., Lee, Y. W., Lee, Y. M., Song, K. W., Park, M. H., Nam, Y. S. and Ahn, H. C. (2003) Bio-artificial skin composed of gelatin and (1 –> 3), (1 –> 6)-beta-glucan, *Biomaterials,* **24**, 2503–2511.

Lee, S. Y., Pereira, B. P., Yusof, N., Selvaratnam, L., Yu, Z., Abbas, A. A. and Kamarul, T. (2009) Unconfined compression properties of a porous poly(vinyl alcohol)-chitosan-based hydrogel after hydration, *Acta Biomaterialia,* **5**, 1919–1925.

Li, W. (2006) Multidimensional HRMAS NMR: A platform for *in vivo* studies using intact bacterial cells, *Analyst,* **131**, 777–781.

Li, Y., Ke, W., Gao, X., Yuan, Y. and Shen, K. (2005) Effect of melt vibration on mechanical properties of injection molding and rheology, *Journal of Macromolecular Science, Part B,* **44**, 289–301.

Lim, D. W., Choi, S. H. and Park, T. G. (2000) A new class of biodegradable hydrogels stereocomplexed by enantiomeric oligo(lactide) side chains of poly(HEMA-g-OLA)s, *Macromolecular Rapid Communications,* **21**, 464–471.

Lohse, D. J. (2005) The influence of chemical structure on polyolefin melt rheology and miscibility, *Polymer Reviews,* **45**, 289–308.

Lozinsky, V. I. (2002) Cryogels on the basis of natural and synthetic polymers: Preparation, properties and application, *Uspekhi Khimii,* **71**, 559–585.

Lozinsky, V. I., Plieva, F. M., Galaev, I. Y. and Mattiasson, B. (2001) The potential of polymeric cryogels in bioseparation, *Bioseparation,* **10**, 163–188.

Ma, P. X. and Zhang, R. Y. (2001) Microtubular architecture of biodegradable polymer scaffolds, *Journal of Biomedical Materials Research,* **56**, 469–477.

Mancuso, A. and Glickson, J. D. (2004) Applications of NMR spectroscopy and imaging to the study of immobilised cell physiology. In: Nedovic, V. and Willaert, R. (eds.), *Fundamentals of Cell Immobilisation Biotechnology*, Springer-Verlag New York Inc.

Manju, S., Muraleedharan, C. V., Rajeev, A., Jayakrishnan, A. and Joseph, R. (2011) Evaluation of alginate dialdehyde cross-linked gelatin hydrogel as a biodegradable sealant for polyester vascular graft, *Journal of Biomedical Materials Research Part B-Applied Biomaterials,* **98B,** 139–149.

Mason, C. and Dunnill, P. (2008) A brief definition of regenerative medicine, *Regenerative Medicine,* **3**, 1–5.

Mcinnes, F. J., Thapa, P., Baillie, A. J., Welling, P. G., Watson, D. G., Gibson, I., Nolan, A. and Stevens, H. N. E. (2005) *In vivo* evaluation of nicotine lyophilised nasal insert in sheep, *International Journal of Pharmaceutics,* **304**, 72–82.

Meng, D. C., Erol, M. and Boccaccini, A. R. (2010) Processing technologies for 3D nanostructured tissue engineering scaffolds, *Advanced Engineering Materials*, **12**, B467–B487.

Mikos, A. G. and Temenoff, J. S. (2000) Formation of highly porous biodegradable scaffolds for tissue engineering, *Electronic Journal of Biotechnology*, **3**, 1–6.

Mikos, A. G., Thorsen, A. J., Czerwonka, L. A., Bao, Y., Langer, R., Winslow, D. N. and Vacanti, J. P. (1994) Preparation and characterization of poly(L-Lactic Acid) foams, *Polymer,* **35**, 1068–1077.

Mironov, V., Trusk, T., Kasyanov, V., Little, S., Swaja, R. and Markwald, R. (2009) Biofabrication: a 21st century manufacturing paradigm, *Biofabrication,* **1**, Article number: 022001.

Mithieux, S. M., Rasko, J. E. J. and Weiss, A. S. (2004) Synthetic elastin hydrogels derived from massive elastic assemblies of self-organized human protein monomers, *Biomaterials,* **25**, 4921–4927.

Mooney, D. J., Baldwin, D. F., Suh, N. P., Vacanti, L. P. and Langer, R. (1996a) Novel approach to fabricate porous sponges of poly(D,L-lactic-co-glycolic acid) without the use of organic solvents, *Biomaterials,* **17**, 1417–1422.

Mooney, D. T., Mazzoni, C. L., Breuer, C., Mcnamara, K., Hern, D., Vacanti, J. P. and Langer, R. (1996b) Stabilized polyglycolic acid fibre based tubes for tissue engineering, *Biomaterials,* **17**, 115–124.

Mu, Y. H., Li, Y. B., Wang, M. B., Xu, F. L., Zhang, X. and Tian, Z. Y. (2006) Novel method to fabricate porous n-HA/PVA hydrogel scaffolds. In: Kim, H. S., Li, Y. B. and Lee, S. W. (eds.), *Eco-Materials Processing and Design VII.* Zurich-Uetikon: Trans Tech Publications Ltd.

Nagahara, S. and Matsuda, T. (1996) Hydrogel formation via hybridization of oligonucleotides derivatized in water-soluble vinyl polymers, *Polymer Gels and Networks,* **4**, 111–127.

Nandivada, H., Jiang, X. and Lahann, J. (2007) Click chemistry: Versatility and control in the hands of materials scientists, *Advanced Materials,* **19**, 2197–2208.

Nehrer, S., Breinan, H. A., Ramappa, A., Young, G., Shortkroff, S., Louie, L. K., Sledge, C. B., Yannas, I. V. and Spector, M. (1997) Matrix collagen type and pore size influence behaviour of seeded canine chondrocytes, *Biomaterials,* **18**, 769–776.

Nie, Z. and Kumacheva, E. (2008) Patterning surfaces with functional polymers, *Nat Mater,* **7**, 277–290.

Nijenhuis, K. T. and Winter, H. H. (1989) Mechanical-properties at the gel point of a crystallizing polyvinyl-chloride solution, *Macromolecules,* **22**, 411–414.

Nouailhas, H., El Ghzaoui, A., Li, S. M. and Coudane, J. (2011) Stereocomplex-induced gelation properties of polylactide/poly(ethylene glycol) diblock and triblock copolymers, *Journal of Applied Polymer Science,* **122**, 1599–1606.

Nunes, M. C., Raymundo, A. and Sousa, I. (2006) Rheological behaviour and microstructure of pea protein/[kappa]-carrageenan/starch gels with different setting conditions, *Food Hydrocolloids,* **20**, 106–113.

O'brien, F. J., Harley, B. A., Yannas, I. V. and Gibson, L. (2004) Influence of freezing rate on pore structure in freeze-dried collagen-GAG scaffolds, *Biomaterials,* **25**, 1077–1086.

O'brien, F. J., Harley, B. A., Yannas, I. V. and Gibson, L. J. (2005) The effect of pore size on cell adhesion in collagen-GAG scaffolds, *Biomaterials,* **26**, 433–441.

Ogushi, Y., Sakai, S. and Kawakami, K. (2007) Synthesis of enzymatically-gellable carboxymethyl cellulose for biomedical applications, *Journal of Bioscience and Bioengineering,* **104**, 30–33.

Oh, S. H., Kang, S. G., Kim, E. S., Cho, S. H. and Lee, J. H. (2003) Fabrication and characterization of hydrophilic poly(lactic-co-glycolic acid)/poly(vinyl alcohol) blend cell scaffolds by melt-molding particulate-leaching method, *Biomaterials,* **24**, 4011–4021.

Omidian, H., Hashemi, S. A., Sammes, P. G. and Meldrum, I. (1998) A model for the swelling of superabsorbent polymers, *Polymer,* **39**, 6697–6704.

Osaki, K. (1993) Polymer dynamics and rheology, *International Journal of Polymeric Materials,* **20**, 265–269.

Ovsianikov, A., Deiwick, A., Van Vlierberghe, S., Dubruel, P., Moller, L., Drager, G. and Chichkov, B. (2011) Laser fabrication of three-dimensional CAD scaffolds from photosensitive gelatin for applications in tissue engineering, *Biomacromolecules,* **12**, 851–858.

Park, S. A., Lee, S. H. and Kim, W. (2011) Fabrication of hydrogel scaffolds using rapid prototyping for soft tissue engineering, *Macromolecular Research,* **19**, 694–698.

Park, S. H., Kim, T. G., Kim, H. C., Yang, D.-Y. and Park, T. G. (2008) Development of dual scale scaffolds via direct polymer melt deposition and electrospinning for applications in tissue regeneration, *Acta Biomaterialia,* **4**, 1198–1207.

Pek, Y. S., Spector, M., Yannas, I. V. and Gibson, L. J. (2004) Degradation of a collagen-chondroltin-6-sulfate matrix by collagenase and by chondroitinase, *Biomaterials,* **25**, 473–482.

Peltola, S. M., Melchels, F. P. W., Grijpma, D. W. and Kellomaki, M. (2008) A review of rapid prototyping techniques for tissue engineering purposes, *Annals of Medicine,* **40**, 268–280.

Peppas, N. A., Bures, P., Leobandung, W. and Ichikawa, H. (2000) Hydrogels in pharmaceutical formulations, *European Journal of Pharmaceutics and Biopharmaceutics,* **50**, 27–46.

Peppas, N. A. and Merrill, E. W. (1977) Crosslinked (polyvinyl-alcohol) hydrogels as swollen elastic networks, *Journal of Applied Polymer Science,* **21**, 1763–1770.

Perez, E. M. S., Lopez, J. G., Iglesias, M. J., Ortiz, F. L., Toresano, F. and Camacho, F. (2011) HRMAS-nuclear magnetic resonance spectroscopy characterization of tomato 'flavor varieties' from Almeria (Spain), *Food Research International,* **44**, 3212–3221.

Peter X, M. (2004) Scaffolds for tissue fabrication, *Materials Today,* **7**, 30–40.

Petka, W. A., Harden, J. L., Mcgrath, K. P., Wirtz, D. and Tirrell, D. A. (1998) Reversible hydrogels from self-assembling artificial proteins, *Science,* **281**, 389–392.

Pfister, A., Landers, R., Laib, A., Hubner, U., Schmelzeisen, R. and Mulhaupt, R. (2004) Biofunctional rapid prototyping for tissue-engineering applications: 3D bioplotting versus 3D printing, *Journal of Polymer Science Part a-Polymer Chemistry,* **42**, 624–638.

Pillay, V. and Fassihi, R. (1999) A new method for dissolution studies of lipid-filled capsules employing nifedipine as a model drug, *Pharmaceutical Research,* **16**, 333–337.

Pourjavadi, A. and Kurdtabar, M. (2007) Collagen-based highly porous hydrogel without any porogen: Synthesis and characteristics, *European Polymer Journal,* **43**, 877–889.

Pourjavadi, A., Kurdtabar, M. and Ghaseazadeh, H. (2008) Salt- and pH-resisting collagen-based highly porous hydrogel, *Polymer Journal,* **40**, 94–103.

Pourjavadi, A., Sadeghi, M., Hashemi, M. M. and Hosseinzadeh, H. (2006) Synthesis and absorbency of gelatin-graft-poly(sodium acrylate-co-acrylamide) superabsorbent hydrogel with salt and pH-responsiveness properties, *E-Polymers*, Article Number: 057.

Qin, Y. M. (2008) Alginate fibres: an overview of the production processes and applications in wound management, *Polymer International,* **57**, 171–180.

Ramadhar, T. R., Amador, F., Ditty, M. J. T. and Power, W. P. (2008) Inverse H-C ex situ HRMAS NMR experiments for solid-phase peptide synthesis, *Magnetic Resonance in Chemistry,* **46**, 30–35.

Ramakrishnan, S., Gerardin, C., Prud, Apos and Homme, R. K. (2004) Syneresis of Carrageenan Gels: NMR and rheology, *Soft Materials,* **2**, 145–153.

Rasteiro, M. G. and Antunes, E. (2005) Correlating the Rheology of PVC-Based Pastes with Particle Characteristics, *Particulate Science and Technology,* **23**, 361–375.

Ratner, B. D. (2004) Scanning electron microscopy. In*:* Ratner, B. D., Hoffman, A. S., Schoen, F. J. and Lemons, J. E. (eds.), *Biomaterials Science.* 2nd ed.: Elsevier Academic Press.

Reignier, J. and Huneault, M. A. (2006) Preparation of interconnected poly(epsilon-caprolactone) porous scaffolds by a combination of polymer and salt particulate leaching, *Polymer,* **47**, 4703–4717.

Ren, L., Tsuru, K., Hayakawa, S. and Osaka, A. (2001) Sol-gel preparation and *in vitro* deposition of apatite on porous gelatin-siloxane hybrids, *Journal of Non-Crystalline Solids,* **285**, 116–122.

Rios, H. F., Lin, Z., Oh, B., Park, C. H. and Giannobile, W. V. (2011) Cell- and gene-based therapeutic strategies for periodontal regenerative medicine, *Journal of Periodontology,* **82**, 1223–1237.

Risbud, M. (2001) Tissue engineering: implications in the treatment of organ and tissue defects, *Biogerontology,* **2**, 117–125.

Rnjak-Kovacina, J., Wise, S. G., Li, Z., Maitz, P. K. M., Young, C. J., Wang, Y. and Weiss, A. S. (2011) Tailoring the porosity and pore size of electrospun synthetic human elastin scaffolds for dermal tissue engineering, *Biomaterials,* **32**, 6729–6736.

Rosso, F., Giordano, A., Barbarisi, M. and Barbarisi, A. (2004) From cell-ECM interactions to tissue engineering, *Journal of Cellular Physiology,* **199**, 174–180.

Rousselot (2011) How to use gelatin? [Online]. Available: http://www.rousselot.com/en/applications/how-to-use-gelatine/ [Accessed 13/12 2011].

Roy, A. D., Jayalakshmi, K., Dasgupta, S., Roy, R. and Mukhopadhyay, B. (2008) Real time HR-MAS NMR: application in reaction optimization, mechanism elucidation and kinetic analysis for heterogeneous reagent catalyzed small molecule chemistry, *Magnetic Resonance in Chemistry,* **46**, 1119–1126.

Rueda, J., Suica, R., Komber, H. and Voit, B. (2003a) Synthesis of new polymethyloxazoline hydrogels by the 'macroinitiator' method, *Macromolecular Chemistry and Physics,* **204**, 954–960.

Rueda, J. C., Komber, H., Cedron, J. C., Voit, B. and Shevtsova, G. (2003b) Synthesis of new hydrogels by copolymerization of poly(2-methyl-2-oxazoline) bis(macromonomers) and N-vinylpyrrolidone, *Macromolecular Chemistry and Physics*, **204**, 947–953.

Rueda, J. C., Komber, H. and Voit, B. (2005) Synthesis of new amphiphilic and lypophilic polymer networks containing 2-methyl- and 2-nonyl-2-oxazoline by the macroinitiator method, *Journal of Polymer Science Part a-Polymer Chemistry,* **43**, 122–128.

Sakai, S., Ogushi, Y. and Kawakami, K. (2009) Enzymatically crosslinked carboxymethyl cellulose-tyramine conjugate hydrogel: Cellular adhesiveness and feasibility for cell sheet technology, *Acta Biomaterialia,* **5**, 554–559.

Schoof, H., Apel, J., Heschel, I. and Rau, G. (2001) Control of pore structure and size in freeze-dried collagen sponges, *Journal of Biomedical Materials Research,* **58**, 352–357.

Schurz, J. (1996) Rheology of synovial fluids and substitute polymers, *Journal of Macromolecular Science, Part A,* **33**, 1249–1262.

Seema, A. and Kutty, S. K. N. (2005) Rheology of short nylon-6 fiber reinforced styrene-butadiene rubber, *International Journal of Polymeric Materials,* **54**, 933–948.

Sell, S. A., Mcclure, M. J., Garg, K., Wolfe, P. S. and Bowlin, G. L. (2009) Electrospinning of collagen/biopolymers for regenerative medicine and cardiovascular tissue engineering, *Advanced Drug Delivery Reviews,* **61**, 1007–1019.

Shapiro, M. J. and Gounarides, J. S. (2000) High resolution MAS-NMR in combinatorial chemistry, *Biotechnology and Bioengineering,* **71**, 130–148.

Shin, I., Szamosi, J. and Tobing, S. (1991) Two-level factorial study of the rheology and foaming of bromobutyl rubber solutions, *International Journal of Polymeric Materials,* **15**, 103–106.

Simpson, A. J., Kingery, W. L., Shaw, D. R., Spraul, M., Humpfer, E. and Dvortsak, P. (2001) The application of H-1 HR-MAS NMR spectroscopy for the study of structures and associations of organic components at the solid–Aqueous interface of a whole soil, *Environmental Science and Technology,* **35**, 3321–3325.

Smewing, J. (1998) Analysing the textural properties of cosmetics, *Cosmetics and Toiletries Manufacture Worldwide*, 249–253.

Soeda, T. (1995) The function on food-processing for the cold-gel prepared from heated soy protein isolate – studies on the gelation of soy protein during the cold-storage.4, *Journal of the Japanese Society for Food Science and Technology-Nippon Shokuhin Kagaku Kogaku Kaishi,* **42**, 672–676.

Sperinde, J. J. and Griffith, L. G. (1997) Synthesis and characterization of enzymatically-cross-linked poly(ethylene glycol) hydrogels, *Macromolecules,* **30**, 5255–5264.

Sperinde, J. J. and Griffith, L. G. (2000) Control and prediction of gelation kinetics in enzymatically cross-linked poly(ethylene glycol) hydrogels, *Macromolecules,* **33**, 5476–5480.

Stacey, E. and Blachford, L. (2002) *Gelatin* [Online]. gale cengage. available: http://www.madehow.com/Volume-5/Gelatin.html [Accessed 19 November 2011].

Steppe, K., Cnudde, V., Girard, C., Lemeur, R., Cnudde, J. P. and Jacobs, P. (2004) Use of X-ray computed microtomography for non-invasive determination of wood anatomical characteristics, *Journal of Structural Biology,* **148**, 11–21.

Stern, C., Frick, A. and Weickert, G. (2007) Relationship between the structure and mechanical properties of polypropylene: Effects of the molecular weight and shear-induced structure, *Journal of Applied Polymer Science,* **103**, 519–533.

Stevens, A. and Lowe, J. (1997) Steuncellen en de extracellulaire matrix. *Histologie van de mens.* Houten: Bohn Stafleu Van Loghum.

Tabata, Y. (2009) Biomaterial technology for tissue engineering applications, *Journal of the Royal Society Interface,* **6**, S311–S324.

Tamari, S. (2004) Optimum design of the constant-volume gas pycnometer for determining the volume of solid particles, *Measurement Science and Technology,* **15**, 549–558.

Tamari, S. and Aguilar-Chavez, A. (2005) Optimum design of gas pycnometers for determining the volume of solid particles, *Journal of Testing and Evaluation,* **33**, 135–138.

Tanahashi, M., Kohsaka, N., Mori, M., Hatao, T., Katsumura, A. and Takeda, K. (2006) Fatigue-fracture surface of polycarbonate subjected to heating/cooling cycles under longitudinal confinement, *Kobunshi Ronbunshu,* **63**, 767–773.

Telis, V. R. N., Telis-Romero, J. and Gabas, A. L. (2005) Solids rheology for dehydrated food and biological materials, *Drying Technology,* **23**, 759–780.

Tesch, R., Ramon, O., Ladyzhinski, I., Cohen, Y. and Mizrahi, S. (1999) Water sorption isotherm of solution containing hydrogels at high water activity, *International Journal of Food Science and Technology,* **34**, 235–243.

The Organ Procurement and Transplantation Network. (2012). *National Data Report (waiting list, overall by organ)* [Online]. Richmond, Virginia, USA: Health Resources and Services Administration, U.S. Department of Health and Human Services. Available: http://optn.transplant.hrsa.gov/latestData/rptData.asp [Accessed 13 May 2012].

Tillet, G., Boutevin, B. and Ameduri, B. (2011) Chemical reactions of polymer crosslinking and post-crosslinking at room and medium temperature, *Progress in Polymer Science,* **36**, 191–217.

Toman, P. D., Chisholm, G., Mcmullin, H., Gieren, L. M., Olsen, D. R., Kovach, R. J., Leigh, S. D., Fong, B. E., Chang, R., Daniels, G. A., Berg, R. A. and Hitzeman, R. A. (2000) Production of recombinant human type I procollagen trimers using a four-gene expression system in the yeast Saccharomyces cerevisiae, *Journal of Biological Chemistry,* **275**, 23303–23309.

Treloar, L. R. G. (1944) Stress–strain data for vulcanized rubber under various types of deformation, *Transactions of the Faraday Society,* **40**, 59–70.

Tsioptsias, C., Paraskevopoulos, M. K., Christofilos, D., Andrieux, R. and Panayiotou, C. (2011) Polymeric hydrogels and supercritical fluids: The mechanism of hydrogel foaming, *Polymer,* **52**, 2819–2826.

Ulubayram, K., Eroglu, I. and Hasirci, N. (2002) Gelatin microspheres and sponges for delivery of macromolecules, *Journal of Biomaterials Applications,* **16**, 227–241.

Valentini, M., Ritota, M., Cafiero, C., Cozzolino, S., Leita, L. and Sequi, P. (2011) The HRMAS-NMR tool in foodstuff characterisation, *Magnetic Resonance in Chemistry,* **49**, S121–S125.

Van Tienen, T. G., Heijkants, R. G. J. C., Buma, P., De Groot, J. H., Pennings, A. J. and Veth, R. P. H. (2002) Tissue ingrowth polymers and degradation of two biodegradable porous with different porosities and pore sizes, *Biomaterials*, **23**, 1731–1738.

Van Vlierberghe, S., Cnudde, V., Dubruel, P., Masschaele, B., Cosijns, A., De Paepe, I., Jacobs, P. J. S., Van Hoorebeke, L., Remon, J. P. and Schacht, E. (2007) Porous gelatin hydrogels: 1. Cryogenic formation and structure analysis, *Biomacromolecules*, **8**, 331–337.

Van Vlierberghe, S., Dubruel, P., Lippens, E., Cornelissen, M. and Schacht, E. (2009) Correlation between cryogenic parameters and physico-chemical properties of porous gelatin cryogels, *Journal of Biomaterials Science-Polymer Edition*, **20**, 1417–1438.

Van Vlierberghe, S., Dubruel, P., Lippens, E., Masschaele, B., Van Hoorebeke, L., Cornelissen, M., Unger, R., Kirkpatrick, C. J. and Schacht, E. (2008) Toward modulating the architecture of hydrogel scaffolds: curtains versus channels, *Journal of Materials Science-Materials in Medicine,* **19**, 1459–1466.

Van Vlierberghe, S., Dubruel, P. and Schacht, E. (2011a) Biopolymer-based hydrogels as scaffolds for tissue engineering applications: a review, *Biomacromolecules*, **12**, 1387–1408.

Van Vlierberghe, S., Fritzinger, B., Martins, J. C. and Dubruel, P. (2010) Hydrogel network formation revised: high-resolution magic angle spinning nuclear magnetic resonance as a powerful tool for measuring absolute hydrogel cross-link efficiencies, *Applied Spectroscopy,* **64**, 1176–1180.

Van Vlierberghe, S., Schacht, E. and Dubruel, P. (2011b) Reversible gelatin-based hydrogels: Finetuning of material properties, *European Polymer Journal,* **47**, 1039–1047.

Vanvlierberghe, S., Cnudde, V., Dubruel, P., Masschaele, B., Cosijns, A., Depaepe, I., Jacobs, P. J. S., Vanhoorebeke, L., Remon, J. P. and Schacht, E. (2007) Porous gelatin hydrogels: 1. Cryogenic formation and structure analysis, *Biomacromolecules*, **8**, 331–337.

Vanvlierberghe, S., Dubruel, P., Lippens, E., Cornelissen, M. and Schacht, E. (2009) Correlation between cryogenic parameters and physico-chemical properties of porous gelatin cryogels, *Journal of Biomaterials Science-Polymer Edition*, **20**(10), 1417–1438.

Veis, A. (1964) *The Macromolecular Chemistry of Gelatin,* New York, Academic Press.

Wang, X., Kim, H. J., Wong, C., Vepari, C., Matsumoto, A. and Kaplan, D. L. (2006) Fibrous proteins and tissue engineering, *Materials Today,* **9**, 44–53.

West, J. L. (2011) Protein-patterned hydrogels: Customized cell microenvironments, *Nat Mater,* **10**, 727–729.

Whang, K., Thomas, C. H., Healy, K. E. and Nuber, G. (1995) A novel method to fabricate bioabsorbable scaffolds, *Polymer,* **36**, 837–842.

Wolfe, S. V., Tod, D. A. and Rarde (1989) Characterization of engineering polymers by dynamic mechanical analysis, *Journal of Macromolecular Science, Part A,* **26**, 249–272.

Yang, J. S., Xie, Y. J. and He, W. (2011) Research progress on chemical modification of alginate: A review, *Carbohydrate Polymers,* **84**, 33–39.

Yannas, I. V. (2001) *Tissue and Organ Regeneration in Adults*, New York, Springer.

Zaleskas, J. M., Kinner, B., Freyman, T. M., Yannas, I. V., Gibson, L. J. and Spector, M. (2004) Contractile forces generated by articular chondrocytes in collagen-glycosaminoglycan matrices, *Biomaterials,* **25**, 1299–1308.

Zhou, C. and Wu, Q. (2011) A novel polyacrylamide nanocomposite hydrogel reinforced with natural chitosan nanofibers, *Colloids and Surfaces B: Biointerfaces,* **84**, 155–162.

13

Titanium biomedical foams for osseointegration

F. CAUSA, Interdisciplinary Research Centre on Biomaterials (CRIB), University of Naples Federico II, Italy and Center for Advanced Biomaterials for Health Care (IIT@CRIB), Istituto Italiano di Tecnologia, Italy, N. GARGIULO, University of Naples Federico II, Italy, E. BATTISTA, Center for Advanced Biomaterials for Health Care (IIT@CRIB), Istituto Italiano di Tecnologia, Italy and P. A. NETTI, Interdisciplinary Research Centre on Biomaterials (CRIB), University of Naples Federico II and Center for Advanced Biomaterials for Health Care (IIT@CRIB), Istituto Italiano di Tecnologia, Italy

DOI: 10.1533/9780857097033.2.391

Abstract: This chapter describes the state of the art of titanium foam for tissue attachment and, in particular, for implant osseointegration as the final application for bone tissue reconstruction. The chapter first introduces a description of the titanium alloys used for biomedical applications. Next, a section on the processing techniques for the foaming of the titanium or titanium alloys, as well as the surface treatments for the control of physical and chemical surface properties, is given. This overview aims at emphasizing the range of technological approaches to obtain functional biomedical foams. A section on methods for endowing titanium surfaces with biomolecules for tissue integration is also included. Finally, a survey on tissue response to material implantation is presented, with a focus on the titanium interfaces previously described.

Key words: titanium, foam, surface, bio-activation, bio-interface, bone interactions.

13.1 Introduction: Titanium for biomedical applications

Titanium for biomedical applications can be used either pure or combined with other elements in specifically designed alloys. As stated in the ASTM F67 standard (2006), all four grades of commercially pure titanium are considered suitable for surgical implant production: in practice, the choice will depend on the mechanical features required for specific applications.

As regards to titanium alloys, there are at least 15 different types that can be applied in biomedical devices (Niinomi, 1998). Historically, the titanium alloy most used for implant manufacturing was Ti–6Al–4V: compared to other grades of pure titanium, this alloy has higher tensile and yield strength and lower elongation, while keeping similar reduction of area and elastic modulus (Niinomi, 1998). From the microstructural point of view, the crystal structure of pure titanium is close-packed hexagonal (α phase), while Ti–6Al–4V also contains the metastable, body-centred cubic (β) phase. Due to its considerable mechanical properties, Ti–6Al–4V was extensively proposed for hard tissue replacement; however, it has recently been evidenced that *in vitro* conditions can induce corrosion and ion release from this kind of alloy, despite the presence of a pristinely compact passive layer (Garcìa-Alonso *et al*., 2003). These findings raised significant biocompatibility issues, considering also that, *in vivo*, the integrity of passive layers can be compromised not only because of chemical factors, but also as a result of mechanical stresses, such as fretting phenomena (Hanawa, 2004). Such concerns have stimulated the challenge for producing ever more reliable titanium alloys; in particular, tissue reaction studies have identified Nb, Zr and Ta as non-toxic elements, as they do not cause any adverse reaction in human body (Elias *et al*., 2006). For this reason, alloys based on β-Ti, such as Ti–Nb–Zr and Ti–Nb–Zr–Ta, are currently considered good candidates for the replacement of Ti–6Al–4V in biomedical applications; with respect to the latter, such alloys have also a lower elastic modulus (Elias *et al*., 2006), which is a key factor for reducing the resorption of adjacent bone tissues due to the great difference in modulus between the implant device and adjacent bone tissues (Zhou *et al*., 2004). Moreover, Ti–Nb–Zr–Ta alloys can perform significantly well in terms of wear resistance, particularly when surface-treated (Samuel *et al*., 2008). For all these reasons, Ti–Nb–Zr and Ti–Nb–Zr–Ta alloys are currently considered among the best starting materials in the production of Ti-based foams for biomedical applications; as a very recent example, Maya *et al*. (2012) produced Ti–Nb–Zr porous alloys with values of Young's modulus in the 0.3–1.4 GPa range (i.e., closely comparable with those of natural bone) and excellent biocompatibility in subcutaneous as well as in bone tissue.

13.2 Titanium foam processing and surface treatments

At present, titanium foam processing is always based on powder metallurgy, because of the extreme reactivity of liquid titanium (Dunand, 2004). Within this technological approach, two main groups of processes can be identified: the first relies on powder sintering, while the second is based on the

Table 13.1 Summary of various Ti foaming methods

	Technique	References
Powder sintering	Sintering of uniform powder preforms	Asaoka *et al.*, 1985; Dunand, 2004
	Sintering of non-uniform powder preforms in presence of either a blowing gas or a solid space-holder	Hurysz *et al.*, 1998; Tuchinskiy and Loutfy, 2003; Dunand, 2004
	Sintering of powders previously deposited on a sacrificial porous scaffold	Kupp *et al.*, 2002; Dunand, 2004
Expansion of pressurized pores	Creep expansion processes	Kearnes *et al.*, 1988; Martin, 1996; Dunand, 2004
	Superplastic expansion processes	Davis *et al.*, 2001; Dunand, 2004
Alternative techniques	Freeze casting	Singh *et al.*, 2010
	Rapid prototyping	
	Conversion of porous TiO_2 precursors to metallic Ti foams	

expansion of pressurized pores obtained during a preliminary powder densification step. A summary of these processes is given in Table 13.1.

The partial sintering of pristinely unbound, preformed Ti powders with uniform size distribution is the most straightforward technique to produce porous foams. The basic process variables that can be tuned in this case are treatment temperature and time; in particular, porosity decreases and mechanical properties usually increase with increasing treatment time. Process kinetics can be accelerated by means of pressure sintering (Taylor *et al.*, 1993; Schuh *et al.*, 2000). The main limitation of the uniform powder sintering approach is that the size and shape of pores are strongly dependent on the initial size and shape of the titanium powders. When spherical powders are used, the maximum achievable porosity is generally 50%, and the pores show pronounced cusps at the sintering necks: these are weak points where cracks can easily initiate under fatigue conditions (Asaoka *et al.*, 1985). In order to solve at least the problem of the low pore fraction, crimpled titanium wires may be used instead of powders (Murray and Semple, 1981). An alternative approach is sintering hollow powders: in this way, porosity can be significantly increased, but the mechanical properties of the resulting foams are rather poor (Sypeck *et al.*, 1998).

Sintering of non-uniform powder preforms in the presence of a blowing gas allows generation of large, secondary pores by letting a gas pass through a preform of titanium powders (voids between powder particles constitute the primary pores). When sintering occurs, the primary pores are promptly closed,

while the secondary porosity is preserved in both shape and volume. The gas blowing approach can be also combined with the use of hollow powders, in order to achieve porosity values higher than 80% (Hurysz *et al.*, 1998). The main advantage of this technique is that the secondary porosity can be tuned independently of the characteristics of the starting powders. On the other hand, the main drawbacks are: the coarse pore size range of the secondary porosity; the need for a binder to be mixed with titanium powders during the pre-forming process (it is a possible contamination source); and the residual primary porosity that can occur after the sintering process. In particular, the last issue cannot even be solved by means of pressure sintering, because it would cause the collapse of the secondary pores (Dunand, 2004). Such limitations can be partially overcome by using solid space holders instead of a gas as secondary porogen agent. Space holders are usually solid materials that can be removed at low temperature, minimizing the contamination of the titanium powders. The metal/space-holder powder mixture can also be pressed, thus providing enough green strength to prevent collapse during the space-holder removal and sintering steps (Dunand, 2004). Among the possible variants of this approach, one of the most interesting variants considers the preliminary extrusion of rods made of a sacrificial core and of titanium powders held together by a polymer binder (Tuchinskiy and Loutfy, 2003). The rods are then cut and poured into a die to undergo preliminary compression. A first low-temperature treatment removes the core and the binder, while the successive sintering step produces titanium foams containing elongated secondary pores. By this way, the possibility to build honeycomb structures could be taken into account (Tuchinskiy and Loutfy, 2003).

Taking inspiration from space-holder-based sintering, there is another approach that uses sacrificial polymer scaffolds coated with repeatedly deposited layers of titanium powder/binder mixtures. In this case, the pre-sintering treatment removes the scaffold and the binder; from the following sintering process, a reticulated open-cell foam, held together by hollow titanium struts, is obtained (Kupp *et al.*, 2002). In this type of foam, three different types of porosity can be identified: a primary porosity inside the struts (if sintering is carried out at relatively low temperatures), a secondary porosity corresponding to the space previously occupied by the scaffold and an open tertiary porosity due to the voids between the struts.

The second main group of techniques for titanium foaming comprises creep and superplastic expansion processes. Creep expansion processes are in turn divided into argon expansion processes and low-density core processes. In the first case (Kearnes *et al.*, 1988), powders are packed into a steel canister, which is evacuated and backfilled with argon gas. Powder densification is then performed by means of hot isostatic pressing: during this phase, argon is entrapped within the titanium matrix as micron-sized bubbles. When the resulting billet is cooled and extracted from the canister, it undergoes

another thermal treatment (or evacuation) step: by this means, gas bubbles expand, thus generating porosity. In the low-density core process (Martin, 1996), the canister, which is made of Ti–6Al–4V, becomes itself part of the porous structure: before starting the foaming process, it is filled with particles of commercial-purity Ti and 60Al–40V alloy. Because of the flat geometry of the canister, it is converted into the face-sheets of a sandwich structure. The creep expansion processes usually exhibit slow kinetics and allow only for small porosities. A possible solution to these issues is to induce superplasticity in the titanium matrix during foaming: with respect to creep, superplastic deformation is dominated by faster strain/foaming rates and higher tensile ductility/terminal porosity (Davis *et al*., 2001; Dunand, 2004).

Apart from the two main groups of processes just described, alternative techniques for titanium foaming, such as those in Table 13.1, have been recently designed. For an in-depth description of such techniques, the reading of reviews, such as Singh *et al*. (2010), is strongly recommended. The main advantages of these methods with respect to more traditional ones, rest in the possibility to achieve, on the one hand, simpler fabrication procedures and, on the other hand, a finer control of foam structures.

Surface modification of pure titanium and titanium alloys is often performed in order to improve their biological, chemical and mechanical properties. The literature on this topic is massively vast: for this reason, only a survey will be given here, suggesting the consultation of other sources, such as the very comprehensive review by Liu *et al*. (2004). A summary of the processes that will be described here is shown in Table 13.2.

Table 13.2 Summary of various Ti surface modification methods

	Technique	References
Physical methods	Cutting and turning	Bagno *et al.*, 2004
	Smoothing	Taborelli *et al.*, 1997
	Blasting	Aparicio *et al.*, 2003
Chemical methods	Acid treatment	Schwartz *et al.*, 1996
	H_2O_2 treatment	Tengvall and Lunstrom, 1992
Sol-gel coatings	TiO_2 coatings	Kozhukharov *et al.*, 1993
	Ca phosphate coatings	Partenfelder *et al.*, 1993; Gross *et al.*, 1998
	TiO_2/hydroxyapatite coatings	Milella *et al.*, 2001; Kim *et al.*, 2004
Anodization	Anodization in aqueous electrolytes	Gong *et al.*, 2001; Mor *et al.*, 2003
	Anodization in buffered aqueous electrolytes	Cai *et al.*, 2005
	Anodization in polar organic electrolytes	Macak *et al.*, 2006; Prakasam *et al.*, 2007; Yoriya *et al.*, 2007
	Anodization in non-F^- containing electrolytes	Allam *et al.*, 2008

13.2.1 Physical methods

First of all, there are different treatments that are currently defined as 'physical', since they generally allow modifying surface characteristics by the application of external forces. In particular, cutting and turning techniques can be coupled on the basis of the characteristic dimensions of the defects impressed on the metallic surface (Bagno and Di Bello, 2004). However, this method tends to produce rough and irregular surfaces with a very low degree of finish. For this reason, pure titanium and titanium alloy surfaces can also undergo a smoothing process using grit-paper and/or diamond cloth (Taborelli *et al*., 1997). During such treatment, it is mandatory to avoid damaging the surface through scratching; it is then useful to put the metallic surface in contact with a sequence of particles having progressively smaller sizes. Another issue that can occur during the smoothing process is related to the possible embedding of abrasive particles into the metallic matrix: this phenomenon is usually known as abrasive pollution, and it can be dealt with by means of successive removal processes, such as solvent cleaning and sonication. Similarly to smoothing, blasting processes also rely on the use of abrasive particles but, in this case, they are forced against the surface by a dragging fluid (Aparicio *et al*., 2003). Blasting methods also share with smoothing ones the problems related to abrasive pollution, that are potentially responsible for modifications in the chemical and physical interaction features of treated surfaces.

13.2.2 Chemical methods

Different from physical techniques for treating titanium and its alloys, chemical techniques mainly rely on chemical reactions occurring at the interface between the metal phase and a solution. In particular, acid treatment is often used as a preliminary surface-finishing process to remove oxide layers and contaminating agents. This technique mainly uses mixed acid solutions (Schwartz *et al*., 1996): indeed, aqueous solutions containing 10–30 vol% HNO_3 and 1–3 vol% HF can currently be considered standard solutions for acid pre-treatment of titanium surfaces. In particular, hydrofluoric acid is known to promptly attack TiO_2 passive layers, thus forming soluble TiF_6^{3-} complexes and gaseous hydrogen. Diffusion of gaseous hydrogen in titanium lattice can cause embrittlement of the surface layer, but keeping the HNO_3/HF ratio between 1 and 10 to minimize the formation of free hydrogen (ASTM, 2011). After having polished Ti surfaces, a chemical treatment often performed to improve their bioactivity relies on the use of H_2O_2 solutions: in this way, Ti-peroxy gel coatings are developed on the metal substrate (Tengvall and Lunstrom, 1992) that can induce the

formation of apatite when soaked in a simulated body fluid (Li *et al.*, 1994). Usually, a porous, amorphous titania gel layer can be obtained by treating Ti in a H_2O_2/0.1 M HCl solution. Coating thickness and porosity can be tuned by adjusting the treatment time.

13.2.3 Sol-gel processes

Porous TiO_2 coatings can also be obtained by means of sol-gel processes. Apart from biomedical applications, sol-gel-derived titania coatings are widely used in the optical, electrical and catalytic fields (Kozhukharov *et al.*, 1993). Usually, a Ti alkoxide precursor (such as tetraisopropyl orthotitanate) is hydrolysed in the presence of a homogeneous acid catalyst and the resulting sol is cast on the metal substrate by dip/spin coating to undergo the successive gelation process (Peltola *et al.*, 1998). A final calcination step (temperatures > 500°C) leads to the partial/complete crystallization of the thin oxide film. A major concern about this surface modification technique is the bonding strength between the coating and the substrate: from this point of view, good results can be achieved by an alkali pre-treatment of the substrate (Pätsi *et al.*, 1998).

Sol-gel-derived TiO_2 coating mainly finds its purpose in the biomedical field because of its capacity to induce the precipitation of calcium phosphate species at the interface with body fluids: to achieve this goal, a more effective approach is directly coating such compounds on Ti substrates. Calcium phosphate (in particular, hydroxyapatite) coatings are currently of common use in orthopaedic applications. The sol-gel technique is a fairly simple way to produce calcium phosphate coatings on pure titanium and Ti alloys because of the relatively low temperature at which the process is carried out. However, the choice of the phosphorus precursor may become a significant issue. Indeed, monophosphates are not good gel formers unless coupled with aqueous solutions of polyphosphates. Moreover, the excessive reactivity (particularly in aqueous solution) of phosphate esters and phosphoric acid, together with their distinct trend to form crystalline salts by complexation, makes these species practically unemployable in the sol-gel synthesis (Liu *et al.*, 2004). Possible workarounds to these issues rely on the choice of phosphorus sources, such as chlorophosphines (Partenfelder *et al.*, 1993) and triethyl phosphite (Gross *et al.*, 1998), and the main calcium phosphate phase usually obtained by these ways is hydroxyapatite (HA).

The aforementioned sol-gel-derived hydroxyapatite coatings are strongly bioactive but show weak adhesion to Ti substrates. On the other hand, TiO_2 coatings, as also described above, can strongly adhere to the metal phase; however, their bioactivity is limited. Therefore, composite titania/

hydroxyapatite coatings should represent the best solution in both adhesion and bioactivity terms (Liu *et al*., 2004). As an example, Milella *et al*. (2001) prepared TiO_2/HA composite coatings by pre-mixing two distinct (one containing TiO_2, the other one containing HA) sols at different volume ratios and coating the metal substrate with the resulting suspensions. As expected, the resultant composite thin layer showed very good adhesion strength. Alternatively to this approach, Kim *et al*. (2004) deposited sol-gel-derived hydroxyapatite on titanium by means of a titania intermediate layer produced by a sol-gel technique as well.

13.2.4 Anodization

Despite the good results given by the surface modification techniques based on sol-gel coating, another class of processes, relying on the anodization of titanium substrates, recently drew attention in several fields, including the biomedical one. The main reason for such interest resides in the fact that, when carried out under specific conditions, titanium anodization leads to the formation, on its surface, of one-dimensional highly ordered TiO_2 nanotube arrays with unique properties. At the moment, the several different approaches for Ti anodization can be grouped in four distinct generations (Rani *et al*., 2010). In particular, the first generation TiO_2 nanotube arrays were fabricated on Ti foils in two-electrode electrochemical cells using dilute HF aqueous solutions at constant anodizing voltages below 20 V and anodizing times of a few tens of minutes (Gong *et al*., 2001; Mor *et al*., 2003). In this way, nanotube arrays of sub-micrometric lengths could usually be prepared; also pore diameters were practically limited to very few tens of nanometres. In order to achieve higher tube lengths, a second generation of anodization techniques, based on the use of buffered aqueous electrolytes, was developed. Indeed, Cai *et al*. (2005) employed fluoride salts in the electrolytic environment, along with buffer solutions, in order to fine-tune the pH. By means of this second generation synthesis method, nanotubes of up to approximately 5 μm (i.e., an order of magnitude longer compared to their first generation counterparts) could be obtained. A third evolution was achieved when inorganic electrolytes started to be replaced by organic ones, such as dimethyl sulfoxide (DMSO), ethylene glycol (EG) and glycerol, for the electrolyte formulation in TiO_2 nanotube syntheses (Rani *et al.*, 2010). In particular, typical DMSO-based electrolytes contain 1–6% HF aqueous solution; the anodization voltages are usually varied in the 10–70 V range, while anodization times could vary from 20 to 90 h (Yoriya *et al*., 2007). By this way, tube lengths and diameters of over 100 μm and 100 nm, respectively, could be achieved. A major drawback of this technique was the trend to develop TiO_2 nanotube bundles

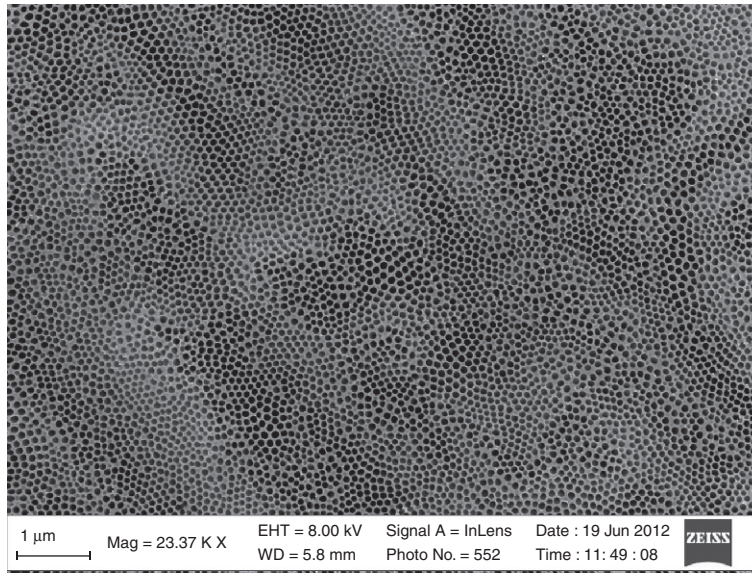

13.1 Top view of a TiO_2 nanotube array obtained by anodization in an EG-based electrolyte for short treatment times.

that significantly decreased the array order. This issue can be solved using EG-based solutions (containing small quantities of NH_4F and water) as the electrolyte (Prakasam *et al.*, 2007). In this case, anodization times can vary from 1 to more than 100 h: when short times are used, highly ordered, strongly substrate-adhering arrays can be obtained, as reported in Fig. 13.1, while tube lengths and diameters slightly below 100 µm and 100 nm can be achieved, respectively. In order to increase these values, anodization times have to be prolonged, but, at the same time, the adhesion of the array drastically decreases, making this approach useless for surface treatment purposes. A possible workaround to this issue could be presented by anodization techniques that employ glycerol-based electrolytes (Macak *et al.*, 2006). In particular, when using this kind of solutions, it is possible to grow strongly substrate-adhering nanotube arrays, such as reported in Fig. 13.2, whose average tube diameter is much higher than 100 nm (as in the case of DMSO-based processes), and whose order degree is only slightly lower than that found in optimized EG-based syntheses. Third generation fabrication methods for TiO_2 nanotube arrays should then meet almost all possible needs in terms of morphological tunability. However, recent literature is reporting new synthesis techniques that rely on the use of fluoride-free electrolytes, which can be considered fourth generation anodization processes (Allam *et al.*, 2008).

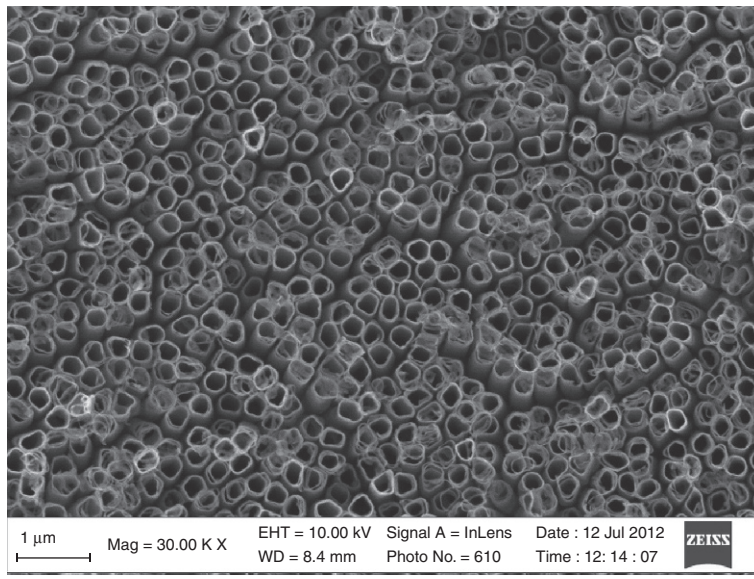

13.2 Top view of a TiO_2 nanotube array obtained by anodization in a glycerol-based electrolyte.

13.3 Bio-activation of titanium surfaces

This section will briefly review chemical modifications to control the interaction of titanium surfaces either towards small and large molecules (protein or drugs) or towards cell to guide their adhesion and fate in general. We defined these kinds of treatments 'bio-functionalization' as bioactive compounds are loaded onto titanium surfaces.

Bioactivating treatments, aimed to change mostly the chemistry of the surfaces rather than the topography, began to be developed in 1990s by using hydroxyapatite or other forms of calcium phosphate (CaP) coating. The high impact on the compatibility with tissues and the osteoconducive ability are supported by a number of studies (Dhert, 1994; Lacefield, 1998; Geesink, 2002). Different techniques have been applied to produce CaP coatings as plasma spray, deposition via magnetron sputtering, electrophoretic deposition, hot isostatic pressing, sol-gel deposition, pulsed laser deposition, ion beam dynamic mixing deposition, electrospray deposition, biomimetic deposition and electrolytic deposition (Saldana *et al.*, 2006). The resultant coating layers differ mainly in terms of uniformity, the adhesion strength to the metallic surface, and the thickness ranging from the micrometres (i.e. plasma spray) to the nanometres (i.e. ion beam deposition). The application to commercial products has been optimized matching the end use of implant (Jonge *et al.*, 2008).

Other treatments able to confer protein repellency are related to poly(ethylene glycol) (PEG) deposition onto titanium surfaces by adsorption with copolymers such as PLL-g-PEG (Huang *et al.*, 2001) or through electrodeposition. In the latter case, aminated PEG molecules have been covalently linked on the surfaces through oxime formation between titanium OH and amino groups on the polymer. In this way, the possibility was demonstrated to tune the amount of PEG immobilized and its shape on the surface (random/brush/U-shape) (Tanaka *et al.*, 2007).

Bio-functionalization was usually possible by previous intermediate treatments. Silanizing agents and alkylphosphonic acids have been successfully used to provide functional groups to the titanium surfaces. Self-assembled monolayers (SAM) achieved with these reagents provide chemically and structurally well-defined surfaces that can often be manipulated using standard synthetic methodologies. A problem related to the application of immobilized biomolecules via silanization techniques is the hydrolysis of siloxane films when exposed to aqueous (physiological) conditions (Kämmerer *et al.*, 2012). Alkylphosphonic SAMs are more robust under physiological conditions, and have been used to provide ordered monolayers of carboxyl functional groups as well as hydroxyls (Sinn *et al.*, 2009; Song *et al.*, 2009). Beside the use of SAMs, alkylphosphonic acids have been used in combination with peptides to coat titanium on the surfaces of the native oxide. More recently, Kessler group proposed a simple one-step coating procedure by synthesizing cyclic RGD (arginine-glycine-aspartic acid) peptides, well known as strong cell adhesion promoters, with a multimeric four-branched phosponic acid (Auernheimer *et al.*, 2005).

The latest alternative approaches are represented by the use of specific peptides able to recognize titanium surfaces and oligonucleotide mediated attachment and release. The work on self-assembled EAK (glutamic acid-alanine-lysine) oligopeptides showed the ability of glutamate and lysine residues to interact specifically with the Ti surface. In this work the adsorption was highlighted experimentally and by simulations due to the coordination of carbonyl oxygen to Ti^{4+} and the stabilization by hydrogen bonding between NH_2 and surface active hydroxyl groups. The specific adsorption on TiO_2 of large peptides containing RGD sequences linked to EAK peptides in different combination (PetpA H-RGD-AEAEAKAKAEAEAKAK-NH2 or PeptB H-RGD-AAKAEAEAAEKAKAEK-NH_2) showed different conformations when adsorbed on the surfaces. The PeptB seems to assume a disordered configuration, while the PeptA assumes a beta sheet conformation linking the surface through the -NH_2 terminus, exposing the RGD at interface (Monti *et al.*, 2008; Vallee *et al.*, 2010). More interestingly, a method to PEGylate titanium surfaces was achieved selecting specific adsorbing peptides by using a phage display technique. The resultant peptides were coupled to PEG (MW 3400) and assessed to verify the coating ability and

antifouling properties. This method was claimed by the author to be generalizable as modification to confer protein and cell resistance (Khoo *et al.*, 2009).

Another valuable approach was used to anchor osteogenic growth factors and at the same time to slowly release from titanium surfaces to enhance the osteogenic activity of the implant. Such an approach was defined as nanomechanical anchorage, where the molecules can be linked at high extent and released. To this aim the authors immobilized a 5′ phosphate terminated 31-mer oligonucleotide onto anodized titanium surface (Beutner *et al.*, 2009), a complementary strand was conjugated to rhBMP and a prolonged release over a period of 4 weeks was demonstrated (Schliephake *et al.*, 2012).

13.4 Bone interactions at the bio-interface

Titanium metal and its alloy have been extensively used as implant materials in orthopaedic and dental applications because of their excellent mechanical and corrosion resistance. A stable oxide layer spontaneously forms when exposed to oxygen conferring biocompatibility to the surface. However osseointegration of titanium implants is influenced by several factors, including porosity of the foam, presence of a bioactive additional layer, chemical composition at the interface and surface roughness.

Because of the three-dimensional environment it provides, titanium foam is thus considered to be adequate material for promoting desirable implant–bone interactions. Indeed, the interconnective porous structure of titanium foam can itself play an important role in osteogenesis. The optimal pore diameter for *in vivo* osteoconduction is thought to be in the micrometric range. In particular, porous titanium with pore size ranging between 50 and 400 μm was considered appropriate substrate for osteogenic cell adhesion, proliferation and production of mineralized matrix (Rosa *et al.*, 2008). 50% in volume in interconnected porosity is enough to significantly increase bone filling, bone-implant contact area compared to dense titanium control (Wazen *et al.*, 2009). It has also been shown that porous TiO_2 scaffold can achieve higher porosity, surface-to-volume ratio and pore interconnectivity of the commonly used scaffolds such as Bio-Oss® (Geistlich Pharma AG, Switzerland) and BoneCeramic® (Institute Straumann, Switzerland) (Sabetrasekh *et al.*, 2011). Recently, more sophisticated techniques in porosity and structural control, such as free-form-fabrication of Ti6Al4V, were used for the realization of complex porous structures showing a long-term biocompatibility *in vivo* (Palmquist *et al.*, 2011).

A thin layer of calcium phosphate or hydroxyapatites is currently introduced on titanium surfaces to enhance the osteoconducibility of the

implants. The calcium phosphate plasma-sprayed layer is 30–50 μm thick, chemically interlocked with pre-roughened metallic surfaces and, therefore, subjected to delaminations (Lacefield, 1998), while sol-gel-formed calcium phosphate coatings are more effective and compatible with porous titanium alloy implant (Tachè *et al*., 2004). CaP-coated implants display significant increase in the area of bone ingrowth and greater bone-to-implant contact when compared with native titanium material (Nguyen *et al*., 2004). In the case of titanium fibre mesh, CaP coating leads to ectopic bone formation after *in vitro* culturing with bonelike tissue, while only calcification without tissue organization was observed on titanium meshes.

Chemical and physical characteristics of titanium surface also have an effect on the interactions between implant and bone. Since hydrophilicity plays an important role in protein adsorption and cell attachment to materials, several reports have focused on the hydrophilicity profile of surface modified titanium implants. To this aim, the photo-catalytic effect has been used to increase wettability of the anatase form of titanium surface, with significant advantages in term of implant incorporation into the tissue (Sawase *et al.*, 2007). Furthermore, crystallinity plays a role in apatite formation *in vivo* with apatite formation at the crystalline titanium surface (Wu and Nancollas 1998; Uchida *et al*., 2003). Oxidation by electrochemical methods is also used to change surface chemistry and to incorporate Mg or Ca ions on implant surfaces, improving the integration with the bone (Sul *et al*., 2005). Moreover, anodization techniques can improve the osteointegration with possibility of immediate implant loading (Degidi *et al*., 2006). Plasma-sprayed or chemical treatments (immersion in NaOH and water solution), followed by thermal treatment (heating to 600°C), spontaneously form a very thin layer of calcium phosphate on the titanium surface *in vivo*, thus enhancing bone integration (Fujibayashi *et al*., 2004; Takemoto *et al*., 2005).

Finally, surface roughness is correlated to an enhancement of bone ingrowth, changing upon the type of treatments performed (physical methods, chemical methods or anodization). Acid-etched micro-texture on the surface of sintered porous titanium implant positively affect the extent of bone ingrowth for biological fixation (Hacking *et al*., 2003).

However, the pore structure of titanium foam is considered more effective in osseointegration than some cases of surface bio-activation. Indeed, Ti–6Al–4V sintered foam showed improved early implant stability and accelerated healing response with respect to plasma-sprayed implants (Simmons *et al*., 1999) as well as structured porous titanium surface exhibiting osteoconductive properties exceeding those of smooth, high crystalline CaP coating (Xiropaidis *et al*., 2004).

13.5 Future trends

Much effort has already been devoted to the development of processing techniques to precisely control the porosity structure of titanium foam, even though there is still room to ameliorate the bone integration of implants. The improvement of the titanium implants in the next years will be strongly related to advancements in material science, nanotechnology and biotechnology to control the interface between the tissue and the materials surface. In this respect, cell behaviour can be controlled via biochemical modification, surface topography and their combinations.

The RGD (Arg-Gly-Asp) motif present in a number of proteins including fibronectin and fibrinogen is known to interact specifically with cell surface integrin receptors, so functionalization of surfaces with the RGD motif can be a way to enhance osteoblast functions. Although RGD has been shown to enhance osteoblast activities, it lacks selectivity (Morra, 2006). Thus, attention is now increasingly directed towards bone morphogenetic proteins (BMP), a class of signalling molecules known to promote bone formation by both osteoconduction and osteoinduction (Li and Wozney, 2001; Harwood and Giannoudis, 2005). Since BMPs act locally, direct introduction into the body is not desirable because of potentially adverse effects such as unwanted ectopic bone formation. BMP-2 adsorbed on porous titanium oxide implant surfaces was shown to have an osteoconductive effect, which was surface and dose dependent in a rat ectopic model (Hall *et al*., 2007). For substrates with adsorbed BMP, a complicating factor is the tuning of the kinetics of release to achieve an optimum local concentration.

On the other hand, it is generally accepted that protein adsorption and cell behaviour can be affected by nanotopography and nanostructures at the interface (Texeira *et al*., 2003; Rechendorff *et al*., 2006; Scopelliti *et al*., 2010). Even if an implant surface can be designed with the nanotopography for optimizing osteoblast functions, the presence of different types of proteins and the dynamic nature of the *in vivo* environment may compromise its efficacy.

However, highly ordered titania nanotube arrays with high specific surface area and surface energy have been fabricated by anodization of pure titanium plates or titanium alloys, and *in vitro* and *in vivo* experiments have revealed that this nanoscaled topography can guide enhanced cellular migration on the surface, promote differentiation and matrix production of bone cells, and enhance both short- and long-term osseointegration (Popat *et al*., 2007). The hollow tubes also constitute an excellent platform for drug delivery and immobilization of various functional molecules such as antimicrobials, pharmaceutics and growth factors (De Santo *et al*., 2012; Gulati *et al*., 2012). This may represent the next step towards an improvement of

titanium foam performance based on synergistic combination between topological modification and biochemical function.

13.6 Sources of further information and advice

Several books address aspects related to structural design and processing of titanium foams, but their applications in bone reconstruction have resulted in a dedicated book. Three different books to consult from mechanical design and technological perspectives are reported: Development, synthesis, and characterization of novel titanium foams by Emilie Auguste Steinhoff, edited by ProQuest UMI Dissertation Publishing, 2012; Cellular Materials in Nature and Medicine by Lorna J. Gibson, Michael F. Ashby and Brendan A. Harley, edited by Cambridge University Press, 2010; Metal Foams: A Design Guide from M.F. Ashby, A.G. Evans, N.A. Fleck, L.J. Gibson, J.W. Hutchinson and H.N.G. Wadley, edited by Butterworth-Heinemann, 2000.

A number of websites report interesting results from research groups working on titanium foams for bone integration. Fraunhofer Institute for Manufacturing and Advanced Materials in Dresden reports about a titanium foams to replace injured bones. It deals with flexible yet rigid like a human bone material, and immediately capable of bearing loads. An implant, made of titanium foam, resembles the inside of a bone in terms of its structural configuration (website: http://www.fraunhofer.de/en/press/research-news/2010/09/titanium-foams-replace-injured-bones.html). Furthermore, bone ingrowth in titanium foam developed by the Industrial Material Institute of the National Research Council Canada (NRC-IMI) is also well reported on the Web. The micro-CT reconstruction shows the bone osseointegration in a 4 mm diameter, 50% porous, titanium plug in a rabbit femur after 6 weeks (website: http://www.youtube.com/watch?v=hdscnna5r1Q).

13.7 References

Allam N K, Shankar K and Grimes C A (2008), 'Photoelectrochemical and water photoelectrolysis properties of ordered TiO_2 nanotubes fabricated by Ti anodization in fluoride-free HCl electrolytes', *J Mater Chem*, **18**, 2341–2346. DOI: 10.1039/B718580D.

Aparicio C, Javier Gil F, Fonseca C, Barbosa M and Planell J A (2003), 'Corrosion behaviour of commercially pure titanium shot blasted with different materials and sizes of shot particles for dental implant applications', *Biomaterials*, **24**, 263–273. DOI: 10.1016/S0142-9612(02)00314-9.

Asaoka K, Kuwayama N, Okuno O and Miura I (1985), 'Mechanical properties and biomechanical compatibility of porous titanium for dental implants', *J Biomedical Mater Research*, **19**, 699–713. DOI: 10.1002/jbm.820190609.

ASTM Standard B600 – 11 (2011), '*Standard Guide for Descaling and Cleaning Titanium and Titanium Alloy Surfaces*', ASTM International, West Conshohocken, PA. DOI: 10.1520/B0600-11, www.astm.org.

ASTM Standard F67 (2006), '*Standard Specification for Unalloyed Titanium, for Surgical Implant Applications*', ASTM International, West Conshohocken, PA. DOI: 10.1520/F0067-06, www.astm.org.

Auernheimer J, Zukowski D, Dahmen C, Kantlehner M, Enderle A, Goodman A L and Kessler H (2005), 'Titanium implant materials with improved biocompatibility through coating with phosphonate-anchored cyclic RGD peptides', *Chem Bio Chem*, **6**, 2034–2040. DOI: 10.1002/cbic.200500031.

Bagno A and Di Bello C (2004), 'Surface treatments and roughness properties of Ti-based biomaterials', *J Mater Sci – Mater Med*, **15**, 935–949. DOI: 10.1023/B:JMSM.0000042679.28493.7f.

Beutner R, Michael J, Förster A, Schwenzer B and Scharnweber D (2009), 'Immobilization of oligonucleotides on titanium based materials by partial incorporation in anodic oxide layers', *Biomaterials*, **30**, 2774–2781. DOI: 10.1016/j.biomaterials.2009.01.047.

Cai Q, Paulose M, Varghese O K and Grimes C A (2005), 'The effect of electrolyte composition on the fabrication of self-organized titanium oxide nanotube arrays by anodic oxidation', *J Mater Res*, **20**, 230–236. DOI: 10.1557/JMR.2005.0020.

Davis N G, Teisen J, Schuh C and Dunand D C (2001), 'Solid-state foaming of titanium by superplastic expansion of argon-filled pores', *J Mater Res*, **16**, 1508–1519. DOI: 10.1557/JMR.2001.0210.

De Santo I, Sanguigno L, Causa F, Monetta T and Netti P A (2012), 'Exploring doxorubicin localization in eluting TiO(2) nanotube arrays through fluorescence correlation spectroscopy analysis', *Analyst*, 7 November 2012, **137**(21), 5076–5081. DOI: 10.1039/c2an36052g.

Degidi M, Perrotti V and Piattelli A (2006), 'Immediately loaded titanium implants with a porous anodized surface with at least 36 months of follow-up', *Clin Implant Dent*, **8**(4), 169–177. DOI: 10.1111/j.1708-8208.2006.00008.x.

Dhert W J A (1994), 'Retrieval studies on CaP-coated implants', *Med. Prog. Technol*, **20**, 143–154.

Dunand D C (2004), 'Processing of titanium foams', *Adv Eng Mater*, **6**, 369–376. DOI: 10.1002/adem.200405576.

Elias L M, Schneider S G, Schneider S, Silva H M and Malvisi F (2006), 'Microstructural and mechanical characterization of biomedical Ti-Nb-Zr(-Ta) alloys', *Mater Sci Eng A*, **432**, 108–112. DOI: 10.1016/j.msea.2006.06.013.

Fujibayashi S, Neo M, Kim H M, Kokubo T and Nakamura T (2004), 'Osteinduction of porous bioactive titanium metal', *Biomaterials*, **25**, 443–450. DOI: 10.1016/S0142-9612(03)00551-9.

García-Alonso M C, Saldaña L, Vallés G, González-Carrasco J L, González-Cabrero J, Martínez, M E, Gil-Garay E and Munuera L (2003), '*In vitro* corrosion behaviour and osteoblast response of thermally oxidised Ti6Al4V alloy', *Biomaterials*, **24**, 19–26. DOI: 10.1016/S0142-9612(02)00237-5.

Geesink R G (2002), 'Osteoconductive coatings for total joint arthroplasty', *Clin. Orthop. Relat Res*, **395**, 53–65.

Gong D, Grimes C A, Varghese O K, Hu W, Singh R S, Chen Z and Dickey E C (2001), 'Titanium oxide nanotube arrays prepared by anodic oxidation', *J Mater Res*, **16**, 3331–3334. DOI: 10.1557/JMR.2001.0457.

Gross K A, Chai C S, Kannangara G S K, Ben-Nissan B and Hanley L (1998), 'Thin hydroxyapatite coatings via sol-gel synthesis', *J Mater Sci Mater Med*, **9**, 839–843. DOI: 10.1023/A:1008948228880.

Gulati K, Aw M S, Findlay D and Losic D (July 2012), 'Local drug delivery to the bone by drug-releasing implants: perspectives of nano-engineered titania nanotube arrays', *Ther Deliv*, **3**(7), 857–873. DOI: 10.4155/tde.12.66.

Hacking S A, Harvey E J, Tanzer M, Krygier J J and Bobyn J D (2003), 'Acid-etched microtexture for enhancement of bone growth into porous-coated implants', *J Bone Joint Surg Br*, **85**(8), 1182–1189. DOI: 10.1302/0301-620X.85B8.14233.

Hall J, Sorensen R G, Wozney J M and Wikesjö U M E (2007), 'Bone formation at rhBMP-2- coated titanium implants in the rat ectopic model', *J Clin Periodontol*, **34**, 444–451. DOI: 10.1111/j.1600-051X.2007.01064.x.

Hanawa T (2004), 'Metal ion release from metal implants', *Mater Sci Eng C*, **24**, 745–752. DOI: 10.1016/j.msec.2004.08.018.

Hanawa T (2011), 'A comprehensive review of techniques for biofunctionalization of titanium' *J Periodontal Implant Sci*, **41**, 263–272. DOI: 10.5051/jpis.2011.41.6.263.

Hanawa T and Ota M (1992), 'Characterization of surface-film formed on titanium in electrolyte using XPS'. *Appl Surf Sci*, **55**, 269–276. DOI: 10.1016/0169-4332(92)90178-Z.

Harwood P J and Giannoudis P V (2005), 'Application of bone morphogenetic proteins in orthopedic practice: their efficacy and side effects', *Expert Opin Drug Saf*, **4**, 75–89. DOI: 10.1517/14740338.4.1.75.

Haugen H J, Monjo M, Rubert M, Verket A, Lyngstadaas S P, Ellingsen J E, Ronold H J and Wohlfahrt J C (2012), *Acta Biomaterialia*, DOI:10.1016/j.actbio.2012.09.009.

Huang NP, Michel R, Voros J, Textor M, Hofer R, Rossi A, Elbert D L, Hubbell J A and Spencer N D (2001), 'Poly(L-lysine)-g-poly(ethylene glycol) layers on metal oxide surfaces: surface-analytical characterization and resistance to serum and fibrinogen adsorption', *Langmuir*, **17**, 489–498. DOI: 10.1021/la000736+.

Huang Y H, Xiropaidis A V, Sorensen R G, Albandat J M, Hall J and Wikesjo U M E (2005), 'Bone formation at titanium porous oxide (TiUnite TM) oral implants in type IV bone', *Clin Oral Impl Res*, **16**, 105–111. DOI:10.1111/j.1600-0501.2004.01086.x.

Hurysz K M, Clark J L, Nagel A R, Hardwicke C U, Lee K J, Cochran J K and Sanders T H (1998), 'Steel and titanium hollow sphere foams', in Schwartz D S, Shih D S, Evans A G and Wadley H N G (eds.), *Porous and Cellular Materials for Structural Applications*, Pittsburgh, MRS, 191–203. DOI: 10.1557/PROC-521-191.

Jonge L T, Leeuwenburgh S C, Wolke J G and Jansen J A (2008), 'Organic–Inorganic surface modifications for titanium implant surfaces', *Pharm Res*, **25**, 2357–2369. DOI: 10.1007/s11095-008-9617-0.

Kämmerer P W, Gabriel M, Al-Nawas B, Scholz T, Kirchmaier C M and Klein M O (2012), 'Early implant healing: promotion of platelet activation and cytokine release by topographical, chemical and biomimetical titanium surface modifications *in vitro*', *Clin Oral Implants Res*, **23**(4), 504–510. DOI: 10.1111/j.1600-0501.2011.02153.x.

Kearnes M W, Blenkinsop P A, Barber A C and Farthing T W (1988), 'Manufacture of a novel porous metal', *Intern J Powder Metall*, **24**, 59–64.

Khoo X, Hamilton P, O'Toole G A, Snyder B D, Kenan D J and Grinstaff M W (2009), 'Directed assembly of PEGylated-peptide coatings for infection-resistant titanium metal', *J Am Chem Soc*, **131**(31), 10992–10997. DOI: 10.1021/ja9020827.

Kim H- W, Koh Y- H, Li L- H, Lee S and Kim H- E (2004), 'Hydroxyapatite coating on titanium substrate with titania buffer layer processed by sol-gel method', *Biomaterials*, **25**, 2533–2538. DOI: 10.1016/j.biomaterials.2003.09.041.

Kozhukharov V, Trapalis Ch and Samuneva B (1993), 'Sol-gel processing of titanium-containing thin coatings – Part III Properties', *J Mater Sci*, **28**, 1283–1288. DOI: 10.1007/BF01191965.

Kupp D, Claar D, Flemmig K, Waag U and Goehler H (2002), 'Processing of controlled porosity titanium-based materials', in Ghosh A, Sanders T and Claar D, *Processing and Properties of Lightweight Cellular Metals and Structures*, Warrendale, TMS, 61–72.

Lacefield W R (1998), 'Current status of ceramic coatings for dental implants', *Implant Dent*, **7**, 315–322.

Li P, Kangasniemi I, de Groot K and Kokubo T (1994), 'Bonelike hydroxyapatite induction by a gel-derived titania on a titanium substrate', *J Am Ceram Soc*, **77**, 1307–1312. DOI: 10.1111/j.1151–2916.1994.tb05407.x.

Li RH and Wozney JM (2001), 'Delivering on the promise of bone morphogenetic proteins', *Trends Biotechnol*, **19**, 255–265. DOI: 10.1016/S0167-7799(01)01665-1.

Liu X, Chu P K and Ding C (2004), 'Surface modification of titanium, titanium alloys, and related materials for biomedical applications', *Mater Sci Eng, R*, **47**, 49–121. DOI: 10.1016/j.mser.2004.11.001.

Macak J M, Aldabergerova S, Ghicov A and Schmuki P (2006), 'Smooth anodic TiO_2 nanotubes: annealing and structure', *Physica Status Solidi A Appl Res*, **203**, R67–R69. DOI: 10.1002/pssa.200622214.

Martin R L (McDonnell Douglas Corporation) (1996), Integral porous-core metal bodies and in situ method of manufacture thereof. US patent application 5,564,064. 8 October 1996.

Maya A E A, Grana D R, Hazarabedian A, Kokubu G A, Luppo M I and Vigna G (2012), 'Zr-Ti-Nb porous alloys for biomedical application', *Mater Sci Eng C*, **32**, 321–329. DOI: 10.1016/j.msec.2011.10.035.

Milella E, Cosentino F, Licciulli A and Massaro, C (2001), 'Preparation and characterisation of titania/hydroxyapatite composite coatings obtained by sol-gel process', *Biomaterials*, **22**, 1425–1431. DOI: 10.1016/S0142-9612(00)00300-8.

Monti S, Caravetta V, Battochio C, Iucci G and Polzonetti G (2008). 'Peptide/TiO_2 Surface interactions: A theoretical and experimental study on the structure of adsorbed ALA-GLU and ALA-LYS', *Langmuir*, **24**, 3205–3214. DOI: 10.1021/la702956t.

Mor G K, Varghese O K, Paulose M, Mukherjee N and Grimes C A (2003), 'Fabrication of tapered, conical-shaped titania nanotubes', *J Mater Res*, **18**, 2588–2593. DOI: 10.1557/JMR.2003.0362.

Morra M (2006), 'Biochemical modification of titanium surfaces: peptides and ECM proteins', *Eur Cell Mater*, **12**, 1–15.

Murray G A W and Semple J C (1981), 'Transfer of tensile loads from a prosthesis to bone using porous titanium', *J Bone Joint Surg-Br*, **63**, 138–141.

Nguyen HQ, Deporter DA, Pilliar RM, Valiquette N and Yakubovich R (2004), 'The effect of the sol-gel-formed calicium phosphate coating on bone ingrowth and osteoconductivity of porous –surfaced Ti alloy implants', *Biomaterials*, **25**, 865–876, DOI:10.1016/S0142-9612(03)00607-0.

Niinomi M (1998), 'Mechanical properties of biomedical titanium alloys', *Mater Sci Eng A*, **243**, 231–236. DOI: 10.1016/S0921-5093(97)00806-X.

Palmquist A, Snis A, Emanuelsson L, Browne M and Thomsen P (2011), 'Long-term biocompatibility and osseointegration of electron beam melted, free-form-fabricated solid and porous titanium alloy: Experimental studies in sheep', *J Biomater Appl*, 29 December 2011(Epub ahead of print). DOI: 10.1177/0885328211431857.

Partenfelder U, Engel A and Russel C (1993), 'A pyrolytic route for the formation of hydroxyapatite/fluoroapatite solid solutions', *J Mater Sci Mater Med*, **4**, 292–295. DOI: 10.1007/BF00122283.

Pätsi M E, Hautaniemi J A, Rahiala H M, Peltola T O and Kangasniemi I M O (1998), 'Bonding strengths of titania sol-gel derived coatings on titanium', *J Sol–Gel Sci Technol*, **11**, 55–66. DOI: 10.1023/A:1008684815735.

Peltola T, Pätsi M, Rahiala H, Kangasniemi I and Yli-Urpo A (1998), 'Calcium phosphate induction by sol-gel-derived titania coatings on titanium substrates *in vitro*', *J Biomed Mater Res*, **41**, 504–510. DOI: 10.1002/(SICI)1097-4636(19980905)41:3<504::AID-JBM22>3.0.CO;2-G.

Popat K C, Leoni L, Grimes C A and Desai T A (2007), 'Influence of engineered titania nanotubular surfaces on bone cells', *Biomaterials*, **28**, 3188–3197. 10.1016/j.biomaterials.2007.03.020.

Prakasam H E, Shankar K, Paulose M, Varghese O K and Grimes C A (2007), 'A new benchmark for TiO_2 nanotube array growth by anodization', *J Phys Chem C*, **111**, 7235–7241. DOI: 10.1021/jp070273h.

Rani S, Roy S C, Paulose M, Varghese O K, Mor G K, Kim S, Yoriya S, Latempa T J and Grimes C A (2010), 'Synthesis and applications of electrochemically self-assembled titania nanotube arrays', *Phys Chem Chem Phys*, **12**, 2780–2800. DOI: 10.1039/B924125F.

Rechendorff K, Hovgaard M B, Foss M, Zhdanov V P and Besenbacher F (2006), 'Enhancement of protein adsorption induced by surface roughness', *Langmuir*, **22**, 10885–10888. DOI: 10.1021/la0621923.

Rosa A L, Crippa G E, de Oliveira P T, Taba Jr M, Lefebvre L -P and Beloti M M (2008), 'Human alveolar bone cell proliferation, expression of osteoblastic phenotype, and matrix mineralization on porous titanium produced by powder metallurgy', *Clin Oral Impl Res*, **20**, 472–481. DOI: 10.1111/j.I600-0501.2008.01662.x.

Sabetrasekh R, Tiainen H, Lyngstadaas SP, Reseland J and Haugen H (2011), 'A novel ultraporous titanium dioxide ceramic with excellent biocompatibility', *J Biomater Appl*, **25**, 559–580. DOI: 10.1177/0885328209354925.

Saldana L, Gonzalez-Carrasco JL, Rogriguez M, Munuera L and Vilaboa N (2006), 'Osteoblast reponce to plasma-spray porous Ti6Al4V coating on substrates of identical alloy', *J Biomed Mater Res*, **77A**, 608–617. DOI:10.1002/jbm.a.30671.

Samuel S, Nag S, Scharf T W and Banerjee R (2008), 'Wear resistance of laser-deposited boride reinforced Ti-Nb-Zr-Ta alloy composites for orthopedic implants', *Mater Sci Eng C*, **28**, 414–420. DOI: 10.1016/j.msec.2007.04.029.

Sawase T, Jimbo R, Wennerberg A, Suketa N, Tanaka Y and Atsuta M (2007), 'A novel characteristic of porous titanium oxide implants', *Clin Oral Impl Res*, **18**, 680–685. DOI: 10.1111/j.1600-0501.2007.01404.x.

Schliephake H, Bötel H, Förster A, Schwenzer B, Reichert J and Scharnweber D (2012), 'Effect of oligonucleotide mediated immobilization of bone morphogenic proteins on titanium surfaces', *Biomaterials*, **33**, 1315–1322. DOI: 10.1016/j.biomaterials.2011.10.027.

Schuh C, Noël P and Dunand D C (2000), 'Enhanced densification of metal powders by transformation-mismatch plasticity', *Acta Mater*, **48**, 1639–1653. DOI: 10.1016/S1359-6454(00)00018-5.

Schwartz Z, Martin J Y, Dean D D, Simpson J, Cochran D L and Boyan B D (1996), 'Effect of titanium surface roughness on chondrocyte proliferation, matrix production, and differentiation depends on the state of cell maturation', *J Biomed Mater Res*, **30**, 145–155. DOI: 10.1002/(SICI)1097-4636(199602)30:2<145::AID-JBM3>3.0.CO;2-R.

Scopelliti PE, Borgonovo A, Indrieri M, Giorgetti L, Bongiorno G, Carbone R, Podestà A and Milani P (2010), 'The effect of surface nanometre-scale morphology on protein adsorption', *PLOS ONE*, **5**, e11862. DOI: 10.1371/journal.pone.0011862.

Simmons C A, Valiquette N and Pilliar R M (1999), 'Osseointegration of sintered porous-surfaced and plasma spray-coated omplants: An animal model study of early post implantation healing response and mechanical stability', *J Biomed Mater Res*, **47**, 127–138. DOI: 10.1002/(SICI)1097-4636(199911)47:2<127::AID-JBM3>3.0.CO;2-C.

Singh R, Lee P D, Dashwood R J and Lindley T C (2010), 'Titanium foams for biomedical applications: A review', *Mater Technol*, **25**, 127–136. DOI: 10.1179/175355510X12744412709403.

Sinn MA, Addai-Mensah J and Losic D (2009), 'A multi-drug delivery system with sequential release using titania nanotube arrays' *Chem. Commun*, **48**, 3348–3350. DOI: 10.1039/C2CC17690D.

Song Y -Y, Schmidt-Stein F, Bauer S and Schmuki P (2009) 'Amphiphilic TiO_2 nanotube arrays: An actively controllable drug delivery system', *J Am Chem Soc*, **131**, 4230–4232. DOI: 10.1021/ja810130h.

Sul YT, Johansson C, Byon E and Albrektsson T (2005), The bone response of oxidized bioactive and non-bioactive titanium implants, *Biomaterials*, **26**, 6720–6730, DOI:10.1016/j.biomaterials.2005.04.058.

Sypeck D J, Parrish P A and Hayden H N G (1998), 'Novel hollow powder porous structures', in Schwartz D S, Shih D S, Evans A G and Wadley H N G (eds.), *Porous and Cellular Materials for Structural Applications*, Pittsburgh, MRS, 205–210.

Taborelli M, Jobin M, François P, Vaudaux P, Tonetti M, Szmukler-Moncler S, Simpson J P and Descouts P (1997), 'Influence of surface treatments developed for oral implants on the physical and biological properties of titanium: (I) Surface characterization', *Clin Oral Impl Res*, **8**, 208–216. DOI: 10.1034/j.1600-0501.1997.080307.x.

Takemoto M, Fujibayashi S, Neo M, Suzuki J, Kokubo T and Nakamura T (2005), 'Mechanical properties and osteoconductivity of porous bioactive titanium', *Biomaterials*, **26**, 6014–6023. DOI: 10.1016/j.biomaterials.2005.03.019.

Taylor N, Dunand D C and Mortensen A (1993), 'Initial stage hot pressing of monosized Ti and 90% Ti-10% TiC powders', *Acta Metall Mater*, **41**, 955–965. DOI: 10.1016/0956-7151(93)90030-V.

Teixeira A I, Abrams G A, Bertics P J, Murphy C J and Nealey P F (2003), 'Epithelial contact guidance on well-defined micro- and nanostructured substrates', *J Cell Sci*, **116**, 1881–1892. DOI:10.1242/jcs.00383.

Tengvall P and Lunstrom I (1992), 'Physico-chemical considerations of titanium as a biomaterial', *Clin Mater*, **9**, 115–134. DOI: 10.1016/0267-6605(92)90056-Y.

Tuchinskiy L and Loutfy R (2003), 'Titanium foams for medical applications' in Shrivastava S (ed.), *Medical Device Materials – Proceedings of the Materials and Processes for Medical Devices Conference*, Metals Park, ASM, 377–381.

Uchida M, Kim H -M, Kokubo T, Fujibayashi T and Nakamura T (2003), 'Structural dependence of apatite formation on titania gels in a simulated body fluid', *J Biomed Mater Res*, **64A**, 164–170. DOI: 10.1002/jbm.a.10414.

Vallee A, Hummblot V and Praidier C M (2010), 'Peptide Interactions with Metal and Oxide Surfaces', *Acc Chem Res*, **43**, 1297–1306. DOI: 10.1021/ar100017n.

Vehof J W M, van den Dolder J, de Ruijter J E, Spauwen P H M and Jansen J A (2003), 'Bone formation in CaP-coated and noncoated titanium fiber mesh', *J Biomed Mater Res*, **64A**, 417–426. DOI: 10.1002/jbm.a.10288.

Wazen R M, Lefebvre L -P, E Baril and A Nanci (2009), 'Initial evaluation of bone ingrowth into a novel porous titanium coating', *J Biomed Mater Res Part B: Appl Biomater*, **94B**, 64–71. DOI: 10.1002/jbm.b.31624.

Wu W and Nancollas G H (1998), 'Kinetics of heterogeneous nucleation of calcium phosphates on anatase and rutile', *J Coll Inter Sci*, **199**, 206–211. DOI: 10.1006/jcis.1997.5329.

Xiropaidis A V, Qahash M, Lim W H, Shanaman R H, Rohrer M D, Wikesjö U M and Hall J (2004), 'Bone- implant contact at calcium phosphate-coated and porous titanium oxide (TiUnite™)-modified oral implants', *Clin Oral Impl Res*, **16**, 532–539. DOI: 10.1111/j.I600-0501.2005.01126.x.

Yoriya S, Paulose M, Varghese O K, Mor G K and Grimes C A (2007), 'Fabrication of vertically oriented TiO_2 nanotube arrays using dimethyl sulfoxide electrolytes', *J Phys Chem C*, **111**, 13770–13776. DOI: 10.1021/jp074655z.

Zhou Y L, Niinomi M and Akahori T (2004), 'Effects of Ta content on Young's modulus and tensile properties of binary Ti-Ta alloys for biomedical applications', *Mater Sci Eng A*, **371**, 283–290. DOI: 10.1016/j.msea.2003.12.011.

This page intentionally left blank

Index